Autodesk® Simulation
Accuracy Verification Examples Manual

Version 2012

Table of Contents

Accuracy Verification Examples Listed by Analysis Type

Static Stress with Linear Material Models

Other

Introduction

This manual was written to assure the customer that the Autodesk Simulation Mechanical /Multiphysics 2012 performs consistently and accurately within its defined scope. It contains a large number of Accuracy Verification Examples (AVEs), which compare analysis results with theory for cases taken from well-known engineering reference books. The software should produce results that are consistent with the material presented in this manual.

How to Access the Models

Model files including results for each example can be accessed by downloading and unzipping the file named AutodeskSimulation_ave_archives.zip. Use the "Application button: Archive: Retrieve" command to locate and open the desired model archive, then restore the model to the desired location on your local or network drive.

How to Use This Manual

This manual is divided into a table of contents, this introduction and three chapters. Chapter 1 acquaints you with the definitions and finite element concepts used throughout the software. Chapter 2 presents a verified analysis of a simple bar to illustrate a variety of concepts and to give you a "feel" for finite element modeling considerations. Chapter 3 presents the AVEs. It contains abstracts of all AVEs, two tables that index the AVEs by analysis type used and elements used, respectively, and the descriptions of the AVEs. The descriptions provide a full discussion of each problem, including all information you would need to recreate the problem on your own. You can use the supplied model files to rerun the analyses, if desired. The results you obtain may differ by an insignificant amount because of potential changes in output format or processing options as well as the number of significant digits for math calculations on your particular computer.

Differences in Processor Output Files

If you experience deviations from the results in this manual, here are a few things to consider before assuming that there is a problem.

The results for the verification examples in this manual were obtained using processors that were near current at the original time of publication. The version number of the processor used on a given input file can be found on the header line in the processor output file. If you find that your processors are out-of-date, contact your account representative in order to upgrade to the current versions.

You may also experience deviations if you are using the same versions of the processors listed, but on a different hardware platform. All results posted in this manual were obtained running on a PC workstation. If you are running on a different hardware platform, or analyzing a very large model using a different amount of memory, you might notice a slight difference in the results due to round-off errors. These differences, however, should be very small (typically far less than 0.1%) for significant results.

It should be emphasized, differences may occur that are not at all significant. For example, the weight and center of gravity processor typically produces very accurate results because it doesn't lump element masses at the nodes but instead integrates over the volume of the elements. However, for a model centered at the origin it usually doesn't report exactly zero coordinates for the center of gravity; it may likely give values something like 2.E-6 for a model with dimensions the order of 1, due to round-off error in the calculations or in the nodal coordinates. That is a very accurate answer for the position of the center of gravity, even though the percentage error from zero is infinite. But when the compiler used to build the program changes, those tiny values may change noticeably (maybe even the sign of some value will change), but the results will still be very accurate answers.

Similarly, in a model with maximum stress components on the order of 10,000 psi, a difference of 0.02 psi in a perpendicular stress component is probably a symptom of round-off error. Identical situations should produce identical calculations, but changing the compiler or the math library or the order in which the calculations are done will often give answers that are slightly, but insignificantly, different.

The "% Difference" in these examples is defined as follows:

$$\% \text{ Difference} = \left[\frac{\text{Model value - theoretical value}}{\text{theoretical value}} \text{ X } 100 \right]$$

Chapter 1: Elementary Finite Element Concepts

A physical mechanical system is modeled by using elements, such as plate elements (Figure 1-1). Material properties, such as Young's Modulus, Poisson's Ratio, thermal expansion coefficients and density, are then assigned to the elements. Let's see how you would model and analyze a simple bar.

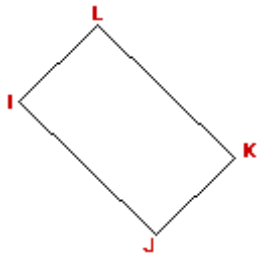

Figure 1-1: A Sample Plate Element

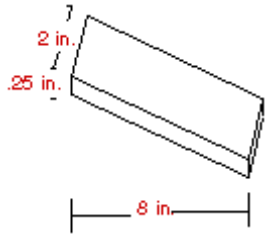

Figure 1-2: A Simple Bar

Models are constructed of elements by locating points in space (nodes) using coordinates in the global coordinate system.

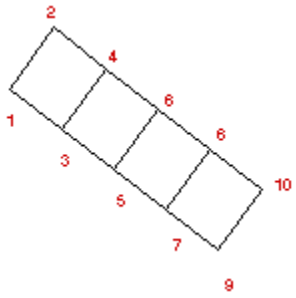

Figure 1-3: An FEA Model Showing Node Numbering

This plate (thin shell) model has 10 nodes and 4 elements. The elements are defined by the way in which the nodes are connected. For example, element number 4 is defined by nodal order 7, 9, 10 and 8. Note that this element is not referred to as being defined by nodes 7, 8, 9, and 10. When you are referring to an element by the nodes which define it, it is often important to know the order in which the nodes define the element. Therefore, if you have to refer to an element by the nodes that define it, it is a good practice to refer to nodes by the order in which they define the element.

Each node has six potential degrees of freedom (DOF). This means that a given node may displace in three translational degrees of freedom, referred to as Tx (Translation in the X direction), Ty (Translation in the Y direction) and Tz (Translation in the Z direction).

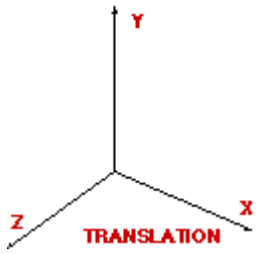

Figure 1-4: Translational Degrees of Freedom

Each node may also displace in three rotational degrees of freedom, referred to as Rx (Rotation in the X direction), Ry (Rotation in the Y direction) and Rz (Rotation in the Z direction). Translation refers to the movement of a node along the X, Y, or Z axes (or any combination of the three), while rotation refers to the movement of a node about the X, Y or Z axes (or any combination). Some element types do not use all of these degrees of freedom, for example, 2-D elements use only Ty and Tz.

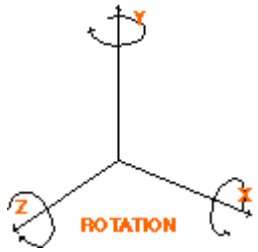

Figure 1-5: Rotational Degrees of Freedom

Boundary conditions are set by restricting various degrees of freedom. For example, if the bar is built into a wall, all degrees of freedom at the connection to the wall are fixed (restricted). These would be nodes 1 and 2 in Figure 1-6, below.

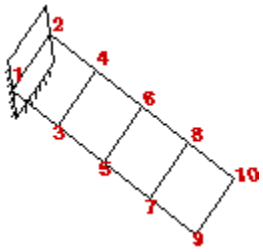

Figure 1-6: Nodal Boundary Conditions for a Bar Fixed to a Wall

Table 1-1 shows the restrictions imposed on translations and rotation of the nodes in the design in Figure 1-6. Degrees of freedom are defined using a binary format, where 0 means that the node is free to move and 1 means that the node is fixed in the degree of freedom. Boundary conditions are added to nodes 1 and 2 to indicate that these nodes are fully fixed.

Table 1-1: Restrictions on Translations and Rotation of the Nodes in Figure 1-6

Node Number	Tx	Ty	Tz	Rx	Ry	Rz
1	1	1	1	1	1	1
2	1	1	1	1	1	1
3	0	0	0	0	0	0
4	0	0	0	0	0	0
5	0	0	0	0	0	0
6	0	0	0	0	0	0
7	0	0	0	0	0	0
8	0	0	0	0	0	0
9	0	0	0	0	0	0
10	0	0	0	0	0	0

Note: Conventions: 0 = Free, 1 = Fixed

In stress analysis, loads can be applied directly at nodes or indirectly via elements.

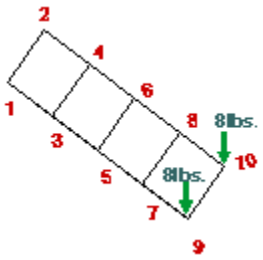

Figure 1-7: An FEA Model Showing Nodal Loads

In this case, a force of 16 lbs is applied to the end of the cantilevered bar. Additionally, you could specify pressure or thermal loads on the elements of the bar. For some elements, thermal loads may be applied by specifying nodal temperatures. For others, element temperatures may be specified.

Nodal loads are referenced in terms of the global coordinate system, just like node locations.

Element loads are applied in the local coordinate systems. Each type of element has a different local coordinate system. Figure 1-8 illustrates the local coordinate system used in plate/shell elements.

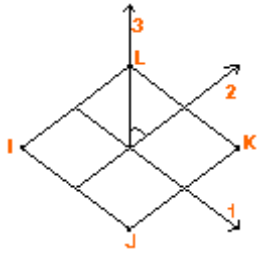

Figure 1-8: Local Coordinate System (Plate/Shell)

Figure 1-9 is an illustration of the local coordinate system for beam elements.

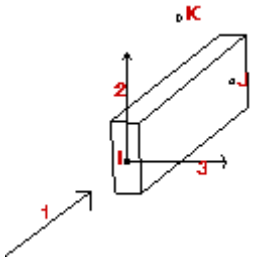

Figure 1-9: Local Coordinate System (Beam)

Stresses are frequently referred to using the local coordinate system rather than the global coordinate system. However, principal stresses are independent of the coordinate system, which makes results based on principal stresses, such as von Mises stresses and stress intensities, easier to relate to engineering requirements.

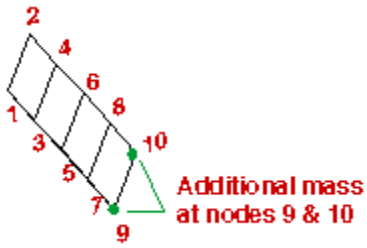

Figure 1-10: Additional Mass in Dynamic Analysis

In dynamic analysis, additional mass can be added to the system by adding nodal masses, which are analogous to nodal loads.

Mass is entered in terms of the global coordinates, like nodal forces. Stresses produced by dynamic response are usually referred to using the local coordinate system.

Once the model and forces/masses have been entered into the system, the following situation exists:

- A force vector {F} or mass matrix [M] has been defined.
- A stiffness matrix [K] has been defined.

The linear stress system will solve one of the following equations.

Static Stress Analysis

$$\{F\} = [K] \{D\}$$

where:

- {D} = the displacement vector. Stresses are back-calculated from this vector.

Modal Analysis

$$[K] \times [D] = [M] \times [D] \times [W]^2$$

where:

- [D] = displacement matrix (mode shapes)
- $[W]^2$ = diagonal matrix containing eigenvalues (natural frequencies)

Dynamic Response

$$[M] \{\ddot{U}\} + [C] \{\dot{U}\} + [K] \{U\} = [R] (t)$$

where:

- [M] = mass matrix
- [C] = damping matrix
- [K] = stiffness matrix
- $\ddot{U}$ = acceleration
- $\dot{U}$ = velocity
- {U} = displacement
- R(t) = any time-dependent loading function (It may be equal to $-M\ddot{U}_g$ for cases of ground motion, such as earthquakes.)

You can obtain either stresses and displacement histories with respect to time or maximum displacements and corresponding stresses.

Bandwidth

One of the variables affecting computer processing speed is the "bandwidth," which is defined by the following.

For any element, the bandwidth is defined as:

(Highest Node Number - Lowest Node Number + 1) * (# DOF per node)

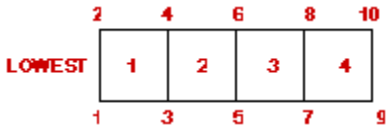

Figure 1-11: Node Numbering (Low Bandwidth)

Figure 1-11 shows a one node numbering scheme that yields a low bandwidth. In Figure 1-11, the bandwidth for element 4 = (10 - 7 + 1) x 6 = 24. Note that in this case, the bandwidth is the same for all elements.

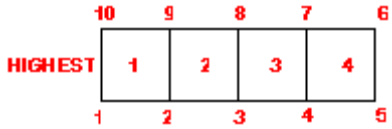

Figure 1-12: Node Numbering (High Bandwidth)

Figure 1-12 shows a node numbering scheme that would yield a very high bandwidth for this geometry.

The bandwidth for element number `1 = (10 - 1 + 1) x 6 = 60`

The bandwidth is an important factor in determining the solution time and storage requirements for the stiffness matrix for your entire model. The highest possible bandwidth for any element in your model is the bandwidth for the entire model. This makes it very important that the smallest possible bandwidth is achieved.

In classical finite element modeling, and even today with some other finite element systems, you must spend a considerable amount of time trying to minimize the bandwidth. This is done using techniques such as careful numbering and adding of the nodes in your model to minimize the maximum difference between the node numbers in any element. Some finite element systems even use separate programs to do this, but this alters the node numbers in your model. A routine to minimize the bandwidth is built into the processors. The execution of this routine is totally transparent. For this reason, when using the software, you usually do not have to worry about the bandwidth of your model.

Chapter 2: Sample Analysis of Skewed Elements

One of the questions that frequently arises in finite element modeling is, "How does the use of skewed elements affect the accuracy of the analysis of my model?" As a general rule, significant skewness can be tolerated if the main interest is displacements in a static analysis case or the determination of natural frequencies. Often, the main impact of irregular elements relates to stress determination, though there can be an impact on the overall stiffness matrix in some situations.

Even in this case, a relatively large amount of irregularity can be tolerated in many situations, and there are options that can reduce the sensitivity of the analysis to badly shaped elements. It is impossible, however, to present any standard guidelines or "rules of thumb" to determine in advance just how much irregularity in the shapes of the elements is acceptable.

To help determine the accuracy of analysis results, Precision dithered displays are available. The Precision display highlights areas of a model where a finer mesh will provide more accurate results.

The sample problem presented in this chapter illustrates the effect of skewed elements on stress results. The sample problem consists of a plate that is 10" long, 4" wide and 0.5" thick, completely fixed at one end. The plate is loaded across the free end with the equivalent of 500 lb of force perpendicular to the plate and 5,000 lb of force applied at the free end, stretching the plate away from the fixed end, as Figure 2-1 illustrates.

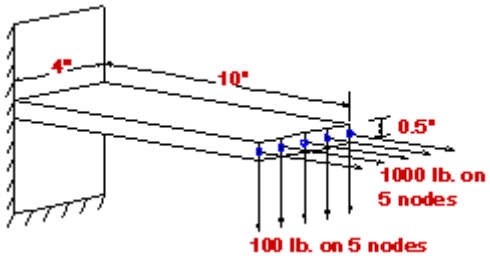

Figure 2-1: Cantilever Plate with Force Applied at the Free End

Two models were developed and processed. In each model the plate is divided into 40 elements. In Case 1, "skewuss", the elements are exactly square, having 1" on each side, as Figure 2-2 shows. Figure 2-3 shows the deflected plate, with the deflections being scaled up by a factor of 10.

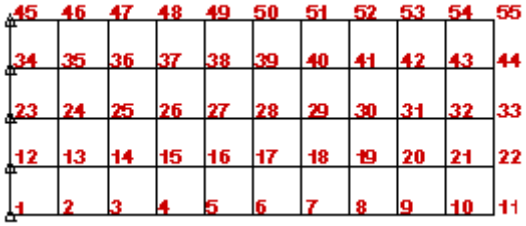

Figure 2-2: Square Elements in Example "skewuss"

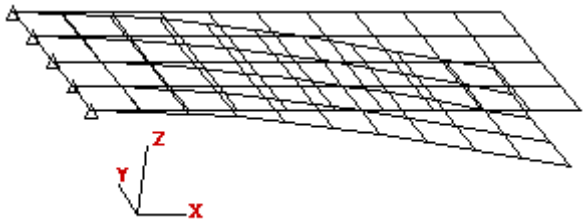

Figure 2-3: Deflected "skewuss" Model Superimposed on the Original Model

In the second case "skewss", the same plate is modeled with 40 elements. However, as Figure 2-4 shows, the elements are very badly skewed. During analysis two warning messages are given, showing that the extreme skewedness has affected the stiffness matrix. In this case, results are not significantly affected, but a very simple method (besides remeshing or dividing the two most badly skewed quadrilaterals into pairs of triangles) can be used to improve the matrix. Simply use the reduced shear plate element formulation which is less sensitive to badly shaped elements than the default Veubecke formulation. Figure 2-5 shows the deflected plate with the deflections being scaled up by a factor of 10.

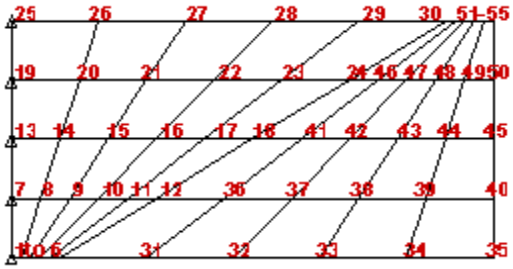

Figure 2-4: Model "skewss" Showing Skewed Elements

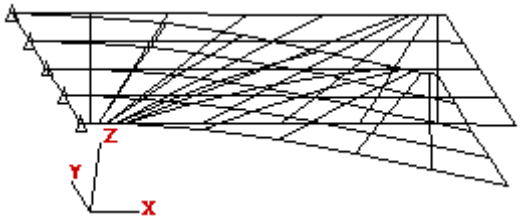

Figure 2-5: Deflected, Skewed Model Superimposed on Original "skewss"

At this point the reader is encouraged to further research the effect of irregular elements on a case-by-case basis as the engineering situation warrants. As a further point of interest, let us compare the high stresses reported by the two models with numbers calculated by hand, using simple beam theory:

$$Z = \frac{bh^2}{6} = \frac{4 \times 0.5^2}{6} = 0.1667 \text{ in}^3$$

$$I = \frac{bh^3}{12} = \frac{4 \times 0.5^3}{12} = 0.041667 \text{ in}^4$$

$$Mx = 100 \times 5 \times 10 = 5000 \text{ inches lb (moment)}$$

$$Sm = \frac{1000 \times 5}{4 \times 0.5} = 2500 \text{ psi (membrane stress)}$$

$$Sb = \frac{Mx}{Z} = \frac{5000}{0.1667} = 30000 \text{ psi (bending stress)}$$

$$Sx = Sm + Sb = 30000 + 2500 = 32500 \text{ psi}$$

where:

- b = 4"
- h = .5"

The maximum stress computed by simple beam theory is within 10.24% of the results reported by both finite element analyses. The theoretical results are based on beam theory as compared with actual plate bending and stretching behavior. The plate model can provide a beam solution by setting the Poisson ratio to zero. In such a case, the difference between beam theory and the plate results is less than 1%. Regarding the deflection of the free end, the beam theory calculation yields the following result:

$$DY = \frac{WL^3}{3EI} = \frac{500 \times 10^3}{3 \times 3.0 \times 10^7 \times 0.041667} = 0.1333 \text{ inches}$$

where:

- W = 500 lb (transverse end force)
- L = 10"
- E = 3.0 x 10^7 psi
- I = 0.041667 in^4

This compares to a value of 0.1283" from Case 1, "skewuss", and a value of 0.1278" from Case 2, "skewss".

Note: The analysis is probably more accurate because it accounts for the curling of the bar.

Chapter 3: Accuracy Verification Examples

This chapter presents abstracts of all examples, an index of AVEs by analysis type used, an index of AVEs by elements used and the AVE descriptions.

Autodesk Simulation Automated Test

Autodesk Simulation Automated Test is a program that is installed on a system when the AVE files are installed. This program will run all, or a selected set, of AVE models and compare the results to the accepted values. This can be executed by navigating to the directory where the AVE files were installed and double clicking on the AlgorScript.exe file.

The following information must be provided:

Path to the AVE folder: Press the **"…"** button to the right of this field and navigate to the AVES directory where the AVE files were installed on the machine.

Path to the Autodesk Simulation installation: Press the **"…"** button to the right of this field and navigate to the directory where Autodesk Simulation is installed on the machine.

Path to the testing folder: Press the **"…"** button to the right of this field and navigate to the directory to which the AVE models will be unarchived and analyzed.

Start at AVE number: Specify the number corresponding to the first AVE that will be analyzed.

Stop at AVE number: Specify the number corresponding to the last AVE that will be analyzed.

AVE type filter: All of the AVE models between the **"Start at AVE number"** and **"Stop at AVE number"** will be performed that fall into the analysis types selected in this section. Pressing the **"Sync with License"** button will select the analysis types which are available with the current license setup.

Once the necessary information is specified, press the **"Start"** button. The selected AVE models will be unarchived and analyzed automatically. Depending on how many models are being analyzed, this process could take a considerable amount of time.

Abstracts of All Accuracy Verification Examples

AVE - 1: Flat Circular Plate of Constant Thickness (2-D) – A flat, annular, circular plate of 0.5" constant thickness with its outer edge simply supported and inner edge free is analyzed for stress and deflection under a 50 lbf/in uniform annular line load located at the inner edge. The model is constructed of 2-D axisymmetric elements.

AVE - 2: Flat Circular Plate of Constant Thickness (3-D) – A flat, annular, circular plate of constant thickness with its outer edge simply supported, inner edge free and the load located at the inner edge is analyzed for stress and deflection. The model is constructed of 3-D solid brick elements.

AVE - 3: Thin-Walled Cylinder with Uniform Axial Load – A thin-walled cylinder under uniform axial load is analyzed for axial stress and deflection.

AVE - 4: Thick Cylindrical Disk under Uniform Radial Pressure – A thick-walled cylindrical disk that has uniform internal radial pressure is analyzed for hoop stress and radial deflection. The model uses 3-D brick elements.

AVE - 5: Rectangular Plate with All Edges Simply Supported and Uniform Pressure – A rectangular plate with all edges simply supported and uniform pressure over a central rectangular area is analyzed for maximum stress. The model uses 3-D plate elements.

AVE - 6: Flat Rectangular Plate with Three Edges Simply Supported – A flat rectangular plate (10" x 5" x 0.25") with 3 edges simply supported and one edge free under uniform pressure loading is analyzed for maximum stress. The model uses 3-D plate elements.

AVE - 7: Cantilever Beam with Nodal Force – A uniform cross-section cantilever beam with fixed-free boundary conditions at the ends is analyzed for deflection under a center point loading. The model uses beam elements.

AVE - 8: Toroidal Shell under Uniform Internal Pressure – A toroidal shell under uniform internal pressure is analyzed for stress and deflection. The model represents one octant of an inner tube with symmetry boundary conditions imposed at all the edges. The model uses 3-D brick elements.

AVE - 9: Beam Guided at the Left and Fixed at the Right – A uniform cross-section beam with fixed-guided boundary conditions at the ends is analyzed for moment and deflection under a center point loading. The model uses beam elements.

AVE - 10: Thick-Walled Spherical Vessel under Uniform Internal Pressure – A thick-walled spherical vessel under uniform internal pressure is analyzed for radial stress and deflection. The model represents one octant of a sphere with symmetry boundary conditions imposed at all edges. The model uses 3-D brick elements.

AVE - 11: Thick-Walled Cylindrical Vessel under Uniform Internal Radial Pressure – A thick-walled cylindrical vessel under uniform internal pressure is analyzed for hoop stress and radial deflection. The model represents part of one quarter of a thick cylinder with mirror symmetry boundary conditions imposed at the symmetry planes. The model uses 3-D brick elements.

AVE - 12: Hollow Cylinder with Thick Walls and Temperature Gradient – A thick-walled cylindrical vessel under uniform logarithmic temperature gradient throughout the thickness is analyzed for thermal stress. The model uses 3-D brick elements.

AVE - 13: Lid Driven Cavity – Fluid flow analysis is used to analyze a lid driven cavity problem solved at Reynolds number = 400. An incompressible viscous fluid is trapped in a square 2-D box (1" x 1") and the top wall moves at a constant velocity of 1. As a result, the fluid is set in motion. The model uses 2-D elements.

AVE - 14: Flat Rectangular Plate with All Edges Fixed and Uniform Pressure Loading – A flat rectangular plate with all edges fixed under a uniform pressure loading is analyzed for maximum stress and deflection. A quarter-symmetry model is analyzed with symmetry boundary conditions applied at the symmetric edges. The model uses 3-D plate elements.

AVE - 15: Flat Rectangular Plate with Two Sides Fixed, Two Sides Simply Supported and Uniform Load – A flat rectangular plate (20" x 10" x 0.1") with the two short sides fixed, the two long sides simply supported and a uniform 10 psi load is analyzed for maximum stress and deflection. A quarter-symmetry model is analyzed with symmetry boundary conditions applied at the symmetry edges. The model uses 3-D plate elements.

AVE - 16: Uniform Beam with Both Ends Fixed – A uniform beam with both ends fixed is analyzed for eigenvalues and frequencies. The beam is 10" long. It is made of steel and has a 1" x 1" square cross-section. No load is applied to the beam. The model uses beam elements.

AVE - 17: Thick-walled Cylindrical Vessel under Uniform External Pressure Modeled in 3-D – A thick-walled cylindrical vessel under uniform external pressure is analyzed for radial stress and deflection. The model represents one quarter of a thick cylinder with symmetry boundary conditions imposed at the symmetric edges. For this example, we chose an outside radius of 10" and an inside radius of 5" with external pressure of 50 psi. Steel material properties were used. The model used 3-D brick elements.

AVE - 18: Thick-walled Cylindrical Vessel under Uniform External Pressure Modeled in 2-D – A thick-walled cylindrical vessel under uniform external radial pressure is analyzed for hoop stress and radial deflection. For this example, we chose an outside radius of 10" and an inside radius of 5" with an external pressure of 50 psi. Steel material properties were used. The model used 2-D axisymmetric elements.

AVE - 19: Thin-walled Conical Vessel under Uniform Internal Pressure with Tangential Edge Supports – A thin-walled conical vessel under uniform internal pressure is analyzed for stress and deflection. The model represents one quarter of a cone with symmetry boundary conditions imposed at the symmetric edges. The model uses 3-D brick elements.

AVE - 20: Straight Bar with Lower End Fixed and Upper End Free – A straight bar is used to model a column with constant cross section under a compressive loading. Because of the loading, a buckling analysis was performed to determine when the bar will become elastically unstable. The model uses beam elements.

AVE - 21: Wide-flange Beam with Equal Flanges – The "Inquire:XY Moment of Inertia…" command of FEA Editor is used to provide the area, moments of inertia, and radii of gyration for a model of a wide-flange beam with equal flanges.

AVE - 22: Circular Disc Rotating about Its Own Axis with Uniform Angular Velocity Modeled in 2-D – A homogeneous circular disc of conical cross section, which rotates about its own axis with a uniform angular velocity, is analyzed for tensile radial stress and tangential inertia stress. The model uses 2-D axisymmetric elements.

AVE - 23: Circular Disc Rotating about Its Own Axis with Uniform Angular Velocity Modeled in 3-D – A homogeneous circular disc of conical cross section, which rotates about its own axis with a uniform angular velocity, is analyzed for tensile radial stress and tangential inertia stress. The model uses 3-D brick elements.

AVE - 24: Thin-walled Cylindrical Shell under an Axisymmetric Radial-End Load – A long, thin-walled cylindrical shell under an axisymmetric radial-end load is analyzed for maximum stress and deflection. A quarter-symmetry model is used with symmetry boundary conditions applied at the symmetry edges. The model uses 3-D plate elements.

AVE - 25: Test of the Capabilities of the 'dt/dh' Option for the Plate Element – A flat plate of uniform thickness with fixed edges and a uniform linear temperature gradient between the two faces of the plate is analyzed for maximum stress. This accuracy verification example tests the capabilities of the "dt/dh" option for the plate element. The "dt/dh" option enables the user to model a linear temperature gradient in the local 3 direction, which is through the thickness of the plate element.

AVE - 26: Rectangular Plate under Uniform Load Producing a Large Deflection – A rectangular plate, held, not fixed, is under uniform load which produces a large deflection. Because of the large deformation (relative to the plate thickness), a nonlinear analysis was performed using Mechanical Event Simulator with the pressure loading feature. The model uses nonlinear shell elements.

AVE - 27: Solid Circular Plate Section of Constant Thickness with Uniform Load – A solid circular plate section of constant thickness with a uniformly distributed load over the entire surface and the edges simply supported is analyzed for maximum stress. The model uses 3-D plate elements.

AVE - 28: Thin Closed Circular Ring with Circular Cross Section – A thin, closed, circular ring with circular cross section under uniform compressive loading is analyzed for deflection and moments. The model uses beam elements.

AVE - 29: Thick-walled Cylindrical Vessel under Uniform Internal Radial Pressure – A thick-walled cylindrical vessel under uniform internal radial pressure (longitudinal pressure zero or externally balanced) is analyzed for hoop stress and radial deflection. The model uses 2-D axisymmetric elements.

AVE - 30: Ceramic Strip with Radiation and Convection – This example involves a thermal analysis of a ceramic plate with combined convection and radiation environment applied at the top, the bottom surface fully insulated and the sides being held at constant temperature using temperature boundary elements. The model uses 2-D thermal elements.

AVE - 31: Two Masses and Three Massless Springs with an Applied Forced Harmonic Vibration – A two degrees-of-freedom (DOF) system consisting of two masses coupled with three massless springs is analyzed for steady state displacements and natural frequencies due to forced harmonic response. The model uses beam elements.

AVE - 32: Steady-State Heat Loss of a Steam Pipe with Nonconcentric Insulation – A steam pipe that is surrounded by nonconcentric insulation is analyzed to determine the steady-state heat loss. The model uses 2-D thermal elements and temperature boundary elements.

AVE - 33: Elastic Instability of a Flat Plate under Pure Shear Load – A flat rectangular plate with all edges fixed under a pure shear load is analyzed to determine the buckling load under which the plate will become unstable. The model uses 3-D plate elements.

AVE - 34: Ceramic Embedded in a High Thermal Conductivity Material – A ceramic strip is embedded in a high-thermal-conductivity material so that the sides are maintained at constant temperature. The bottom surface is insulated and the top surface is exposed to a convection environment. Transient thermal analysis is performed to find the temperature distribution as the ceramic cools. The model uses 2-D thermal elements and temperature boundary elements.

AVE - 35: Motion of a Two-DOF System Subjected to Random Vibration – A two degrees of freedom (DOF) mass and spring system is subjected to a random vibration environment (or "white noise"). First, the natural frequencies are extracted from the modal analysis, and then a random vibration restart analysis is performed to determine the displacements for the system subjected to an input power spectral density (PSD) applied in the vertical (X) direction. The analysis uses beam elements.

AVE - 36: Interference Analysis of Two Concentric Thick-walled Rings – Two concentric thick-walled rings or circular plates, with different material properties, are subjected to a temperature increase in order to perform an interference analysis. Tangential stress is determined at the inner surfaces of the two rings. The model uses 2-D plane stress elements.

AVE - 37: Circular Flat Plate with Edge Clamped and Concentrated Load Applied at Center – A circular flat plate of constant thickness under point loading at the center with all edges fixed is analyzed for maximum deflection. The model uses 3-D plate elements.

AVE - 38: Thick-walled Spherical Vessel under Uniform Internal Pressure – A thick-walled, spherical vessel under uniform internal pressure is analyzed for radial stress and deflection. Due to symmetry, one octant of the sphere is modeled with symmetry boundary conditions applied at the edges. Two models are analyzed, one using 3-D brick elements and the other using tetrahedral elements.

AVE - 39: Forced Harmonic Response Analysis of a Spring-Mass-Damper System – A single degree of freedom spring-mass-damper system is analyzed for steady-state displacements, phase angle and natural frequencies due to forced harmonic vibration applied to the mass. The model uses beam elements.

AVE - 40: Solid Sphere Analyzed to Find Weight, Center of Gravity and Mass Moment of Inertia – A 1.0 inch radius solid sphere is analyzed for weight, center of gravity and mass moment of inertia. The model uses 2-D axisymmetric elements.

AVE - 41: Natural Frequency Analysis of a Graphite/Epoxy Laminated Composite Square Plate – A simply supported, square, graphite/epoxy laminated composite plate is analyzed for natural frequencies and mode shapes. The laminate material is comprised of 9 different layers. The model uses thick plate composite elements.

AVE - 42: Mid-span Deflection of a Uniform Steel Beam Simply Supported at Both Ends – A steel beam with uniform cross section, which is simply supported at both ends and under uniform distributed triangular loading, is analyzed for deflection and moments. The model uses beam elements.

AVE - 43: Stress Relaxation of a Tightened Bolt Due to Thermal Creep – A bolt with a length of 10 inches and a cross-sectional area of one square inch is tightened to an initial stress (σ_0) of 1000 psi. The bolt is held at a fixed displacement for a long period of time (t = 1000 hrs.) at a temperature at which thermal creep occurs. The stress in the bolt is determined at various times during creep relaxation. Small-strain, small-deformation theory is used. The model uses beam elements.

AVE - 44: Deflection Analysis of a Helical Spring Under Compressive Loading – A closely coiled solid helical spring of circular cross-section is subjected to a compressive load and analyzed for deflection. The model consists of only a single complete turn of the spring.

AVE - 45: Nonlinear Radiation Heat Transfer Analysis of a Cylindrical Disk with Internal Heat Generation – A hollow cylindrical disk, with internal heat generation, is exposed to a radiation environment. A steady-state heat transfer analysis is performed to determine the radiation surface temperature. Due to symmetry, only one quarter of the cylinder is modeled. For comparison, the problem is analyzed using three different element types: 8-node hexahedral brick, 4-node tetrahedral and 10-node tetrahedral.

AVE - 46: Shear Force and Bending Moment Analysis of a Beam under Distributed Loading – A beam with square cross-section, under nodal force and distributed loading, is analyzed for shear force and bending moment.

AVE - 47: Thermal Stress Analysis of a Thick-walled Cylindrical Vessel Under Temperature Gradient – A thick-walled cylindrical vessel under uniform logarithmic temperature gradient throughout the thickness is analyzed for thermal stress. The model uses 2-D axisymmetric elements.

AVE - 48: Elastic Stability of a Flat Plate under a Pure Axial Load – A flat, rectangular plate with all edges simply supported under compressive axial load is analyzed to determine the critical load under which the plate will become elastically unstable (i.e., when buckling will occur). The model uses 3-D plate elements.

AVE - 49: Concrete Frame Structure Subjected to Distributed Loading – A concrete frame structure under distributed loading is analyzed for bending moment and deflection. The model uses beam elements.

AVE - 50: Solid Aluminum Cylinder Exposed to a Convection Environment and Allowed to Cool – A long, solid aluminum cylinder is exposed to a convection environment and allowed to cool. A transient thermal analysis is performed to determine the temperature at a certain radius after 1 minute. The model uses 2-D axisymmetric thermal elements.

AVE - 51: Fluid Flow between Two Plates – The fluid flow between two plates (the bottom plate is stationary and the top plate moves) is calculated with 3-D unsteady fluid flow analysis. The model uses 3-D solid brick elements.

AVE - 52: 2-D Laminar Flow over a Backward Facing Step – Laminar fluid flow over a backward facing step is calculated with 2-D steady fluid flow analysis. The flow is analyzed for Reynolds number 100. The model uses 2-D planar elements.

AVE - 53: Linear Mode Shape with Load Stiffening Analysis on a Simply Supported Continuous Beam – A Linear Mode Shapes and Natural Frequencies with Load Stiffening analysis is performed on a simply supported continuous steel beam under compressive axial loading. The model uses beam elements.

AVE - 54: Thick-walled Spherical Shell Subjected to Uniform Internal Pressure of Gradually Increasing Magnitude – A nonlinear stress analysis is performed for a thick-walled spherical shell subjected to uniform internal pressure of gradually increasing magnitude. Two load cases are considered: 1) the shell just turns plastic and 2) the shell turns completely plastic. One radian of half of the shell was modeled using 2-D axisymmetric elements.

AVE - 55: Nonlinear Heat Flow Analysis of a Solid Cylinder – A Steady-State Heat Transfer analysis is performed to determine the temperature distribution in a solid cylinder exposed to one convection temperature along the top surface and another convection temperature along the bottom surface. The thermal conductivity of the cylinder varies with the temperature. The model uses 2-D axisymmetric elements and temperature boundary elements.

AVE - 56: Response Spectrum Analysis of a Simple Beam – A Linear Response Spectrum (Modal Superposition) analysis is performed to determine moment, force and stress results for a cantilever beam with mass at the end subjected to a response spectrum load.

AVE - 57: Cantilever Beam with a Gap at the Tip – A cantilever beam is subjected to a concentrated load at the tip. An elastic support is below the tip. There is a gap between the beam tip and the elastic support. A compression-only gap element is used to find the deflection of the beam and the reaction of the elastic support.

AVE - 58: Transient Thermal Analysis of a Solid Wall with Internal Heat Generation – A transient thermal analysis of a solid wall with internal heat generation is performed to determine the temperature at the center of the wall as a function of time. The problem is analyzed with two models: one using 2-D thermal elements and the other using 3-D thermal brick elements.

AVE - 59: Steady-State Heat Transfer Analysis of a Fin Immersed in a Cooling Fluid – A fin with one end held at a constant temperature and the other end insulated is immersed in a cooling fluid, which is modeled with convection. A Steady-State Heat Transfer analysis is performed to determine the temperature along the fin. The model uses 2-D thermal elements and temperature boundary elements.

AVE - 60: Nonlinear Radiation Heat Transfer Analysis of a Cylinder with Internal Heat Generation – A hollow cylindrical disk, with internal heat generation, is exposed to a radiation environment. A Steady-State Heat Transfer analysis is performed to determine the external surface temperature. The model uses 3-D thermal brick elements.

AVE - 61: Continuous Beam, Simply Supported at the Ends, Under a Uniformly Distributed Load – A three-span continuous beam subjected to a uniformly distributed load is analyzed to determine the reactions at supports and the maximum moment of the beam.

AVE - 62: Design Spectrum with a Specified Maximum Ground Acceleration – A beam structure with the bottom fixed and a lump mass at the top is analyzed by the response spectrum analysis method to determine the maximum relative displacement for a design spectrum with a specified maximum ground acceleration.

AVE - 63: Slab with Internal Charge Density Distribution – An Electrostatic Field Strength and Voltage analysis is performed for a slab with an internal charge density distribution to determine the voltage distribution inside the slab. The model uses 3-D electrical solid elements.

AVE - 64: Thermal Deflection Analysis of a Plate with One End Fixed and the Other End Guided – A plate with one end guided and the other end fixed is subjected to one temperature on the bottom and a different temperature on the top over half its length. A Linear Static Stress analysis is performed to determine the moments at both ends and the deflection at the guided end. The model uses 3-D plate elements.

AVE - 65: Torsion of an Elastic Beam with a Channel Cross-Section – An elastic beam with a channel cross-section is restrained against torsion on one end and free to twist on the other. Two opposing forces are applied to the intersections of the web and the flanges at the free end, which produces a torsional moment. A linear static stress analysis is performed to determine displacements. The model uses 3-D plate elements.

AVE - 66: Multidimensional Transient Heat Transfer Analysis – A heated stainless steel cylinder is quenched by submersion in an oil bath. A Transient Heat Transfer analysis is performed to determine the temperatures at the center of the cylinder, at the center of a circular face, and at the mid-height of the side at three minutes into the cooling process. The model uses 2-D axisymmetric elements.

AVE - 67: Fundamental Frequency and Static Lateral Deflections of a Loaded Shaft – A simply supported shaft loaded by masses is analyzed to determine the fundamental frequency and also the static lateral deflections of the shaft.

AVE - 68: Annular Plate with a Uniformly Distributed Pressure – An annular plate under a uniformly distributed pressure, with the outer edge simply supported and the inner edge guided, is analyzed to determine displacement and stress. For comparison, the problem is modeled three different ways using 2-D, plate and brick elements.

AVE - 69: Nonlinear Static Analysis of a Simply Supported Plate – A square plate with simply supported edges is subjected to a uniform pressure load. A nonlinear static stress analysis is performed to determine the maximum deflection. The model uses nonlinear plate/shell elements. For comparison, the problem is modeled using two different mesh densities and thicknesses.

AVE - 70: A Combined Beam/Plate Model – A flange beam with a plate attached to the top flange is simply supported on both ends and has a uniform load applied along the span of the beam. The structure is modeled as a combined beam/plate element model. The moment of inertia and section modulus are calculated for the combined model. A Linear Static Stress analysis is performed to determine stress.

AVE - 71: Creep Analysis of a Thick-walled Cylinder – Determine the stationary state stress distribution in a thick-walled cylinder made of a Norton Power Creep Law material when loaded by internal pressure. Due to the symmetry of the loading and geometry, a 2-D axisymmetric analysis was run instead of modeling the entire 3-D cylinder. A small displacement, constant pressure solution was obtained for a duration of 10,000 hours. It was observed that at a time of approximately 2400 hours, the stresses in the cylinder had come to a state of equilibrium.

AVE - 72: Shear Flow in a Simply Supported Beam – A simply supported beam has a rectangular cross section of 1 inch high by 0.5 inches wide. The beam is 10 inches long. A load of 80 pounds is applied at the center of the beam. This causes a constant shear on the end of the beam. A 2-D model was analyzed. The shear stress was calculated for various vertical locations and compared to the results.

AVE - 73: Dynamic Analysis of a Beam Model – A propped beam has two concentrated loads. Determine the ultimate values of the two concentrated loads (i.e., at collapse of the beam structure) if they are increased at such a rate that they remain in the same proportion to each other. A nonlinear dynamic analysis was run to determine the collapse of the structure. The analysis was able to predict the onset of gross deformation, which occurs following reaching plasticity at the right location of the loading in the model. The model uses nonlinear beam elements.

AVE - 74: Thermal Stress Analysis of a Pinned Beam/Truss Structure – The software was used to model and analyze the thermal stress interactions in a pinned beam/truss structure, which consists of a brass cylinder and a steel rod pinned to a rigid linkage bar. The goal of the analysis was to thermally load the brass cylinder and find the resultant deflections and stresses. During the linear static stress analysis, the temperature of the brass cylinder was raised, which caused the material to expand axially. The steel rod remained at the same temperature and resisted expansion. The analysis results indicated maximum stress in the brass cylinder. The model uses beam and truss elements.

AVE - 75: Dynamic Nonlinear Analysis of a Beam Model with a Gravity Load – Two slender rods are joined by a shared pinned node. If the system is released from rest from a particular starting angle, determine the velocity of a particular endpoint. The problem was modeled using 2-D elements and solved using the nonlinear stress analysis software.

AVE - 76: Linear Stress Analysis of a Beam Model – A continuous beam is modeled using beam elements. Reaction force results are compared with theoretical results.

AVE - 77: Two Cylindrical Shells with Internal Pressure Loading – Two cylindrical shells of different thicknesses are subjected to an internal pressure loading. The goal is to find the radial deflection at the common circumference between the two shells. The model uses 2-D axisymmetric linear elements.

AVE - 78: Spring and Collar Slide Down Vertical Rod – A collar slides without friction along a vertical rod. A spring is attached to the collar. If the collar is released from rest, determine its velocity. Because the orientation of the truss is changing with time, MES software was used to solve this problem. The model uses nonlinear 2-D and truss elements.

AVE - 79: Slender Pivoting Rod and Compressed Spring – A slender rod is pivoted about a point which is 1 ft from the end. The other end is pressed against a spring until the spring is compressed 1 inch. The rod is then in a horizontal position. If the rod is released from this position, determine its angular velocity and the reaction at the pivot as the rod passes through a vertical position. An Mechanical Event Simulation was done using nonlinear 2-D and truss elements.

AVE - 80: Dynamic Analysis of an 8-kg Body Using Damping and a Dashpot – An 8-kg body attached to a spring is moved to the right of the equilibrium position and released from rest. Determine its displacement at a specific time given damping. An Mechanical Event Simulation was done using nonlinear 2-D and general contact elements.

AVE - 81: Transient Heat Transfer Analysis of a Semi-Infinite Pressure Loading – A semi-infinite, aluminum cylinder is subjected to a convection on one end and around the perimeter. The goal of the analysis is to determine the temperatures at the center of the cylinder and the surface at 1 minute after being exposed to the environment. A 3-D, 90° sector of the cylinder was modeled for an Transient Heat Transfer analysis using 3-D thermal brick elements.

AVE - 82: Mechanical Event Simulation of a Slider-Crank Mechanism – The common configuration of a reciprocating engine is that of a slider-crank mechanism. An Mechanical Event Simulation is conducted to determine the velocity of the piston. The model uses nonlinear beam and 3-D brick elements.

AVE - 83: Mechanical Event Simulation of a Lunar Lander – A lunar lander is descending onto the moon's surface with a certain velocity when its retro-engine is fired. The engine produces a thrust that varies with the time and then cuts off. Calculate the velocity of the lander at a certain time, assuming it has not yet landed. An model of a lunar lander was built using truss and 3-D solid elements. A Mechanical Event Simulation was performed to calculate velocity at the specified time.

AVE - 84: Fluid Flow Drag Analysis of Flow across a Flat Plate – A sharp, flat plate is immersed parallel to a stream of air of a certain velocity. Find the drag on one side of the plate. A 2-D model was built using planar elements. The model was analyzed using 2-D steady-state fluid flow analysis processor for the calculation of reaction forces. The values for the nodes along the bottom surface of the model (excluding the nodes of the inlet face) were summed. The sum was used to calculate drag.

AVE - 85: Mechanical Event Simulation of a Basketball Being Shot into a Hoop – An Mechanical Event Simulation is performed to determine the projectile motion of a basketball. The basketball is shot from a certain distance away and below the center of the basketball rim. The goal of the analysis is to find the vertical and horizontal displacement of the ball after a certain time. The model uses nonlinear beam and shell and 3-D kinematic elements.

AVE - 86: Heat Flux Transient Heat Transfer Analysis – A block is exposed to an environment such that a known heat flux is imposed on the surface. The specific heat changes as a function of temperature. Find the final bulk temperature after a certain time, if the block starts at a certain temperature. 2-D orthotropic elements were used in order to specify temperature-dependent material properties for the Transient Heat Transfer analysis.

AVE - 87: Mechanical Event Simulation of a Grinder Shaft under Torsion – A grinder has an abrasive wheel mounted at each end of the shaft and a belt-driven sheave at the center. When turning, the wheel is accidentally jammed, causing it to stop "instantly". Estimate the resulting maximum torsional stress and deflection of the shaft. A 3-D model of the shaft and grinding wheel was created and a Mechanical Event Simulation analysis was performed.

AVE - 88: Mechanical Event Simulation of a Chain with Weights at the Hinges – Four weightless rods of equal length are hinged together to form a hanging chain. Find the angles for this closed kinematic chain, given the length of each rod and the loads. A 3-D brick element model was built to represent the four rods. A Mechanical Event Simulation analysis was performed to determine the displacements at points of interest. The angles were then calculated from the displacements.

AVE - 89: Transient Thermal Analysis of a Cooling Copper Wire – A copper wire is heated by a short circuit to 300 °F before a slow-blow fuse burns out and all heating ceases. Determine how long it will take for the wire temperature to drop to 120 °F. A 2-D model of the wire cross-section was created. A transient heat transfer analysis was performed to determine the number of hours required for the wire to cool to the target temperature.

AVE - 90: Heat Flux Loading on a Hollow Cylinder – A hollow cylinder has uniform temperature over the ends and the outer surface. On the inner surface, a prescribed heat flux is applied to the central part of the surface, while the ends of the inner surface are insulated. An axisymmetric section of the cylinder is modeled using 2-D elements. A Steady-State Heat Transfer analysis is performed to determine the temperature at a point of interest.

AVE - 91: Mechanical Event Simulation of a Cylinder Rolling inside a Curved Surface – A cylinder is rolling inside a curved surface. Determine the period of small oscillations. A 2-D model of the cylinder and curved surface is created. A Mechanical Event Simulation analysis is performed to determine the times when the cylinder reaches the maximum elevation. The average period is calculated from these times.

AVE - 92: Mechanical Event Simulation of a Flyball-Governor – A flyball-governor apparatus consists of four identical arms (solid cylindrical rods) and two spheres. At the base, and rotating with the system, is a cylinder. Initially, the system is rotating at a certain speed, which is maintained by a force at the base. If the force is changed, what is the angular velocity of the system? A 3-D model is created and a Mechanical Event Simulation is performed to determine the displacement of the node at the end of one arm, which is used to measure the period of revolution.

AVE - 93: Steady-State Heat Transfer Analysis of a Pipe Buried in Earth – A horizontal pipe is buried in earth. Given the difference in temperature between the pipe wall and the earth surface, calculate the heat lost by the pipe. For comparison, both 2-D and 3-D models are created and analyzed by steady-state heat transfer analysis.

AVE - 94: 3-D Truss System under a Point Load and Uniform Temperature Increase – This example is a simple model of a 3-D truss system with 7 elements. Two load cases are applied independently: a 1,000-lb. point load and a uniform temperature increase of 50 degrees Fahrenheit. This problem verifies the accuracy of the truss element and illustrates the use of the element load multiplier to applied temperature.

AVE - 95: Weight, Center of Gravity and Mass Moment of Inertia Analysis of a Straight Bar – A steel bar is analyzed for weight, center of gravity and mass moment of inertia. This example verifies the accuracy of the Mass Properties Analysis processor for truss elements.

AVE - 96: 6-Story, 2-Bay Frame Structure under Uniformly Distributed Loading – This example is a plane frame example using beam elements with distributed loads. This example verifies the accuracy of the beam element and illustrates the use of uniform distributed loads. Two load cases are used: point loads and distributed loads. The point load case is equivalent to the distributed load case to illustrate that equivalent results can be obtained by different methods. With beam element, distributed loads can be assigned directly to the elements.

AVE - 97: Earthquake Response of a 10-Story Plane Frame – A ten-story plane frame is subjected to a response spectrum load representing an earthquake. The analysis is performed in two parts: a modal analysis to obtain mode shapes and frequencies, followed by a response spectrum analysis to calculate stresses and deflections.

AVE - 98: Frequency Response Analysis of a Two Degrees of Freedom System – A two degrees of freedom system is subjected to a sinusoidal force applied at the second node. This example explores the different options that can be used to obtain the steady-state frequency response of a structure, namely loads with the same frequency, multiple frequencies and the same frequency with different phase angles. The model uses beam elements.

AVE - 99: Weight, Center of Gravity and Mass Moment of Inertia Analysis of a Square Beam – This AVE involves a weight, center of gravity and mass moment of inertia analysis of a beam model using beam elements. This example verifies the accuracy of the Mass Properties Analysis Processor for beam elements.

AVE - 100: Torsion of a Box Beam – A box beam is subjected to torsion using point loads. The torsion is produced by nodal loads at opposite edges of the beam. A 3-D model is created using membrane elements for a linear static stress analysis.

AVE - 101: Weight, Center of Gravity and Mass Moment of Inertia Analysis of a Circular Plate – A circular plate is analyzed for weight, center of gravity and mass moment of inertia. The plate is modeled with membrane elements. This example verifies the accuracy of the Mass Properties Analysis processor for membrane elements.

AVE - 102: Thick-walled Cylinder under Both Pressure and Temperature Loadings – This example involves a thick-walled cylinder with temperature and pressure applied. This illustrates the axisymmetric form of the 2-D element. It also illustrates the use of the load case multipliers to apply both the thermal and pressure loads.

AVE - 103: Stress Concentration around a Hole – This example involves stress concentration around a hole obtained by a plane stress analysis. A uniform pressure load is applied. Orthotropic material properties are used. The model uses 2-D plate elements.

AVE - 104: Spherical Cap with Pressure – This example involves a spherical cap with uniform pressure. There are several ways to set up this problem. Using 2-D axisymmetric elements as shown in this example is the easy way. This problem verifies the accuracy of the 2-D element and shows how to apply uniform pressure to this type of element.

AVE - 105: Cylindrical Tube under Forced Response with Direct Integration – A cylindrical tube with a suddenly applied constant radial ring load is analyzed using the direct integration method. The model uses 2-D elements.

AVE - 106: Cylindrical Tube under Forced Response with Modal Superposition – A cylindrical tube with a point load is analyzed using the modal superposition method.

AVE - 107: Patch Test with Constant Stress – This patch test consists of applying a constant stress loading to a group (patch) of elements and showing that all elements in the patch will have the same stress. Incompatible modes are suppressed in this example. A static analysis using 2-D plane stress elements is performed.

AVE - 108: Weight, Center of Gravity and Mass Moment of Inertia Analysis of a Circular Plate – A circular plate is analyzed for weight, center of gravity, and mass moment of inertia. The plate is modeled with 2-D plane stress elements.

AVE - 109: Thick-walled Cylinder under Centrifugal and Pressure Loading – This example is an analysis of a thick-walled cylinder with centrifugal force and pressure applied as two separate load cases. This problem illustrates the ability to automatically generate centrifugal loading.

AVE - 110: Cantilever Beam Eigenvalues – A cantilever beam is modeled with 3-D solid elements. A Linear Mode Shapes and Natural Frequencies analysis is performed to verify natural frequencies.

AVE - 111: Weight, Center of Gravity and Mass Moment of Inertia Analysis of a Square Beam – A square steel beam is analyzed for weight, center of gravity and mass moment of inertia. The beam is modeled with 3-D brick elements.

AVE - 112: Weight, Center of Gravity and Mass Moment of Inertia Analysis of a Solid Sphere – A solid sphere is analyzed for weight, center of gravity and mass moment of inertia. The sphere is modeled with 3-D brick elements.

AVE - 113: Spherical Cap with Uniform Pressure – This example involves a spherical cap with uniform pressure. Due to symmetry, only a five-degree wedge of the shell is modeled for the Linear Static Stress analysis.

AVE - 114: Equilateral Triangle with Linear Thermal Gradient – This problem is a rare example of the application of temperature difference through thickness in plate element analysis. In this case, a triangular wing is modeled and the through thickness temperature gradient is applied using the element load case multipliers. A plate element model is created and a Linear Static Stress analysis is performed to find the deflections along the X axis.

AVE - 115: Simply Supported Anisotropic Plate – This example involves a simply supported plate with anisotropic material properties and a uniform pressure applied perpendicular to the surface. A plate element model is created using quarter-symmetry and orthogonal boundary conditions. A Linear Static Stress analysis is performed. Results are compared with the Timoshenko method.

AVE - 116: Rectangular Plate with All Edges Clamped – A square plate with all of its edges clamped is subjected to a uniform pressure load normal to the plate. Various mesh densities are used, and the resulting maximum deflection is compared to that predicted by the Timoshenko method. This example shows the reliability of the plate/shell element in bending analysis.

AVE - 117: Linear Mode Shape Analysis with Load Stiffening, Simply Supported Beam – This beam load stiffening problem models a steel beam which is simply supported under compressive axial loading. This example verifies the accuracy of the Linear Mode Shapes and Natural Frequencies Analysis with Load Stiffening processor for plate elements.

AVE - 118: Thin-walled Cylinder with a Uniform Axial Load – This example is taken from formulas for membrane stresses and deformations in thin-walled pressure vessels. It is a thin-walled cylinder with a uniform axial loading, which is analyzed for axial stress and deflection.

AVE - 119: Thick-walled Cylinder under Centrifugal and Pressure Loading – This verification example is a thick-walled cylinder with pressure and centrifugal force applied as two separate load cases modeled using tetrahedral elements.

AVE - 120: Weight, Center of Gravity and Mass Moment of Inertia Analysis of a Solid Sphere – This example involves a weight, center of gravity and mass moment of inertia analysis of a solid spherical model using tetrahedral elements. This example verifies the accuracy of the Mass Properties Analysis Processor for tetrahedral elements.

AVE - 121: Two Cantilever Beams Connected by a Tension-Only Element at the Tip – Two parallel cantilever beams, connected by a tension-only cable at the free ends, are subjected to a concentrated load. A tension-only gap element is used to find the tip deflection.

AVE - 122: L-Shaped Pipe System Subjected to Temperature Load – An L-shaped pipe system is subjected to a uniformly distributed load, a temperature increase and gravity. Due to the interaction of the gravity, temperature load and the uniformly distributed load, only a portion of the pipe contacts the support. Ten zero-gap compression-only gap elements are used to find the reactions. The pipe is modeled with beam elements.

AVE - 123: An Internally Pressurized Cylinder – A sector of an internally pressurized cylinder is modeled using both thin thick composite elements. Three different mesh densities are considered. Radial displacements and hoop stresses are calculated and compared to theoretical results.

AVE - 124: Simply Supported Square Laminate Subjected to a Uniform Pressure Load – A simply supported square laminate is subjected to a uniform lateral pressure. The laminate material is comprised of 9 different lamina (layers). Due to symmetry, a quarter sector was modeled with symmetry boundary conditions. This problem is modeled both thin thick composite elements. Two different laminate thicknesses and three different mesh densities are considered. The goal of the Linear Static Stress analysis is to find the maximum deflection of the central laminate.

AVE - 125: Clamped Circular Plate with a Point Load – A thick, circular plate is subjected to a center point load. The symmetric nature of this problem allows a one-quarter model to be used. The plate is modeled with sandwich elements. These elements include a transverse shear deflection for the core layer. The goal of the Linear Static Stress analysis is to find displacements at various points along the plate radius.

AVE - 126: Large Deformation and Large Strain for a Rubber Sheet – A bell-shaped rubber sheet is subjected to a uniformly distributed load at the end surface. The rubber material is assumed to be a Mooney-Rivlin type. Because the sheet is symmetrical, only half of it is modeled using 2-D plane stress elements.

AVE - 127: Plastic Analysis of a Thick-walled Cylinder – A thick-walled hollow cylinder is subjected to internal pressure that varied with time. The material of the cylinder is assumed to obey the von Mises yield condition. Because the cylinder is axisymmetrical, only one sector of it with a one radian angle is modeled using 2-D axisymmetric elements. Since displacements and strains were small, the analysis of the cylinder was carried out using the materially nonlinear-only formulation.

AVE - 128: Static Large Displacement Analysis of a Spherical Shell – A spherical shell is subjected to a concentrated apex load. The shell is axisymmetrical, therefore 2-D axisymmetric elements are used in the model. The goal of the analysis is to determine the deflection at the apex of the shell.

AVE - 129: Static Analysis of a Simply Supported Plate – A simply supported plate is subjected to a concentrated load at the center. The material is assumed to be isotropic. Only small displacement is considered. Because the plate is symmetrical, only a quarter of it is modeled. 3-D elements are used. The goal of the analysis is to determine the deflection at the plate center.

AVE - 130: Natural Frequencies for a Simply Supported Plate – The geometric and material properties for this plate are identical to those in AVE 140. Because the plate and loading are symmetrical, only one-quarter of the plate is modeled. 3-D elements are used. The goal of the analysis is to determine natural frequencies.

AVE - 131: Dynamic Analysis of a Simply Supported Plate under Concentrated Load – A simply supported plate is subjected to a concentrated load applied at the center. The material is assumed to be isotropic. The goal of the analysis is to determine the dynamic displacement at the point of applied load at a specific time.

AVE - 132: Wall with Internal Heat Generation – A solid wall has a distributed internal heat generation. Taking advantage of symmetry, only half the thickness of the wall is modeled. The goal of the Steady-State Heat Transfer analysis is to determine the temperature distribution inside the wall.

AVE - 133: Plane Couette Flow – This example involves steady-state viscous flow between two parallel plates (Couette flow). The top plate moves with constant speed and the bottom plate is fixed at zero velocity. The model consists of 2-D fluid elements. A Steady Fluid Flow analysis is performed to determine fluid velocity.

AVE - 134: Axisymmetric Flow through a Circular Pipe – This example involves steady-state viscous flow in a circular pipe (Poiseuille flow). An axisymmetric model of the pipe system is created using 2-D fluid elements. A Steady Fluid Flow analysis is performed to determine the fluid velocity in the Z direction.

AVE - 135: Axisymmetric Flow past a Sphere at Re=10 – This example involves an axisymmetric flow past a sphere at Reynolds number = 10. An axisymmetric model of the sphere system is created using 2-D fluid elements. A Steady Fluid Flow analysis is performed.

AVE - 136: Flow past a Circular Cylinder at Re=40, 100 – This example involves a flow past a circular cylinder at Reynolds number = 40 and 100. The cylinder system is modeled using 2-D fluid elements and a Steady Fluid Flow analysis is performed. A reasonable flow field is obtained showing the formation of eddies.

AVE - 137: 3-D Fluid Flow – This verification example is a driven 3-D cavity flow at Reynolds number = 400. Fluid is entrapped in a 3-D box, and the top wall moves, setting the fluid in motion. The mesh used consists of 3-D fluid elements.

AVE - 138: DDAM Shock Analysis of Heavy Equipment Mounted on the Deck of a Surface Ship –
A piece of heavy equipment is deck-mounted on a surface ship and a design check of a proposed foundation is made for the elastic-plastic category in the athwartship direction. The equipment is considered to be a rigid body, but, because of unsymmetrical foundation stiffness and location of the center of gravity, the system rotates as it translates. A two-degrees-of-freedom system is used to check the foundations. The DDAM results compare very favorably with analytical hand calculations.

AVE - 139: DDAM Shock Analysis of a Ship's Rudder System – A ship's rudder system, consisting of the bearing housing and foundation, the rudder stock and the rudder carrier key, are modeled as a mass-spring system. The system is analyzed for a vertical shock load.

AVE - 140: Pressure Drop in a Straight Pipe – Laminar fluid flow is analyzed inside a 10" long straight pipe with a 2" diameter to determine the pressure drop from frictionless losses.

AVE - 141: Linear Static Stress Analysis of a Laminated Strip – A simply supported laminated strip, which consists of seven layers with varying orientation, is subjected to a 10 N/mm line load at the center. Results for displacement and bending stresses compare well to NAFEMS benchmark results.

AVE - 142: Distance for Stopping a Car – A 2895-lb weight traveling at 88 ft/s is analyzed to determine the distance it takes to stop given a specified coefficient of friction between the weight and a concrete surface.

AVE - 143: Body-to-Body Radiation between Two Cylinders – Two concentric cylinders with different emissivities in a heated room undergo body-to-body radiation. Steady-State Heat Transfer analysis results for the temperature of the outer cylinder are in close agreement with the theoretical solution for this example.

AVE - 144: Nonlinear Displacement of a Bar with an Axial Load – A bar made of nonlinear material has an axial load (4000 N) applied to it and undergoes displacement past the yield point of the material.

AVE - 145: Tapered Axisymmetric Thick Shell Subjected to a Pressure Load – A tapered axisymmetric thick shell that has a pressure load applied to it is analyzed for hoop stress.

AVE - 146: Contact Pressure Analysis of a Punch-Foundation System – A punch has a uniform pressure load (40,000 N/m^2) applied to its top surface, which causes the punch to contact a foundation. An Static Stress with Linear Material Models analysis is performed to calculate the contact pressure.

AVE - 147: Acceleration Analysis of a Piston-Crank Mechanism – The motion of a piston-crank mechanism is analyzed via Mechanical Event Simulation with Nonlinear Materials. The acceleration of the piston is calculated for a particular instant and the results are compared to the theoretical solution.

AVE - 148: Natural Frequencies Analysis of a Pin-Ended Double Cross Structure – A double cross structure with its ends pinned is modeled with beam elements. Linear Mode Shapes and Natural Frequencies analysis results for the first 16 natural frequencies closely match the NAFEMS reference solution.

AVE - 149: Electrostatic Field Strength Analysis of a Spherical Electron Cloud – The electric field intensity of a spherical electron cloud is calculated by Electrostatic Field Strength and Voltage analysis. The results for the electric field magnitude at various radii from the electron cloud center are compared to the theoretical solution.

AVE - 150: Steady-State Heat Transfer Analysis of a Rod with an Adiabatic Tip – A long rectangular rod, which has its base maintained at 300F by heating equipment, is assumed to have an adiabatic tip because the tip area is approximately 1% of the total surface. Steady-State Heat Transfer analysis results for the temperature at 3 inches above the base is compared to the theoretical solution.

AVE - 151: Natural Frequency Analysis of a Flat Circular Plate – A flat circular plate of uniform thickness and radius has its outer edge fully fixed. A Linear Mode Shapes and Natural Frequencies analysis was performed to obtain the first natural frequency of the plate for comparison to the theoretical solution.

AVE - 152: Cylinder/Sphere under Uniform Internal Pressure – A thin-shelled cylinder/sphere combination is subjected to a uniform internal pressure of 1 MPa. Static stress analysis results are in close agreement with the NAFEMS reference solution.

AVE - 153: Heat Generation in a Wire due to Electrical Current – A stainless steel wire passes an electrical current of 200 Amps and is submerged in a 110°C fluid. Multiphysics capabilities are used to determine the temperature at the center of the wire. First, an Electrostatic Current and Voltage analysis is done to get the voltage distribution and then the voltage results are used as input to a Steady-State Heat Transfer analysis to get the temperature distribution.

AVE - 154: Natural Frequency (Modal) Analysis of a Cantilevered Beam – A 10-m beam with a square cross-section (0.125 m x 0.125 m) is rigidly supported on one end. A Natural Frequency (Modal) analysis is performed to obtain the first modal frequency of the beam for comparison to the theoretical solution.

AVE - 155: Tapered Plate with Gravity – A flat, tapered plate (4m x 4m x 2m) is fully constrained at one edge. A Static Stress with Linear Material Models analysis is performed to determine the stresses at a point of interest due to the acceleration of gravity. The analysis results closely correlate with the NAFEMS benchmark solution.

AVE - 156: Rectangular Plate Held by Three Wires – A thin, rectangular plate is held in position by three inextensible wires. A Mechanical Event Simulation with Nonlinear Material Models is performed to determine the acceleration of the plate when one of the wires is cut.

AVE - 157: Effect of Fins on Heat Transfer from a Steam Pipe – Heated steam flows through an aluminum pipe with an outer diameter of 3 cm and a temperature that is maintained at 120°C. To determine the effect of adding cooling fins to the pipe, Steady-State Heat Transfer analyses are conducted on models of the pipe without fins and with fins.

AVE - 158: Velocity and Reaction Force from a Crate Being Dragged across the Floor – A 100-kg crate is initially at rest on a smooth horizontal floor. A Mechanical Event Simulation with Nonlinear Material Models is performed to simulate the crate being dragged for 10 seconds by a 200-N force acting at a 45° angle from parallel to the floor. The calculated velocity and normal force results are compared to the theoretical solution.

AVE - 159: Heat Transfer between Hot- and Cold-Water Pipes – Two pipes run parallel to each other in a concrete block. One pipe has hot water (70°C) running through it and the other pipe contains running cold water (15°C). A Steady-State Heat Transfer analysis is performed to calculate the temperature distribution. Results environment capabilities are used to determine the heat transfer between the pipes, and they are compared to the theoretical solution

AVE - 160: Axisymmetric Vibration of a Simply Supported Annular Plate – An annular plate (with an inner radius of 1.8 m, radial length of 4.2 m and thickness of 0.6 m) is simply supported at its bottom outer edge. A Natural Frequency (Modal) analysis is performed to calculate the natural frequencies and mode shapes.

AVE - 161: Natural Frequency (Modal) Analysis of a Cantilever Beam with Off-Center Point Masses – A cantilever beam (10 m long) with a circular cross section (0.5 m in diameter) is fixed at one end and has two off-center point masses at its free end (10,000 kg and 1,000 kg, respectively, both 2 m from the end of the beam). A Natural Frequency (Modal) analysis is performed to calculate the first six natural frequencies and mode shapes, which closely correspond to the NAFEMS benchmark solution.

AVE - 162: Steady-State Heat Transfer Analysis of a Coal Powder Stockpile – A 2-m-deep layer of fine coal powder generates heat volumetrically due to a reaction between the coal particles and atmospheric gases. A Steady-State Heat Transfer analysis is performed to calculate the temperature of the upper surface.

AVE - 163: Bending and Wrinkling of a Pretensioned Beam-like Membrane – A beam-like rectangular plate membrane is tensioned by a uniform normal stress in both the X and Y directions and subject to an in-plane bending moment applied on its two ends. As the bending moment is increased, a band of vertical wrinkles appears along the compressed edge. A Mechanical Event Simulation with Nonlinear Material Models is performed to determine the stress in the membrane and the relation between the bending moment and the overall curvature of the beam-like membrane.

AVE - 164: Displacement of a Restraining Rod Attached to a Beam – A horizontal beam carries a triangular distributed load and is simply supported near one end and is restrained by a thin aluminum rod at the other end. A Static Stress with Linear Material Models analysis is run to determine the displacement of the beam at the restrained end.

AVE - 165: MES of a Parallelogram Linkage Used to Transfer a Crate between Platforms – A parallelogram linkage is used to transfer crates from one platform to another and is hydraulically operated by an actuator. A Mechanical Event Simulation with Nonlinear Material Models is conducted to solve for the axial force where a rod connects to the middle of the platform at time = 0.01 s and 1.00 s.

AVE - 166: Beam with Spring Support under Distributed Load – A horizontal beam is fixed on one end and supported by a spring at the other end and a distributed load is applied on the top of the beam. A Static Stress with Linear Material Models analysis is performed to determine the deflection of the beam and the force in the spring.

AVE - 167: Flow through a Tube with Fixed Heat Flux – Water flows through a tube with its outer surface subjected to a heat flux load, which warms the fluid. A Steady Fluid Flow analysis is performed to obtain the velocity results for the fluid and then the fluid flow results are input as a load to a Steady-State Heat Transfer analysis to find the temperature at the outlet of the tube.

AVE - 168: Body-to-Body Radiation Heat Transfer in the Frustum of a Cone – A frustum of a cone has its base heated while its top is held at a constant temperature and the side is perfectly insulated on the outside. A Steady-State Heat Transfer analysis is performed to determine the temperature of the bottom and side surfaces.

AVE - 169: Steady Fluid Flow through a Circular Tube – A circular tube has fluid flowing through it. A Steady Fluid Flow analysis is performed to determine the maximum velocity of the fluid flow in the tube.

AVE - 170: Circular Plate with Fixed Edges under Uniform Pressure Load – A circular plate is fixed at the edges and is subjected to a uniform pressure load. A Static Stress with Linear Material Models analysis is run to find the maximum displacement in the plate.

AVE - 171: Force on the Actuator of a Hydraulic-Lift Table – A hydraulic-lift table, which consists of a platform and two identical linkages with hydraulic cylinders, is used to raise a crate. A Mechanical Event Simulation with Nonlinear Material Models is performed to determine the force on the actuator when the linkage is at a particular angle.

AVE - 172: Heat Transfer Rate of a Heat Exchanger Wall with Pin Fins on One Side – A heat exchanger wall separates a stream of hot liquid from a stream of cold gas. The cold side of the wall has pin fins arranged in a square pattern. A Steady-State Heat Transfer analysis is performed to determine the total heat transfer rate for the heat exchanger wall.

AVE - 173: First Natural Frequency of a Rectangular Flat Plate with All Edges Fixed – A square flat plate has all four edges fixed. A Natural Frequency (Modal) analysis is run to determine the first natural frequency of vibration due to the plate's own weight under gravity loading.

AVE - 174: Heat Transfer through Thin Plate – A cylindrical plate is subjected to a temperature load at one end and a convection load across the outer surface. A Steady State Heat Transfer analysis is run to find the temperature of the plate on the unheated end.

AVE - 175: Maximum Fluid Velocity – Fluid flow through a simple pipe is model using pressure loads. A Steady Fluid Flow analysis is performed to determine the maximum velocity of the fluid through the pipe.

AVE - 176: Angular Deflection of a Steel Step Shaft – A long shaft made of a hollow and solid region joined by a step is subjected to several torsional loads with one fixed boundary condition. A Static Stress with Linear Material Models analysis is performed to determine the rotation of the shaft at the free end.

AVE - 177: Deflection of Simply Support Beam and Spring System– A beam supported both at two ends and in the middle by a spring experiences dynamic loading from a falling block. A Mechanical Event Simulation with Nonlinear Material Models is performed to determine the maximum bending stress of the beam and the contact force between the beam and the block.

AVE - 178: Temperature Drop across Contact – Two stainless steel cylinders are brought into contact and subjected to a temperature difference across their combined length of 100 C. A Steady State Heat Transfer analysis is run to find the temperature drop across the cylinders due to contact resistance.

AVE - 179: Natural Frequency of a Flat Plate– A rectangular flat plate has three edges fully fixed and a fourth that is simply supported. A Natural Frequency (Modal) analysis is run to determine the first natural frequency of vibration due to the plate's own weight under gravity loading.

AVE - 180: Deflection of Truss – A truss construction is fixed on one end with several loads applied to different points in the truss. A Static Stress with Linear Material Models analysis is run to find the maximum x and y displacements of the free end of the truss.

AVE - 181: MES Thermal Loading of Shell Composite – A composite shell experiences a constant thermal load of 100 ºF. A Mechanical Event Simulation with Nonlinear Material Models is performed to determine the maximum stress tensor in the principal directions.

AVE - 182: Deflection of a Spring Supported Beam – A square beam is supported by 7 identical springs and is loaded at the center. A static stress analysis is performed to find the maximum bending stress and deflection.

AVE - 183: MES of Force Accelerated Block – A brick is dragged across a surface by a 500 N force. A MES is performed to determine the maximum sustained velocity of the block.

AVE - 184: Radiation between two Cylinders – Two concentric cylinders radiate both to each other and the environment. A Steady-State Heat Transfer analysis is utilized with body-to-body radiation to find the temperature of the outer cylinder.

AVE - 185: Outlet Velocity of 3D Fluid Tank with Sudden Contraction Loss – Fluid drains along a pipe from a large tank. An Unsteady Fluid Flow analysis is used to determine the maximum fluid velocity after four seconds.

AVE - 186: Steady-State Heat Transfer along a Rod – A bar is subjected to a point load and an ambient environment. A Steady-State Heat analysis is used to find the temperature of the rod at a given distance from the point load.

AVE - 187: Natural Frequency of Beam, Spring, and Mass System – A mass and spring are attached to a stiff rod. A Natural Frequency (Modal) analysis is performed to determine the natural frequency of the system.

AVE - 188: Notched Plate – A simple notched plate experiences pressure loading and fixed boundary constraints. A Linear Static analysis was used to find the maximum stress of the plate.

AVE - 189: MES Deflection of a Spring Supported Beam – A square cantilever beam is supported by a spring and loaded by a force at one end. A MES is performed to determine the maximum deflection.

AVE - 190: Flow of Steam through an Insulated Pipe – Steam is flowing through an insulated pipe. A steady-state heat transfer analysis is used to determine the temperature on the interior and exterior surfaces of the pipe.

AVE - 191: Airflow over a Hill – Wind is blowing over a hill. A steady fluid flow analysis is used to determine the velocity profile along the hillside.

AVE - 192: Heat Lost through the Walls of a Furnace – A furnace is kept at a constant temperature. A steady-state heat transfer analysis is used to determine the heat lost.

AVE - 193: Natural Frequency of a Simply Supported Beam with a Mass in the Middle – A simply supported beam has a concentrated mass located at the center. A Natural Frequency (Modal) analysis is performed to determine the natural frequency of the system.

AVE - 194: Contact Pressure between a Punch and Foundation – A pressure is applied to a punch which contacts a foundation. A static stress analysis was performed to determine the contact pressure between the punch and foundation.

AVE - 195: MES Deflection of a Pointer Due to Thermal Expansion – A pointer is connected to aluminum and steel bars. A MES is performed in order to determine the deflection of the tip of the pointer with respect to a scale when the temperature increases.

AVE - 196: Natural Frequency of a Weighing Platform – A weighing platform consists of a mass, two levers and a spring. A Natural Frequency (Modal) analysis is performed to determine the period of the system.

AVE - 197: Axial and Bending Forces Acting on a Wide Flanged Beam – Forces are applied in three directions to a cantilever beam with a wide-flanged cross-section. A static stress analysis was performed to calculate the maximum stress in the beam.

AVE - 198: MES of a Pinned Rod Released from Rest – A pinned rod is originally at a 45º angle to the horizontal. A MES is performed in order to determine the velocity at the tip when the rod becomes horizontal. The results are within one percentage point of the theoretical results.

AVE - 199: MES of a Pinned Reinforced Concrete Beam – A rectangular concrete beam is reinforced with reinforcing rods. A uniform pressure is applied along the length. A MES is performed in order to determine the maximum vertical deflection.

AVE - 200: Riks Analysis of a Curved Cylindrical Shell – A curved cylindrical shell is loaded at the center by a nodal force. A Riks analysis is performed to determine the load vs. deflection results.

Index of Accuracy Verification Examples by Analysis Type Used

AVE #	Accuracy Verification Example Title	Static Stress with Linear Material Models	Linear Natural Frequency (Modal)	Linear Response Spectrum	Linear Random Vibrations	Linear Frequency Response	Linear Transient Stress (Direct Integration)	Linear Transient Stress (Modal Superposition)	Dynamic Design Analysis Method (DDAM)	Linear Critical Load Buckling	Steady-state Heat Transfer	Transient Heat Transfer	Steady Fluid Flow	Unsteady Fluid Flow	Electrostatic Current & Voltage	Electrostatic Field Strength & Voltage	Mechanical Event Simulation with Linear & Nonlinear Material Models	Weight & Center of Gravity
001	Flat Circular Plate of Constant Thickness (2-D)	X																
002	Flat Circular Plate of Constant Thickness (3-D)	X																
003	Thin-Walled Cylinder with Uniform Axial Load	X																
004	Cylindrical Disk with Uniform Internal Radial Pressure	X																
005	Rectangular Plate with All Edges Simply Supported and Uniform Pressure	X																
006	Flat Rectangular Plate with Three Edges Simply Supported	X																
007	Cantilever Beam with Nodal Force	X																
008	Toroidal Shell Under Uniform Internal Pressure	X																
009	Beam Guided at the Left and Fixed at the Right	X																
010	Thick-Walled Spherical Vessel Under Uniform Internal Pressure	X																
011	Thick-Walled Cylindrical Vessel Under Uniform Internal Radial Pressure	X																
012	Hollow Cylinder with Thick Walls and Temperature Gradient	X																
013	Lid Driven Cavity												X					
014	Flat Rectangular Plate with All Edges Fixed and Uniform Pressure Loading	X																
015	Flat Rectangular Plate with Two Sides Fixed, Two Sides Simply Supported and Uniform Load	X																
016	Uniform Beam with Both Ends Fixed		X															
017	Thick-walled Cylindrical Vessel Under Uniform External Pressure Modeled in 3-D	X																
018	Thick-walled Cylindrical Vessel Under Uniform External Pressure Modeled in 2-D	X																
019	Thin-Walled Conical Vessel Under Uniform Internal Pressure with Tangential Edge Supports	X																

AVE #	Accuracy Verification Example Title	Static Stress with Linear Material Models	Linear Natural Frequency (Modal)	Linear Response Spectrum	Linear Random Vibrations	Linear Frequency Response	Linear Transient Stress (Direct Integration)	Linear Transient Stress (Modal Superposition)	Dynamic Design Analysis Method (DDAM)	Linear Critical Load Buckling	Steady-state Heat Transfer	Transient Heat Transfer	Steady Fluid Flow	Unsteady Fluid Flow	Electrostatic Current & Voltage	Electrostatic Field Strength & Voltage	Mechanical Event Simulation with Linear & Nonlinear Material Models	Weight & Center of Gravity
020	Straight Bar with Lower End Fixed and Upper End Free									X								
021	Wide-flange Beam with Equal Flanges																	
022	Circular Disc Rotating about Its Own Axis with Uniform Angular Velocity Modeled in 2-D	X																
023	Circular Disc Rotating about Its Own Axis with Uniform Angular Velocity Modeled in 3-D	X																
024	Thin-walled Cylindrical Shell Under an Axisymmetric Radial-End Load	X																
025	Test of the Capabilities of the 'dt/dh' Option for the Plate Element	X																
026	Rectangular Plate Under Uniform Load Producing a Large Deflection																X	
027	Solid Circular Plate Section of Constant Thickness with Uniform Load	X																
028	Thin Closed Circular Ring with Circular Cross Section	X																
029	Thick-walled Cylindrical Vessel Under Uniform Internal Radial Pressure	X																
030	Ceramic Strip with Radiation										X							
031	Two Masses and Three Massless Springs with an Applied Forced Harmonic Vibration					X												
032	Steady-state Heat Loss of a Steam Pipe with Nonconcentric Insulation										X							
033	Elastic Instability of a Flat Plate Under Pure Shear Load									X								
034	Ceramic Embedded in a High Thermal Conductivity Material											X						
035	Motion of a Two-DOF System Subjected to Random Vibration				X													
036	Interference Analysis of Two Concentric Thick-walled Rings	X																
037	Circular Flat Plate with Edge Clamped and Concentrated Load Applied at Center	X																

AVE #	Accuracy Verification Example Title	Static Stress with Linear Material Models	Linear Natural Frequency (Modal)	Linear Response Spectrum	Linear Random Vibrations	Linear Frequency Response	Linear Transient Stress (Direct Integration)	Linear Transient Stress (Modal Superposition)	Dynamic Design Analysis Method (DDAM)	Linear Critical Load Buckling	Steady-state Heat Transfer	Transient Heat Transfer	Steady Fluid Flow	Unsteady Fluid Flow	Electrostatic Current & Voltage	Electrostatic Field Strength & Voltage	Mechanical Event Simulation with Linear & Nonlinear Material Models	Weight & Center of Gravity
038	Thick-walled Spherical Vessel Under Uniform Internal Pressure	X																
039	Forced Harmonic Response Analysis of a Spring-Mass-Damper System					X												
040	Solid Sphere Analyzed to Find Weight, Center of Gravity and Mass Moment of Inertia																	X
041	Natural Frequency of a Gr./Epoxy Laminated Composite Square Plate		X															
042	Mid-span Deflection of a Uniform Steel Beam Simply Supported at Both Ends	X																
043	Stress Relaxation of a Tightened Bolt Due to Thermal Creep																X	
044	Deflection Analysis of a Helical Spring Under Compressive Loading	X																
045	Nonlinear Radiation Heat Transfer Analysis of a Cylindrical Disk with Internal Heat Generation										X							
046	Shear Force and Bending Moment Analysis of a Beam Under Distributed Loading	X																
047	Thermal Stress Analysis of a Thick-walled Cylindrical Vessel Under Temperature Gradient	X																
048	Elastic Stability of a Flat Plate Under a Pure Axial Load									X								
049	Concrete Frame Structure Subjected to Distributed Loading	X																
050	Solid Aluminum Cylinder Exposed to a Convection Environment and Allowed to Cool											X						
051	Fluid Flow between Two Plates													X				
052	2-D Laminar Flow over a Backward Facing Step												X					
053	Linear Mode Shape with Load Stiffening Analysis on a Simply Supported Continuous Beam		X															
054	Thick-Walled Spherical Shell Subjected to Uniform Internal Pressure																X	

AVE #	Accuracy Verification Example Title	Static Stress with Linear Material Models	Linear Natural Frequency (Modal)	Linear Response Spectrum	Linear Random Vibrations	Linear Frequency Response	Linear Transient Stress (Direct Integration)	Linear Transient Stress (Modal Superposition)	Dynamic Design Analysis Method (DDAM)	Linear Critical Load Buckling	Steady-state Heat Transfer	Transient Heat Transfer	Steady Fluid Flow	Unsteady Fluid Flow	Electrostatic Current & Voltage	Electrostatic Field Strength & Voltage	Mechanical Event Simulation with Linear & Nonlinear Material Models	Weight & Center of Gravity
055	Nonlinear Heat Flow Analysis of a Solid Cylinder										X							
056	Response Spectrum Analysis of a Simple Beam			X														
057	Cantilever Beam with a Gap at the Tip	X																
058	Transient Thermal Analysis of a Solid Wall with Internal Heat Generation											X						
059	Steady-State Heat Transfer Analysis of a Fin Immersed in a Cooling Fluid										X							
060	Nonlinear Radiation Heat Transfer Analysis of a Cylindrical Disk with Internal Heat Generation										X							
061	Continuous Beam, Simply Supported at the Ends, Under a Uniformly Distributed Load	X																
062	Design Spectrum with a Specified Maximum Ground Acceleration			X														
063	Slab with Internal Charge Density Distribution															X		
064	Thermal Deflection Analysis of a Plate	X																
065	Torsion of an Elastic Beam with a Channel Cross-Section	X																
066	Multidimensional Transient Heat Transfer Analysis											X						
067	Fundamental Frequency and Static Lateral Deflections of a Loaded Shaft		X															
068	Annular Plate with a Uniformly Distributed Pressure	X																
069	Nonlinear Static Analysis of a Simply Supported Plate																X	
070	A Combined Beam/Plate Model	X																
071	Creep Analysis of a Thick-Walled Cylinder																X	
072	Shear Flow in a Simply Supported Beam	X																

AVE #	Accuracy Verification Example Title	Static Stress with Linear Material Models	Linear Natural Frequency (Modal)	Linear Response Spectrum	Linear Random Vibrations	Linear Frequency Response	Linear Transient Stress (Direct Integration)	Linear Transient Stress (Modal Superposition)	Dynamic Design Analysis Method (DDAM)	Linear Critical Load Buckling	Steady-state Heat Transfer	Transient Heat Transfer	Steady Fluid Flow	Unsteady Fluid Flow	Electrostatic Current & Voltage	Electrostatic Field Strength & Voltage	Mechanical Event Simulation with Linear & Nonlinear Material Models	Weight & Center of Gravity
073	Dynamic Analysis of a Beam Model																X	
074	Thermal Stress Analysis of a Pinned Beam/Truss Structure	X																
075	Dynamic Nonlinear Analysis of a Beam Model with a Gravity Load																X	
076	Linear Stress Analysis of a Beam Model	X																
077	Two Cylindrical Shells with Internal Pressure Loading	X																
078	Spring and Collar Slide Down Vertical Rod																X	
079	Slender Pivoting Rod and Compressed Spring																X	
080	Dynamic Analysis of an 8-kg Body Using Damping and a Dashpot																X	
081	Transient Heat Transfer Analysis of a Semi-Infinite Pressure Loading											X						
082	Mechanical Event Simulation of a Slider-Crank Mechanism																X	
083	Mechanical Event Simulation of a Lunar Lander																X	
084	Fluid Flow Drag Analysis of Flow across a Flat Plate												X					
085	Mechanical Event Simulation of a Basketball Being Shot into a Hoop																X	
086	Heat Flux Transient Heat Transfer Analysis											X						
087	Mechanical Event Simulation of Grinder Shaft Under Torsion																X	
088	Mechanical Event Simulation of a Chain with Weights at the Hinges																X	
089	Transient Thermal Analysis of a Cooling Copper Wire											X						
090	Heat Flux Loading on a Hollow Cylinder										X							
091	Mechanical Event Simulation of a Cylinder Rolling inside a Curved Surface																X	

AVE #	Accuracy Verification Example Title	Static Stress with Linear Material Models	Linear Natural Frequency (Modal)	Linear Response Spectrum	Linear Random Vibrations	Linear Frequency Response	Linear Transient Stress (Direct Integration)	Linear Transient Stress (Modal Superposition)	Dynamic Design Analysis Method (DDAM)	Linear Critical Load Buckling	Steady-state Heat Transfer	Transient Heat Transfer	Steady Fluid Flow	Unsteady Fluid Flow	Electrostatic Current & Voltage	Electrostatic Field Strength & Voltage	Mechanical Event Simulation with Linear & Nonlinear Material Models	Weight & Center of Gravity
092	Mechanical Event Simulation of a Flyball-Governor																X	
093	Steady-State Heat Transfer Analysis of a Pipe Buried in Earth										X							
094	3-D Truss System under a Point Load and Uniform Temperature Increase	X																
095	Weight, Center of Gravity and Mass Moment of Inertia Analysis of a Straight Bar																	X
096	6-Story, 2-Bay Frame Structure under Uniformly Distributed Loading	X																
097	Earthquake Response of a 10-Story Plane Frame			X														
098	Frequency Response Analysis of a Two Degrees of Freedom System					X												
099	Weight, Center of Gravity and Mass Moment of Inertia Analysis of a Square Beam																	X
100	Torsion of a Box Beam	X																
101	Weight, Center of Gravity and Mass Moment of Inertia Analysis of a Circular Plate																	X
102	Thick-Walled Cylinder under Both Pressure and Temperature Loadings	X																
103	Stress Concentration around a Hole	X																
104	Spherical Cap with Pressure	X																
105	Cylindrical Tube under Forced Response with Direct Integration						X											
106	Cylindrical Tube under Forced Response with Modal Combination							X										
107	Patch Test with Constant Stress	X																
108	Weight, Center of Gravity and Mass Moment of Inertia Analysis of a Circular Plate																	X
109	Thick-Walled Cylinder under Centrifugal and Pressure Loading	X																
110	Cantilever Beam Eigenvalues		X															

AVE #	Accuracy Verification Example Title	Static Stress with Linear Material Models	Linear Natural Frequency (Modal)	Linear Response Spectrum	Linear Random Vibrations	Linear Frequency Response	Linear Transient Stress (Direct Integration)	Linear Transient Stress (Modal Superposition)	Dynamic Design Analysis Method (DDAM)	Linear Critical Load Buckling	Steady-state Heat Transfer	Transient Heat Transfer	Steady Fluid Flow	Unsteady Fluid Flow	Electrostatic Current & Voltage	Electrostatic Field Strength & Voltage	Mechanical Event Simulation with Linear & Nonlinear Material Models	Weight & Center of Gravity
111	Weight, Center of Gravity and Mass Moment of Inertia Analysis of a Square Beam																	X
112	Weight, Center of Gravity and Mass Moment of Inertia Analysis of a Solid Sphere																	X
113	Spherical Cap with Uniform Pressure	X																
114	Equilateral Triangle with Linear Thermal Gradient	X																
115	Simply Supported Anisotropic Plate	X																
116	Rectangular Plate with All Edges Clamped	X																
117	Linear Mode Shape Analysis with Load Stiffening, Simply Supported Beam		X															
118	Thin-Walled Cylinder with a Uniform Axial Load	X																
119	Thick-Walled Cylinder	X																
120	Weight, Center of Gravity and Mass Moment of Inertia Analysis of a Solid Sphere																	X
121	Two Cantilever Beams Connected by a Tension-Only Element at the Tip	X																
122	L-Shaped Pipe System Subjected to Temperature Load	X																
123	An Internally Pressurized Cylinder	X																
124	Simply Supported Square Laminate Subjected to a Uniform Pressure Load	X																
125	Clamped Circular Plate with a Point Load	X																
126	Large Deformation and Large Strain for a Rubber Sheet																X	
127	Plastic Analysis of a Thick-Walled Cylinder																X	
128	Static Large Displacement Analysis of a Spherical Shell																X	
129	Static Analysis of a Simply Supported Plate																X	
130	Natural Frequencies for a Simply Supported Plate																X	

AVE #	Accuracy Verification Example Title	Static Stress with Linear Material Models	Linear Natural Frequency (Modal)	Linear Response Spectrum	Linear Random Vibrations	Linear Frequency Response	Linear Transient Stress (Direct Integration)	Linear Transient Stress (Modal Superposition)	Dynamic Design Analysis Method (DDAM)	Linear Critical Load Buckling	Steady-state Heat Transfer	Transient Heat Transfer	Steady Fluid Flow	Unsteady Fluid Flow	Electrostatic Current & Voltage	Electrostatic Field Strength & Voltage	Mechanical Event Simulation with Linear & Nonlinear Material Models	Weight & Center of Gravity
131	Dynamic Analysis of a Simply Supported Plate under Concentrated Load																X	
132	Wall with Internal Heat Generation										X							
133	Plane Couette Flow with pressure gradient												X					
134	Axisymmetric Flow through a Circular Pipe												X					
135	Axisymmetric Flow past a Sphere at Re = 10												X					
136	Flow past a Circular Cylinder at Re = 40, 100												X					
137	3-D Fluid Flow												X					
138	DDAM Shock Analysis of Heavy Equipment Mounted on the Deck of a Surface Ship								X									
139	DDAM Shock Analysis of a Ship's Rudder System								X									
140	Pressure Drop in a Straight Pipe												X					
141	Linear Static Stress Analysis of a Laminated Strip	X																
142	Distance for Stopping a Car																X	
143	Body-to-Body Radiation between Two Cylinders										X							
144	Nonlinear Displacement of a Bar with an Axial Load																X	
145	Tapered Axisymmetric Thick Shell Subjected to a Pressure Load	X																
146	Contact Pressure Analysis of a Punch-Foundation System	X																
147	Acceleration Analysis of a Piston-Crank Mechanism																X	
148	Natural Frequencies Analysis of a Pin-Ended Double Cross Structure		X															
149	Electrostatic Field Strength Analysis of a Spherical Electron Cloud															X		
150	Steady-State Heat Transfer Analysis of a Rod with an Adiabatic Tip										X							
151	Natural Frequency Analysis of a Flat Circular Plate		X															

AVE #	Accuracy Verification Example Title	Static Stress with Linear Material Models	Linear Natural Frequency (Modal)	Linear Response Spectrum	Linear Random Vibrations	Linear Frequency Response	Linear Transient Stress (Direct Integration)	Linear Transient Stress (Modal Superposition)	Dynamic Design Analysis Method (DDAM)	Linear Critical Load Buckling	Steady-state Heat Transfer	Transient Heat Transfer	Steady Fluid Flow	Unsteady Fluid Flow	Electrostatic Current & Voltage	Electrostatic Field Strength & Voltage	Mechanical Event Simulation with Linear & Nonlinear Material Models	Weight & Center of Gravity
152	Cylinder/Sphere under Uniform Internal Pressure	X																
153	Heat Generation in a Wire due to Electrical Current										X				X			
154	Natural Frequency (Modal) Analysis of a Cantilever Beam		X															
155	Tapered Plate with Gravity	X																
156	Rectangular Plate Held by Three Wires																X	
157	Effect of Fins on Heat Transfer from a Steam Pipe										X							
158	Velocity and Reaction Force from a Crate Being Dragged across the Floor																X	
159	Heat Transfer between Hot- and Cold-Water Pipes										X							
160	Axisymmetric Vibration of a Simply Supported Annular Plate		X															
161	Natural Frequency (Modal) Analysis of a Cantilever Beam with Off-Center Point Masses		X															
162	Steady-State Heat Transfer Analysis of a Coal Powder Stockpile										X							
163	Bending and Wrinkling of a Pretensioned Beam-like Membrane																X	
164	Displacement of a Restraining Rod Attached to a Beam	X																
165	MES of a Parallelogram Linkage Used to Transfer a Crate between Platforms																X	
166	Beam with Spring Support under Distributed Load	X																
167	Flow through a Tube with Fixed Heat Flux										X		X					
168	Body-to-Body Radiation Heat Transfer in the Frustum of a Cone										X							
169	Steady Fluid Flow through a Circular Tube												X					
170	Circular Plate with Fixed Edges under Uniform Pressure Load	X																
171	Force on the Actuator of a Hydraulic-Lift Table																X	

AVE #	Accuracy Verification Example Title	Static Stress with Linear Material Models	Linear Natural Frequency (Modal)	Linear Response Spectrum	Linear Random Vibrations	Linear Frequency Response	Linear Transient Stress (Direct Integration)	Linear Transient Stress (Modal Superposition)	Dynamic Design Analysis Method (DDAM)	Linear Critical Load Buckling	Steady-state Heat Transfer	Transient Heat Transfer	Steady Fluid Flow	Unsteady Fluid Flow	Electrostatic Current & Voltage	Electrostatic Field Strength & Voltage	Mechanical Event Simulation with Linear & Nonlinear Material Models	Weight & Center of Gravity
172	Heat Transfer Rate of a Heat Exchanger Wall with Pin Fins on One Side										X							
173	First Natural Frequency of a Rectangular Flat Plate with All Edges Fixed		X															
174	Heat Transfer through Thin Plate										X							
175	Maximum Fluid Flow												X					
176	Angular Deflection of Steel Step Shaft	X																
177	Deflection of Beam and Spring System																X	
178	Temperature Difference Across Contact										X							
179	Natural Frequency of a Flat Plate		X															
180	Deflection of Truss	X																
181	MES Thermal Loading of Shell Composite																X	
182	Deflection of a Spring Supported Beam	X																
183	MES of Force Accelerated Block																X	
184	Radiation between two Cylinders										X							
185	Outlet Velocity of Fluid Tank													X				
186	Steady-State Heat Transfer along a Rod										X							
187	Natural Frequency of a Beam, Spring and Mass System		X															
188	Notched Plate	X																
189	MES Deflection of a Spring Supported Beam																X	
190	Flow of Steam through an Insulated Pipe										X							
191	Airflow over a Hill												X					
192	Heat Lost through the Walls of a Furnace										X							
193	Simply Supported Beam with a Mass in the Middle		X															
194	Contact Pressure between a Punch and Foundation	X																

AVE #	Accuracy Verification Example Title	Static Stress with Linear Material Models	Linear Natural Frequency (Modal)	Linear Response Spectrum	Linear Random Vibrations	Linear Frequency Response	Linear Transient Stress (Direct Integration)	Linear Transient Stress (Modal Superposition)	Dynamic Design Analysis Method (DDAM)	Linear Critical Load Buckling	Steady-state Heat Transfer	Transient Heat Transfer	Steady Fluid Flow	Unsteady Fluid Flow	Electrostatic Current & Voltage	Electrostatic Field Strength & Voltage	Mechanical Event Simulation with Linear & Nonlinear Material Models	Weight & Center of Gravity
195	MES Deflection of a Pointer Due to Thermal Expansion																X	
196	Natural Frequency of a Simply Supported Beam with a Mass in the Middle		X															
197	Axial and Bending Forces Acting on a Wide Flanged Beam	X																
198	MES of a Pinned Rod Released from Rest																X	
199	MES of a Reinforced Concrete Beam																X	
200	Riks Analysis of a Curved Cylindrical Shell																X	

Index of Accuracy Verification Examples by Elements Used

AVE #	Accuracy Verification Example Title	Truss	Beam	Membrane	2-D	3-D Brick	3-D Plate/Shell	Boundary	3-D Enhanced Brick	10-node Tetrahedral	Spring	Rigid	Gap	Thin Shell Composite	Thick Shell Composite	3-D Nonlinear Truss	3-D Nonlinear Beam	3-D General Contact	2-D Nonlinear	3-D Nonlinear	Nonlinear Shell	3-D Kinematic	3-D Nonlinear Membrane	Thermal Boundary	3-D Thermal Plate	4-node Tetrahedral	10-node Tetrahedral	Thermal Brick	2-D Thermal	3-D Electro-boundary	Electrical Solid	2-D Electrostatic	2-D Fluid	3-D Fluid	Dynamic Contact	Actuator
001	Flat Circular Plate of Constant Thickness (2-D)				X																															
002	Flat Circular Plate of Constant Thickness (3-D)					X																														
003	Thin-Walled Cylinder with Uniform Axial Load			X		X	X																													
004	Cylindrical Disk with Uniform Internal Radial Pressure and Longitudinal Pressure of Zero					X																														
005	Rectangular Plate with All Edges Simply Supported and Uniform Pressure						X																													
006	Flat Rectangular Plate with Three Edges Simply Supported						X																													
007	Cantilever Beam with Nodal Force		X																																	
008	Toroidal Shell Under Uniform Internal Pressure					X																														
009	Beam Guided at the Left and Fixed at the Right		X																																	
010	Thick-Walled Spherical Vessel Under Uniform Internal Pressure					X																														
011	Thick-Walled Cylindrical Vessel Under Uniform Internal Radial Pressure					X																														
012	Hollow Cylinder with Thick Walls and Temperature Gradient					X																														

AVE #	Accuracy Verification Example Title	Truss	Beam	Membrane	2-D	3-D Brick	3-D Plate/Shell	Boundary	3-D Enhanced Brick	10-node Tetrahedral	Spring	Rigid	Gap	Thin Shell Composite	Thick Shell Composite	3-D Nonlinear Truss	3-D Nonlinear Beam	3-D General Contact	2-D Nonlinear	3-D Nonlinear	Nonlinear Shell	3-D Kinematic	3-D Nonlinear Membrane	Thermal Boundary	3-D Thermal Plate	4-node Tetrahedral	10-node Tetrahedral	Thermal Brick	2-D Thermal	3-D Electro-boundary	Electrical Solid	2-D Electrostatic	2-D Fluid	3-D Fluid	Dynamic Contact	Actuator
013	Lid Driven Cavity																																X			
014	Flat Rectangular Plate with All Edges Fixed and Uniform Pressure Loading						X																													
015	Flat Rectangular Plate with Two Sides Fixed, Two Sides Simply Supported and Uniform Load						X																													
016	Uniform Beam with Both Ends Fixed		X																																	
017	Thick-walled Cylindrical Vessel Under Uniform External Pressure Modeled in 3-D					X																														
018	Thick-walled Cylindrical Vessel Under Uniform External Pressure Modeled in 2-D				X																															
019	Thin-Walled Conical Vessel Under Uniform Internal Pressure with Tangential Edge Supports					X																														
020	Straight Bar with Lower End Fixed and Upper End Free		X																																	
021	Wide-flange Beam with Equal Flanges	Demonstration of FEA Editor's "Inquire:XY Moment of Inertia…" capability. No elements are used.																																		
022	Circular Disc Rotating about Its Own Axis with Uniform Angular Velocity Modeled in 2-D				X																															
023	Circular Disc Rotating about Its Own Axis with Uniform Angular Velocity Modeled in 3-D					X																														

AVE #	Accuracy Verification Example Title	Truss	Beam	Membrane	2-D	3-D Brick	3-D Plate/Shell	Boundary	3-D Enhanced Brick	10-node Tetrahedral	Spring	Rigid	Gap	Thin Shell Composite	Thick Shell Composite	3-D Nonlinear Truss	3-D Nonlinear Beam	3-D General Contact	2-D Nonlinear	3-D Nonlinear	Nonlinear Shell	3-D Kinematic	3-D Nonlinear Membrane	Thermal Boundary	3-D Thermal Plate	4-node Tetrahedral	10-node Tetrahedral	Thermal Brick	2-D Thermal	3-D Electro-boundary	Electrical Solid	2-D Electrostatic	2-D Fluid	3-D Fluid	Dynamic Contact	Actuator
024	Thin-walled Cylindrical Shell Under an Axisymmetric Radial-End Load						X																													
025	Test of the Capabilities of the 'dt/dh' Option for the Plate Element						X																													
026	Rectangular Plate Under Uniform Load Producing a Large Deflection																				X															
027	Solid Circular Plate Section of Constant Thickness with Uniform Load						X																													
028	Thin Closed Circular Ring with Circular Cross Section		X																																	
029	Thick-walled Cylindrical Vessel Under Uniform Internal Radial Pressure				X																															
030	Ceramic Strip with Radiation																							X					X							
031	Two Masses and Three Massless Springs with an Applied Forced Harmonic Vibration		X																																	
032	Steady-state Heat Loss of a Steam Pipe with Nonconcentric Insulation																							X					X							
033	Elastic Instability of a Flat Plate Under Pure Shear Load						X																													
034	Ceramic Embedded in a High Thermal Conductivity Material																							X					X							

AVE #	Accuracy Verification Example Title	Truss	Beam	Membrane	2-D	3-D Brick	3-D Plate/Shell	Boundary	3-D Enhanced Brick	10-node Tetrahedral	Spring	Rigid	Gap	Thin Shell Composite	Thick Shell Composite	3-D Nonlinear Truss	3-D Nonlinear Beam	3-D General Contact	2-D Nonlinear	3-D Nonlinear	Nonlinear Shell	3-D Kinematic	3-D Nonlinear Membrane	Thermal Boundary	3-D Thermal Plate	4-node Tetrahedral	10-node Tetrahedral	Thermal Brick	2-D Thermal	3-D Electro-boundary	Electrical Solid	2-D Electrostatic	2-D Fluid	3-D Fluid	Dynamic Contact	Actuator
035	Motion of a Two-DOF System Subjected to Random Vibration		X																																	
036	Interference Analysis of Two Concentric Thick-walled Rings				X																															
037	Circular Flat Plate with Edge Clamped and Concentrated Load Applied at Center						X																													
038	Thick-walled Spherical Vessel Under Uniform Internal Pressure					X				X																										
039	Forced Harmonic Response Analysis of a Spring-Mass-Damper System		X																																	
040	Solid Sphere Analyzed to Find Weight, Center of Gravity and Mass Moment of Inertia				X																															
041	Natural Frequency of a Gr./Epoxy Laminated Composite Square Plate														X																					
042	Mid-span Deflection of a Uniform Steel Beam Simply Supported at Both Ends		X																																	
043	Stress Relaxation of a Tightened Bolt Due to Thermal Creep																		X																	
044	Deflection Analysis of a Helical Spring Under Compressive Loading		X			X																														

AVE #	Accuracy Verification Example Title	Truss	Beam	Membrane	2-D	3-D Brick	3-D Plate/Shell	Boundary	3-D Enhanced Brick	10-node Tetrahedral	Spring	Rigid	Gap	Thin Shell Composite	Thick Shell Composite	3-D Nonlinear Truss	3-D Nonlinear Beam	3-D General Contact	2-D Nonlinear	3-D Nonlinear	Nonlinear Shell	3-D Kinematic	3-D Nonlinear Membrane	Thermal Boundary	3-D Thermal Plate	4-node Tetrahedral	10-node Tetrahedral	Thermal Brick	2-D Thermal	3-D Electro-boundary	Electrical Solid	2-D Electrostatic	2-D Fluid	3-D Fluid	Dynamic Contact	Actuator
045	Nonlinear Radiation Heat Transfer Analysis of a Cylindrical Disk with Internal Heat Generation																									X	X	X								
046	Shear Force and Bending Moment Analysis of a Beam Under Distributed Loading		X																																	
047	Thermal Stress Analysis of a Thick-walled Cylindrical Vessel Under Temperature Gradient				X																															
048	Elastic Stability of a Flat Plate Under a Pure Axial Load						X																													
049	Concrete Frame Structure Subjected to Distributed Loading		X																																	
050	Solid Aluminum Cylinder Exposed to a Convection Environment and Allowed to Cool																												X							
051	Fluid Flow between Two Plates																																X			
052	2-D Laminar Flow over a Backward Facing Step																															X				
053	Linear Mode Shape with Load Stiffening Analysis on a Simply Supported Continuous Beam		X																																	

AVE #	Accuracy Verification Example Title	Truss	Beam	Membrane	2-D	3-D Brick	3-D Plate/Shell	Boundary	3-D Enhanced Brick	10-node Tetrahedral	Spring	Rigid	Gap	Thin Shell Composite	Thick Shell Composite	3-D Nonlinear Truss	3-D Nonlinear Beam	3-D General Contact	2-D Nonlinear	3-D Nonlinear	Nonlinear Shell	3-D Kinematic	3-D Nonlinear Membrane	Thermal Boundary	3-D Thermal Plate	4-node Tetrahedral	10-node Tetrahedral	Thermal Brick	2-D Thermal	3-D Electro-boundary	Electrical Solid	2-D Electrostatic	2-D Fluid	3-D Fluid	Dynamic Contact	Actuator
054	Thick-Walled Spherical Shell Subjected to Uniform Internal Pressure																		X																	
055	Nonlinear Heat Flow Analysis of a Solid Cylinder																							X					X							
056	Response Spectrum Analysis of a Simple Beam		X																																	
057	Cantilever Beam with a Gap at the Tip		X										X																							
058	Transient Thermal Analysis of a Solid Wall with Internal Heat Generation																											X	X							
059	Steady-State Heat Transfer Analysis of a Fin Immersed in a Cooling Fluid																							X					X							
060	Nonlinear Radiation Heat Transfer Analysis of a Cylindrical Disk with Internal Heat Generation																											X								
061	Continuous Beam, Simply Supported at the Ends, Under a Uniformly Distributed Load		X																																	
062	Design Spectrum with a Specified Maximum Ground Acceleration		X																																	
063	Slab with Internal Charge Density Distribution																														X					
064	Thermal Deflection Analysis of a Plate						X																													

AVE #	Accuracy Verification Example Title	Truss	Beam	Membrane	2-D	3-D Brick	3-D Plate/Shell	Boundary	3-D Enhanced Brick	10-node Tetrahedral	Spring	Rigid	Gap	Thin Shell Composite	Thick Shell Composite	3-D Nonlinear Truss	3-D Nonlinear Beam	3-D General Contact	2-D Nonlinear	3-D Nonlinear	Nonlinear Shell	3-D Kinematic	3-D Nonlinear Membrane	Thermal Boundary	3-D Thermal Plate	4-node Tetrahedral	10-node Tetrahedral	Thermal Brick	2-D Thermal	3-D Electro-boundary	Electrical Solid	2-D Electrostatic	2-D Fluid	3-D Fluid	Dynamic Contact	Actuator
065	Torsion of an Elastic Beam with a Channel Cross-Section						X																													
066	Multidimensional Transient Heat Transfer Analysis																												X							
067	Fundamental Frequency and Static Lateral Deflections of a Loaded Shaft		X																																	
068	Annular Plate with a Uniformly Distributed Pressure				X	X	X																													
069	Nonlinear Static Analysis of a Simply Supported Plate																				X															
070	A Combined Beam/Plate Model		X				X																													
071	Creep Analysis of a Thick-Walled Cylinder																		X																	
072	Shear Flow in a Simply Supported Beam				X																															
073	Dynamic Analysis of a Beam Model																X																			
074	Thermal Stress Analysis of a Pinned Beam/Truss Structure	X	X																																	
075	Dynamic Nonlinear Analysis of a Beam Model with a Gravity Load																		X																	
076	Linear Stress Analysis of a Beam Model		X					X																												
077	Two Cylindrical Shells with Internal Pressure Loading				X																															

AVE #	Accuracy Verification Example Title	Truss	Beam	Membrane	2-D	3-D Brick	3-D Plate/Shell	Boundary	3-D Enhanced Brick	10-node Tetrahedral	Spring	Rigid	Gap	Thin Shell Composite	Thick Shell Composite	3-D Nonlinear Truss	3-D Nonlinear Beam	3-D General Contact	2-D Nonlinear	3-D Nonlinear	Nonlinear Shell	3-D Kinematic	3-D Nonlinear Membrane	Thermal Boundary	3-D Thermal Plate	4-node Tetrahedral	10-node Tetrahedral	Thermal Brick	2-D Thermal	3-D Electro-boundary	Electrical Solid	2-D Electrostatic	2-D Fluid	3-D Fluid	Dynamic Contact	Actuator
078	Spring and Collar Slide Down Vertical Rod															X			X																	
079	Slender Pivoting Rod and Compressed Spring															X			X																	
080	Dynamic Analysis of an 8-kg Body Using Damping and a Dashpot																	X	X																	
081	Transient Heat Transfer Analysis of a Semi-Infinite Pressure Loading																											X								
082	Mechanical Event Simulation of a Slider-Crank Mechanism																X			X																
083	Mechanical Event Simulation of a Lunar Lander															X				X																
084	Fluid Flow Drag Analysis of Flow across a Flat Plate																															X				
085	Mechanical Event Simulation of a Basketball Being Shot into a Hoop																X				X	X														
086	Heat Flux Transient Heat Transfer Analysis																												X							
087	Mechanical Event Simulation of Grinder Shaft Under Torsion																			X																
088	Mechanical Event Simulation of a Chain with Weights at the Hinges																			X																
089	Transient Thermal Analysis of a Cooling Copper Wire																												X							
090	Heat Flux Loading on a Hollow Cylinder																												X							
091	Mechanical Event Simulation of a Cylinder Rolling inside a Curved Surface																		X																X	
092	Mechanical Event Simulation of a Flyball-Governor	X	X																																	

AVE #	Accuracy Verification Example Title	Truss	Beam	Membrane	2-D	3-D Brick	3-D Plate/Shell	Boundary	3-D Enhanced Brick	10-node Tetrahedral	Spring	Rigid	Gap	Thin Shell Composite	Thick Shell Composite	3-D Nonlinear Truss	3-D Nonlinear Beam	3-D General Contact	2-D Nonlinear	3-D Nonlinear	Nonlinear Shell	3-D Kinematic	3-D Nonlinear Membrane	Thermal Boundary	3-D Thermal Plate	4-node Tetrahedral	10-node Tetrahedral	Thermal Brick	2-D Thermal	3-D Electro-boundary	Electrical Solid	2-D Electrostatic	2-D Fluid	3-D Fluid	Dynamic Contact	Actuator
093	Steady-State Heat Transfer Analysis of a Pipe Buried in Earth																											X	X							
094	3-D Truss System under a Point Load and Uniform Temperature Increase	X																																		
095	Weight, Center of Gravity and Mass Moment of Inertia Analysis of a Straight Bar	X																																		
096	6-Story, 2-Bay Frame Structure under Uniformly Distributed Loading		X																																	
097	Earthquake Response of a 10-Story Plane Frame		X																																	
098	Frequency Response Analysis of a Two Degrees of Freedom System		X																																	
099	Weight, Center of Gravity and Mass Moment of Inertia Analysis of a Square Beam		X																																	
100	Torsion of a Box Beam			X																																
101	Weight, Center of Gravity and Mass Moment of Inertia Analysis of a Circular Plate			X																																
102	Thick-Walled Cylinder under Both Pressure and Temperature Loadings				X																															
103	Stress Concentration around a Hole				X																															

AVE #	Accuracy Verification Example Title	Truss	Beam	Membrane	2-D	3-D Brick	3-D Plate/Shell	Boundary	3-D Enhanced Brick	10-node Tetrahedral	Spring	Rigid	Gap	Thin Shell Composite	Thick Shell Composite	3-D Nonlinear Truss	3-D Nonlinear Beam	3-D General Contact	2-D Nonlinear	3-D Nonlinear	Nonlinear Shell	3-D Kinematic	3-D Nonlinear Membrane	Thermal Boundary	3-D Thermal Plate	4-node Tetrahedral	10-node Tetrahedral	Thermal Brick	2-D Thermal	3-D Electro-boundary	Electrical Solid	2-D Electrostatic	2-D Fluid	3-D Fluid	Dynamic Contact	Actuator
104	Spherical Cap with Pressure				X																															
105	Cylindrical Tube under Forced Response with Direct Integration				X																															
106	Cylindrical Tube under Forced Response with Modal Combination				X																															
107	Patch Test with Constant Stress				X																															
108	Weight, Center of Gravity and Mass Moment of Inertia Analysis of a Circular Plate				X																															
109	Thick-Walled Cylinder under Centrifugal and Pressure Loading					X		X																												
110	Cantilever Beam Eigenvalues					X																														
111	Weight, Center of Gravity and Mass Moment of Inertia Analysis of a Square Beam					X																														
112	Weight, Center of Gravity and Mass Moment of Inertia Analysis of a Solid Sphere					X																														
113	Spherical Cap with Uniform Pressure						X																													
114	Equilateral Triangle with Linear Thermal Gradient						X																													

AVE #	Accuracy Verification Example Title	Truss	Beam	Membrane	2-D	3-D Brick	3-D Plate/Shell	Boundary	3-D Enhanced Brick	10-node Tetrahedral	Spring	Rigid	Gap	Thin Shell Composite	Thick Shell Composite	3-D Nonlinear Truss	3-D Nonlinear Beam	3-D General Contact	2-D Nonlinear	3-D Nonlinear	Nonlinear Shell	3-D Kinematic	3-D Nonlinear Membrane	Thermal Boundary	3-D Thermal Plate	4-node Tetrahedral	10-node Tetrahedral	Thermal Brick	2-D Thermal	3-D Electro-boundary	Electrical Solid	2-D Electrostatic	2-D Fluid	3-D Fluid	Dynamic Contact	Actuator
115	Simply Supported Anisotropic Plate						X																													
116	Rectangular Plate with All Edges Clamped						X																													
117	Linear Mode Shape Analysis with Load Stiffening, Simply Supported Beam						X																													
118	Thin-Walled Cylinder with a Uniform Axial Load						X																													
119	Thick-Walled Cylinder							X		X																										
120	Weight, Center of Gravity and Mass Moment of Inertia Analysis of a Solid Sphere									X																										
121	Two Cantilever Beams Connected by a Tension-Only Element at the Tip		X										X																							
122	L-Shaped Pipe System Subjected to Temperature Load		X										X																							
123	An Internally Pressurized Cylinder													X	X																					
124	Simply Supported Square Laminate Subjected to a Uniform Pressure Load													X	X																					
125	Clamped Circular Plate with a Point Load														X																					
126	Large Deformation and Large Strain for a Rubber Sheet																		X																	

AVE #	Accuracy Verification Example Title	Truss	Beam	Membrane	2-D	3-D Brick	3-D Plate/Shell	Boundary	3-D Enhanced Brick	10-node Tetrahedral	Spring	Rigid	Gap	Thin Shell Composite	Thick Shell Composite	3-D Nonlinear Truss	3-D Nonlinear Beam	3-D General Contact	2-D Nonlinear	3-D Nonlinear	Nonlinear Shell	3-D Kinematic	3-D Nonlinear Membrane	Thermal Boundary	3-D Thermal Plate	4-node Tetrahedral	10-node Tetrahedral	Thermal Brick	2-D Thermal	3-D Electro-boundary	Electrical Solid	2-D Electrostatic	2-D Fluid	3-D Fluid	Dynamic Contact	Actuator
127	Plastic Analysis of a Thick-Walled Cylinder																		X																	
128	Static Large Displacement Analysis of a Spherical Shell																		X																	
129	Static Analysis of a Simply Supported Plate																			X																
130	Natural Frequencies for a Simply Supported Plate																			X																
131	Dynamic Analysis of a Simply Supported Plate under Concentrated Load																			X																
132	Wall with Internal Heat Generation																							X				X								
133	Plane Couette Flow																															X				
134	Axisymmetric Flow through a Circular Pipe																															X				
135	Axisymmetric Flow past a Sphere at Re = 10																															X				
136	Flow past a Circular Cylinder at Re = 40, 100																															X				
137	3-D Fluid Flow																																X			
138	DDAM Shock Analysis of Heavy Equipment Mounted on the Deck of a Surface Ship		X																																	
139	DDAM Shock Analysis of a Ship's Rudder System		X																																	

AVE #	Accuracy Verification Example Title	Truss	Beam	Membrane	2-D	3-D Brick	3-D Plate/Shell	Boundary	3-D Enhanced Brick	10-node Tetrahedral	Spring	Rigid	Gap	Thin Shell Composite	Thick Shell Composite	3-D Nonlinear Truss	3-D Nonlinear Beam	3-D General Contact	2-D Nonlinear	3-D Nonlinear	Nonlinear Shell	3-D Kinematic	3-D Nonlinear Membrane	Thermal Boundary	3-D Thermal Plate	4-node Tetrahedral	10-node Tetrahedral	Thermal Brick	2-D Thermal	3-D Electro-boundary	Electrical Solid	2-D Electrostatic	2-D Fluid	3-D Fluid	Dynamic Contact	Actuator
140	Pressure Drop in a Straight Pipe																																X			
141	Linear Static Stress Analysis of a Laminated Strip													X																						
142	Distance for Stopping a Car																		X																X	
143	Body-to-Body Radiation between Two Cylinders																							X												
144	Nonlinear Displacement of a Bar with an Axial Load																		X																	
145	Tapered Axisymmetric Thick Shell Subjected to a Pressure Load				X																															
146	Contact Pressure Analysis of a Punch-Foundation System				X								X																							
147	Acceleration Analysis of a Piston-Crank Mechanism															X	X																			
148	Natural Frequencies Analysis of a Pin-Ended Double Cross Structure		X																																	
149	Electrostatic Field Strength Analysis of a Spherical Electron Cloud				X																									X		X				
150	Steady-State Heat Transfer Analysis of a Rod with an Adiabatic Tip					X																														
151	Natural Frequency Analysis of a Flat Circular Plate						X																													
152	Cylinder/Sphere under Uniform Internal Pressure						X																													
153	Heat Generation in a Wire due to Electrical Current																												X							
154	Natural Frequency (Modal) Analysis of a Cantilever Beam		X																																	

AVE #	Accuracy Verification Example Title	Truss	Beam	Membrane	2-D	3-D Brick	3-D Plate/Shell	Boundary	3-D Enhanced Brick	10-node Tetrahedral	Spring	Rigid	Gap	Thin Shell Composite	Thick Shell Composite	3-D Nonlinear Truss	3-D Nonlinear Beam	3-D General Contact	2-D Nonlinear	3-D Nonlinear	Nonlinear Shell	3-D Kinematic	3-D Nonlinear Membrane	Thermal Boundary	3-D Thermal Plate	4-node Tetrahedral	10-node Tetrahedral	Thermal Brick	2-D Thermal	3-D Electro-boundary	Electrical Solid	2-D Electrostatic	2-D Fluid	3-D Fluid	Dynamic Contact	Actuator
155	Tapered Plate with Gravity						X																													
156	Rectangular Plate Held by Three Wires	X					X																													
157	Effect of Fins on Heat Transfer from a Steam Pipe																										X								
158	Velocity and Reaction Force from a Crate Being Dragged across the Floor																		X																
159	Heat Transfer between Hot- and Cold-Water Pipes																											X							
160	Axisymmetric Vibration of a Simply Supported Annular Plate				X																														
161	Natural Frequency (Modal) Analysis of a Cantilever Beam with Off-Center Point Masses				X																														
162	Steady-State Heat Transfer Analysis of a Coal Powder Stockpile																											X							
163	Bending and Wrinkling of a Pretensioned Beam-like Membrane																						X												
164	Displacement of a Restraining Rod Attached to a Beam	X	X																																
165	MES of a Parallelogram Linkage Used to Transfer a Crate between Platforms															X	X		X																
166	Beam with Spring Support under Distributed Load								X		X																								
167	Flow through a Tube with Fixed Heat Flux																										X						X		

AVE #	Accuracy Verification Example Title	Truss	Beam	Membrane	2-D	3-D Brick	3-D Plate/Shell	Boundary	3-D Enhanced Brick	10-node Tetrahedral	Spring	Rigid	Gap	Thin Shell Composite	Thick Shell Composite	3-D Nonlinear Truss	3-D Nonlinear Beam	3-D General Contact	2-D Nonlinear	3-D Nonlinear	Nonlinear Shell	3-D Kinematic	3-D Nonlinear Membrane	Thermal Boundary	3-D Thermal Plate	4-node Tetrahedral	10-node Tetrahedral	Thermal Brick	2-D Thermal	3-D Electro-boundary	Electrical Solid	2-D Electrostatic	2-D Fluid	3-D Fluid	Dynamic Contact	Actuator
168	Body-to-Body Radiation Heat Transfer in the Frustum of a Cone																												X							
169	Steady Fluid Flow through a Circular Tube																																X			
170	Circular Plate with Fixed Edges under Uniform Pressure Load						X																													
171	Force on the Actuator of a Hydraulic-Lift Table																	X		X																X
172	Heat Transfer Rate of a Heat Exchanger Wall with Pin Fins on One Side																											X							
173	First Natural Frequency of a Rectangular Flat Plate with All Edges Fixed						X																												
174	Heat Transfer through Thin Plate																											X							
175	Maximum Fluid Flow																																X		
176	Angular Deflection of Steel Step Shaft					X																													
177	Deflection of Beam and Spring System		X								X																								

AVE #	Accuracy Verification Example Title	Truss	Beam	Membrane	2-D	3-D Brick	3-D Plate/Shell	Boundary	3-D Enhanced Brick	10-node Tetrahedral	Spring	Rigid	Gap	Thin Shell Composite	Thick Shell Composite	3-D Nonlinear Truss	3-D Nonlinear Beam	3-D General Contact	2-D Nonlinear	3-D Nonlinear	Nonlinear Shell	3-D Kinematic	3-D Nonlinear Membrane	Thermal Boundary	3-D Thermal Plate	4-node Tetrahedral	10-node Tetrahedral	Thermal Brick	2-D Thermal	3-D Electro-boundary	Electrical Solid	2-D Electrostatic	2-D Fluid	3-D Fluid	Dynamic Contact	Actuator
178	Temperature Difference Across Contact																											X								
179	Natural Frequency of a Flat Plate						X																													
180	Deflection of Truss	X																																		
181	MES Thermal Loading of Shell Composite													X																						
182	Deflection of a Spring Supported Beam		X								X																									
183	MES of Force Accelerated Block																		X																	
184	Radiation between two Cylinders																												X							
185	Outlet Velocity of Fluid Tank																																X			
186	Steady-State Heat Transfer along a Rod	X																																		
187	Natural Frequency of a Beam, Spring and Mass System		X								X																									
188	Notched Plate				X																															
189	MES Deflection of a Spring Supported Beam															X	X																			
190	Flow of Steam through an Insulated Pipe																												X							
191	Airflow over a Hill																															X				

AVE #	Accuracy Verification Example Title	Truss	Beam	Membrane	2-D	3-D Brick	3-D Plate/Shell	Boundary	3-D Enhanced Brick	10-node Tetrahedral	Spring	Rigid	Gap	Thin Shell Composite	Thick Shell Composite	3-D Nonlinear Truss	3-D Nonlinear Beam	3-D General Contact	2-D Nonlinear	3-D Nonlinear	Nonlinear Shell	3-D Kinematic	3-D Nonlinear Membrane	Thermal Boundary	3-D Thermal Plate	4-node Tetrahedral	10-node Tetrahedral	Thermal Brick	2-D Thermal	3-D Electro-boundary	Electrical Solid	2-D Electrostatic	2-D Fluid	3-D Fluid	Dynamic Contact	Actuator
192	Heat Lost through the Walls of a Furnace																											X								
193	Simply Supported Beam with a Mass in the Middle		X																																	
194	Contact Pressure between a Punch and Foundation					X							X																							
195	MES Deflection of a Pointer Due to Thermal Expansion																X																			
196	Natural Frequency of a Weighing Platform	X				X					X	X																								
197	Axial and Bending Forces Acting on a Wide Flanged Beam		X																																	
198	MES of a Pinned Rod Released from Rest																X																			
199	MES of a Reinforced Concrete Beam																			X																
200	Riks Analysis of a Curved Cylindrical Shell																				X															

AVE - 1 Flat Circular Plate of Constant Thickness (2-D)

Reference

Roark, R. J. and Young, W. C., *Roark's Formulas for Stress and Strain*, Fifth Edition, New York: McGraw-Hill, 1975, page 334, Table 24, Case 1a.

Problem Description

A flat, annular, circular plate of 0.5" constant thickness with its outer edge simply supported and inner edge free is analyzed for stress and deflection under a 50 lbf/in uniform annular line load located at the inner edge.

The association between degrees of freedom and bending in elements is confusing to many FEA users. The commonly used term "element's degree of freedom" is technically incorrect because the degrees of freedom that are supported by an element do not associate directly with the element, but rather with the nodes that define it. It is correct, however, to associate certain element types with certain nodal degrees of freedom.

Active vs. Inactive

A degree of freedom is either active or inactive. An active degree of freedom affects the element's solution, whereas an inactive degree of freedom does not. An active degree of freedom also becomes part of the stiffness matrix, while an inactive degree of freedom does not. A maximum of six active degrees of freedom (three translational and three rotational) are possible at a node. In Autodesk Simulation, the default active degrees of freedom are automatically defined for every node depending on the element type.

Table 1-1 gives the default degrees of freedom for many common linear elements. Some element types do not require all of the six available degrees of freedom. For instance, truss, 2-D axisymmetric, 2-D continuum, and 3-D continuum elements all need fewer than six degrees of freedom.

Table 1-1. (0 = Active, 1 = Inactive)

Element Type	Translation			Rotation		
	X	Y	Z	X	Y	Z
Truss	0	0	0	1	1	1
Beam	0	0	0	0	0	0
2-D Axisymmetric	1	0	0	1	1	1
2-D Continuum	1	0	0	1	1	1
3-D Continuum (Bricks)	0	0	0	1	1	1
Plate	0	0	0	0	0	1

Degrees of Freedom vs. Type of Analysis

The available degrees of freedom do not necessarily determine the kinds of structures that a particular element type can model. For instance, an engineer could model a structural I-beam by using plate or 3-D brick elements, if needed.

For the truss element, however, the absence of rotational degrees of freedom does determine the types of structures it can realistically be used to analyze. A truss element resists axial forces but does not resist or transmit moments, so it is essentially equivalent to a beam element with ball joints at both ends.

Unlike a beam element, a truss element cannot accept a moment load applied to its nodes, while it can accept nodal forces. Therefore, truss elements should only be used to model 2-D structures that have pinned joints or 3-D structures with ball joints.

The connection between 2-D and 3-D continuum element's degrees of freedom and the type of structures these elements can analyze is not always clear. For example, either 2-D or 3-D continuum elements can be used to model a cantilever beam with a rectangular cross-section and an end load. Stresses generated would be caused by a bending moment. At first glance, it might appear to a person new to FEA that the active degrees of freedom would prevent the element from adequately representing the effects. These elements, however, will correctly analyze the model because they properly interpret the translations caused by the bending moment. These elements will not support a moment applied to the nodes. Moments are applied as force couples, which is more realistic.

Degrees of Freedom vs. Boundary Conditions

The relationship between degrees of freedom and boundary conditions is also often unclear. Degrees of freedom are inherent to an element's formulation whereas boundary conditions are assigned by the user. By applying a boundary condition to a node, the user can constrain one or all of the active degrees of freedom. The user may further restrict a node, but cannot release a default degree of freedom. For example, if the rotational degrees of freedom are inactive for an element type, then setting a boundary condition to free those degrees of freedom has no effect.

Inactive degrees of freedom do not tie a model down or prevent the "rigid body modes encountered" message. Tying two nodes of a brick model down in all three translation directions (for example, Txyz), still allows the model to rotate about an axis that passes through both of these constrained points. Fixing a third node in a direction perpendicular to the plane created by the three nodes will prevent the model from rotating.

Autodesk Simulation Solution

For this example, the following values are used:

- a = 24 in (outer radius)
- b = 12 in (inner radius)
- w = 50 lbf/in (uniform annular line load)
- t = 0.5 in (thickness)
- b/a = 0.5
- E = 27.5E6 psi (Young's Modulus)
- ν = 0.3 (Poisson's Ratio)

(Refer to AVE 002 for the theoretical solution to this problem.)

Four different mesh densities were tested. The line load was applied using nodal forces, which, for axisymmetric elements, are interpreted as per radian.

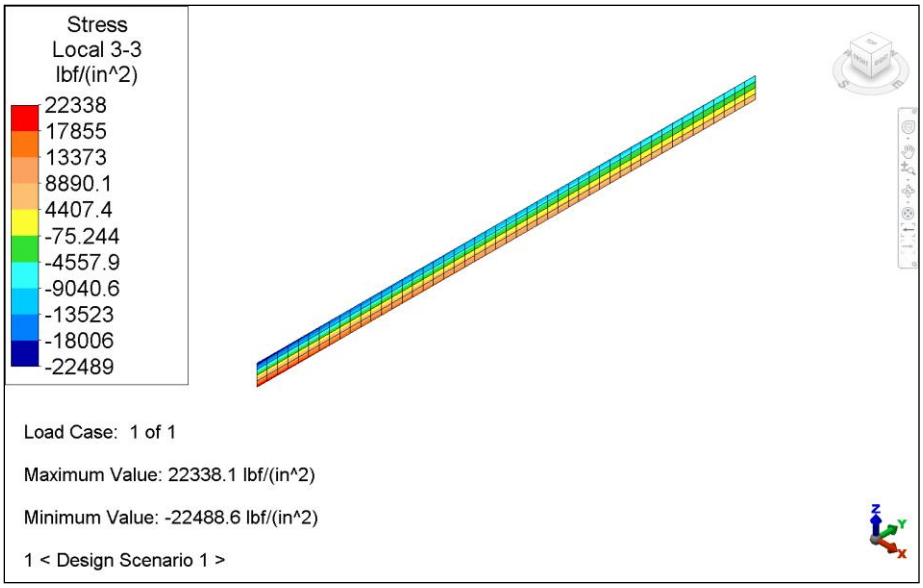

Figure 1-1. Stress contour (S-tensor in 33 direction: S33)

As shown in Table 1-2, the deflections generated using 2-D axisymmetric elements with the Linear Static Stress processor very nearly match theoretical deflections, even with a coarse mesh. With a mesh of 2 x 24, the differences between theoretical stresses and the analysis results are within 0.3%. Furthermore, with a 1 x 12 mesh, the stresses are still within 1.9% of each other. (The stresses are read away from the application of the nodal forces.)

These percentages show that it is acceptable to use 2-D or 3-D continuum elements in problems involving bending.

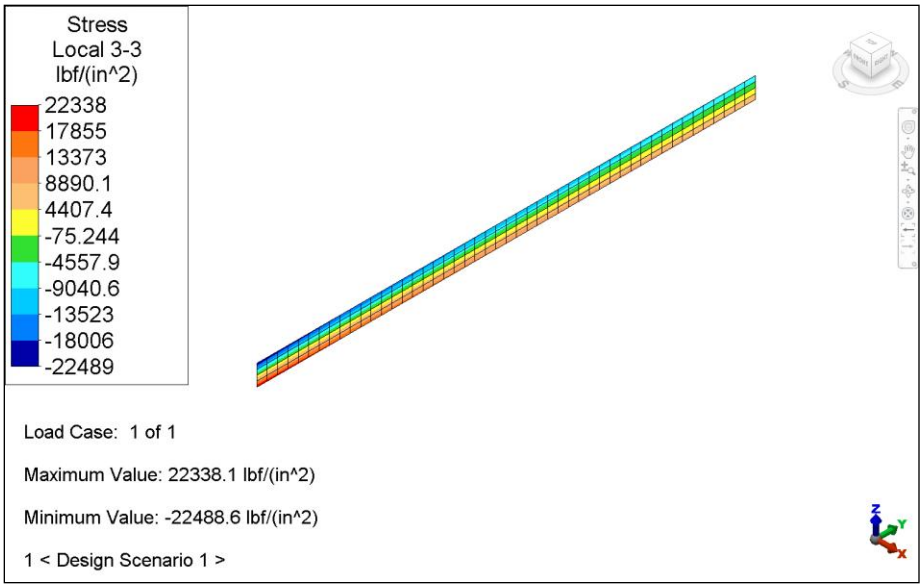

Figure 1-1. Stress contour (S-tensor in 33 direction: S33)

Table 1-2. Comparison of Results

	Theory	2-D Axisymmetric			
		1x12 Mesh	2x24 Mesh	3x36 Mesh	4x48 Mesh
Vertical Deflection (inch)	-0.4247	-0.4245	-0.4247	-0.4247	-0.4247
% Difference	NA	-0.05	0	0	0
Sigma 33 (psi) (hoop stress)	22,340	22,748	22,390	22,345	22,338
% Difference	NA	1.83	0.22	0.02	-0.01

The model is constructed in the YZ plane where the Y coordinate corresponds to the radial dimension. For the results, the local axis 3 corresponds to the hoop direction; thus, the stress tensor S33 will show the hoop stress.

Note: The supplied archive file includes the densest mesh (4 x 48) only.

AVE - 2 Flat Circular Plate of Constant Thickness (3-D)

Reference

Roark, R. J. and Young, C. W., *Roark's Formulas for Stress and Strain*, 5th Edition, New York: McGraw-Hill, 1975, Page 334, Table 24, Case 1a.

Problem Description

Accuracy Verification Example 001 compares analysis results with theoretical results found in Case 1a from Roark and Young. Case 1a analyzes a flat, annular, circular plate of constant thickness with its outer edge simply supported, inner edge free, and the load located at the inner edge. The model analyzed for the comparison was constructed of 2-D axisymmetric elements. Analysis results were shown to be within 0.1% of the Roark and Young Case 1a theoretical answer.

Theoretical Solution

The theoretical stress and vertical deflection are shown below.

σ (hoop stress at inner radius) = $\frac{6M}{t^2} = \frac{6(.7757)(50)(24)}{(0.5)^2}$ = 22340.16 psi

vertical deflection = $K_y \frac{wa^3}{D} = \frac{-0.1934(50)(24)^3}{314789}$ = -0.4247 inch

Where:

- M = moment = $K_m$wa
- K_m = 0.7757 (based on b = 12 in a = 24 in)
- w = 50 lbs/in
- t = 0.5 in
- E = 27.5E6 psi (Young's Modulus)
- ν = 0.3 (Poisson's Ratio)
- K_y = -0.1934 (based on a and b)
- D = $Et^3/12(1-\nu^2)$ = 314,789

Autodesk Simulation Solution

To further expand on this point, the Roark and Young theory was again compared to analysis results. This time, the model analyzed for the comparison consisted of brick elements. The results yielded a maximum hoop stress of 22,497.06 psi (the average of the top and bottom faces), which is within 0.70% of the theoretical solution.

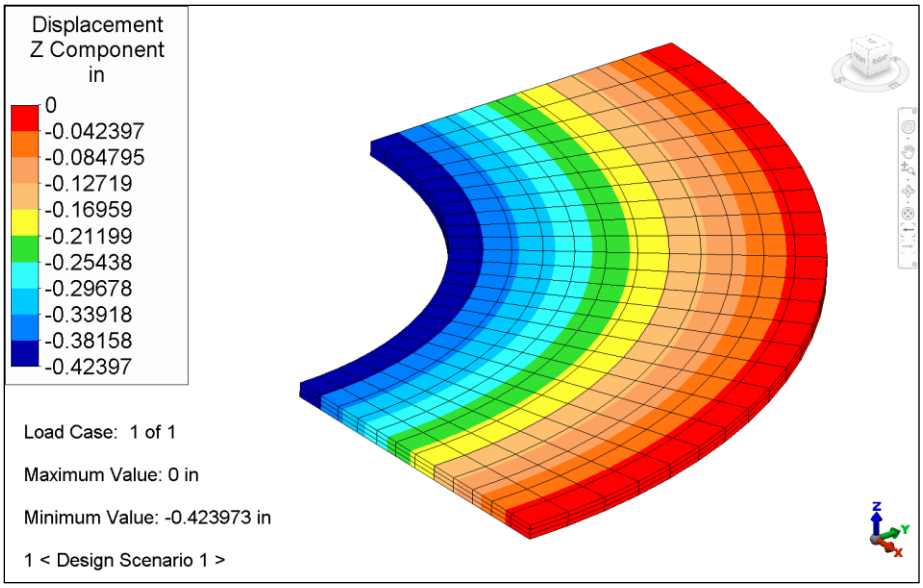

Figure 2-1. The vertical (Z) displacement vector display of the quarter-section model of the annular, circular plate referred to in Roark and Young, Case 1a. The vertical deflection at the inside radius is -0.42397 in.

The problem was modeled by constructing a 90-degree portion of the annular, circular plate. The plate was modeled in the xy plane with the following boundary conditions:

- Along the outer radius, Tz at the bottom
- Along the X-axis, TyRxz fixed along the entire face (for symmetry)
- Along the Y-axis, TxRyz fixed along the entire face (for symmetry)

As explained in AVE 001, the rotational boundary conditions (R_{xz} and R_{yz}) are strictly not needed for brick elements. We included them in the model as an indication of the symmetry condition.

The mesh consisted of 12 elements along the radius and 24 elements along the circumference and 3 elements along the thickness.

An annular line load of 50 lbs/in was applied as a force at each node along the top of the inner radius by dividing the total load for a 12 inch radius by ¼ (it is one quarter of a circle) and by the number of nodes on the inner radius. (This included applying half the load to nodes along symmetry planes.)

Table 2-1. Comparison of Results

Vertical Deflection			Stress		
Deflection (inch)		% Difference	Sigma (psi)		% Difference
Theory	Analysis		Theory	Analysis	
-0.4247	-0.4240	-0.16	22340.16	22493.94	0.69

AVE - 3 Thin-Walled Cylinder with Uniform Axial Load

Reference

Roark, R. J. and Young, W. C., *Roark's formulas for Stress and Strain*, Fifth Edition, New York: McGraw-Hill, 1975, page 448, Table 29, Case 1A.

Problem Description

This accuracy verification example is taken from formulas for membrane stresses and deformations in thin-walled pressure vessels. In this example, a thin-walled cylinder under uniform axial load is analyzed for axial stress and deflection.

Theoretical Solution

For this example the following values are used:

- p = 1,000 lb/linear in (uniform axial load)
- t = 0.1 in (cylinder thickness)
- E = 30 x 10^6 psi (Young's Modulus)
- z = 12 in (length of cylinder)
- R = mean radius = 5 inches
- σ_1 = p/t = 1,000/0.1 = 10,000 psi (applied axial stress)
- Δz = pz/Et = (1,000 * 12)/(30E6 * 0.1) = 0.004 in (deflection)

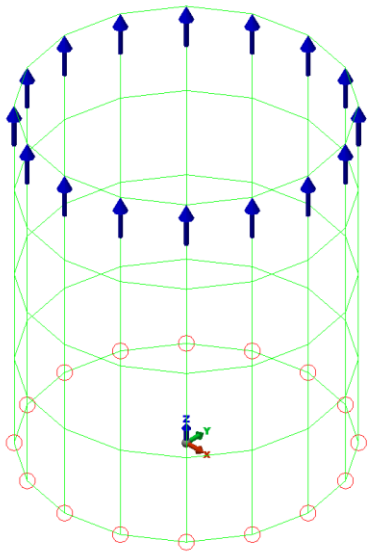

Figure 3-1. Thin-walled cylinder with loading and boundary conditions.

Autodesk Simulation Solution

The mean radius of the cylinder is modeled in FEA Editor as a 3-D shape and the thickness assigned using membrane elements. The mean radius of the cylinder is 5 inches and the height (in the Z direction) is 12 inches. The mesh consists of 4 divisions along the length of the cylinder and 16 divisions along the circumference. To simulate the unrestrained cylinder in the reference, all nodes on the base were restrained in the Z direction (Tz), the nodes on the X axis were restrained in Y translation (Ty) and the nodes on the Y axis were restrained in X translation (Tx). These last two conditions are required for model stability. The nodal loads are calculated as:

- Total load = (1000 lb/in)(2)(π)(5) = 31415.93 lb
- F applied = total load/node = 31415.93/16 = 1963.49 lb

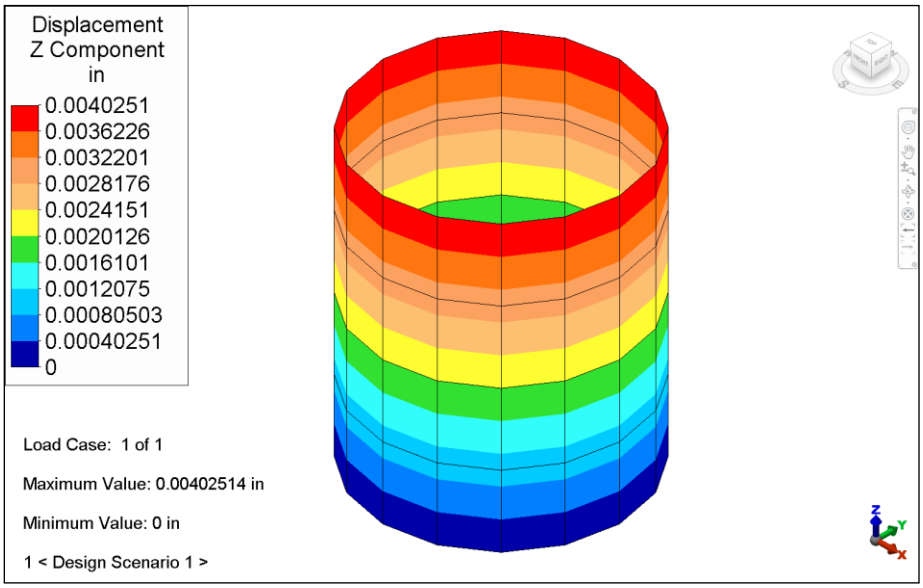

Figure 3-2. Axial deflection contour (dz) of the cylindrical shell (using membrane elements) referred to in Roark and Young, Table 29, Case 1A.

The model uses membrane elements with E and t the same as above:

- Longitudinal stress (S-tensor:Vector:Z) = 10065 psi
- Longitudinal displacement (Z deflection) = 0.00403 in

Model using plate elements:

- Longitudinal stress (S-tensor:Vector:Z) = 10065 psi
- Longitudinal displacement (Z deflection) = 0.00403 in

Model using brick elements:

- Longitudinal stress (S-tensor:Vector:Z) = 10000 psi
- Longitudinal displacement (Z deflection) = 0.00403 in

Table 3-1. Comparison of Results

	Theory	Analysis		
		Membrane Elements	**Plate Elements**	**Brick Elements**
Vertical Deflection (inch)	0.004	0.00403	0.00403	0.00403
% Difference	NA	0.75	0.75	0.75
Sigma (1) (psi)	10000.00	10064	10073	10000
% Difference	NA	0.64	0.73	0

Note: The supplied archive file includes the membrane element model only please refer to AVE - 118 for the plate element model.

AVE - 4 Thick Cylindrical Disk under Uniform Radial Pressure

Reference

Roark, R. J. and Young, W. C., *Roark's Formulas for Stress and Strain*, Fifth Edition, New York: McGraw-Hill, 1975, page 504, Table 32, Case 1A

Problem Description

A thick-walled cylindrical disk that has uniform internal radial pressure is analyzed for stress and deflection. The disk is free to deflect in the radial and longitudinal directions.

Theoretical Solution

σ_{max} = q*((a*a + b*b)/(a*a - b*b)) = 1667 psi (hoop stress at inner radius)

Δ_{max} = ((q*b)/E)((a*a + b*b)/(a*a - b*b) + v) = 1.967E-4 inch (radial displacement at the inner radius)

Where:

- q = 1000 radial pressure (psi)
- a = 6 outer radius (inch)
- b = 3 inner radius (inch)
- ν = 0.3 Poisson's Ratio
- E = 30E6 Young's Modulus (psi)

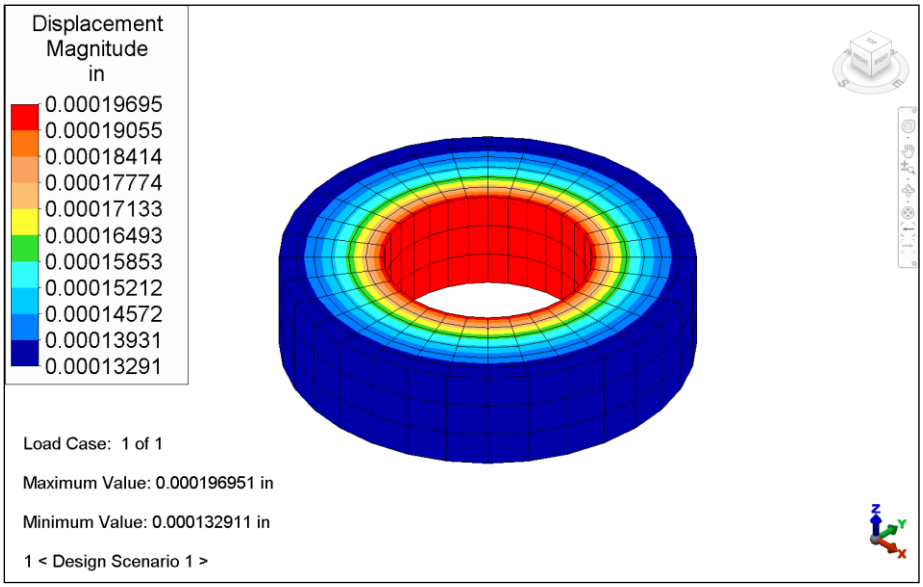

Figure 4-1. A displacement magnitude vector display of the thick-walled cylinder referred to in Roark and Young, Table 32, Case 1A. (See also note 2.)

Autodesk Simulation Solution

The model is composed of 576 brick elements (3 along the length, 6 through the thickness and 32 around the circumference). The inner radius is 3 inches and the outer radius is 6 inches. The length is 3 inches. The model is fixed at four points on one end to allow the cylinder to expand longitudinally and radially per the case in Roark's. These 4 points are not restrained in their axial direction. A uniform internal pressure of 1000 psi is applied. The results generated by the Linear Static Stress Analysis processor are:

- σ_{max} = 1697 psi (hoop stress)
- Δ_{max} = 1.961E-4

Table 4-1. Comparison of Results

Delta max (inch)		% Difference	sigma max (psi)		% Difference
Theory	**Analysis**		**Theory**	**Analysis**	
1.967e-4	1.962e-4	-0.3	1667	1697	1.8

Notes:

1. The hoop stress is obtained by viewing the stress tensor in the X direction and then reading the stress at a node on the Y axis. (At this location, the X direction corresponds to the hoop stress.) Likewise, the Y direction stress tensor shows the hoop stress for any node on the X axis.
2. The maximum displacement magnitude in the magnitude plot includes the effect of axial deflection as well as radial deflection. Thus, the radial deflection given above was obtained from the X displacement or Y displacement display.

AVE - 5 Rectangular Plate with All Edges Simply Supported and Uniform Pressure

Reference

Roark, R. J. and Young, W. C., Roark's Formulas for Stress and Strain, Fifth Edition, New York: McGraw-Hill, 1975, page 387, Table 26, Case 1C

Problem Description

A rectangular plate with all edges simply supported and uniform pressure over a central rectangular area is analyzed for maximum stress.

Theoretical Solution

sigma max = $(\beta W)/t^2$ parallel to the short edge = 11,264 psi

Where:

- $W = qa_1b_1$
- q = 100 uniform pressure (psi)
- a = 20 length of rectangular plate (inch)
- b = 10 width of rectangular plate (inch)
- a_1 = 8 length of central rectangular area (inch)
- b_1 = 4 width of central rectangular area (inch)
- t = 0.5 thickness of rectangular plate (in)
- β = 0.88 value from Case 1C Table using a = 2b, $a_1/b = 0.8$, and $b_1/b = 0.4$.
- ν = 0.3 Poisson's Ratio

Autodesk Simulation Solution

The model is composed of 200 3-D plate/shell elements drawn in the X-Y plane. Each element is one-inch square. There are 20 elements along edge "a" and 10 along edge "b". The boundary conditions are set at Txz on the short edges of the plate and Tyz on the long edges (to satisfy Roark's definition of "simply supported"). The plate elements are 0.5 inches thick. Any material can be used provided that Poisson's Ratio = 0.3 and the two moduli are compatible with this. A pressure of 100 psi is applied to an 8" x 4" rectangular area at the center of the plate. The long edge of the loaded area is parallel to the long edge of the plate. The results generated by the Linear Static Stress Analysis processor are:

σ_{max} = 11,255 psi

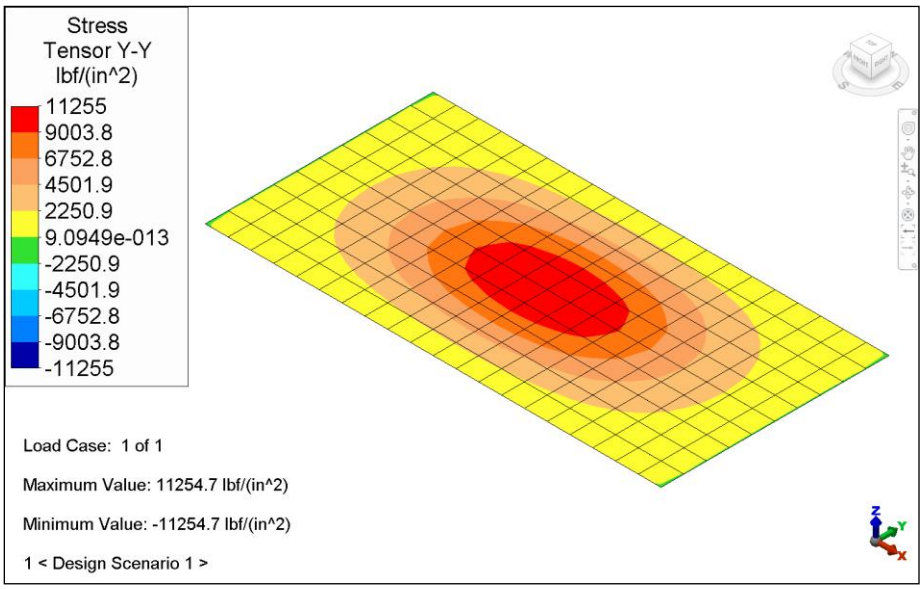

Figure 5-1. An Syy tensor stress contour of the rectangular plate referred to in Roark and Young, Table 26, Case 1C.

Table 5-1. Comparison of Results

σ_{max} (psi)		% Difference
Theory	**Analysis**	
11,264	11,255	-0.08

AVE - 6 Flat Rectangular Plate with Three Edges Simply Supported

Reference

Roark, R. J. and Young, W. C., *Roark's Formulas for Stress and Strain*, Fifth Edition, New York: McGraw-Hill, 1975, page 389, Table 26, Case 2A.

Problem Description

A flat rectangular plate 10" x 5" x 0.25" with 3 edges simply supported and free on the fourth and a uniform 50 psi load is analyzed for maximum stress.

Theoretical Solution

Maximum stress: sigma max = Bqb*b/(t*t) = 15,800 psi parallel to free edge

Where:

- t = 0.25 thickness (inch)
- q = 50 uniform pressure (psi)
- a = 10 length of long side of plate (inch)
- b = 5 length of short side of plate (in)
- B = 0.79 parameter from Roark and Young table based on a/b = 2
- ν = 0.3 Poisson's Ratio

Autodesk Simulation Solution

The model is composed of 200 3-D plate/shell elements drawn in the X-Y plane. Each element is one-half inch square. There are 20 elements along edge "a" and 10 along edge "b". The boundary conditions are set at Tyz on both "a" edges and at Txz on one of the "b" edges. Any material can be used provided that Poisson's Ratio = 0.3 and the two moduli are compatible with this. The plate elements are 0.25 inches thick. A pressure of 50 psi is applied to the entire plate. The Linear Stress Analysis processor was used for the analysis.

Max Stress in the "b" direction = 15,772 psi

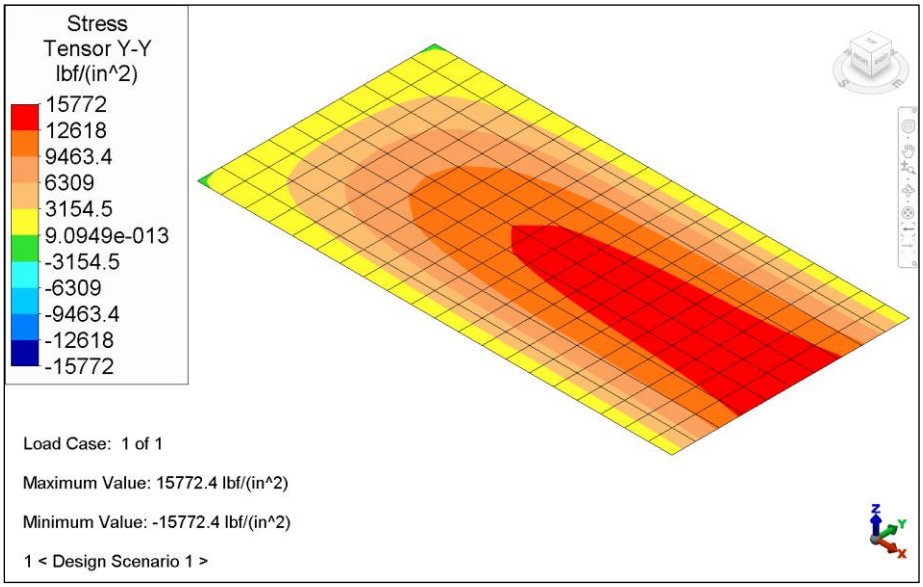

Figure 6-1. Front view of the problem in Roark and Young Table 26, Case 2A. Stress tensor Y-Y contours are shown.

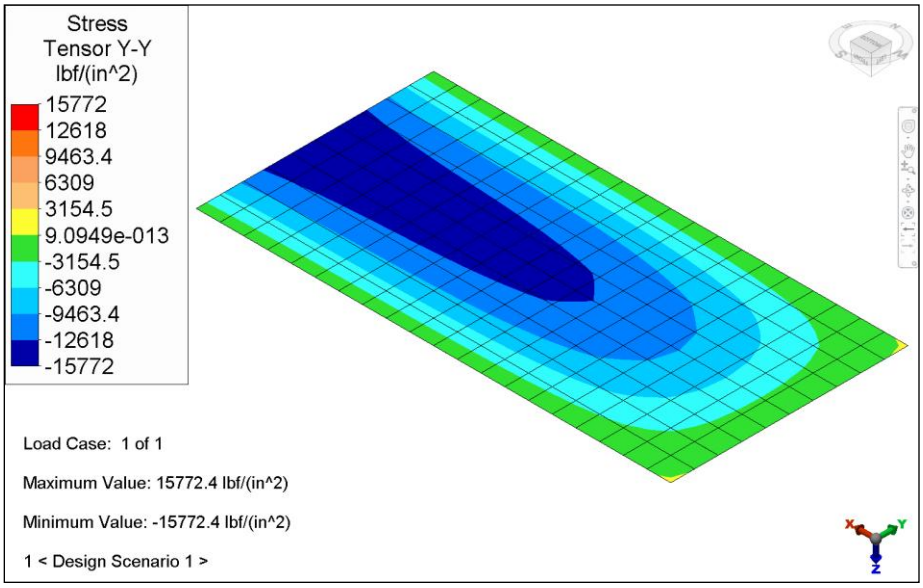

Figure 6-2. Backside view of the problem in Roark and Young Table 26, Case 2A.

Table 6-1. Comparison of Results

σ_{max} (psi)		% Difference
Theory	**Analysis**	
15,800	15,772	0.18

AVE - 7 Cantilever Beam with Nodal Force

Reference

Roark, R. J. and Young, W. C., *Roark's Formula for Stress and Strain*, Fifth Edition, New York: McGraw-Hill, 1975, page 96, Table 3, Case 1A.

Problem Description

A 16" long cantilever beam, which is fixed at one end and free at the other, is made of steel and has a 1" x 1" square cross-section. A 100-lb downward force is applied at the center of the beam. The beam is analyzed for deflection.

Theoretical Solution

The deflection at the free end of the beam is given as:

$$y_A = \frac{-W}{6EI}(2l^3 - 3l^2a + a^3) = -0.01706667 \text{ inch}$$

Where:

- W = 100 applied force (lb)
- E = 30E6 modulus of elasticity (psi)
- I = 1/12 moment of inertia (inch^4)
- l = 16 length of beam (inch)
- a = 8 distance from free end of beam to applied load (inch)

Autodesk Simulation Solution

The beam is modeled with two beam elements, each of which is 8" long. A force of 100 lbs is applied at the center of the beam in the negative Y direction. One end of the beam has boundary conditions that fix all three translations and rotations.

The results generated by the Linear Static Stress Analysis Processor are:

* y_A = -0.017149 inch

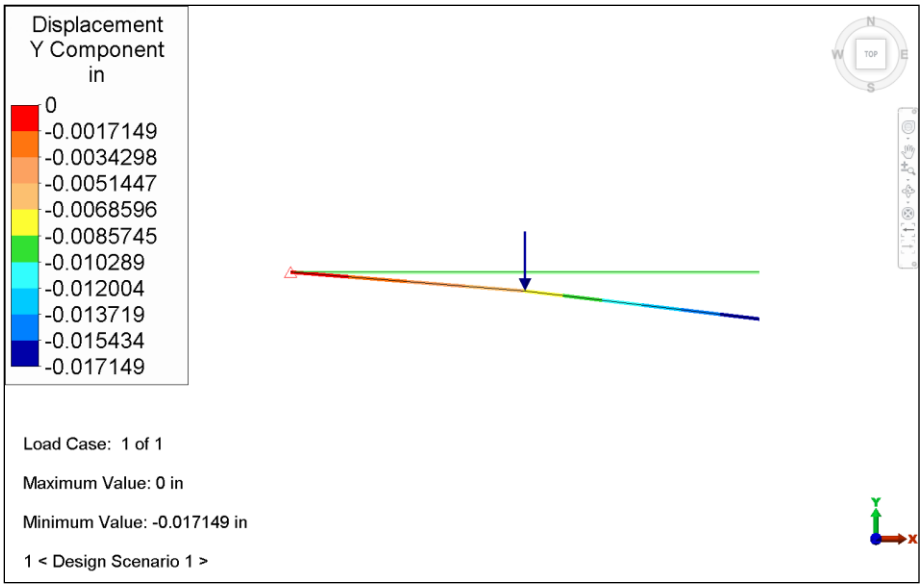

Figure 7-1. Undisplaced and displaced views of the cantilever beam in Roark and Young's Table 3, Case 1A.

Table 7-1. Comparison of Results

Comparison of Results		
y_A (inch)		% Difference
Theory	Analysis	
-0.017067	-0.017149	0.48

Note: This example demonstrates that a coarse mesh such as this will give accurate deflections and stresses at the nodes. To get a deflection or stress distribution along the length of the beam, more elements would be used.

AVE - 8 Toroidal Shell under Uniform Internal Pressure

Reference

Roark, R. J. and Young, W. C., *Roark's Formulas for Stress and Strain*, Fifth Edition, New York: McGraw-Hill, 1975, page 454, Table 29, Case 5A.

Problem Description

A toroidal shell under uniform internal pressure is analyzed for stress and deflection. The model represents one octant of an inner tube with symmetric boundary conditions imposed at all the edges. We use a total outside diameter of 30.4", an outside width of 10.4", and a wall thickness of 0.2". An internal pressure of 35 psi is applied.

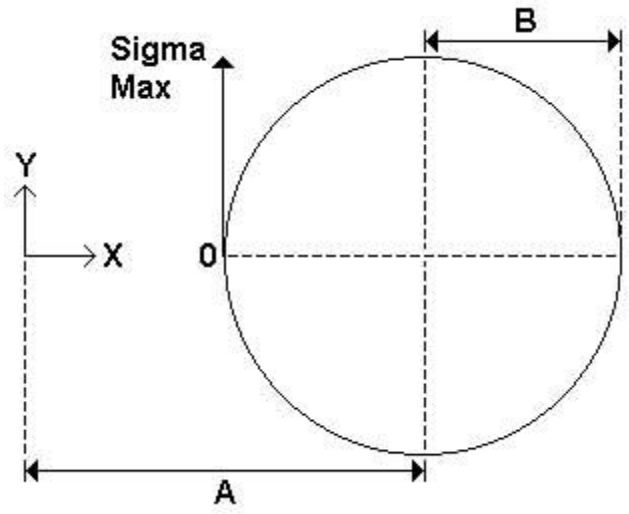

Figure 8-1. A diagram shows a cross-section of the toroidal shell. The cross-section is revolved around the Y axis.

Theoretical Solution

Sigma is maximum meridional stress (occurring inside the shell).

$$\sigma_{max} = \left(\frac{QB}{2T}\right)\left(\frac{2A-B}{A-B}\right)$$ at point 0 = 1312.5 psi

Where:

- A = 10" radius to center
- B = 5" radius air space
- Q = 35 psi internal pressure
- T = 0.2" wall thickness

Autodesk Simulation Solution

The problem can be analyzed as 2-D axisymmetric elements, 3-D plate elements, or 3-D brick elements. ***Brick elements*** are used for this example. Due to symmetry, one-eighth of the entire torus was modeled. Eighteen elements were used in the meridional and circumferential directions and one element along the thickness.

The appropriate boundary conditions were applied to each symmetry plane, as follows:

- X-Symmetry (Tx,Ry,Rz) to all nodes along the edge surface lying in the YZ plane.
- Y-Symmetry (Ty,Rx,Rz) to all nodes along the edge surface lying in the XZ plane.
- Z-Symmetry (Tz,Rx,Ry) to all nodes along the edge surface lying in the XY plane.

The toroidal model that is constructed has 722 nodes and 324 brick elements. An arbitrary set of material properties were assigned as follows:

- Mass Density = 0.0001 $lb_f \cdot s^2/in/in^3$
- E=250,000 psi
- Poisson's Ratio=0.4

The result of interest is the YY stress tensor, which is a function of the load and geometry only and is not affected by the material properties.

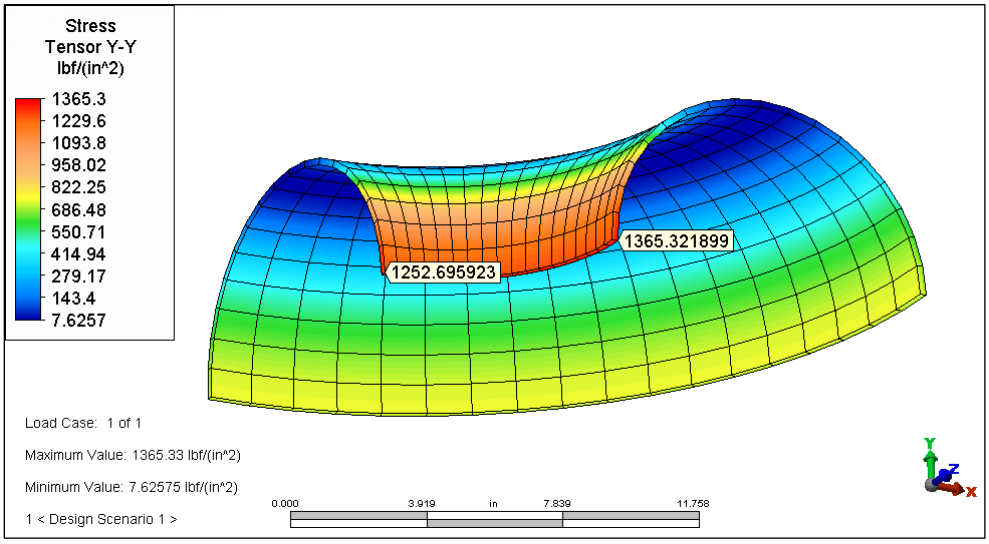

Figure 8-2. A stress tensor display showing Y-direction stress of the toroidal model constructed for Roark and Young's Table 29, Case 5A.

The numbers used in the Roark and Young formula are thin wall (average stress). Thus, the average of the y-direction stress at the inside and outside of the torus is:

- σ_{max} = (1/2)(1252.7 + 1365.3 psi) = 1309.0 psi

Table 8-1. Comparison of Results

σ_{max} (psi)		% Difference
Theory	**Analysis**	
1312.5	1309	-0.3

AVE - 9 Beam Guided at the Left and Fixed at the Right

Reference

Roark, R. J. and Young, W. C., *Formulas for Stress and Strain*, Fifth Edition, New York: McGraw-Hill, 1975, page 96, Table 3, Case 1b.

Problem Description

Case 1b is a beam that is guided at the left end (A) and fixed at the right (B). A concentrated downward load is applied at a distance "a" from the left end of the beam. The model analyzed is a 16" long steel beam with a 1" x 1" square cross-section. A 100 pound downward force is applied at the center of the beam.

Theoretical Solution

$R_A = 0$

$y_B = 0$

$\theta_A = 0$

$\theta_B = 0$

$$M_A = \frac{W(L-a)^2}{2L} = 200 \text{ inch lb}$$

$$M_B = \frac{-W(L^2-a^2)}{2L} = -600 \text{ inch lb}$$

$$y_A = \frac{-W}{12EI}(L-a)^2(L+2a) = -6.827E-3 \text{ inch}$$

$R_B = W = 100$

Where:

- W = 100 applied force (lb)
- E = 30E6 modulus of elasticity (psi)
- I = 1/12 moment of inertia (inch^4)
- L = 16 length of beam (inch)
- a = 8 distance from guided end of beam to applied load (inch)

Autodesk Simulation Solution

The beam is modeled with ten beam elements. The cross sectional properties are manually entered and the shear area values have been omitted since the theoretical results do not include shear effects. A force of 100 lbs is applied at the center of the beam in the negative Y direction. The right end of the beam is completely fixed (TxyzRxyz) and the left end of the beam is fixed except for X and Y translations (TzRxyz). The results generated by the Static Stress Analysis Processor are:

- $R_A = 0.0$
- $\theta_A = 0.0$
- $M_A = 200.0$ in lb
- $y_A = -0.00682694$ inch
- $y_B = 0.0$
- $\theta_B = 0.0$
- $M_B = -600.0$ in lb
- $R_B = 100.0$ lb

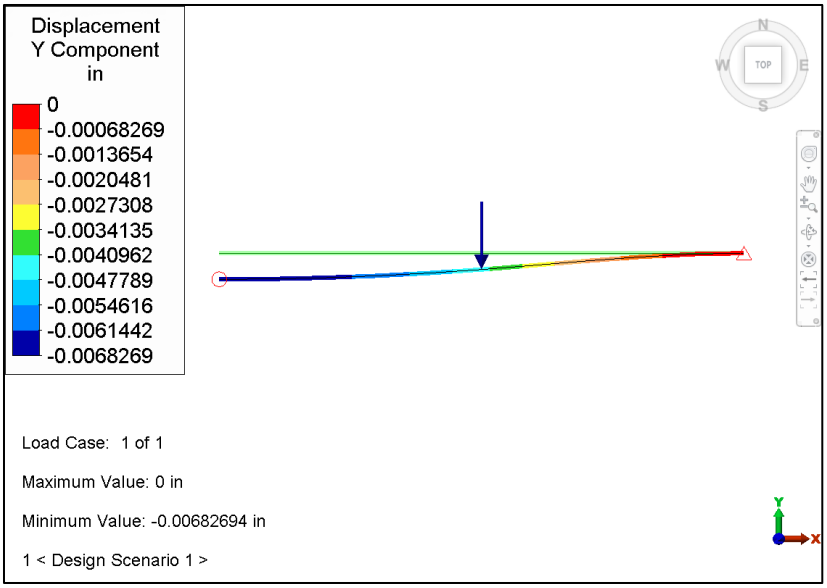

Figure 9-1. Undisplaced and displaced views of the beam in Roark and Young's Table 3, Case 1b.

Table 9-1. Comparison of Results (M_A and M_B)

M_A (lb-in)		%	M_B (lb-in)		%	yA (lb-in)		%
Theory	**Analysis**	**Difference**	**Theory**	**Analysis**	**Difference**	**Theory**	**Analysis**	**Difference**
200	200.0	0.00	-600	-600.0	0.00	-6.827e-3	-6.827e-3	0.00

Notes:

1. Reaction forces and moments can be obtained by viewing the shear and moment results in the beam elements in Superview or in the stress output file (*.s* file) by activating the "Stress data" checkbox in the "Output" tab of the "Analysis Parameters" dialog.
2. The deflections can be obtained from either Results interface or the summary file (*.L* file) by activating the "Displacement/eigenvector data" checkbox in the "Output" tab of the "Analysis Parameters" dialog.
3. The slopes θ_A and θ_B can be obtained from the summary file (*.L* file) by activating the "Displacement/eigenvector data" checkbox in the "Output" tab of the "Analysis Parameters" dialog.

AVE - 10 Thick-Walled Spherical Vessel under Uniform Internal Pressure

Reference

Roark, R. J. and Young, W. C., *Roark's Formulas for Stress and Strain*, Fifth Edition, New York: McGraw-Hill, 1975, page 506, Table 32, Case 2a.

Problem Description

A thick-walled spherical vessel under uniform internal pressure is analyzed for radial stress and deflection. For this example, we chose an outside radius of 10" and an inside radius of 7" with an internal pressure of 10,000 psi. Steel material properties were used.

Theoretical Solution

$\sigma_1 = \sigma_2$ is the normal stress in the hoop or tangential direction at radius r.

$$\sigma_1 = \left(\frac{qb^3}{2r^3}\right)\left(\frac{a^3+2r^3}{a^3-b^3}\right)$$

Δb is the radial displacement at the inside radius.

$$\Delta b = \left(\frac{qb}{E}\right)\left(\frac{(1-\nu)(a^3+2b^3)}{2(a^3-b^3)}+\nu\right)$$

Where:

* a = 10 inch outside radius
* b = 7 inch inside radius
* q = 10,000 psi internal pressure
* ν = 0.3 Poisson's Ratio
* E = 30E+6 psi Young's Modulus

for r = 7 inches

* σ_1 = 12,831.05 psi
* Δb = 0.002796 inch

Autodesk Simulation Solution

One-eighth of the spherical thick shell is modeled using 3-D brick elements. Care is taken to get a smooth mesh with smaller elements at the inside radius where the high stresses were expected. The resulting mesh has 546 nodes and 375 brick elements with 5 layers of elements through the thickness.

Analyzed stress tensor contour:

* S_{22} max = 12,881.9 psi ($S_{22} = S_{yy}$ = hoop stress on XZ plane)

Analyzed displacement vector contour:

* translation max = 0.002795 inch

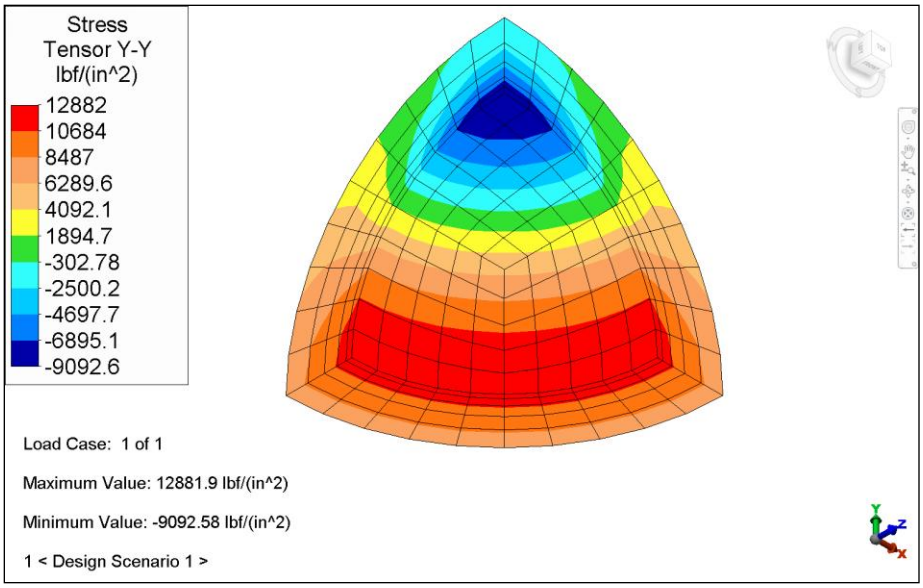

Figure 10-1. A stress contour of the model created for Roark and Young's Table 32, Case 2a.

Table 10-1. Comparison of Results

Translation max (inch)		% Difference	Sigma 2 (psi)		% Difference
Theory	Analysis		Theory	Analysis	
0.002796	0.002795	-0.11	12831.05	12,881.9	0.40

AVE - 11 Thick-Walled Cylindrical Vessel under Uniform Internal Radial Pressure

Reference

Roark, R. J. and Young, W. C., *Roark's Formulas for Stress and Strain*, Fifth Edition, New York: McGraw-Hill, 1975, page 504, Table 32, Case 1a.

Problem Description

A thick-walled cylindrical vessel under uniform internal pressure is analyzed for hoop stress and radial deflection. For this example, we chose an outside radius of 10" and an inside radius of 7", with an internal pressure of 10,000 psi. Steel material properties are used.

Theoretical Solution

σ_2 is the normal stress in the hoop or tangential direction at radius r.

$$\sigma_2 = \left(\frac{qb^2}{r^2}\right)\left(\frac{a^2+r^2}{a^2-b^2}\right)$$

Δb is the radial displacement at the inside radius.

$$\Delta b = \left(\frac{qb}{E}\right)\left(\frac{a^2+b^2}{a^2-b^2}+\nu\right)$$

Where:

* a = 10 outside radius (inch)
* b = 7 inside radius (inch)
* q = 10,000 internal pressure (psi)
* ν = 0.3 Poisson's ratio
* E = 30E+6 Young's modulus (psi)

for r = 7:

* σ_2 = 29,216 psi
* Δb = 0.007517"

Autodesk Simulation Solution

An 8" section of one quarter of the thick cylindrical shell is modeled using 3-D solid elements. The resulting mesh has 594 nodes and 400 elements with five layers of elements through the thickness. Symmetry boundary conditions are applied such that the model represents 1/8 of the actual object. (Z Symmetry on the XY cut-plane, Y Symmetry on the XZ cut-plane and X Symmetry on YZ cut-plane.) A pressure of 10,000 psi is applied at the inner surface of the vessel.

From the Results interface, Stress tensor display:

* S Y-Y max = 29,254 psi - the hoop stress at the inside radius.

From Results Interface, X displacement vector display:

* translation max = 0.007514" - the displacement at the inside radius.

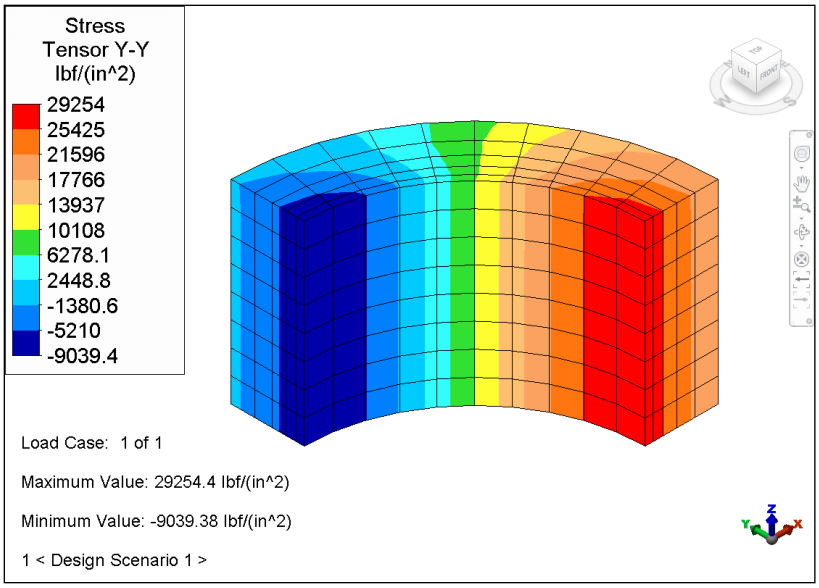

Figure 11-1. An 8" section of one quarter of the thick cylindrical shell described in Table 32, Case 1a. Note that S22 (equivalent to Syy for brick elements) represents the hoop stress only on the face of the bottom of the view.

Table 11-1. Comparison of Results

Translation Max (inch)		% Difference	S22 Max (psi)		% Difference
Theory	Analysis		Theory	Analysis	
0.007517	0.007514	0.04	29,216	29,254	0.13

AVE - 12 Hollow Cylinder with Thick Walls and Temperature Gradient

Reference

Roark, R. J. and Young, W. C., *Roark's Formulas for Stress and Strain*, Fifth Edition, New York: McGraw-Hill, 1975, page 585, Section 15.6, Case 16.

Problem Description

A thick-walled cylindrical vessel under uniform logarithmic temperature gradient throughout the thickness is analyzed for thermal stress. There is a temperature difference of ΔT between the outside surface and the inside surface of the cylinder. The ends of the cylinder are not constrained. The solution is valid away from the ends of the cylinder. The internal temperature distribution is logarithmic throughout the thickness (i.e., a steady-state temperature distribution). For this example, an outside radius of 2" and an inside radius of 1" were used with a temperature difference of 10°F.

Theoretical Solution

Outer surface:

$$\sigma_t = \frac{\Delta T \alpha E}{2(1-\nu)\log_e\left(c/b\right)}\left(1 - \frac{2b^2}{c^2-b^2}\log_e\frac{c}{b}\right)$$ tension = 998 psi circumferential stress

Inner surface:

$$\sigma_t = \frac{\Delta T \alpha E}{2(1-\nu)\log_e\left(c/b\right)}\left(1 - \frac{2c^2}{c^2-b^2}\log_e\frac{c}{b}\right)$$ compression = -1574 psi circumferential stress

Where:

* $\Delta T = 10^oF$ temperature difference (hotter on inside than outside)
* α = 6E-6/^{o}F coefficient of thermal expansion
* E = 30E6 psi modulus of elasticity
* ν = 0.3 Poisson's ratio
* c = 2 inches outside radius
* b = 1 inch inside radius

Autodesk Simulation Solution

One-eighth of the thick-walled cylinder is modeled with 3-D brick elements. The mesh consists of 9 elements through the thickness (with smaller elements near the inside where the stress is higher), 8 elements around the circumference, and 8 elements along the length (4 inches in our model). Symmetry conditions of T_z are applied to the nodes at z = 0, conditions of T_y are applied to the nodes at Y = 0 and T_x to the nodes at X=0.

If the temperatures were known at each radial position (easy to calculate with the help of a heat transfer book), the temperatures could be applied manually to the model. Alternatively, a steady-state heat transfer analysis could be performed to calculate the temperature distribution, then use these results for the stress model. (The supplied archive uses the latter approach.)

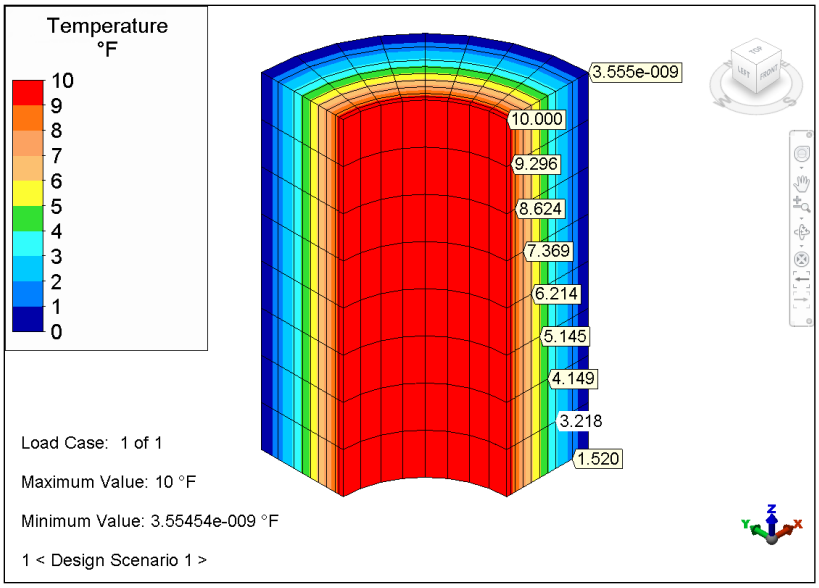

Figure 12-1. The temperature results at various radial positions.

From the Results interface, the stress tensor display:

Outer surface:

* σ_t = 984 psi

Inner surface:

* σ_t = -1560 psi

Both results are taken at the symmetry face along the length; that is, the face farthest from the free end.

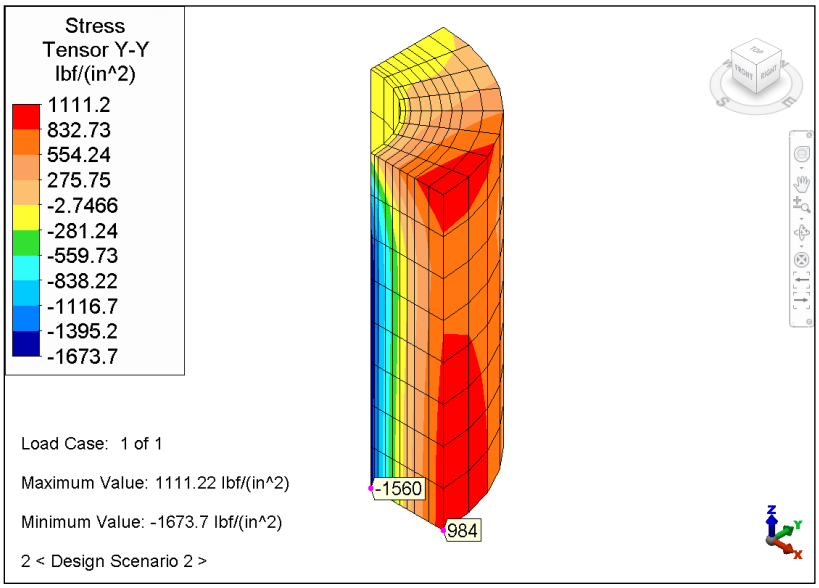

Figure 12-2. A stress contour of the model created for Roark and Young's Section 15.6, Case 16. Note that S22 (equivalent to Syy for brick elements) represents the hoop stress only on the face at the bottom of this view.

Table 12-1. Comparison of Results

σ_t (Outer Surface) (psi)		% Difference	σ_t (Inner Surface) (psi)		% Difference
Theory	**Analysis**		**Theory**	**Analysis**	
998	984	-1.4	-1574	-1560	-0.9

AVE - 13 Lid Driven Cavity

Reference

Brooks, A., Hughes, T. J. R. and Liu, W. K., *Review of Finite Element Analysis of Incompressible Viscous Flows by the Penalty Function Formulation*, Journal of Computational Physics, 30 (1979).

Problem Description

Fluid Flow Analysis capabilities are used to analyze a lid driven cavity problem solved at Reynolds number = 400.

The lid driven cavity problem is popular in computational fluid dynamics because of the simplicity of the geometry and boundary conditions. Many incompressible fluid flow codes are validated with this problem.

An incompressible viscous fluid is trapped in a square 2-D box (1" x 1") and the top wall moves at a constant velocity of 1 in/s. As a result, the fluid is set in motion. The Reynolds number is defined as:

$$\mathrm{Re} = \frac{1}{\nu}$$

Where:

* $\nu = \mu / \rho$ kinematic viscosity
* μ = dynamic viscosity
* $\rho = 1$ mass density

Autodesk Simulation Solution

A model with a mesh of 20 x 20 elements is constructed with $\mu = 0.025$. The y-velocity component at y = 0.5 and the z-velocity component at z = 0.5 are shown on the graph below. The results are plotted with "X"s and data obtained by Hughes & Liu is plotted as a dashed line. The results are essentially in perfect agreement.

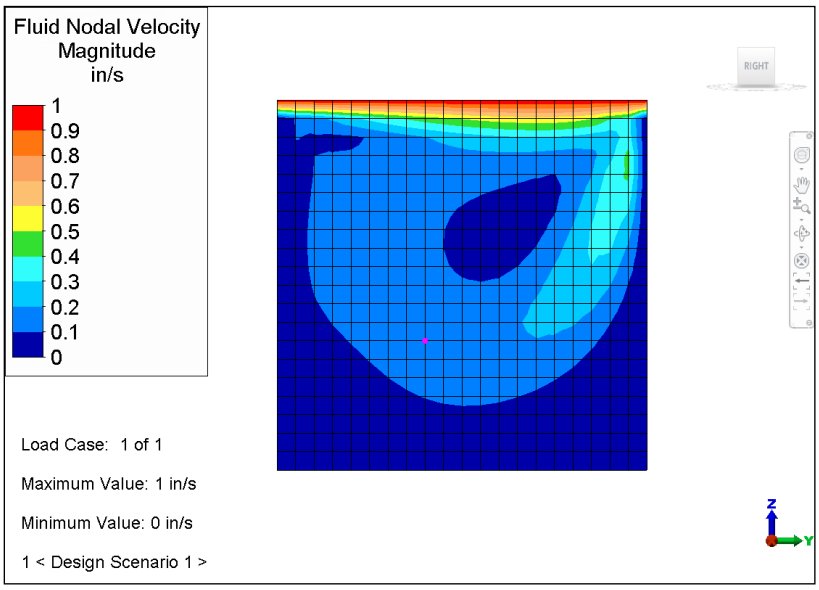

Figure 13-1. Steady-state velocity for the lid driven cavity at Re = 400.

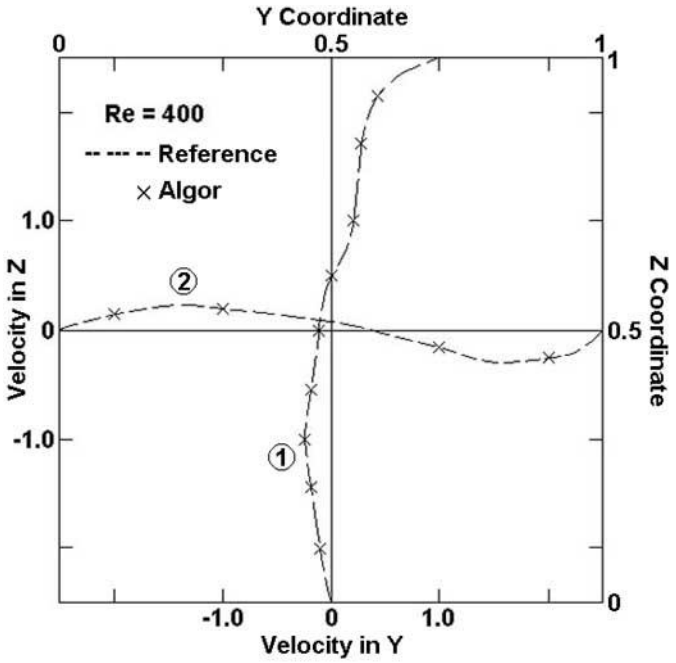

Figure 13-2. Line 1 shows the Y velocity versus the Z coordinate. Line 2 shows the Z velocity versus the Y coordinate.

AVE - 14 Flat Rectangular Plate with All Edges Fixed and Uniform Pressure Loading

Reference

Roark, R. J. and Young, W. C., *Roark's Formulas for Stress and Strain*, Fifth Edition, New York: McGraw-Hill, 1975, page 392, Table 26, Case 8A.

Problem Description

A flat rectangular plate with all edges fixed under a uniform pressure loading is analyzed for maximum stress and deflection.

Theoretical Solution

The maximum stress will occur at the center of the long edge with a value of:

$\sigma_{max} = \beta_1 q b^2/t^2 = 28{,}650$ psi

Where:

* q = 100 uniform pressure (psi)
* a = 12 length of plate (inch)
* b = 6 width of plate (inch)
* t = 0.25 thickness of plate (inch)
* $\beta_1 = 0.4974$ value from case 8A with a/b = 2
* $\nu = 0.3$ Poisson's Ratio

Autodesk Simulation Solution

One quarter of the plate is modeled in the X-Y plane with 3-D plate/shell elements by using symmetry boundary conditions (24 elements along the long edge and 12 elements along the short edge). Because the stress is maximum at the center of the long edge, one element at this location was further subdivided into 17 elements using a geometric progression with an adjacent ratio of 1.333.

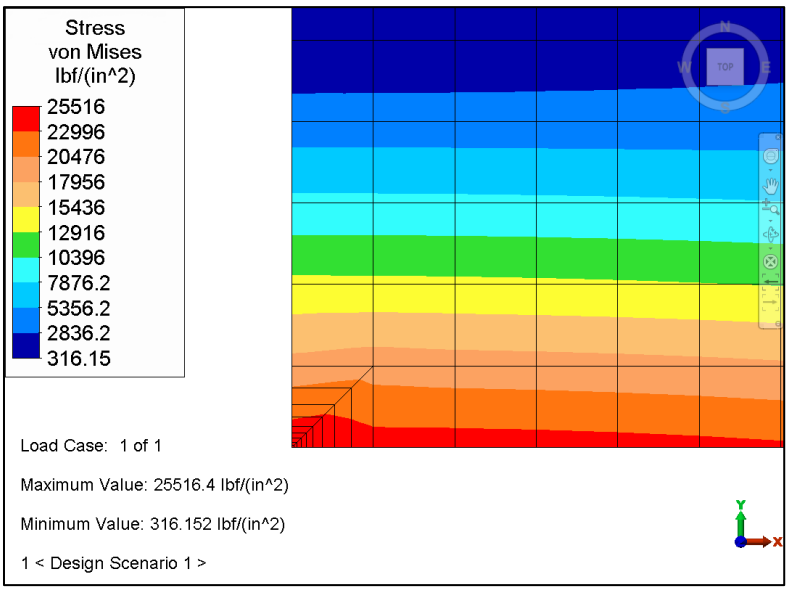

Figure 14-1. A close-up display of the mesh at the corner where stress is maximum.

The nodes at X = 6 and Y = -3 are fully constrained. To apply symmetry conditions, the nodes at Y = 0 are constrained in T_yR_{xz}, while the nodes at X = 0 are constrained in T_xR_{yz}. The model is processed with the linear static stress analysis processor. The S_{yy} stress tensor contour is shown in Figure 14-2 below. The maximum stress is:

σ_{max} = 28,682 psi

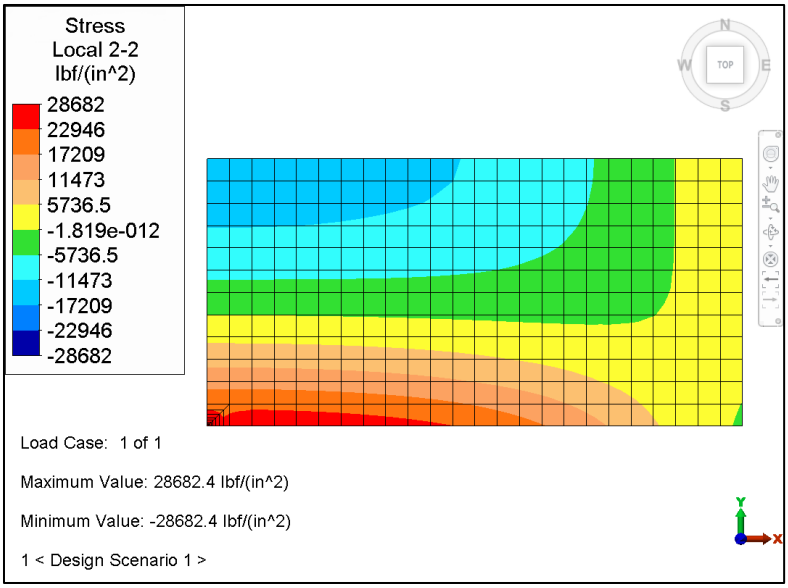

Figure 14-2. Results display of the stress tensor in the Local Y direction (S_{22})

Table 14-1. Comparison of results

σ_{max} (psi)		% Difference
Theory	**Analysis**	
28,650	28,682	0.11

AVE - 15 Flat Rectangular Plate with Two Sides Fixed, Two Sides Simply Supported and Uniform Load

Reference

Roark, R. J. and Young, W. C., *Roarks's Formulas for Stress and Strain*, Fifth Edition, New York: McGraw-Hill, 1975, page 390, Table 26, Case 5A.

Problem Description

A flat rectangular plate 20" x 10" x 0.1", with the two short sides fixed, the two long sides simply supported and a uniform 10 psi load is analyzed for maximum stress and deflection.

Theoretical Solution

The maximum stress occurs at the center of the short edge and has a value of:

* maximum stress = $\beta qb^2/(t^2)$ = 71460 psi

The maximum vertical deflection occurs at the center of the plate and has a value of:

* maximum deflection = $-\alpha qb^4/Et^3$ = -0.3073 inch

Where:

* t = 0.1 thickness (inch)
* q = 10 uniform pressure (psi)
* a = 20 length of long side of plate (inch)
* b = 10 length of short side of plate (inch)
* β = 0.7146 parameter from Roark and Young
* E = 30E6 Young's Modulus
* ν = 0.3 Poisson's Ratio
* α = 0.0922 parameter from Roark and Young

Autodesk Simulation Solution

The plate was modeled in the X-Y plane using 1/4 symmetry and is composed of 214 3-D plate/shell elements. There are 20 elements along edge "a" and 10 elements along edge "b". The center of the short edge was meshed finer to achieve higher accuracy. (One element was subdivided into 15 elements using a geometric progression with an adjacent ratio of 2.)

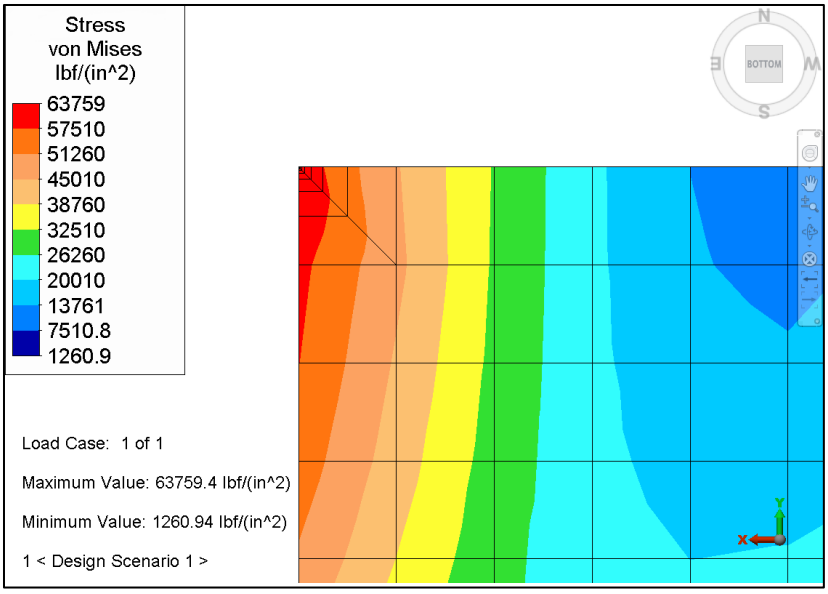

Figure 15-1. A close-up display of the mesh at the corner where stress is maximum.

The boundary conditions are set at T_{yz} along edge "a" and fixed along edge "b". The symmetry boundary conditions along the edge at x=0 are set to T_xR_{yz}. The symmetry boundary conditions along the edge at y=5 are set to T_yR_{xz}. The plate elements are 0.10 inch thick. A pressure of 10 psi is applied on the top surface of the plate.

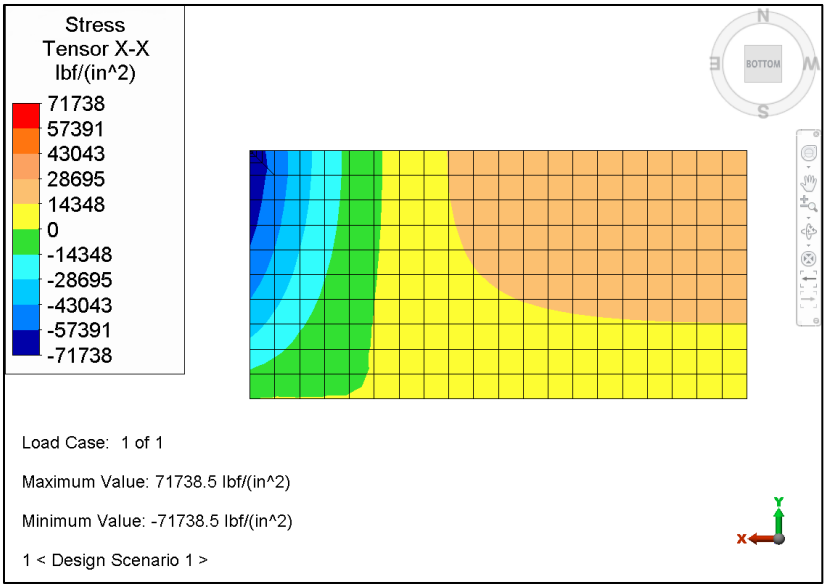

Figure 15-2. A stress tensor display (Sxx) of the top surface of the plate.

Table 15-1. Comparison of Results

	Theory	Analysis	% Difference
Maximum Vertical Deflection (inch)	-0.3073	-0.3064	0.29
Maximum Stress (Sxx) (psi)	71460	71738	0.39

AVE - 16 Uniform Beam with Both Ends Fixed

Reference

Roark, R. J. and Young, W. C., *Roark's Formulas for Stress and Strain*, Fifth Edition, page 576, New York: McGraw-Hill, 1975, Table 36, Case 2B.

Problem Description

A uniform beam with both ends fixed is analyzed for eigenvalues and frequencies. The beam is 10" long. It is made of steel and has a 1" x 1" square cross-section. No load is applied to the beam.

Theoretical Solution

The natural frequencies of the beam are given as:

$$f_n = \frac{K_n}{2\pi}\sqrt{\frac{EIg}{wL^4}}$$

Where:

* g = 386.4 in/sec^2 gravity
* w = 0.2836 uniform load per unit length including beam weight (lb/in)
* E = 3E7 modulus of elasticity (psi)
* I = 1/12 moment of inertia (inch^4)
* L = 10 length of beam (inch)
* K_n = parameter from Roark and Young table

Autodesk Simulation Solution

The beam is modeled with 50 beam elements, each of which is 0.2" long. The cross sectional properties are manually entered and the shear area values have been omitted since the theoretical results do not include shear effects.

Both ends of the beam are fixed in translation and rotation (TxyzRxyz). Since the theoretical frequencies consider bending only, boundary conditions of all other nodes are set to TxzRxy. The results generated by Linear Mode Shapes and Natural Frequencies processor are presented in the table below. One of the bending mode shapes is shown in Figure 16-1 below.

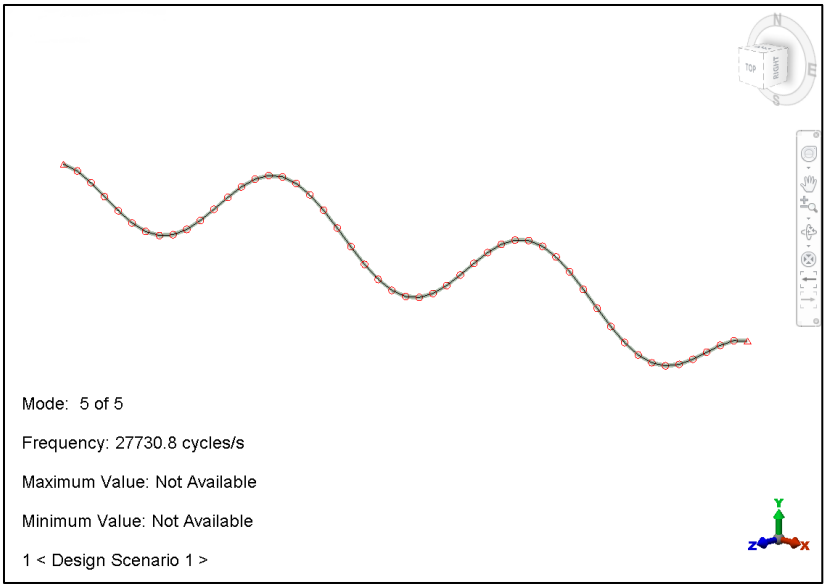

Figure 16-1. The Results display shows the second bending mode shapes of the beam in Roark and Young Table 36, Case 2B.

Table 16-1. Comparison of Results

Mode	K_n (Roark)	Natural Frequencies, f_n (Hz)		% Difference
		Roark	Analysis	
1	22.4	2081	2078	-0.14
2	61.7	5731	5728	-0.05
3	121	11240	11230	-0.09
4	200	18580	18564	-0.09
5	299	27770	27731	-0.14

AVE - 17 Thick-walled Cylindrical Vessel under Uniform External Pressure Modeled in 3-D

Reference

Roark, R. J. and Young, W. C., *Roark's Formulas for Stress and Strain*, Fifth Edition, New York: McGraw-Hill, 1975, page 504, Table 32, Case 1C.

Problem Description

A thick-walled cylindrical vessel under uniform external pressure is analyzed for radial stress and deflection. For this example, we chose an outside radius of 10" and an inside radius of 5" with external pressure of 50 psi. Steel material properties were used.

Theoretical Solution

σ_2 is the normal stress in the hoop or circumferential direction at radius r.

$$\sigma_2 = -\frac{qa^2\left(b^2+r^2\right)}{r^2\left(a^2-b^2\right)}$$

Δb is the radial displacement of the inside radius.

$$\Delta b = -\frac{q}{E}\frac{2a^2b}{a^2-b^2}$$

Where:

* a = 10 outside radius (in)
* b = 5 inside radius (in)
* q = 50 external pressure (psi)
* E = 30E+6 Young's Modulus (psi)

For r = 5 inches:

* σ_2 = -133.33 psi
* Δb = -2.2222E-5 in

Autodesk Simulation Solution

A 13" long section of one-quarter of the thick cylindrical vessel was modeled using 3-D solid elements. The resulting mesh has 1470 nodes and 1080 elements with 9 layers of elements through the thickness, 9 around the circumference and 15 along the length. A finer mesh was constructed on the inside radius where the stress is higher. Mirror symmetry boundary conditions are applied such that the model represents one-eighth of the actual object: Tz for the bottom surface and Ty along the y=0 plane and Tx along the x=0 plane. From the Results interface:

Stress tensor display, hoop stress at inner radius

Sxx = -133.12

Y displacement display, radial displacement of inner radius translation = -2.2203E-5

The stress and displacements were taken at the symmetry plane in the X-Y plane remote from the effects of the free end.

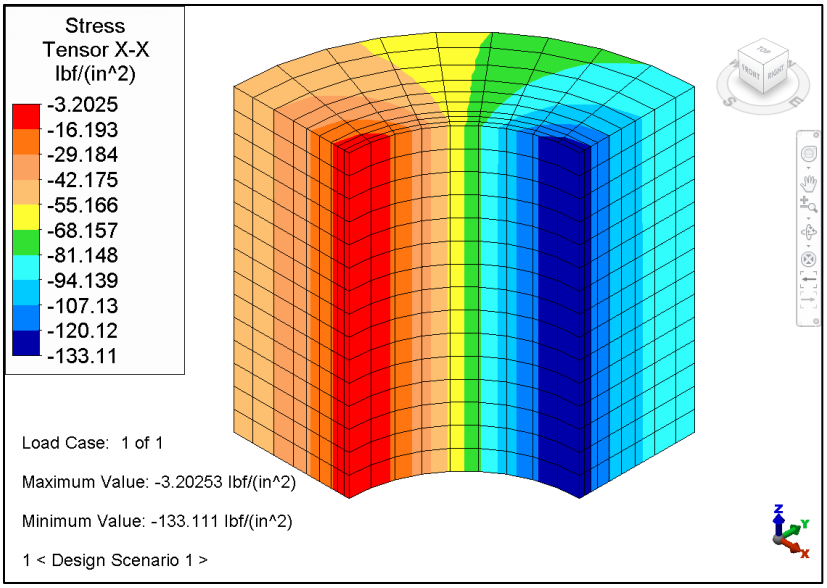

Figure 17-1. An Sxx stress tensor display (hoop stress for the right cross-sectional surface).

Table 17-1. Comparison of Results

Radial Displacement of the Inside Radius (inch)		% Difference	σ_2 (psi)		% Difference
Theory	**Analysis**		**Theory**	**Analysis**	
-2.2222E-5	-2.2203E-5	-0.09	-133.33	-133.11	-0.16

AVE - 18 Thick-walled Cylindrical Vessel under Uniform External Pressure Modeled in 2-D

Reference

Roark, R. J. and Young, W. C., *Roark's Formulas for Stress and Strain*, Fifth Edition, New York: McGraw-Hill, 1975, page 504, Table 32, Case 1C.

Problem Description

A thick-walled cylindrical vessel under uniform external radial pressure is analyzed for hoop stress and radial deflection. For this example, we chose an outside radius of 10" and an inside radius of 5" with an external pressure of 50 psi. Steel material properties were used.

Theoretical Solution

σ_2 is the normal stress in the hoop or circumferential direction at radius r.

$$\sigma_2 = -\frac{qa^2\left(b^2+r^2\right)}{r^2\left(a^2+b^2\right)}$$

Δb is the radial displacement of the inside radius.

$$\Delta b = -\frac{q}{E}\frac{2a^2b}{a^2-b^2}$$

Where:

* a = 10 outside radius (in)
* b = 5 inside radius (in)
* q = 50 external pressure (psi)
* ν = 0.3 Poisson's Ratio
* E = 30E+6 Young's Modulus (psi)

For r = 5 inches

* σ_2 = -133.33 psi
* Δb = -2.2222E-5 in

Autodesk Simulation Solution

The cylindrical vessel was modeled using 2-D axisymmetric elements. A 6 x 20 mesh was used (120 elements). Pressure was applied on the outside edge. Mirror symmetry boundary conditions were applied at the base (T_z) such that the model represents 1/2 of the actual object. The model is 20" long.

Results from the Linear Static Stress Processor (at r = b) are:

* Stress tensor display in the X direction (hoop stress)
  Sxx = - 132.24 psi
* Displacement in the Y direction (radial displacement)
  Translation = -2.2334E-5

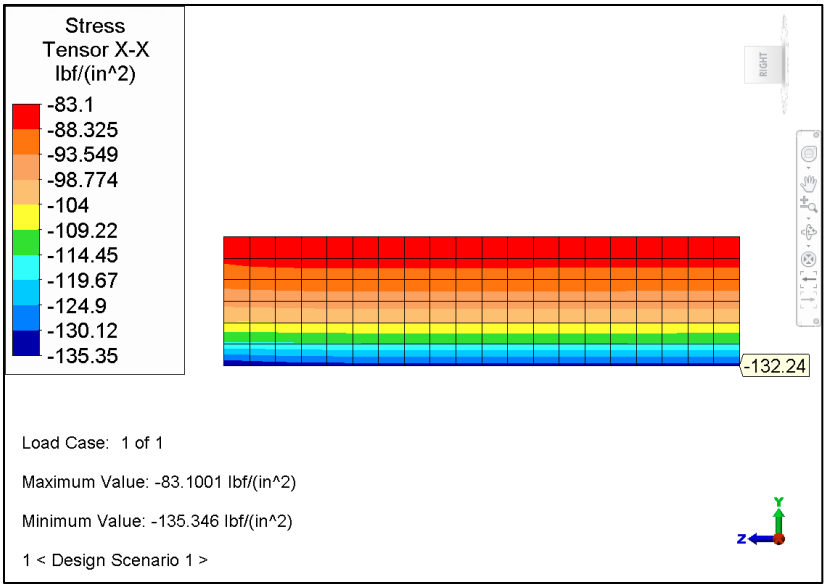

Figure 18-1. A 2-D axisymmetric model of the thick-walled cylindrical vessel described in Table 32, Case 1C. The stress in the X direction (hoop stress) is shown.

Table 18-1. Comparison of Results

Translation (inch)		% Difference	Sxx (psi)		% Difference
Theory	Analysis		Theory	Analysis	
-2.2222E-5	-2.2334E-5	0.50	-133.33	-132.24	0.82

AVE - 19 Thin-walled Conical Vessel under Uniform Internal Pressure with Tangential Edge Supports

Reference

Roark, R. J. and Young, W. C., *Roark's Formulas for Stress and Strain*, Fifth Edition, New York: McGraw-Hill, 1975, page 449, Table 29, Case 2A.

Problem Description

A thin-walled conical vessel under uniform internal pressure with tangential edge supports. A pressure of 10 psi, wall thickness of 0.10" and an angle of 30 degrees were chosen. Steel material properties were used.

Theoretical Solution

The meridional stress (σ_1) and the circumferential, or hoop stress (σ_2) at radius of curvature R is given as:

$$\sigma_1 = \frac{qR}{2t\cos\alpha}$$

$$\sigma_2 = \frac{qR}{t\cos\alpha}$$

and radial displacement (ΔR) of a circumference as:

$$\Delta R = \frac{qR^2}{Et\cos\alpha}\left(1 - \frac{\nu}{2}\right)$$

* q = 10 internal pressure (psi)
* E = 3E+7 Young's Modulus (psi)
* ν = 0.3 Poisson's Ratio
* α = 30 conical angle (degrees)
* t = 0.10 wall thickness (in)

At R = 4.013 inch:

* σ_1 = 231.69 psi
* σ_2 = 463.38 psi
* ΔR = 5.269E-5 inches

Autodesk Simulation Solution

The problem can be analyzed as an axisymmetric model composed of 2-D elements, 3-D plate elements or 3-D brick elements. An additional coordinate system was specified with an axis along the 30 degree slant of the part to get accurate tangential stress values.

In this case, the model was constructed of 720 brick elements using 1/4 symmetry. Elastic boundary elements were used for tangential edge support. The static stress processor was used to analyze the model. The following results were averaged at the inside (node number 1447) and outside (node number 1448) nodes closest to the radius R, and measured at the nodes in the XY plane (a local coordinate system was used to obtain the σ_1 results):

* $\sigma_1 = (235.15 + 217.91)/2 = 226.53$ psi
* $\sigma_2 = (471.26 + 446.09)/2 = 458.68$ psi
* $\Delta R = (5.339E\text{-}5 + 5.163E\text{-}5)/2 = 5.251E\text{-}5$ inch

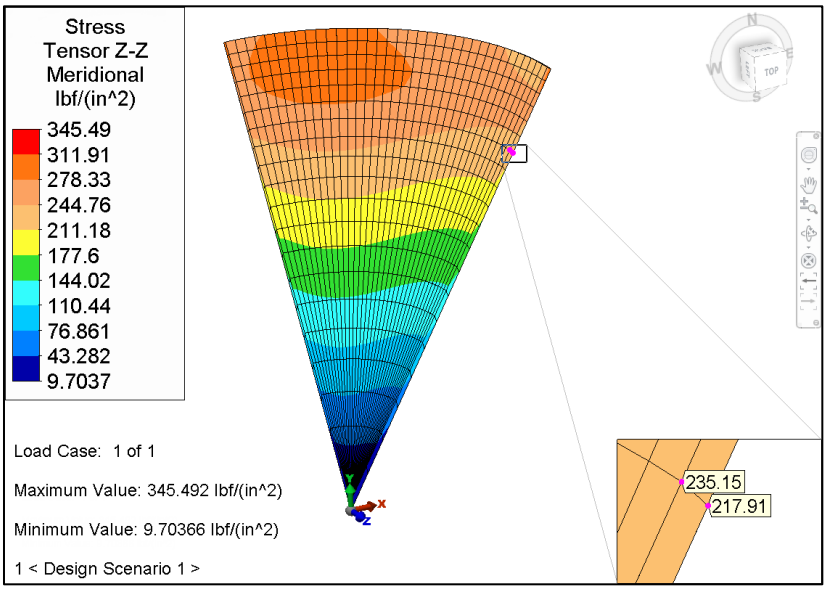

Figure 19-1. A meridional stress contour display of the conical pressure vessel. ZZ is meridional component of the local (rectangular) coordinate system on the face in the XY plane.

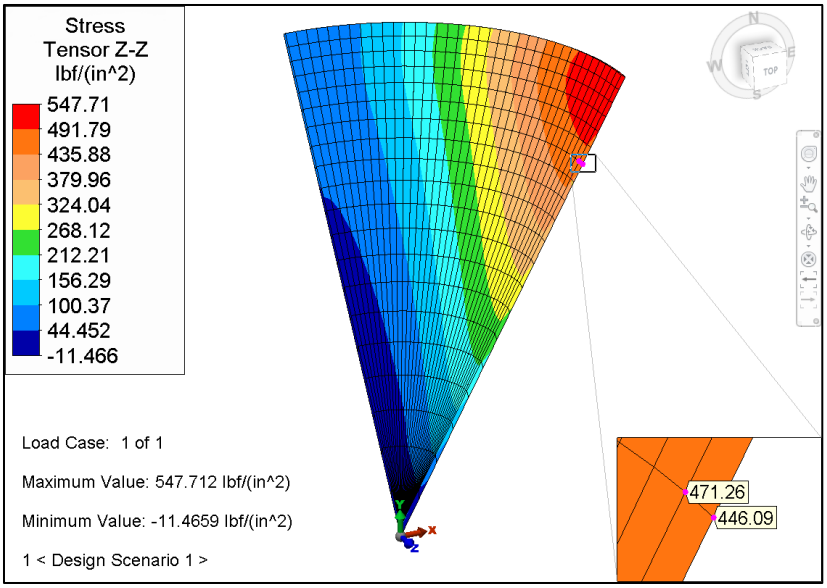

Figure 19-2. An Szz stress contour display of the conical pressure vessel. Szz is the hoop stress on the face in the XY plane.

Table 19-1. Comparison of Results

σ_1 (psi)		%	σ_2 (psi)		%	ΔR (inch)		%
Theory	**Analysis**	**Difference**	**Theory**	**Analysis**	**Difference**	**Theory**	**Analysis**	**Difference**
231.69	226.53	-2.2	463.38	458.68	-1.0	5.269E-5	5.251E-5	-0.34

AVE - 20 Straight Bar with Lower End Fixed and Upper End Free

Reference

Roark, R. J. and Young, W. C., *Roark's Formulas for Stress and Strain*, Fifth Edition, New York: McGraw-Hill, 1975, page 534, Table 34, Case 1A.

Problem Description

Case 1A is a straight bar with the lower end fixed and upper end free. The bar is 10 inches long, made of steel and has a constant circular cross-section of 0.5 inches in diameter. A 10 lb downward load is applied with no intermediate load. Because of the loading, a buckling analysis was performed to determine when the bar will become elastically unstable.

Theoretical Solution

The load at which the bar will buckle is given as:

$$P_1 = K\pi^2 \frac{EI}{l^2}$$

Where:

* E = 30E6 modulus of elasticity (psi)
* I = 0.003068 moment of inertia (in^4)
* l = 10 length of bar (in)
* K = 0.25 parameter from Roark and Young table ($P_2/P_1 = 0$)

The result is:

* P_1 = 2270.97 lbs

Autodesk Simulation Solution

The bar is modeled with 10 beam elements, each of which is 1 inch long. A force of 10 lbs is applied at the top of the bar in a negative Y direction. The bottom of the bar has all translations and rotations fixed.

The results generated by the Linear Critical Buckling Load processor are:

- Buckling load multiplier = 226.841 (from Summary file)
- Buckling load = 226.841(10-lb applied load) = 2268.41 lbf

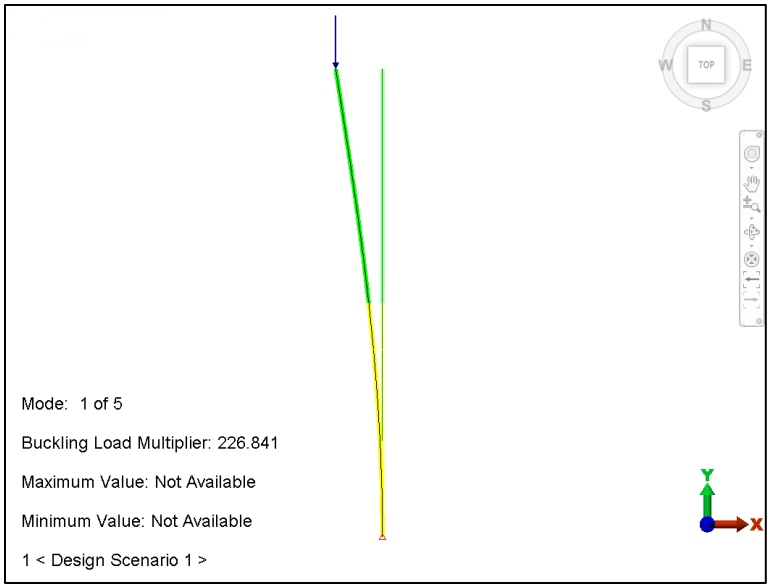

Figure 20-1. Model of straight bar created for Roark and Young's Table 34, Case 1A. The figure shows both undeformed and deformed views.

Table 20-1. Comparison of Results

	Theory	Analysis	% Difference
Buckling Load Multiplier	227.1	226.841	0.11
Buckling Load	2270.97 lbf	2268.41 lbf	0.11

AVE - 21 Wide-flange Beam with Equal Flanges

Reference

Young, Warren C., *Roark's Formulas for Stress and Strain*, Sixth Edition, page 64, Table 1, Case 6.

Problem Description

This verification problem tests the capabilities of the "2D Moment of Inertia" command in FEA Editor. The "Moment of Inertia" menu is used to provide the area and moments of inertia for any closed outline that is drawn in any plane.

Table 1, Case 6 is a wide-flange beam with equal flanges. For this example, we chose a web depth of 4", a flange width of 6", a flange thickness of 1", and a web thickness of 1".

Theoretical Solution

* $A = 2bt + t_w d$
* $I_1=[((b(d + 2t)^3)/12) - (((b - t_w)d^3)/12)]$ where axis 1 is perpendicular to the web
* $I_2 = [((b^3t)/6) + ((t_w^3d)/12)]$ where axis 2 is parallel to the web
* b = 6 flange width (in)
* d = 4 depth of web (in)
* t = 1 flange thickness (in)
* t_w = 1 web thickness (in)

$A = 16.0$ in^2

$I_1 = 81.333$ in^4

$I_2 = 36.333$ in^4

Autodesk Simulation Solution

The outline of the flange was drawn in the Y-Z plane in FEA Editor. The following results were obtained with the "Moment of Inertia" menu using 2,000 divisions:

- Area = 16.01 in^2
- $I_{yy} = 81.373$ in^4
- $I_{zz} = 36.369$ in^4

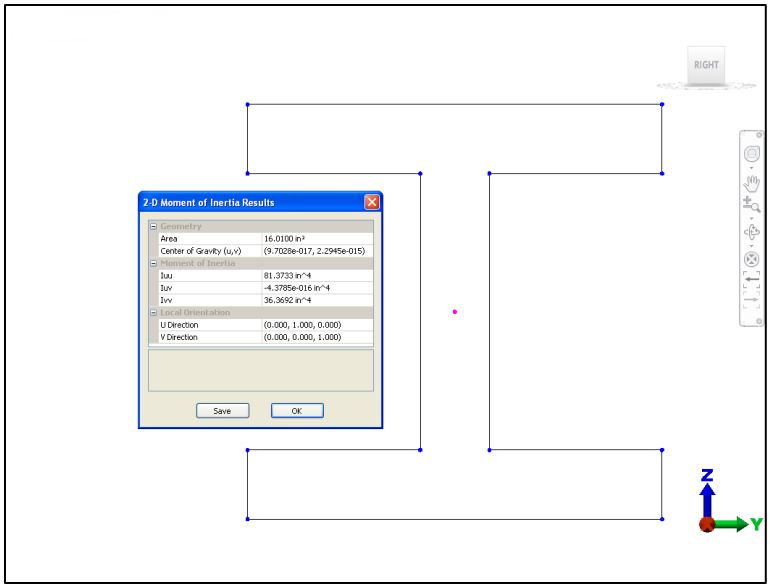

Figure 21-1. Wide-flange beam model in FEA Editor

Table 21-1. Comparison of Results

	Theory	Analysis	% Difference
Area (in^2)	16.0	16.01	0.06
I_{yy} (in^4)	81.333	81.373	0.05
I_{zz} (in^4)	36.333	36.369	0.10

AVE - 22 Circular Disc Rotating about Its Own Axis with Uniform Angular Velocity Modeled in 2-D

Reference

Roark, R. J. and Young, W. C., *Roark's Formulas for Stress and Strain*, Sixth Edition, New York: McGraw-Hill, 1989, page 705, Section 15.2, Case 9.

Problem Description

A homogeneous circular disc of conical cross section which rotates about its own axis with a uniform angular velocity of 2500 rpm is analyzed for tensile radial stress and tangential inertia stress. The disc has a 4 inch radius hole, an outer radius of 20 inches, a 1.5 inch inner thickness, and a 0.5 inch outer thickness. Steel material properties were used.

Theoretical Solution

At any point a distance of r inches from the center, the tensile radial (σ_r) and tangential (σ_t) inertia stresses are given by:

$\sigma_r = TK_r + Ap_1 + Bp_2$

$\sigma_t = TK_t + Aq_1 + Bq_2$

Where:

* $T = 0.0000282R^2N^2\delta$
* R is the radius to the apex of the cone
* N is the speed in RPM
* δ is the weight density

The parameters K_r, K_t, p_1, q_1, and q_2 are given in Roark and Young for a range of r/R from 0 to 1.0. Parameters A and B were found by setting the radial stress at the inner and outer surfaces to a known value (0 in this case) and solving the equations simultaneously. The parameters used for this example are:

	r/R	**K_r**	**K_t**	**p_1**	**q_1**	**p_2**	**q_2**
Inner Rim	0.143	0.1778	0.1746	1.618	1.558	-33.99	42.252
Outer Rim	0.714	0.1055	0.1424	4.056	2.883	-0.5247	3.027
r = 8.4	0.300	0.1761	0.1767	1.898	1.738	-6.371	10.89

- δ = 0.2836 Density (lb/in^3)
- R = 28 Conical disk radius (in)
- E = 30E+06 Young's modulus (psi)
- ν = 0.3 Poisson's ratio
- T = 39,188 Equation coefficient
- A = -998.95 Derived from equations
- B = 157.44 Derived from equations

The stresses at r = 8.4 in. from the center are:

* σ_r = 4001.9 psi
* σ_t = 6902.9 psi

Autodesk Simulation Solution

The circular disc was modeled using 160 2-D axisymmetric elements. One node was constrained in the z-direction to prevent rigid body motion. The loading is centrifugal with a rotation rate of 2500 rpm and the axis orientation set to the Z direction. The stress results at r =8.4 in. are:

* σ_r = 3984.45 psi stress tensor in Y direction
* σ_t = 7030.24 psi stress tensor in X direction

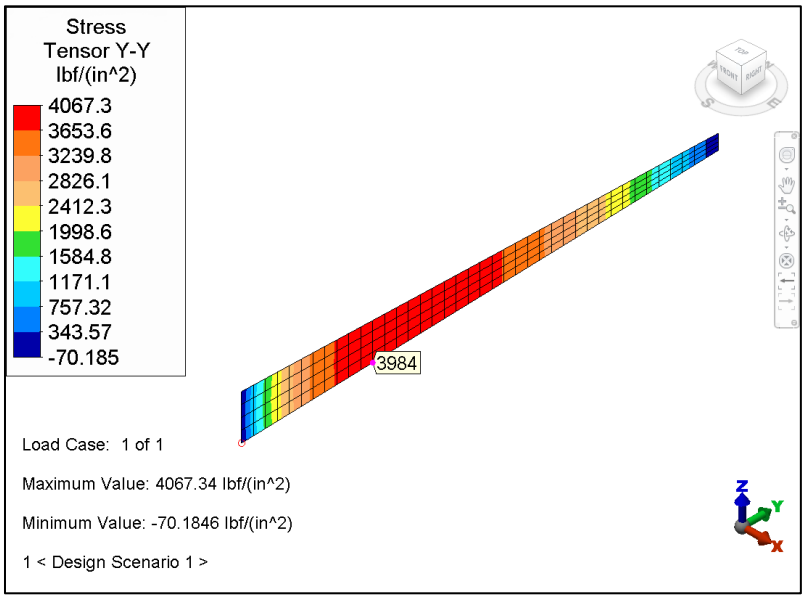

Figure 22-1. Stress results for the homogeneous circular disc of conical section. The Syy stress shown corresponds to the radial stress.

Table 22-1. Comparison of Results

σ_r (psi)		% Difference	σ_t (psi)		% Difference
Theory	**Analysis**		**Theory**	**Analysis**	
4001.9	3984.45	-0.43	6902.9	7030.24	1.84

Note: This problem was reanalyzed in Accuracy Verification Example 023 using 3-D solid (brick) elements.

AVE - 23 Circular Disc Rotating about Its Own Axis with Uniform Angular Velocity Modeled in 3-D

Reference

Roark, R. J. and Young, W. C., *Roark's Formulas for Stress and Strain*, Sixth Edition, New York: McGraw-Hill, 1989, page 705, Section 15.2, Case 9.

Problem Description

A homogeneous circular disc of conical cross section which rotates about its own axis with a uniform angular velocity of 2500 rpm is analyzed for tensile radial stress and tangential inertia stress. The disc has a 4 inch radius hole, an outer radius of 20 inches, a 1.5 inch inner thickness, and a 0.5 inch outer thickness. Steel material properties were used.

Theoretical Solution

At any point a distance of r inches from the center, the tensile radial σ_r and tangential σ_t inertia stresses are given by:

$\sigma_r = TK_r + Ap_1 + Bp_2$

$\sigma_t = TK_t + Aq_1 + Bq_2$

Where:

* $T = 0.0000282R^2N^2\delta$
* R is the radius to the apex of the cone
* N is the speed in RPM
* δ is the weight density

The parameters K_r, K_t, p_1, q_1, and q_2 are given in Roark and Young for a range of r/R from 0 to 10. Parameters A and B were found by setting the radial stress at the inner and outer surfaces to a known value (0 in this case) and solving the equations simultaneously. The parameters used for this example are:

	r/R	K_r	K_t	p_1	q_1	p_2	q_2
Inner Rim	0.143	0.1778	0.1746	1.618	1.558	-33.99	42.252
Outer Rim	0.714	0.1055	0.1424	4.056	2.883	-0.5247	3.027
r = 8.4	0.300	0.1761	0.1767	1.898	1.738	-6.371	10.89

- δ = 0.2836 Density (lb/in^3)
- R = 28 Conical disk radius (in)
- E = 30E+06 Young's modulus (psi)
- ν = 0.3 Poisson's ratio
- T = 39,188 Equation coefficient
- A = -998.95 Derived from equations
- B = 157.44 Derived from equations

The stresses at r = 8.4 in. from the center are:

* σ_r = 4001.9 psi
* σ_t = 6902.9 psi

Autodesk Simulation Solution

The disc was modeled using 2880 3-D solid brick elements. Symmetric boundary conditions were used for one quarter of the model. In addition, one node at the inner rim was constrained in the z-direction to prevent rigid body motion. The loading is centrifugal with a rotation rate of 2500 rpm and the axis orientation set to the Z direction. The stress results r = 8.4 in are:

* σ_r = 3977.48 psi stress tensor in Y direction at Y-Z symmetry plane
* σ_t = 7017.97 psi stress tensor in X direction at Y-Z symmetry plane

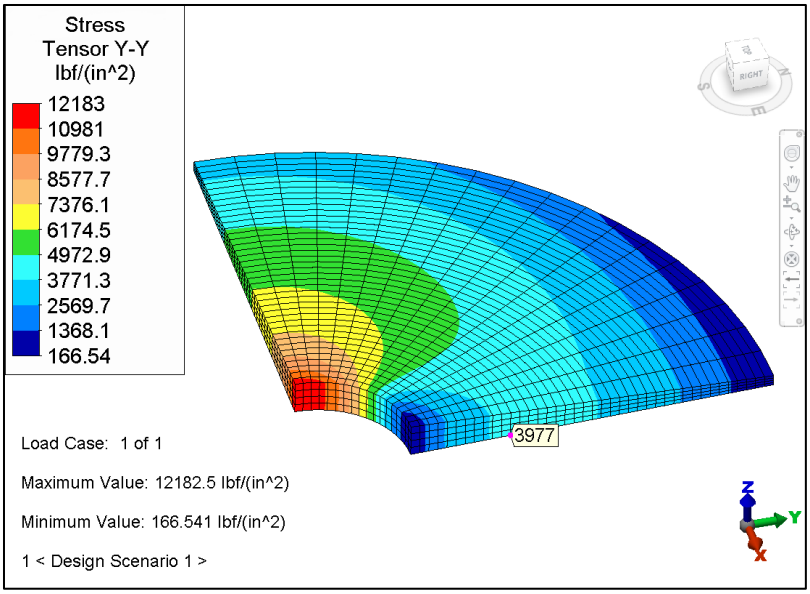

Figure 23-1. Stress results for the homogeneous circular disc of conical section. The Syy stress for nodes at the the Y-Z plane corresponds to the radial stress.

Table 23-1. Comparison of Results

σ_r (psi)		% Difference	σ_t (psi)		% Difference
Theory	**Analysis**		**Theory**	**Analysis**	
4001.9	3977.48	0.59	6902.9	7017.97	1.67

Note: This problem was analyzed in Accuracy Verification Example 022 using 2-D axisymmetric elements. The difference between the analyses using 2-D axisymmetric and 3-D solid brick elements are:

* σ_r = 0.17% difference
* σ_t = 0.17% difference

AVE - 24 Thin-walled Cylindrical Shell under an Axisymmetric Radial-End Load

Reference

Roark, R. J. and Young, W. C., *Roark's Formulas for Stress and Strain*, Sixth Edition, New York: McGraw-Hill, 1989, page 533, Table 29, Case 8.

Problem Description

A long, thin-walled cylindrical shell under an axisymmetric radial-end load is analyzed for maximum stress and deflection. The loaded end is free and the tube is long enough such that the support conditions have no effect ($\lambda l > 6$). For this example, we chose a total length of 5 inches and a radius of 2.5 inches. A 50 lb/in radial end load and steel material properties were used.

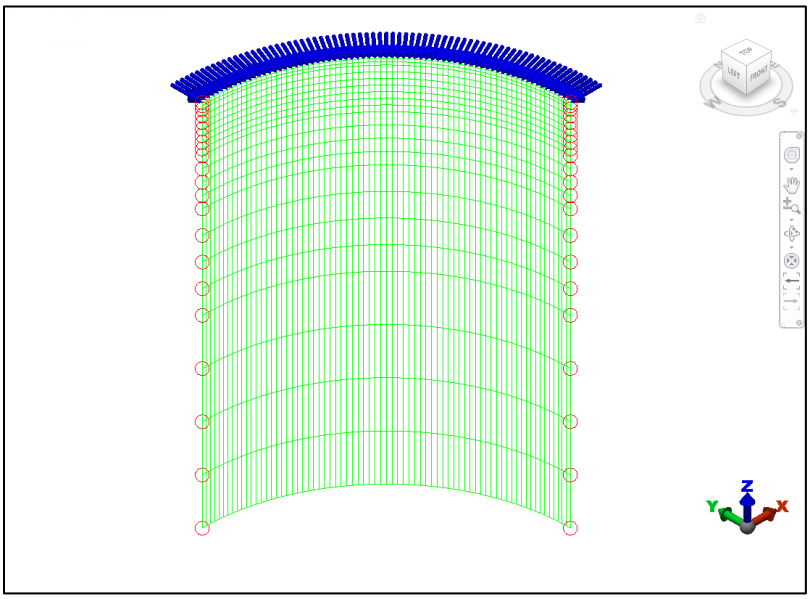

Figure 24-1. FEA model of the cylindrical shell with loading and boundary conditions.

Theoretical Solution

The longitudinal stress (σ_1) for this case is zero everywhere. The maximum radial displacement (Δy) and circumferential or hoop stress (σ_2) are respectively given as:

$$\Delta y = -\frac{V_O}{2D\lambda^3}$$

$$\sigma_2 = -\frac{2V_O\lambda R}{t}$$

Where:

$$* \quad \lambda = \left[\frac{3(1-\nu^2)}{R^2 t^2}\right]^{\frac{1}{4}}$$

* $D = \frac{Et^3}{12(1-\nu^2)}$
* V_O = 50 Radial end load (lb/in)
* R = 2.5 Cylinder radius (in)
* t = 0.1 Cylinder wall thickness (in)
* E = 30e+6 Young's modulus (psi)
* ν = 0.3 Poisson's ratio

Maximum values (at the loaded end) are:

* Δy = -5.356 e-4 in
* σ_2 = 6427 psi

Autodesk Simulation Solution

The cylindrical shell was modeled using 1,512 plate/shell elements and 1/4 symmetry boundary conditions (T_yR_{xz} on the y=0 edge, and T_xR_{yz} on the x=0 edge with one node fixed T_z for solution stability). Note that the longitudinal axis is the z-axis. Results from the linear stress processor at the loaded end are:

* Radial displacement = -5.343 e-4 in
* Circumferential stress = 6463 psi average

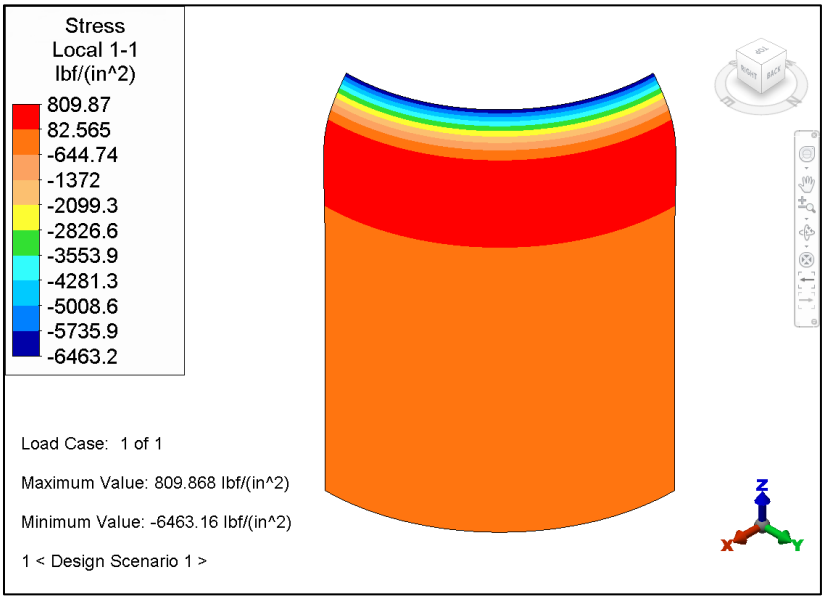

Figure 24-2. Hoop stress (σ_2) contour for the thin cylindrical shell.

Table 24-1. Comparison of Results

	Theory	Analysis	% Difference
Radial Displacement (Δy) (inch)	-5.356e-4	-5.343e-4	0.24
Circumferential Stress (σ_2) (psi)	6427	6463	0.56

AVE - 25 Test of the Capabilities of the 'dt/dh' Option for the Plate Element

Reference

Young, Warren C., *Roark's Formulas for Stress and Strain*, Sixth Edition, page 721, Case 5.

Problem Description

This verification example tests the capabilities of the "dt/dh" option for the plate element. The "dt/dh" option allows the user to model a linear temperature gradient in the element's local 3 direction, which is through the thickness.

A flat plate of uniform thickness with fixed edges and a uniform linear temperature gradient between the two faces of the plate is analyzed for maximum stress. For this example, we chose a 6" x 12" x 1" thick plate with a temperature difference of 100 degrees between opposite faces.

Theoretical Solution

Maximum resulting bending stress:

$$\sigma_B = \frac{1}{2}\Delta T \gamma \frac{E}{(1-\nu)}$$ = 13,928.57 psi at the center

Where:

* ΔT = 100 Temperature difference (^oF)
* γ =6.5E-06 Thermal expansion coefficient
* E = 30E+06 Modulus of elasticity (psi)
* ν = 0.3 Poisson's ratio

Autodesk Simulation Solution

The plate was modeled in FEA Editor with 72 plate elements. All nodes on the edges of the plate were fully constrained. The "delta T thru thickness" temperature gradient was specified in the "Element Definition" data entry screen.

The bending stress tensor (S11) results from the analysis is:

* σ_B = 13928.57 psi

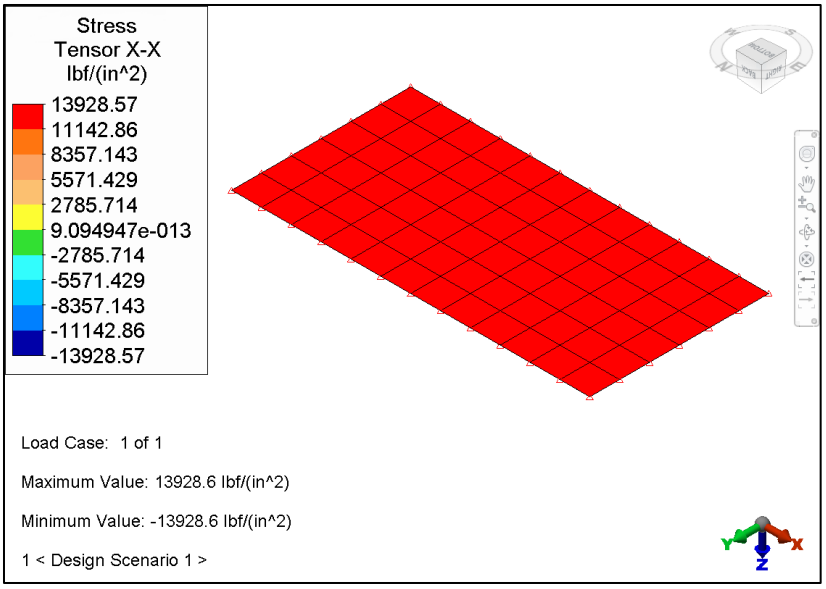

Figure 25-1. Stress tensor (S11) display from the Results environment.

Table 25-1. Comparison of Results

σ_B (psi)		% Difference
Theory	**Analysis**	
13,928.57	13,928.57	0.0

AVE - 26 Rectangular Plate under Uniform Load Producing a Large Deflection

Reference

Roark, R. J. and Young, W. C., *Roark's Formulas for Stress and Strain*, Fifth Edition, McGraw-Hill, New York, 1975, page 408.

Problem Description

The case described is a rectangular plate, held, not fixed, under uniform load producing a large deflection. The model is a square 36" x 36" x 0.1046" plate made of steel. A 0.5 psi pressure load is applied to the plate. Because of the large deformation (relative to the plate thickness), a nonlinear analysis was performed using MES with the pressure loading feature.

Theoretical Solution

From Roark and Young, the relationships among load, deflection and stress are interpolated as:

$y/t = 1.76$

$\sigma b^2/Et^2 = 20.40$

based on $qb^4/Et^4 = 247.9$

Where:

* q = 0.5 applied pressure load (psi)
* E = 28.3E6 modulus of elasticity (psi)
* t = 0.1046 plate thickness (in)
* b = 36 plate length (in)
* ν = 0.316 Poisson's ratio

Deflection (calculated from above formula) at plate center:

y = 0.184 in

The stress due to diaphragm and bending stresses (calculated from the above formula) at the plate center:

σ = 4874 psi

Autodesk Simulation Solution

Due to geometric symmetry, only 1/4 of the plate was modeled using 36 high-order shell elements. A 0.5 psi load was applied normal to the plate. The two edges of the plate were held, but not fixed (T_{xyz} applied only).

The results of the nonlinear static stress analysis by Mechanical Event Simulation (MES) processor are:

Deflection at plate center:

* y = 0.184 in

Stress at plate center:

* σ = 4640 psi on tension side

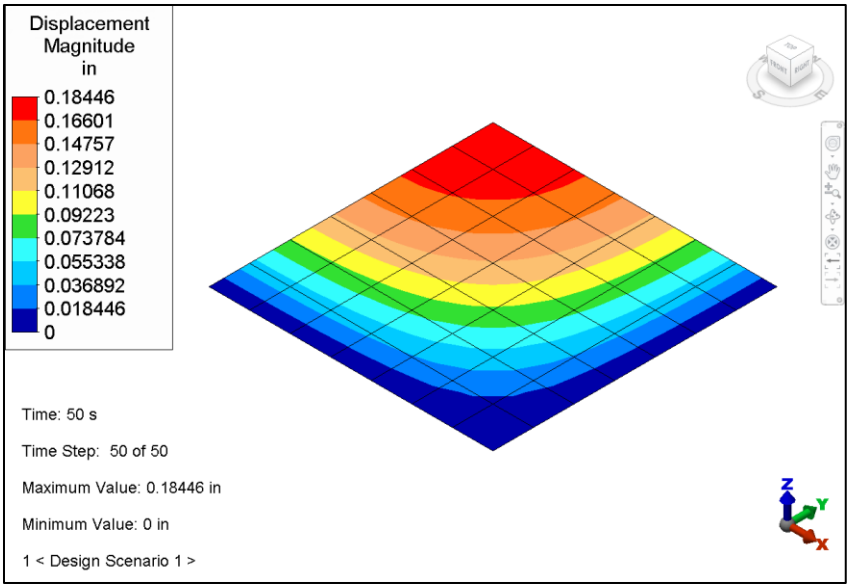

Figure 26-1. Nonlinear displaced shape and displacement contour from MES

Table 26-1. Comparison of Results

Comparison of Results			
	Theory	**Analysis**	**% Difference**
y (inch)	0.184	0.184	0
σ (psi)	4874	4640	-4.8

AVE - 27 Solid Circular Plate Section of Constant Thickness with Uniform Load

Reference

Young, Warren C., *Roark's Formulas for Stress and Strain*, Sixth Edition, page 437, Table 24, Case 27.

Problem Description

A solid circular plate section of constant thickness with a uniformly distributed load over the entire surface and the edges simply supported is analyzed for maximum stress. A 60^o section was used with a radius of 10 inches and a thickness of 0.1 inches. A 10-psi pressure load was applied normal to the section. Steel material properties were used.

Theoretical Solution

σ_r and σ_t are radial and tangential stresses in the section, respectively. The maximum values of these stresses are given by:

$$\sigma_r = \beta \frac{qa^2}{t^2}$$

$$\sigma_t = \beta_1 \frac{qa^2}{t^2}$$

Where:

* a = 10 radius (inches)
* t = 0.1 plate thickness (inches)
* q = 10 applied pressure (psi)
* β = 0.147 parameter from Table 24, Roark and Young for 60^o
* β_1 = 0.155 parameter from Table 24, Roark and Young for 60^o
* ν = 0.3 Poisson's ratio

For a 60^o angle section:

* σ_r = 14,700 psi
* σ_t = 15,550 psi

Autodesk Simulation Solution

The circular section was modeled using 800 plate/shell elements. A 20 x 40 mesh (tangential and radial, respectively) was used. Simply supported boundary conditions were applied to all edges (T_{xyz} applied only).

In order to use the local element orientations to view the radial and tangential stresses, the Element Definition was set such that the "Orient i Node" option was selected for the "Nodal Order method". A coordinate to define the element's in-plane orientation was manually entered.

Results from the Linear Static Stress processor are:

* $\sigma_r = \sigma_{22}$ = 14,651 psi
* $\sigma_t = \sigma_{11}$ = 15,385 psi

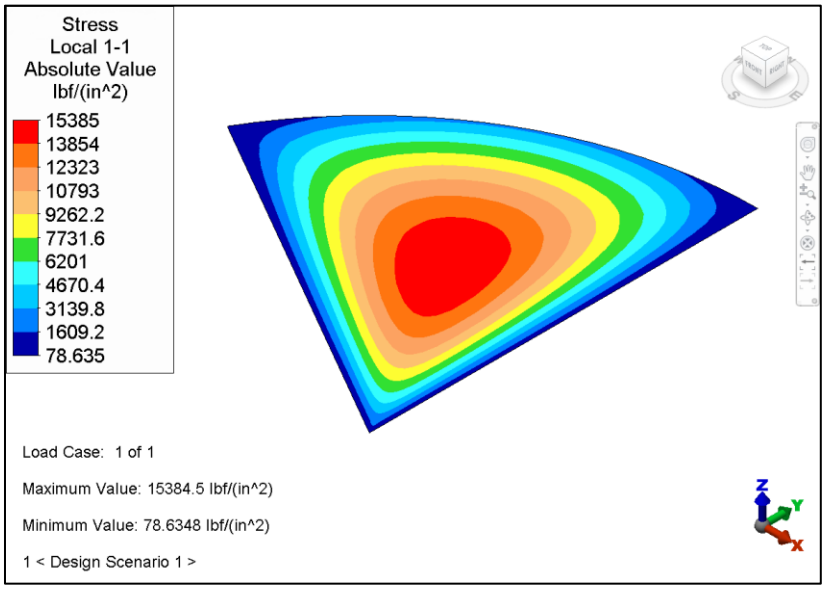

Figure 27-1. Tangential (σ_{11}) stress contour (absolute value)

Table 27-1. Comparison of Results

	Theory	**Analysis**	**% Difference**
$\sigma_r = \sigma_{22}$ (psi)	14,700	14,651	0.33
$\sigma_t = \sigma_{11}$ (psi)	15,550	15,385	1.06

AVE - 28 Thin Closed Circular Ring with Circular Cross Section

Reference

Young, Warren C., *Roark's Formulas for Stress and Strain*, Sixth Edition, page 263, Table 17, Case 1.

Problem Description

This example is a thin closed circular ring with circular cross section. Two concentrated loads of 100 lbs are applied at the top and bottom of the ring acting toward the center. Steel material properties are used. We want to find the internal moments and deflections of the ring.

Theoretical Solution

The moment at the top load location (M_A), change in horizontal diameter (D_H), and change in vertical diameter (D_V) from Roark's formulae are:

$$M_A = \frac{WRK_2}{\pi}$$

$$D_H = \frac{WR^3}{EI}\left(\frac{K_1}{2} - K_2 + \frac{2K_2^2}{\pi}\right)$$

$$D_V = \frac{-WR^3}{EI}\left(\frac{\pi K_1}{4} - \frac{2K_2^2}{\pi}\right)$$

$K_1 = 1 - \alpha + \beta \approx 1$ for thin rings

$K_2 = 1 - \alpha \approx 1$ for thin rings

Where:

* A = 0.031416 beam cross sectional area (in^2)
* R = 10 radius of ring (in)
* W = 100 applied force (lb)
* E = 3e7 modulus of elasticity (psi)
* ν = 0.3 Poisson's ratio
* I2 = I3 = 7.854e-5 moment of inertia (in^4)
* Z2 = Z3 = 7.854e-4 section moduli (in^4)

M_A = 318.31 lb-in

D_H = 5.7983 in

D_V = -6.3143 in

Autodesk Simulation Solution

The circular ring was modeled with 52 beam elements of circular cross section. A force of 100 lbs was applied at the top and bottom nodes in the Y direction. The model was constrained with T_{xz} at the top and bottom nodes, and with T_{yz} at the two side nodes. The results from the Static Stress Analysis processor are:

* M_A = 317.92 lb-in
* D_H = 5.782 in
* D_V = -6.298 in

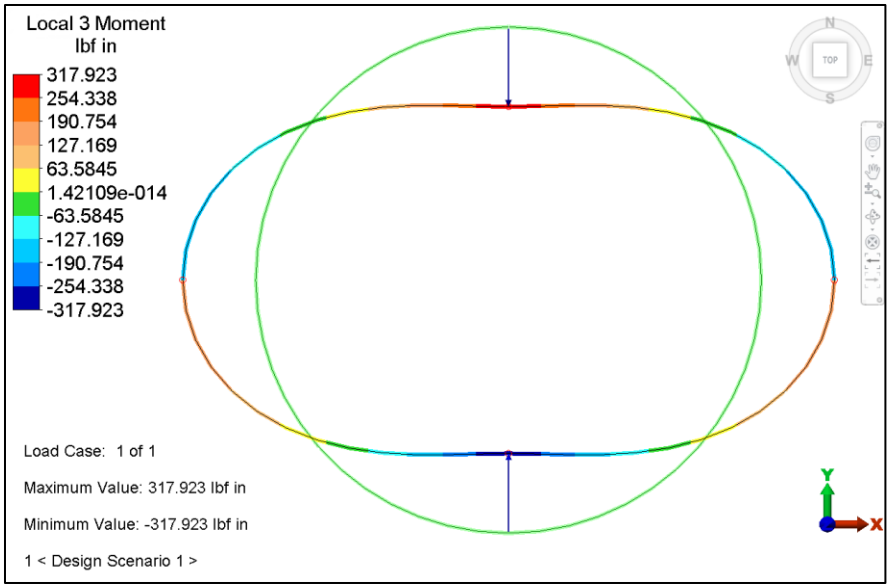

Figure 28-1. Moment contour. The figure shows both undeformed and deformed views.

Table 28-1. Comparison of Results

M_A (lb-in)		%	D_H (in)		%	D_V (in)		%
Theory	**Analysis**	**Difference**	**Theory**	**Analysis**	**Difference**	**Theory**	**Analysis**	**Difference**
318.31	317.92	0.12	5.7983	5.782	0.28	-6.3143	-6.298	0.26

AVE - 29 Thick-walled Cylindrical Vessel under Uniform Internal Radial Pressure

Reference

Roark, R. J. and Young, W. C., *Roark's Formulas for Stress and Strain*, Fifth Edition, New York, McGraw-Hill, 1975, page 504, Table 32, Case 1A.

Problem Description

A thick-walled cylindrical vessel under uniform internal radial pressure (longitudinal pressure zero or externally balanced) is analyzed for hoop stress and radial deflection. For this example, we chose an outside radius of 10 inches and an inside radius of 7 inches, with an internal pressure of 10,000 psi. Steel material properties were used.

Theoretical Solution

σ_2 is the normal stress in the hoop or tangential direction at radius r.

$$\sigma_2 = \left(\frac{qb^2}{r^2}\right)\left(\frac{a^2+r^2}{a^2-b^2}\right)$$

Δb is the radial displacement at the inside radius.

$$\Delta b = \left(\frac{qb}{E}\right)\left(\frac{a^2+b^2}{a^2-b^2}+\nu\right)$$

Where:

* a = 10 outside radius (in)
* b = 7 inside radius (in)
* q = 10,000 internal pressure (psi)
* ν = 0.3 Poisson's ratio
* E = 30E+6 Young's modulus

For r = 7:

* σ_2 = 29,216 psi
* Δb = 0.007517 in

Autodesk Simulation Solution

A 4-inch section of the thick cylindrical shell is modeled, but mirror symmetry boundary conditions are added to simulate an 8-inch long cylinder. This problem was previously analyzed (AVE - 11) using 3-D brick elements. For comparison we use 2-D axisymmetric elements in the current model. The resulting mesh has 121 nodes and 100 elements with 10 layers of elements through the thickness. Results were taken from the lower left corner of the model.

1. Stress Tensor X-X (hoop stress for a 2-D axisymmetric model) at the inside radius = 29,198 psi
2. Y displacement at the inside radius = 0.007517 in

Note: These results are taken at the node on the symmetry plane. This is the node farthest from the effects of the free face, which Roark and Young are not considering in this case.

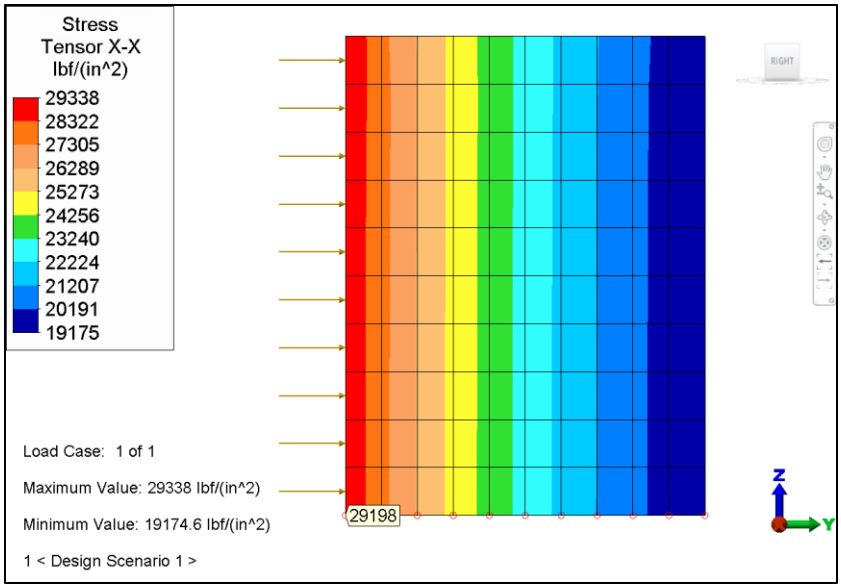

Figure 29-1. An 8-inch section of the thick cylindrical shell described in Case 1A. Notice that S_{XX} represents the hoop stress for 2-D axisymmetric elements.

Table 29-1. Comparison of Results

Delta (inch)		% Difference	σ_2 (psi)		% Difference
Theory	**Analysis**		**Theory**	**Analysis**	
0.007517	0.007517	0.0	29,216	29,198	0.06

The results using brick elements (AVE - 11) were essentially the same.

AVE - 30 Ceramic Strip with Radiation and Convection

Reference

Holman, J. P., *Heat Transfer*, Fifth Edition, New York: McGraw-Hill, 1981, page 96, Example 3-8.

Problem Description

This Accuracy Verification Example will test the nonlinear iteration capabilities of the thermal analysis processor. The test problem is a 0.02 meter wide, by 0.01 meter high ceramic strip. The bottom surface of the strip is perfectly insulated. The sides are held at a constant 900^{o}C. The top is exposed to a combined convection and radiation environment with the following conditions:

* T = 50^{o}C ambient temperature
* h = 50 W/m^{2o}C film coefficient
* ε = 0.7 emissivity

In addition, the following parameters are used in the analysis:

* k = 3.0 W/m^{o}C thermal conductivity of ceramic
* σ = 5.669e-8 W/m^{2o}K^{4} Stefan-Boltzmann constant
* T_{ABS} = 273 conversion from ^{o}C to ^{o}K

Theoretical Solution

The following three points were chosen from the reference for comparison with the analysis results:

T2 - middle of the strip on the top surface

T5 - middle of the strip at the midline

T8 - middle of the strip on the bottom surface

The reference employs a Gauss-Seidel iterative technique to obtain the following steady-state temperatures for these points:

T2 = 711^{o}C (984^{o}K)

T5 = 791^{o}C (1064^{o}K)

T8 = 815^{o}C (1088^{o}K)

Autodesk Simulation Solution

The ceramic strip was modeled with 1152 2-D planar thermal elements. Applied temperatures were applied to the nodes on the sides of the strip to hold them at the prescribed temperature of 900^{o}C. The radiation and convection conditions were applied to the top surface (surface #2).

Since the governing equation for radiation is a nonlinear function, an iterative procedure must be used to update the nodal temperatures between processor runs until the temperatures from two successive iterations converge to within an acceptance criteria. The processor fully automates this iteration process.

After 5 iterations, the temperature results calculated by the thermal analysis processors are:

* T2 = 703.783 ^{o}C
* T5 = 787.454 ^{o}C
* T8 = 813.530 ^{o}C

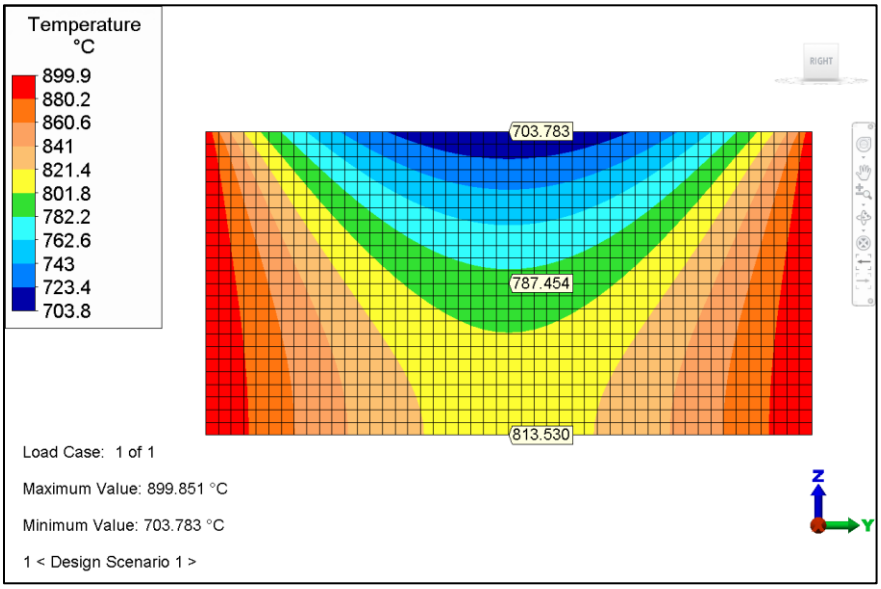

Figure 30-1. Temperature results of the ceramic strip.

Table 30-1. Comparison of Results

Point Name	Temperature (^{o}C)		% Difference
	Theory	Analysis	
T2	711	703.783	1.02
T5	791	787.454	0.45
T8	815	813.530	0.18

AVE - 31 Two Masses and Three Massless Springs with an Applied Forced Harmonic Vibration

Reference

Thomson, William T., *Theory of Vibration with Applications*, Second Edition, Englewood Cliffs, N.J.: Prentice-Hall, Inc., 1981, page 143, Example 5.3-1.

Problem Description

This Accuracy Verification Example tests the capabilities of the Linear Frequency Response processor. The problem is a two degrees-of-freedom (DOF) system consisting of two masses, coupled with three massless springs, with a forced harmonic vibration applied to one of the masses. The system is analyzed for steady state displacements and natural frequencies due to forced harmonic response.

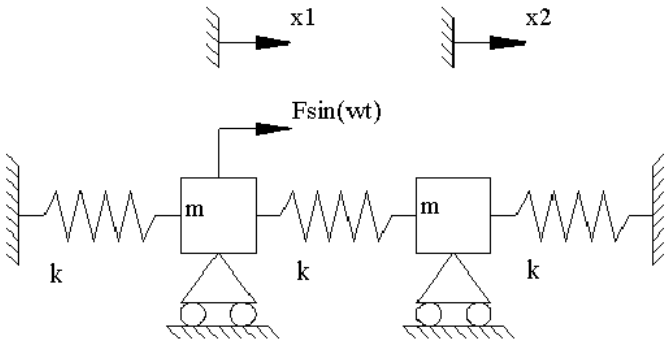

Figure 031-1: Diagram of the two degrees-of-freedom system from Example 5.3-1.

Theoretical Solution

The reference provides the following formulas for the steady-state vibration amplitudes, X_1 and X_2, and the two natural frequencies of the system:

$$\omega_1 = \sqrt{k/m}$$

$$\omega_2 = \sqrt{3k/m}$$

$$X_1 = \frac{\left(2k - m\omega^2\right)F}{m^2\left(\omega_1^2 - \omega^2\right)\left(\omega_2^2 - \omega^2\right)}$$

$$X_2 = \frac{kF}{m^2\left(\omega_1^2 - \omega^2\right)\left(\omega_2^2 - \omega^2\right)}$$

The following parameters were used for this analysis:

* k = 100 lb/in. spring rate
* m = 1.0 lb-sec^2/in mass
* ω =20 rad/sec = 3.1831 Hz exciting frequency
* F = 100 lb force

The results of substituting these values into the above formulas are as follows:

* ω_1 = 10 rad/sec
* ω_2 = 17.32 rad/sec
* X_1 = 0.666 in
* X_2 = 0.333 in

Autodesk Simulation Solution

The springs were modeled with 6 massless beam elements using FEA Editor. Each beam element is 5 inches long, making each spring 10 inches long. The two end nodes were fully constrained and all other nodes were permitted to translate in the axial direction only. Lumped masses can be added in FEA Editor. The stiffnesses of the beam elements were determined using the following formula:

k = AE/L axial stiffness of beam = 100 lb/in (given)

One set of parameters that satisfies this is:

* A = 1 in^2 area of beam
* E = 1000 psi modulus of elasticity
* L = 10" length of a spring

Because the Linear Frequency Response analysis processor uses a modal superposition technique, the file was first run through the Linear Mode Shapes and Natural Frequencies analysis processor. The analysis type was then changed to Linear Frequency Response, and the Analysis Parameters screen was used to enter the forced harmonic vibration information. Then a forced harmonic response analysis was run. The natural frequencies computed by the Linear Mode Shapes and Natural Frequencies analysis processor and the peak amplitudes computed by the Linear Frequency Response analysis processor were as follows:

* ω_1 = 10.0 rad/sec (0% difference from the theoretical solution)
* ω_2 = 17.32 rad/sec (0% difference)
* X_1 = 0.666 in (0% difference)
* X_2 = 0.333 in (0% difference)

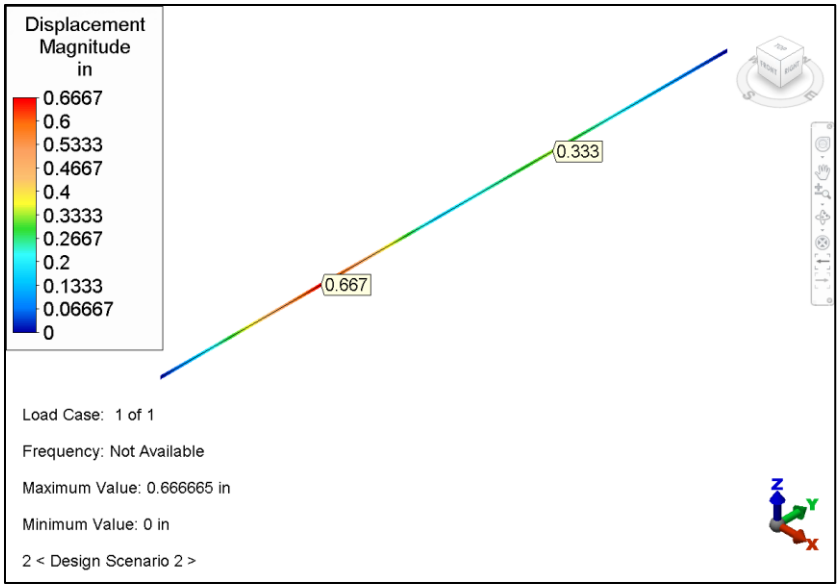

Figure 31-1. Displacement at the nodes where the masses are located.

Table 31-1. Comparison of Results

	Theory	**Analysis**	**% Difference**
ω_1 (rad/sec)	10	10.0	0.0
ω_2 (rad/sec)	17.32	17.32	0.0
X_1 (inch)	0.666	0.666	0.0
X_2 (inch)	0.333	0.333	0.0

AVE - 32 Steady-State Heat Loss of a Steam Pipe with Nonconcentric Insulation

Reference

Giedt, W.H., *Principles of Engineering Heat Transfer*, First Edition, D. Van Nostrand Company, Inc.

Problem Description

In this problem, a steam pipe is surrounded by insulation. The pipe is located 3.25 inches off from the centerline of the insulation cylinder. The diameter of the pipe is 6.5 inches. The outside diameter of the insulation cylinder is 16.25 inches. The temperature of the pipe's outer wall is held at 212°F, and the temperature of the outside of the insulation is held at 70°F (air temperature). Determine the steady-state heat loss of the steam pipe with nonconcentric insulation.

Theoretical Solution

The heat flow rate is:

$$q = \frac{2\pi kl\left(t_i - t_0\right)}{\cosh^{-1}\left(\frac{y_i}{r_i}\right) - \cosh^{-1}\frac{y_0}{r_0}}$$

The following parameters were used:

* k = 0.0045 BTU/hr/in°F conductivity of insulation
* l = 1 in length of pipe run
* t_i = 212°F pipe temperature
* t_o = 70°F air temperature
* r_o = 8.125 in radius of insulation cylinder
* r_i = 3.25 in radius of pipe

The y values are evaluated as shown below:

$$y_i = \frac{r_0^2 - r_i^2 - a^2}{2a} = 6.9063$$

and,

$$y_0 = \frac{r_0^2 - r_i^2 + a^2}{2a} = 10.1563$$

Using a value of 3.25" for a, the offset of the centers of the pipe and the insulation, the following steady-state heat flow rate is obtained:

q = 5.792 BTU/hour

Autodesk Simulation Solution

The insulation was modeled using 2000 2-D planar elements.

Fixed temperatures were imposed on the inside and outside of the insulation. The resulting temperature profile is shown above. The heat flow predicted is:

- q into insulation (all Faces within Surface 2) = 5.619 BTU/hour
- q out of insulation (all Faces within Surface 3) = 5.878 BTU/hour

The slight difference between the heat into the pipe versus the heat out of the insulation is due to the heat flux calculation. Heat fluxes are calculated at the element centroid, so the heat flux through the face is based on a projection of the heat flux times the area of the face. Around the pipe, the area of the face is slightly smaller than the "centroid" area, leading to an underestimate of the heat flux. The opposite occurs around the insulation. A finer mesh in the radial direction would decrease the difference.

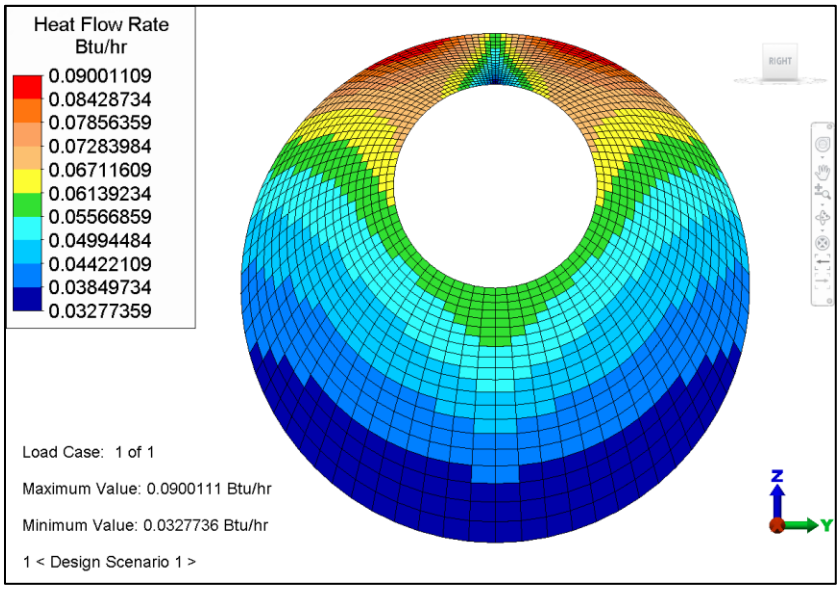

Figure 32-1. Heat flow rate is shown for the insulation section. The image is captured without using the smoothing option. "Results Options", "Maximum Value" setting was utilized.

Table 32-1. Comparison of Results

Heat Flow Rate q (BTU/hour)					
Heat into Insulation			Heat out of Insulation		
Theory	**Analysis**	**% Difference**	**Theory**	**Analysis**	**% Difference**
5.792	5.618	-3.0	5.792	5.878	1.5

AVE - 33 Elastic Instability of a Flat Plate under Pure Shear Load

Reference

Timoshenko, S. P. and Gere, J. M., *Theory of Elastic Stability*, McGraw-Hill, New York, 1961, pages 379-383.

Problem Description

This verification problem involves determining the critical load at which a flat plate under a pure shear load will become elastically unstable (i.e., when buckling will occur). The rectangular plate analyzed is submitted to the action of shearing forces uniformly distributed along the edges, which are simply supported.

Theoretical Solution

The critical load at which the plate will become unstable is defined as

$$\tau_{cr} = k\frac{\pi^2 D}{b^2 h}$$

Where:

* $D = \frac{Eh^3}{12(1-\nu^2)}$

and k is a constant depending on the ratio a/b = 2. The values used for this analysis were:

* D = 915.75
* a = 20 length of plate long side (in)
* b = 10 length of plate short side (in)
* E = 10e6 modulus of elasticity (psi)
* ν = 0.3 Poisson's ratio
* h = 0.1 plate thickness (in)
* k = 6.6 constant based on a/b=2 ratio

τ_{cr} = 5965.15 psi

Autodesk Simulation Solution

The plate was modeled using a 20 x 40 mesh (800 elements) and was simply supported on all edges (T_z applied). In addition, corner nodes were constrained to avoid rigid-body solutions. The node at the origin has Txyz; the diagonally opposite node has Tz; and the remaining two nodes have Txz. The plate elements were loaded along the edge using nodal forces based on a 10 psi shear load (0.5 lbs on each edge node and 0.25 lbs at each corner node). The lower cutoff buckling load factor was set to -1000 in order to calculate a potential negative critical buckling load multiplier.

The buckling load multiplier (BLM) calculated by the processor was:

BLM = -599.37

The critical load at which the plate will buckle is, therefore:

τ_{cr} = (Absolute Value of BLM) x (Applied Load) = 5993.7

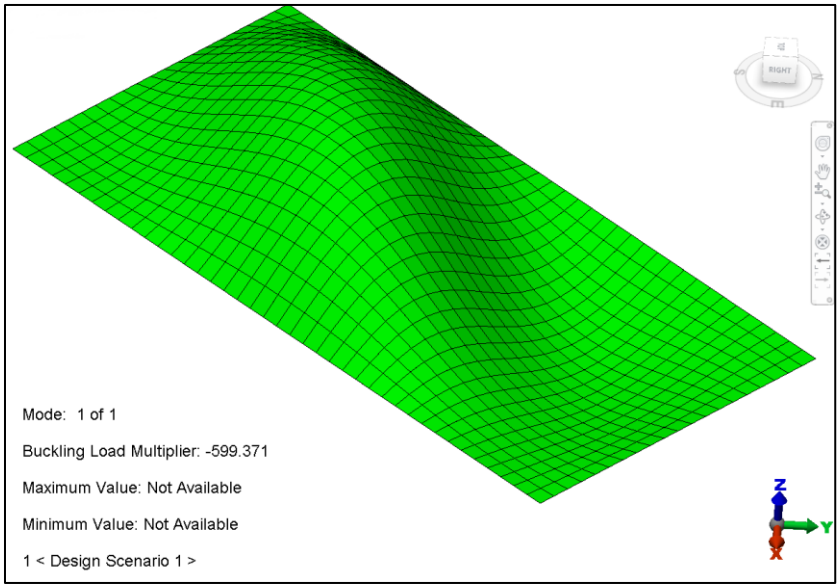

Figure 33-1. Buckling mode shape for the lowest buckling eigenvalue.

Table 33-1. Comparison of Results

τ_{cr} (BLM x Applied Load) (psi)		% Difference
Theory	**Analysis**	
5965.15	5993.7	0.48

AVE - 34 Ceramic Embedded in a High Thermal Conductivity Material

Reference

Holman, J. P., *Heat Transfer*, Fifth Edition, New York: McGraw-Hill, 1981, pages 148-149, Problem 4-11.

Problem Description

A 1 x 2 cm ceramic strip is embedded in a high-thermal-conductivity material so that the sides are maintained at 300^{o}C. The bottom surface is insulated. At time zero the ceramic is uniform in temperature at 300^{o}C. The top surface is then exposed to a convection environment. We want to find the temperature distribution as the ceramic cools.

Theoretical Solution

A finite difference method was used to solve for the temperature distribution in the ceramic.

The following parameters were also used:

* T = 50 ambient convection temp. (^{o}C), top surface
* h = 200 convection coefficient (W/m^{2})
* k = 3.0 conduction coefficient (W/m^{o}C)
* p = 1600 density (kg/m^{3})
* c = 0.80 specific heat (kJ/kg^{o}C)

The temperature distribution at a distance of 0.5 cm from a side and after cooling for 12 seconds is:

* T (top surface) = 243.32^{o}C
* T (center of strip) = 279.87^{o}C
* T (bottom surface) = 289.71^{o}C

Autodesk Simulation Solution

The ceramic strip was modeled using a 40 by 40 mesh of 2-dimensional planar thermal elements. Due to symmetry, only one-half of the strip was modeled. Applied temperatures were used to maintain the left side at 300°C. Using a time step of 2 seconds, the Transient Thermal Processor solved for the following temperature distribution at a time of 12 seconds (time step 6):

* T (top surface) = 239.46°C
* T (center of strip) = 280.37°C
* T (bottom surface) = 290.41°C

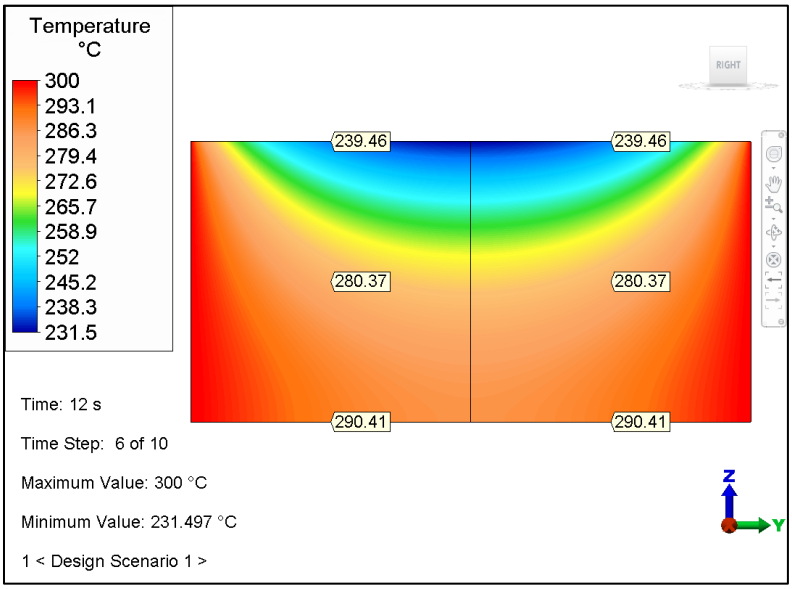

Figure 34-1. Temperature distribution of a ceramic strip at a time of 12 seconds. XZ Mirror plane has been activated to show the full strip.

Table 34-1. Comparison of Results

Nodal Temperature	Temperature (°C) at time = 12 s		% Difference
	Theory	Analysis	
T (top surface)	243.32	239.46	6.8%
T (center of strip)	279.87	280.37	2.5%
T (bottom surface)	289.71	290.41	6.8%

Note: Transient thermal analysis calculates temperature change. Hence, the correct way to compare the percentage difference is to compare the temperature changes between theory and the results. Therefore, the above values were calculated as follows:

$$\% \text{ difference} = \frac{\left(T_{initial} - T_{final}\right)_{Theory} - \left(T_{initial} - T_{final}\right)_{ALGOR}}{\left(T_{initial} - T_{final}\right)_{Theory}} \times 100$$

$$\% \text{ difference} = \frac{\left(T_{final}\right)_{ALGOR} - \left(T_{final}\right)_{Theory}}{\left(T_{initial} - T_{final}\right)_{Theory}} \times 100$$

AVE - 35 Motion of a Two-DOF System Subjected to Random Vibration

Reference

Hurty, W. C., Rubenstein, M. F., *Dynamics of Structures*, Englewood Cliffs, N.J.: Prentice-Hall, Inc., 1964, pages 402 - 405.

Problem Description

This verification problem involves determining the motion of a two degrees of freedom (DOF) mass and spring system subjected to a random vibration environment (or "white noise"). The displacements are determined for the system subjected to an input power spectral density (PSD) applied in the vertical (X) direction.

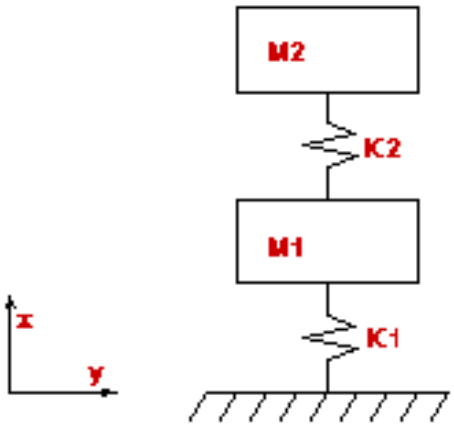

Figure 35-1. Two-DOF dynamic system subjected to a random vibration.

Theoretical Solution

Using the modal method from Hurty and Rubenstein, the mean square response is:

$$X^2(x) = \sum_{r=1}^{2} \frac{U_r(x)^2 \times m_r \times G(\omega) \times \omega_r \times 2\pi}{\omega_r^4 \times 8 \times \beta}$$

Where:

* $U_r(x)$ = normalized mode shapes (inches)
* m_r = mass (lb-sec^2/in) = M1 = M2 = 75 (lb-sec^2/in)
* ω_r = natural frequency (rad/sec)
* $G(\omega)$ = 10e6 input spectral density (g^2/cps)
* β = 0.01 viscous damping

The values of the spring constants are:

* K1 = 100,000 lb/in
* K2 = 150,000 lb/in

Hurty and Rubenstein solutions are:

$x^2(1)$ = 14.135, x(1) = 3.7597
$x^2(2)$ = 27.172, x(2) = 5.2126

Autodesk Simulation Solution

The two-DOF mass and spring system was modeled using 10 beam elements, with concentrated mass located at nodes 10 and 14. Other dimensions and properties of the model include:

* Length from origin to M1 = 30 in
* Length from M1 to M2 = 20 in
* Area = 0.1 in^2
* Mass Density = 0
* Young's Modulus = 3.0e7
* Poisson's Ratio = 0.3

The above beam properties will produce the given spring constants based on K = AE/L.

A Natural Frequency (Modal) analysis was run to extract the first two modes (normalized to the mass matrix) which are:

ω(1) = 23.632 rad/sec, and

ω(2) = 69.100 rad/sec

Then a Linear Random Vibration analysis was run with the approximation method. The PSD of 0.15 g^2/cps in the X-direction was input using the "Analysis Parameters" screen. The responses are:

x(1) = 3.763

x(2) = 5.217

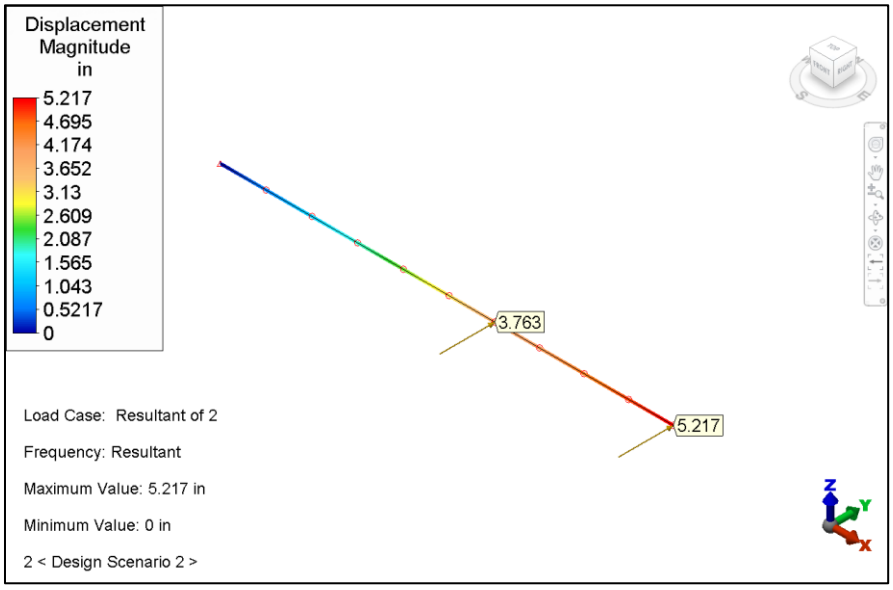

Figure 35-2. Displacement at the node where mass 1 and 2 are located. ("Resultant" option is activated)

Table 35-1. Comparison of Results

	Theory	Analysis	% Difference
x(1) (inch)	3.7597	3.763	0.09
x(2) (inch)	5.2126	5.217	0.08

AVE - 36 Interference Analysis of Two Concentric Thick-walled Rings

Reference

Burgreen, D., *Elements of Thermal Stress Analysis*, Jamaica, N.Y.: C.P. Press, 1971, pages 204-211.

Problem Description

Two concentric thick-walled rings or circular plates, with different material properties, are subjected to a temperature increase in order to perform an interference analysis. A ring with an inside radius of 3" and an outside radius of 4" is to have an inner ring with a wall thickness of 1" forced into it. An interference between the rings of 0.01 inches is obtained when they are held at the elevated temperature. We want to find the tangential stresses at the inner surfaces of the two rings.

Theoretical Solution

The tangential stresses at the inner surfaces of the two rings are given as:

$$\Delta = -R_j(\alpha_1 - \alpha_2)(T_d - T_o) = .01 \text{ interference}$$

$$\sigma_{1t} = -\frac{\dfrac{2R_j^2 E_1}{R_j^2 - R_i^2}\left[(\alpha_1 - \alpha_2)(T_o - T_d)\right]}{\dfrac{E_1}{E_2}\left(\dfrac{R_o^2 + R_j^2}{R_o^2 - R_j^2}\right) + \dfrac{R_j^2 + R_i^2}{R_j^2 - R_i^2} + \dfrac{E_1}{E_2}\nu_2 - \nu_1}$$

$$\sigma_{2t} = \frac{\dfrac{R_o^2 + R_j^2}{R_o^2 - R_j^2}E_1\left[(\alpha_1 - \alpha_2)(T_o - T_d)\right]}{\dfrac{E_1}{E_2}\left(\dfrac{R_o^2 + R_j^2}{R_o^2 - R_j^2}\right) + \dfrac{R_j^2 + R_i^2}{R_j^2 - R_i^2} + \dfrac{E_1}{E_2}\nu_2 - \nu_1}$$

Where:

* α_1 = 13.3 e-6 (thermal expansion coefficient - inner ring 1)
* α_2 = 9.6 e-6 (thermal expansion coefficient - outer ring 2)
* R_i = 2 (inner ring 1 inner radius, inches)
* R_j = 3 (inner ring 1 outer radius, inches)
* R_o = 4 (outer ring 2 outer radius, inches)
* E_1 = 10.3 e+6 (Elastic modulus, inner ring 1, psi)
* E_2 = 27.6 e+6 (Elastic modulus, outer ring 2, psi)
* ν_1 = 0.334 (Poisson's ratio, inner ring 1)
* ν_2 =0.304 (Poisson's ratio, outer ring 2)
* T_d = 70 (stress-free reference temperature, ^oF)
* T_o = 970.9 (final temperature of rings, ^oF)

The solution for the inner surfaces is

σ_{1t} (inner ring) = -33,295 psi

σ_{2t} (outer ring) = 33,030 psi

Autodesk Simulation Solution

The rings were modeled using 2-D plane stress elements. Due to symmetry, only one-quarter of the object was modeled by applying T_z to all nodes on the surface parallel to the y-axis, and applying T_y to all nodes on the surface parallel to the z-axis. The mesh was generated with the Two-Dimensional Mesh Generation capability, with a global mesh density of 1000 and mesh refinements (element size h=0.05 within 0.5" radius) placed at the inside radius of each ring on the Z axis, resulting in 2756 elements.

The following information was entered:

For part 1 (ring 1):

* thickness = 1
* stress free reference temperature = 70

For part 2 (ring 2):

* thickness = 1
* stress free reference temperature = 70 F

For the "Analysis Parameters:Thermal/Electrical" tab, the default nodal temperature = 970.9 F

The linear static stress analysis processor solved for the following stresses:

σ_{1t} (inner ring) = -33,410 psi

σ_{2t} (outer ring) = 33,106 psi

These stress values are obtained using smoothed stress tensor results (Y-Y direction at the inner radius for both parts along the Z axis). To view the stress on the inside of the outer cylinder, the inner cylinder must be made hidden.

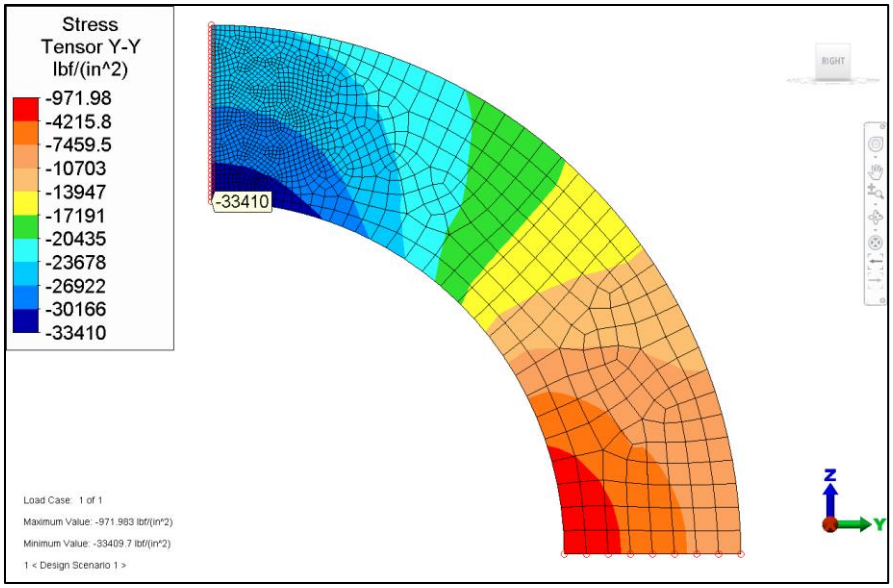

Figure 36-1. Vector stress tensor (Y direction) contour display of the inner ring. The elements of the outer ring are hidden in this display.

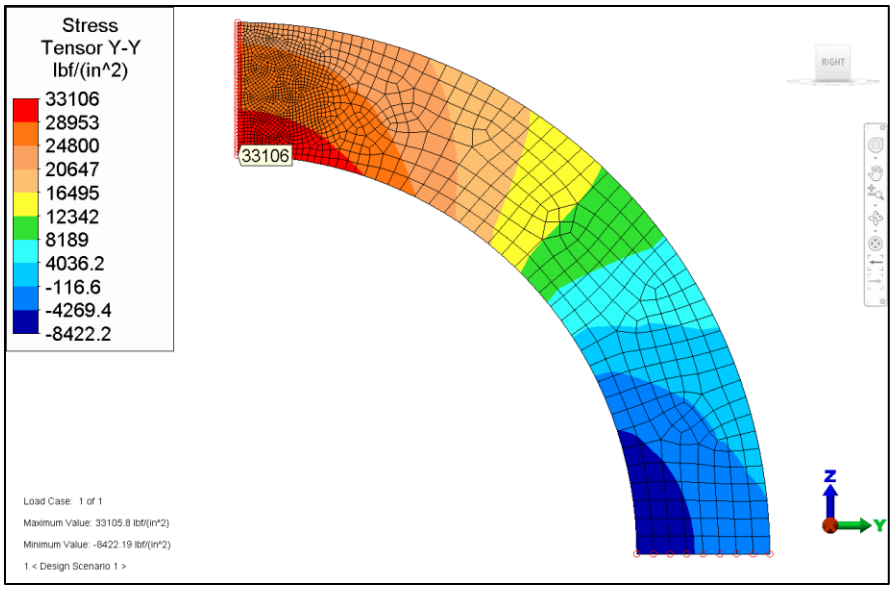

Figure 36-2. Vector stress tensor (Y direction) contour display of the outer ring. The elements of the inner ring are hidden in this display.

Table 36-1. Comparison of Results

σ_{1t} (inner ring) (psi)		% Difference	σ_{2t} (outer ring) (psi)		% Difference
Theory	**Analysis**		**Theory**	**Analysis**	
-33,295	-33,410	0.35	33,030	33,106	0.23

AVE - 37 Circular Flat Plate with Edge Clamped and Concentrated Load Applied at Center

Reference

Timeshenko and Woinowsky-Krieger, *Theory of Plates and Shells*, McGraw-Hill Book Company, Inc., 1959, pages 67-69.

Problem Description

The subject problem is a circular flat plate with the edge clamped. A concentrated load is acting at the center. We want to find the maximum deflection at a given distance from the center of the plate.

Theoretical Solution

The maximum deflection at any distance r from the center of the plate is given in the reference as follows:

$$w = \frac{Pr^2}{8\pi D}\log\frac{r}{a} + \frac{P}{16\pi D}\left(a^2 - r^2\right)$$

$$w = \frac{Pa^2}{16\pi D} \text{ at } r = 0$$

$$D = \frac{Eh^3}{12\left(1-\nu^2\right)}$$

Where:

* P = 1.0 concentrated load (lbs)
* a = 1.1125 plate radius (inches)
* E = 30.0e6 modulus of elasticity (psi)
* ν = 0.3 Poisson's ratio
* h = 0.02 plate thickness (inches)
* D = 21.978 inch-lbs

The solution for deflection at the center of the plate (r = 0) is:

* w = 0.00112 inches

Autodesk Simulation Solution

One quarter of the circular plate was modeled using 80 3-D plate elements. Symmetry boundary conditions were applied. The plate was modeled in the XZ-plane, and nodes along the Z-axis were constrained in T_xR_{yz}, and nodes along the X-axis were constrained in T_zR_{xy}. The outer edge of the plate was fully constrained.

A 0.25-lb nodal force was applied at the center node in the Y-direction to simulate a 1-lb force on the full model. The model was processed using the Linear Static Stress analysis processor. The calculated Y-displacement results are:

* max. Y-displacement = 0.0011054 in

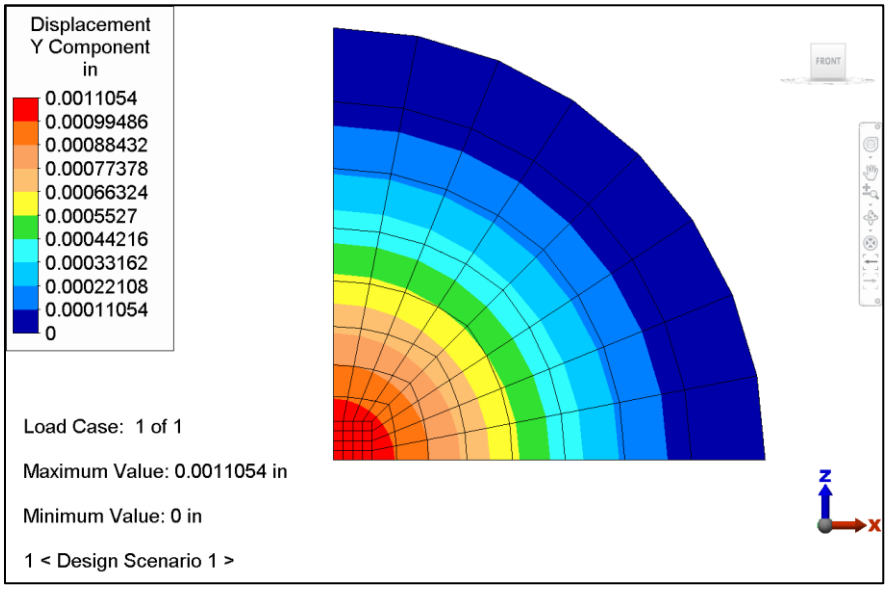

Figure 37-1. Y-displacement display of point loaded circular plate (1/4-symmetry model).

Table 37-1. Comparison of Results

Maximum Y-Displacement (inch)		% Difference
Theory	**Analysis**	
0.00112	0.0011054	1.30

AVE - 38 Thick-walled Spherical Vessel under Uniform Internal Pressure

Reference

Roark, R. J. and Young, W. C., *Roark's Formulas for Stress and Strain*, Fifth Edition, New York: McGraw-Hill, 1975, page 506, Table 32, Case 2a.

Problem Description

A thick-walled, spherical vessel under uniform internal pressure is analyzed for radial stress and deflection. For this example, we chose an outside radius of 10" and an inside radius of 7". Internal pressure of 10,000 psi was applied and steel material properties were used. This AVE is similar to AVE - 10. The main difference is the use of tet elements with midside nodes.

Theoretical Solution

$\sigma_1 = \sigma_2$ is the normal stress in the hoop or tangential direction at radius r.

$$\sigma_1 = \left(\frac{qb^3}{2r^3}\right)\left(\frac{a^3+2r^3}{a^3-b^3}\right)$$

Δb is the radial displacement at the inside radius.

$$\Delta b = \left(\frac{qb}{E}\right)\left(\frac{(1-\nu)(a^3+2b^3)}{2(a^3-b^3)}+\nu\right)$$

Where:

* a = 10 inches (outside radius)
* b = 7 inches (inside radius)
* q = 10,000 psi (internal pressure)
* ν = 0.3 Poisson's ratio
* E = 30E6 psi (Young's modulus)

For r = 7 inches

* σ_1 = 12831.05 psi
* Δb = 0.002796 inches

Autodesk Simulation Solution

Due to symmetry, only one octant of the spherical vessel was modeled. Mirror symmetry boundary conditions were used at the edges on the XY, YZ and ZX planes.

For purposes of comparison, the problem was first modeled using 3-D brick elements. The results were as follows:

* σ_1 max = 12,627.89 psi
* Δb = 0.002878 inches

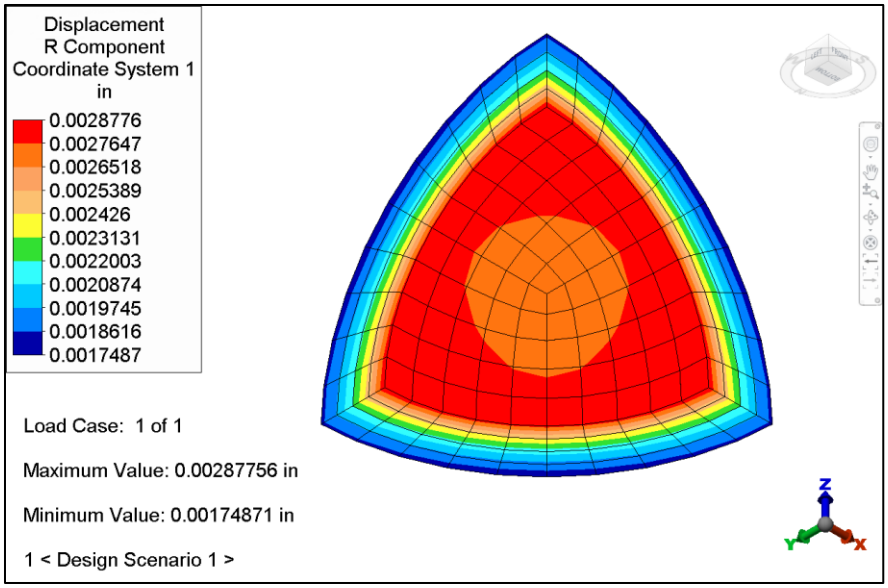

Figure 38-1. Displacement contours for the model with brick elements.

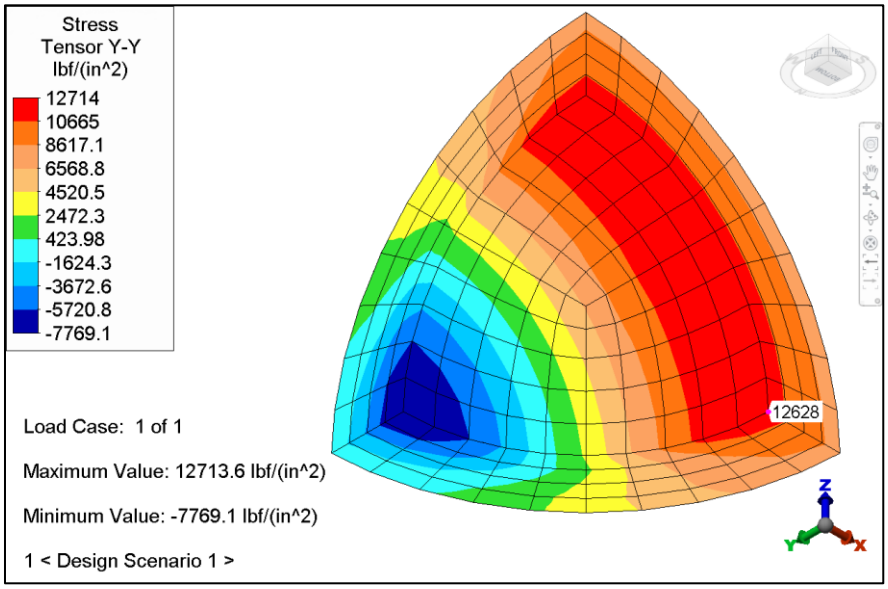

Figure 38-2. Stress contours for the model with brick elements.

Next, the mesh was recreated using 3-D, solid tetrahedral elements. The Element Definition data entry screen enabled us to specify either 4-node (midside nodes not included) or 10-node (midside nodes included) tetrahedral elements. For the first case, we used 4-node elements to do a quick check of the displacements and stresses. We then re-"check" the mesh with 10-node elements for the final, high-accuracy result. In essence, we performed a quick convergence analysis with the "flip of a switch". However, midsides nodes must be constrained to ensure accurate results. This is most easily accomplished by defining surface boundary conditions

The stress analysis results using 10-node tetrahedra were:

σ_1 max = 12,757.67psi

Δb = 0.0028 in

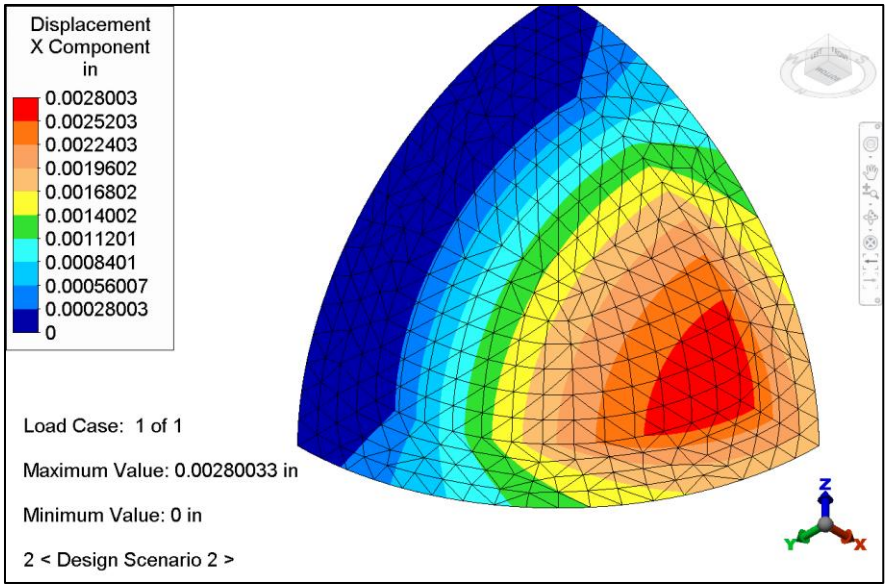

Figure 38-3. Displacement contours for the model with 10-node tetrahedral elements.

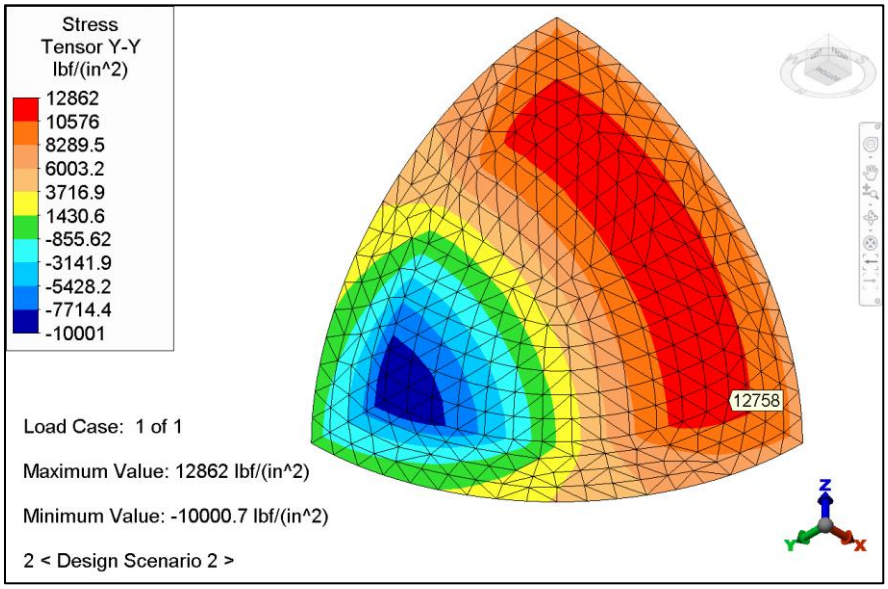

Figure 38-4. Stress contours for the model with 10-node tetrahedral elements.

Table 38-1. Comparison of Results

	Theory	Brick Elements		Tetrahedral Elements	
		Analysis	% Difference	Analysis	% Difference
σ_1 max (psi)	12,831.05	12,627.89	1.58	12,757.67	0.57
Δb (inch)	0.002796	0.002878	2.93	0.0028	0.14

AVE - 39 Forced Harmonic Response Analysis of a Spring-Mass-Damper System

Reference

Thompson, W.T., *Theory of Vibration with Applications*, Second Edition, Englewood Cliffs, N.J.: Prentice-Hall, Inc., 1981, page 49.

Problem Description

A single degree of freedom spring-mass-damper system is analyzed for steady-state displacements, phase angle and natural frequencies due to forced harmonic vibration applied to the mass. A machine of weight W is supported on springs of stiffness k. A harmonic disturbing force of magnitude F_0 and frequency ω_n acts on the mass. Determine the displacement in terms of peak amplitude X, phase angle ψ and frequency ω_n. The viscous damping coefficient is c.

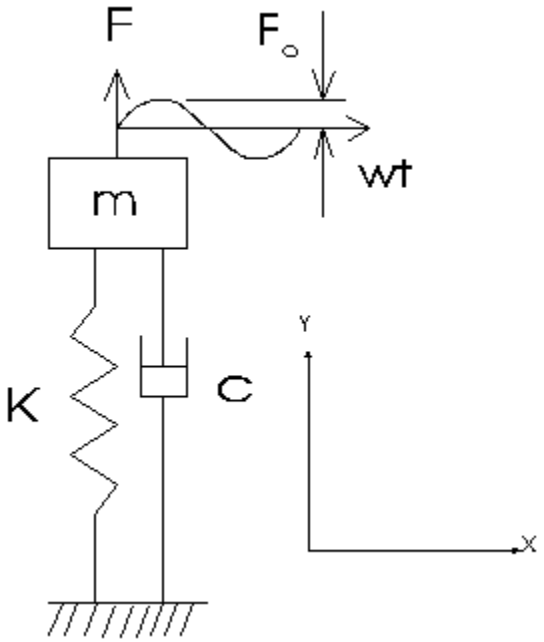

Figure 39-1. Spring-mass-damper system.

Theoretical Solution

From vibration theory, the following can be derived:

$$x = \frac{F_0}{\sqrt{\left(k - m\omega^2\right)^2 + \left(c\omega\right)^2}}, \text{ and}$$

$$\psi = \tan^{-1}\frac{c\omega}{\left(k - m\omega^2\right)}$$

$m = W/g$

$g = 386.40$ in/sec^2

Where:

* m = 0.5 lb-s^2/in
* k = 200 lb/in
* $\omega = \omega_n = \sqrt{\frac{k}{m}}$ = 20 rad/sec
* F_0 = 10.016 lb
* $\xi = \frac{c}{2m\omega_n}$ = damping ratio = 0.3
* c = 6 lb-sec/in

Autodesk Simulation Solution

The springs were modeled with 10, beam elements connected in series, each 1 inch long. The ground node was fully constrained and the other nodes were permitted to translate in the axial direction only. The lumped mass was added in the FEA Editor.

The axial stiffness of the beam elements is AE/L. By setting the area A to 1.0 in^2 and the modulus of elasticity E to 2000 psi, the desired spring stiffness K of 200 lb/in was obtained.

The dynamic linear modal analysis was performed for one natural frequency using the Linear Mode Shapes and Natural Frequencies analysis processor. A non-zero mass density is required for the beam elements to obtain a solution, but the value should be small so that the beam's mass has a negligible effect on the answer. Then the analysis type was changed to Linear Frequency Response and the "Analysis Parameters" screen was used to specify the forced harmonic vibration information and a restart analysis was run using the frequency response processor.

The natural frequency computed by the Linear Mode Shapes and Natural Frequencies analysis processor and the peak amplitude and phase angle computed by the Linear Frequency Response analysis processor are given below in tabular format along with the theoretical solutions.

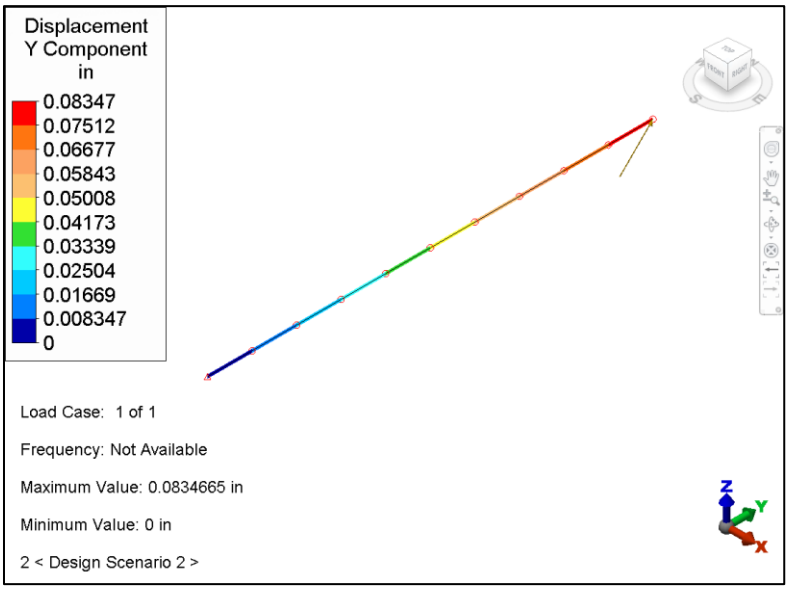

Figure 39-2. Displacement contours (SRSS) in the Y direction.

Table 39-1. Comparison of Results

	Theory	Analysis	% Difference
ω_n (rad/sec)	20.00	20.0	0.0
Amplitude (in)	0.083	0.083	0.0
Phase Angle ϕ (deg)	90	90	0.0

The frequency and forced amplitude can be found from Result interface (Results Options: Response type: SRSS) or the summary files. The phase angle is obtained only from the summary file.

AVE - 40 Solid Sphere Analyzed to Find Weight, Center of Gravity and Mass Moment of Inertia

Reference

Ellis, R. and Gulick, D., *Calculus with Analytic Geometry*, HBJ, New York, 1978, page 913.

Problem Description

A 1.0 inch radius solid sphere is analyzed for weight, center of gravity and mass moment of inertia.

Theoretical Solution

The mass moment of inertia equation for a solid sphere is given as:

$$I = \frac{8\rho\pi r^5}{15}$$

Where:

* r = 1.0 radius of sphere (in)
* ρ = 7.34E-4 mass density (lb-s^2/in^4)

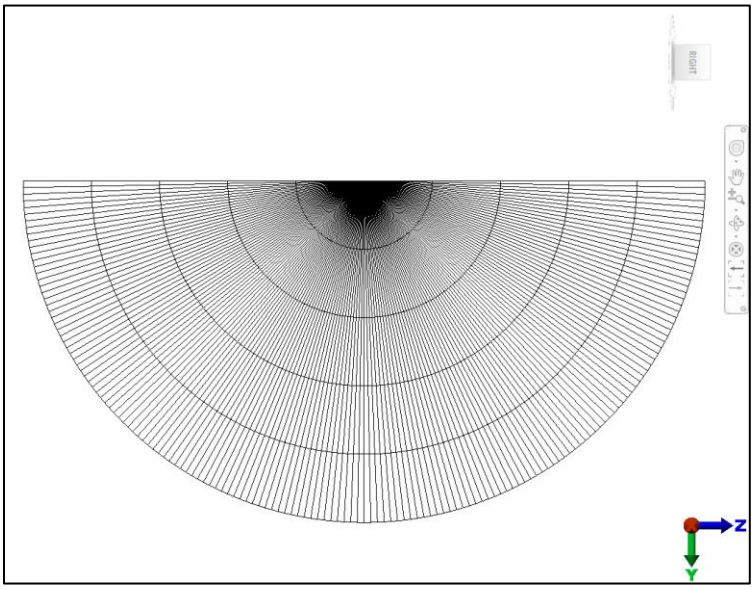

Figure 40-1. The 1.0 inch radius solid sphere was modeled with 800 2-D axisymmetric elements.

Autodesk Simulation Solution

The sphere was modeled with 800 2-D axisymmetric elements. Steel material properties were used. In the results interface, the "Tools:Weight and Center of Gravity…" command was used to access the pop-up window for calculating weight, center of gravity, and mass moment of inertia (g=386.4 in/s^2). The results are given in tabular format below.

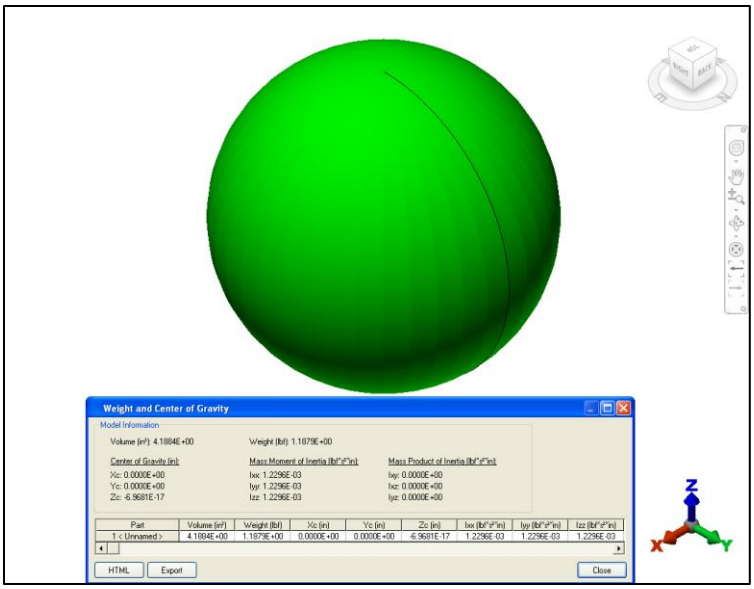

Figure 40-2. The weight, center of gravity and mass moment of inertia

Table 40-1. Comparison of Results

	Theory	Analysis	% Difference
Volume, V (in^3)	4.19	4.19	0.0
Weight, W (lb)	1.188	1.188	0.0
X_C (inch)	0.00	0.00	0.0
Y_C (inch)	0.00	0.00	0.0
Z_C (inch)	0.00	0.00	0.0
Mass Moment of Inertia, X Axis (lb-s^2-in)	0.00123	0.00123	0.0
Mass Moment of Inertia, Y Axis (lb-s^2-in)	0.00123	0.00123	0.0
Mass Moment of Inertia, Z Axis (lb-s^2-in)	0.00123	0.00123	0.0

AVE - 41 Natural Frequency Analysis of a Graphite/Epoxy Laminated Composite Square Plate

Reference

Ashton, J. E., and Whitney, J. M., *Theory of Laminated Plates*, Technomic Publishing Co., Inc., Stamford, Connecticut, 1970, p. 70.

Problem Description

A simply supported graphite/epoxy laminated composite 1in x 1in square plate with nine layers alternating at 0^o and 90^o [0/90]s with respect to the global Z axis is analyzed for natural frequencies and mode shapes. Thicknesses of the layers at 0^o and 90^o are 0.001 inch and 0.00125 inch respectively.

Theoretical Solution

The following material properties are given in material principal directions:

* EX = 40E6 psi (Modulus of elasticity)
* EY = 1E6 psi (Modulus of elasticity)
* NUXY = 0.25 (Poisson's Ratio)
* GXY = 0.6E6 (Shear Modulus)
* GXZ = 0.6E6 (Shear Modulus)
* GYZ = 0.5E6 (Shear Modulus)
* Density = 1.0 lb. s^2/in^4 (Mass density)

Autodesk Simulation Solution

Due to symmetry only a quarter of the plate was modeled. Simply supported boundary conditions (T_{xyz} R_z) were applied along the outer edges and symmetry boundary conditions were applied along the symmetry edges.

> **Note:** The use of symmetry to reduce the size of dynamics problems can result in missing modes that do not have the symmetry of the reduced model. In this example, the antisymmetric mode shapes are excluded.

256 composite elements (16 x 16 mesh) were used for analyzing the mode shapes. The Natural Frequency (modal) processor was used for the analysis. The first four natural frequencies of the plate are presented below in tabular form along with the theoretical solution.

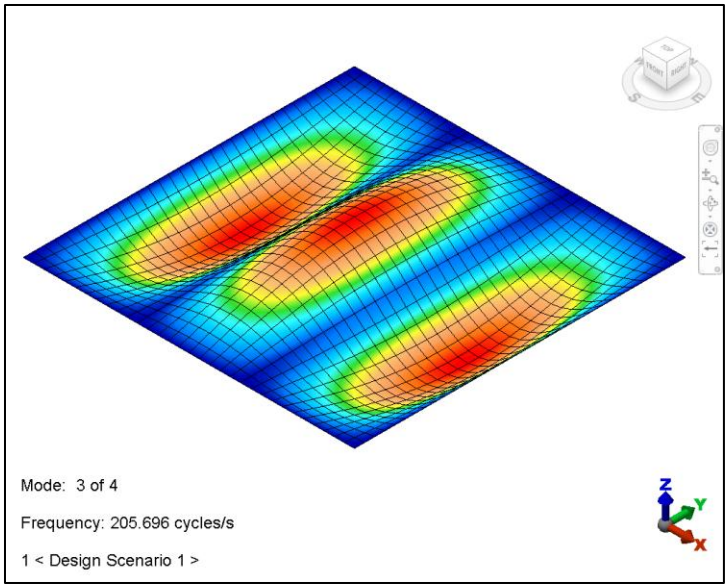

Figure 41-1. This deflected natural frequency analysis contour shows the 3rd mode shape of the laminated composite plate with 2 active mirror planes.

Table 41-1. Comparison of Results

Mode	Frequency (Hz)		% Difference
	Theoretical	Analysis	
1	30.064	30.044	0.07
2	167.113	166.96	0.09
3	205.867	205.70	0.08
4	270.579	268.75	0.68

AVE - 42 Mid-span Deflection of a Uniform Steel Beam Simply Supported at Both Ends

Reference

Pytel, A. and Singer, F. L., *Strength of Materials*, Fourth Edition, Harper & Row Publishers, New York, 1987, p. 193.

Problem Description

A steel beam, 10" long with a 1" x 1" cross-section, is simply supported at both ends. Determine the mid-span deflection with non-uniformly distributed triangular loading.

Theoretical Solution

The mid-span deflection of the beam is given as:

$$\delta = \left(\frac{9}{1920}\right)\left(\frac{w_o L^4}{EI}\right)$$

Where:

* w_o = 100 lb/in (uniform distributed triangular loading)
* E = 30E6 psi (modulus of elasticity)
* I = 1/12 in^4 (moment of inertia)
* L = 10 in (length of beam)

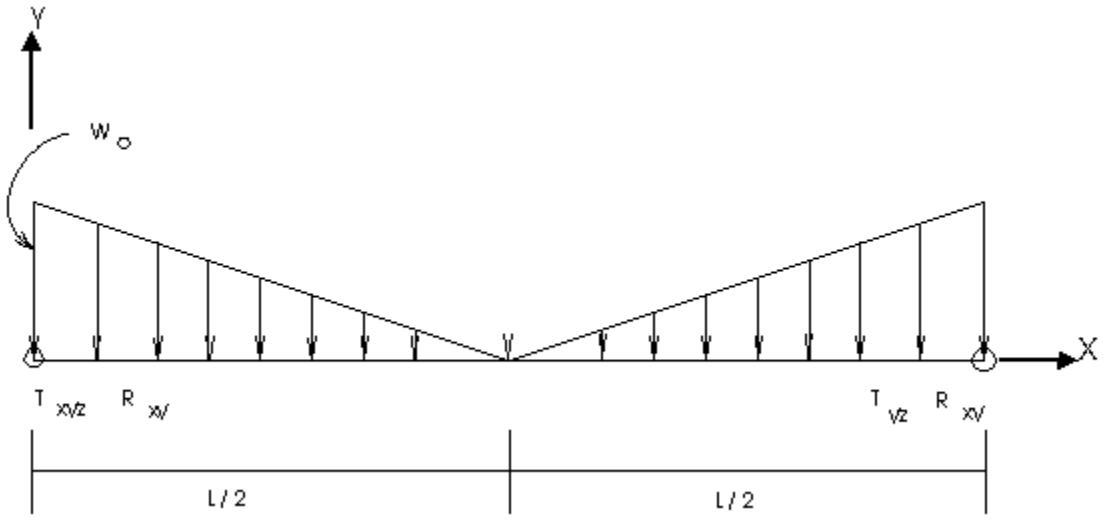

Figure 42-1. Uniform distributed loading is illustrated in this drawing.

Autodesk Simulation Solution

The beam was modeled with two beam elements, each 5 inches long. For simulating the simply supported boundary conditions, one end of the beam has TxyzRxy fixed and the other end of the beam has TyzRxy fixed.

This problem demonstrates the FEA Editor's non-uniformly distributed loading capacity for beam elements. To apply a non-uniformly distributed force, the "Beam Distributed Load" command was used. A force magnitude of 100 lbf/in on the fixed end and a 0 lbf/in in the center of the beam was entered for the selected beam members.

The reference results and the Linear Static Stress analysis processor results are given below in tabular form.

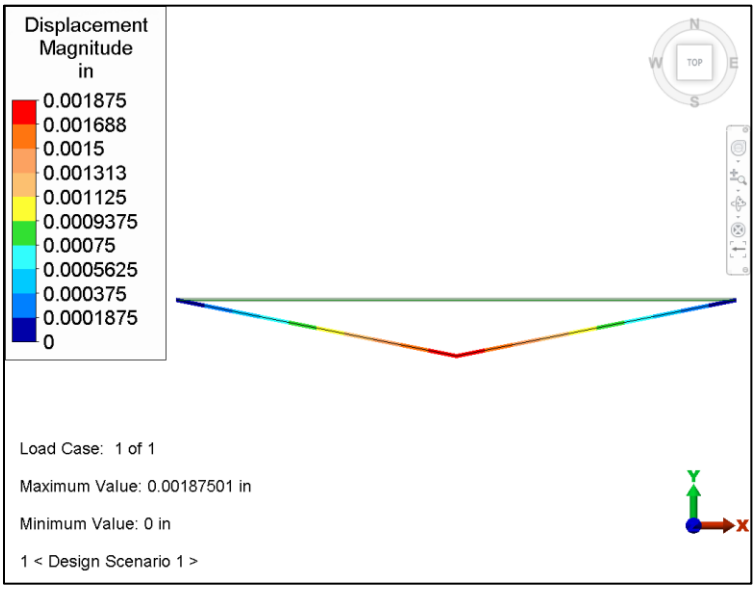

Figure 42-2. Displacement magnitude contour. Both deflected and undeflected beams are shown.

Table 42-1. Comparison of Results

Mid-span Deflection Δ (in)		% Difference
Reference	**Analysis**	
1.875e-3	1.875e-3	0.0

AVE - 43 Stress Relaxation of a Tightened Bolt Due to Thermal Creep

Reference

Timoshenko, S., *Strength of Materials, Part II, Advanced Theory and Problems*, Third Edition, Van Nostrand Co., Inc., New York, 1956, p. 530.

Problem Description

A bolt with a length of 10 inches and a cross-sectional area of one square inch is tightened to an initial stress (σ_0) of 1000 psi. The bolt is held at a fixed displacement for a long period of time (t = 1000 hrs.) at a temperature at which thermal creep occurs. Determine the stress in the bolt at various times during creep relaxation. Small-strain, small-deformation theory is used.

Theoretical Solution

The bolt material has a creep strain rate given by:

$$\dot{\xi}_c = k\sigma^n$$

From this equation using:

$$\frac{d\sigma}{dt} = -\dot{\xi}_c E = -k\sigma^n E$$

and integrating over the time period from "0" to "t" we get stress at any time instant "t" as:

$$\sigma_t = \left[\sigma_0^{1-n} + k(n-1)Et\right]^{1/(1-n)}$$

Where:

* E = 3.E7 psi (Young's Modulus)
* σ_0 =1000 psi (initial stress)
* k = 4.8E-30/hr. (creep strain relaxation constant)
* n = 7
* t = 1000 hrs (time period)

Autodesk Simulation Solution

One 2-D plane stress continuum element was used for this visco-elastic material model for nonlinear creep analysis. Boundary condition Tyz was used at the lower left corner node and Ty at the upper left corner to simulate the tightened bolt fixities at the left end. To obtain the 1000 psi preload, prescribed displacements were applied to the right end. The magnitude of the displacement was 0.000333 inch (deflection = $\sigma_0 L/E$) where the length L is given in the problem statement (10 inches). The MES with Nonlinear Material Models analysis type was used for the analysis.

A total of 1000 solution steps and 100 timestep iterations for each solution step were used to apply the preload over a short time interval (1 hr), but the results were output every 100 steps (100 hours). The second-order time integration method and a creep strain calculation tolerance of 5E-2 were entered in the Element Definition data entry screen. This solution is both a time-hardening and strain-hardening solution.

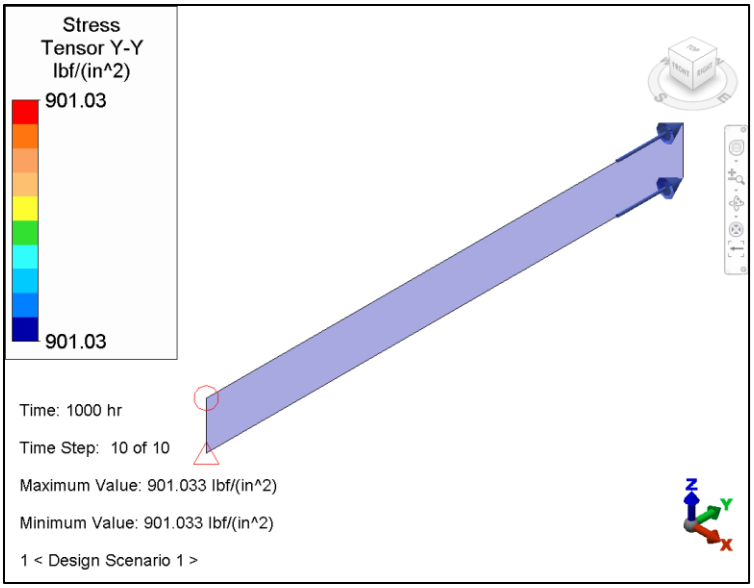

Figure 43-1. Stress Tensor (Y-Y) results of the last time step.

The theoretical stress results and comparative analytical stress results at various time-instants are given below in tabular form. The results demonstrate the accuracy and effectiveness of the visco-elastic power creep capability of the MES with Nonlinear Material Models stress analysis processor.

Table 43-1. Comparison of Results

Time Instant (hours)	Maximum Stress (psi)		% Difference
	Theory	Analysis (Syy)	
t = 200	973.78	973.10	0.07
t = 400	951.73	951.16	0.06
t = 600	932.76	932.26	0.05
t = 800	916.15	915.72	0.05
t = 1000	901.42	901.03	0.04

AVE - 44 Deflection Analysis of a Helical Spring Under Compressive Loading

Reference

Popov, E. P., *Introduction to Mechanics of Solids*, Prentice-Hall, Inc., Englewood Cliffs, New Jersey, 1968, p. 274.

Problem Description

A closely coiled solid helical spring of circular cross-section is subjected to a compressive load F. The diameter of the spring is d and the coil radius is $\bar{r}$ (distance from the axis of the spring to the centroid of the spring's cross-sectional area).

For modeling simplicity, only a single complete turn of the spring is analyzed (i.e., N = 1).

Theoretical Solution

For a helical spring, the deflection Δ under compressive load F is defined by the relation:

$$\Delta = \frac{64\,F\bar{r}^3 N}{Gd^4}$$

Where:

- F = 1.0 lb (Compressive load)
- $\bar{r}$ = 3.0 in (Coil radius)
- d = 0.5 in (Spring diameter)
- G = 1.154E7 psi (Shear modulus)
- N = 1 (Number of turns)

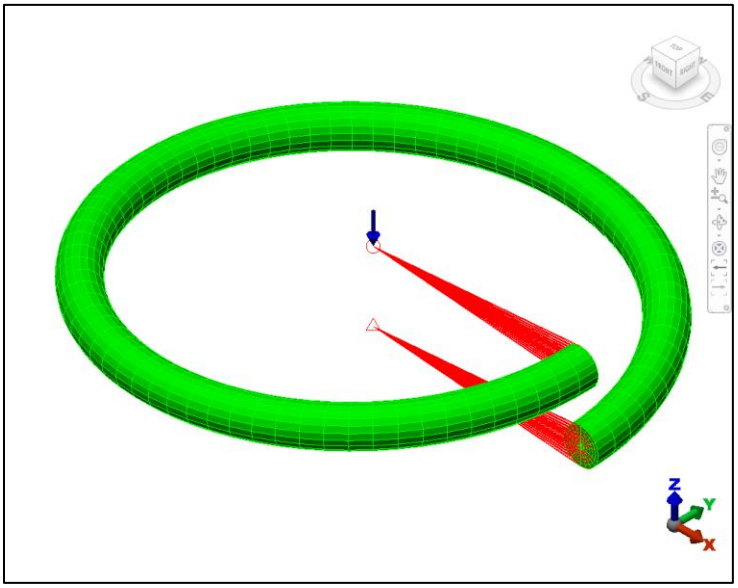

Figure 44-1. A light-shaded display of the model shows the helical spring turn with rigid elements for axial loading.

Autodesk Simulation Solution

A total of 9600 brick elements were generated for the analysis. The forces and boundary conditions to simulate the compressive loading on the turn of the spring were applied to the ends of rigid elements, each extending from the axis of the spring to the respective end circles of the spring mesh. The lower rigid elements were fully fixed on one end. The upper rigid elements were fixed in all directions on one end except for Tz. To transmit the forces and moments into the spring, each rigid element was connected to every node on the face of the spring coil, for a total of 242 rigid elements.

The theoretical and analytical solutions are given below in tabular form.

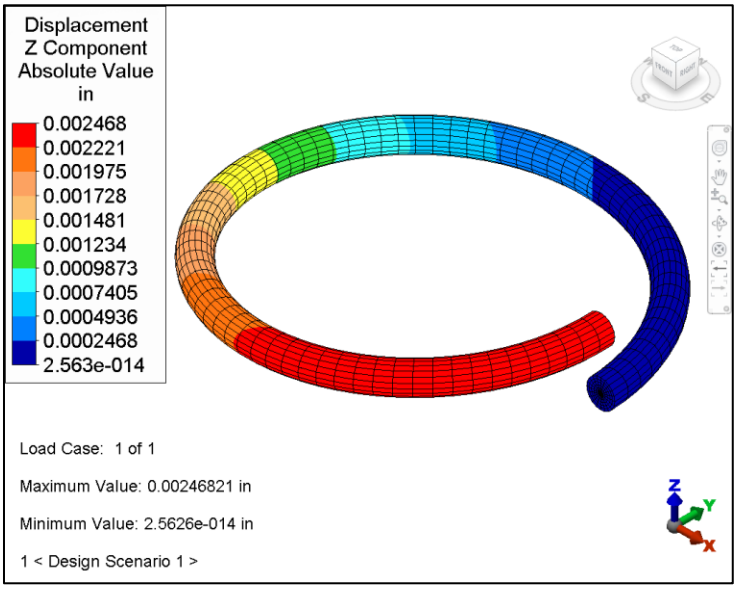

Figure 44-2. The Z displacement results in absolute value format is shows the commpressed shape of the helical spring model.

Table 44-1. Comparison of Results

Deflection, Δ (in)		% Difference
Theory	Analysis	
0.002396	0.002468	3.01

AVE - 45 Nonlinear Radiation Heat Transfer Analysis of a Cylindrical Disk with Internal Heat Generation

Reference

Holman, J. P., *Heat Transfer*, Fifth Edition, McGraw-Hill Book Company, New York, 1981, p 13.

Problem Description

A hollow cylindrical disk with an external radius of 1.5 inches and an inner radius of 0.5 inches is exposed to a radiation environment (T_{rad} = 70°F, F_{rad} = 0.26). It has internal heat generation elements along the inner edge. We want to compute the radiation surface temperature.

Theoretical Solution

An ideal radiator, or blackbody, emits energy at a rate proportional to the fourth power of the absolute temperature of the body. Therefore:

$q = F\sigma A(T_1^4 - T_2^4)$

Where:

- q/Vol. = 388 BTU/sec in^3
- $q = \text{Vol.} \times \left({}^{q}\!/_{\text{Vol.}} \right) = \pi\left[(0.55)^2 - (0.5)^2\right](0.1) \times 388 = 6.3994$ BTU/sec

  (where the heat generation is assigned to the inner 0.05 inches of the radius)
- T_2 = 70°F (radiation temperature at the inner radius)
- r = 1.5 in (external radius of the cylindrical disk)
- h = 0.1 in (height of the cylindrical disk)
- A = 1.5 x 0.1 x 2π = 0.9425 in^2 (radiation area)
- σ = 3.3 E-15 BTU/sec R^4 in^2 (Stephen-Boltzman constant)
- F = 0.26 (radiation emissivity function)

Solving for radiation surface temperature we get:

T_1 = 9431.8 R = 8971.8 °F (theory) where 460 °F was used for the conversion from °F to R.

Autodesk Simulation Solution

Due to the circular symmetry, only one quarter of the cylinder was modeled. In order to determine which solid element type can provide accurate results with the most efficient use of computing resources, the problem was analyzed using brick elements, and tetrahedral elements with and without midside nodes. The same surface mesh size (0.1 in) was used to create the brick mesh and the tetrahedral mesh.

The steady-state heat transfer analyses are independent of the thermal conductivity, but the models used a value of 1.887e-3 BTU/(sec-in-°F).

The analyses were performed using the nonlinear iterations specified on the Advanced tab. Using a default nodal temperature setting of 9000°F (initial guess), the analysis converged to the final solution within 20 iterations for the brick model and the tetrahedral models with a relaxation parameter of 0.25 and a corrective tolerance of 0.01.

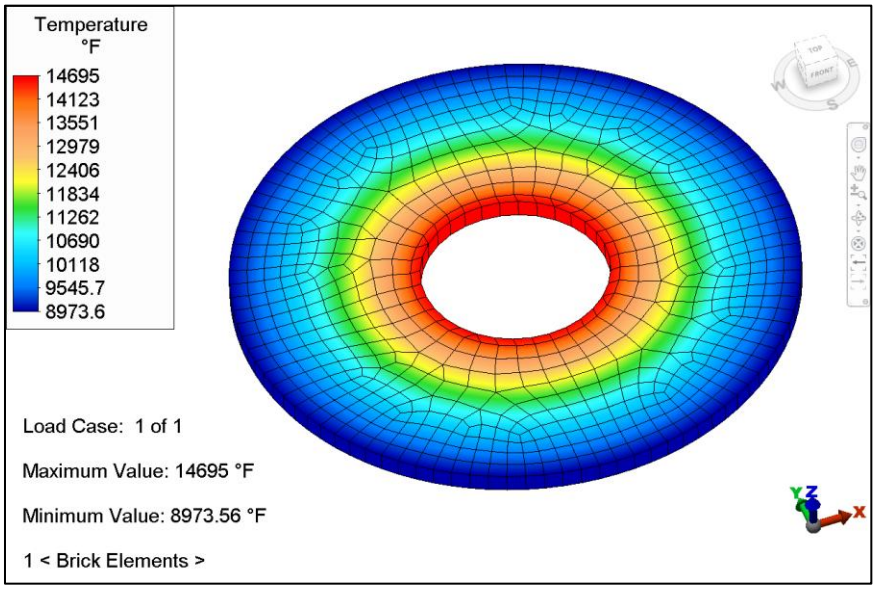

Figure 45-1. The 1/4 section model of the cylindrical disk was meshed and analyzed using three different element types. Here the temperature results from brick elements are shown.

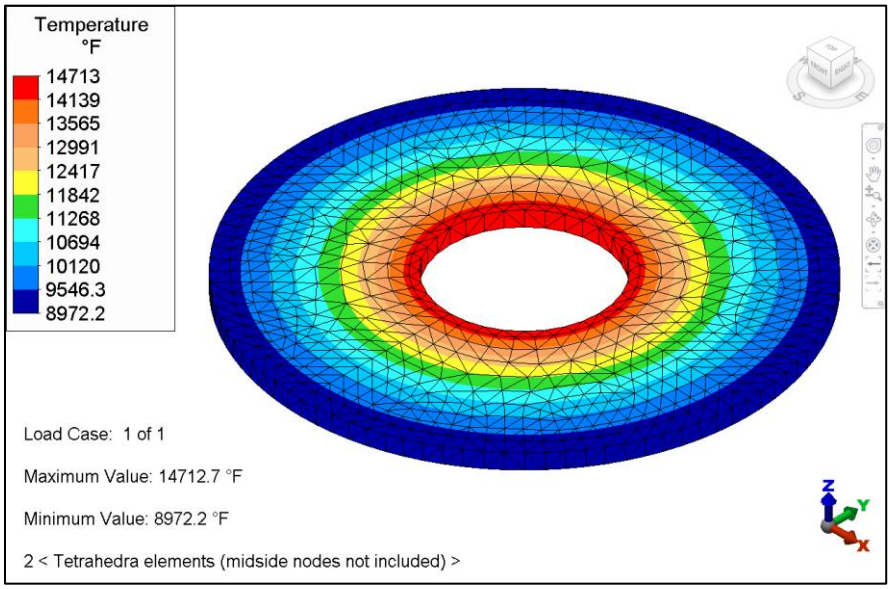

Figure 45-2. Tetrahedra elements without midside nodes. (2 mirror planes were activated to show the full model)

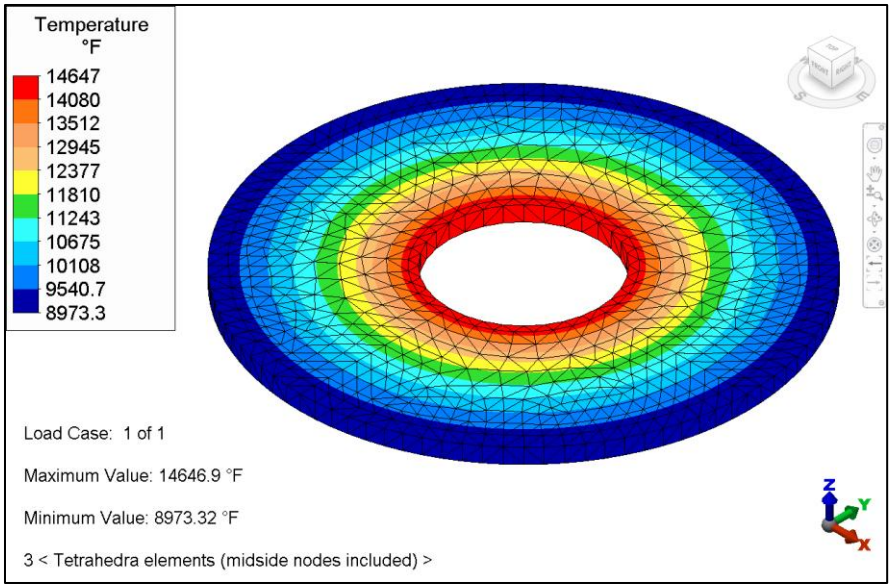

Figure 45-3. Tetrahedra elements with midside nodes. (2 mirror planes were activated to show the full model)

Comparison of Element Types

The CAD model was created in Autodesk Inventor 2011. The results demonstrate that brick elements provided accurate results with the fewest elements.

Obtaining similar results with tetrahedral elements required more elements and computing resources. However, tetrahedral elements provided a useful comparison to analysis results using brick elements. The results also demonstrate the accuracy of the Steady-State Heat Transfer analysis processor.

Table 45-1. Comparison of Results

	Theory	Brick elements	Tetrahedra elements without midside nodes	Tetrahedra elements with midside nodes
Number of Elements	NA	180	1648	1648
Radiation Temperature (°F)	8971.8	8973.56	8972.2	8973.32
% Difference	NA	0.02	0.00	0.02

AVE - 46 Shear Force and Bending Moment Analysis of a Beam under Distributed Loading

Reference

Popov, E. P., *Introduction to Mechanics of Solids*, Prentice-Hall, Inc., Englewood Cliffs, New Jersey, 1968, p. 39.

Problem Description

Shear force and bending moment analysis of a beam under distributed loading. The beam is loaded as shown in the figure below. The problem involves computation of shear and bending-moment diagrams for the beam under distributed loading using the summation procedure. It demonstrates the Result's environment shear force and bending moment diagram display capability.

Theoretical Solution

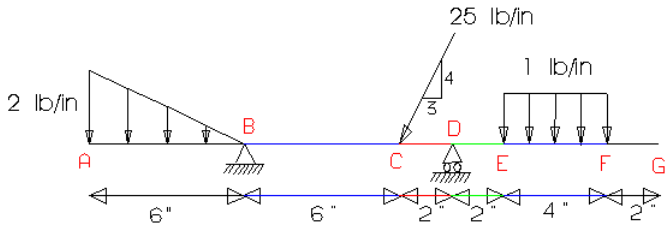

Figure 46-1. Loading of beam.

We compute the reactions first. Using $\sum M = 0$ the vertical reactions at B and D are computed as 12 lbs. and 18 lbs., respectively. With reactions known, the summation of the forces gives the shear force diagram. The total downward force from A to B is 6 lbs., which is the positive ordinate of the shear diagram.

At B, an upward reaction of 12 lbs. moves the ordinate of shear diagram upward to +6 lbs. No forces are applied to the beam between B and C, hence there is no change in the value of shear. At C, the 20 lbs. downward component of the concentrated load lowers the value of shear to -14 lbs.

Between E and F, a uniformly distributed load acts downward. An increase in shear takes place at a constant rate of 1 lb/in. At F, shear becomes zero (final check). Next, we get the moment at different points by integrating shear areas. Therefore we get:

- $M_B = -2/3 * 6 * 6 = -24$ lbs.-in.
- $M_C = M_B + 6 * (6) = 12$ lbs.-in.
- $M_D = M_C - 14 * (2) = -16$ lbs.-in.
- $M_E = M_D + 4 * (2) = -8$ lbs.-in.
- $M_F = M_E + 1/2 * 4 * (4) = 0$ lbs.-in.

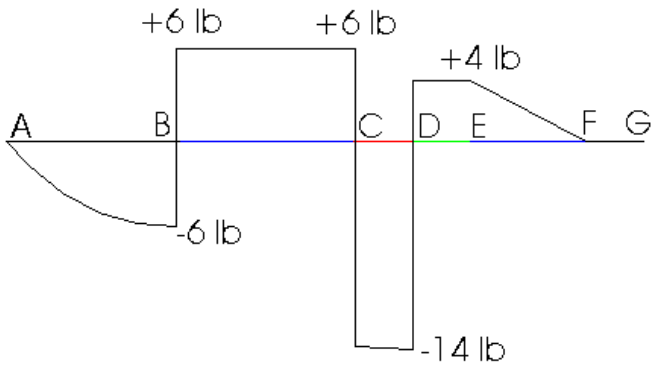

Figure 46-2. Shear force diagram.

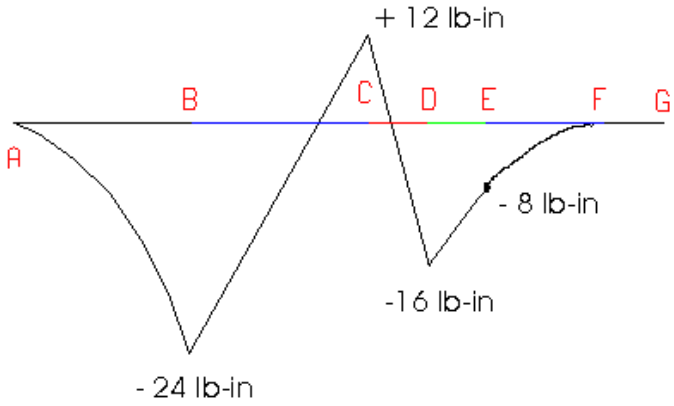

Figure 46-3. Bending moment diagram.

Autodesk Simulation Solution

The beam has pinned boundary conditions (TxyzRxy) at B and is simply supported at D (TyzRxy). A triangular distributed loading (2 to 0 lb/in) is applied from A to B. A linearly distributed loading (1 lb/in) is applied from E to F. A nodal force of magnitude 25 lbs. is applied at point C at a gradient of 4/3. Six beam elements were used.

The following geometric and material properties for the beam are necessary for the FEA model even though they are not required for shear and bending moments calculations.

- E = 3E7 psi (Young's modulus)
- A = 1 in^2 (Beam cross-sectional area)
- L = 22 in (Length of the beam)
- I = 0.0833 in^4 (Moment of inertia)

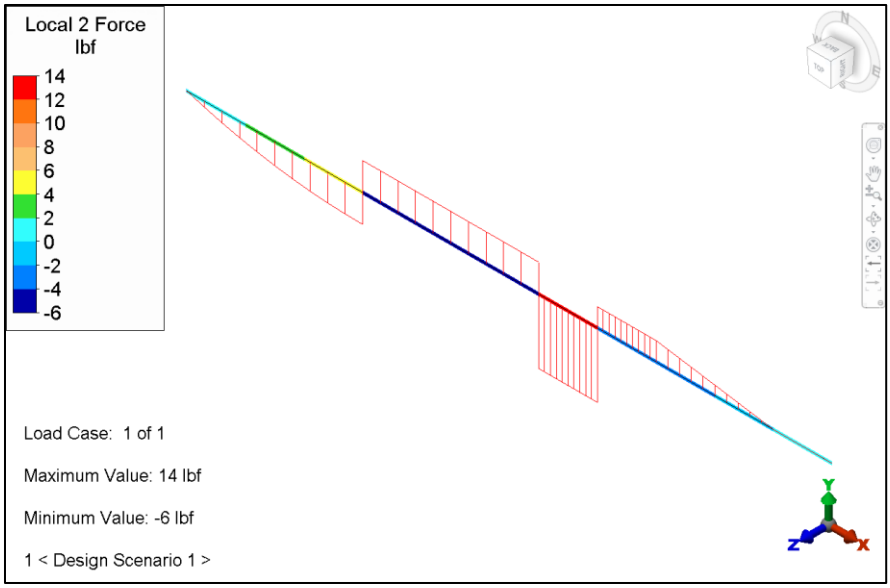

Figure 46-4. Shear force diagram and Local 2 direction force results.

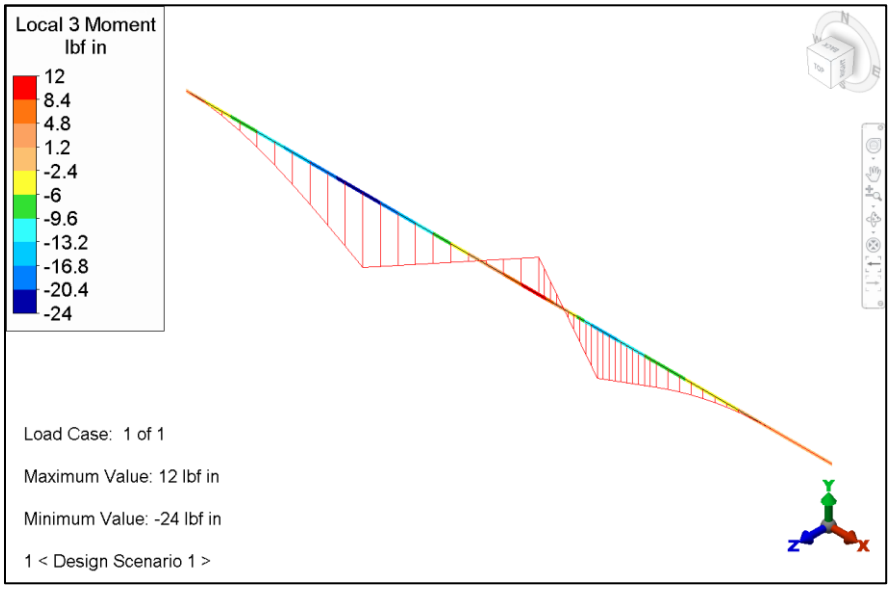

Figure 46-5. Bending moment diagram and Local 3 direction moment results

The theoretical and analytical solutions are given below in tabular form. The results demonstrate the accuracy of the Linear Static Stress analysis processor.

Table 46-1. Comparison of Results

Bending Moment (lb-in)	Theory	Analysis	% Difference
M_B	-24.00	-24.00	0.0
M_C	+12.00	+12.00	0.0
M_D	-16.00	-16.00	0.0

AVE - 47 Thermal Stress Analysis of a Thick-walled Cylindrical Vessel Under Temperature Gradient

Reference

Roark, R.J. and Young, W.C., *Roark's Formulas for Stress and Strain*, Fifth Edition, McGraw-Hill, New York, 1975, p. 585, problem 16.

Problem Description

In this example, we analyze a hollow cylinder with thick walls. There is a temperature difference (ΔT) between the outside and inside surfaces. The same geometry was analyzed in AVE - 12 using brick elements.

The solution is valid away from the ends of the cylinder. The steady-state temperature distribution is logarithmic through the thickness; that is, a steady-state temperature distribution. For this example, an outside radius of 2" and an inside radius of 1" was considered with a temperature difference of 10^{o}F.

Theoretical Solution

Outer surface tangential stress (tension):

$$\sigma_t = \frac{\Delta T \alpha E}{2(1-\nu)\log_e\left(c/b\right)}\left[1 - \frac{2b^2}{c^2 - b^2}\log_e\left(c/b\right)\right]$$

Inner surface tangential stress (compression):

$$\sigma_t = \frac{\Delta T \alpha E}{2(1-\nu)\log_e\left(c/b\right)}\left[1 - \frac{2c^2}{c^2 - b^2}\log_e\left(c/b\right)\right]$$

Where:

- $\Delta T = 10^{o}$F (temperature difference, hotter on the inside than outside)
- α = 6E-6/^{o}F (coefficient of thermal expansion)
- c = 2" (outside radius)
- b = 1" (inside radius)
- ν = 0.3 (Poisson's ratio)
- E = 30E+6 (Young's modulus)

Autodesk Simulation Solution

The cylindrical vessel was modeled using 2-D axisymmetric elements. Care was taken to get a smooth mesh with smaller elements at the inside radius where the high stresses were expected. The resulting mesh had 528 nodes and 480 elements. Symmetry boundary conditions of Tz were applied along the nodes z = 0.

The model was analyzed with the Steady-State Heat Transfer analysis processor. Nodal temperatures were then transferred to the Linear Static Stress analysis processor. The theoretical and analytical results are shown in the table below.

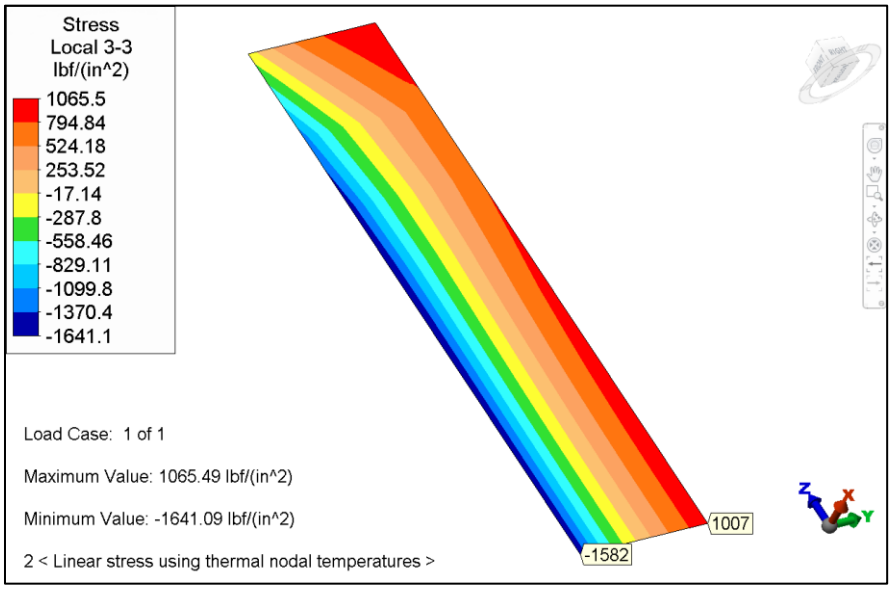

Figure 47-1. Stress contours (Local 3-3) for the model of the thick-walled cylinder.

Table 47-1. Comparison of Results

	Theory	Analysis	% Difference
σ_{33} Outer Surface (psi)	997.75	1007	0.93
σ_{33} Inner Surface (psi)	-1573.68	-1582	0.53

AVE - 48 Elastic Stability of a Flat Plate under a Pure Axial Load

Reference

Roark, R. J. and Young, W. C., *Roark's Formulas for Stress and Strain*, Fifth Edition, McGraw-Hill, New York, 1975, p. 550.

Problem Description

The verification problem involves determining the critical load at which a flat plate under a pure axial load will become elastically unstable (i.e., when buckling will occur). The square plate is subjected to compressive axial forces uniformly distributed along facing edges, which are simply supported. The plate measures 20" x 20" x 0.5".

Theoretical Solution

The critical load at which the plate will become unstable is defined as:

$$\sigma' = \kappa \frac{E}{1-\nu^2}\left(\frac{t}{b}\right)^2 = 67{,}788 \text{ psi}$$

Where:

- t = 0.50" (plate thickness)
- a = 20" (length of plate)
- b = 20" (width of plate)
- E = 30E6 psi (Young's modulus)
- ν = 0.3 (Poisson's ratio)
- κ = 3.29 (parameter from Roark and Young table for a/b = 1)

Autodesk Simulation Solution

One quarter of the plate was modeled with 400 3-D plate/shell elements using simply supported boundary conditions (Tx) at all exterior edges. Symmetry boundary conditions Tz Rxy and Ty Rxz were applied at the symmetry edges. The plate elements were 0.50 inches thick.

The Linear Critical Buckling Load analysis type was used. The plate elements were loaded along the edge using nodal forces based on a 1 lb compressive axial nodal load (giving 4 psi axial stress, which is multiplied by the buckling load multiplier to give the critical compressive stress σ').

* Analyzed Critical Compressive stress:
= 4 psi x 16964.7
= 67,858 psi

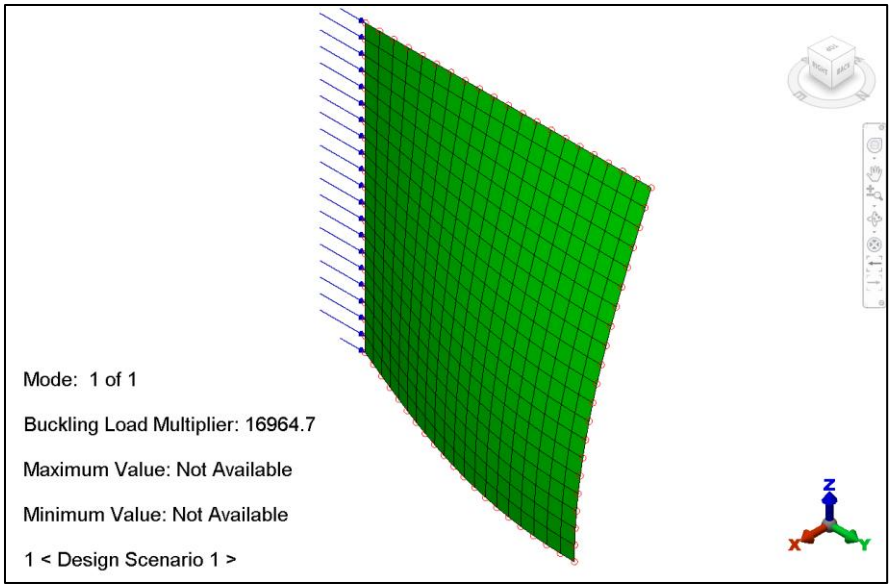

Figure 48-1. Displaced shape for the quarter-symmetry model of the flat plate under a pure axial load.

The theoretical and analysis solutions are provided in the following table.

Table 48-1. Comparison of Results

σ' (sigma x BLM) psi		
Theory	**Analysis**	**% Difference**
67,788	67,858	0.10

Note: The use of symmetry in a buckling analysis to reduce problem size is not recommended unless the buckling mode is known to have the exact same symmetry as used in the geometry and loading. For this model and this loading, using symmetry led to the right answer, but in general it can be a risky shortcut to assume the shape of the answer before performing the analysis.

AVE - 49 Concrete Frame Structure Subjected to Distributed Loading

Reference

Wang, Chu-Kia, *Introductory Structural Analysis*, Prentice-Hall, New York, 1973, p. 356.

Problem Description

A concrete frame structure measuring 20 ft across and 16 ft high is subjected to a distributed loading. The dimensions and loadings for the frame are shown in the drawing below. We will analyze the concrete frame's bending moment.

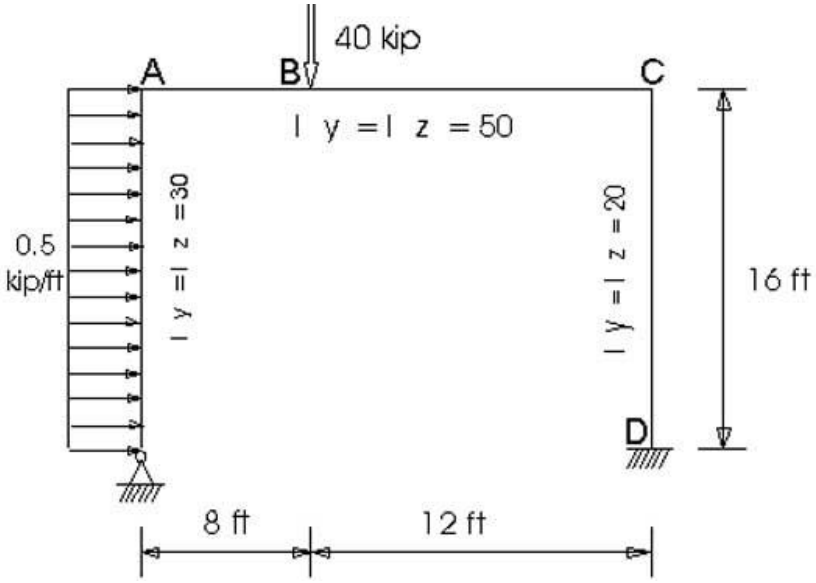

Figure 49-1. Loadings and dimensions.

Theoretical Solution

The theoretical results are obtained using the force method: consistent deformation using reactions as redundant. The values used for the computation are:

- w_o = 0.5 kips/ft (uniform distributed loading as shown above)
- E = 710310 psi (modulus of elasticity for concrete)
- ν = 0.2 (Poisson's ratio for concrete)
- A = 10 in^2 (beam cross-sectional area)
- P = 40 kips (force applied at the top beam)

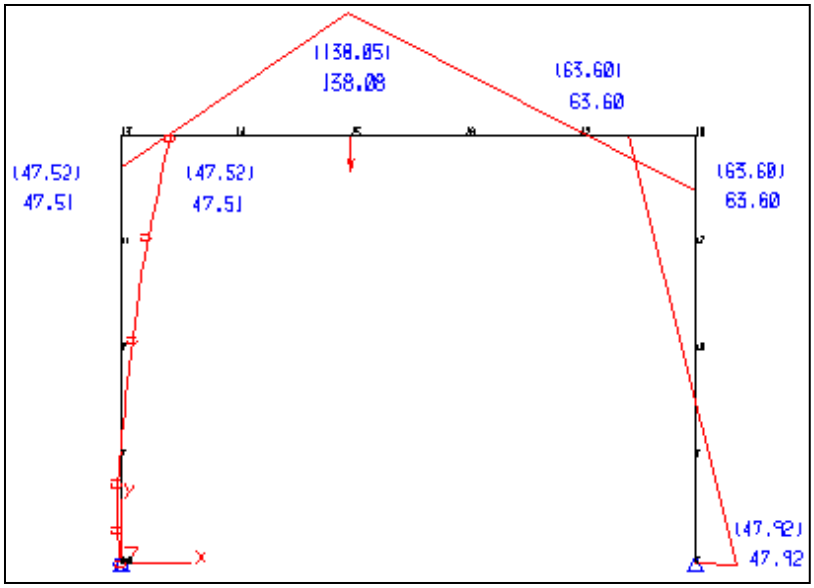

Figure 49-2. The bending moment diagram (ft-kips) for the concrete frame. The theoretical values are in parentheses; the converted results are below.

Autodesk Simulation Solution

Four beam elements were used to model each column. Five elements were used to model the cross-beam. To simulate the simply supported boundary conditions at one end of the beam, Txyz Rxy is fixed. At the other end, Txyz Rxyz is fixed. This problem demonstrates the uniformly distributed loading capability of Autodesk Simulation.

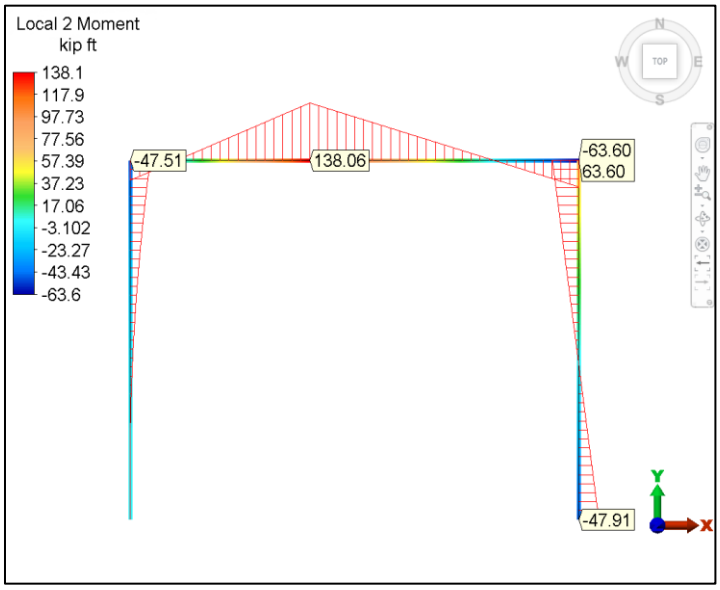

Figure 49-3. The Bending moment diagram and local 2 Moment for the concrete frame model.

The table below shows theoretical and analysis results from the Linear Static Stress Analysis processor. Note that the dimensions, properties of the model use inches as the unit of length and pounds as the unit of force, while the theoretical results and the figure abve and the table below use feet and kips.

Table 49-1. Comparison of Results

Bending Moment (ft-kips)			% Difference
Location	**Theory**	**Analysis**	
A	47.52	47.51	0.02
B	138.05	138.06	0.01
C	63.60	63.60	0.00
D	47.92	47.91	0.02

AVE - 50 Solid Aluminum Cylinder Exposed to a Convection Environment and Allowed to Cool

Reference

Holman, J. P., *Heat Transfer*, Fifth Edition, McGraw Hill, Inc., New York, page 129.

Problem Description

A long, solid aluminum cylinder 5 cm in diameter and initially at a temperature of 200^o C is suddenly exposed to a convection environment of 70^o C and allowed to cool with a convection coefficient of 525 W/m^2*°C. Find the temperature at a radius of 1.25 cm after 1 minute.

Theoretical Solution

The following parameters were used:

- T = 70 °C (ambient convection temperature)
- h = 525 W/(m^2*°C) (convection coefficient)
- k = 215 W/(m*°C) (conduction coefficient)
- ρ = 2700 kg/m^3 (density)
- c_p = 900 J/(kg*^{o}C) (specific heat)
- T_{init} = 200 ^{o}C (initial temperature)
- α = 8.4x10^5 m^2/s (thermal expansion coefficient)

The Heisler charts discussed in the reference were used to first determine the temperature along the axis of the cylinder and then compute the temperature for a radius of 1.25 cm (r/r_0 = 0.5):

- θ_0/θ_i = 0.38 (from fig. 4-10, Holman)
- θ/θ_0 = 0.98 (from fig. 4-13, Holman)
- $\theta/\theta_i = (\theta_0/\theta_i)(\theta/\theta_0)$ = (0.38)(0.98) = 0.372
- $\theta = T - T_\infty = 0.372\theta_i$ = 0.372(200-70) = 48.4
- T = 70 + 48.4 = 118.4 ^{o}C

Autodesk Simulation Solution

The cylindrical rod was modeled using a 40 x 40 mesh of 2-D axisymmetric thermal elements. The long cylindrical rod was represented by specifying no boundary condition on the ends of the rod (i.e., insulated rod ends).

Convection was applied to the outer surface of the cylinder. An event end time of 60 seconds and 6 total steps were requested from the processor. The Transient Thermal Analysis processor calculated the temperature and heat flux values at every time step.

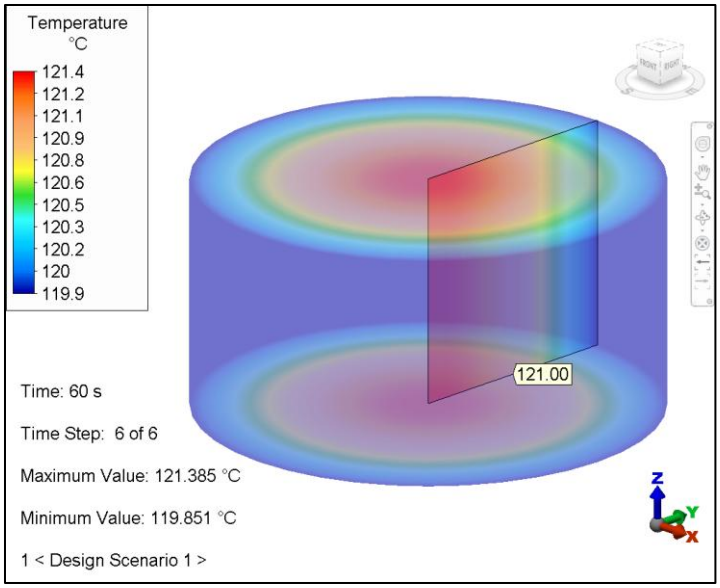

Figure 50-1. Temperature distribution for the axisymmetric model of a cylinder at a time of 60 seconds.

Table 50-1. Comparison of Results

Temperature (°C)		% Difference
Theory	**Analysis**	
118.4	121	2.2

AVE - 51 Fluid Flow between Two Plates

Reference

Chung, T. J., *Finite Element Analysis in Fluid Dynamics*, McGraw-Hill, Inc., New York, 1978.

Problem Description

In this problem, we will analyze 3-D fluid flow between two plates. The bottom plate is stationary while the top plate moves. The problem is used to demonstrate the 3-D Unsteady Fluid Flow Analysis processor.

Theoretical Solution

The analytical solutions shown in the chart below are taken from the reference. The following parameters were used:

- ρ = 0.00242 lbf x s^2/in/in^3 (Mass density)
- v = 0.00362 lbf x s/in^2 (Dynamic viscosity)
- V_y = 0.1 in/s (Velocity)

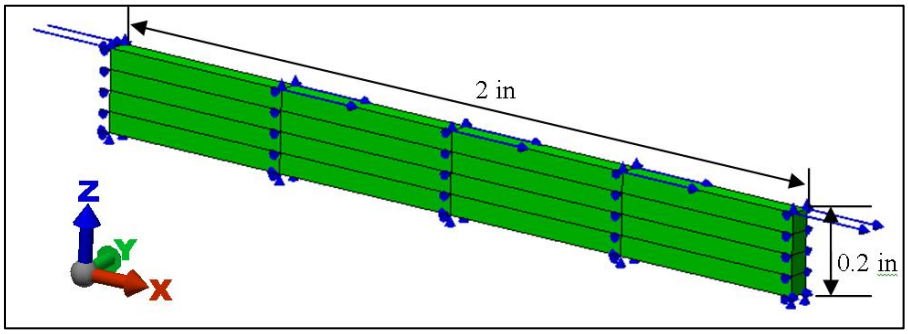

Figure 51-1. Illustration of the construction and loading of the 3-D solid "brick" model.

Autodesk Simulation Solution

A 1x4x4 mesh of 3-D solid "brick" elements were used to model the problem. The nodes at the bottom were fixed using velocity boundary conditions and the velocity was applied in the x direction as shown in the drawing (with Vy and Vz set to 0). Symmetric boundary conditions are set at the two surface nodes at depth direction to zero restrain velocity in y direction. Note that the element depth value in y direction does not contribute to result, but affect element quality. Finally the reference pressure has to be set at the inlet surface. Here we are using inlet/outlet boundary condition.

A backward difference time integration scheme was used for time marching algorithm in segregated formulation. The load curve of a single load interval was designed with 100 time steps with a starting time of 0.0 and an ending time of 0.01 sec. The starting and ending load factor were both set to 1.0. This simulates a sudden impulsive motion.

The 3-D Unsteady Fluid Flow Analysis Processor performed the time history analysis. The velocities at nodes 19, 39 and 43 are compared in the chart below.

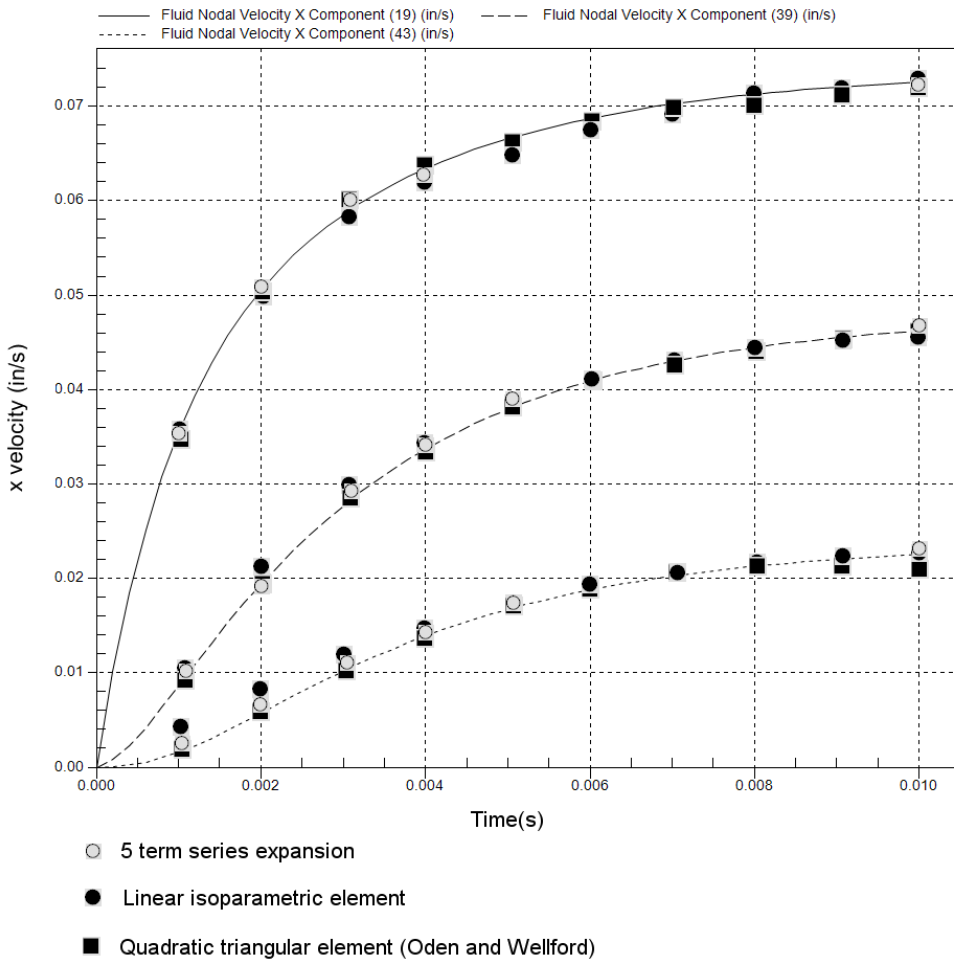

Figure 51-2. Time history of the Y velocity at nodes 19, 34 and 49. Both the analytical and software solutions are shown.

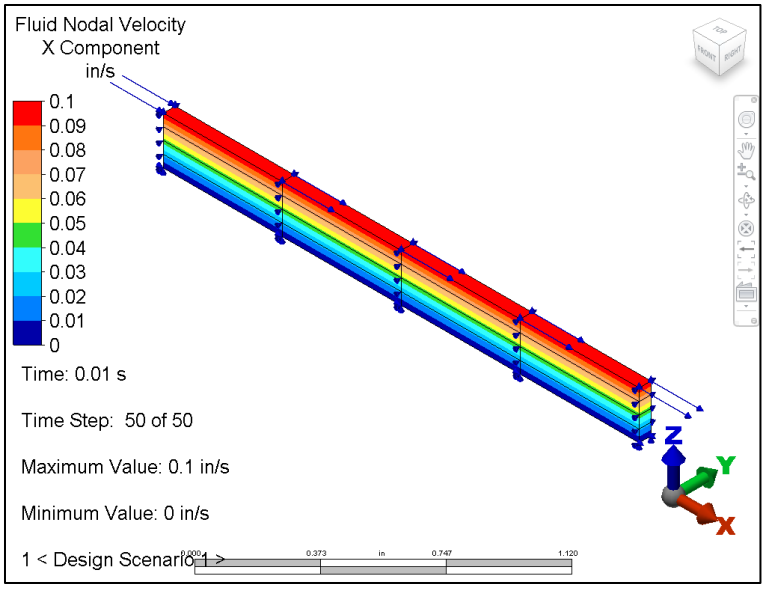

Figure 51-3. Velocity contour of X component in 3-D transient Couette flow problem.

AVE - 52 2-D Laminar Flow over a Backward Facing Step

Reference

Armaly, B. F., Durst, F., Pereira J. C. F. and Schonung, B., *Experimental and Theoretical Investigation of Backward Facing Step Flow*, J. Fluid Mech., p. 473-496, 1983.

Problem Description

The geometry and boundary conditions for this classical CFD problem are shown in Figure 053-1 below. The aspect ratio of the backward facing step (h) to the overall cross-sectional width is 1:2, and the total length in horizontal direction is 30h.

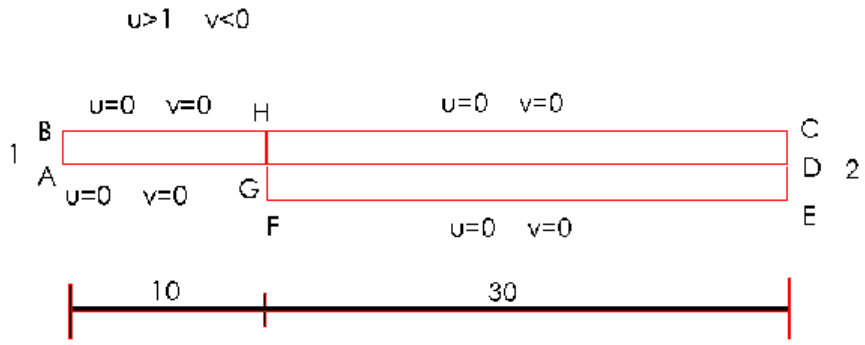

Figure 52-1. Illustration of the geometry and boundary conditions for the backward facing step model.

Theoretical Solution

A fully developed parabolic velocity profile is formed at the inlet boundary, GH, by prescribing a linear velocity profile at edge AB. The flow was analyzed for Reynolds number 100.

Autodesk Simulation Solution

The problem was modeled with 2-D planar elements and analyzed using the Steady Fluid Flow analysis processor. A fully structured mesh of 40 x 150 was used for the region ABCD and 40 x 100 for the region GFED. The Reynolds number is based on the bulk velocity (1.0) at the inlet boundary and the cross-sectional width of the entire domain (2.0).

The following properties were used for the analysis:

- ρ = 1.0 Mass density (ML^{-3})
- μ = 0.02 Dynamic viscosity ($ML^{-1}\ T^{-1}$)
- V_y = 1.0 Velocity (LT^{-1})

The reattachment length can be determined in Results interface as follows. Display the Y Velocity and inquire to get the Y velocity values at the nodes from the backward facing step on downstream in the Y direction (one node up from the bottom). Find the two adjacent nodes with -Y and +Y velocity values closest to zero. Linear interpolation between the nodes gives the precise location where Y velocity is zero. One can also use the Path Plot feature. The distance from the backward facing step to this location is the reattachment length.

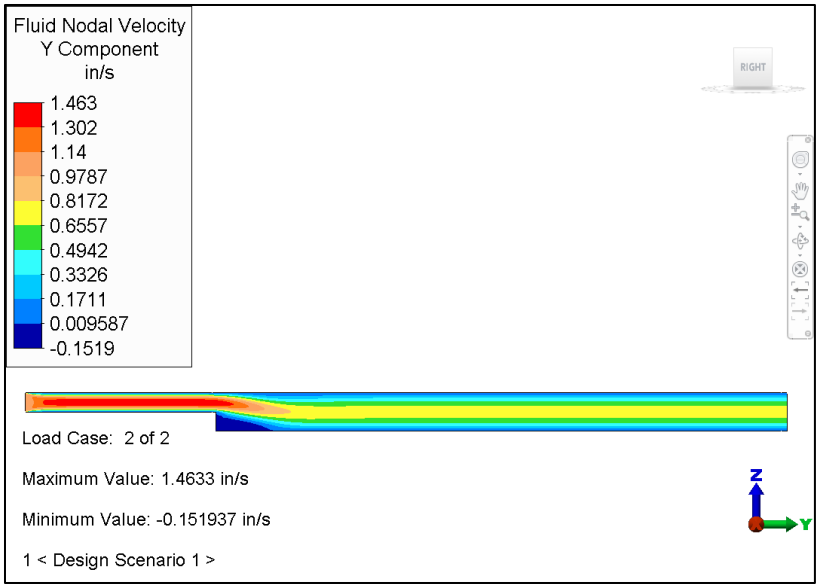

Figure 52-2. The velocity plot of the backward facing step for Reynolds Number = 100.

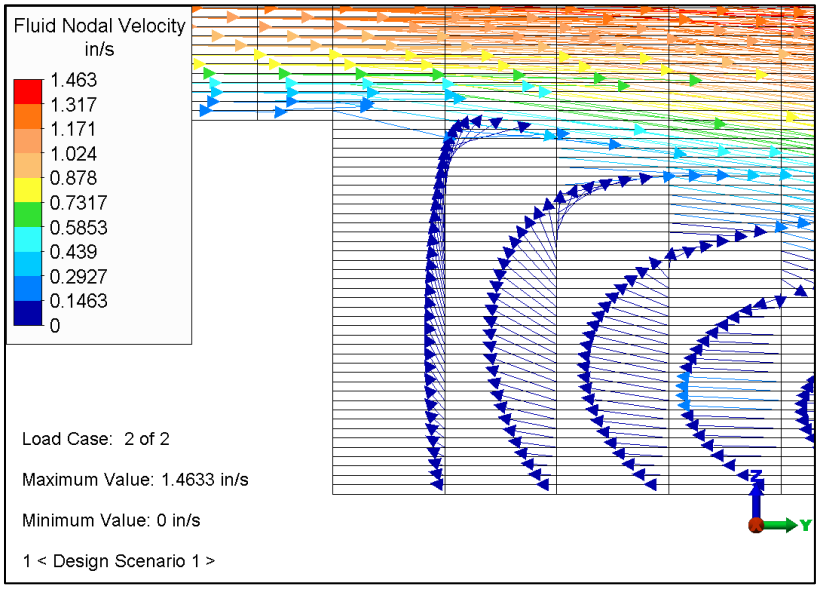

Figure 52-3. A zoomed-in view of the vector plot.

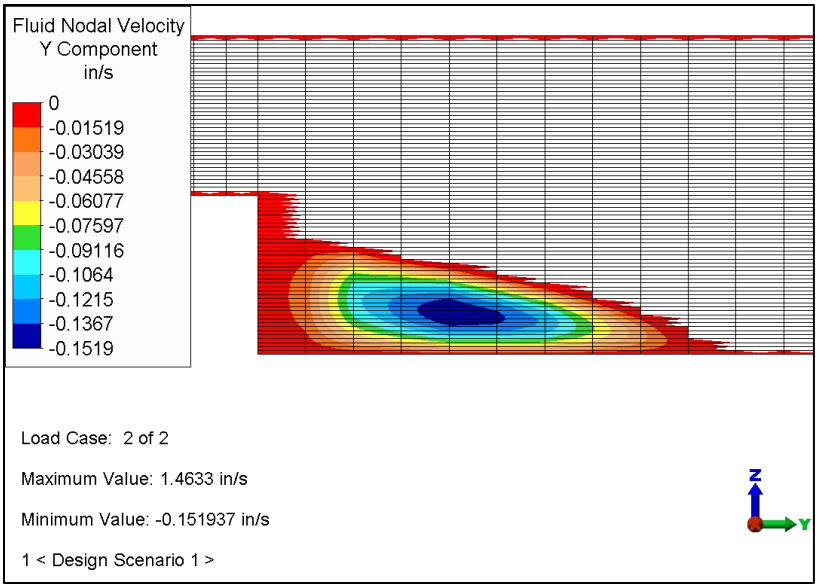

Figure 52-4. The recirculating zone behind the backward facing step. This display shows the Y velocity in part of the model with auto range feature deactivated and a specified range with a maximum value of zero. All the results above 0 are hidden.

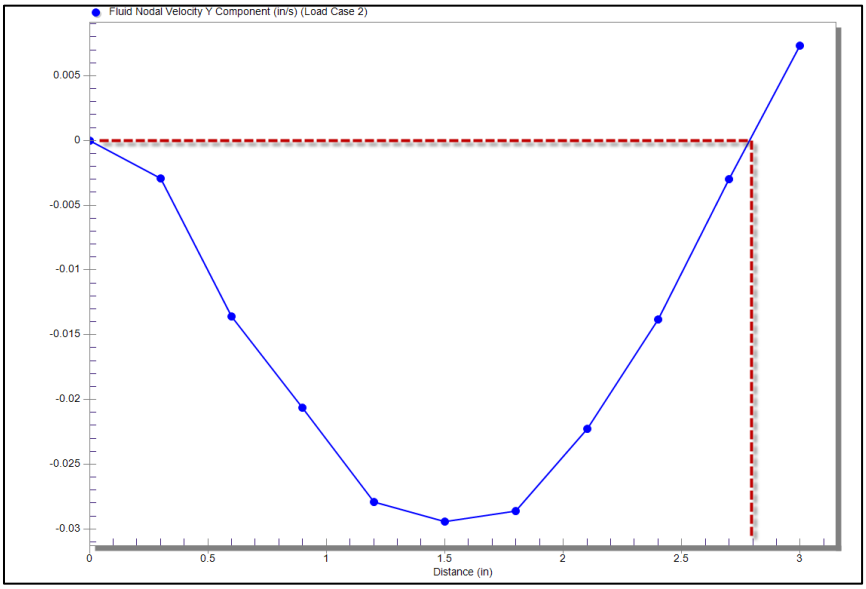

Figure 52-5. Y velocity values at the nodes from the backward facing step on downstream in the Y direction (one node up from the bottom)

Table 52-1. Comparison of Results

Reattachment Length		% Difference
Reference	Analysis	
3.00	2.8	6.67

AVE - 53 Linear Mode Shape with Load Stiffening Analysis on a Simply Supported Continuous Beam

Reference

Timoshenko, S., Weaver, W. and Young, D. H., *Vibration Problems in Engineering*, New York: Wiley, 1974, pp. 454-455.

Problem Description

In this problem, we perform a linear mode shape with load stiffening analysis on a simply supported continuous beam. The problem utilizes a 2" x 8" x 200" steel beam which is simply supported under compressive axial loading of 20,000 lbs.

Theoretical Solution

The theoretical solutions were derived using a FORTRAN program developed from the reference. The theoretical problem formulation is as follows:

The frequency equation is given by:

$$\omega_i = \frac{1}{2\pi}\frac{i^2\pi^2}{l^2}\sqrt{\frac{(EI)}{(\rho A)}\left(1 \pm \frac{Sl^2}{i^2 EI\pi^2}\right)} \text{ Hz}$$

Where:

- i = (1,2,3 ...) for different mode shapes
- l = 200 in (length of the beam)
- E = 30E6 psi (modulus of elasticity)
- I = $bh^3/12$ in^4 (area moment of inertia)
  = 85.3 in^4 for bending in the XY plane
  = 5.33 in^4 for bending in the XZ plane
- ρ = 7.324E-4 $lb(s^2)/in^4$ (mass density)
- A = 16 in^2 (cross-sectional area)
- S = 20,000 lb (axial load)
- +/- = denotes tensile or compressive load, respectively

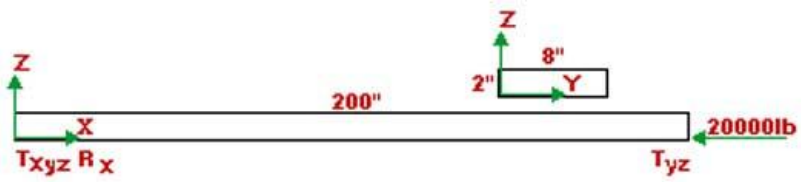

Figure 53-1. Line drawing shows the beam orientation and dimensions.

Autodesk Simulation Solution

The geometry was modeled with 20 beam elements. The analysis results were obtained using the Linear Mode Shapes and Natural Frequencies with Load Stiffening analysis processor.

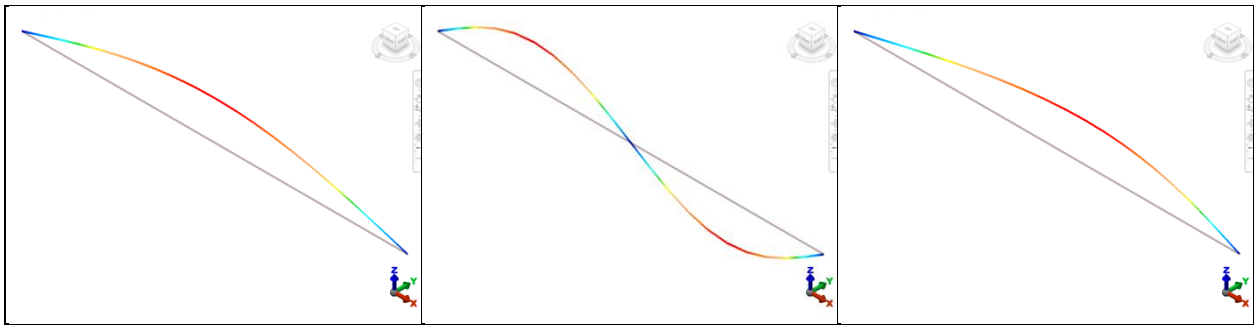

Figure 53-2. Three example mode shapes of the simply supported continuous beam. The gray line is the non-deflected beam

The theoretical and computed frequencies for vibrations in the XY and XZ planes are shown in the table below.

Table 53-1. Comparison of Results

Analysis Mode Number	Modal Plane	Frequency (Hz)		% Difference
		Theory	Analysis	
1	XZ	3.2211	3.2211	0.00
2	XZ	17.147	17.147	0.00
3	XY	18.058	18.058	0.00
4	XZ	40.105	40.104	0.00
5	XZ	72.223	72.215	0.01
6	XY	73.113	73.113	0.00
7	XZ	113.51	113.48	0.03
8	XZ	163.97	163.86	0.07
9	XY	164.87	164.86	0.01
10	XZ	223.61	223.31	0.13

AVE - 54 Thick-walled Spherical Shell Subjected to Uniform Internal Pressure of Gradually Increasing Magnitude

Reference

Chakrabarty, J., *Theory of Plasticity*, McGraw-Hill, New York, 1987, pages 307-311.

Problem Description

A thick-walled spherical shell is subjected to uniform internal pressure of gradually increasing magnitude.

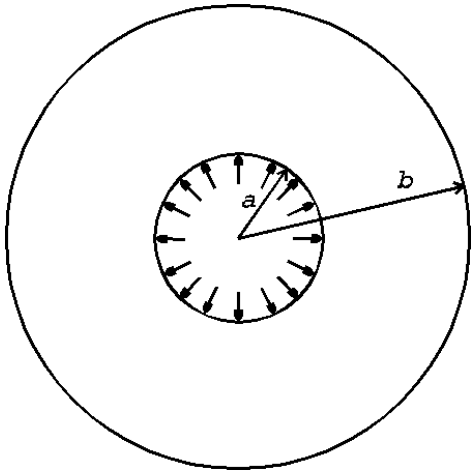

Figure 54-1. A thick-walled spherical shell, whose internal and external radii are a and b respectively, is subjected to uniform internal pressure p of gradually increasing magnitude.

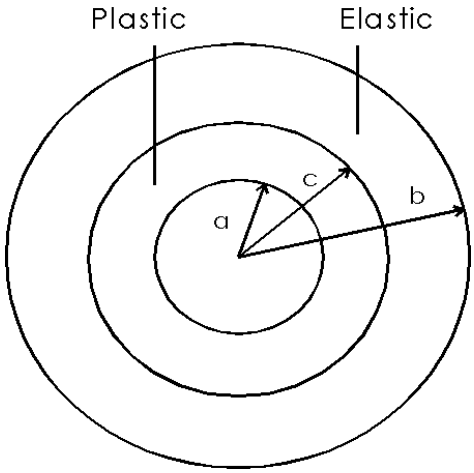

Figure 54-2. The shell is axisymmetric. The material of the shell is assumed to behave in an elastic-perfectly plastic manner. Von Mises yield criterion with the associated flow rule is used to model the plastic flow. Plasticity spreads from the inside surface to the outer surface as shown.

Theoretical Solution

Theoretical solutions for the two limit cases, as plasticity progresses from the inside surface to the outside surface, are considered: Case 1 (the beginning) in which the shell just turns plastic (i.e., the inside surface just becomes plastic); and Case 2 (the end) in which the shell turns completely plastic (i.e., the outside surface just becomes plastic). Two variables are considered: the displacement (radial) of the inside surface and the pressure.

Case 1 just plastic:

$$u_i = \frac{ya}{3E}\left\{(1+\nu)+2(1-2\nu)\frac{a^3}{b^3}\right\} = 0.001116$$

$$p = \frac{2y}{3}\left(1-\frac{a^3}{b^3}\right) = 21000$$

Case 2 fully plastic:

$$u_i = \frac{ya}{E}\left\{(1-\nu)\frac{b^3}{a^3}-2(1-2\nu)\log_e\left(\frac{b}{a}\right)\right\} = 0.0122346$$

$$p = 2y\log_e\left(\frac{b}{a}\right) = 49906.6$$

Where:

- y = 36,000 psi (yield stress of material)
- E = 30 x 10^6 psi (Young's modulus)
- ν = 0.29 (Poisson's ratio)
- Strain hardening modulus = 96,171 psi
- a = 2 in (internal radius of shell)
- b = 4 in (external radius of shell)
- u_i = inside surface radial displacement
- p = pressure applied (psi)

Autodesk Simulation Solution

One radian of half of the shell was modeled using axisymmetric elements. Mild steel material properties were used. Pressure was applied. The dimensions and material properties are shown above.

The analysis results were obtained using the MES nonlinear stress analysis processor. A simple ramp loading curve and a Total Lagrangian analysis formulation were used.

The theoretical and computed results are compared in the table below.

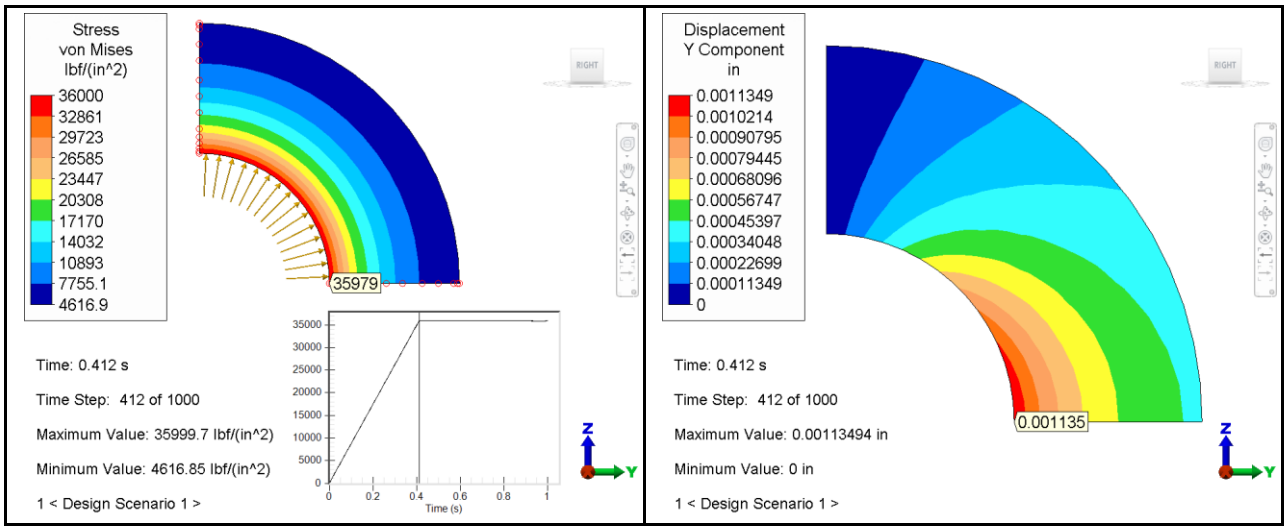

Figure 54-3. A von Mises stress contour and Displacement (Y component) of the thick-walled spherical shell when it is half-plastic. (Time = 0.412 s)

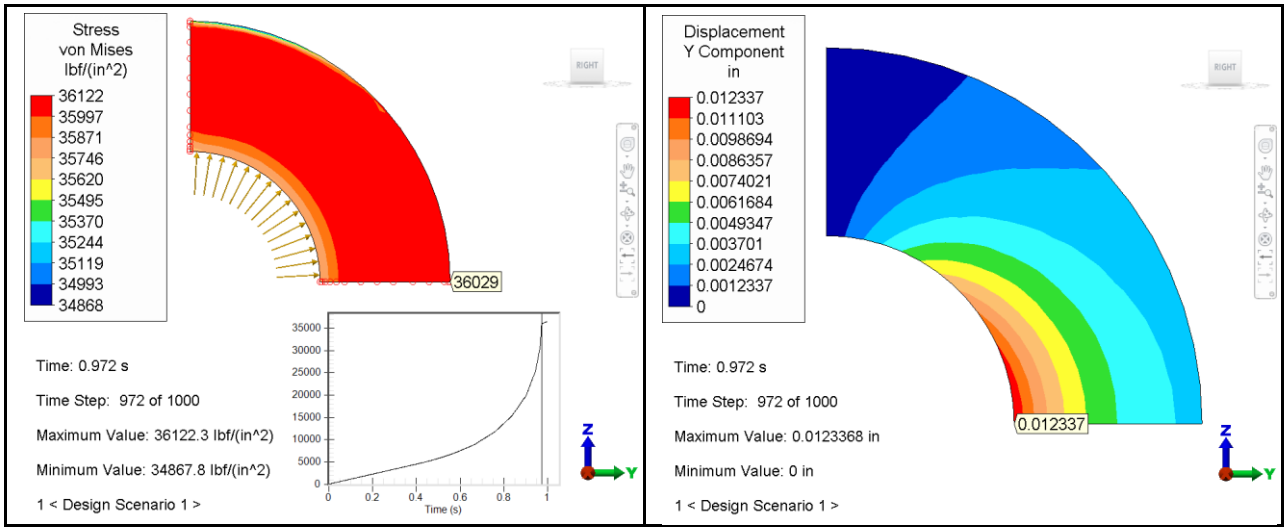

Figure 54-4. A von Mises stress contour and Displacement (Y component) of the thick-walled spherical shell when it is fully-plastic (Time = 0.972 s)

Table 54-1. Comparison of Results

	Just Plastic (Case 1)			Fully Plastic (Case 2)		
	Theory	**Analysis**	**% Difference**	**Theory**	**Analysis**	**% Difference**
Pressure (psi)	21000	21424	2.02	49906.6	50544	1.28
Displacement (in)	0.001116	0.001135	1.70	0.0122346	0.0123368	0.84

AVE - 55 Nonlinear Heat Flow Analysis of a Solid Cylinder

Reference

Holman, J. P., *Heat Transfer*, Fifth Edition, New York: McGraw-Hill Book Company, 1981, p. 31.

Problem Description

A solid cylinder is exposed to a convection temperature T_1 along the top surface and T_4 along the bottom surface. The outside wall is insulated. The thermal conductivity of the cylinder material is known to vary with temperature according to the given function: $K(T) = C_0 + C_1T$. Find the temperature distribution in the cylinder for two cases:

1) K = constant (i.e., $C_1 = 0$)

2) K = K(T)

Theoretical Solution

The heat transfer process may be represented by the resistance network as shown in Figure 55-1 below.

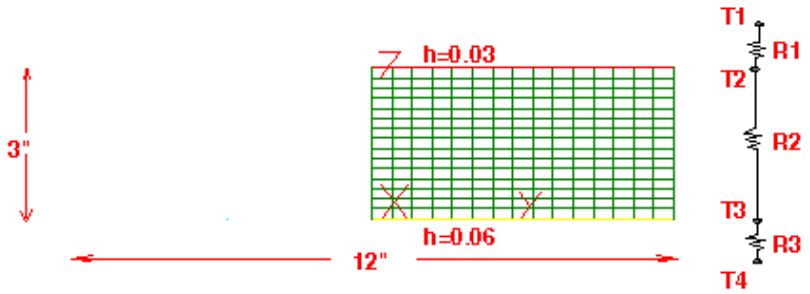

Figure 55-1. The resistance network and dimensions for the axisymmetric solid cylinder model.

The overall heat transfer by convection is expressed in terms of an overall heat-transfer coefficient U, defined by the relation:

$$q = UA\Delta T$$

Where:

$$U = \frac{1}{R_1 + R_2 + R_3} = \frac{1}{\frac{1}{h_1} + \frac{\Delta x}{K} + \frac{1}{h_2}}$$

Where:

- h_1 = 0.03 BTU/min*in^2*^{o}F (convection coefficient of the top surface)
- h_2 = 0.06 BTU/min*in^2*^{o}F (convection coefficient of the bottom surface)
- Δx = 3.0 in (height of the cylinder)
- d = 12 in (diameter of the cylinder)
- $A = \pi d^2/4$ = 113.10 in^2 (surface area)
- T_1 = 2000^{o}F (convection temperature of the top surface)
- T_4 = 200^{o}F (convection temperature of the bottom surface)
- K = Average thermal conductivity of the cylinder in BTU/min*in*^{o}F

Autodesk Simulation Solution

A 1/2-section of the cylinder was modeled using 225 2-D axisymmetric elements. The top and bottom surfaces were made to have different surface numbers for convenient specification of the different convection coefficients and temperatures in the surface data definition screens. The results demonstrate the accuracy of the Steady-State Heat Transfer Analysis processor.

Case 1

- K = 0.02 BTU/min*in*^{o}F (constant)
- $R_1 = 1/h_1 = 33.33$ (convection resistance)
- $R_2 = \Delta x/K = 150$ (conduction resistance)
- $R_3 = 1/h_2 = 16.67$ (convection resistance)
- $R_T = R_1 + R_2 + R_3 = 200$
- $U = 1/R_T = 1/200$
- $T_2 = T_1 - [(R_1/R_T)* \Delta T] = 1700^{o}$F (theory) (temperature of cylinder top surface)
- $T_3 = T_1 - [(R_1 + R_2)/R_T]* \Delta T = 350^{o}$F (theory) (temperature of cylinder bottom surface)
- $q = UA\Delta T = 1017.9$ BTU/min (theory)

A temperature contour for Case 1 is shown below.

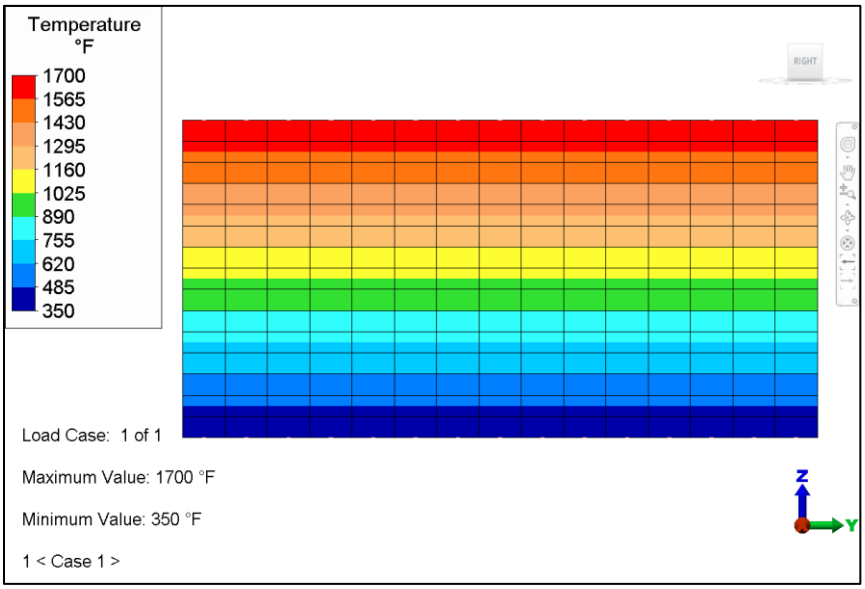

Figure 55-2. Temperature results for Case 2.

The following table shows the results for Case 1, generated by the Steady-State Heat Transfer Analysis processor after four iterations.

Table 55-1. Comparison of Results for Case 1

	Theory	Analysis	% Difference
T_2 (°F)	1700	1700	0.0
T_3 (°F)	350	350	0.0
q (BTU/min)	1017.9	1017.9	0.0

Case 2

K = 0.02 + T/200,000 BTU/min*in*^{o}F (nonlinear conduction coefficient)

For this case, the function from T_1 to T_2 is integrated to compute the heat rate:

$$q = \int_{T_1}^{T_2} UA\,dT = A\int_{T_1}^{T_2} U\,dT$$

After performing the necessary integration we get:

$$q = \frac{A}{50}\left[T - 1200\ln\left(1+\frac{T}{1600}\right)\right]_{200}^{2000} = 1211.68\ BTU/min$$

- R_T = 168.01
- $T_2 = T_1 - [(R_1/R_T)* \Delta T] = 1642.91^{o}F$ (theory)
- $T_3 = T_1 - [\{(R_1 + R_2)/R_T\}* \Delta T] = 378.60^{o}F$ (theory)

Autodesk Simulation provides values for element heat flux, element heat rate, and overall heat rate through a surface (q). A temperature contour for Case 2 is shown below.

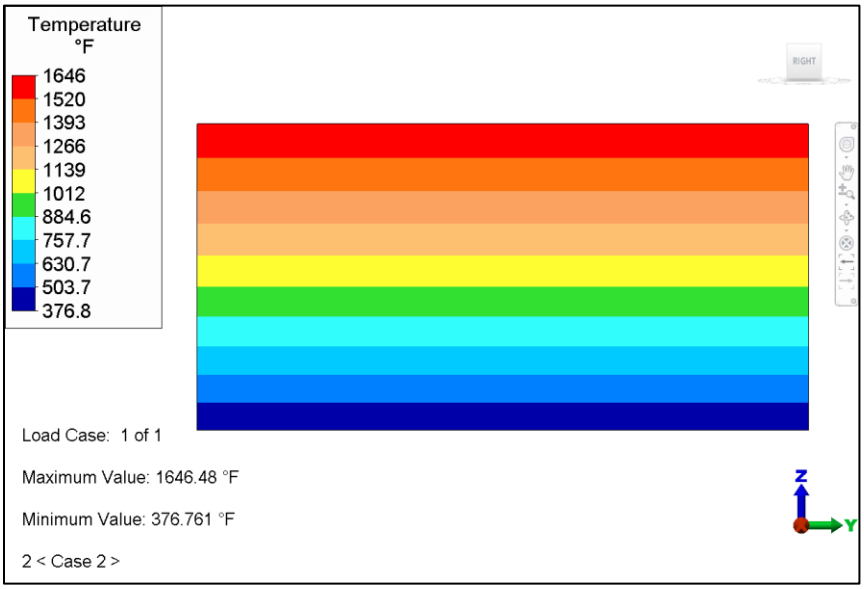

Figure 55-3. Temperature results for Case 2.

The following table shows the results for Case 2, generated by the Steady-State Heat Transfer Analysis processor after four iterations.

Table 55-2. Comparison of Results for Case 2

	Theory	Analysis	% Difference
T_2 (°F)	1642.91	1646.48	0.22
T_3 (°F)	378.60	376.76	0.49
q (BTU/min)	1211.68	1199.46	1.01

AVE - 56 Response Spectrum Analysis of a Simple Beam

Reference

Weaver, W., Timoshenko, S. P. and Young, D. H., *Vibration Problems in Engineering*, New York: John Wiley & Sons, Inc., 1990.

Problem Description

A cantilever beam with mass at the end (see Figure 56-1 below) is excited by ground motion, characterized by a response spectrum. A response spectrum is a plot of the maximum response (i.e., maximum acceleration, velocity, or displacement) to a specified dynamic ground motion on all possible single degree-of-freedom systems.

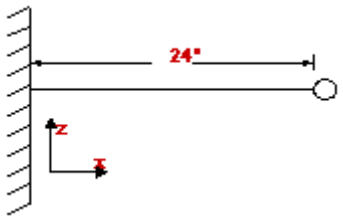

Figure 56-1. The cantilever beam with mass at end subjected to response spectrum input.

Theoretical Solution

Natural Frequency

The theoretical solution for natural frequencies is as follows:

$$K = \frac{3EI}{L^3} = \frac{3(30\times10^6)(1)}{24^3} = 6510.41667 \text{ lb/in} \quad \text{(spring constant of beam)}$$

$$f_1 = \frac{1}{2\pi}\sqrt{\frac{K}{M}} = \frac{1}{2\pi}\sqrt{\frac{6510.41667}{0.1294}} = 35.699 \text{ hertz} \quad \text{(natural frequency)}$$

(agrees with the Linear Mode Shapes and Natural Frequencies Analysis Processor)

$$\delta_{static} = \frac{W}{K} = \frac{50}{6510.4} = 0.768\times10^{-2} = 0.00768 \quad \text{(static deflection)}$$

Where:

- f_{lss} = 35.699 Hz (natural frequency)
- E = 30 x 10^6 psi (Young's modulus)
- I = 1.00 in^4 (moment of inertia)
- S = 0.5 in^3 (section modulus)
- L = 24 in (length)
- W = 50 lb (weight)
- g = 386.4 in/sec^2 (gravity)
- M = W/g = 0.1294 lbm (mass)

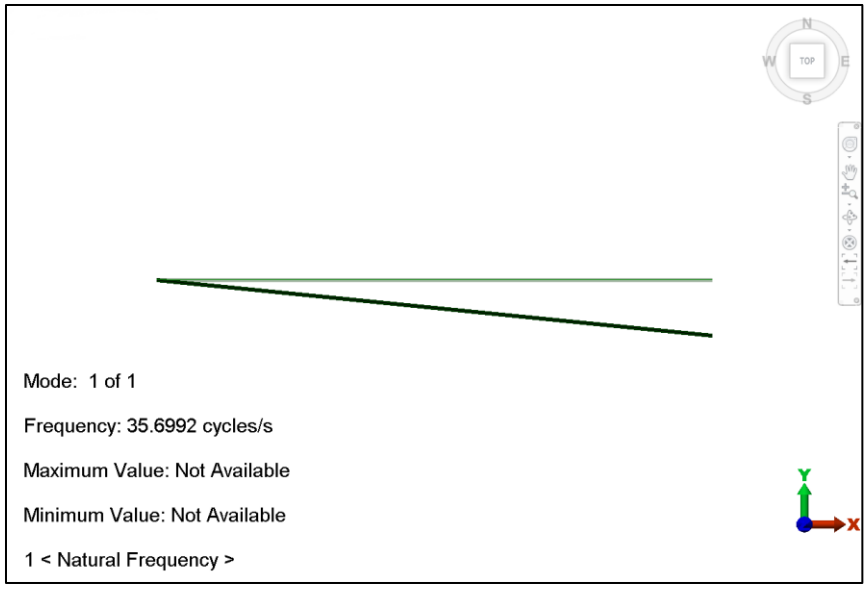

Figure 56-2. Results display of natural frequency for the cantilever beam with mass at end.

Table 56-1. Comparison of Results

Frequency (Hz)		% Difference
Theory	Analysis	
35.699	35.699	0.0

Response Spectrum

At 5% critical damping, find the steady-state response. First, check the eigenvector, Φ (mode shape) and the modal participation factor, Γ.

$\{\Phi\}^T[M]\{\Phi\} = 1$ for mass normalization

$$[M] = \begin{bmatrix} 0.1294 & 0 & 0 \\ 0 & 0.1294 & 0 \\ 0 & 0 & 0.1294 \end{bmatrix}$$

Φ_z is the displacement of the mass in the Z direction. For the X and Y directions, Φ = 0.

For Z, $\Phi_z^2 M = 1$

$$\Phi_z = \sqrt{\frac{1}{0.1294}} = 2.7799$$

(agrees with the Linear Mode Shapes and Natural Frequencies Analysis Processor)

Γ is the participation factor in the Z direction.

$$\Gamma = \frac{\Phi\ M}{\Phi^T M \Phi} = 0.35972$$

(agrees with the Linear Response Spectrum Analysis Processor)

Table 56-2. Comparison of Results

	Theory	Analysis	% Difference
Normalized Modal Y Displacement (in)	2.7799	2.7799	0.0
Maximum Displacement Response (in)	0.0768	0.0768	0.0
Participation Factor Y Direction	0.35972	0.35972	0.0

$$\text{Magnification factor} = \frac{1}{2\zeta} = \frac{1}{2(0.05)} = 10$$

The peak of the response spectrum output is 10.0 g for a 1 g input. The theoretical maximum response is:

$10\delta_{st}$ = 0.0768"

The Linear Response Spectrum Analysis Processor result is 0.0768" with displacement input, and 0.076790" with acceleration input.

The difference with displacement input is 0%, and the difference with acceleration input is 0.013%.

Moments, Stresses and Forces

A check of moments, stresses and forces gives the following:

Theory:

- M = (50)(24)(10) = 12000 lbf-in
- Force = (50)(10) = 500 lbf
- R_z = 500 lbf
- Stress = M/S = 12000/0.5 = 24000 psi

Table 56-3. Comparison of Results

	Theory	Analysis	% Difference
Moment (lbf-in)	12000	12000	0.0
Shear Force (R_z) (lbf)	500	500	0.0
Stress (psi)	24000	24000	0.0

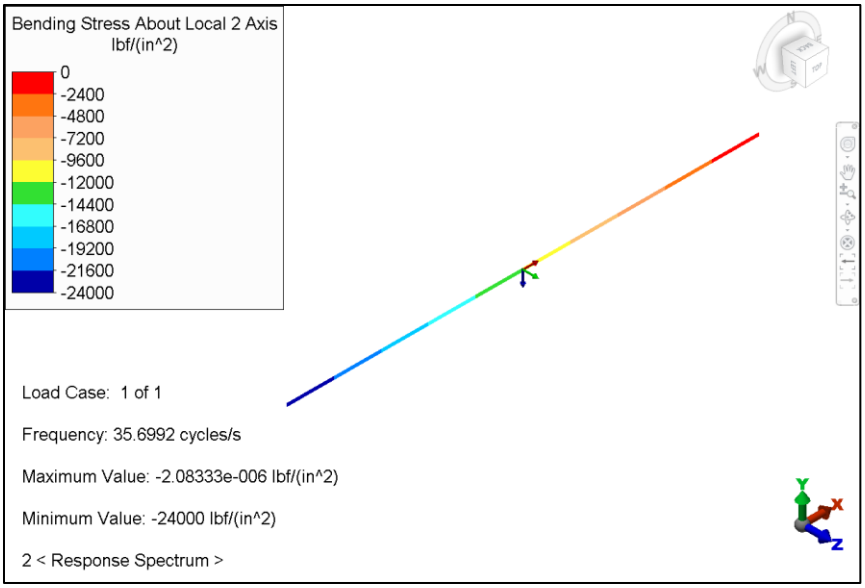

Figure 56-3. Results display of bending stress in the cantilever beam with mass at end subjected to response spectrum input.

AVE - 57 Cantilever Beam with a Gap at the Tip

Reference

Vanderbilt, M. Daniel, *Matrix Structural Analysis*, New York: Quantum Publishers, Inc., 1974.

Problem Description

A 100-inch long cantilever beam is subjected to a concentrated load of 810.0 lb at the tip, as shown in Figure 57-1 below. An elastic support with a stiffness of 202.5 lb/inch is 0.5 inch below the tip.

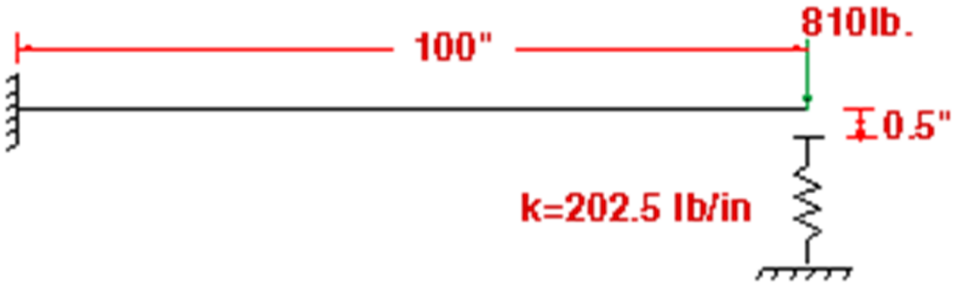

Figure 57-1. Diagram of the cantilever beam with loading and boundary conditions.

The problem parameters are:

- E = 30.0 x 10^6 psi (Young's modulus)
- Area = 9.0 in^2 (cross-sectional area)
- Iy = Iz = 6.75 in^4 (moment of inertia)
- Sy = Sz = 4.5 in^3 (section modulus)
- d = 0.5 inch (gap)

Find:

- The deflection at the tip of the beam
- The reaction of the elastic support

Theoretical Solution

The analytic solution can be found as follows:

$$R = \frac{3 \times E \times I \times d}{4 \times L^3} - \frac{P}{4}$$

$$R = \frac{3 \times 30\,E6 \times 6.75 \times 0.5}{4 \times 100^3} - \frac{810}{4}$$

R = -126.5625 lb

$$\text{Def} = -0.5 - \frac{126.5625}{202.5} = -1.125 \text{ in}$$

Autodesk Simulation Solution

For Linear Static Stress Analysis with gap elements, a compression with gap element with 0.5-inch initial gap space was used to model the gap and spring. Ten beam elements were used to model the cantilever beam. The theoretical and analysis results are given in the table below.

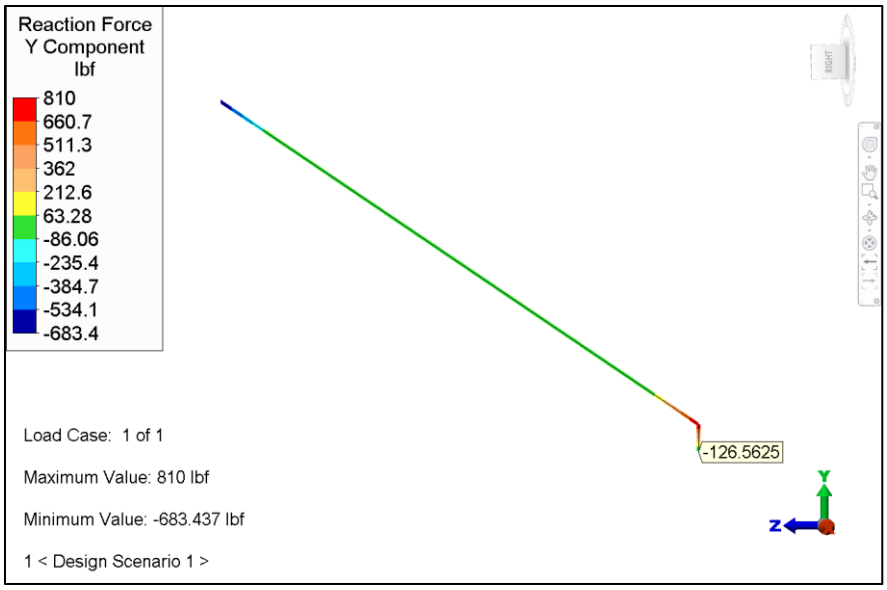

Figure 57-2. Results display of tyhe reaction force in the gap element.

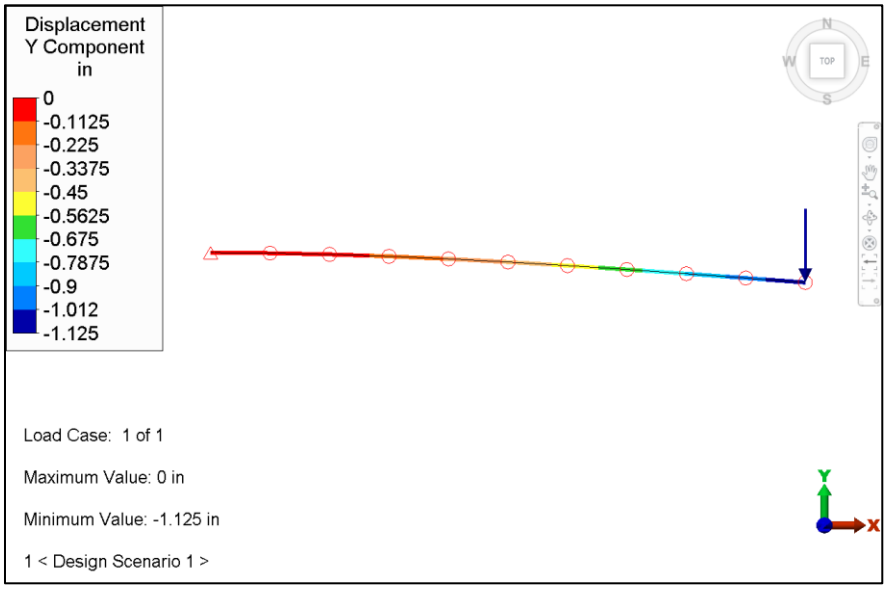

Figure 57-3. Results display of displacements in the cantilever beam model.

Table 57-1. Comparison of Results

	Theory	Analysis	% Difference
R (lb)	-126.5625	-126.563	0.0
Def (in)	-1.125	-1.125	0.0

AVE - 58 Transient Thermal Analysis of a Solid Wall with Internal Heat Generation

Reference

Gebhart, B., *Heat Transfer*, Third Edition, New York: McGraw-Hill.

Problem Description

This example involves a transient thermal analysis of a solid wall with internal heat generation. A long wall is initially at a temperature of 0°F. A uniform internal heat generation is applied to the entire wall. The two sides of the wall are held at a temperature of 0°F. The temperature at the center of the wall is computed as a function of time.

This problem was analyzed first with 2-D thermal elements (case one), and then with thermal brick elements (case two).

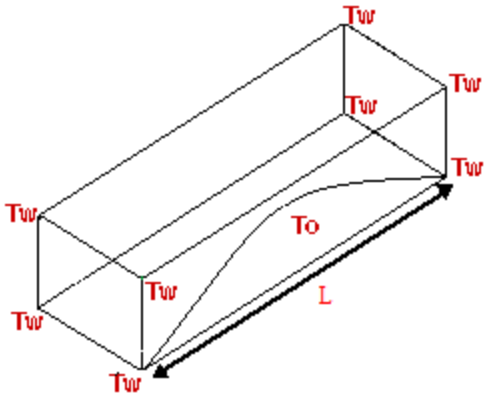

Figure 58-1. Diagram of the thermal FE model of the wall with internal heat generation.

Theoretical Solution

The analytic solution is an infinite series, which converges within 20 terms for the transient under consideration here.

The solution is:

$$T = \frac{q'''L^2}{2K}\left(\frac{x}{L} - \left(\frac{x}{L}\right)^2\right) - \frac{4q'''L^2}{K\pi^3}\sum_{n=1,3,5}^{\infty}\frac{1}{n^3}e^{-\left(\frac{n\pi}{L}\right)^2\alpha\tau}\sin\left(\frac{n\pi x}{L}\right)$$

Where:

- $\alpha = \text{diffusivity} = \frac{K}{\rho c_p} = 0.01\frac{in^2}{sec}$ for $\rho = 0.01\frac{lbm}{in^3}$
- L = 10 inches (thickness of wall)
- K = 1.4 x 10^{-5} BTU/sec*in*°F (thermal conductivity)
- q''' = 0.0001 BTU/sec*in^3 (volumetric heat generation rate)
- T = temperature at x into the wall at time, τ
- x = distance into the wall (inches)

- τ = time (seconds)

Autodesk Simulation Solution

The results were computed using 1000 time steps with 10-second intervals between time steps. The results were output every 100 time steps and are shown in the table below.

> **Note:** The heat input is applied as a steady-state load of heat generation on the part, even though it is a transient analysis. The results reported in the table below are maximum temperatures for each time step from the Results environment within Autodesk Simulation. The analytic values were computed using a sperate FORTRAN program.

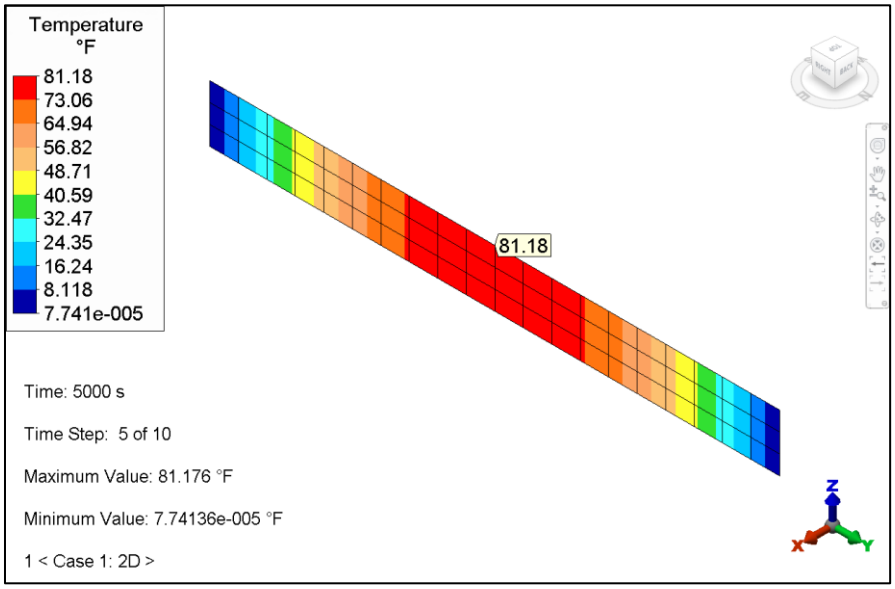

Figure 58-2. Results display of temperature contours for case one at 5000 seconds.

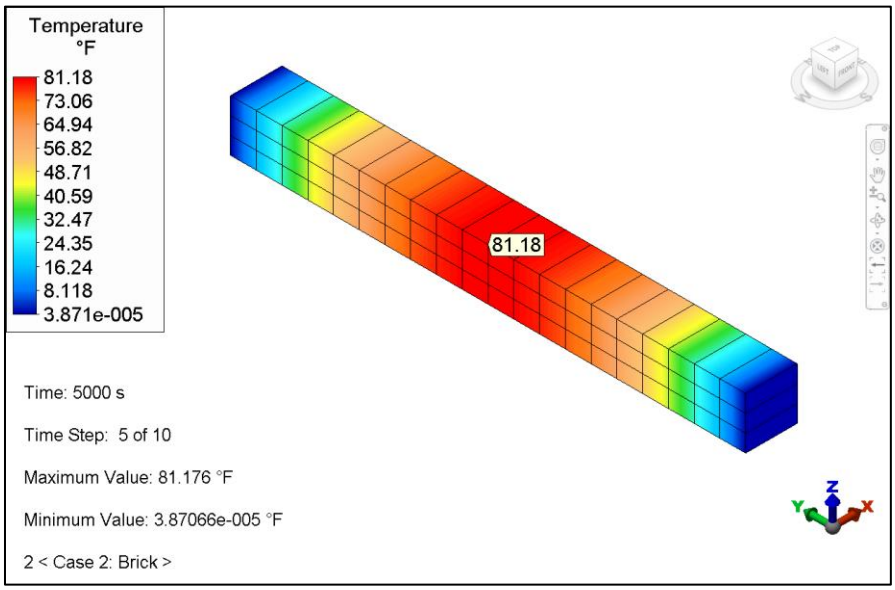

Figure 58-3. Results display of temperature contours for case two at 5000 seconds.

Table 58-1. Comparison of Results

Midplane Temperatures vs. Time					
		Case One: 2-D Elements		Case Two: Brick Elements	
Time (sec)	Analytic Solution (°F)	Analysis Solution (°F)	% Difference	Analysis Solution (°F)	% Difference
1000	32.78	32.66	0.37	32.66	0.37
2000	54.58	54.43	0.27	54.43	0.27
3000	67.99	67.85	0.21	67.85	0.21
4000	76.21	76.10	0.14	76.10	0.14
5000	81.26	81.18	0.10	81.18	0.10
6000	84.36	84.30	0.07	84.30	0.07
7000	86.26	86.22	0.05	86.22	0.05
8000	87.43	87.40	0.03	87.40	0.03
9000	88.15	88.13	0.02	88.13	0.02
10000	88.59	88.57	0.02	88.57	0.02

AVE - 59 Steady-State Heat Transfer Analysis of a Fin Immersed in a Cooling Fluid

Reference

Holman, J. P., *Heat Transfer*, Third Edition, New York: McGraw-Hill, 1981.

Problem Description

In this problem, a fin with one end held at a temperature of 1070°F is immersed in a fluid, which is at a temperature of 70°F. The other end of the fin is completely insulated. We want to find the steady state temperature along the fin.

The fin is considered to be much wider than it is thick. This way, only one slice of the fin needs to be analyzed.

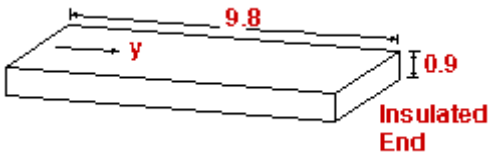

Figure 59-1. Dimensions of the fin that is immersed in a fluid.

Theoretical Solution

This problem has a closed form solution, which is reported in J.P. Holman's "Heat Transfer." The following is the analytical solution:

$$T_y = (T_0 - T_a)\left[\frac{e^{-my}}{1+e^{-2ml}} + \frac{e^{my}}{1+e^{2ml}}\right] + T_a$$

Where:

- $m = \sqrt{\frac{hp}{KA}}$
- A = 0.9 in^2 (area of the cross section)
- h = 0.1 (surface convection film coefficient)
- K = 5.0 (thermal conductivity of the fin)
- l = 9.8 in (length of the fin)
- p = 2.0 in (convection perimeter of the fin)
- t = 1 in (depth of the model)
- $T_a = 70^o$ (fluid temperature)
- $T_0 = 1070^o$F
- y = distance along the length

Autodesk Simulation Solution

The model was built using temperature boundary elements, which provided the capability to hold the high-temperature end at 1070°F.

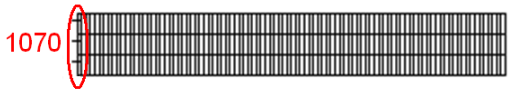

Figure 59-2. 2-D finite element mesh with temperature boundaries.

Notice that the elements are in a fine mesh along the length of the fin. This is because the temperature drops exponentially along the length of the fin. A highly accurate analysis requires the use of this fine mesh when a high temperature gradient occurs. The analysis results are compared to the theoretical solution in the following table. Notice that the results are in close agreement even in the region next to the hot wall, where the temperature changes greatly in a short distance.

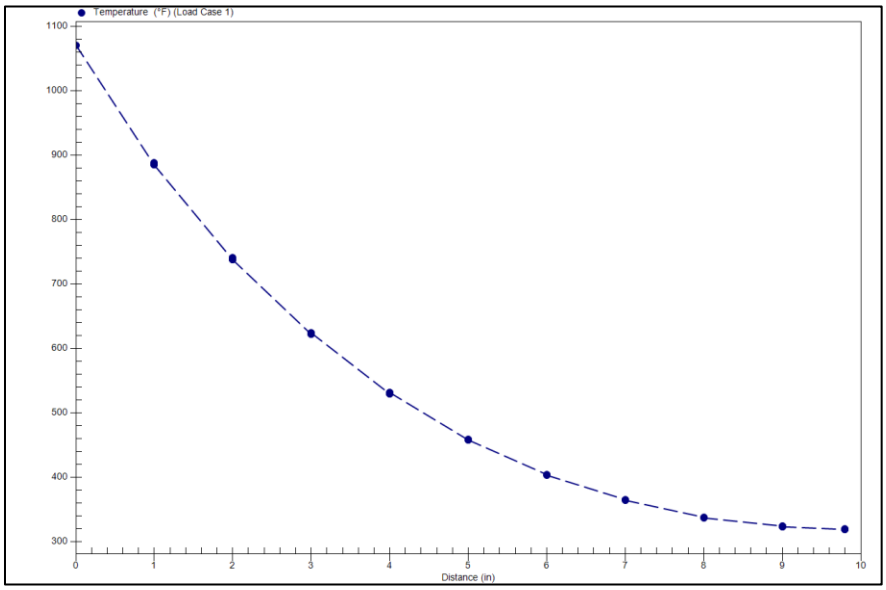

Figure 59-3. Path-plot of temperature contours in the fin model.

Table 59-1. Comparison of Results

Distance Z (in)	Temperature (°F)		% Difference
	Theoretical	Analysis (avg. of 4 nodes along the thickness)	
0	1070.00	1069.98	0.00
1	886.63	886.32	0.04
2	739.69	739.64	0.01
3	622.63	622.77	0.03
4	530.21	530.48	0.05
5	458.33	458.69	0.08
6	403.77	404.18	0.10
7	364.10	364.55	0.12
8	337.55	338.02	0.14
9	322.93	323.41	0.15
9.8	319.37	319.86	0.15

AVE - 60 Nonlinear Radiation Heat Transfer Analysis of a Cylinder with Internal Heat Generation

Reference

Holman, J. P., *Heat Transfer*, Fifth Edition, New York: McGraw-Hill Book Company, 1981.

Problem Description

A cylinder with internal heat generation is exposed to a radiation environment (T_{rad}= 70ºF, F = 0.26). It has internal heat generation elements along the inner edge, where there is a tiny hole along the axis of the cylinder. We want to find the radiation surface temperature along the outer edge. Note that the same problem was analyzed in AVE - 45 with slightly different dimentions using 3D elements.

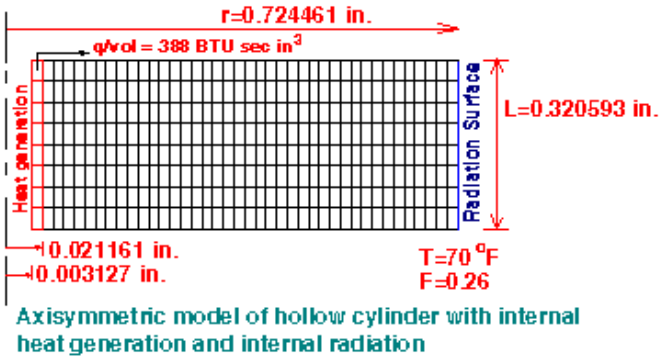

Figure 60-1. Diagram of the axisymmetric FE model of the cylinder with dimensions and thermal properties.

Theoretical Solution

The axisymmetric model for the heat transfer process is shown in the figure above. Since an ideal radiator, or blackbody, emits energy at a rate proportional to the fourth power of the absolute temperature of the body:

$q = F \sigma A (T_1^4 - T_2^4)$

Where:

- $\frac{q}{\text{Volume}} = 388 \frac{\text{BTU}}{\text{sec} * \text{in}^3}$
- $q = \text{Volume} \times \left(\frac{q}{\text{Volume}} \right) = \frac{\pi \left[(0.021161)^2 - (0.003127)^2 \right] (0.320593)}{2\pi} \times 388$
- $q = 0.027242 \frac{\text{BTU}}{\text{sec}}$ (per radian)
- T_2 = 70ºF (radiation temperature)
- r = 0.724461 in (radius of the cylinder)
- L = 0.320593 in (height of the cylinder)
- A = r x L = 0.724461 x 0.320593 = 0.232257 $\text{in}^2 \frac{\text{radiation area}}{\text{radian}}$

- $\sigma = 3.3 \times 10^{-15} \frac{BTU}{sec * in^2 * °F^4}$ (Stephen-Boltzman constant)
- F = 0.26 (radiation emissivity function)
- $k = 0.0018866 \frac{BTU}{sec * in * °F}$ (conduction coefficient)

Solving for radiation surface temperature yields:
T_1= 2959.842ºF (theory)

Autodesk Simulation Solution

The cylinder was modeled with 320 2-D axisymmetric elements. The inner layer of elements was defined using a different part number from the rest of the model for convenient specification of internal heat generation. The outer surface was defined using a unique surface number for specifying ambient temperature and radiation function.

Analysis was performed after setting the nonlinear analysis options on the "Advanced" tab of the "Analysis Parameters" screen. Without setting any prior nodal temperature (that is, as an initial guess), the analysis converged to the final solution within 17 iterations with a relaxation parameter $\alpha = 0.25$.

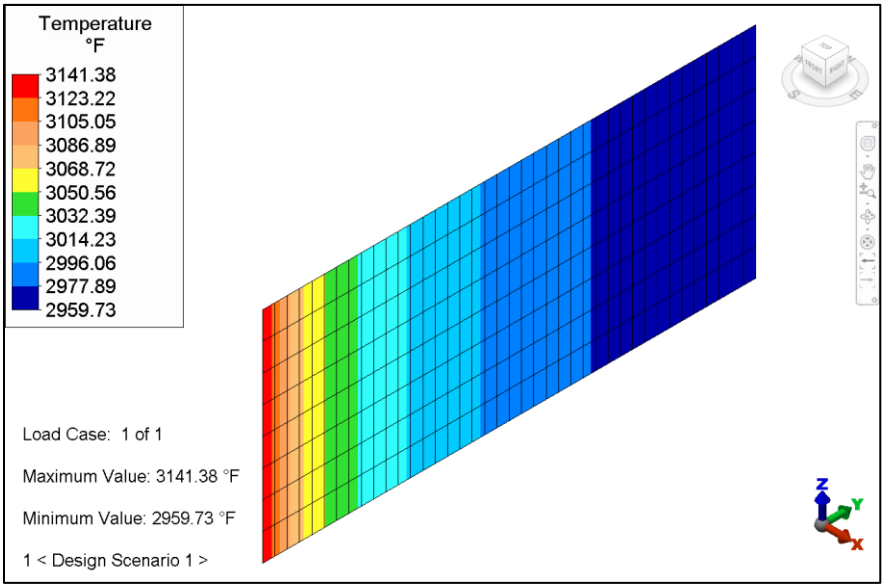

Figure 60-2. Results display of temperature contours in the axisymmetric model of a cylinder with internal heat generation in a radiation environment.

The table below compares the theoretical and analysis results. The results demonstrate the accuracy of the Steady-State Heat Transfer Analysis Processor.

Table 60-1. Comparison of Results

Radiation Temperature (°F)		% Difference
Theory	Analysis	
2959.842	2959.73	0.004

AVE - 61 Continuous Beam, Simply Supported at the Ends, Under a Uniformly Distributed Load

Reference

Pytel, A. and Singer, F. L., *Strength of Materials*, New York: Harper & Row Publishers, 1987.
Manual of Steel Construction, Ninth Edition, Chicago, American Institute of Steel Construction, Inc., 1989.

Problem Description

A three-span continuous beam, 360 inches long, is subjected to a uniformly distributed load of 100 lb/inch. The following are the material and area properties:

- E = 30 x 10^6 psi
- Poisson's ratio = 0.3
- Weight density = 0.2836 lb/in^3
- Cross section = 2 in x 5 in

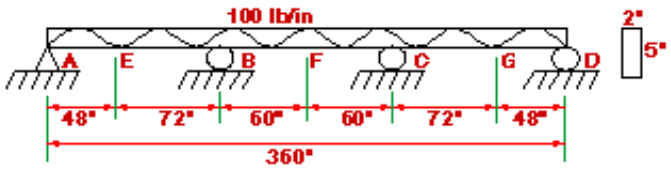

Figure 61-1. This diagram illustrates the characteristics of the three-span continuous beam with loading and boundary conditions.

Find the reactions at the supports and the maximum moment of the beam.

Theoretical Solution

The analytical solutions can be obtained from the reference given above.

Where:
- ω = 100 lb/inch
- l = 120 inches

Then,
- $R_D = R_A = 0.4\ \omega\ l = 4800$ lb
- $R_C = R_B = 1.1\ \omega\ 1 = 13200$ lb
- $M_F = 0.025\ \omega\ l^2 = 36{,}000$ lb-in
- $M_B = M_C = -0.1\ \omega\ l^2 = 144{,}000$ lb-in
- $M_E = M_G = (\omega x)\left(\frac{x}{2}\right)\Big|_{x=48} = \frac{\omega(x)^2}{2} = 115{,}200$ in-lb

Autodesk Simulation Solution

The beam is divided into 6 beam elements with unequal span. The end points of each beam element are intentionally set at the points where the maximum moments in each span occur (A - G). Each beam element is loaded with a uniformly distributed load of 100 lb/inch over the entire element length. FEA Editor was used to create the model for analysis by the Linear Stress Analysis Processor.

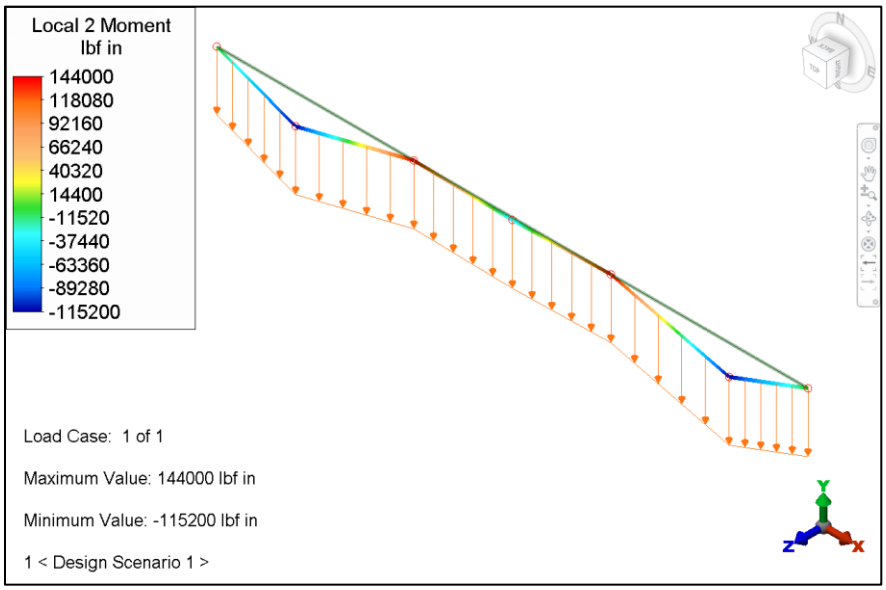

Figure 61-2. Results display of moments in the continuous beam with simple supports at the ends. The displaced and original shapes are shown as well.

The tables below compare the results:

Table 61-1. Comparison of Results for Support Reactions

Location	Theory (lb)	Analysis (lb)	% Difference
A, D	4800	4800	0.0
B, C	13200	13200	0.0

Table 61-2. Comparison of Results for Moments

Location	Theory (lb-in)	Analysis (lb-in)	% Difference
B, C	144000	144000	0.0
E, G	115200	115200	0.0
F	36000	36000	0.0

AVE - 62 Design Spectrum with a Specified Maximum Ground Acceleration

Reference

Paz, Mario, *Structural Dynamics - Theory and Computation*, New York: Van Nostrand Reinhold Company, 1980.

Problem Description

A structure is modeled as a single mass system with a natural period of T = 1 sec. Using the response spectrum analysis method, determine the maximum relative displacement for a design spectrum with a maximum ground acceleration equal to 0.32 g.

Theoretical Solution

In the reference, the following results are calculated from a basic design spectra with a frequency (f) of 1 cycle per second and 10% critical damping. The results were adjusted to the 0.32-g maximum ground acceleration.

S_D = 9.5 x 0.32 = 3.04 in
S_v = 60 x 0.32 = 19.2 in/sec
S_a = 0.95 x 0.32 g = 0.304 g

Autodesk Simulation Solution

A model was constructed along the Y axis with the bottom node fully fixed and TxRyz boundary conditions applied to all other nodes. A lump mass was specified in force units at the top node.

The following values were used:

f = 1 Hz (frequency)
T = 1 sec (period)
W = 1000 lbs at top (weight)
l = 42 in (length)
E = 30 x 10^6 psi (Young's modulus)
I = 0.08333 in^4 (moment of inertia)
g = 386.4 in/sec^2 (gravity)

A linear mode shapes and natural frequencies analysis was run, which gave the natural frequency for the model. Then a restart analysis was prepared using a Linear Response Spectrum analysis. The following data was specified in the "Response Spectrum Analysis Input" table.

Period (sec)	Amplitude (g)
0.5	0.304
1.5	0.304

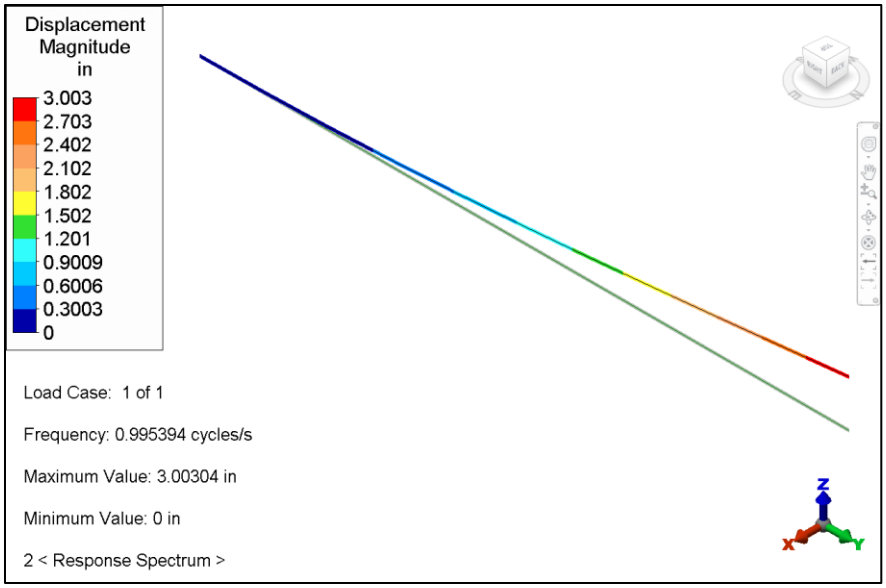

Figure 62-1. Maximum displacement from the Linear Response Spectrum analysis.

The theoretical results and analysis results are compared in the table below.

Table 62-1. Comparison of Results

Maximum Displacement (inches)		% Difference
Theory	**Analysis**	
3.04	3.003	1.22

AVE - 63 Slab with Internal Charge Density Distribution

Reference

Holman, J. P., *Heat Transfer*, Fifth Edition, New York: McGraw-Hill Book Company, 1981.

Problem Description

This accuracy verification is an electrostatic "field and volt" analysis of a slab with an internal charge density distribution. A plane slab 40 millimeters thick has a distributed charge density of 1E-9 coulomb / mm^3. The voltage distribution inside the wall is desired. The dielectric constant of the material is 56470 (unit less). The external voltage is held at 70 volts.

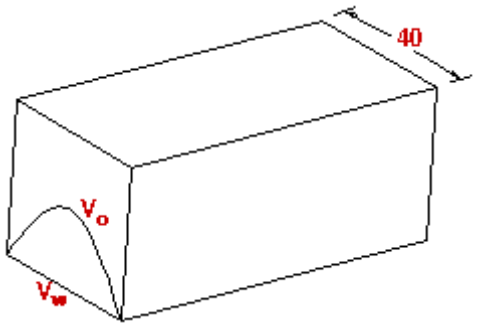

Figure 63-1. Diagram of the slab with internal charge density distribution.

Theoretical Solution

V_o = 470 volts (maximum voltage)
V_w = 70 volts (external voltage)

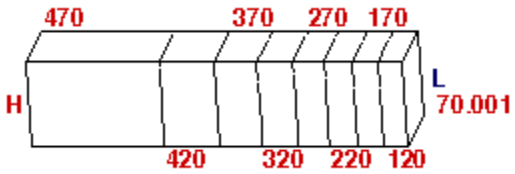

Figure 63-2. Voltage distribution.

Autodesk Simulation Solution

Taking advantage of symmetry, only half the thickness of the slab needs to be analyzed. At the center, the derivative of voltage with respect to thickness is 0, which means that the midplane can be treated as an insulated surface. The voltage boundary element is used to maintain a voltage of 70 volts at the outside of the slab. A voltage boundary element stiffness of 1e10 A/V is used. (This is equivalent to the stiffness of a boundary element in a stress analysis.)

It can readily be shown that the voltage is a parabolic function of distance and that the maximum voltage is at the midplane. This maximum voltage has a value of 470 volts. This is exactly the value computed by the Electrostatic Analysis processor.

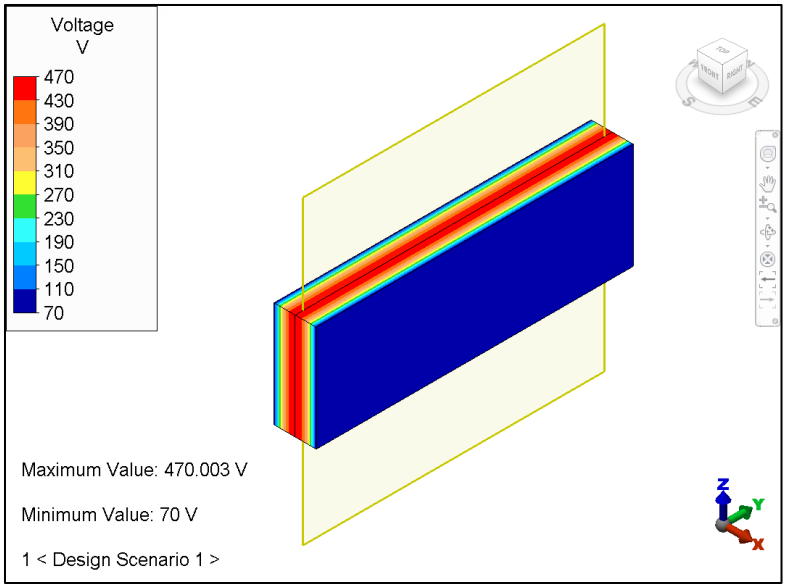

Figure 63-3. Results display of the voltage field in the symmetrical model of the slab with an internal charge density distribution. Y-Z Mirror Plane is activated to show the full model.

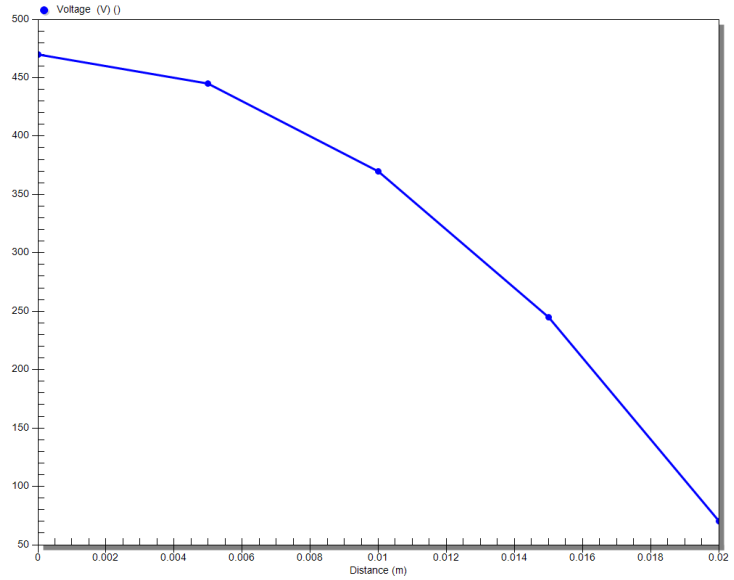

Figure 63-4. Voltage distribution across 5 nodes through the thickness of the symmetrical model. Zero distance, shown on the X axis of this graph, represents the symmetry plane.

Table 63-1. Comparison of Results

Maximum Voltage (Volts)		% Difference
Theory	Analysis	
470	470	0.0

AVE - 64 Thermal Deflection Analysis of a Plate with One End Fixed and the Other End Guided

Reference

Young, Warren C., *Roark's Formulas for Stress and Strain*, McGraw-Hill Book Company, Sixth Edition, 1989, case 6b, p. 111.

Problem Description

A 6-inch long, by 0.375-inch wide, by 0.25-inch thick plate, with the left end guided and the right end fixed, is subjected to uniform temperatures of 270°F on the bottom and 135°F on the top over half its length as shown in Figure 64-1. The change in temperature throughout the thickness for the remaining length is 0°F. The moments at both ends and the deflection at the left end are required.

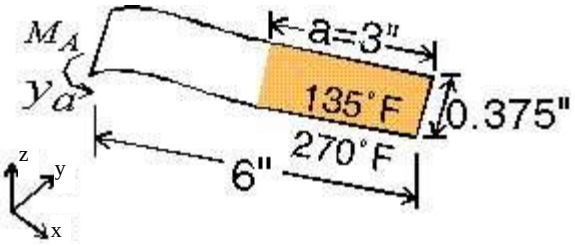

Figure 64-1. Diagram of the plate model.

The plate is made out of steel with a Young's modulus of 30 x 10^6 psi and a coefficient of thermal expansion of 6.5 x 10^{-6}in/(in-°F).

Theoretical Solution

The solution for this problem is given by Roark on page 111, Reference No. 6b in Table 3 of Article 7.1. Because the Roark solution is based on conventional beam element theory, there is no rotational constraint about the X axis for this mode. Furthermore, the Roark solution ignores the Poisson's ratio effects, therefore, a Poisson's ratio of 0.0 is used in the analysis.

$$M_A = \frac{-EI\gamma}{lt}(T_2 - T_1)(l - a)$$

$$z_A = \frac{a\gamma}{2t}(T_2 - T_1)(l - a)$$

Where:

E = 30 x 10^6 psi (Young's modulus)

I = Moment of inertia, which for this plate is $\frac{bt^3}{12} = \frac{0.375 \times .25^3}{12} = 4.883 \times 10^{-4}\ \text{in}^4$

l = 6 in (length of plate)

γ = 6.5 x 10^{-6}in/(in-°F) (thermal expansion coefficient)

t = 0.25 in (thickness)

T_2 = 270°F (temperature on bottom)

T_1 = 135°F (temperature on top)

a = 3 in (length of plate subjected to dT/dh)

The calculated results are M_A= M_B= -25.7 in-lbs and z_A= 0.0158 in. The total moment of 25.7 in-lbs can be converted into the moment per unit width by dividing by 0.375 in., which yields -68.6 in-lbs/in.

Autodesk Simulation Solution

The model shown in Figure 64-2 was created in FEA Editor. For the plate elements, the value of the thermal gradient, dT/dh, and a point, PP (PPx, PPy, PPz) are required to define the local 3 axis of the plate element to orient dT/dh correctly.

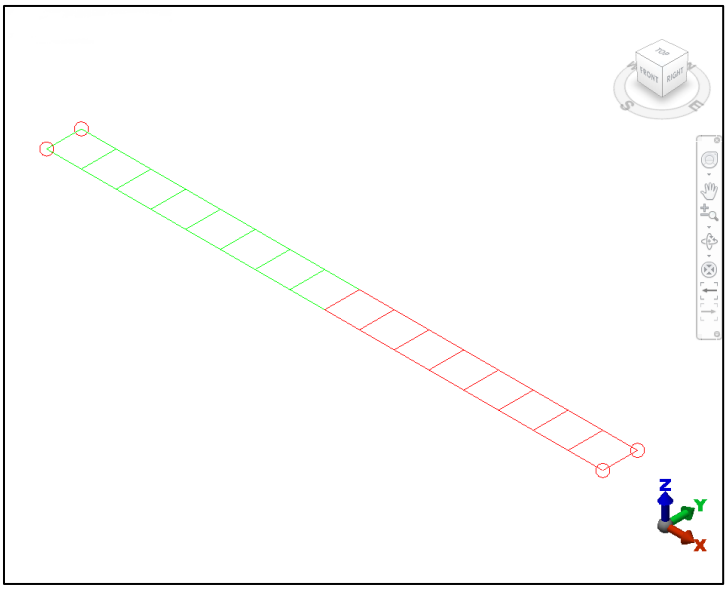

Figure 64-2. The model created in FEA Editor.

When point PP is placed on the cooler side, dT/dh is positive. For this problem, we need a positive thermal gradient in the -Z direction; therefore, the orientation point, PP, was chosen as 3,3,1. The temperature gradient through the thickness of the plate, dT/dh, is equal to (270-135)/(0.25) or 540^{o}F/in.

The material properties, the plate thickness of 0.25 and the temperature gradient, dT/dh were defined using the Element Data Control window. The temperature gradient was only applied to the part 2 (red) elements, since only half the plate is subjected to the temperature gradient.

A linear static stress analysis was performed. The displacement calculated by the software is 0.0158 in, as shown in Figure 64-3. The moment per unit width calculated at the ends is 68.6 in-lbs/in as shown in Figure 64-4. These values are exactly the same as those calculated for the Roark solution. However, there is a discontinuity in the moments in the isotropic plate solution, where the dT/dh changes from 540°F/in to 0°F/in. This discontinuity can be eliminated by using an orthotropic plate with a coefficient of thermal expansion of 0 in the width direction (0.375 in). The shear modulus was calculated for the orthotropic plate element to be 15 x 10^6 psi, by using G=E/(2*(1+υ)), with υ = 0. The results from the orthotropic plate model are shown in Figure 64-5.

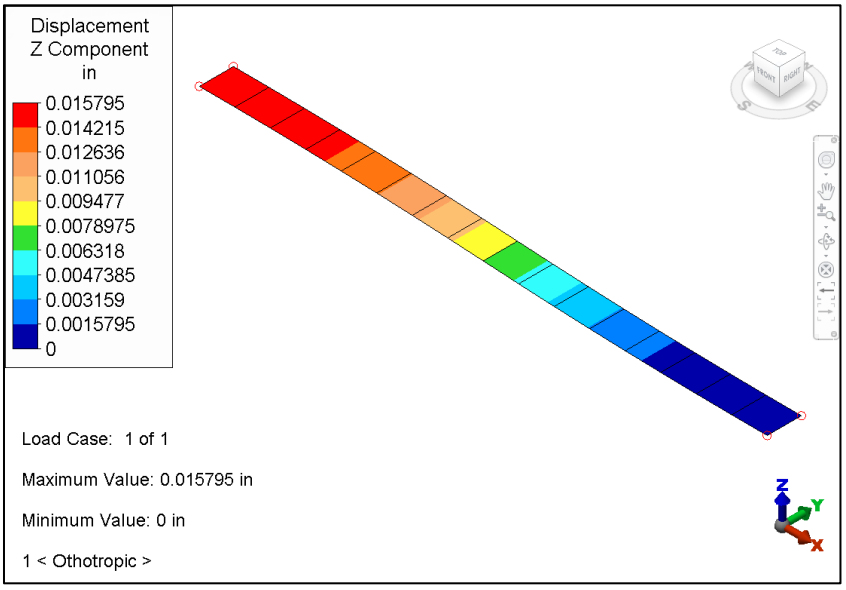

Figure 64-3. Displacement results in the Z direction.

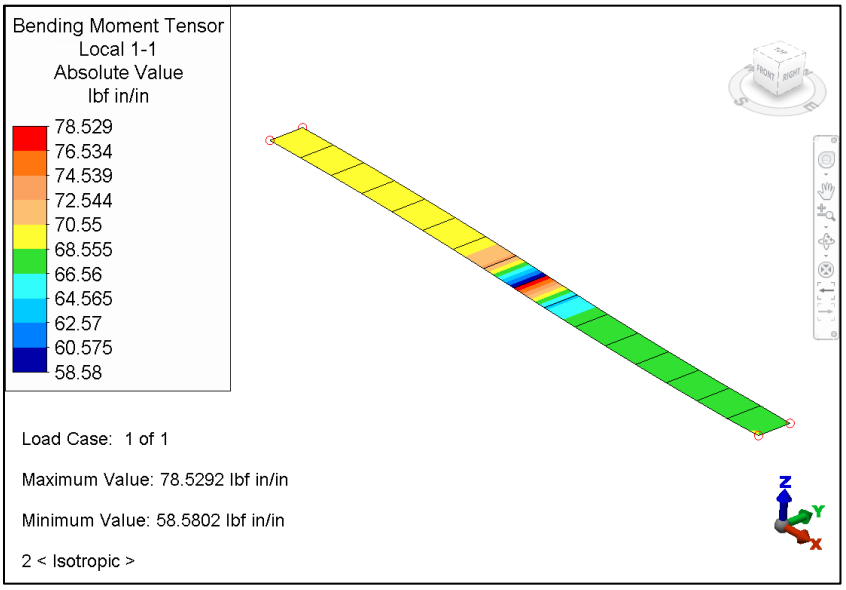

Figure 64-4. The moment results using isotropic plate elements.

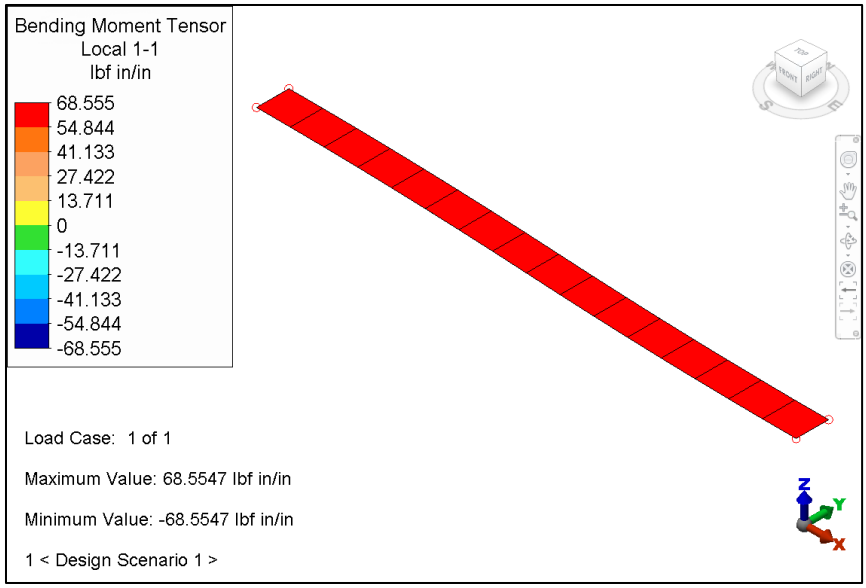

Figure 64-5. The moment results using orthotropic plate elements.

Table 64-1. Comparison of Results

	Theory	Analysis	% Difference
Displacement in Z Direction (in)	0.0158	0.0158	0.0
Moment per Unit Width (in-lbs/in)	68.6	68.6	0.0

AVE - 65 Torsion of an Elastic Beam with a Channel Cross-Section

Reference

Blodgett, Omer W., *Design of Welded Structures,* Chapter 2.10, Cleveland: James F. Lincoln Arc Welding Foundation, 1966.

Problem Description

The problem of torsion of an elastic beam with a channel cross-section has been analyzed utilizing the software. The material is steel with a Young's modulus of 30,000 ksi, and a Poisson's ratio of 0.3. That material is considered to be isotropic. Therefore, the shear modulus is G = 30,000/[2(1 + 0.30)] = 11,540 ksi.

The beam span (L) is 72 inches, the web of the channel is h=36 inches and its flanges (b) are 10 inches deep. The thickness (t) of both the web and the flanges is one inch. The beam is restrained against torsion on one end and free to twist on the other. Two opposing forces with a magnitude of 4,000 pounds are applied to the intersections of the web and the flanges at the free end. These forces are perpendicular to the axis of the beam and to the web of the channel, and produce a torsional moment (T) of 4,000 x 36 = 144,000 lb-in or 144 kip-in.

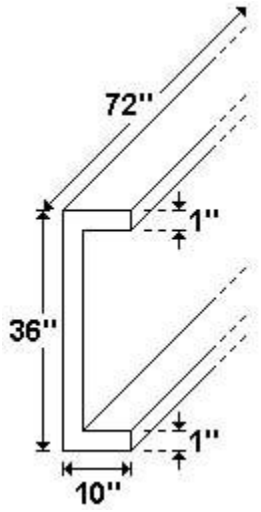

Figure 65-1. Diagram of the beam with channel cross-section.

Theoretical Solution

The formulas for calculating torsional stiffness properties and rotations in thin-walled open cross-sections presented in Tables 21 and 22 of the reference text have been used for the purpose of comparison with closed form solutions.

The flanges of the channel were not included. In this case, the reference gives the following formula for the torsional rotation,θ:

$\theta = TL/(KG)$

T, L and G have been previously defined, and K is the torsional stiffness constant.

For this case, we have $K = ht^3/3$ (i.e., $K = 36 \times 1^3/3 = 12$ in^4).

Therefore, $\theta = 144 \times 72/(12 \times 11{,}540) = 0.0749$ radians = 4.291 degrees.

Autodesk Simulation Solution

The model shown above was built using 32 plate elements. A linear static stress analysis was performed to determine displacements. The results are compared to theoretical results in the table below.

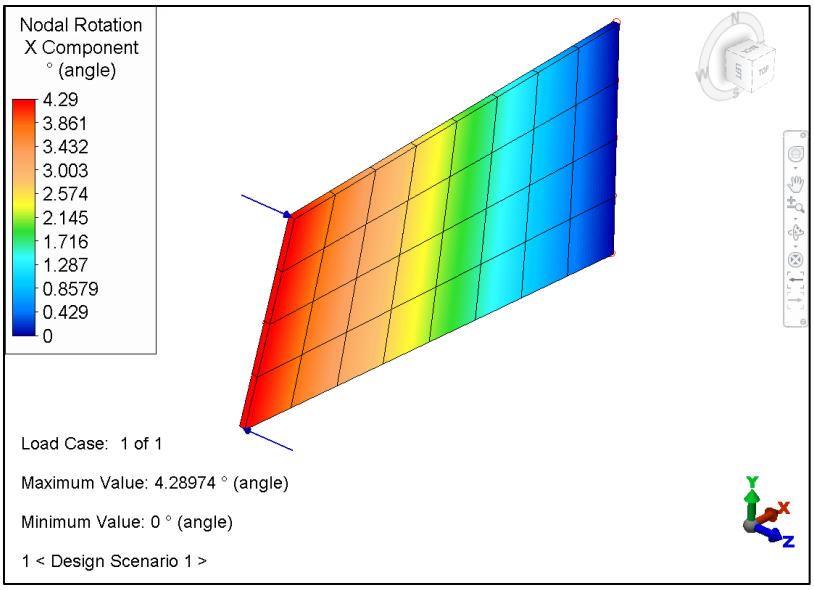

Figure 65-2. Nodal rotation (X component) of the channel without flanges. 3D visualization is active.

Table 65-1. Comparison of Results

	Theoretical	Analysis	% Difference
θ (degrees)	4.291	4.290	0.02

AVE - 66 Multidimensional Transient Heat Transfer Analysis

Reference

Incropera, Frank and DeWitt, David, *Introduction to Heat Transfer*, John Wiley & Sons, New York, 1990, pp. 266-270.

Problem Description

A stainless steel cylinder (AISI 304), initially at 600K, is quenched by submersion in an oil bath maintained at 300K with a convection coefficient of h = 500 W/m^2K. The length of the cylinder is 60 mm and the diameter is 80 mm. We must determine the temperatures at the center of the cylinder, at the center of a circular face, and at the mid-height of the side at three minutes into the cooling process.

Theoretical Solution

The following material properties for stainless steel (AISI 304) were used in *Introduction to Heat Transfer*.

- density = 7900 kg/m^3
- conduction coefficient = 17.4 W/m K
- specific heat = 526 J/kg K

Autodesk Simulation Solution

FEA Editor was used to create a model of the cylinder cross-section. Because the cylinder is axially symmetrical, only one quarter of the cross-section was modeled. 2-D axisymmetric elements were used.

The model was created in the Y-Z plane with the lower left corner (actually, the exact center of the cylinder) located at the origin (0,0,0). Orientation in the Y-Z plane is a modeling requirement when using 2-D axisymmetric elements.

The unit system was specified as Metric mks (SI). First, a rectangle was added with the appropriate dimensions in meters (DY = 0.040, DZ = 0.030).

Next, a dense mesh was constructed using the four corners of the rectangle. A coarse mesh is not recommended for heat transfer analysis. The next step was to change the surface number of the lines which form the top and right sides. (Note: this surface number was used later in the Surface Control window to indicate the elements exposed to the convection conditions.) In this case, the entire mesh was surface 1 (green), but the top and right sides were updated to surface 2 (red).

A line was added in the upper right corner of the model. The purpose of this operation was to divide the single corner quadrilateral element into two individual triangular elements. The heat transfer analysis software does not permit boundary conditions to be applied to more than one side of a 2-D element.

Additional model data were specified, including the element type, material properties (mass density, thermal conductivity and specific heat), and convection properties of the external surfaces. In the "Analysis Parameters" screen, the number of time steps and the time step size were specified for analysis. On the "Multipliers" tab, the convection multiplier was activated. On the "Options" tab, the default nodal temperature was set to 600K. A load curve was set up for times 0 to 180 with factors of 1, indicating a constant loading.

Results obtained from the analysis agree very closely with the reference, indicating the accuracy of the Transient Heat Transfer Analysis processor.

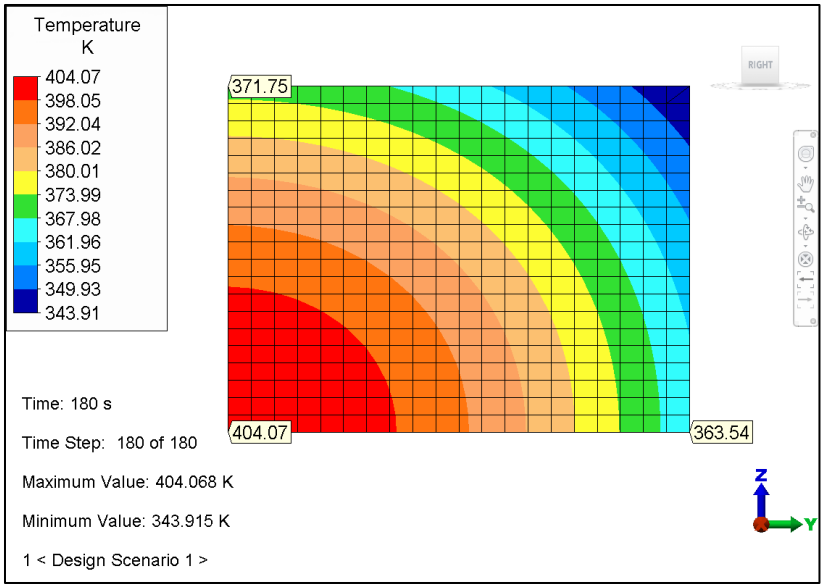

Figure 66-1. Results display of temperature contours in the 2-D axisymmetric model of the stainless steel cylinder. Results for the final time step of the analysis are shown.

The following table compares results from the reference and the analysis.

Table 66-1. Comparison of Results

Temperature at 3 minutes (K)			
	Theoretical	**Analysis**	**% Difference**
Center of Cylinder	405	404.07	0.23
Center of Top Circular Face	372	371.75	0.07
Mid-height of Side	366	363.54	0.67

AVE - 67 Fundamental Frequency and Static Lateral Deflections of a Loaded Shaft

Reference

Thomson, William T., *Mechanical Vibrations*, Second Edition, Prentice-Hall, Inc., New Jersey, 1953, p. 202.

Problem Description

The shaft in Figure 67-1 is simply supported on both ends. Determine the fundamental frequency of the shaft when 300- and 500-pound masses are clamped to it. Also determine the static lateral deflections of the shaft under the action of the transverse loads (300- and 500-pound weights).

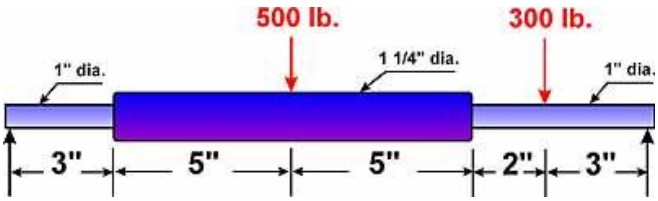

Figure 67-1. Diagram of the shaft with varying diameter and two mass loadings.

Theoretical Solution

The following values where obtained in *Mechanical Vibrations*.

- Displacement at 500-lb. Load = 0.0256 in.
- Displacement at 300-lb. Load = 0.0159 in.
- First Natural Frequency = 1240 c.p.m. = 20.7 Hz

Autodesk Simulation Solution

FEA Editor was used to model the shaft in 1-inch segments. The 1-inch diameter section was defined on layer 1 (green) and the 1.25-inch diameter section was defined on layer 2 (red). Boundary conditions were added to the end nodes to simulate simple support (TxyzRxy). The beam element type was specified. Sectional properties were added to the beams as shown in below table

Table 67-1. Sectional properties of beams

Layer #	Diameter (inches)	Area (in^4)	Torsional Constant (in^4)	Moment of Inertia (in^4)	Sectional Modulus (in^3)
1	1	0.785398	.098175	.049087	.098175
2	1.25	1.227185	.239864	.119842	.191748

Lumped masses were added in the FEA Editor. These were input as 500 lbf and 300 lbf, respectively.

Note: lbm stands for pounds mass, which is the unit for mass in the English unit system.

The following material properties were specified:

- $E = 29 \times 10^6$ psi (Young's modulus)
- $\nu = 0.3$ (Poisson's ratio)
- $\rho = 0.283$ lbs/in^3 (mass density, input as $0.283/386.4 = 7.324 \times 10^{-4}$ to include gravity)

Shear deformations were not enabled. A Linear Mode Shapes and Natural Frequencies analysis was performed on the model. Figure 67-2 shows the first natural frequency of 20.5 Hz.

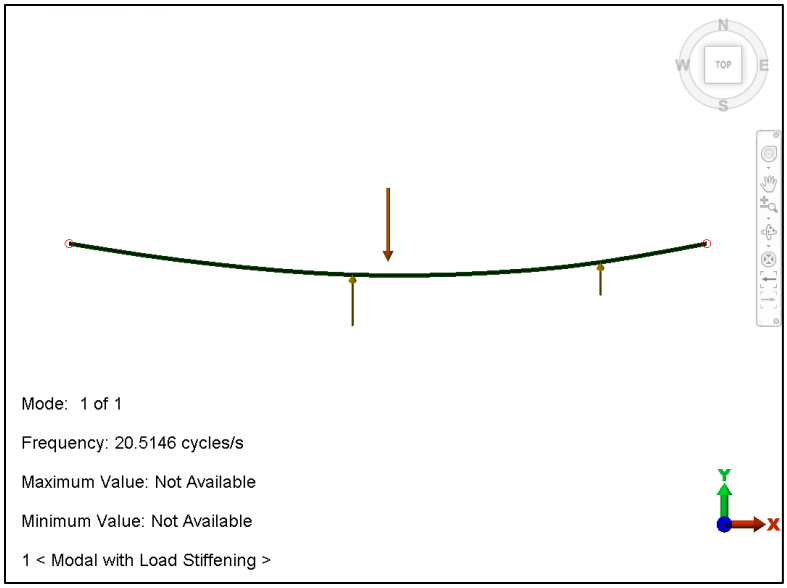

Figure 67-2. Results display of the first mode shape at 20.5 Hz.

Thomson also calculated the static deflection at the points of load. In FEA Editor, nodal forces of 500 and 300 pounds were added to the model for a Linear Static Stress analysis. Note that shear deformation was not enabled (shear area = 0).

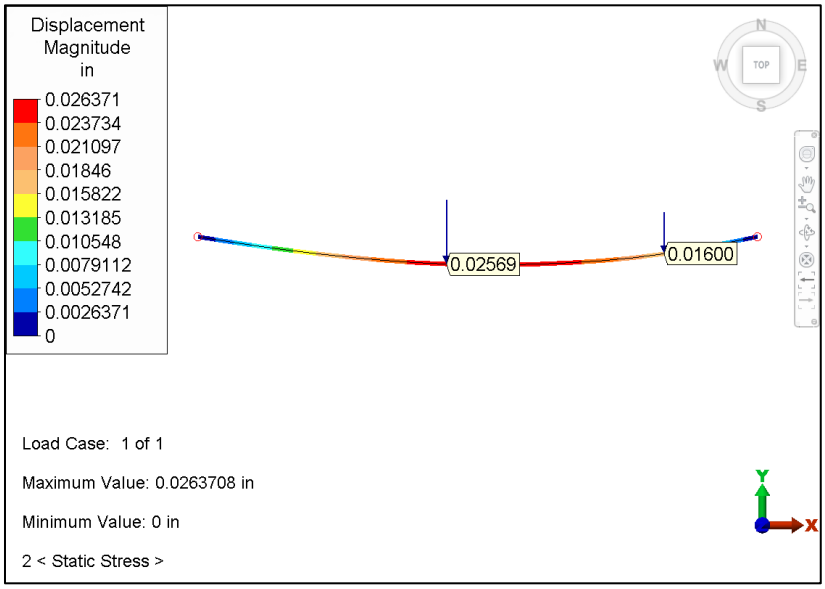

Figure 67-3. Results display of deflections in the shaft model. Probes are added to the 2 loading points.

The following table compares analysis results to the referenced solution. The results compare extremely well with the results calculated by Thomson.

Table 67-2. Comparison of Results

	Theoretical	Analysis	% Difference
Displacement at 500-lb. Load (inches)	0.0256	0.0257	0.39
Displacement at 300-lb. Load (inches)	0.0159	0.0160	0.63
First Natural Frequency (Hertz)	20.7	20.5	0.97

AVE - 68 Annular Plate with a Uniformly Distributed Pressure

Reference

Young, W. C., *Roark's Formulas for Stress & Strain*, Sixth Edition, McGraw-Hill, New York, 1989, Case 2b, page 405.

Problem Description

The sixth edition of Roark's *Formulas for Stress & Strain* was used to verify the displacements and stresses predicted by the two-dimensional axisymmetric elements, plate elements and brick elements.

The model chosen for this accuracy verification example was an annular plate with a uniformly distributed pressure (*q*) of 10 psi over the entire plate. The outer edge of the plate was simply supported and the inner edge is guided (fixed against rotation, but free to translate).

The plate has an outside radius of 5 inches, an inside radius of 2.5 inches and a thickness of 0.25 inches. Young's modulus was set to 30 x 10^6 psi and the Poisson's ratio was set to 0.3.

Theoretical Solution

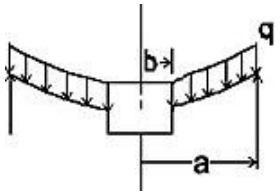

Figure 68-1. A diagram of the annular plate with a uniformly distributed pressure.

Outside radius, a =	5 in.
Inside radius, b =	2.5 in.
Young's Modulus, E =	30 x 10^6 psi
Thickness, t =	0.25 in.
Poisson's ratio, v =	0.3
Pressure, q =	10 psi
Plate constant, D =	$\frac{Et^3}{12(1-v^2)} = 42{,}926$

At b/a = 0.5 then:

K_{yb} =	-0.0103
K_{Mrb} =	0.1223
Moment, M =	$K_{Mrb}\, qa^2$
Stress, s =	$\frac{6M}{t^2} = \frac{6(K_{Mrb} qa^2)}{t^2} = \frac{6(0.1223)(10)(5)^2}{(0.25)^2} = 2{,}935\,\text{psi}$ (σ_{xx} at inner edge)
Displacement, y =	$\frac{(K_{yb})qa^4}{D} = \frac{-0.0103(10)5^4}{42{,}926} = -0.0015$ in (at inner edge of plate)

Autodesk Simulation Solution

Using the two-dimensional elements, a displacement of 0.0015135 in, and a stress of 2,935 psi were predicted.

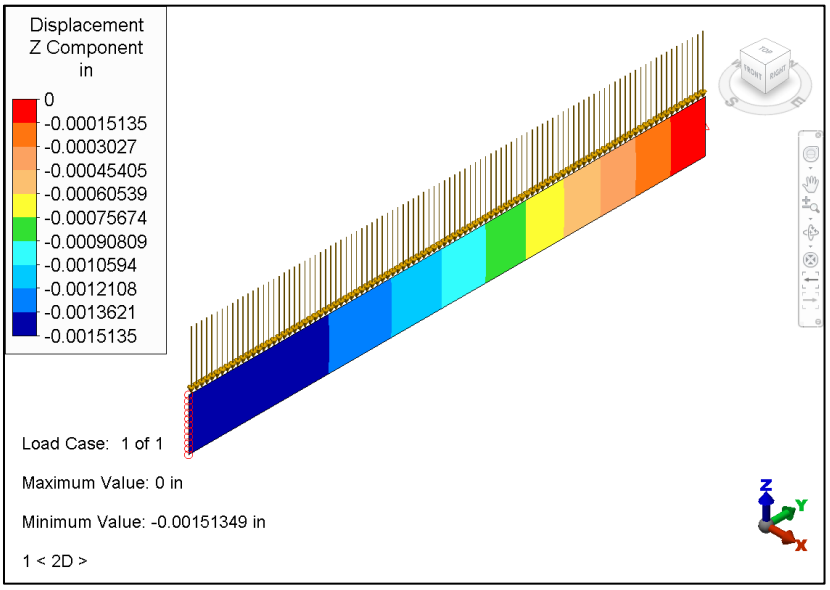

Figure 68-2. Vertical displacement results for the 2-D model.

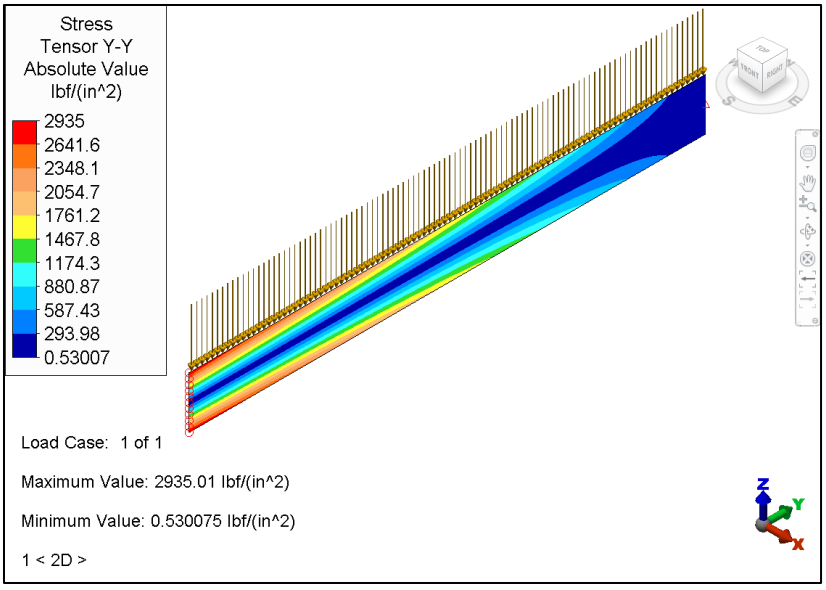

Figure 68-3. Stress results (absolute value) for the 2-D model.

The plate elements predicted a similar displacement value but a slightly lower stress value of 2,880.4 psi (due to the large stress gradient at the edge) as shown in Figures below.

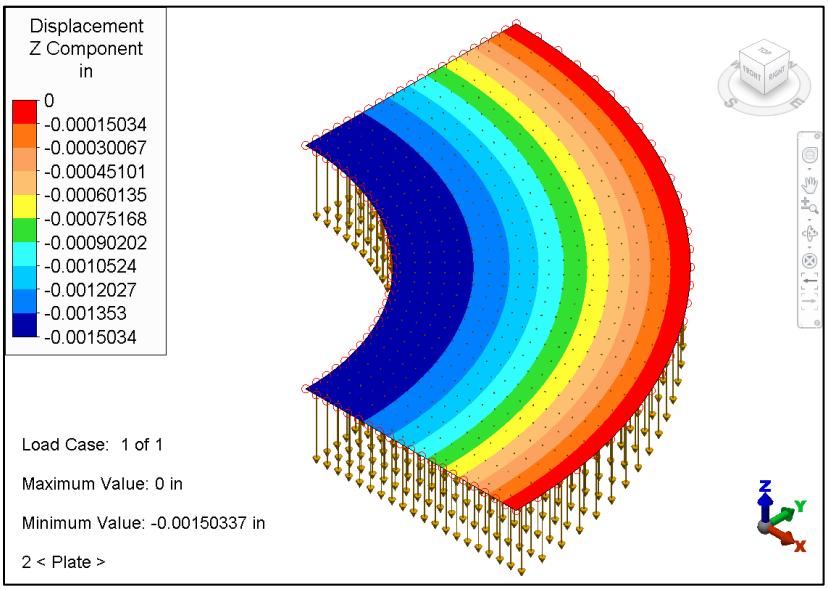

Figure 68-4. Vertical displacement results for the plate model.

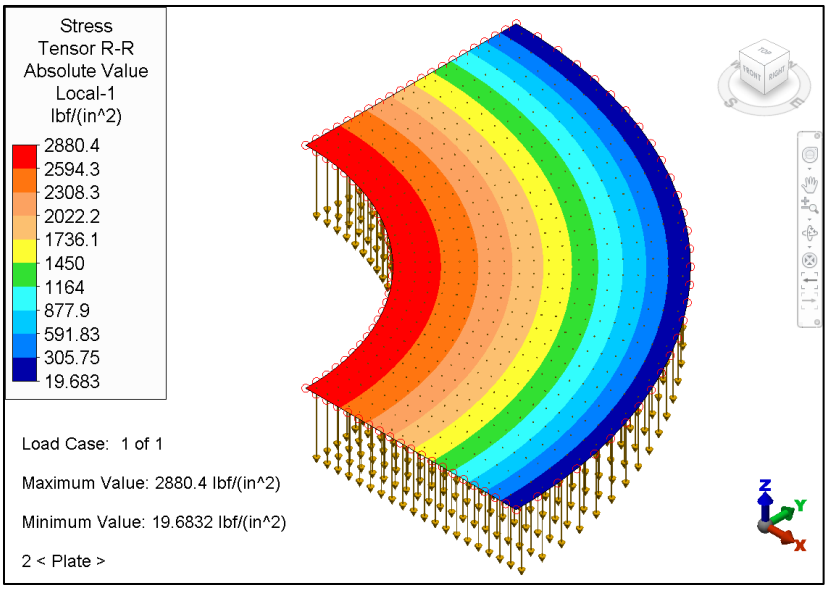

Figure 68-5. Stress results (absolute value) for the plate model.

A brick element model, shown in Figures below, was created by using the "Modify:Copy…" command with the "Join All Copies" option active to extrude the plate model mesh and create two brick elements through the thickness. The brick element produced acceptable results (deflection of 0.0015133 in, stress of 2912.3 psi), which illustrate that a planar mesh can easily be converted into an acceptable brick mesh.

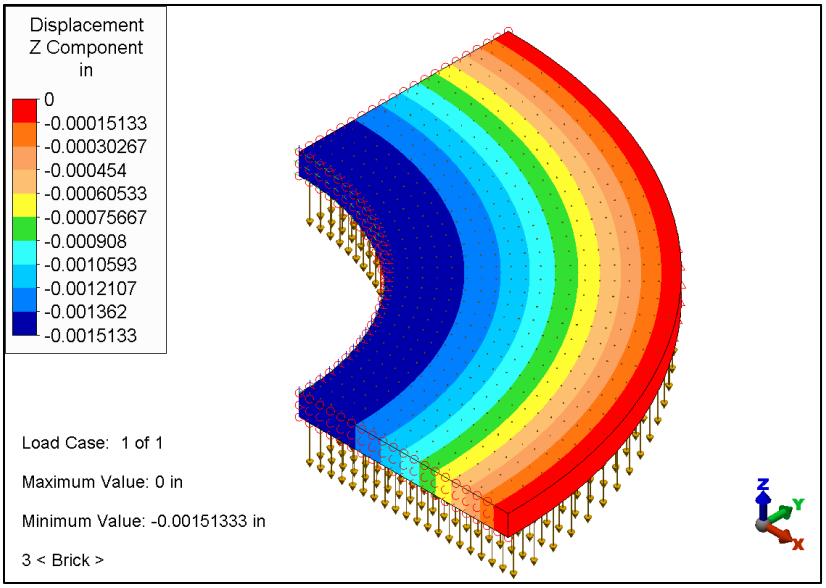

Figure 68-6. Vertical displacement results for the brick model.

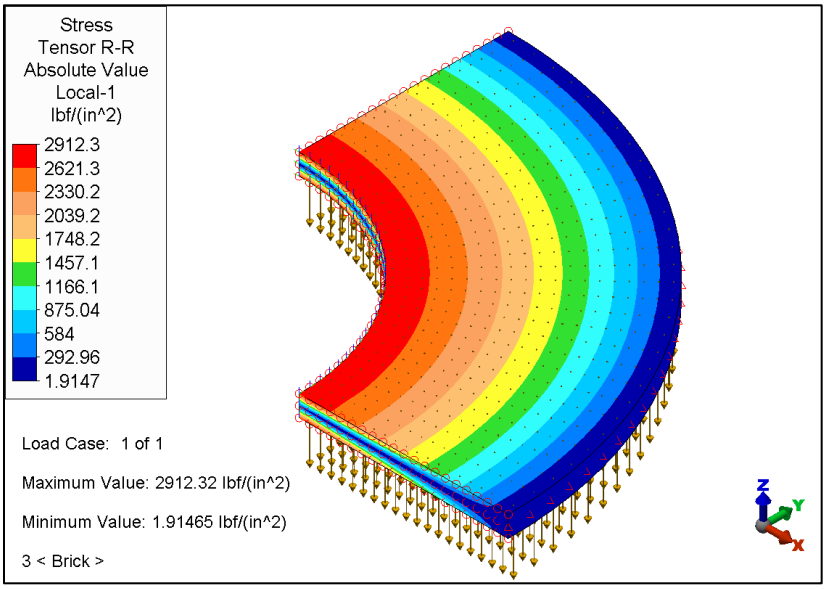

Figure 68-7. Stress results (absolute value) for the brick model.

Table 68-1. Comparison of Results

	Theoretical	Analysis (2-D)	% Difference	Analysis (Plate)	% Difference	Analysis (Brick)	% Difference
Deflection (inches)	-1.5E-3	-1.5135E-3	0.90	-1.5034E-3	0.23	-1.5133E-3	0.89
Stress (psi)	2,935	2,935	0.00	2,880.4	1.86	2,912.3	0.77

AVE - 69 Nonlinear Static Analysis of a Simply Supported Plate

Reference

Timeshenko and Woinowsky-Krieger, *Theory of Plates and Shells*, McGraw-Hill Book Company, Inc., 1959, page 116.

Problem Description

A square plate with simply supported edges is subjected to a uniform pressure load of 1.0 psi. Determine the maximum deflection of the plate.

Theoretical Solution

The analytic result of $W_{max} = 4.4335 * 10^{-9} * t^{-3}$ was obtained using the equation $W_{max} = \alpha * p * a^{4/D}$

Where:
$D = \{E * t^3\} / \{12(1- \nu^2)\}$
$p = 1.0$ psi
$a=1.0$
$E=1 \times 10^7$ psi (Young's modulus)
$\nu = 0.3$ (Poisson's Ratio)
$\alpha = 0.00406$ (From Timoshenko, et. al.)

Autodesk Simulation Solution

The plate was modeled using two different mesh densities (16 x 16 and 32 x 32) and thicknesses (0.01 and 0.001). The boundary conditions used were simply supported along all edges (T_{xyz}). The transverse pressure loading of 1.0 psi was defined.

The nonlinear plate/shell element model was analyzed using the MES Nonlinear Static Analysis Processor to investigate accuracy for various thicknesses and mesh densities.

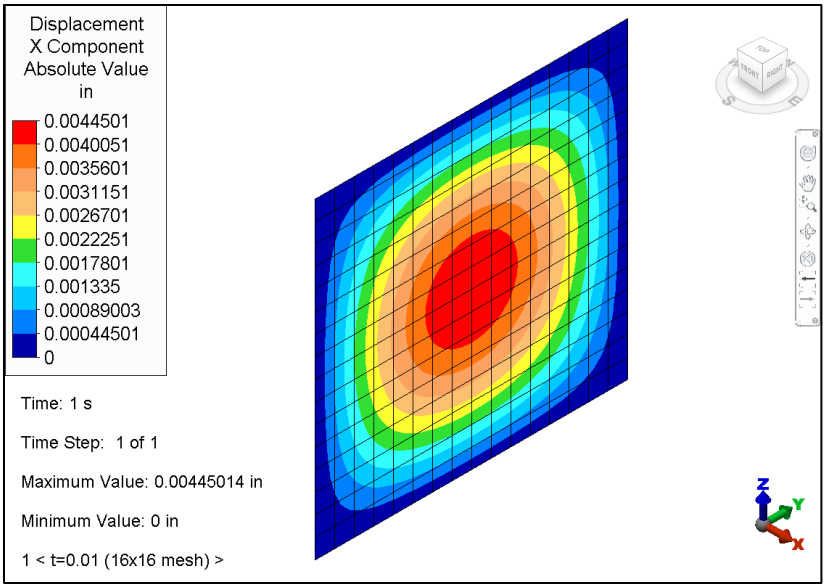

Figure 69-1. The center of the plate was where the maximum displacement occurred after the pressure load was applied.

Comparison of the analysis results using the nonlinear plate/shell element model for 0.01- and 0.001-inch thick plates are shown in the following table. Two mesh densities were used, both utilizing the 8-node nonlinear plate/shell element (shell elements with midside nodes). The plate dimensions, boundary conditions and loadings were the same in both cases.

Table 69-1. Comparison of Results

Design Scenario	Thickness	Theoretical X-Displacement (in)	Analysis X-Displacement (in)	% Difference
1	t=0.01 (16x16 mesh)	0.0044335	0.0044501	0.37
2	t=0.001 (16x16 mesh)	4.4335	4.42579	0.17
3	t=0.01 (32x32 mesh)	0.0044335	0.0044633	0.67
4	t=0.001 (32x32 mesh)	4.4335	4.4351	0.04

AVE - 70 A Combined Beam/Plate Model

References

American Institute of Steel Construction (AISC), *Steel Construction Manual*, Eighth Edition.

Beer, Ferdinand P. and Johnston, Jr., E. Russel, *Vector Mechanics for Engineers, Statics*, Third Edition, pp. 359-364.

Popov, E. P., *Mechanics of Materials*, Second Edition, pp. 125-126.

Problem Description

This problem uses classical equations to calculate the moment of inertia and section modulus of a combined beam/plate model. The moment of inertia and section modulus are then used to calculate the stress of a simply supported beam made from the combined model.

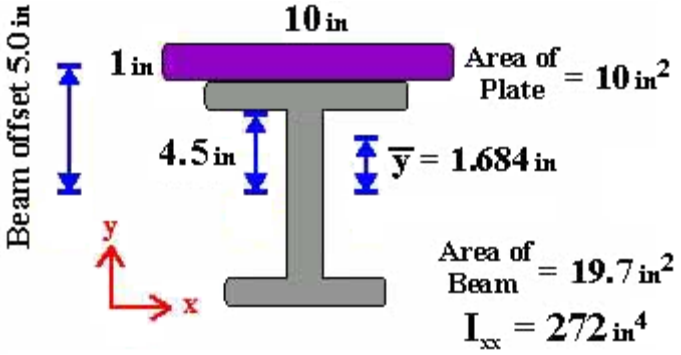

Figure 70-1. Beam/plate model which consists of a W8 x 67-inch wide flange beam with a 10-inch wide by one-inch thick plate attached to the top flange.

Theoretical Solution

The following properties for a W8 x 67-inch wide flange beam are taken from the American Institute of Steel Construction (AISC), *Steel Construction Manual*, Eighth Edition:

- Area (A) = 19.7 in^2
- Moment of inertia about the X-X axis = 272 in^4 (I_3)
- X-X axis section modulus = 60.4 in^3 (S_3)
- Moment of inertia about the Y-Y axis = 88.6 in^4 (I_2)
- Y-Y axis section modulus = 21.4 in^3 (I_2)
- Torsional constant = 5.06 in^4 (J_1)
- Depth of the beam = 9 in (in the y direction)

Using the parallel-axis theorem from *Vector Mechanics for Engineers, Statics*, Third Edition, Beer, Ferdinand P. and Johnston, Jr., E. Russel, pages 359 to 364, the combined moment of inertia is calculated as follows:

$$\bar{y} = \frac{0 \times 19.7 + 10(4.5 + .5)}{(19.7 + 10)} = 1.684 \text{ in}$$

$$I = \frac{1}{12}(10)(1)^3 + 272 + 10(5 - 1.684)^2 + 19.7(1.684)^2 = 438.7 \text{ in}^4$$

Note that the section modulus and moments of inertia are given relative to the center of gravity of the I-beam.

The beam was simply supported on both ends, which were set 240 inches apart. A uniform load of 100 pounds per inch was applied along the span of the beam. The maximum moment, as calculated from the AISC manual, for a simply supported beam for a uniformly distributed load is found on page 2-114 of the AISC, *Steel Construction Manual* and is

$$M = \frac{w(1)^2}{8} = \frac{100(240)^2}{8} = 720{,}000 \text{ inch-pounds}$$

The flexure formula from *Mechanics of Materials*, Second Edition, Popov, E. P., pages 125 to 126 is used to calculate the normal stress for the combined section.

$$\sigma = \frac{My}{I}$$

Autodesk Simulation Solution

Both plate and beam elements were generated in FEA Editor. The plate model has the beam model as its centerline and has 2400 1 x 1 inch elements. It was decoded with the same material properties as the beam and has a thickness of 1 inch. Boundary conditions were added to the left end (TxTyTzRx) and the right end (TyTz) of the beam element. These constraints simulate a simply supported beam. A beam offset of 5 inches and a distributed load of 100 lb/in in the -Y direction was applied.

The stress at the top of the combined section was obtained by looking at the stress tensor in the X direction on the front surface of the plate elements as shown in figure below.

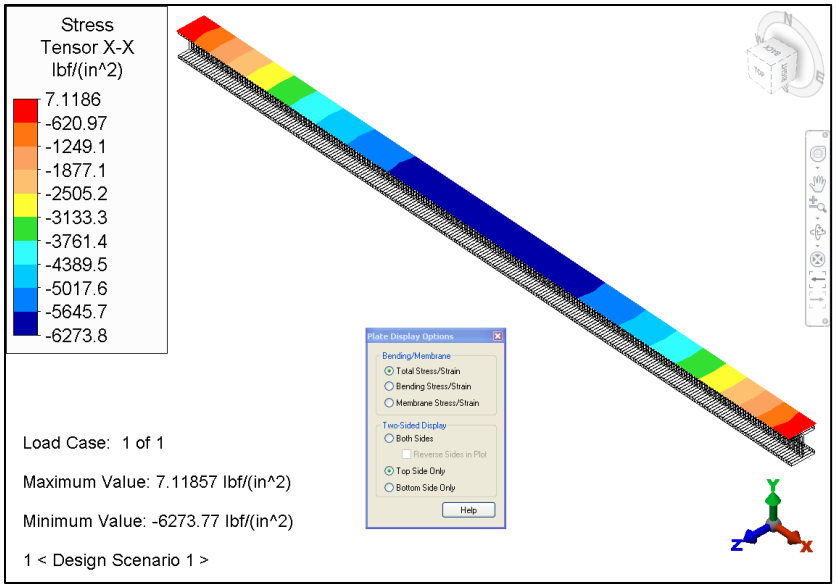

Figure 70-2. Stress tensor X-X for Plate elements (top side only).

The stress at the bottom of the plate elements was obtained by looking at the back side stresses of the plate elements as shown in figure below.

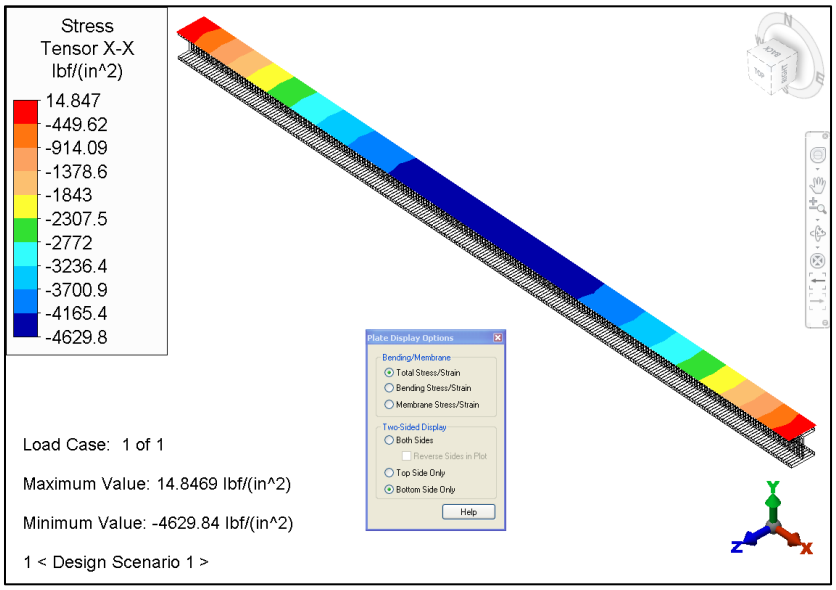

Figure 70-3. Stress tensor X-X for Plate elements (bottom side only).

The stress at the bottom of the combined section can be obtained by looking at the worst stress in the beam elements as shown in figure below. Worst Stress is the combination of axial stress, bending stress about axis 2, and bending stress about axis 3. Positive (+) indicates the beam is in axial tension, and negative (-) indicates the beam is in axial compression.

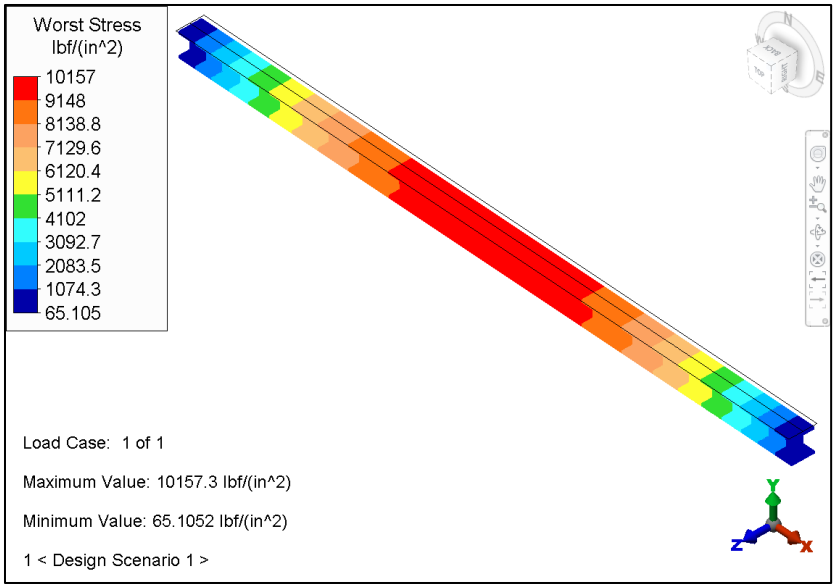

Figure 70-4. Worst stress in the beam elements.

The normal stresses were calculated at the following locations using the moment of inertia of 438.7 in^4 calculated above. These calculated results were compared to the analysis results.

Table 70-1. Comparison of Results

Location	y (in) (refer to Figure 70-1)	Theoretical Stress (psi)	Analysis Stress (psi)	% Difference
Top of Combined Section	(5.5-1.684) = 3.816	6263	6273.8	0.17
Top of Beam Bottom of Plate	(4.5-1.684) = 2.816	4622	4629.84	0.17
Bottom of Beam	(4.5+1.684) = 6.184	10149	10157.3	0.08

AVE - 71 Creep Analysis of a Thick-walled Cylinder

Reference

Odquist, F. K. G., *Mathematical Theory of Creep and Creep Rupture*, Oxford Mathematical Monographs, 1966.

Problem Description

Determine the stationary state stress distribution in a thick-walled cylinder made of a Norton Power Creep Law material when loaded by internal pressure.

$$\varepsilon_c = C_1 \sigma^{C_2} t^{C_3}$$ (Norton Power Creep Law)

Theoretical Solution

$$\frac{\sigma_{hoop}}{p} = q\left[-\left(1-\frac{2}{n}\right)r^{-2/n} + b^{-2/n}\right]$$

$$\frac{\sigma_r}{p} = -q\left[r^{-2/n} - b^{-2/n}\right]$$

$$q = \frac{1}{a^{-2/n} - b^{-2/n}}$$

Where:

a = inside radius
b = outside radius
p = internal pressure
n = creep rate stress exponent
r = radius at point of interest

Autodesk Simulation Solution

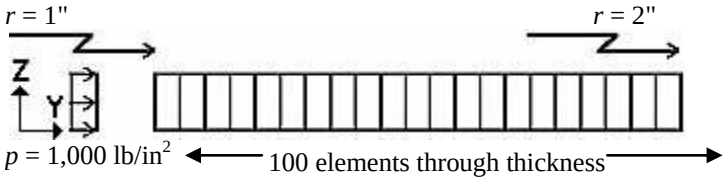

Figure 71-1. Diagram of the creep analysis problem.

Due to the symmetry of the loading and geometry, a 2D axisymmetric analysis was run instead of modeling the entire 3D cylinder. A thin, horizontal slice through the cylinder was modeled, and to model a state of plane strain in the cylinder, translation in the vertical direction (Tz) was constrained on all nodes. The mesh that was used for the analysis had 100 elements through the thickness of the cylinder to better capture the stress gradient.

The constants in the Norton Power Creep Law that were used for this verification example were:

$c^1 = 5 \times 10^{-14}$ in/in/hour
$c^2 = n = 2.0$ in/hour
$c^3 = 1.0$ in/hour

For this analysis, the creep error ratio was set to 0.10.

The cylinder was made out of material with the following properties:

$E = 30 \times 10^6$ psi (Young's modulus)
$\nu = 0.3$ (Poisson's ratio)

A small displacement, constant pressure solution was obtained for a duration of 10,000 hours, divided into 200 time steps of 50 hours each. It was observed that at a time of approximately 2400 hours, the stresses in the cylinder had come to a state of equilibrium. Figure 71-2 plots the predicted stresses through the thickness of the cylinder with the theoretical stresses at the time of 2400 hours.

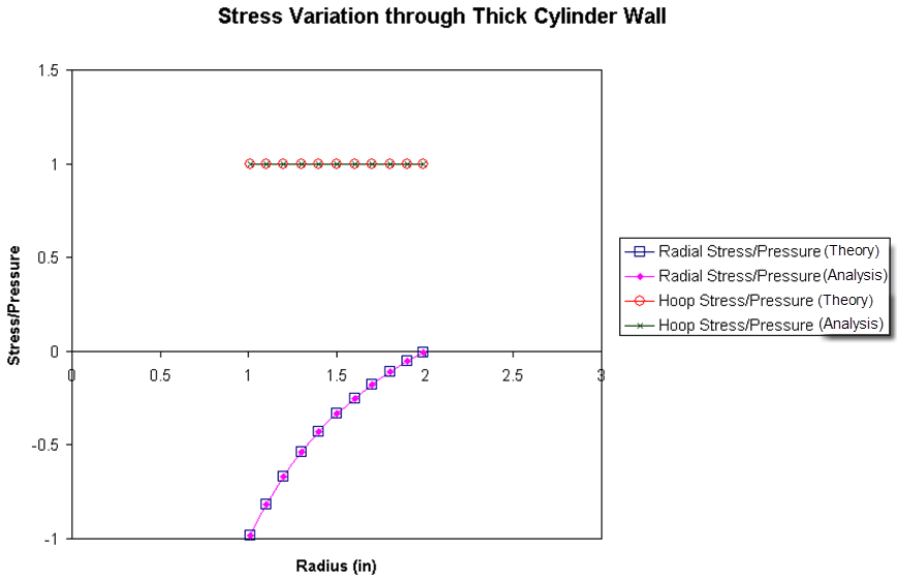

Figure 71-2. Stress variation through the thickness of the thick cylinder at t=2400 hours.

The table below outlines the stress components at r = 1.5 inches at t = 2400 hours, compared to the theoretical stationary state values. From t=2400 hours to the end of the analysis, stress results change by only a very small amount, and at no time after t=2400 hours do the stress results deviate by more than 1% from the theoretical stationary state solution.

Table 71-1. Comparison of Results

	Theoretical (psi)	Analysis (psi)	% Difference
σ_{radial}	-333.33	-333.18	0.05
σ_{hoop}	1000.00	1000.33	0.03

AVE - 72 Shear Flow in a Simply Supported Beam

Reference

Popov, E. P., *Mechanics of Materials*, 2nd Edition, Prentice-Hall, Inc., Englewood Cliffs, NJ, 1976, Section 6-3.

Problem Description

A simply supported beam has a rectangular cross section of 1 inch high by 0.5 inches wide. The beam is 10 inches long. A load of 80 pounds is applied at the center of the beam. This causes a constant shear on the end of the beam as shown in the following shear diagram.

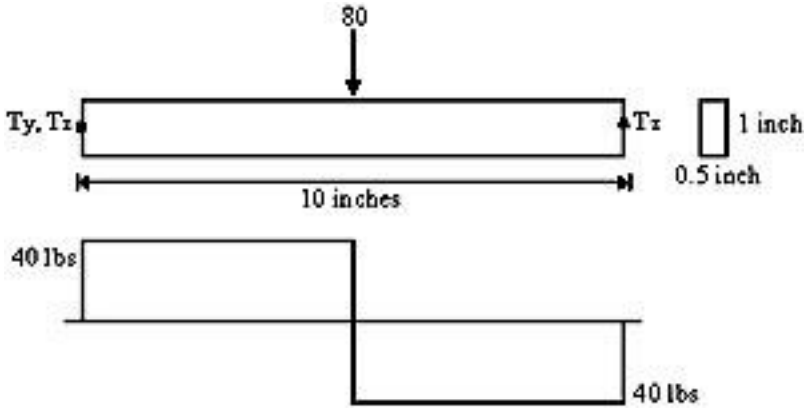

Figure 72-1. Shear diagram of the simply supported beam problem.

Theoretical Solution

Equation 6-5 of Popov predicts the shear flow as follows:

$$q = \frac{VA_{fghi}\bar{y}}{I} = \frac{VQ}{I}$$

The shear flow has units of pounds per inch and is for a unit width. To calculate the actual shear, *q* is divided by the width.

- *Q* is the first or statical moment of area *fghi* around the neutral axis (as shown in Figure 72-2 below).
- $\bar{y}$ is the distance from the neutral axis to the centroid of A_{fghi}.
- *I* is the moment of inertia of the entire cross section.

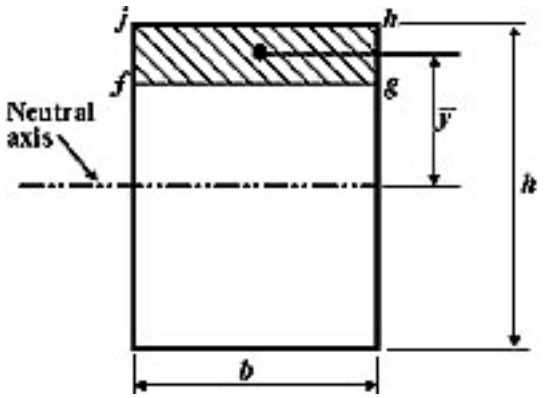

Figure 72-2. The first or statical moment of area *fghi* around the neutral axis

For this example, *V* is constant across half the beam and is 40 pounds. The moment of inertia of this cross section is:

$bh^3/12 = (0.5)(1)^3/12 = 0.04167$ in^4

Q varies depending upon the vertical location at which the shear flow is desired. For the shear flow at the center of the section,

$Q = (0.5)(0.5)(0.25) = 0.0625$ in^3.

The shear flow is then *VQ/I* or (40)(0.0625)/(0.04167) = 60 pounds per inch. Dividing by the width of 0.5, the shear stress at the center is 120 psi.

Autodesk Simulation Solution

The model consists of 16,000 2-D plane stress elements. The model is a rectangle 10 inches long by 1 inch deep. The thickness of the model was specified as 0.5 inches on the "Element Definition" screen. The model was constructed using a uniform mesh with 200 elements along the length and 80 elements through the depth. Fewer elements could have been used to obtain the same level of accuracy if the mesh had been proportioned with more elements towards the outside fibers, since the shear stress is parabolic and varies more rapidly at the outside fibers than at the center.

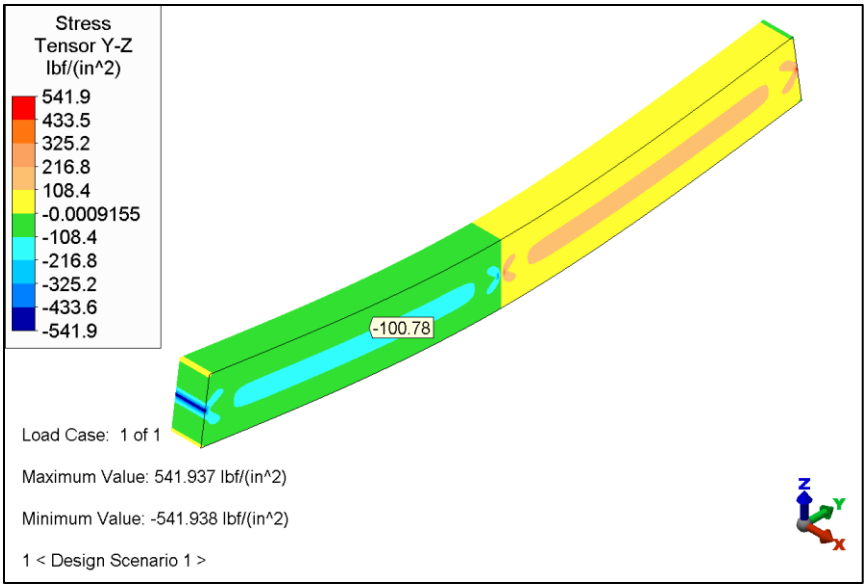

Figure 72-3. Stress tensor results in the entire model (Probe location: Y=2.75, Z=0.7). 3D-Visualization

The shear stress is calculated for various vertical locations and compared to the analysis results in the following table.

Table 72-1. Comparison of Results at Y=2.75

Vertical Location (in)	Area (in^2)	$\bar{y}$ (in)	Q (in^3)	Shear flow q (lb/in)	Shear Stress		
					Theoretical (psi)	Analysis (psi)	% Difference
0.5	0.5	0.25	0.125	60.0	120.0	120.0	0.00
0.6	0.4	0.30	0.120	57.6	115.2	115.2	0.00
0.7	0.3	0.35	0.105	50.4	100.8	100.8	0.00
0.8	0.2	0.40	0.080	38.4	76.8	76.8	0.00
0.9	0.1	0.45	0.045	21.6	43.2	43.2	0.00

The results at y = 2.75 are shown in the above table. The analysis results match the theoretical results with 0.0 percent error. At the point of application of the concentrated load and at the reaction points, there are some edge effects, because the load and reaction were applied as point loads. Away from these edge effects, the shear results are uniform as expected.

AVE - 73 Dynamic Analysis of a Beam Model

Reference

McCormac, Jack C., *Structural Analysis*, Third Edition, pages 565-568.

Problem Description

A propped beam has two concentrated loads as shown in Figure 73-1 (a). Design was performed by the elastic procedure for the 30^k and 50^k loads shown. A W 24 x 84 (S = 197 in^3, Z = 224.0 in^3) beam was selected. We wish to determine the ultimate values of the two concentrated loads (i.e., at collapse of the beam structure) if they are increased at such a rate that they remain in the same proportion to each other. In part (b) of Figure 73-1, the larger load at collapse is equal to P_u and the smaller equal to $0.6P_u$.

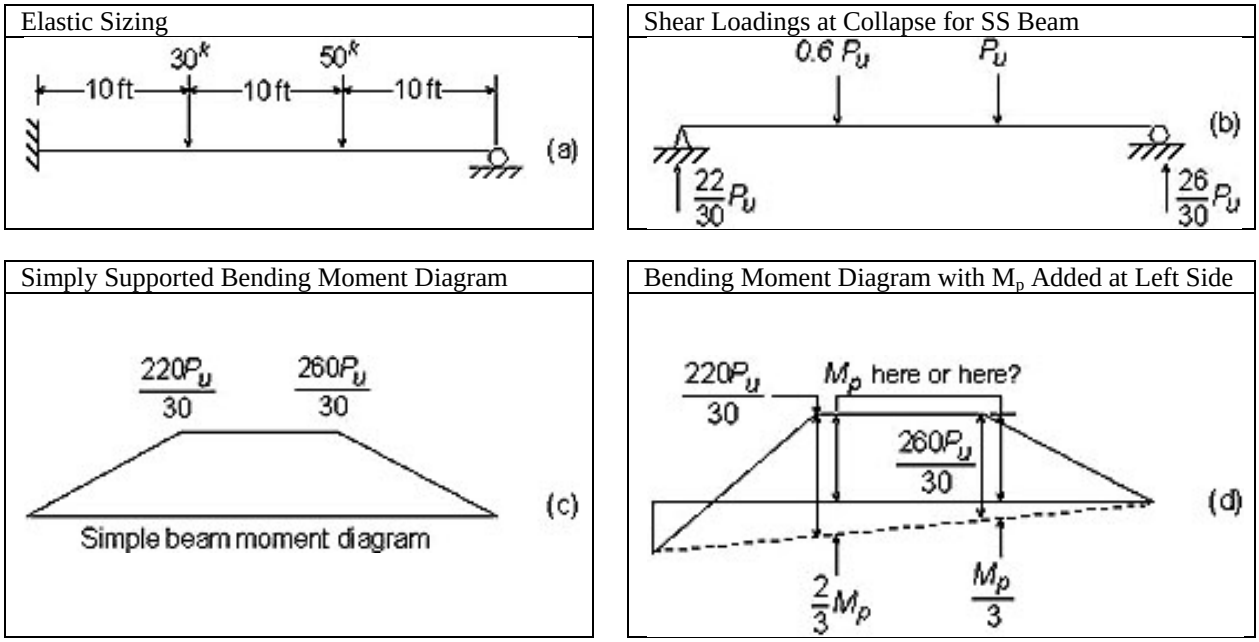

Figure 73-1. A propped beam with two concentrated loads.

As the loads are increased, the left end will reach the plastic moment first. After this plastic hinge forms, the structure will be statically determinate since the right end is a real hinge. The loads may be increased until another plastic hinge forms out in the span at one of the two concentrated loads. Since the point where the second plastic hinge will form is not obvious, we must consider both possibilities.

Theoretical Solution

Should the second plastic hinge be assumed to form at the point of application of the 0.6 P_u concentrated load (see part (d) of Figure 73-1), the values of M_p and P_u can be determined as follows:

$$M_p + \frac{2}{3}M_p = \frac{220\,P_u}{30}$$

$M_p = 4.4P_u$

$P_u = 0.227M_p$

If the second plastic hinge is assumed to form at the point of application of P_u, the values of M_p and P_u would be as follows:

$$M_p + \frac{M_p}{3} = \frac{260 P_u}{3}$$

$M_p = 6.5P_u$

$P_u = 0.154M_p$

The moment at the concentrated load P_u will logically be greater than the moment at the concentrated load $0.6P_u$ and the second plastic hinge will occur at P_u. The numerical value of P_u and the plastic factor of safety can now be calculated.

$$M_p = F_y Z = \frac{(36)(224)}{12} = 672^{'k}$$

$P_u = (0.154)(672) = 103.5^k$

Factor of safety = 103.5/50 = 2.07

If there is any doubt as to whether the correct location of the second plastic hinge has been selected, plot the moment diagrams for the two possibilities as shown in Figure 73-2. If the wrong location is selected, the moment somewhere will exceed the calculated value of M_p. This situation is shown in part (c) of Figure 73-2 where the assumed location of the second plastic hinge under the left load is shown to be impossible.

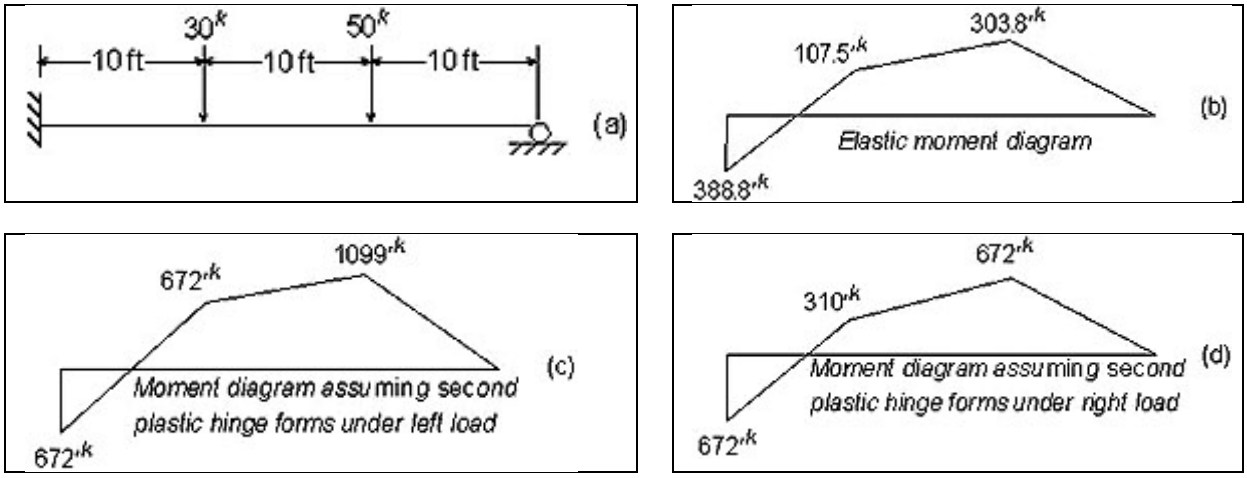

Figure 73-2. Moment diagrams for the two possibilities.

Autodesk Simulation Solution

The nonlinear analysis was run using 300 load steps in the nonlinear dynamic processor. The collapse of the structure occurred at a load factor of 2.09, 0.96% difference from theoretical collapse prediction. The nonlinear analysis was able to predict the onset of gross deformation, which occurs following reaching plasticity at the right location of the loading in the model.

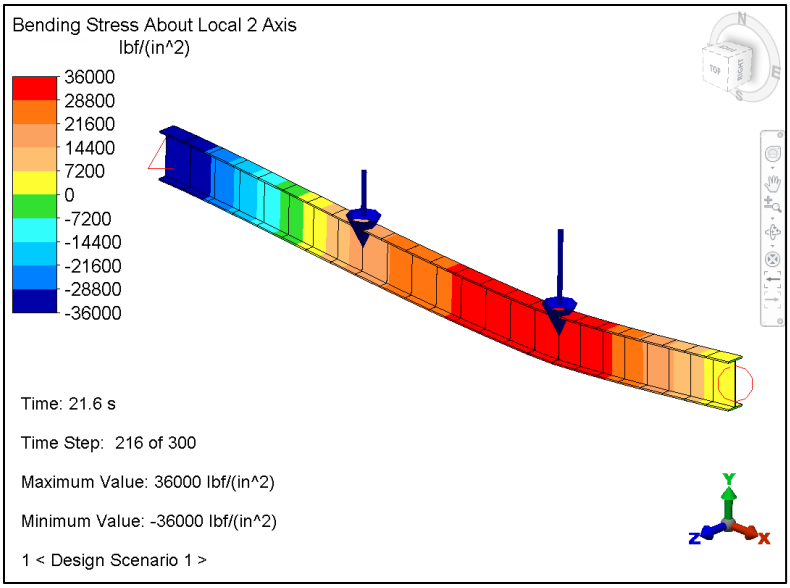

Figure 73-3. 3-D Visualization of deformed shape and Bending Stress about the weak axis.

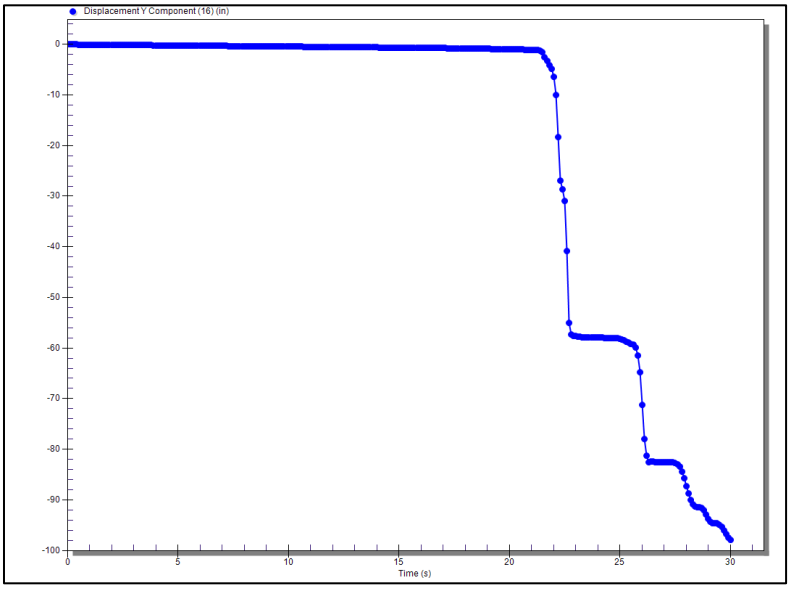

Figure 73-4. Graph of Y displacement of Node 16 vs. time.

Table 73-1. Comparison of Results

	Theoretical	Analysis	% Difference
Load Factor at Collapse	2.07	2.09	0.96

AVE - 74 Thermal Stress Analysis of a Pinned Beam/Truss Structure

Reference

Beer, Ferdinand P. and Johnston, Jr., E. Russell, *Mechanics of Materials*, McGraw-Hill, Inc., 1981, sample problem 2.4, page 58.

Problem Description

The rigid bar *CDE* is attached to a pin support at E and rests on the 30-mm-diameter brass cylinder *BD*. A 22-mm-diameter steel rod *AC* passes through a hole in the bar and is secured by a nut which is snugly fitted when the temperature of the entire assembly is 20°C. The temperature of the brass cylinder is raised to 50°C while the steel rod remains at 20°C. Assuming that no stresses were present before the temperature change, determine the stress in the cylinder.

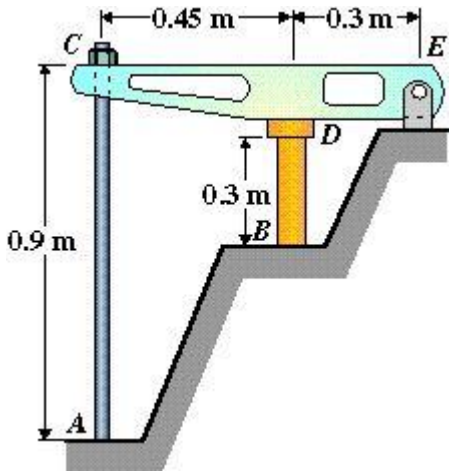

Figure 74-1. Diagram of the pinned beam/truss structure.

Properties of Steel Rod *AC*	**Properties of Brass Cylinder *BD***
E = 200 GPa $\alpha = 12 \times 10^{-6}$/°C	E = 105 GPa $\alpha = 18.8 \times 10^{-6}$/°C

Theoretical Solution

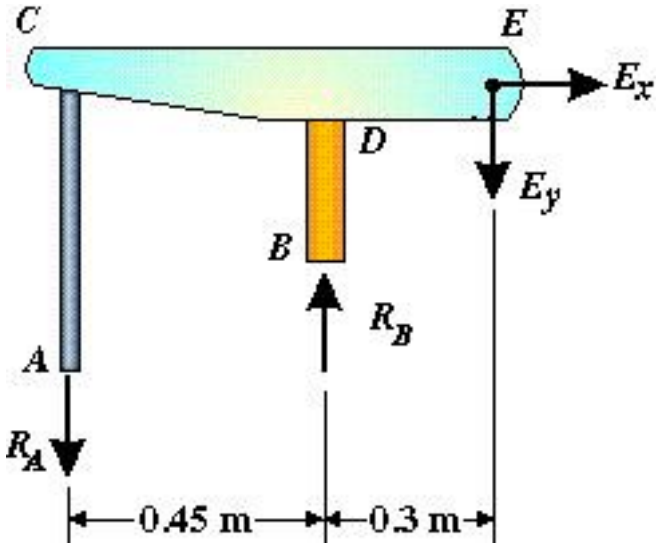

Figure 74-2. Diagram showing R_A and R_B

Statics

Considering the free body of the entire assembly, Beer and Johnston write:

$+\circlearrowleft \sum M_E = 0$:

$R_A\,(0.75\text{ m}) - R_B\,(0.3\text{ m}) = 0$

$R_A = 0.4\,R_B$

Deformations

The method of superposition was used, considering R_B as redundant. With R_B removed, the temperature rise of the cylinder causes point B to move down through δ_T. The reaction R_B causes a deflection δ_1 of the same magnitude as δ_T so that the final deflection of point B will be zero (as shown in Figure 74-3, below).

Deflection δ_T

Due to a temperature rise of 50° - 20° = 30°C, the length of the brass cylinder increases by δ_T.

$\delta_T = L(\Delta T)\alpha = (0.3\text{ m})(30°\text{C})(18.8 \times 10^{-6}/°\text{C}) = 169.2 \times 10^{-6}\text{ m}\downarrow$

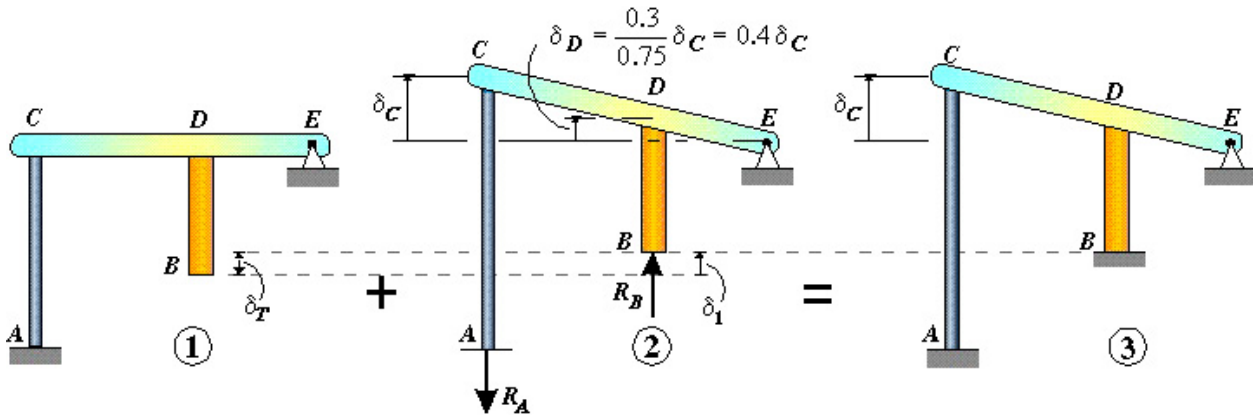

Figure 74-3. Diagram of deflections.

Deflection δ_1

From Figure 083-3, we note that $\delta_D = 0.4\,\delta_C$ and that $\delta_1 = \delta_D + \delta_{B/D.}$

$$\delta_C = \frac{R_A L}{AE} = \frac{R_A (0.9\text{ m})}{\frac{1}{4}\pi (0.022\text{ m})^2 (200\text{ GPa})} = 11.84\times10^{-9}\,R_A \uparrow$$

$\delta_D = 0.4\,\delta_C = 0.4(11.84 \times 10^{-9} R_A) = 4.74 \times 10^{-9} R_A \uparrow$

$$\delta_{B/D} = \frac{R_B L}{AE} = \frac{R_B (0.3\text{ m})}{\frac{1}{4}\pi (0.03\text{ m})^2 (105\text{ GPa})} = 4.04\times10^{-9}\,R_B \uparrow$$

Given that $R_A = 0.4R_B$:

$\delta_1 = \delta_D + \delta_{B/D} = [4.74\,(0.4\,R_B) + 4.04\,R_B]10^{-9} = 5.94 \times 10^{-9} R_B \uparrow$

But $\delta_T = \delta_1$:

169.2×10^{-6} m $= 5.94 \times 10^{-9} R_B$

$R_B = 28.5$ kN

Stress in Cylinder

$$\sigma_B = \frac{R_B}{A} = \frac{28.5\text{ kN}}{\frac{1}{4}\pi (0.03)^2}$$

$\sigma_B = 40.324254$ Mpa

Autodesk Simulation Solution

The software was used to model and analyze the thermal stress interactions in the pinned beam/truss structure, which consists of a brass cylinder and a steel rod pinned to a rigid linkage bar. The goal of the analysis was to thermally load the brass cylinder and find the resultant deflections and stresses. All units were in SI.

The brass cylinder (E = 105 GPa, $\alpha = 18.8 \times 10^{-6}$/°C , diameter = 30 mm) was subjected to a 30°C thermal expansion. The steel rod (E = 200 GPa, $\alpha = 12 \times 10^{-6}$/°C, diameter = 22 mm) was held at a constant temperature. (This was implemented by specifying the stress free reference temperature as -30°C for the brass cylinder and as 0°C for the steel rod.) The cylinder and rod were modeled with truss elements. The rigid bar was represented by two beam elements with artificially stiff properties (area = 1×10^5, $i = 1 \times 10^6$, $s = 1 \times 10^6$, $E = 1 \times 10^{12}$).

The entire model was held in the x direction to force all deflections to remain in the yz plane. Additionally, the trusses were held against translations at their bottom. The rigid bar itself was constrained against movement in the x direction as well as the y and z rotations at all nodes. The pivot node was fully constrained except for the x direction rotation.

During the linear static stress analysis, the temperature of the brass cylinder was raised, which caused the material to expand axially. The steel rod remained at the same temperature and resisted expansion. The analysis results indicated maximum stress in the brass cylinder of 40.34 MPa, a 0.05% difference from the theoretical solution.

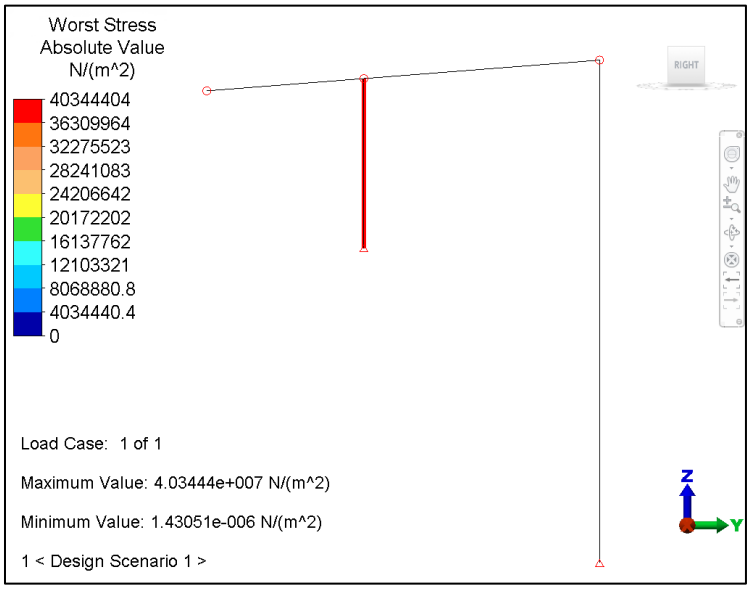

Figure 74-4. Stress results in the model.

Table 74-1. Comparison of Results

	Theoretical (Pa)	Analysis (Pa)	% Difference
Stress in Cylinder	40,324,254	40,344,404	0.05

AVE - 75 Dynamic Nonlinear Analysis of a Beam Model with a Gravity Load

Reference

Beer, Ferdinand P. and Johnston, Jr., E. Russell, *Vector Mechanics for Engineers*, Third Edition, McGraw-Hill, Inc., 1977, sample problem 17.5, p. 790.

Problem Description

Each of two slender rods, as shown in Figure 75-1, is 0.75 m long and has a mass of 6 kg. If the system is released from rest when $\beta = 60°$, determine the velocity of point *D* when $\beta = 20°$.

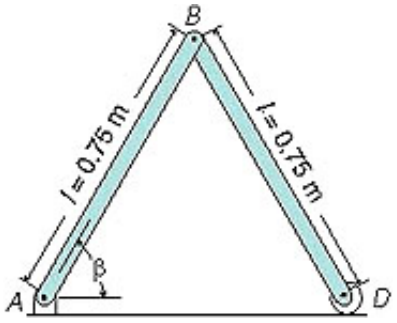

Figure 75-1. Diagram of the hinged rods system.

Theoretical Solution

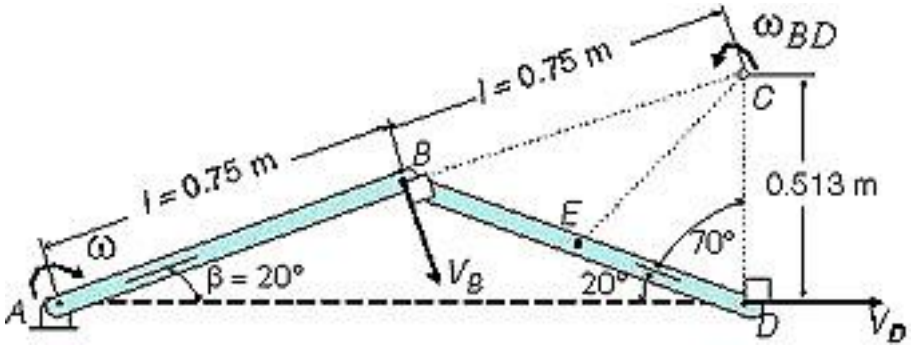

Figure 75-2. Diagram of the hinged rods system with $\beta = 20°$.

Since V_B is perpendicular to the rod *AB* and V_D is horizontal, the instantaneous center of rotation of the rod *BD* is located at *C*. Considering the geometry of Figure 75-2, we obtain

$BC = 0.75$ m

$CD = 2(0.75\text{m}) \sin 20° = 0.513$ m

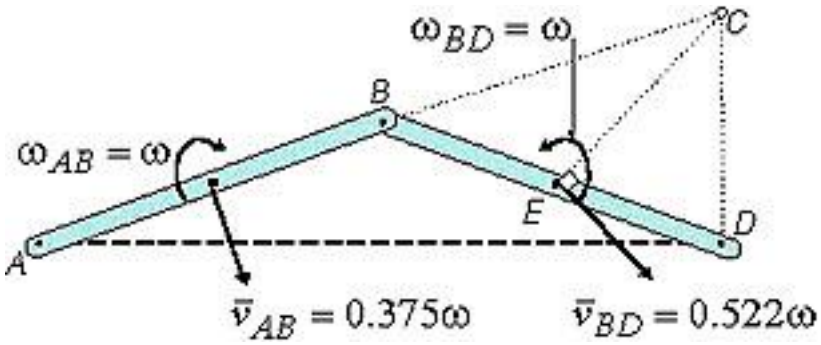

Figure 75-3. Diagram of angular velocities.

Applying the law of cosines to the triangle *CDE*, where *E* is located at the mass center of rod *BD*, we find *EC* = 0.522 m. Denoting by ω the angular velocity of the rod AB, we have:

$\bar{\upsilon}_{AB}$ = (0.375 m) ω

$\bar{V}_{AB} = 0.375\omega \searrow$

υ_B = (0.75 m) ω

$v_B = 0.75\omega \searrow$

Since rod *BD* seems to rotate about point *C*, then:

$\upsilon_B = (BC)\,\omega_{BD}$

(0.75 m) ω = (0.75 m) ω_{BD}

$\omega_{BD} = \omega \circlearrowleft$

$\bar{\upsilon}_{BD} = (EC)\omega_{BD} = (0.522\ )\omega$

$\bar{V}_{BD} = 0.522\omega \searrow$

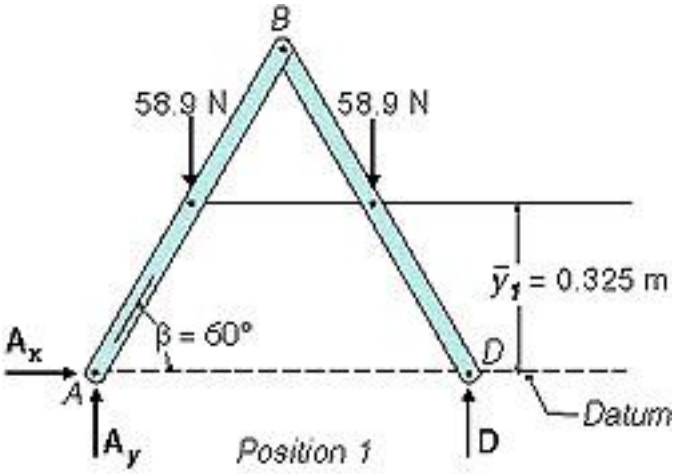

Figure 75-4. Diagram of position 1.

Potential Energy

Choosing the datum as shown, and observing that W = (6 kg)(9.81 m/s^2) = 58.9 N, we have:

$V_1 = 2W\bar{y}_1 = 2(58.9\text{ N})(0.325\text{ m}) = 38.3\text{ J}$

Kinetic Energy

Since the system is at rest, $T_1 = 0$.

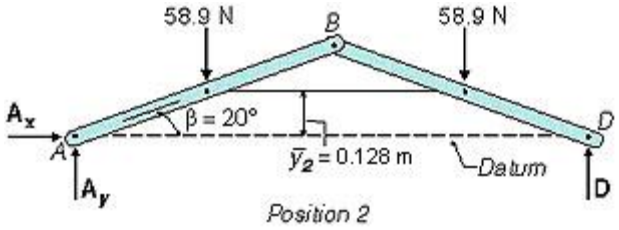

Figure 75-5. Diagram of position 2.

Potential Energy

$V_2 = 2W\bar{y}_2 = 2(58.9\text{ N})(0.128\text{ m}) = 15.1\text{ J}$

Kinetic Energy

$\bar{I}_{AB} = \bar{I}_{BD} = {}^1/_{12}ml^2 = {}^1/_{12}(6\text{ kg})(0.75\text{ m})^2 = 0.281\text{ kg m}^2$

$T_2 = {}^1/_2m\bar{v}^2_{AB} + {}^1/_2\bar{I}_{AB}\omega^2_{AB} + {}^1/_2m\bar{v}^2_{BD} + {}^1/_2\bar{I}_{BD}\omega^2_{BD}$

$= {}^1/_2(6)(0.375\omega)^2 + {}^1/_2(0.281)\omega^2 + {}^1/_2(6)(0.522\omega)^2 + {}^1/_2(0.281)\omega^2$

$= 1.520\omega^2$

Conservation of Energy

$T_1 + V_1 = T_2 + V_2$:

$0 + 38.3\ J = 1.520\omega^2 + 15.1\ J$

$\omega = 3.91$ rad/s

$\omega_{AB} = 3.91$ rad/s ↻

Velocity of Point *D*

$\upsilon_D = (CD)\omega = (0.513\ m)(3.91\ rad/s) = 2.01$ m/s

$V_D = 2.01$ m/s→

Autodesk Simulation Solution

The problem stated above was solved using the MES nonlinear stress analysis software. The two rods were modeled using linear 2-D elements. The mesh was modified to ensure that the rods shared only one coincident node (at point B).

At the bottom of the left rod, the pivot node was fully constrained. On the bottom of the right rod, the pivot node was constrained in all directions except the Y direction, since it is the velocity in the Y direction that we are trying to discover. Additionally, this model employed an impact plane to represent the rod hitting the ground. Since this was a theoretical solution to the body forces of the rods, no damping was used.

The analysis duration was set to 0.75 seconds and a capture rate of 100 results per second was used. Figure 75-6 shows the "Custom Result" graph. Beta is 20degrees between time 0.57 and 0.58 seconds. The following equation was used in the results environment to achieve this custom result. The variable "AB1" was set to the Displacement Y component. this equation outputs the Beta in degrees when one inquires on node # 38 which is the node that exists at point D in Figure 75-1.

acos(((0.75+AB1)^2)/(2*0.75*(0.75+AB1)))*180/3.1415926

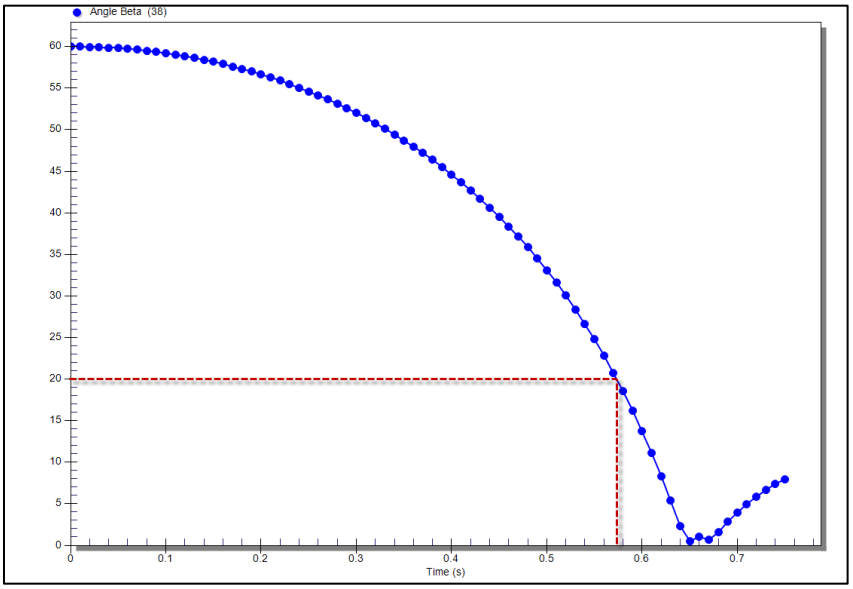

Figure 75-6. The angle Beta over time.

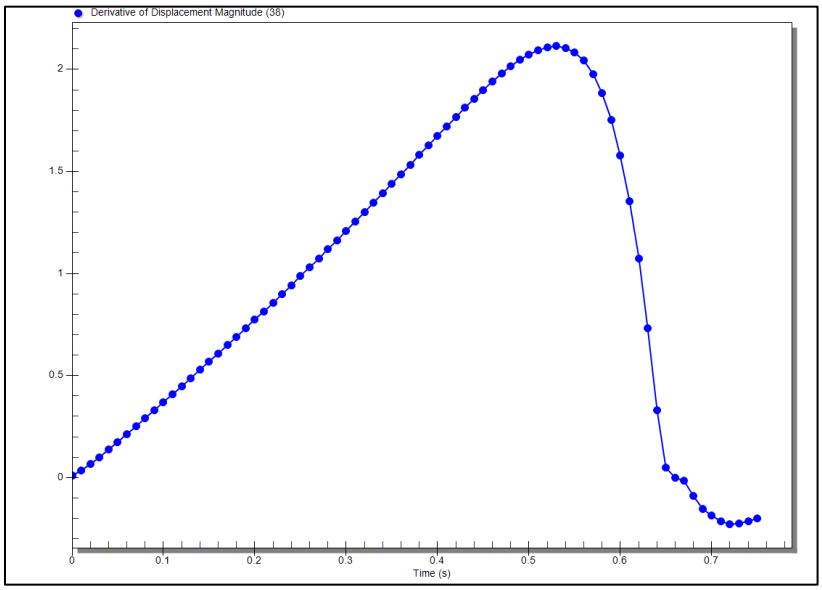

Figure 75-7. Graph of velocity at Point D

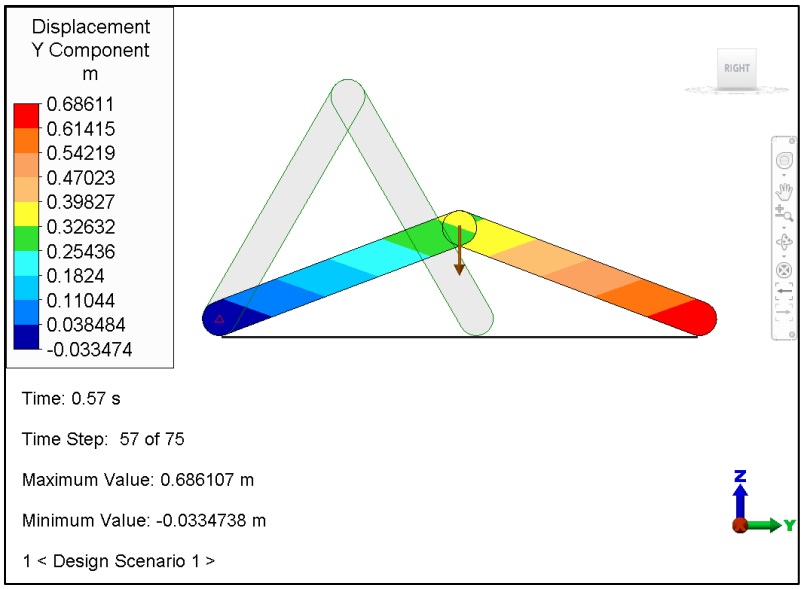

Figure 75-8. Displacement Y component at time = 0.57 seconds

Table 75-1. Comparison of Results

	Theoretical	Analysis*	% Difference
Velocity	2.01 m/s	1.978 m/s	1.59

* Based on velocity of Point D at time = 0.57 seconds

AVE - 76 Linear Stress Analysis of a Beam Model

Reference

McCormac, Jack C., *Structural Analysis*, Third Edition, 1975, pages 388-390.

Problem Description

Given the continuous beam shown in Figure below, find the reactions.

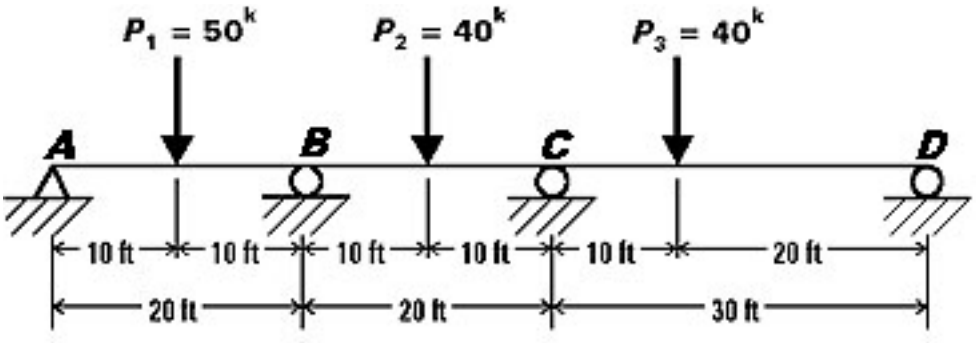

Figure 76-1. Diagram of the beam model.

$E = 29 \times 10^6$ psi
$I = 8147.6$ in^4

Theoretical Solution

The shear and moment diagrams are drawn in the reference as shown in Figure 76-2 and Figure 76-3, below.

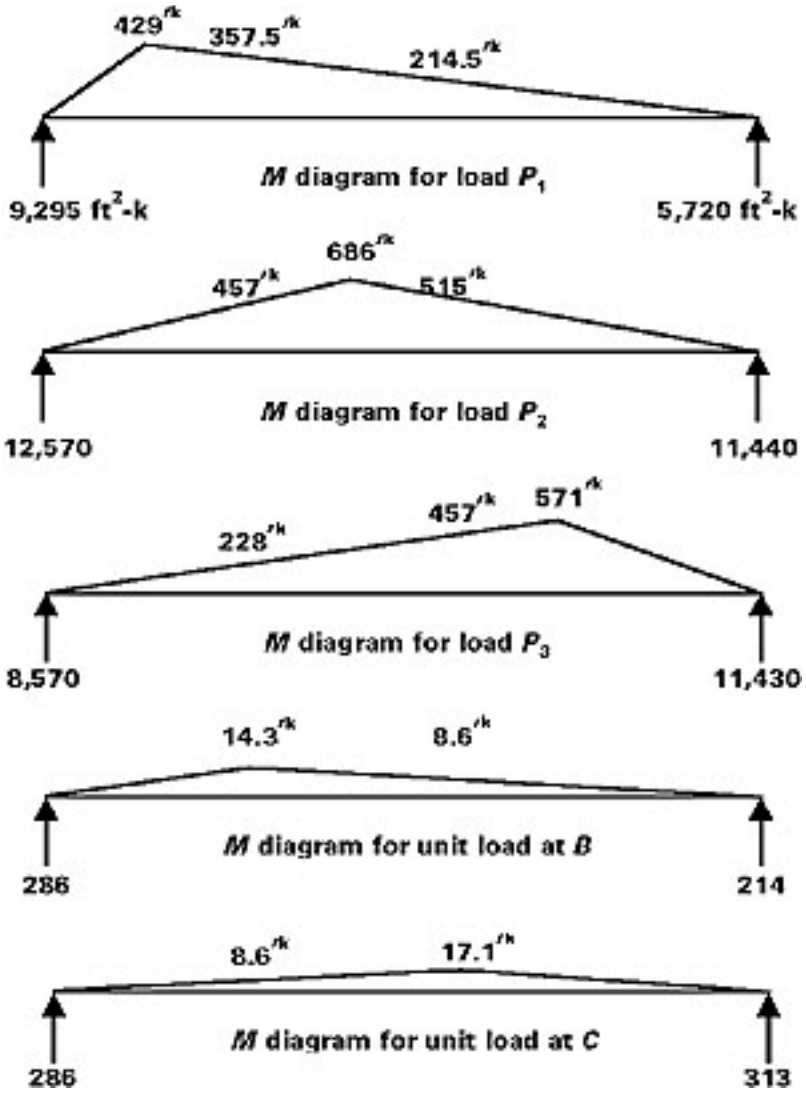

Figure 76-2. Moment diagrams.

δ_B = (5720)(50) - (1/2)(50)(357.5)(16.67) + (12,570 + 8570)(20) - (1/2)(20)(457 + 228)(6.67)

δ_B = 514,350

δ_C = (5720 + 11,440)(30) - (1/2)(30)(214.5 + 515)(10) + (8570)(40) - (1/2)(40)(457)(13.33)

δ_C = 625,300

δ_{bb} = (20)(286) - (1/2)(20)(14.3)(6.67) = 4,765

δ_{cc} = (30)(313) - (1/2)(30)(17.1)(10) = 6,820

$\delta_{cb} = \delta_{bc}$ = (20)(286) - (1/2)(20)(8.6)(6.67) = 5,140

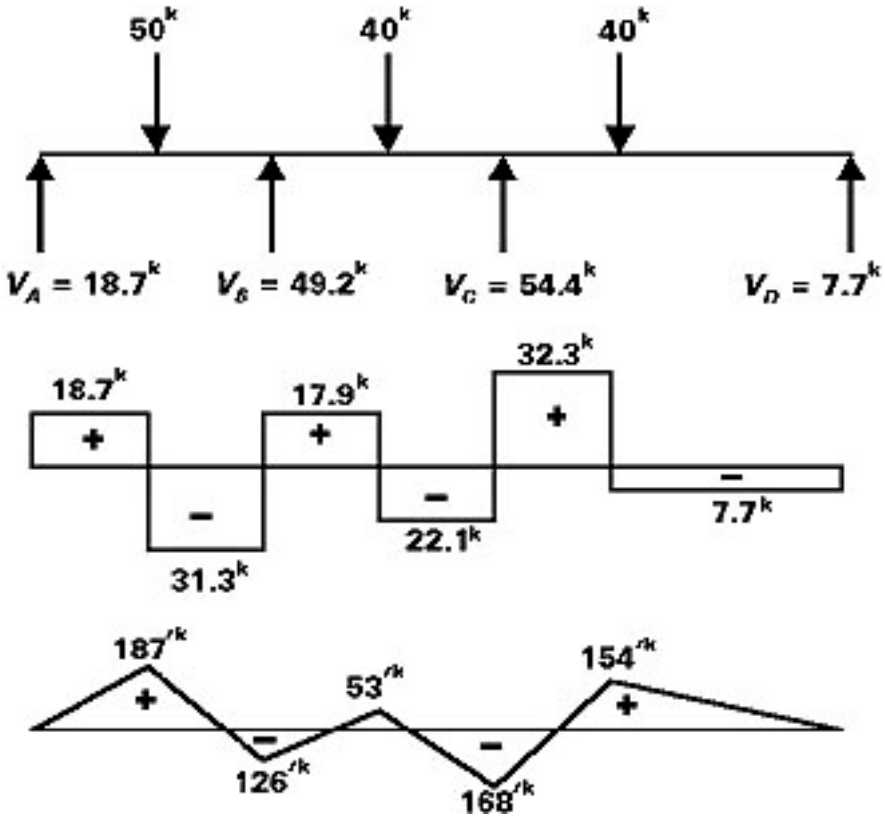

Figure 76-3. Reaction forces and shear and moment diagrams.

By writing the deflection equations,

$$\delta_B + V_B\delta_{bb} + V_c\delta_{bc} = 0$$
$$514{,}350 + 4{,}765V_B + 5{,}140V_C = 0 \quad (1)$$

$$\delta_C + V_B\delta_{cb} + V_C\delta_{cc} = 0$$
$$625{,}300 + 5{,}140V_B + 6{,}820V_C = 0 \quad (2)$$

Simultaneous solution of equations (1) and (2) gives V_B and V_C; values of V_A and V_D are found by statics.

Autodesk Simulation Solution

The beam was modeled using seven beam elements, each 240 inches (10 feet) long. Results are shown in comparison with theoretical results in the table below.

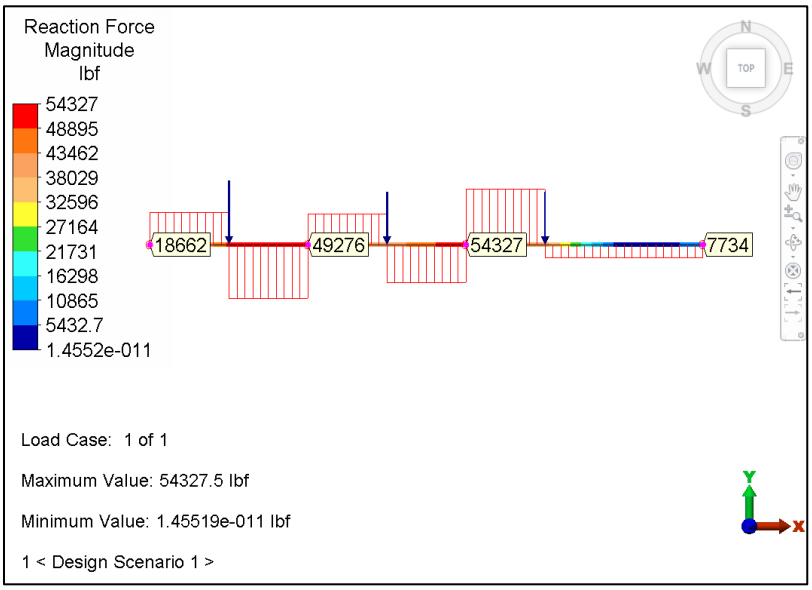

Figure 76-4. Reaction forces and Shear diagram

Table 76-1. Comparison of Results

	Theoretical	Analysis	% Difference
V_A	18.7^k	18.7^k	0.0
V_B	49.2^k	49.3^k	0.2
V_C	54.4^k	54.3^k	0.2
V_D	7.7^k	7.7^k	0.0

AVE - 77 Two Cylindrical Shells with Internal Pressure Loading

Reference

Roark, R. J. and Young, W. C., *Roark's Formulas for Stress and Strain*, Sixth Edition, New York: McGraw-Hill, 1989, Table 31, 1a.

Problem Description

Two cylindrical shells of different thicknesses are subjected to an internal pressure loading. Our goal is to find the radial deflection at the common circumference between the two shells.

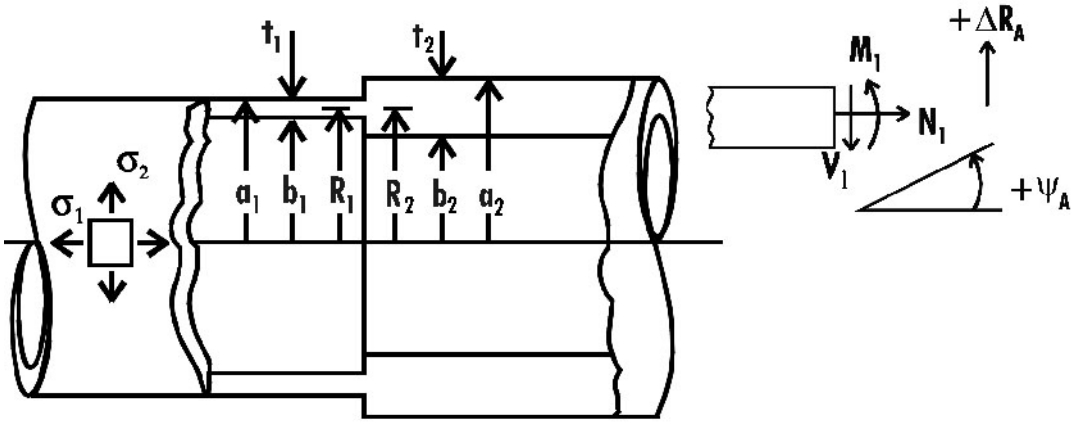

Figure 77-1. Diagram of two cylindrical shells with internal pressure loading (general case, where $b_1 \neq b_2$).

Theoretical Solution

According to Roark and Young, the radial deflection of the common circumference, ΔR_A, is given by the following equation, which is accurate if $R/t > 5$.

$$\Delta R_A = \frac{q R_1^2}{E_1 t_1} K_{\Delta RA}$$

Where:

Thickness (larger O.D. cylinder)	=	t_2	=	2.0 inches
Thickness (smaller O.D. cylinder)	=	t_1	=	1.0 inches
Modulus of Elasticity (same for both cylinders)	=	$E_1 = E_2$	=	3 x 10^7 psi
Inner Radius (same for both cylinders)	=	$b_1 = b_2$	=	19.5 inches
Radius to midplane of small cylinder	=	R_1	=	20 inches
Poisson's Ratio (same for both cylinders)	=	$v_1 = v_2$	=	0.3
Internal Pressure	=	q	=	100 psi
Value from Roark's Table 31, 1a corresponding to R_1/t_1 = 20"/1" = 20 and t_2/t_1 = 2"/1" = 2	=	$K_{\Delta RA}$	=	0.6857

$$\Delta R_A = \frac{q R_1^2}{E_1 t_1} K_{\Delta RA} = \frac{100\,\text{psi}(20\,\text{in})^2}{(3\times10^7\,\text{psi})(1.0\,\text{in})}(.6857) = 9.142667\times10^{-4}$$

(radial deflection at common interface)

Autodesk Simulation Solution

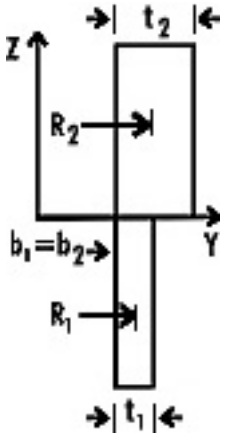

Figure 77-2. Diagram of the 2-D model.

The model was created and meshed in FEA Editor using 2-D axisymmetric linear elements. Boundary conditions were placed at the ends of the model to constrain translation in the z direction on the top and bottom surfaces. The dimensions and parameters defined above for the theoretical solution were used. A comparison between theoretical and analysis solutions may be found in the table below.

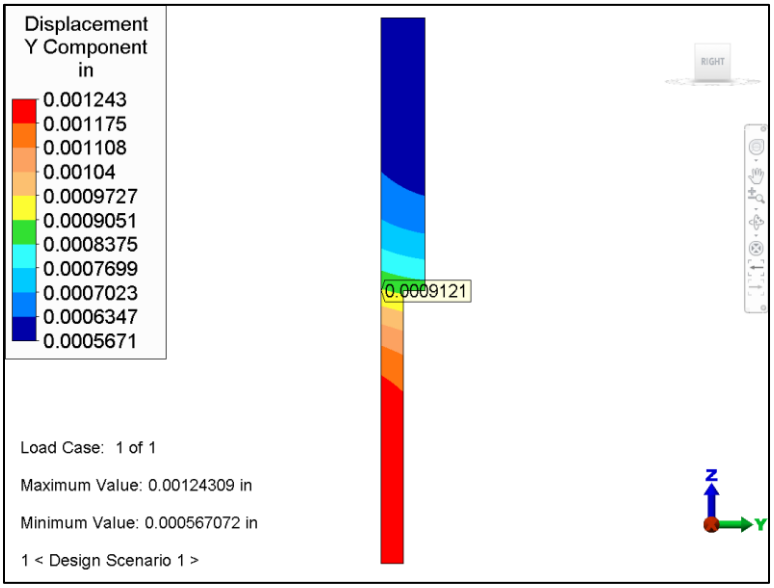

Figure 77-3. Results display of displacement contours with a probe on the node of common circumference.

Table 77-1. Comparison of Results

	Theoretical	Analysis	% Difference
Radial Deflection at Common Circumference	9.142667×10^{-4}	9.121334×10^{-4}	0.23

AVE - 78 Spring and Collar Slide Down Vertical Rod

Reference

Beer, Ferdinand P. and Johnston, Jr., E. Russell, *Vector Mechanics for Engineers, Dynamics*, Third Edition, sample problem 13.6, page 570.

Problem Description

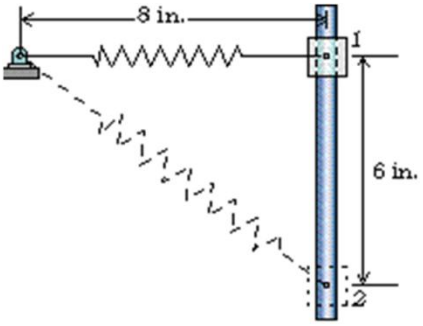

Figure 78-1. Diagram of the spring, collar and rod mechanism.

A 20-lb collar slides without friction along a vertical rod as shown in Figure 78-1. The spring attached to the collar has an undeformed length of 4 in. and a constant of 3 lb/in. If the collar is released from rest in position 1, determine its velocity after it has moved 6 in. to position 2.

Theoretical Solution

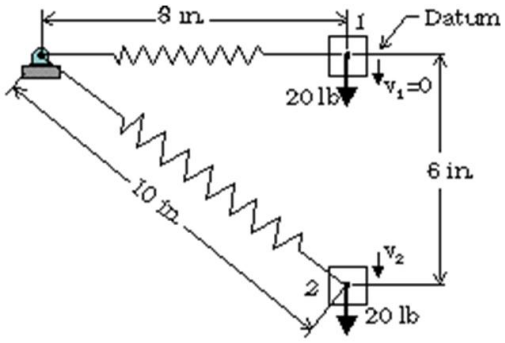

Figure 78-2. Diagram showing datum and velocity.

The elongation of the spring in position 1 is x_1 = 8 in. - 4 in. = 4 in. Therefore, to calculate the potential energy in position 1, we begin by writing

$Ve = ½kx_1^2 = ½(3 \text{ lb/in.})(4 \text{ in.})^2 = 24 \text{ in·lb}$

Choosing the datum as shown, we have $V_g = 0$. Therefore,

$V_1 = V_e + V_g = 24 \text{ in·lb} = 2 \text{ ft·lb}$

Since the velocity in position 1 is zero, $T_1 = 0$, T_1 being the kinetic energy at the initial position.

The elongation of the spring in position 2 is x_2 = 10 in. - 4 in. = 6 in. Therefore, to calculate the potential energy in position 2, we begin by writing

$V_e = ½kx_2^2 = ½(3 \text{ lb/in.})(6 \text{ in.})2 = 54 \text{ in·lb}$

$V_g = Wy = (20 \text{ lb})(-6 \text{ in.}) = -120 \text{ in·lb}$

Therefore the potential energy at position 2 is,

$V_2 = V_e + V_g = 54 - 120 = -66 \text{ in·lb} = -5.5 \text{ ft·lb}$

To calculate the kinetic energy at position 2 , we write

$T_2 = ½mv_2^2 = (½)(20/32.2)v_2^2 = 0.311v_2^2$

Applying the principle of conservation of energy between positions 1 and 2, we write,

$T_1 + V_1 = T_2 + V_2$

$0 + 2 \text{ ft·lb} = 0.311v_2^2 - 5.5 \text{ ft·lb}$

$v_2 = \pm 4.91 \text{ ft/s}$

$v_2 = 4.91 \text{ ft/s}\downarrow$

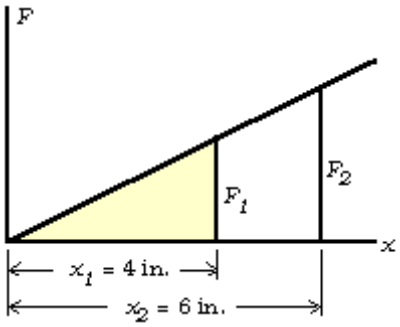

Figure 78-3. Graph of F versus x.

Autodesk Simulation Solution

This problem was modeled in FEA Editor. The collar was drawn in part 1 as a 2 in. x 2 in. square in the YZ plane with its center at the origin. Because only vertical motion is allowed, all nodes were constrained in Ty. The spring was drawn in part 2 as a line between (y=0,z=0) and (y=-8,z=0).

Collar Parameters

- linear 2-D element
- mass density = 0.01294
- Young's modulus = 30 x 10^6
- Poisson's ratio = 0.3
- thickness = 1 in. (given the 4 in. cubic volume)

Spring Parameters

- linear truss element

Properties were determined as follows:

$$k = \frac{P}{\Delta} = \frac{AE}{L} = 3$$

- area, A = 1 in^2.
- length, L = 8 in.
- Young's modulus, E = 24 psi
- initial axial strain = 0.5 (Initial strain is defined as $\Delta L/(L_n + \Delta L)$ where L_n = natural length. Since the spring is stretched from 4 in. at time 0, its initial strain is 50%.)
- density = 0

Other parameters for the spring were defined the same as for the collar.

Global Parameters

- Duration = 0.2 sec.
- Capture rate = 1000 steps per sec.

On the "Load Curves" tab, a constant load curve multiplier of 1 was specified for the duration of the analysis. On the "Acceleration/Gravity" tab, the gravitational constant of 386.4 was set in the -Z direction.

Since the orientation of the truss is changing with time, Mechanical Event Simulation was used to solve this problem.

Results

At a time of 0.185 seconds, the displacement at the center node was 5.997 in. in the -Z direction.

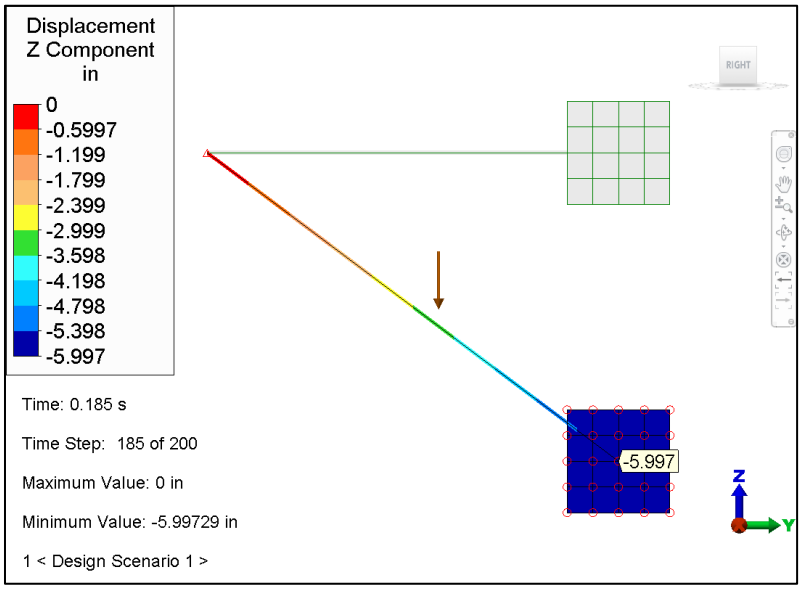

Figure 78-4. Displacement results (Z component)

Velocity result at time 0.185 seconds was 57.969 in./sec. which corresponds closely to the results from Beer and Johnston. The graphing capability was used to graph the displacement and velocity simultaneously.

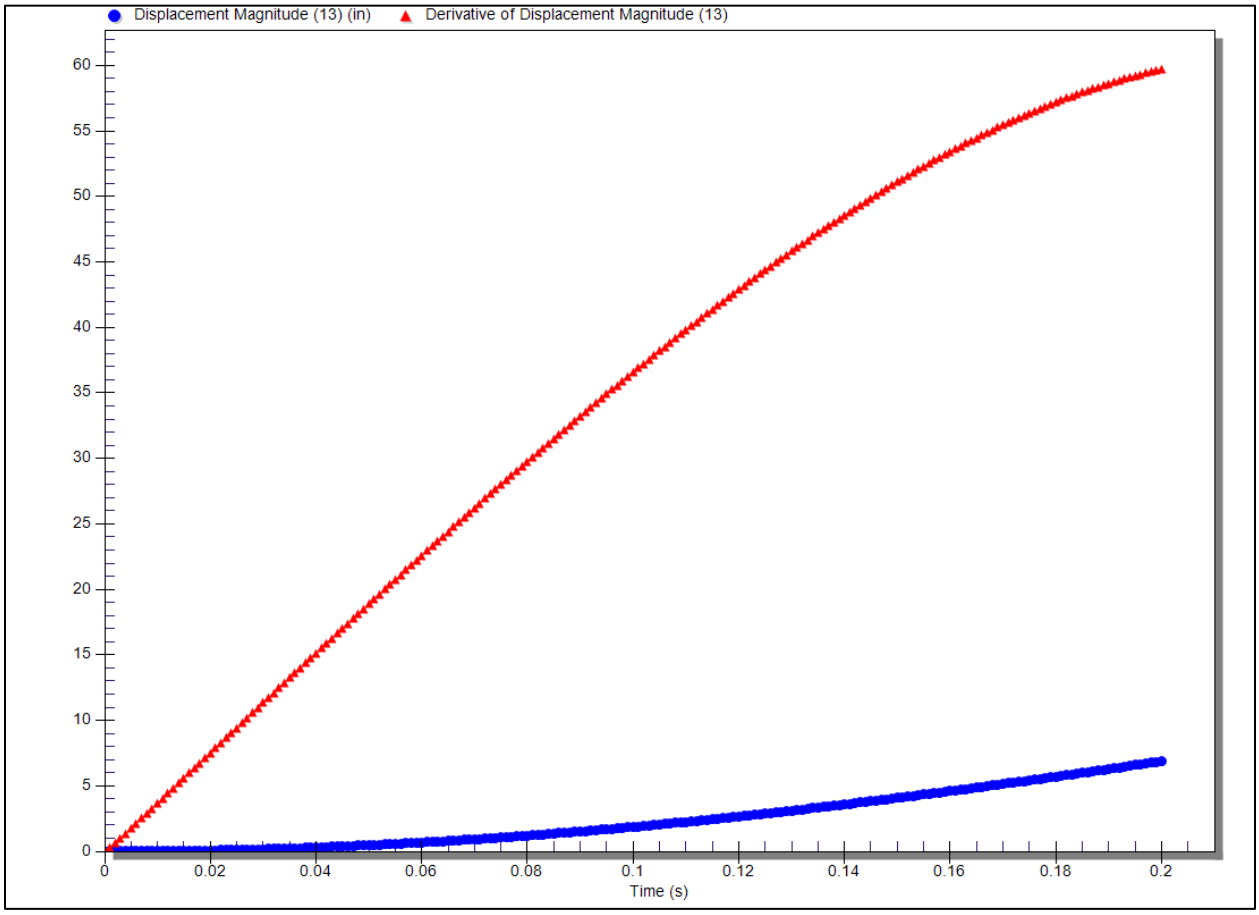

Figure 78-5. Displacement and velocity graph for the node at the center

Table 78-1. Comparison of Results

Velocity at Position 2		
Theory	**Analysis**	**% Difference**
4.91 ft/s	4.83075 ft/s	1.61

AVE - 79 Slender Pivoting Rod and Compressed Spring

Reference

Beer Ferdinand P. and Johnston, Jr., E. Russell, *Vector Mechanics for Engineers, Dynamics*, Third Edition, sample problem 17.4, Page 789.

Problem Description

A 30-lb slender rod *AB* is 5 ft long and is pivoted about a point *O* which is 1 ft from the end *B*. The other end is pressed against a spring of constant k = 1800 lb/in until the spring is compressed 1 in. The rod is then in a horizontal position. If the rod is released from this position, determine its angular velocity and the reaction at the pivot *O* as the rod passes through a vertical position.

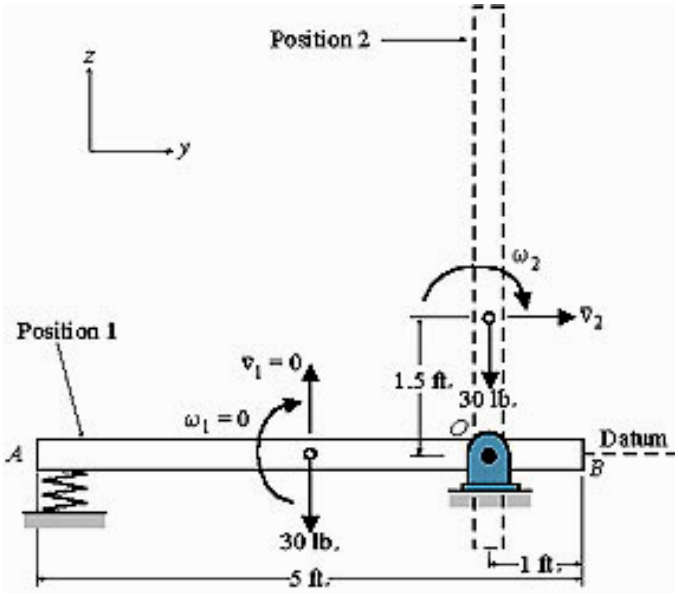

Figure 79-1. Diagram of the pivoting rod and compressed spring system.

Theoretical Solution

Since the spring is compressed 1 inch when in position 1, we have x_1 = 1 in. Therefore, to calculate the potential energy, we begin by writing:

$V_e = \frac{1}{2}kx_1^2 = \frac{1}{2}(1800 \text{ lb/in})(1 \text{ in})^2 = 900 \text{ in·lb}$

Choosing the datum as shown, we have $V_g = 0$; therefore,

$V_1 = V_e + V_g = 900 \text{ in·lb} = 75 \text{ ft·lb}$

Since the velocity in position 1 is zero, the kinetic energy, T_1, also is zero.

The elongation of the spring in position 2 is zero, and we have $V_e = 0$. Since the center of gravity of the rod is now 1.5 ft above the datum, the potential energy is calculated thus:

V_g = (30 lb)(+1.5 ft) = 45 ft lb

$V_2 = V_e + V_g$ = 45 ft lb

Denoting by ω_2 the angular velocity of the rod in position 2, we note that the rod rotates about *O* and write $\bar{v}_2 = \bar{r}\omega_2 = 1.5\omega_2$. To determine the kinetic energy in position 2, we write:

$$\bar{I} = \frac{1}{12}ml^2 = \frac{1}{12}\frac{30\text{ lb}}{32.2\text{ ft/s}^2}(5\text{ ft})^2 = 1.941\text{ lb}\cdot\text{ft}\cdot\text{s}^2$$

$$T_2 = \frac{1}{2}mv_2^2 + \frac{1}{2}\bar{I}\omega_2^2 = \frac{1}{2}\frac{30}{32.2}(1.5\omega_2)^2 + \frac{1}{2}(1.941)\omega_2^2 = 2.019\omega_2^2$$

From the conservation of energy in position 2, we write:

$T_1 + V_1 = T_2 + V_2$: 0+75 ft·lb = $2.019\omega_2^2$ +45 ft·lb

ω_2 = 3.86 rad/s↓

Since ω_2 = 3.86 rad/s, the components of the acceleration of *G* as the rod passes through position 2 are

$\bar{a}_n = \bar{r}\omega^2 = (1.5\text{ ft})(3.86\text{ rad/s})^2 = 22.3\text{ ft/s}^2$ $\quad \bar{a}_n = 22.3\text{ ft/s}^2\downarrow$

$\bar{a}_t = \bar{r}\alpha$ $\quad \bar{a}_t = \bar{r}\alpha\rightarrow$

We express that the system of external forces is equivalent to the system of effective forces represented by the vector of components $m\bar{a}_t$ and $m\bar{a}_n$ attached at *G* and the couple $\bar{I}\alpha$.

+↓$\Sigma M_o = \Sigma(M_o)_{eff}$: $0 = \bar{I}\alpha + m(\bar{r}\alpha)\bar{r}$ $\quad \alpha = 0$

$\pm\rightarrow\Sigma F_x = \Sigma(F_x)_{eff}$: $R_x = m(\bar{r}\alpha)$ $\quad R_x = 0$

+↑$F_y = \Sigma(F_y)_{eff}$: $R_y - 30\text{ lb} = -m\bar{a}_n$

$$R_y - 30\text{ lb} = -\frac{30\text{ lb}}{32.2\text{ ft/s}^2}(22.3\text{ ft/s}^2)$$

R_y = + 9.22 lb

R = 9.22 lb↑

Autodesk Simulation Solution

The model consisted of three parts:

- part 1 – the slender rod (between points A and B)
- part 2 – the spring (at point A)
- part 3 – the pivot (at point O)

Setup

Part 1 consisted of 80 2-D linear elements (1.5 in by 1.5 in) used to represent the 5-ft long slender rod. The origin in FEA Editor was chosen to be point *A*. A height of 3 in and a thickness of 1 in were arbitrarily chosen to approximate the slenderness of the rod. The mass density was calculated to be 4.313×10^{-4} to give the correct weight of 30 lb. The Young's modulus was chosen to be 30×10^{8} to cause the rod to behave as a rigid body.

Part 2 consisted of a single truss element with small displacement. This part was used to represent the spring. The length of the truss was drawn as 3 inches in FEA Editor; therefore, in order to simulate an initial compression of 1 inch, an initial strain of -0.33333333 was used. Since the spring stiffness was specified to be 1800 lb/in, the following equation was solved for the Young's modulus of elasticity, *E* (5400 psi) by setting the area to 1 square in.

$$\frac{P}{\Delta} = \frac{AE}{L} = 1800 \text{ lb/in}$$

The density was set to 0. Since the spring is no longer active after it uncompresses, the following nonlinear stress-strain curve was used.

Table 79-1. Stress vs Strain

Strain (in/in)	Stress (psi)
-1	-5400
0	0
1000	0

The node at point *O* was restrained in the Z and Y directions by a translational boundary condition.

On the "Analysis Parameters" screen, the "Duration" was set to 0.35 sec and the "Capture rate" was set to 10000 steps per second. On the "Load Curves" tab, a constant load curve multiplier of 1 was specified for the duration of the analysis. On the "Accel/Gravity" tab, the gravitational constant of 386.4 in/sec^2 was set in the -Z direction.

Comparison of Results

In the mechanical event simulation, the rod reached position 2 at 0.3422 sec. The analysis predicted a velocity of 69.26 in/s in the Y direction at the center of mass. The results from Beer and Johnston of 3.86 rad/s multiplied by 18 inches gives 69.48. The analysis predicted a reaction of 8.93 lb at point *O* compared to the Beer and Johnston result of 9.22 lb.

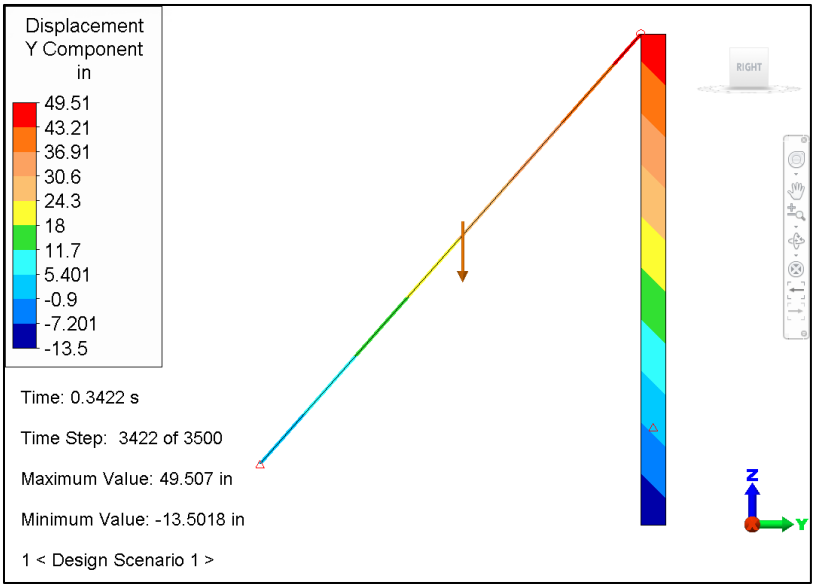

Figure 79-2. Y displacement.

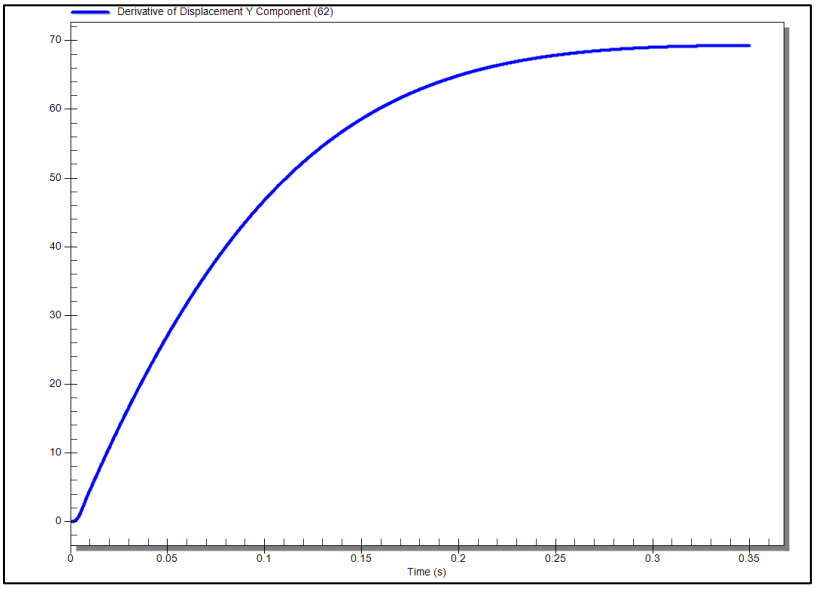

Figure 79-3. Graph of velocity results.

Table 79-2. Comparison of Results

	Theory	Analysis	Difference
Velocity (in/s)	69.48	69.26	0.3%
Reaction (lb)	9.22	8.93	3.1%

Note: Due to size considerations, results for this AVE are not included with the supplied model archive. You can use the archive file to run the analysis on your own.

AVE - 80 Dynamic Analysis of an 8-kg Body Using Damping and a Dashpot

Reference

Meriam, J. L. and Kraige, L. G., *Engineering Mechanics Volume 2: Dynamics*, Fourth Edition, New York: John Wiley & Sons, Inc., 1997, sample problem 8/2, page 610.

Problem Description

An 8-kg body is moved 0.2 m to the right of the equilibrium position and released from rest at time $t = 0$. Determine its displacement at time $t = 2$ sec, given a viscous damping coefficient $c = 20$ N·sec/m, and a spring stiffness $k = 32$ N/m.

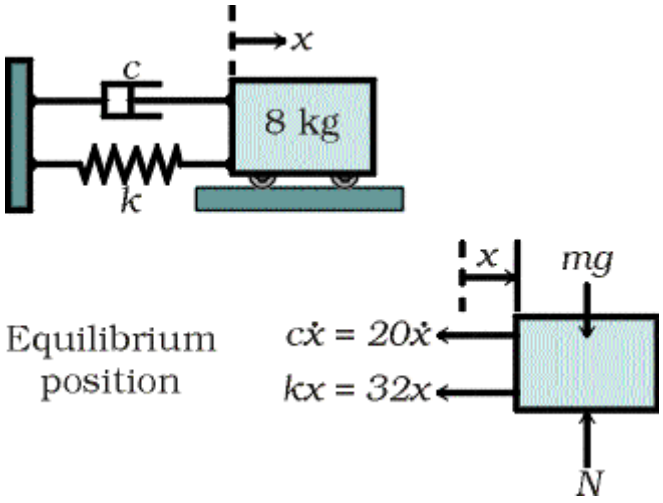

Figure 80-1. Diagram of the 8-kg body system.

Theoretical Solution

In order to determine whether the system is underdamped, critically damped or overdamped, we compute the damping ratio ζ.

$$\omega_n = \sqrt{k/m} = \sqrt{32/8} = 2 \text{ rad/sec}$$

$$\zeta = \frac{c}{2m\omega_n} = \frac{20}{2(8)(2)} = 0.625$$

Since $\zeta < 1$, the system is underdamped. The damped natural frequency is

$$\omega_d = \omega_n \sqrt{1-\zeta^2} = 2\sqrt{1-(0.625)^2} = 1.561 \text{ rad/sec}$$

The motion is given by the equation

$$x = Ce^{-\zeta\omega_n t}\sin(\omega_d t + \psi)$$

Therefore,

$$x = Ce^{-1.25t}\sin(1.561t + \psi)$$

The velocity is then

$$\dot{x} = -1.25Ce^{-1.25t}\sin(1.561t + \psi) + 1.561Ce^{-1.25t}\cos(1.561t + \psi)$$

Evaluating the displacement and velocity at time $t = 0$ gives

$$x_0 = C\sin\psi = 0.2$$

$$\dot{x}0 = -1.25C\sin\psi + 1.561C\cos\psi = 0$$

Solving the two equations for C and ψ yields $C = 0.256$ m. and $\psi = 0.896$ rad. Therefore, the displacement in meters is

$x = 0.256e^{-1.25t} \sin(1.561t + 0.896)$

Evaluation for time $t = 2$ sec. gives $x_2 = -0.0162$ m

(The reference text notes here that the exponential factor $e^{-1.25t}$ is 0.082 at $t = 2$ sec. Hence, $\zeta = 0.625$ represents severe damping, although the motion is still oscillatory.)

Autodesk Simulation Solution

Using FEA Editor, a 1-m square 2-D element was drawn in the YZ plane to represent the 8-kg body. Four 0.2-m prescribed displacements were applied in the positive Y direction, one at each node. Tz constraints were added to the bottom 2 nodes. The square and prescribed displacements were assigned to Part 1.

In Part 2, a 1-m long, general contact element was drawn to perform both the function of the spring and viscous damper. The general contact element is fully constrained on one end and attaches to the 2-D element on the other.

In the general contact data entry screen, under "Unlocked Material Properties", a value of 32 N/m^2 was entered for both the Tensile Young's Modulus and the Compressed Young's Modulus. Under "Damping Parameters", the "Dashpot Coefficient" was set to 20 N·sec/m. The "Cross Sectional Area" was defined as 1.

The 2-D element was defined as a 1-m thick, linear element for Updated Lagrangian Analysis. To give the 1-m cube 8 kg of mass, the density of the 2-D element was defined as 8 kg/m^3. Poisson's ratio was defined as 0.3 and the Young's Modulus as 1×10^9.

The capture rate was defined as 100 steps/sec and the duration was set to 4 sec.

Whereas the reference problem defines $t = 0$ as the moment when the mass is released, an event simulation using prescribed displacements must allow time for displacement to occur. Therefore, the Mechanical Event Simulation was set up to begin 0.2 sec. before the release of the mass. The load curve was defined to apply the 0.2-m prescribed displacements over 0.1 sec and hold the displacements for another 0.1 sec. At time $t = 0.2$ sec, the mass is released to respond to the extended spring. This is accomplished by defining the active range for the prescribed displacement between 0.0 and 0.2 sec (birth = 0 sec and death = 0.2 sec).

Comparison of Results

The Mechanical Event Simulation yielded a displacement of -0.0162 m at 2 sec after the prescribed displacement is released (2.2 sec). Compared to the value obtained from the reference calculations, 0.0162 m, this value matches the reference solution precisely (0.0 % difference).

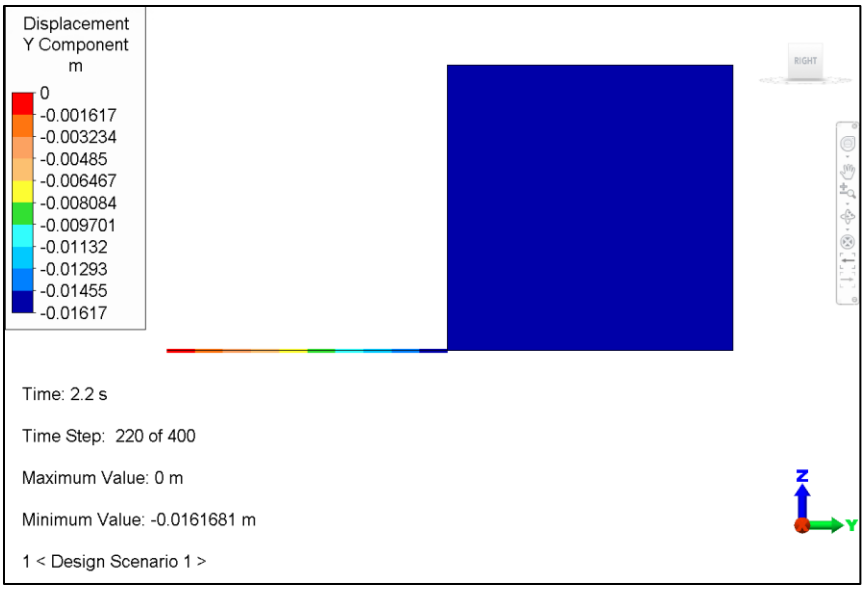

Figure 80-2. Display of displacement results at 2 seconds after the prescribed displacement is released.

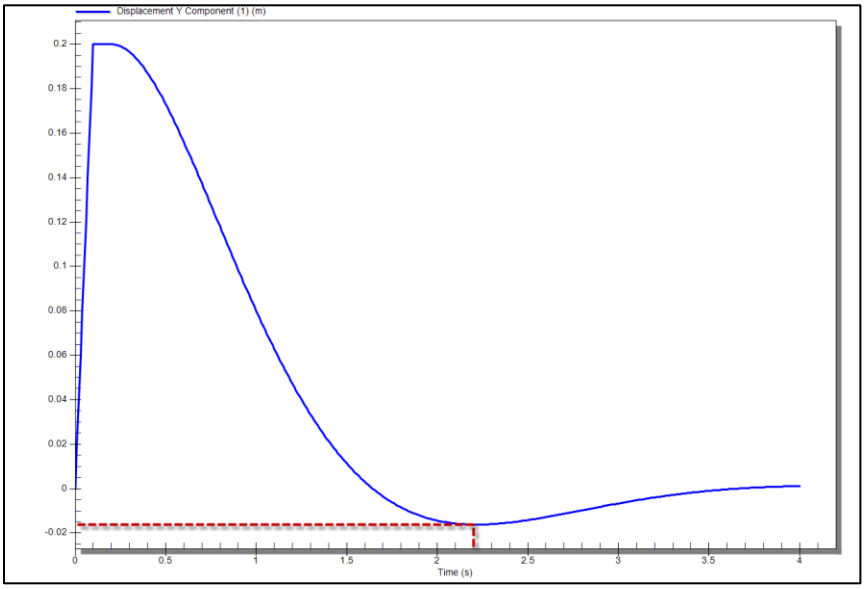

Figure 80-3. Graph of displacement results over time.

Table 80-1. Comparison of Results

	Theoretical	Analysis	% Difference
Displacement (m)	-0.0162	-0.0162	0

AVE - 81 Transient Heat Transfer Analysis of a Semi-Infinite Pressure Loading

Reference

Holman, J. P., *Heat Transfer*, Fifth Edition, McGraw-Hill Book Co., New York, 1981, pp. 132-134.

Problem Description

A semi-infinite, aluminum cylinder initially at 200°C is subjected to a convection at 70°C with h = 525 W/m.^{2}·°C. That is, the convection occurs on one end of the cylinder and around the perimeter. The cylinder is 5 centimeters (cm) in diameter. We must determine the temperatures at:

a) T_1 = the center of the cylinder, and
b) T_2 = the surface,

both at a distance (x) of 10 cm. from the end and 1 minute after being exposed to the environment.

Theoretical Solution

The following conductivity (k) and thermal diffusivity (α) material properties for aluminum were used in the theoretical solution:

k = 215 W/m.·°C
$\alpha = 8.4 \times 10^{-5}$ m^{2}/sec.

Heisler charts were used to combine the temperature solutions for an infinite cylinder and a semi-infinite slab.

For the slab the chart parameters are:

$$\frac{h\sqrt{\alpha\tau}}{k} = \frac{(525)\left[\left(8.4\times10^{-5}\right)(60)\right]^{1/2}}{215} = 0.173$$

$$\frac{x}{2\sqrt{\alpha\tau}} = \frac{0.1}{(2)\left[\left(8.4\times10^{-5}\right)(60)\right]^{1/2}} = 0.704$$

From the Heisler chart:

$$\left(\frac{\theta}{\theta_i}\right)_{\text{semi-infinite slab}} = 1 - 0.036 = 0.964 = S(X)$$

For the infinite cylinder, we calculate both the axis- and surface-temperature ratios. The axis-temperature ratio is:

$$r_0 = 2.5 \text{ cm} \quad \frac{k}{hr_0} = 16.38 \quad \frac{\alpha\tau}{r_0^2} = 8.064 \quad \frac{\theta_0}{\theta_i} = 0.38$$

To find the surface-temperature ratio:

$$\frac{r}{r_0} = 1.0 \quad \frac{\theta}{\theta_0} = 0.97$$

Thus, from the Heisler charts

$$C(\theta) = \left(\frac{\theta}{\theta_i}\right)_{\text{inf cyl}} = \begin{cases} 0.38 & \text{at } r = 0 \\ (0.38)(0.97) = 0.369 & \text{at } r = r_0 \end{cases}$$

The combined solution for the semi-infinite slab and the infinite cylinder is

$$\left(\frac{\theta}{\theta_i}\right)_{\substack{\text{semi-infinite} \\ \text{cylinder}}} = C(\theta)S(x) = \begin{cases} (0.38)(0.964) = 0.366 & \text{at } r = 0 \\ (0.369)(0.964) = 0.356 & \text{at } r = r_0 \end{cases}$$

$T_1 = 70 + 0.366\ (200 - 70) = 117.6$
$T_2 = 70 + 0.356\ (200 - 70) = 116.3$

Autodesk Simulation Solution

FEA Editor was used to create the 2-D cross-section of the cylinder in the Y-Z plane with the centerline of the cylinder and a point 10 cm. from the free end located at the origin. (This makes it easy during post processing to find the nodes of interest.) Finer divisions were used near the surfaces where the thermal gradient will be higher.

After creating the mesh in centimeters, the mesh was scaled to set the units of length to meters (m). The other units used in the analysis were Joule (J), kg., Celsius and seconds (sec), yielding Watts as the units of power.

The top right corner element was split into two triangular elements so that convection conditions could be applied to both the top and side of the cross-section's outside corner. The next step was to change the surface number of the lines that form the top and right sides; that is, the surface of the cylinder. In this case, the entire mesh was created as 1 surface, but the top and right sides were updated to a secondary surface number.

The 3-D, 90° sector of the cylinder was completed by revolving 10 copies of the 2-D model using "Rotate:Copy" with the "Join" switch active.

The 3-D brick element type was selected. Material properties, such as density, specific heat and conduction coefficient, and boundary conditions were assigned.

To derive the specific heat, c_p, the following relationship was used: $\alpha = k/(\rho\, c_p)$ where the density, ρ, of aluminum is approximately 2700 kg./m^3. This yields a value for c_p of 947.97 J./(kg. C°)

The convection coefficient and an ambient temperature were applied to Surface 2. The "Load Curve" was set to "0" since a loading does not change over time

The initial temperature of the model was defined to be 200°C. The solution time step was set to 0.5 seconds, the final solution time was 70 seconds, and the solutions were output every other time step (resulting in output at every second).

To confirm that the extra 30 cm. of cylinder is sufficient to simulate an infinite cylinder, the temperatures of the bottom nodes were checked. Since the temperatures were found not to change axially at the bottom end, we can safely conclude that the extra 30 cm. length is sufficient.

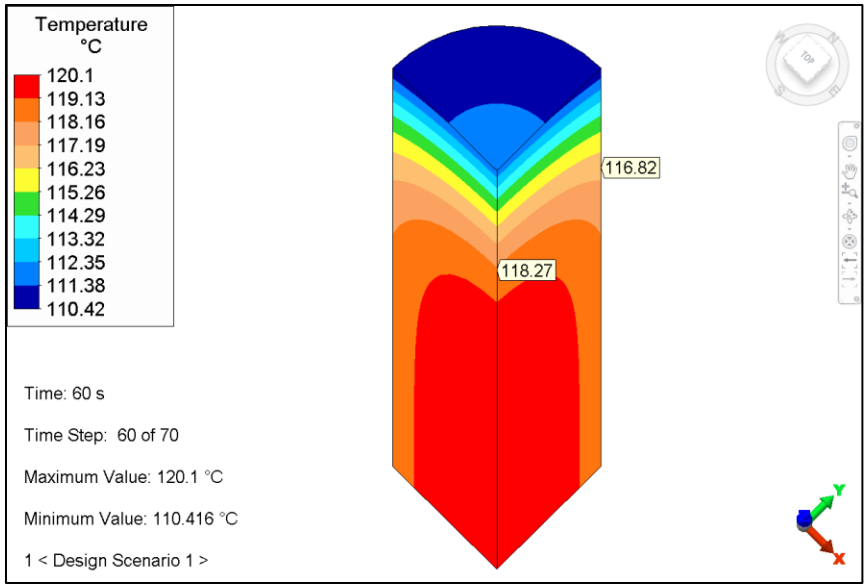

Figure 81-1. Temperature results at T1 and T2, 60 seconds into the analysis.

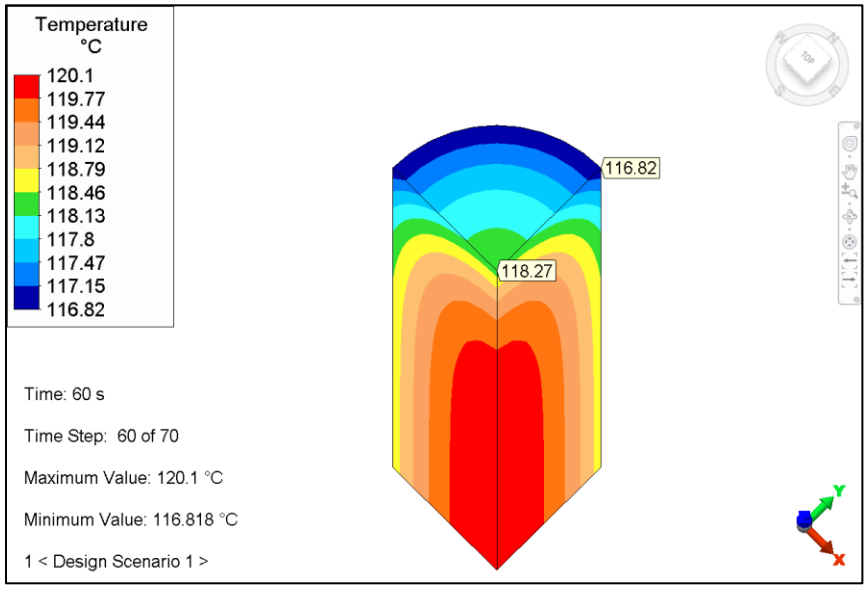

Figure 81-2. Temperature results at T1 and T2, 60 seconds into the analysis. The "Hide Elements" capability was used to show a cross-section of the model at 10 cm.

Table 81-1. Comparison of Results

Temperature at 1 Minute			
	Initial Temperature	**T1 (0,0,0), Center of the Cylinder**	**T2 (0,0.025,0), Surface of the Cylinder**
Theory (°C)	200	117.6	116.3
Analysis (°C)	200	118.3	116.8
% Difference	0.0	0.6	0.4

AVE - 82 Mechanical Event Simulation of a Slider-Crank Mechanism

Reference

Meriam, J. L. and Kraige, L. G., *Engineering Mechanics Volume 2: Dynamics*, Third Edition, New York: John Wiley & Sons, Inc., 1992, sample problem 5/9, page 351.

Problem Description

The common configuration of a reciprocating engine is that of the slider-crank mechanism shown below. At 6 seconds (sec), the rotational velocity (ω) of the crank *BC* is 0.05 rad./sec. and at the position shown below. The crank arm *BC* is 5 inches (in) and *AB* is 14 in. Determine the velocity of the piston *A* at 6 seconds.

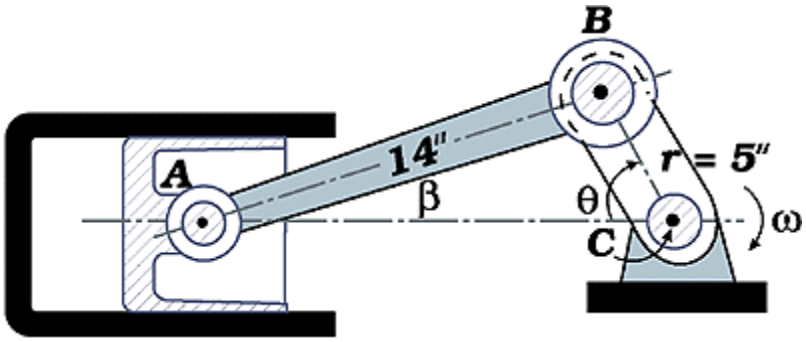

Figure 82-1. Diagram of the slider-crank mechanism.

Theoretical Solution

The velocity of the crank pin *B* as a point on *AB* is easily found, so that *B* will be used as the reference point for determining the velocity of *A* at 6 seconds. The relative-velocity equation may now be written:

$\mathbf{v}_A = \mathbf{v}_B + \mathbf{v}_{A/B}$

The velocity at the pivot point that is common to the two connecting rods (*B*) was computed using the following:

$v_B = r\omega$ = 5 in. (0.05 rad./sec.) = 0.25 in./sec.

and is normal to *BC*. The direction of $\mathbf{v}_A$ is along the horizontal cylinder axis. The direction of $\mathbf{v}_{A/B}$ must be perpendicular to the line *AB* as indicated on the diagram, where the reference point *B* is shown as fixed.

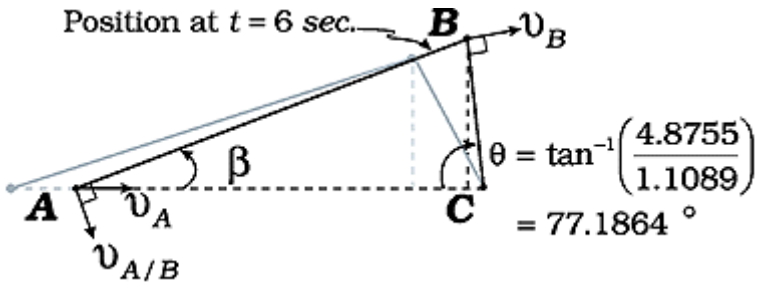

Figure 82-2. Diagram showing velocity.

We obtain this direction by computing the angle β from the law of sines, which gives:

$$\frac{5}{\sin \beta} = \frac{14}{\sin 77.1864}$$

β = 20.38024

We now complete the sketch of the velocity triangle where the angle between $\mathbf{v}_A$ and $\mathbf{v}_{A/B}$ is

90° - β = 90° - 20.38024° = 69.61976°

The second and third angles are

90° - θ = 90° - 77.1864° = 12.8136°

180° - 12.8136° - 69.61976° = 97.56664°

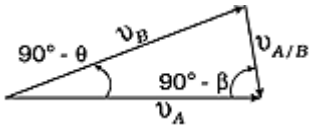

Figure 82-3. Diagram of the velocity triangle.

Solving for $\mathbf{v}_A$ by the law of sines gives

$$\frac{v_A}{\sin 97.56664°} = \frac{0.25}{\sin 69.61976°}$$

v_A = 0.2644 in/sec

Autodesk Simulation Solution

The connecting rod assembly consisted of two rods, each created using solid elements, and connected at the center so as to form a pivot. The model of the connecting rod assembly was generated in FEA Editor, meshed in 2-D using the "Automatic Mesh" commands and then extruded to generate a 3-D solid model, containing 76 solid elements. The left end (*A*) was constrained to move only in the Y-direction. The right pivot point (*C*) had all translational degrees of freedom constrained.

Motion was generated using a prescribed rotation about the connecting rod pivot location (*C*). This rotational velocity was input using a prescribed rotation about the X-axis. The motion was transferred into the connecting rod by means of an arrangement of beam elements.

The analysis was processed using Mechanical Event Simulation. While the analysis was processing, the velocity of the left pivot location was continually viewed. The velocity was displayed by performing the first derivative operation with respect to time on the displacement curve.

The results were obtained at a time of 6 seconds into the analysis.

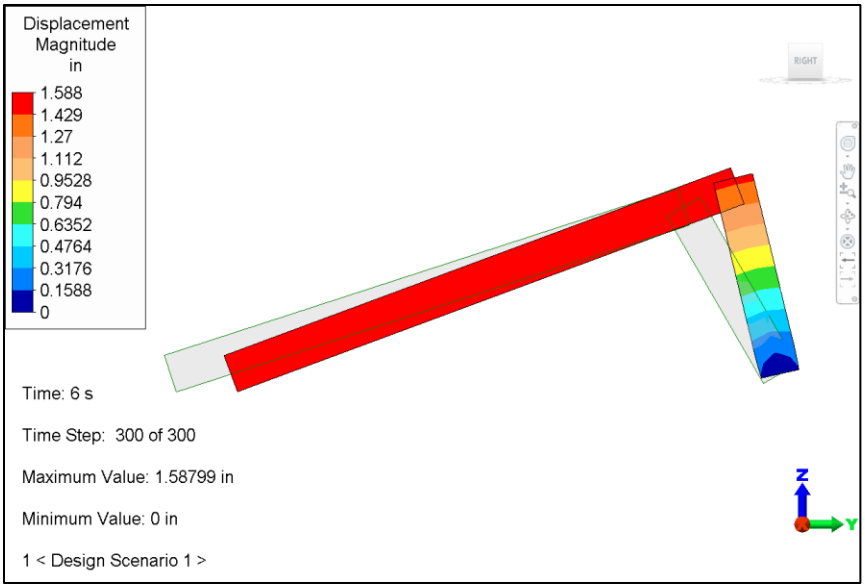

Figure 82-4. This Result display shows the initial and final position of the connecting rod assembly.

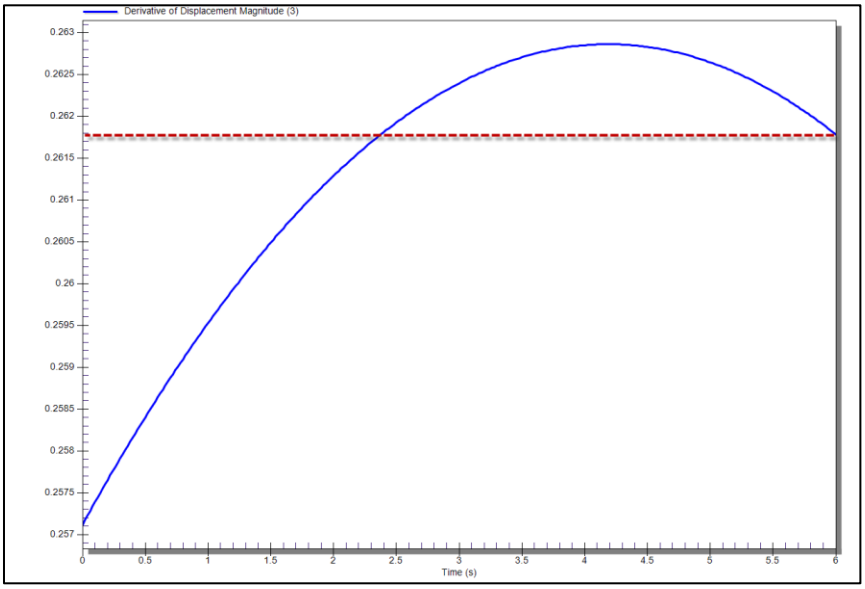

Figure 82-5. Velocity of the piston *A*.

Table 82-1. Comparison of Results

	Theory (in./sec)	Analysis (in./sec)	% Difference
Velocity of A at 6 Seconds	0.2644	0.2618	0.98

AVE - 83 Mechanical Event Simulation of a Lunar Lander

Reference

Meriam, J. L. and Kraige, L. G. *Engineering Mechanics Volume 2: Dynamics*, Third Edition, New York: John Wiley & Sons, Inc., 1992, sample problem 3/185, page 199.

Problem Description

A 200-kg. lunar lander is descending onto the moon's surface with a velocity of 6 m./sec. when its retro-engine is fired. The engine produces a thrust T for 4 sec. that varies with the time as shown in Figure 83-1 and then cuts off. Calculate the velocity of the lander when t = 5 sec, assuming that it has not yet landed. Gravitational acceleration at the moon's surface is 1.62 m/sec^2.

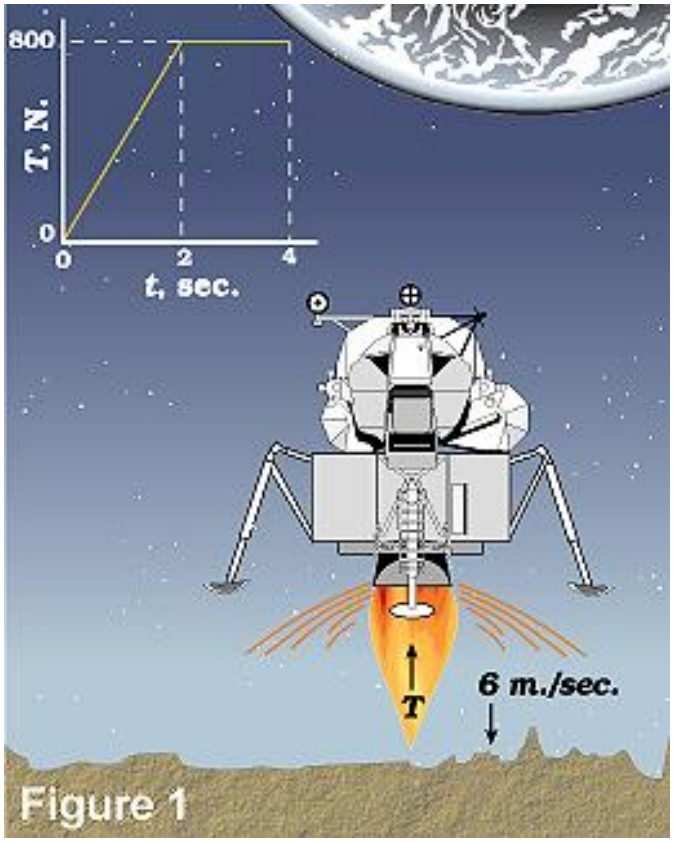

Figure 83-1. Diagram of the lunar lander problem.

Theoretical Solution

The velocity of the lander must be calculated for each of three stages. From 0 to 2 sec. (stage 1), the thrust is ramped up to 800 N. From 2 to 4 sec. (stage 2), the thrust remains constant at 800 N. From 4 to 5 sec. (stage 3), there is no thrust and the lander descends due to a gravitational acceleration of 1.62 m/sec^2.

For each of the three stages, equation 3/23 from the reference is applicable:

$$\int_{t_1}^{t_2} \sum F dt = G_2 - G_1$$

Where:

t_1 = initial time

t_2 = final time

$G = M \cdot V$

V = velocity

Stage 1: The area under the thrust-time curve from 0 to 2 sec. = 1/2*bh*, where *b* = 2 sec. and *h* = 800 N.

$\Sigma F = F_T - F_G$, where F_T is the force due to thrust and F_G is the force due to gravity. Thus,

1/2(2 sec)(800 N) - (200 kg)(1.62 m/sec^2)(2 sec) = $G_2 - G_1$

800 N· sec - 648 N· sec = $M \cdot V_2 - M \cdot V_1$

152 N· sec = $M \cdot V_2 - M \cdot V_1$

152 N· sec + $M \cdot V_1 = M \cdot V_2$

152 N· sec + (200 kg)(-6 m/sec) = (200 kg)(V_2)

-1048 N· sec = (200 kg)(V_2)

-5.24 m/ sec = V_2

At the end of stage 1 the velocity is -5.24 m/sec.

Stage 2: The area under the thrust-time curve from 2 to 4 sec. = *bh*, where *b* = 2 sec. and *h* = 800 N. Thus,

(2 sec)(800 N) - (200 kg)(1.62 m/sec^2)(2 sec) = $G_2 - G_1$

1600 N· sec - 648 N· sec = $M \cdot V_2 - M \cdot V_1$

952 N· sec = $M \cdot V_2 - M \cdot V_1$

952 N· sec + $M \cdot V_1 = M \cdot V_2$

952 N· sec + (200 kg)(-5.24 m/sec) = (200 kg)(V_2)

-96 N· sec = 200 kg.(V_2)

-0.48 m/sec = V_2

At the end of stage 2 the velocity is -0.48 m/sec

Stage 3: There is no thrust. Thus,

(200 kg)(-1.62 m/sec^2)(1 sec) = G_2 - G_1

- 324 N· sec. = M · V_2 - M · V_1

- 324 N· sec. + M · V_1 = M · V_2

-324 N· sec. + (200 kg)(-0.48 m/sec) = (200 kg)(V_2)

-420 N· sec. = 200 kg.(V_2)

-2.1 m/ sec. = V_2

At the end of stage 3 (t = 5 sec), the velocity is -2.1 m/sec.

Autodesk Simulation Solution

A model of a lunar lander was built using truss and 3-D solid elements in FEA Editor. Material properties for steel were used. Using the volume determined by the Weight and Center of Gravity Calculator (5.9542 m^3) and the mass specified in the problem definition (200 kg), a mass density of 33.58973 kg/m^3 was calculated. A negligible mass density (0.0000001 kg/m^3) was specified for the truss elements, which were given an area of 0.01 m^2

The event was defined to last 5 seconds and capture 1000 steps per second. The Displacement Tolerance was specified to be 1 x 10^{-4} and the number of time steps between iterations was set as 5001. By setting this parameter to one more than the total number of steps, we prevent the processor from iterating, thus speeding analysis in this example for which stresses are not considered.

A force of 800 N. was applied to the center node on the bottom of the lander model in FEA Editor. The first load curve was defined as shown to the right to simulate the thruster activity. Note that the thrust cuts out one time step after 4 seconds (4.001 seconds.).

A second load case applies a constant gravity force (specified as 1.62 m/sec^2) in the -Z direction.

First Load Case	
Time	**Multiplier**
0	0
2	1
4	1
4.001	0
5	0
Second Load Case	
Time	**Multiplier**
0	1
5	1

The analysis was processed using Mechanical Event Simulation. The velocity was displayed by performing the first derivative operation with respect to time on the displacement curve.

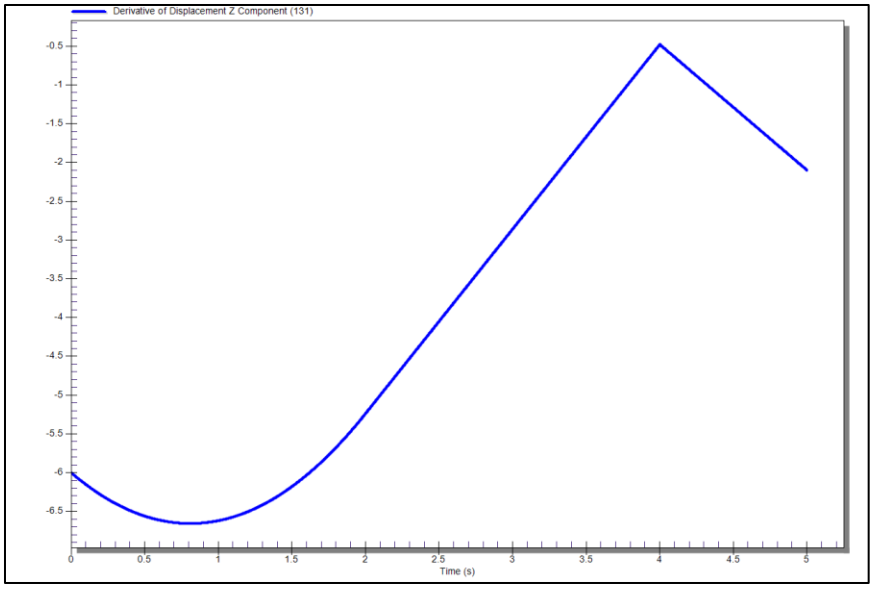

Figure 83-2. Lander's velocity as it descends.

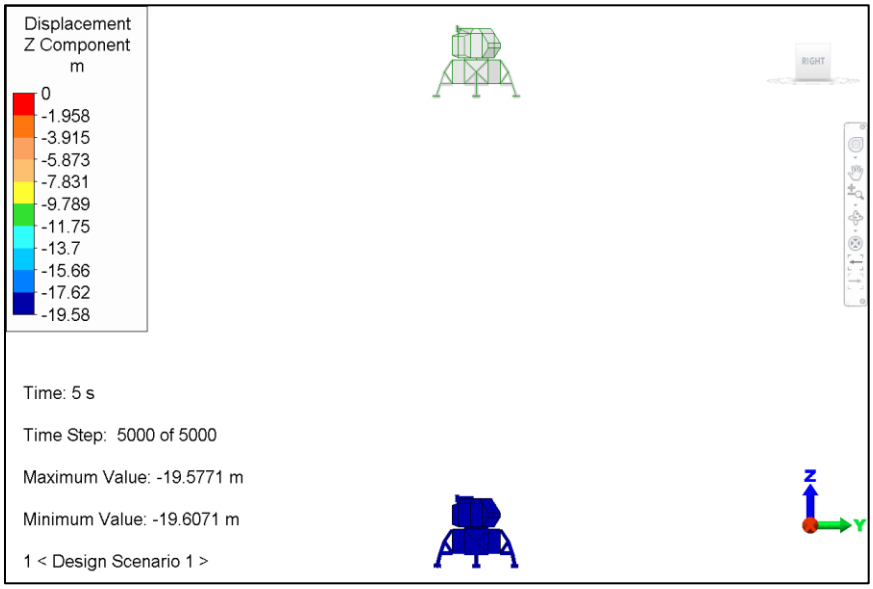

Figure 83-3. Displacement in the model after 5 seconds.

Table 83-1. Comparison of Results

	Velocity at 5 Seconds (m./sec.)
Theory	-2.1
Analysis	-2.097
% Difference	0.143

Note: Due to size considerations, results for this AVE are not included with the supplied model archive. You can use the model files to run the analysis on your own.

AVE - 84 Fluid Flow Drag Analysis of Flow across a Flat Plate

Reference

White, Frank M., *Fluid Mechanics*, McGraw-Hill Book Co., New York, 1979, example 7-3.

Problem Description

A sharp, flat plate with L = 1 m. and b = 3 m. is immersed parallel to a stream of air of velocity 2 m/sec. Find the drag on one side of the plate given the following property values for air:

$\rho = 1.23$ kg/m^3
$\nu = 1.46 \times 10^{-5}$ m^2/sec

Theoretical Solution

The airflow Reynolds number is

$$\frac{VL}{\nu} = \frac{(2.0\ \text{m./sec.})(1.0\ \text{m.})}{1.46\times10^{-5}\ \text{m.}^2\ \text{/sec.}} = 137{,}000$$

Since this value is less than 3×10^6, White assumes that the boundary layer is laminar. According to Eq. 7.26

$$C_D = \frac{2D(L)}{\rho U^2 bL} = \frac{1.328}{Re_L^{1/2}} = 2c_f(L)$$

Thus, the drag coefficient for this problem is

$$C_D = \frac{1.328}{(137{,}000)^{1/2}} = 0.00359$$

The drag on one side in the airflow is

$D = C_D 1/2 \rho U^2 bL = 0.00359(1/2)(1.23)(2.0)^2(3.0)(1.0) = 0.0265$ N

Autodesk Simulation Solution

A 2-D model was built using 24,500 planar elements. The mesh was generated using FEA Editor's arithmetic auto meshing option such that the mesh is finer near the surface of the plate in the Z direction and around the ends of the plate in the Y direction. Velocity boundary conditions were applied to simulate conditions specified in the problem definition

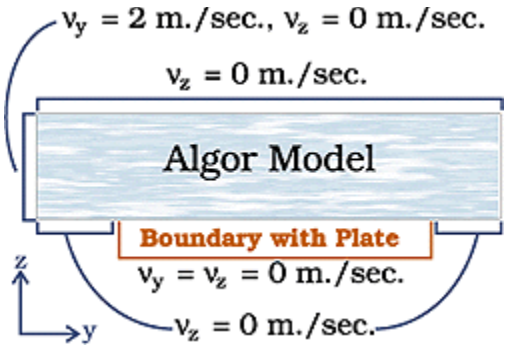

Figure 84-1. Diagram of the model.

The model was processed using the 2-D steady-state fluid flow analysis processor in 1 time step.

The analysis results were then viewed in the Results interface. In order to efficiently find the total drag on the model, the nodes along the plate were selected and the Summary option of the Inquire: Results dialog was used to provide the total drag force of 0.01839 N. This value must be divided in half to get the drag force along the top. This value is 0.0092 N Since the 2-D model represented a 1-m. deep plate and the theoretical calculations specify 3 m, we multiply 0.0092 N by 3 m. to yield 0.0276 N.

Figure 84-2. Reaction force in the Y direction.

Table 84-1. Comparison of Results

	Drag on One Side in the Airflow (N)
Theory	0.0265
Analysis	0.0276
% Difference	4.1

AVE - 85 Mechanical Event Simulation of a Basketball Being Shot into a Hoop

Reference

Lindeburg, M. R., *Mechanical Engineering Reference Manual*, 9th Edition, page 16-5.

Problem Description

The Mechanical Event Simulation (MES) under consideration determines the projectile motion of a basketball. The basketball is shot from 20 ft. away and 3 ft. below the center of the basketball rim.

The initial velocity in the horizontal (Z) direction is = 180 in./sec.(v_z), and the initial vertical (Y) velocity is 300 in./sec. (v_y). The gravitational constant (g) is 386.4 in./sec.^{2} in the -Y direction.

Neglecting air resistance, find the vertical and horizontal displacement of the ball after 1.32 sec.

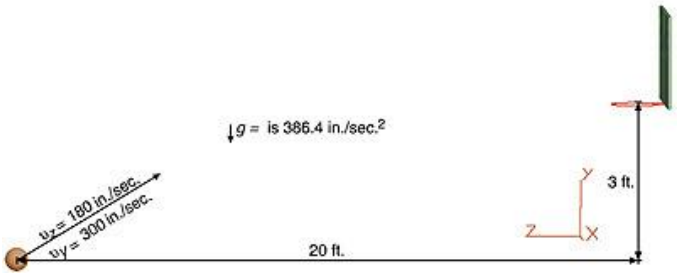

Figure 094-1: Diagram of the basketball shot problem.

Theoretical Solution

The equations for projectile motion are used as follows:

$z(t) = v_z \cdot t$ = (180 in./sec.)(1.32 sec.) = 237.6 in. (or 19.8 ft.)

$y(t) = v_y \cdot t - (1/2)\, g\, t^2$ = 300 in./sec. (1.32 sec.) - (0.5)(386.4 in./sec.^{2})(1.32 sec.)^2
= 396 in. - 336.63168 in. = 59.36832 in. (or 4.94736 ft.)

Autodesk Simulation Solution

In FEA Editor, a basketball backboard and rim were modeled using 83 shell elements and 31 beam elements. A ball was modeled using 180 3-D elements and placed 20 feet away from the center of the rim and three feet below it. Initial velocities of 180 in./sec. in the Z-direction and 300 in./sec. in the Y-direction were specified for the ball.

The "MES with Nonlinear Material Models" analysis type was selected and the event was defined to last 1.5 sec. and capture 500 steps/sec. The gravitational constant used was 386.4 in./sec.^{2} in the -Y direction.

At a time of 1.32 seconds the ball was observed passing through the rim of the basket. Vertical and horizontal displacements were obtained for the node at the center of the ball.

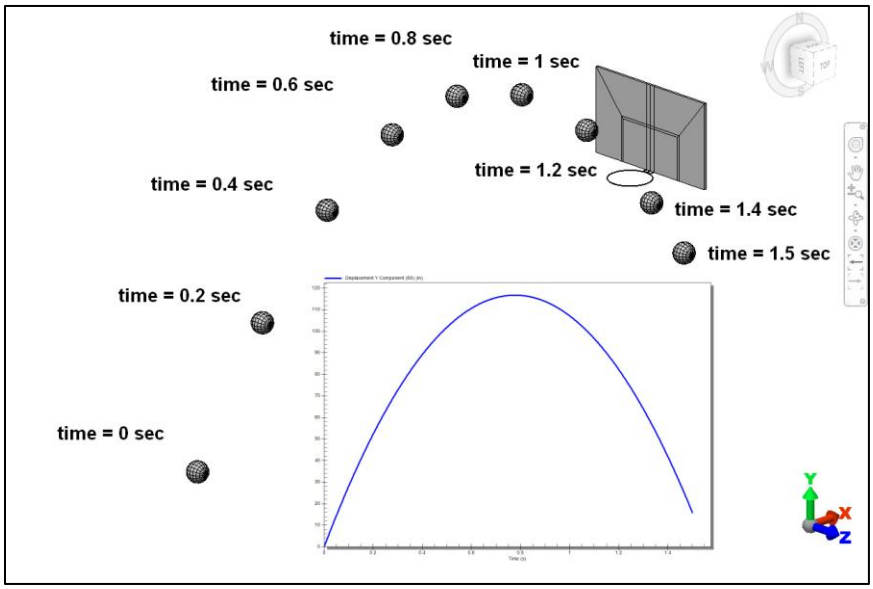

Figure 85-1. Vertical displacement versus time for the center of the basketball.

Table 85-1. Comparison of Results

	Displacement (inches) at time =1.32 sec	
	Horizontal	**Vertical**
Analysis	237.6	59.8468
Theory	237.6	59.36832
Difference	0.00	0.81%

AVE - 86 Heat Flux Transient Heat Transfer Analysis

Reference

Incropera, Frank P. and DeWitt, David P., *Introduction to Heat Transfer*, Second Edition, p. 605.

Problem Description

A block 0.1 m by 0.2 m is exposed to an environment such that a known heat flux is imposed on the surface as shown in Figure 86-1. The mass density is 100 kg/m^3 and the specific heat changes as a function of temperature such that $c_p = 0.15 \cdot T + 7$ J/kg/C°. Find the final bulk temperature after 5 minutes, if the block starts at 20°C.

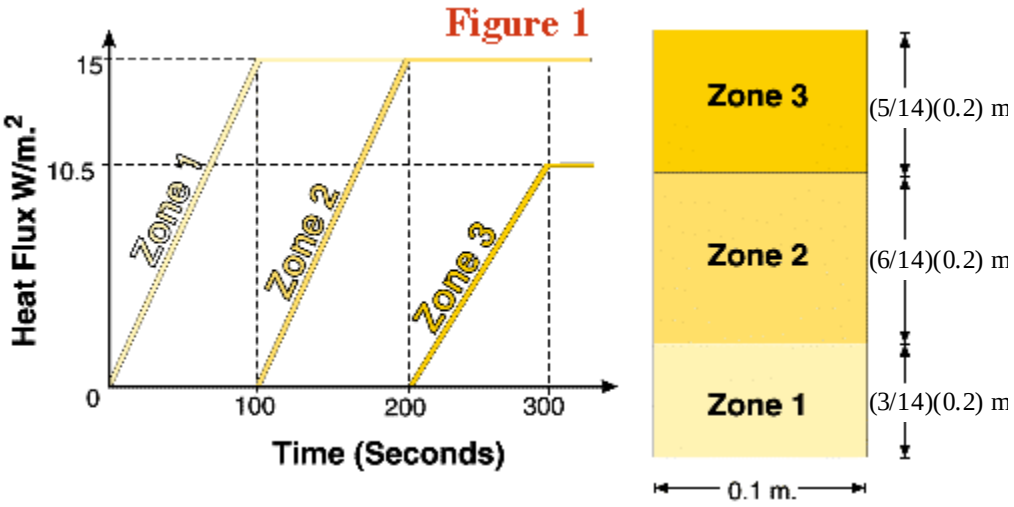

Figure 86-1. Diagram of heat flux.

Theoretical Solution

The total heat applied, Q, must equal the change in heat storage of the block. The total heat $Q = m\int c_p \, dT$ where m is the total mass, c_p is the specific heat as a function of temperature, and dT is the change in temperature. The total heat is summed in the table below.

Zone	Heat Flux (W/m^2)	Surface Area (m^2)	Total Heat Input to 600 Seconds (J)
1	15	0.0186	153.45
2	15	0.0171	115.425
3	10.5	0.0243	89.25
Total	--	--	**358.125**

The total mass will be based on a 0.1 m. thick slice. Integrating the function for c_p gives the following:

$358.125 \text{ J} = (0.1 \text{ m})(0.1 \text{ m})(0.2 \text{ m})(100 \text{ J/kgC°})\int(0.15\,T + 7)\,dT$ $358.125 \text{ J} = 0.2 \text{ J} \cdot (0.075 \cdot T^2 + 7 \cdot T)$

Evaluating the above equation between the initial temperature of 20°C and the final temperature T gives the following quadratic equations:

$$358.125 \text{ J} = 0.2 \text{ J} \cdot \{[0.075 \cdot T^2 + 7 \cdot T] - [0.075 \cdot (20)^2 + 7 \cdot (20)]\}$$

$$0 = 0.075 \cdot T^2 + 7 \cdot T - 1960.625$$

Solution of the above equation gives two values, of which one is the correct physical result, namely:

$T = 121.62°C$

Autodesk Simulation Solution

This example highlights two features that are easily handled with the user interface:

- The capability to use multiple load curves and different activation times.
- The capability to solve transient models with temperature dependent material properties.

A 7- by 2-element mesh was created in FEA Editor and material properties were assigned. 2-D orthotropic elements were used in order to specify temperature-dependent material properties. Since the specific heat is a linear function of temperature, two inputs that bracket the expected temperature range are sufficient, such as specific heats of 7 and 29.5 at 0° and 150°, respectively. A conductivity of 1 W/m·C° was used.

The "Loads" tab on the "Analysis Parameters" screen allows the heat flux to be assigned to the nodes on the perimeter of the model. As seen in Figure 86-2, the "Scale" column can be used to scale the load curve, and the "Activation Time" column indicates when the load curve is applied. Since the shape of the heat load for all three zones is identical, see Figure 86-3, one load curve can be specified in the "Load Curve Input" screen. To account for the temperature dependent material properties, the time steps for matrix reformulation must be set on the "Advanced" tab. In this example, it was specified as "1" as seen in Figure 86-4.

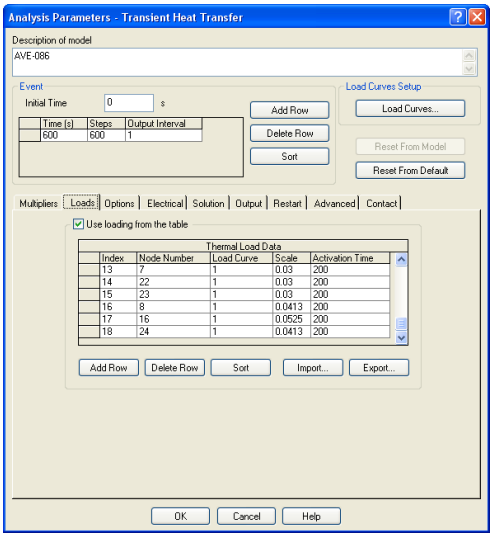

Figure 86-2. Heat flux is assigned to the nodes

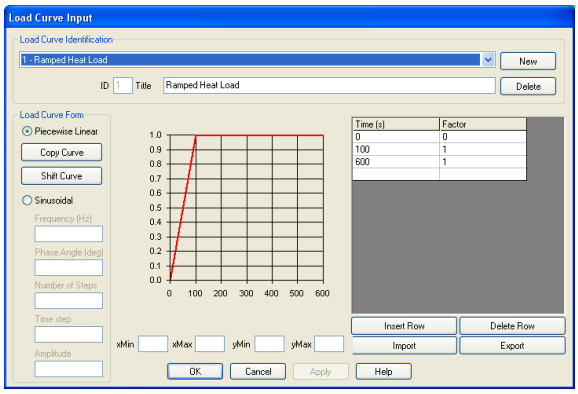

Figure 86-3. One load curve is specified

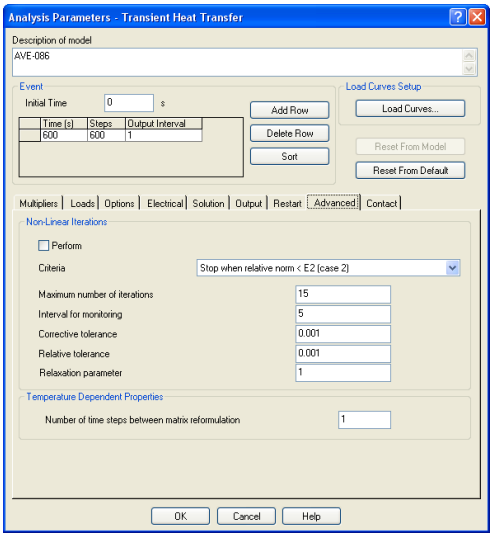

Figure 86-4. Time steps between matrix reformulation is set

From the results with a time step of 1 second, at the time step corresponding to a time of 600 seconds, there is a temperature variation from 121.21°C to 122.07°C. The average of all of the nodal temperatures is 121.79°C.

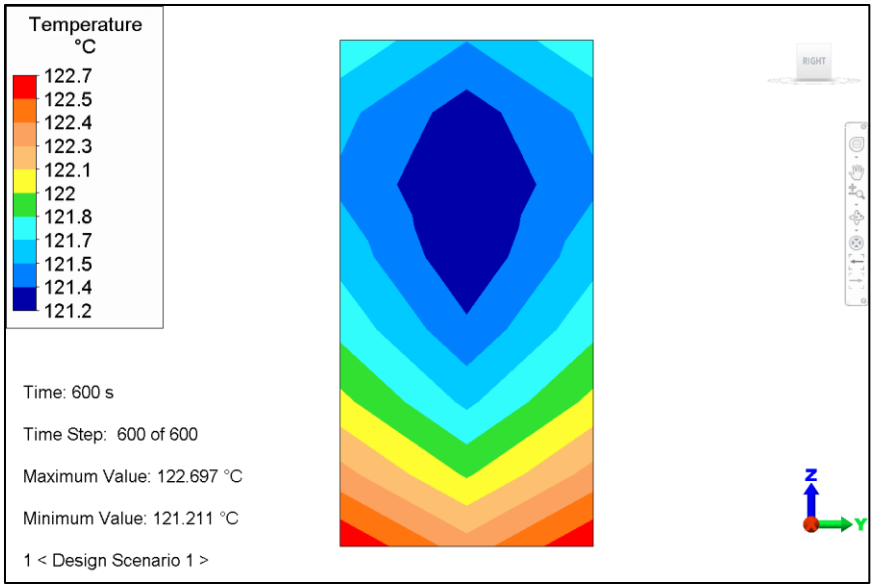

Figure 86-5. Temperature contours at the final time step.

Table 86-1. Comparison of Results

	Average Temperature at 600 Seconds
Theory	121.62°C
Analysis	121.79°C
% Difference	0.17%

The % difference for this thermal model is calculated by

$$\%\ difference = 100 \cdot \frac{Theory\ T - Alg\,or\ T}{Theory\ T - Initial\ T}$$

where the initial temperature is 20°C.

AVE - 87 Mechanical Event Simulation of a Grinder Shaft under Torsion

Reference

Juvinall, Robert C., *Engineering Considerations of Stress, Strain, and Strength*, New York: McGraw-Hill Book Company, page 179. Model contributed by Bill DiMartino, Tandemloc, Inc., Havelock, North Carolina.

Problem Description

Figure 87-1 below shows a grinder with an abrasive wheel mounted at each end of the shaft and a belt-driven sheave at the center. When turning at 2,400 rpm, the 6-inch wheel is accidentally jammed, causing it to stop "instantly." Estimate the resulting maximum torsional stress and deflection of the shaft. The shaft is made of steel (G = 11.5 × 10^6 psi) and its weight may be neglected. The grinding wheels may be considered as solid disks having a density of 0.07 lb./in.^{3}

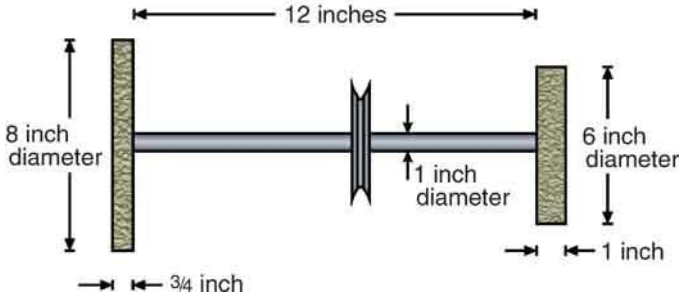

Figure 87-1. Diagram of the grinder shaft problem.

Theoretical Solution

It is the energy in the 8-inch wheel that must be absorbed by the shaft. For this wheel,

$$I = m\frac{r^2}{2} = \frac{(0.07)(16\pi)\left(\frac{3}{4}\right)}{386}\frac{16}{2} = 0.0547 \text{ lb. in. sec.}^2$$

The kinetic energy can be found from the equation:

$$U = \frac{1}{2}I\omega^2 = \frac{1}{2}(0.0547)\left(\frac{2{,}400\times 2\pi}{60}\right)^2 = 1{,}720 \text{ in.}\cdot\text{lb.}$$

The maximum shaft torsional stress can be found from:

$$\tau = 2\sqrt{\frac{UG}{AL}} = 2\sqrt{\frac{1{,}720\left(11.5\times 10^6\right)}{(\pi/4)12}} = 91{,}600 \text{ psi}$$

The reference text goes on to describe how failure would probably occur in this scenario before calculating the theoretical shaft torsional deflection if the shaft were not to fail. Combining the equations $\theta = \tau L/JG$ and $\tau = Tc/J$ gives:

$$\theta = \frac{\tau L}{cG} = \frac{(91{,}600)(12)}{(0.5)(11.5\times10^{6})} = 0.191\ \text{rad.} = 10.9°$$

Autodesk Simulation Solution

The model of the shaft and grinding wheel was built in FEA Editor using a total of 848 elements. The 800 elements that comprise the shaft were assigned to part 1 and defined to have a density (ρ) of 0, since its weight was to be neglected. The 48 elements that comprise the grinding wheel were assigned to part 2 and defined to have a mass density (ρ) of 0.0001813 lb. · sec.^{2}/in.^{4}, calculated by dividing the given density (0.07 lb./in.^{3}) by gravity (386.4 in./sec.^{2}).

The shaft was assigned a Young's modulus *(*E) of 30 x 10^6 psi and a υ of 0.3043. Both parts were given an initial rotational velocity about the X axis of 2,400 rpm. The end of the shaft that does not attach to the grinding wheel was fixed with boundary conditions.

The known deflection is about 11 degrees. If the disk slows uniformly, then the average speed is 1,200 rpm. Thus, to rotate 11 degrees requires 0.0015 sec. Therefore, the event was set to last 0.0025 sec. with a results capture rate of 20,000/sec.

The Mechanical Event Simulation yielded the following results at step number 24 (0.0012 sec.).

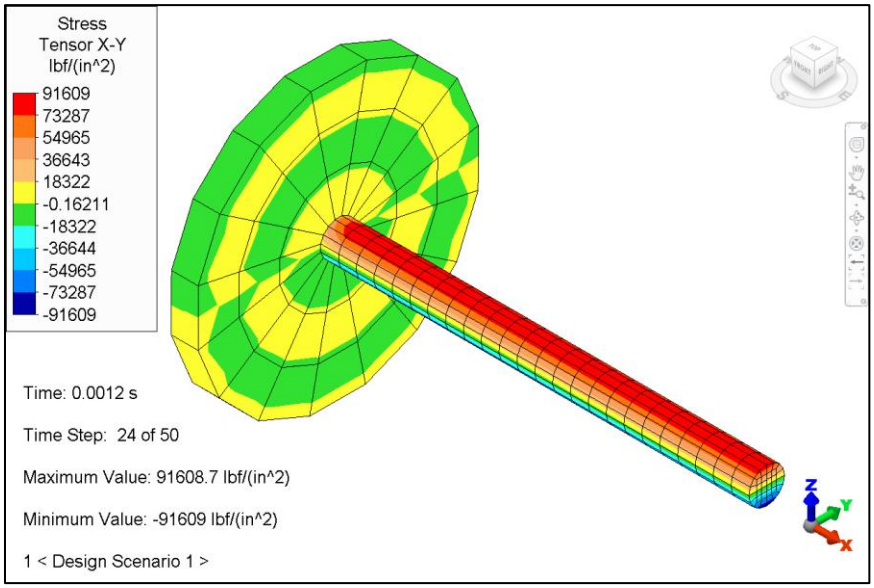

Figure 87-2. The maximum stress of the shaft

Table 87-1. Comparison of Results

	Stress (psi)	Deflection (degrees)
Theory	91,600	10.9
Analysis	91,609 (Sxy)	10.9
% Difference	0.01	0.0

AVE - 88 Mechanical Event Simulation of a Chain with Weights at the Hinges

Reference

Paul, Burton, *Kinematics and Dynamics of Planar Machinery*, Prentice-Hall, Inc., 1979, pp. 379-81.

Problem Description

Four weightless rods of equal length are hinged together to form a hanging chain as shown below.

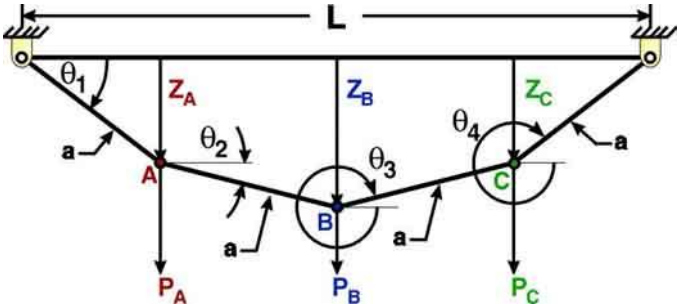

Figure 88-1. Diagram of the hanging chain problem.

Find the angles θ_1, θ_2, θ_3 and θ_4 for this closed kinematic chain, given that the length of each rod is 5 inches and the loads are as follows:

P_A = 5 lbs P_B = 2 lbs P_C = 3 lbs.

As the text points out on page 381, it is difficult to write the explicit expressions of the configuration variables, θ, but the load ratios may be solved directly given the configuration. Therefore, the analysis will be performed first using the given loads. The results will then be verified solving for the load ratios, given the configuration that results from the analysis.

Theoretical Solution

We now verify the solution by calculating the load ratios from the angles that result from the Mechanical Event Simulation.

$$Q_1 = (P_A + P_B + P_C)\cos\theta_1 + \frac{\sin(\theta_1 - \theta_4)}{\sin(\theta_4 - \theta_3)} P_C \cos\theta_3 = 0$$

$$(P_A + P_B + P_C)\cos(1.5) + \frac{\sin(1.5 - 358.77)}{\sin(358.77 - 359.59)} P_C \cos(359.59) = 0$$

$$\frac{P_A + P_B + P_C}{P_C} = \frac{3.328}{0.9997} = 3.329$$

$$Q_2 = (P_B + P_C)\cos\theta_2 + \frac{\sin(\theta_2 - \theta_4)}{\sin(\theta_4 - \theta_3)} P_C \cos\theta_3 = 0$$

$$(P_B + P_C)\cos(0.1364) + \frac{\sin(0.1364 - 358.77)}{\sin(358.77 - 359.59)} P_C \cos(359.59) = 0$$

$$\frac{P_B + P_C}{P_C} = \frac{1.666}{1.0} = 1.666$$

Autodesk Simulation Solution

A 3-D brick model was built to represent the four rods with 6-noded elements representing the hinges at either end of each rod. Each end of the 88-element chain was fixed with boundary conditions. The bricks were 0.2 by 0.25 inches and assigned the properties of Steel ASTM A-36.

The analysis was processed using MES analysis. The event was defined to last 1 second with 500 steps per second -- a sufficient length for the system to reach equilibrium.

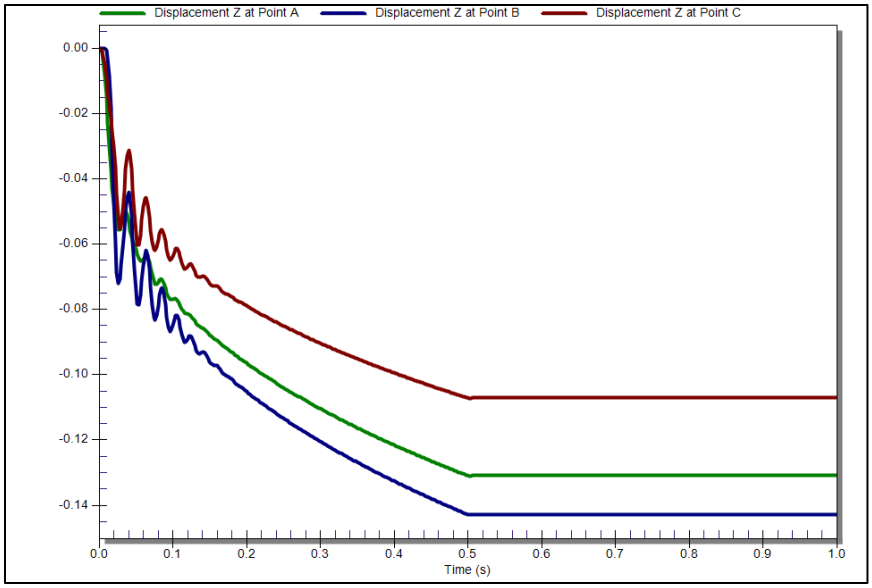

Figure 88-2. Display of displacement versus time for points A, B and C. Note that the forces were applied gradually over 0.5 seconds and were kept constant between time =0.5 and time =1 sec.

The -Z-direction displacements at one second were 0.1309 inch at point A, 0.1428 inch at point B and 0.1071 inch at point C. The angles were then calculated from the displacements as follows:

$$\theta_1 = \tan^{-1}\left(\frac{0.1309}{5}\right) = 1.500°$$

$$\theta_2 = \tan^{-1}\left(\frac{0.1428 - 0.1309}{5}\right) = 0.1364°$$

$$\theta_3 = 360° - \tan^{-1}\left(\frac{0.1428 - 0.1071}{5}\right) = 359.59°$$

$$\theta_4 = 360° - \tan^{-1}\left(\frac{0.1071}{5}\right) = 358.77°$$

Table 88-1. Comparison of Results

	Analysis	Theory	% Difference
$\frac{P_A + P_B + P_C}{P_C}$	3.333	3.329	0.12
$\frac{P_B + P_C}{P_C}$	1.667	1.666	0.06

The load ratios calculated match those used in the analysis almost exactly.

AVE - 89 Transient Thermal Analysis of a Cooling Copper Wire

Reference

Lindeburg, Michael R., *Mechanical Engineering Reference Manual for the PE Exam*, Tenth Edition, p. 34-12.

Problem Description

A 0.03125-in diameter copper wire is heated by a short circuit to 300 °F before a slow-blow fuse burns out and all heating ceases. The ambient temperature is 100 °F and the film coefficient on the wire is 1.65 Btu/hr·ft^2·°F. Use the following copper properties to determine how long it will take for the wire temperature to drop to 120 °F:

conductivity (k): 224 Btu·ft/hr·ft^2·°F

specific heat (c_p): 0.091 Btu/lbm·°F

density (ρ): 558 lbm/ft^3

Theoretical Solution

If the Biot number (Bi) is less than approximately 0.1, the internal thermal resistance of a body is negligible in comparison to the external thermal resistance. In that case, the lumped capacitance method can be used to approximate the transient (time dependent) heat flow to a maximum error less than 7%.

$$T_t = T_\infty + (T_0 - T_\infty)e^{-BiFo}$$

$$= T_\infty + (T_0 - T_\infty)e^{-t/R_t C_t}$$

Where $R_t C_t = \tau = \dfrac{c_p \rho V}{hA}$

$$Bi = \frac{hL_c}{k}$$

L_c for a cylinder $= \dfrac{r}{2} = \dfrac{\dfrac{0.03125\text{ in}}{2} \cdot \dfrac{1\text{ ft}}{12\text{ in}}}{2}$

$$Bi = \frac{1.65 \dfrac{Btu}{hr \cdot ft^2 \cdot °F} \cdot \dfrac{0.03125\text{ in}}{4} \cdot \dfrac{1\text{ ft}}{12\text{ in}}}{224 \dfrac{Btu \cdot ft}{hr \cdot ft^2 \cdot °F}} = 4.8 \times 10^{-6}$$

Since the Biot number is less than 0.1, the lumped capacitance method can be used.

$$\tau = \frac{c_p \rho V}{hA} = \frac{c_p \rho L_c}{h} = \frac{c_p \rho r/2}{h} = \frac{\left(0.091\frac{\text{Btu}}{\text{lbm}\cdot^\circ\text{F}}\right)\left(558\frac{\text{lbm}}{\text{ft}^3}\right)\left(\frac{0.03125\text{ in}}{(2)(2)}\right)\left(\frac{1\text{ ft}}{12\text{ in}}\right)}{1.65\frac{\text{Btu}}{\text{hr}\cdot\text{ft}^2\cdot^\circ\text{F}}}$$

$$= 0.0200 \text{ hr}$$

$$T_t = 120\,^\circ\text{F} = T_\infty + (T_0 - T_\infty)e^{-t/\tau}$$

$$120\,^\circ\text{F} = 100\,^\circ\text{F} + (300\,^\circ\text{F} - 100\,^\circ\text{F})e^{-t/\tau}$$

$$\ln(0.1) = \frac{-t}{0.0200 \text{ hr}}$$

t = 0.0461 hr

Autodesk Simulation Solution

The cross-section of the wire was modeled by meshing a circle and a square. This resulted in 432 two-dimensional plane elements. The outer surface was placed on surface 2 to define the convection. The nodes were assigned an initial temperature of 300 °F. Material properties were entered per the problem statement.

A transient heat transfer analysis was performed using a time step of 0.000461 hours. The results closest to the target temperature are step 101 (120.002-120.003 °F)

Time = 101 steps (0.000461 hr/step) = 0.046561 hours

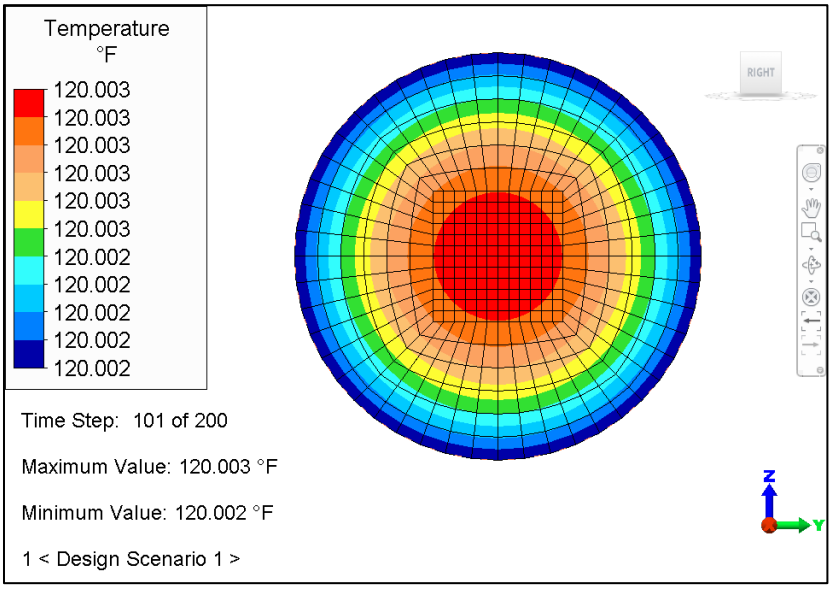

Figure 89-1. Temperature contours at step 101.

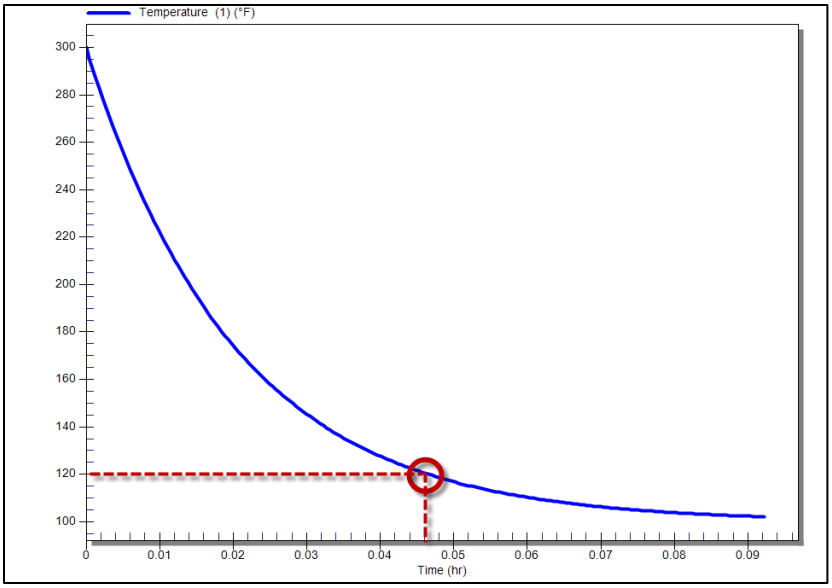

Figure 89-2. Temperature versus time graph

Table 89-1. Comparison of Results

	Analysis	Theory	Difference
Time, hours	0.046561	0.0461	0.99%

The difference is well within the accuracy of the lumped capacitance method used to solve the theoretical problem.

AVE - 90 Heat Flux Loading on a Hollow Cylinder

Reference

Cameron, A. D., Casey, J. A. and Simpson, G. B., *Benchmark Test for Thermal Analyses (Summary)*, Glasgow: NAFEMS, test 15 (iii).

Problem Description

This axisymmetric steady-state heat transfer analysis considers a hollow cylinder. The temperature over the ends and the outer surface of the cylinder is uniform. On the inner surface, a prescribed heat flux is applied to the central part of the surface, while the ends of the inner surface are insulated. Boundary condition details are shown in Figure 90-1 below.

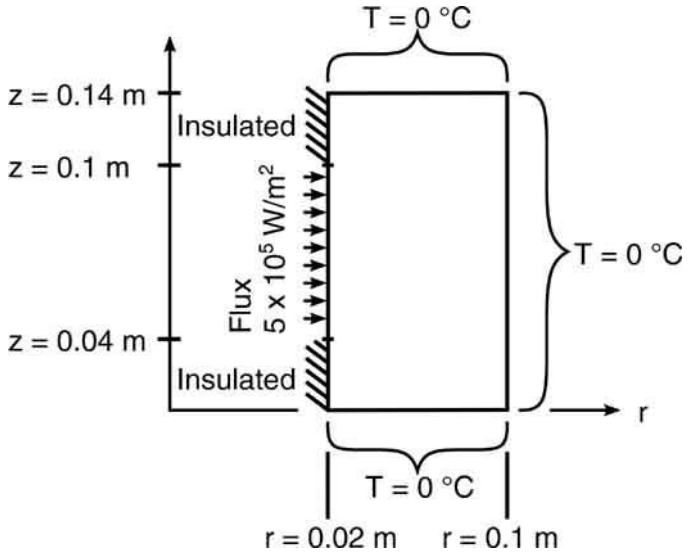

Figure 90-1. Diagram of the hollow cylinder with heat flux loading.

Find the temperature at the point r = 0.04 m, z = 0.04 m given the following material properties:

- Density, ρ = 7,850 kg/m^3
- Specific Heat, C = 460 J/kg · °C
- Thermal Conductivity, K = 52 W/m · °C.

Theoretical Solution

The temperature at the point r = 0.04 m, z = 0.04 m, is given to be 59.82 °C in the reference text.

Autodesk Simulation Solution

The cylinder was drawn in FEA Editor using an 8 by 14 mesh, resulting in 2-D axisymmetric elements 0.01 m square in the Metric mks unit system.

The elements on the central part of the inner surface were changed to surface number 2. A heat flux of 5 x 10^5 J/s/m^2 (5 x 10 5 W/m^2) was then applied as a surface-based load to surface number 2.

"Nodal Applied Temperatures" were added to hold the specified edges at 0 degrees. The stiffness used was based on the recommended value of 100,000 x conductivity/element diagonal length or 100,000 x 52 / 0.01 = 371,000. The "Load case Multipliers" were set as follows:

- Boundary temperature multiplier (for applied temperatures) = 1
- Convection multiplier (for heat flux) = 1
- Radiation multiplier = 0
- Heat generation multiplier = 0.

The analysis was performed using the steady-state heat transfer processor. The resulting temperature was inquired at r = 0.04 m, z = 0.04 m

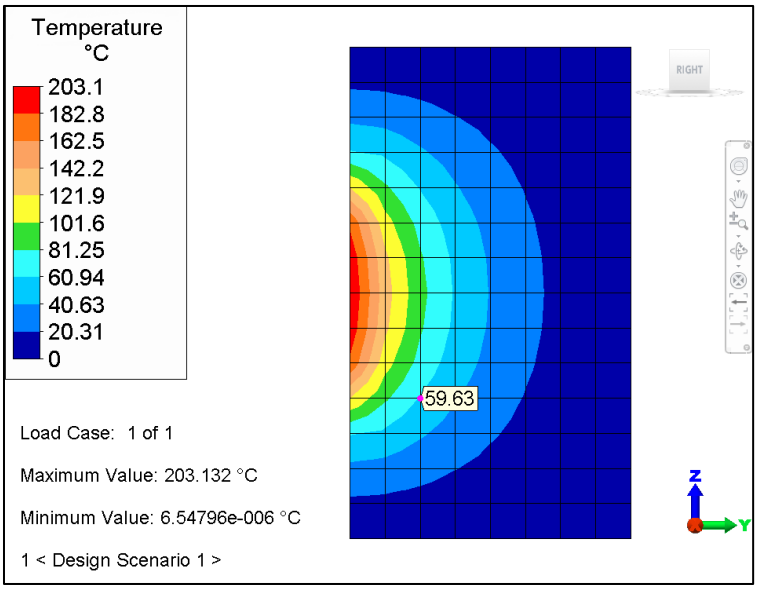

Figure 90-2. Temperature results from the heat transfer analysis. The point of interest is indicated by the probe.

Table 90-1. Comparison of Results

	Theory	Analysis	Difference
Temperature	59.82 C	59.63 C	0.32%

AVE - 91 Mechanical Event Simulation of a Cylinder Rolling inside a Curved Surface

Reference

Beer, F. P. and Johnston, Jr., E. R., *Vector Mechanics for Engineers*, Third Edition, New York: McGraw-Hill Book Company, sample problem 19.4.

Problem Description

Determine the period of small oscillations of a cylinder of radius r = 1 inch, which rolls without slipping inside a curved surface of radius R = 5 inches.

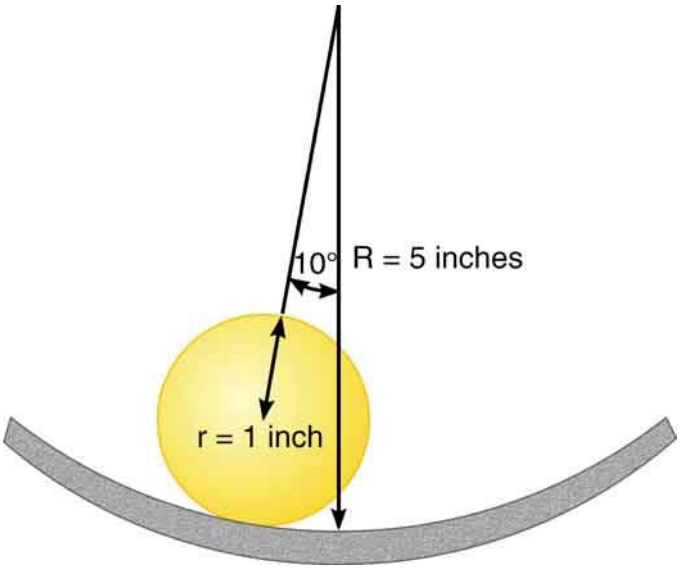

Figure 91-1. Diagram of the cylinder rolling inside a curved surface problem.

Theoretical Solution

Using conservation of energy, the theoretical period is calculated by:

$$\tau = 2\pi\sqrt{\frac{3}{2}\frac{5\,\text{inch}-1\,\text{inch}}{386.4\,\text{inch/sec}^2}} = 0.783\,\text{sec}$$

Autodesk Simulation Solution

The 2-D model of the cylinder and curved surface were drawn in FEA Editor. The curved surface was assigned to part 1 and the cylinder was assigned to part 2. The circumference of the cylinder mesh was created with 10-degree divisions. The cylinder was offset 10 degrees from the vertical and 0.015 inch above the curved surface. The outer surface of the cylinder and the inner curved surface were changed to surface 2.

Surface-to-surface contact was specified between surface 2 of part 1 and surface 2 of part 2. Static friction coefficient and sliding friction coefficient were set to 0.20.

The MES analysis processor was used to analyze the event. The times when the cylinder reaches the maximum elevation are as follows:

R_1 = 0.395 sec L_1 = 0.785 sec
R_2 = 1.195 sec

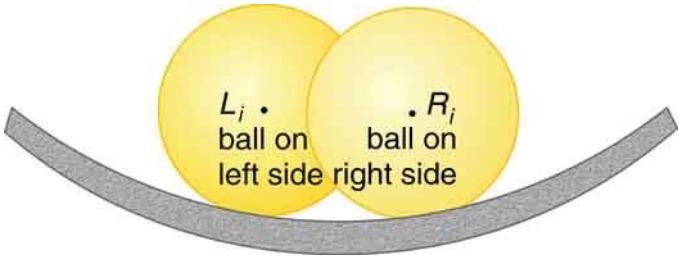

Figure 91-2. Times when the cylinder reaches the maximum elevation.

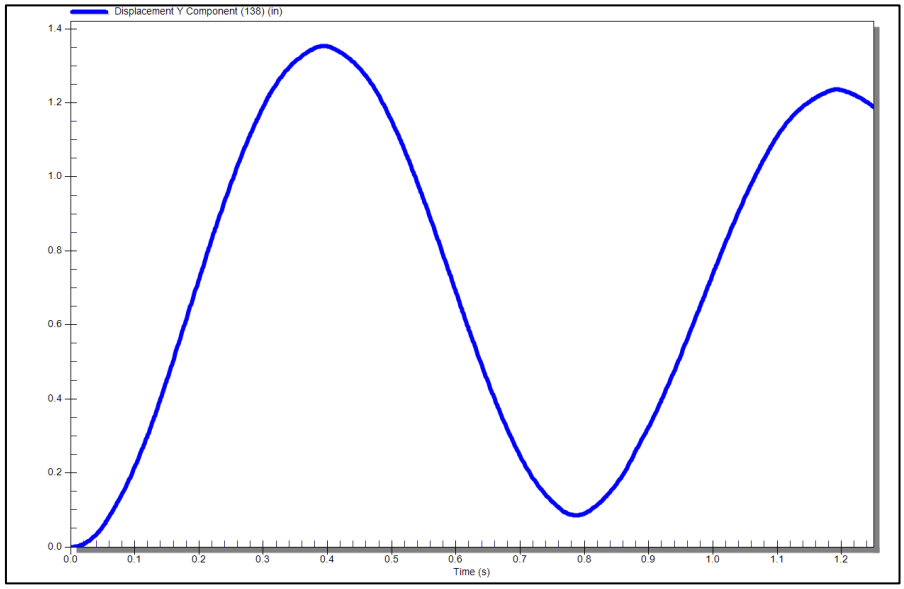

Figure 91-3. Graph of displacement in the Y direction for the center of the cylinder.

The period from R_1 to R_2 = (1.195 sec - 0.395 sec) / 1 cycles = 0.81 sec/cycle.

Table 91-1. Comparison of Results

	Theory	Analysis	% Difference
Period (sec/cycle)	0.783	0.81	3.45

AVE - 92 Mechanical Event Simulation of a Flyball-Governor

Reference

Shames, Irving H., *Engineering Mechanics, v. 2: Dynamics*, Third Edition, Prentice-Hall, 1980, Example 17.10.

Problem Description

A flyball-governor apparatus consists of four identical arms (solid cylindrical rods) each of weight 10 N and two spheres of weight 18 N and radius of gyration 30 mm about a diameter. At the base, and rotating with the system, is a cylinder B of weight 20 N and radius of gyration along its axis of 50 mm. Initially, the system is rotating at speed ω_1 of 500 rpm for $\theta = 45^\circ$. A force F at the base B maintains the configuration shown. If the force is changed so as to decrease θ from 45º to 30º, what is the angular velocity of the system?

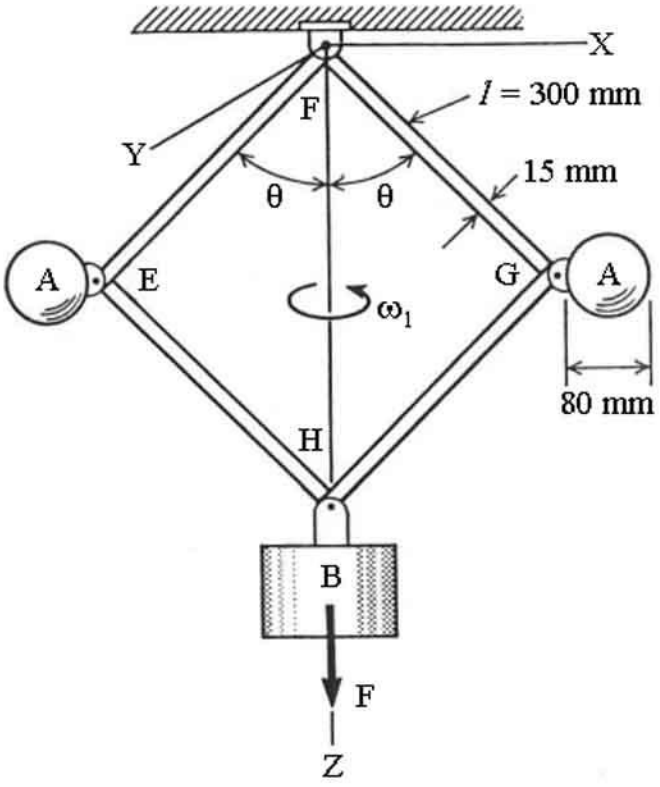

Figure 92-1. Diagram of the flyball-governor apparatus.

Theoretical Solution

Because no external moments act along the axis FH, we have conservation of angular momentum about this axis, which coincides with the Z axis. Note how each body of the governor rotates about this axis. The solution of the problem is obtained by equating the total angular momentum of the system when it has an angle θ of 45° and an angular velocity of 500 rpm to when it has an angle θ of 30° and the unknown angular velocity. As a first step, we calculate the rotational inertia of each body about the Z axis.

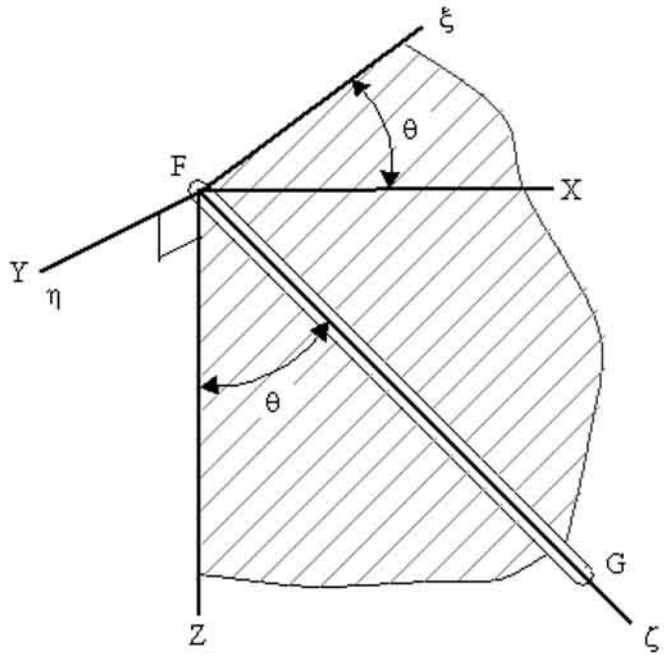

Figure 92-2. Sketch of rod FG including relation between XYZ and ξηζ axes.

First consider the rod FG, which is shown in Figure 92-2. The axes ξηζ are principal axes of inertia for the rod at F. The η axis is collinear with the Y axis, and these are normal to the page. A rotation of angle θ about the η axis relates the ξηζ axis with the XYZ axes. The following expression shows how $I_{\xi\xi}$, $I_{\eta\eta}$ and $I_{\zeta\zeta}$ each contribute to the rotational inertia of the rod FG about the Z axis, (I_{ZZ}) FG

$$\left(I_{ZZ}\right)_{FG} = I_{\xi\xi}\left[\cos\left(\frac{\pi}{2}+\theta\right)\right]^2 + I_{\eta\eta}\left(\cos\frac{\pi}{2}\right)^2 + I_{\zeta\zeta}\left(\cos\theta\right)^2$$

$$= \left[\frac{1}{3}\frac{10}{g}(0.30)^2\right]\sin^2\theta + \left[\frac{1}{2}\frac{10}{g}(0.0075)^2\right]\cos^2\theta \qquad [a]$$

It should be noted that $I_{\zeta\zeta}$ is given by $\frac{1}{2}Mr^2$, where M is the mass of the rod and r is its radius. The rotational inertia about the other two principal axes is given by $1/3\ Ml^2$, where l is the length of the rod. This value for $I_{\xi\xi}$ and $I_{\eta\eta}$ assumes that the rod is slender; which is the case in this example because l/r = 40.

For each sphere, we are given the mass, the radius of gyration and the location of its center relative to the end of the rod, thus

$$\left(I_{ZZ}\right)_{sph} = \frac{18}{g}(0.03)^2 + \frac{18}{g}\left[(0.30)\sin\theta + 0.04\right]^2 \qquad [b]$$

We are also given the mass and the radius of gyration of the cylinder, thus

$$\left(I_{ZZ}\right)_{cyl} = \frac{20}{g}(0.05)^2 \qquad [c]$$

Exploiting the symmetry of the apparatus, we can state that angular momentum along the Z axis is conserved if

$$\left[4(I_{ZZ})_{FG} + 2(I_{ZZ})_{sph} + (I_{ZZ})_{cyl}\right]_{\theta=45°} \frac{(500)(2\pi)}{60} = \left[4(I_{ZZ})_{FG} + 2(I_{ZZ})_{sph} + (I_{ZZ})_{cyl}\right]_{\theta=30°} \frac{(\omega_2)(2\pi)}{60}$$

Substituting the results of equations [a] through [c] into the above conservation statement, and solving for ω_2, gives $\omega_2 = 883$ rpm.

It should be noted that this result was obtained assuming that the governor is composed of rigid parts.

Autodesk Simulation Solution

The event described by the problem statement was replicated using Mechanical Event Simulation. The flyball-governor was modeled using beam elements. These elements allow us to obtain stresses within the rods. Stresses in such slender structures are typically pivotal when designing moving mechanisms. Because we expect insignificant stresses to exist within the spheres and the cylinder, they were not modeled. Instead we added lumped masses to represent their weight and radius of gyration. Finally, truss elements were used to preserve the prescribed offset when attaching the spheres to the ends of the rods; this offset is ½ of 80 mm or 0.04 m.

MES consists of three stages. At the onset of the first stage, all parts of the governor are given an initial axial rotation of 500 rpm about the Z axis. This stage lasts 0.125 seconds, which is long enough to capture over one entire revolution. This is because at 500 rpm a revolution lasts 0.120 seconds. During the first stage, a prescribed displacement is used to maintain the bottom of the cylinder at a constant Z coordinate value. During the second stage, which lasts 0.03 seconds, the prescribed displacement is utilized to linearly move the bottom of the cylinder 0.0956 m in the negative Z direction. This prescribed motion changes the angle θ from 45° to 30°. The third stage is characterized by the new faster rotation rate. Again, we simulate more than an entire period in order to accurately determine this rotation rate.

Figure 92-3 depicts the displacement time traces of two points on the governor. The blue line corresponds to the displacement of the cylinder in the Z direction. Note how this displacement is constant during stages 1 and 3, but depends linearly on time during stage 2. The red line corresponds to the Y displacement of a node at the end of a rod where a sphere is attached. This displacement is sinusoidal during stages 1 and 3. From the plot we obtain periods for stages 1 and 3, respectively. The first revolution rate simply confirms the ability of MES to maintain nearly constant motion of 500 rpm when no loads are applied. The second revolution rate compares well with the analytical result of 883 rpm, and thus confirms the ability of MES to accurately model the motion of an assembly with moving parts. Table 92-1 summarizes these results. It should be pointed out that this accurate solution also produced stresses within the rods.

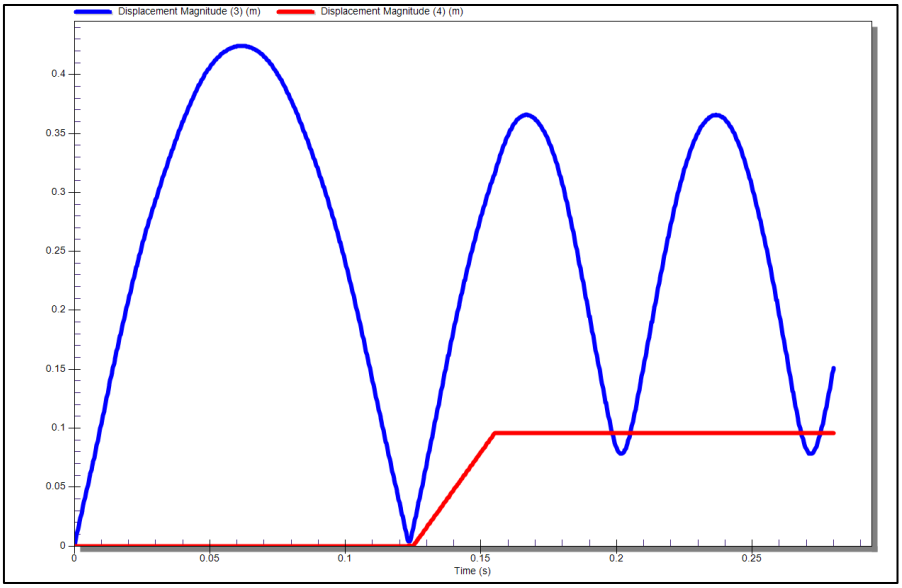

Figure 92-3. Graphical output for the displacement time traces of two nodes on the governor.

The displacement of the node at the end of the arm is used to measure the period of revolution during stages 1 and 3.

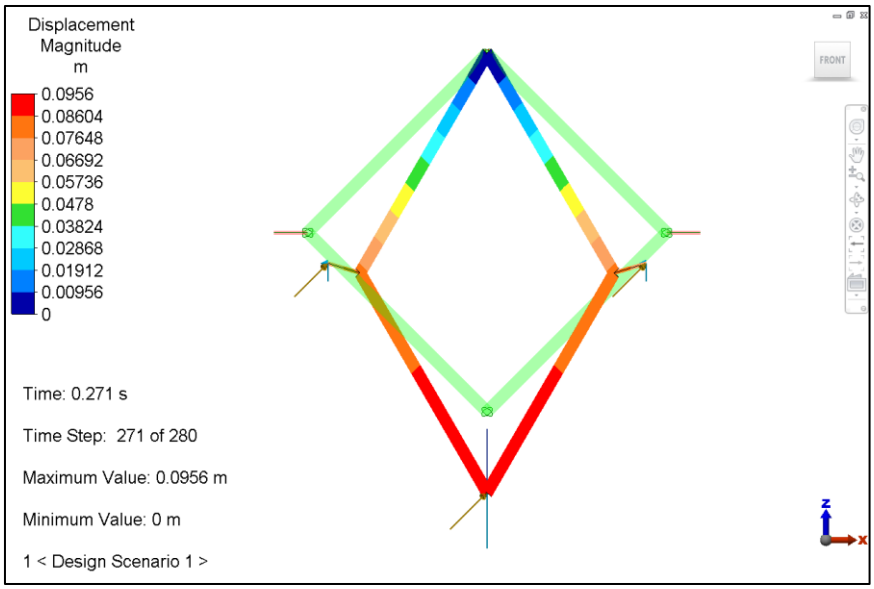

Figure 92-4. Displacement contours at time 0.271 seconds. Note how the flyball-governor elongated.

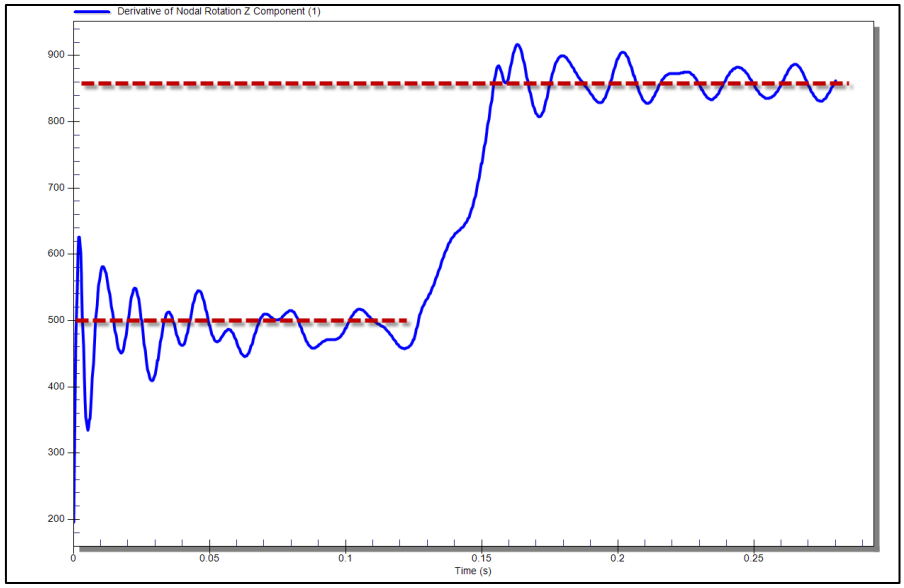

Figure 92-5. Nodal Rotational displacement about the Z axis.

Autodesk Simulation calculates the nodal rotational results in degrees/time units. In this analysis the time units used were seconds. In order to generate the graph shown in Figure 92-5, we used a multiplier if 0.167.

Conversion from [Degrees/second] to [RPM]
Multiplier = [60 sec/minute] / [360 degrees/rotation] = 0.167 (sec.rotation) / (min.deg)

Final rotation rate = 5131.7 degrees /sec x 0.167 (sec.rotation) / (min.deg)
Final rotation rate = 857 RPM

Table 92-1. Comparison of results

	Analytical (RPM)	**MES (RPM)**	**% Difference**
Final Rotation Rate	883	857	2.94

AVE - 93 Steady-State Heat Transfer Analysis of a Pipe Buried in Earth

Reference

Holman, J. P., *Heat Transfer,* Seventh Edition, page 85, example 3-1.

Problem Description

A horizontal pipe 15 cm in diameter and 4 m long is buried in the earth at a depth of 20 cm. The pipe-wall temperature is 75° C, and the earth surface temperature is 5° C. Assuming that the thermal conductivity of the earth is 0.8 W/m·°C, calculate the heat lost by the pipe.

Theoretical Solution

Since D < 3r and L >> r, we may calculate the shape factor of this situation using the equation

$$S = \frac{2\pi L}{\cosh^{-1}(D/r)} = \frac{2\pi(4)}{\cosh^{-1}(20/7.5)} = 15.35 \text{ m}$$

The heat flow is then calculated from

$q = kS\Delta T = (0.8)(15.35)(75 - 5) = 859.6$ W

Autodesk Simulation Solution

Because the pipe is much longer than it's diameter, a first approximation would be to ignore the heat loss from the ends of the pipe and analyze the problem as a two-dimensional model. Whether the problem is solved as two-dimensional or three-dimensional, one question that needs to be resolved is how large does the model need to be to represent a semi-infinite solid.

As the first approximation, the semi-infinite solid is represented by a rectangle 1 m wide by 1 m deep. Due to symmetry, only half of the pipe needs to be modeled. The pipe and ground temperatures can be specified by using either the "Applied Temperatures" or surface-based convection. The convection option was chosen for these analyses, and the specified temperature was obtained by entering a large (1E6) convection coefficient. Other than the pipe wall and surface of the ground, no other heat loads were applied. The "Heat Flow Calculation" option under the “Element Data" screen was set to "Linear Based on BC" so that the heat loss through the surface would be based on the convection boundary condition.

A steady-state heat transfer analysis was performed to obtain the temperature distribution and heat fluxes. The thickness of the 2-D model was set to 4 m to represent the entire length of the pipe. Although the thickness has no effect on the temperature results, the heat flow results do take the thickness into account.

Since the only heat flow is from the pipe to the surface of the ground, the total flow can be summed either around the perimeter of the pipe or on the surface of the ground. The results are given in the table on this page, along with results of several additional models that are variations on the first. Note that all results were multiplied as necessary to represent the full pipe. These models were created to investigate other widths and depths for the semi-infinite ground by extruding the sides of the first mesh. As expected, the larger the domain, the more accurate the solution.

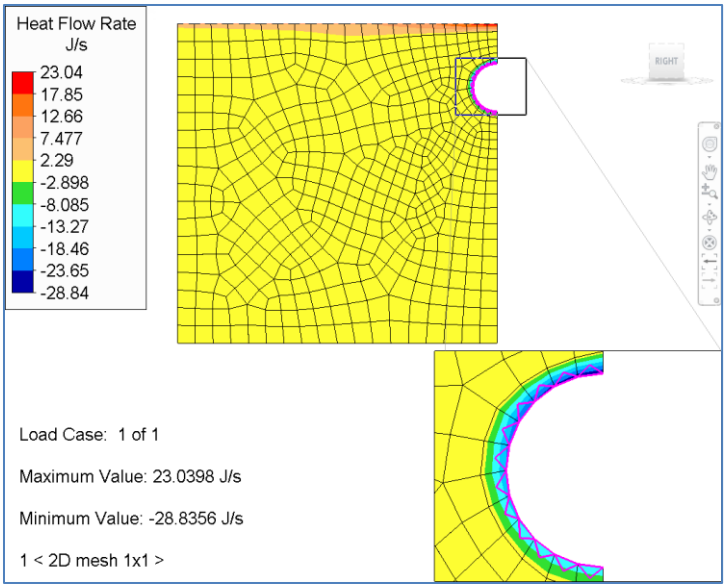

Figure 93-1. For a 2-D version of the model, the heat loss from the pipe was inquired in the results interface by selecting the surface where the pipe would contact the ground and summing the results. Due to half-symmetry, the sum was multiplied by 2 for comparison to the theoretical solution.

Finally, the 1 m by 1 m two-dimensional model was extruded to create a 3-D brick model. Due to symmetry, only one quarter of the model was created. The section of pipe modeled was 2 m long (half the length) with an additional 1 meter of ground extending beyond the end of the pipe. All loads and post-processing were identically applied to the two-dimensional models.

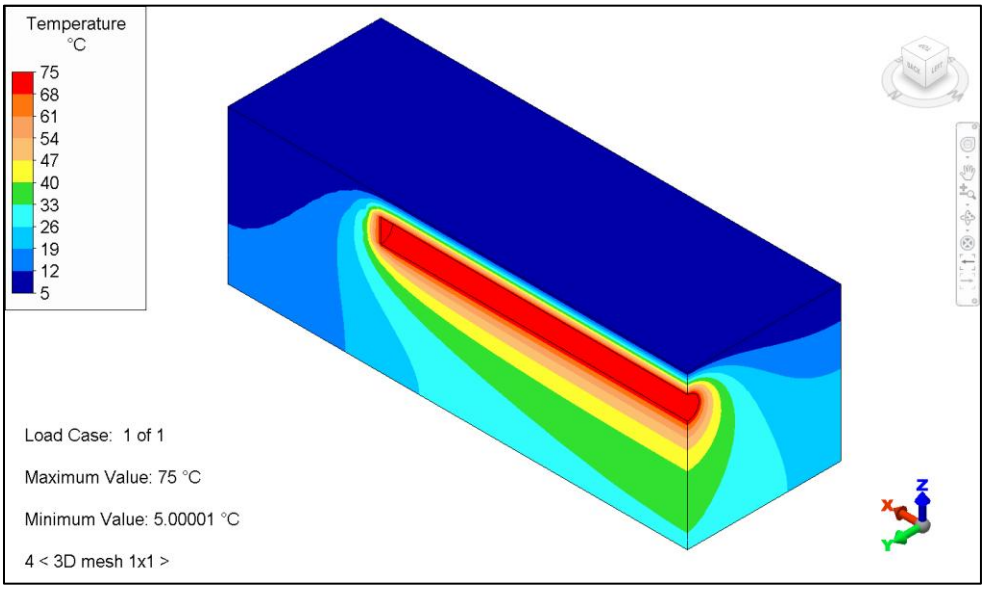

Figure 93-2. Temperature contours for the 3-D brick mesh version of the model.

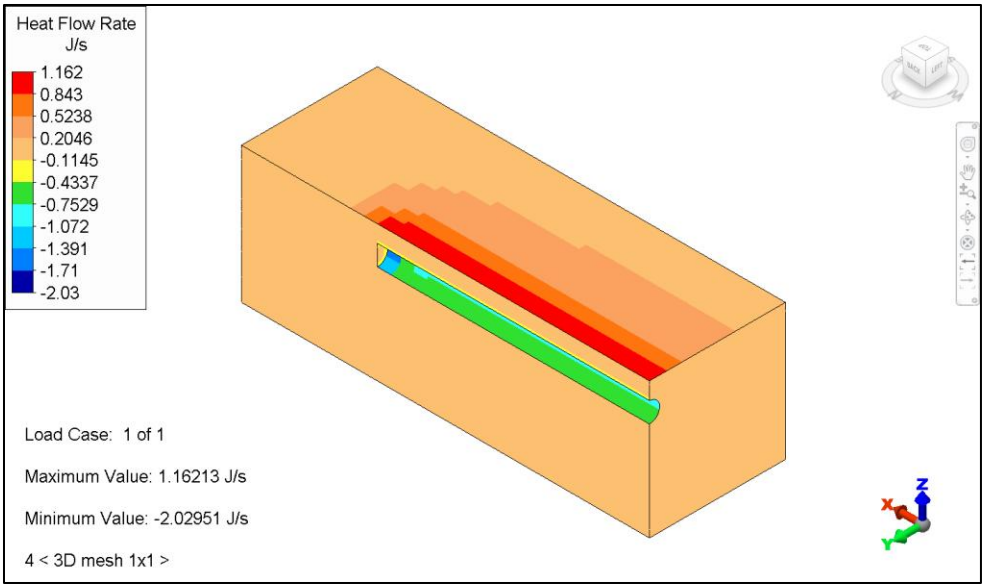

Figure 93-3. Heat flow contours for the 3-D brick mesh version of the model. (Smoothing is turned off)

For the 3-D model, the heat flow was summed on the surface of the ground to obtain heat loss. Due to quarter-symmetry, the sum was multiplied by 4 for comparison to the theoretical solution.

Table 93-1. Comparison of Results

		W (m)	D (m)	T (m)	Heat Flow (W)	% Difference
Theory		∞	∞	∞	859.6	-
Analysis	**2-D Mesh**	1	1	-	831.04	3.32
	2-D Mesh	2	1	-	845.16	1.68
	2-D Mesh	2	2	-	852.96	0.77
	3-D Brick Mesh	1	1	1	893.3	3.92

AVE - 94 3-D Truss System under a Point Load and Uniform Temperature Increase

Reference

Timoshenko, S. P. and Young, D. H., *Theory of Structures*, Second Edition, New York: McGraw-Hill, 1965.

Problem Description

This example is a simple model of a three-dimensional (3-D) truss system with 7 elements. Two load cases are applied independently: a 1,000-lb. point load and a uniform temperature increase of 50 degrees Fahrenheit. This problem verifies the accuracy of the truss element.

Structure Load Case 1:

P = 1000 lb

Structure Load Case 2:

P = 0, uniform temperature increase = 50 ^{o}F

Theoretical Solution

- A = 1.0 in^2 (cross sectional area)
- E = 30 x 10^6 psi (Young's Modulus)
- a = 6.5 x 10^{-6}/^{o}F (coefficient of thermal expansion)

Autodesk Simulation Solution

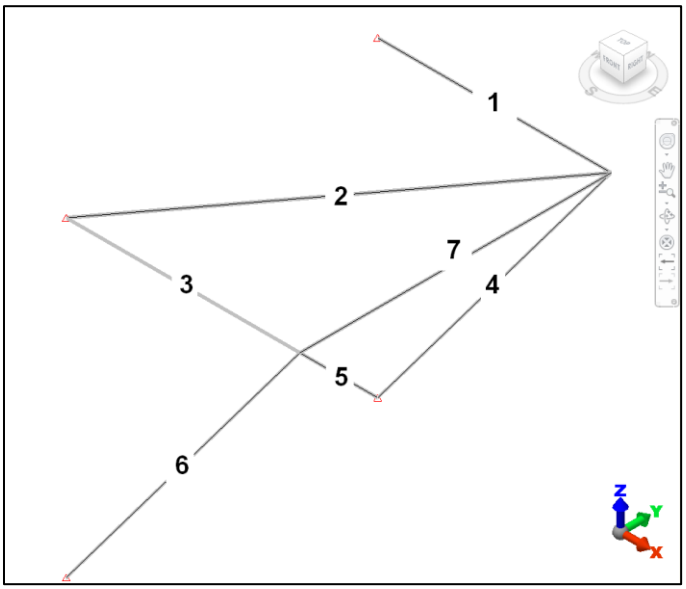

Figure 94-1. Element numbering

The only results given by the reference are the axial stresses in members 2 and 4.

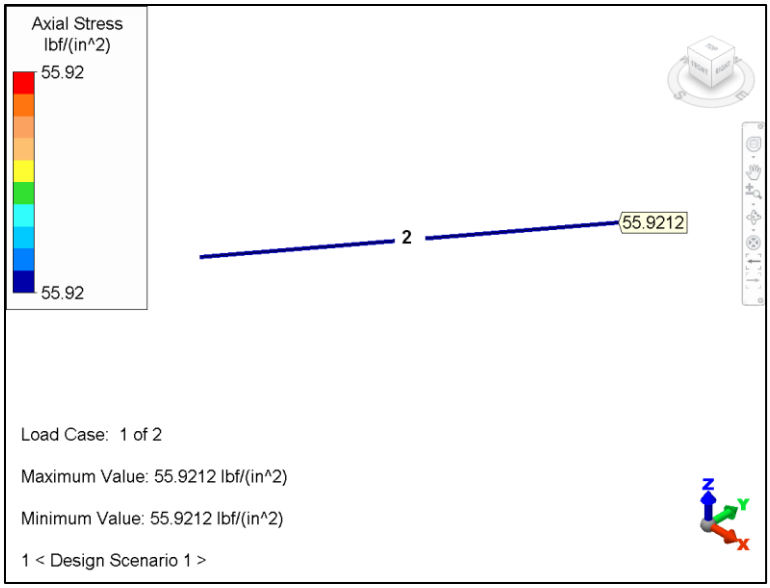

Figure 94-2. Load case 1:axial stress at member 2. All other members are hidden.

Table 94-1. Comparison or Results, Member 2

Load Case	Theory	Analysis	% Difference
1	56	55.92	0.14
2	-1295	-1292	0.23

Force in Truss 3 = `P / (4/5)` for case 1 from $Sigma_z = 0$

Where:

P = 1000 lb

Table 94-2. Comparison or Results, Member 4

Load Case	Theory	Analysis	% Difference
1	-1250	-1250	0.00

AVE - 95 Weight, Center of Gravity and Mass Moment of Inertia Analysis of a Straight Bar

Reference

Beer, Ferdinand P. and Johnston, Jr., E. Russel, *Vector Mechanics for Engineers: Dynamics*, Third Edition, New York: McGraw-Hill, 1977, pp. 937-938.

Problem Description

A straight, 10" long, steel bar of 1 in^2 cross sectional area oriented along the Y axis is analyzed for weight, center of gravity and mass moment of inertia.

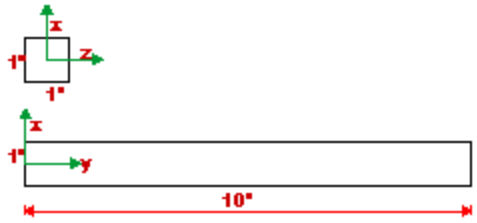

Figure 95-1. Dimensions of the steel bar.

Theoretical Solution

The mass moment of inertia about a transverse axis through one end of the square cross section bar is given by:

$$I_x = I_Z = \rho\alpha^2 l\left(\frac{\alpha^2}{12} + \frac{l^2}{3}\right)$$

Where:

- l = 10.00" (length of beam)
- α = 1.00" (side of square beam)
- ρ = 7.3395 E-4 (lb s^2 / in^4) (mass density)

Autodesk Simulation Solution

The bar is modeled with 10 truss elements, each of which is 1" long. This example verifies the accuracy of the Mass Properties Analysis Processor for truss elements.

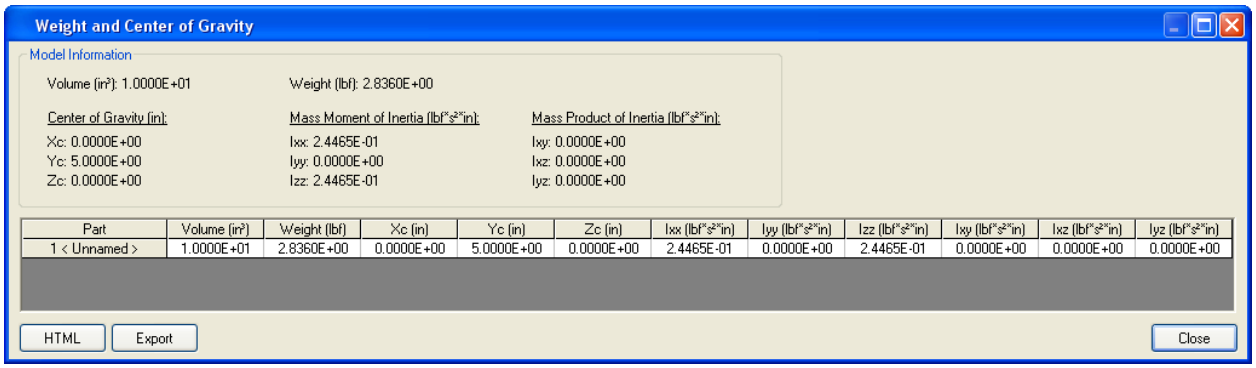

Figure 95-2. Weight, center of gravity and mass moment of inertia calculated by the software.

Table 95-1. Comparison of Results

	Theory	Analysis	% Difference
Volume, V (in^3)	10.00	10.00	0.00
Weight, W (lb)	2.836	2.836	0.00
X_c (inch)	0.00	0.00	0.00
Y_c (inch)	5.00	5.00	0.00
Z_c (inch)	0.00	0.00	0.00
Mass Moment of Inertia X axis (in lb s^2)	0.24526	0.24465	0.25
Mass Moment of Inertia Y axis (in lb s^2)	-	N/A	-
Mass Moment of Inertia Z axis (in lb s^2)	0.24526	0.24465	0.25

Note: Mass Properties Analysis Processor returns a value of 0.0 for the Y axis moment of inertia for this problem because the truss element is a line element having no mass distribution about the axis of the beam. This also accounts for the small difference in the moments of inertia about the other two axes.

See AVE 112 for an example using the brick element on the same problem that eliminates these errors. (Using the slender bar formula of $I_x=I_z= \rho A l^3/3$ gives the same value calculated by the software.)

AVE - 96 6-Story, 2-Bay Frame Structure under Uniformly Distributed Loading

Reference

Toridis, T. G. and Khozeimeh, K., "*Computer Analysis of Rigid Frames*," Computers and Structures 1, 1971.

Problem Description

This example is a plane frame structure under a uniformly distributed loading.

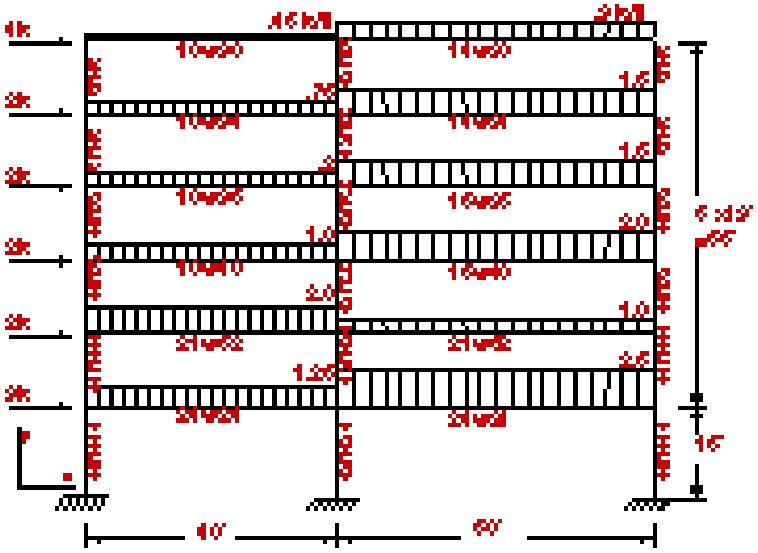

Figure 96-1. The frame and the applied loading from the reference.

Theoretical Solution

The reference article converted the distributed loads to nodal loads and then applied these nodal loads to the structure.

Autodesk Simulation Solution

This example verifies the accuracy of the beam element and illustrates the use of uniform distributed loads. The solution used two structure load cases in solving this problem:

- Using distributed loads directly
- Using equivalent nodal loads (forces and moments)

The point load case is equivalent to the distributed load case to illustrate that equivalent results can be obtained by different methods. With the beam element, distributed loads can be assigned directly to the elements.

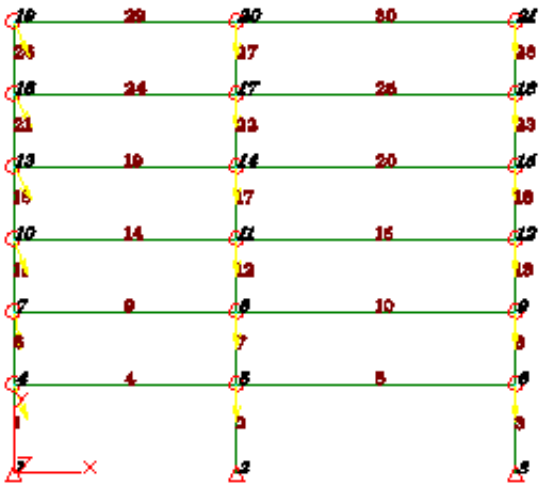

Figure 96-2. Element and node numbering.

Discussion of Results

The nodal deflections produced by both structural load cases are the same, and the beam forces and moments in the columns are the same. The moments calculated by the second structural load case in all the columns and girders are close to those given in the reference.

The beam moments calculated using distributed loads (structural load case 1) in the horizontal members are different (and are more realistic) than those calculated by the reference article. Using nodal loads to emulate a distributed load applies the correct loads to the rest of the model, but does not give the loads (or stresses) in the loaded beam due to the load in that beam itself. Figure 105-3 shows the beam end moments calculated for elements 26 to 30 by the two methods.

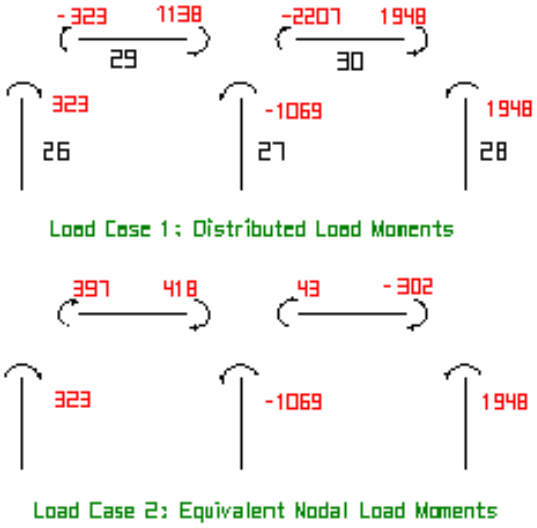

Figure 96-3. Distributed load and equivalent nodal load moments.

The arrow heads in the figure depend on the orientation of the beams. The signs of the moments in the figure are those calculated by the stress processor.

The fixed end moments for elements 29 and 30 are 720 and 2250 in-k respectively. To obtain the actual beam moments, the fixed end moments must be added to the results computed by load case 2. When using the distributed input (load case 1), The software adjusts these moments internally so that the corrected beam moments are output.

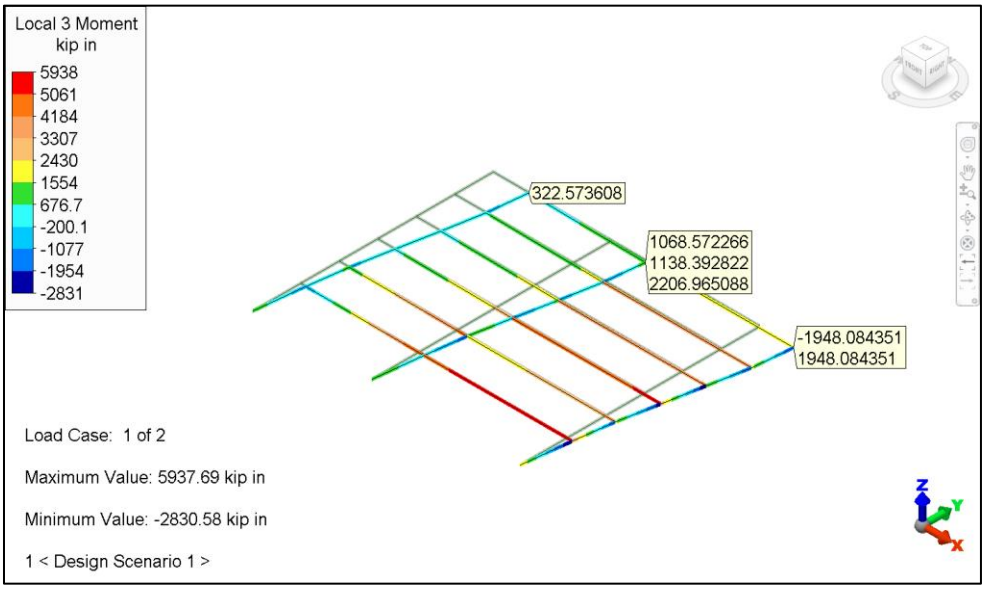

Figure 96-4. Deflected shape and original shape along with moments.

AVE - 97 Earthquake Response of a 10-Story Plane Frame

Reference

No theoretical reference is needed for this problem. This problem is presented for illustrative purposes only.

Problem Description

A ten-story plane frame is subjected to a response spectrum load representing an earthquake. The analysis is performed in two parts: a modal analysis to obtain mode shapes and frequencies, followed by a response spectrum analysis to calculate stresses and deflections.

A 10-story plane frame, as shown in Figure 97-1, was analyzed. Beams of interest are 1, 7, 13, 19 and 25. This is an application example and not a formal verification example. The results provided here are used to check the precision of each new release of the software vs. the previous one.

- E = 30 x 10^6psi
- ν = 0.3
- ρ = 0.283 lb/in^3

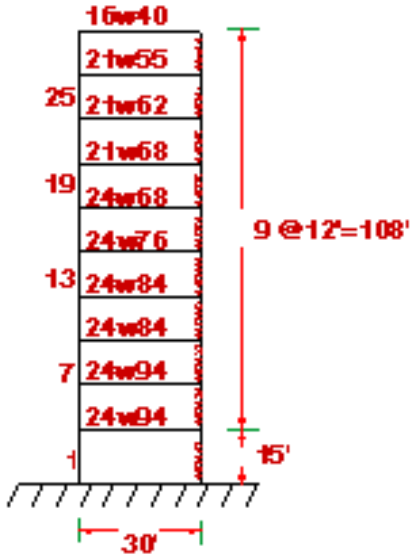

Figure 97-1. FEA model of the 10-story frame.

Autodesk Simulation Solution

The problem is solved in two design scenarios: first the eigen-solution, then the response spectrum analysis with dynamic restart. The response spectrum used represents the 1940 El Centro earthquake.

A theoretical result for this problem is not available. The following tables and figures show the response spectrum results.

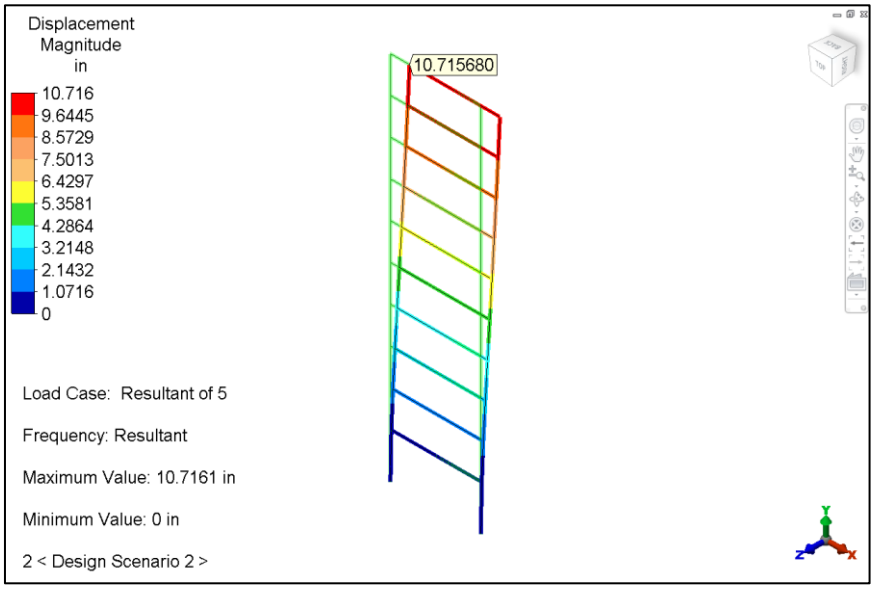

Figure 97-2. Displacement result at node 21. Resultant function is used.

Table 97-1. Nodal Displacements (X direction - Resultant)

Node	Analysis
2	0.497
5	1.390
7	2.522
9	3.753
11	5.010
13	6.266
15	7.483
17	8.640
19	9.712
21	10.716

AVE - 98 Frequency Response Analysis of a Two Degrees of Freedom System

Reference

Thomson, W. T., *Theory of Vibration with Applications, Second Edition*, Englewood Cliffs, NJ: Prentice-Hall, Inc., 1981.

Problem Description

A two degrees of freedom system is subjected to a sinusoidal force applied at the second node. The critical damping ratio for each mode is assumed to be 0.04. Find the steady-state displacement at each node.

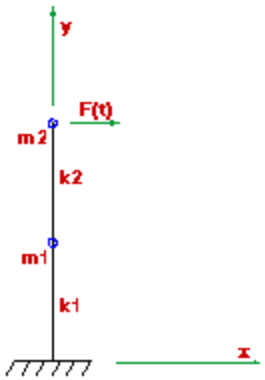

Figure 98-1. FEA model of the two DOF system used for frequency analysis.

Theoretical Solution

Properties shown in Figure 98-1 are given as follows:

- m1 = 150 (lb sec^2)/in
- m2 = 80 (lb sec^2)/in
- Lateral Stiffness (k) = $6EI/l^2$
- k1 = 144000 lb/in
- k2 = 72000 lb/in
- Damping Ratio = 0.04
- F(t) = 20000 x sin(25.13274t) lb

Autodesk Simulation Solution

This example explores the different options that can be used to obtain the steady-state frequency response of a structure, namely loads with the same frequency, multiple frequencies and the same frequency with different phase angles.

Two beam elements with zero mass density were used. Two lumped masses of 150 (lb sec^2)/in and 80(lb sec^2)/in were applied at the two nodes.

The mode shapes and natural frequencies were calculated using the Linear Mode Shapes and Natural Frequencies Processor first. Then, the analysis type was changed and the Linear Frequency Response (Modal Superposition) Processor was used to find the steady-state displacements.

The steady-state X-displacements computed by the Linear Frequency Response Processor are compared to the theoretical results in the following table.

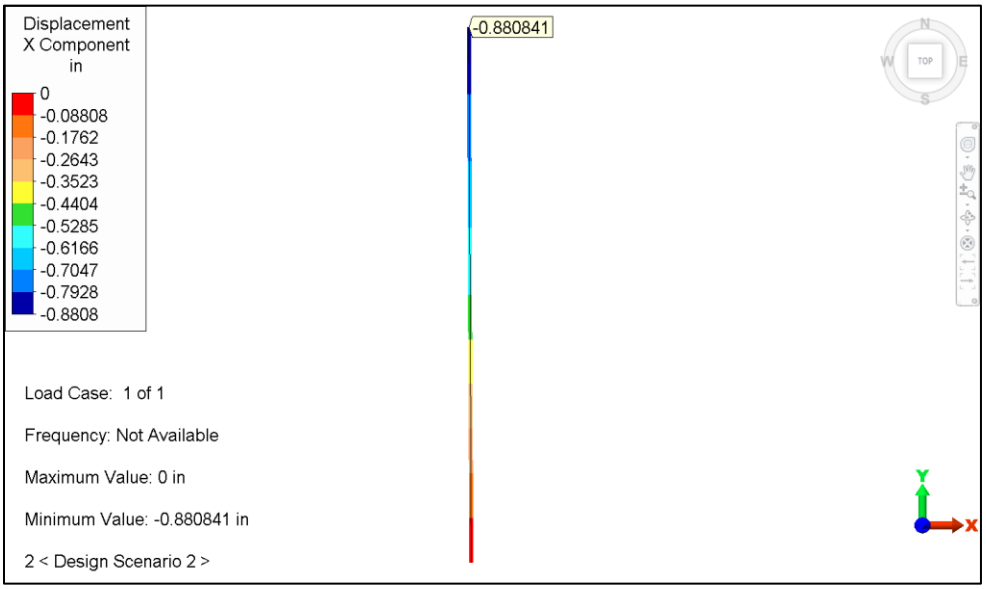

Figure 98-2. Inquiring on the displacement result at node 3.

Table 98-1. Comparison of Results

Node Number	Displacement in X (inch)		% Difference
	Theory	Analysis	
2	0.5402	0.5287	2.13
3	0.9130	0.8808	3.56

AVE - 99 Weight, Center of Gravity and Mass Moment of Inertia Analysis of a Square Beam

Reference

Beer, Ferdinand P. and Johnston, Jr., E. Russel, *Vector Mechanics for Engineers: Dynamics*, Third Edition, New York: McGraw-Hill, 1977, pp. 937-938.

Problem Description

This AVE involves a weight, center of gravity, and mass moment of inertia analysis of a beam model using beam elements. This example verifies the accuracy of the Mass Properties Analysis Processor for beam elements.

A straight 10" long steel beam of 1 in^2 cross-sectional area oriented along the Y axis is analyzed for weight, center of gravity and mass moment of inertia. The problem is the same as AVE - 95 where truss elements were used.

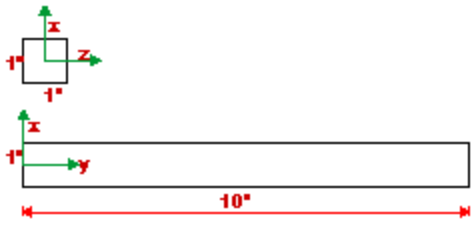

Figure 99-1. Dimensions of the square beam.

Theoretical Solution

The mass moment of inertia about a transverse axis through the centroid of the square cross-section at the end of the bar is given by:

$$I_x = I_z = \bar{I} + m\overline{y^2} = \rho a^2 l\left(\frac{a^2}{12} + \frac{l^2}{3}\right)$$

Where:

- l = 10.00" (length of beam)
- α = 1.00 (side of square beam)
- ρ = 7.3395 E-4 (lb s^2 / in^4) (mass density)

Autodesk Simulation Solution

The beam is modeled with 10 beam elements, each of which is 1" long. In FEA Editor, the "Weight and Center of Gravity…" command was used to calculate the weight, center of gravity and mass moment of inertia for the model.

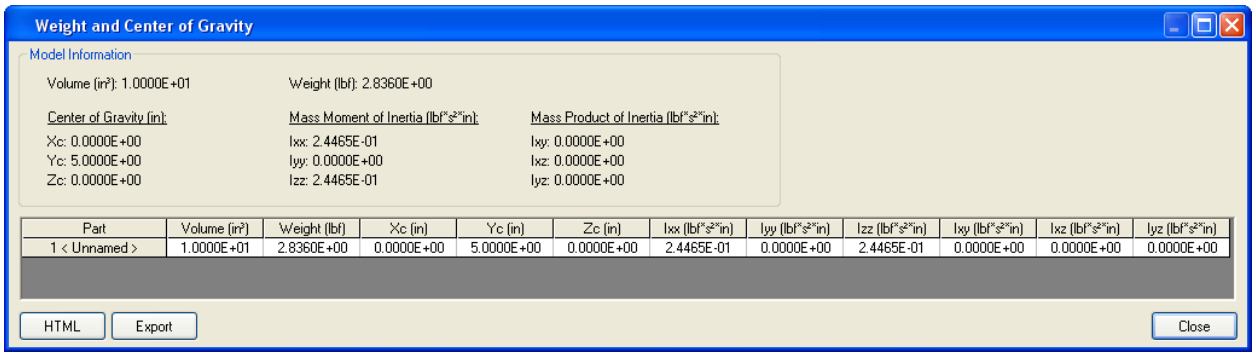

Figure 99-2. Accessing the "Weight and Center of Gravity Calculation" screen.

Table 99-1. Comparison of Results

	Theory	Analysis	% Difference
Volume, V (in^3)	10.00	10.00	0.00
Weight, W (lb)	2.836	2.836	0.00
X_c (inch)	0.00	0.00	0.00
Y_c (inch)	5.00	5.00	0.00
Z_c (inch)	0.00	0.00	0.00
Mass Moment of Inertia X Axis (lb in s^2)	0.24526	0.24465	0.25
Mass Moment of Inertia Y Axis (lb in s^2)	-	Not Applicable	-
Mass Moment of Inertia Z Axis (lb in s^2)	0.24526	0.24465	0.25

Note: The Mass Properties Analysis Processor returns a value of 0.0 for the Y axis moment of inertia for this problem because the beam element is a line element having no mass distribution about the axis of the beam. This also accounts for the small error in the moments of inertia about the other two axes. See AVE 111 for an example using brick element on the same problem, which eliminates these errors. (Using the slender bar formula of $I_x=I_z= \rho A l^3/3$ gives the same value calculated by the software.)

AVE - 100 Torsion of a Box Beam

Reference

Pytel, A. and Singer, F. L., *Strength of Materials*, New York: Harper & Row, 1987.

Problem Description

A box beam is subjected to torsion using point loads. The torsion is produced by nodal loads at opposite edges of the beam.

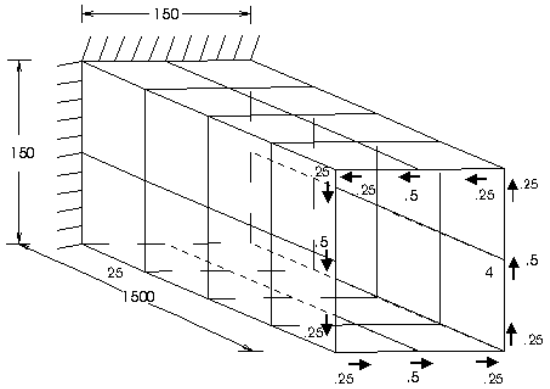

Figure 100-1. Square box beam with loading and boundary conditions.

Theoretical Solution

$$\tau = \frac{T}{2a^2t}$$

$$\Phi = \frac{T}{ta^3G}$$

$$\Theta = \Phi l$$

Where:

- a = 150 in
- t = 3 in (thickness)
- l = 1500 in (length)
- T = 2(1 x 150) = 300 (torque)
- G = 2.8846 (shear modulus)

This gives the following results:

$$\tau = \frac{300}{2(150)^2(3)} = 0.0022222$$

$$\Theta = \frac{(300)(1500)}{(3)(150)^3(2.8846)} = 0.0154074 \text{ rad.}$$

Autodesk Simulation Solution

Membrane elements were used for this application.

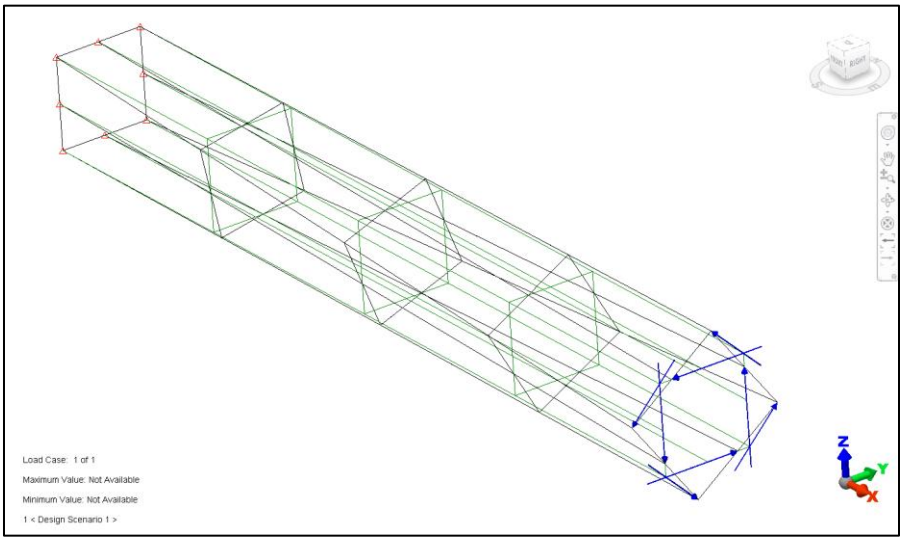

Figure 100-2. Deflected shape superimposed over the original.

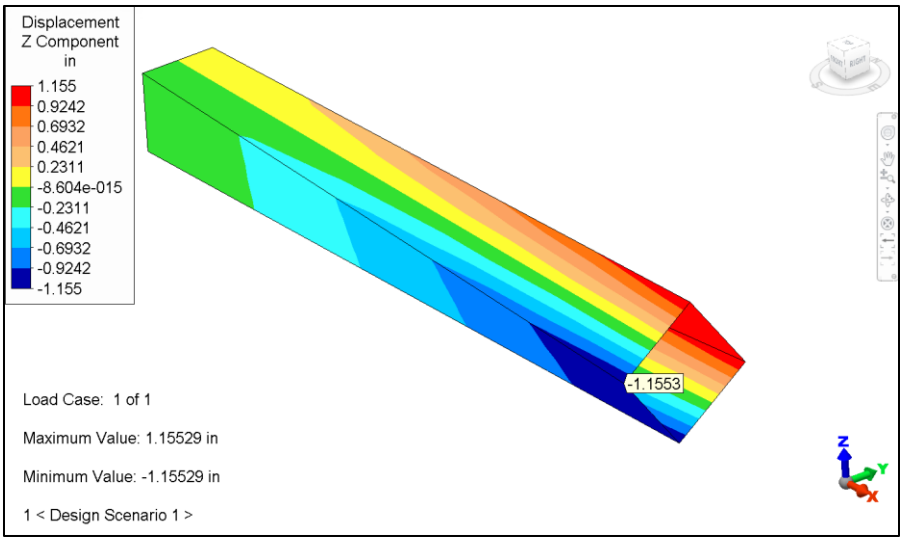

Figure 100-3. Inquiring on the displacement result at node 30.

Results (using displacements from node 30):

$\Theta = \arctan(1.1553/(150/2)) = 0.0154028$ rad.

Table 100-1. Comparison of Results

Θ (radians)		**% Difference**
Theory	**Analysis**	
0.0154074	0.0154028	-0.03

AVE - 101 Weight, Center of Gravity and Mass Moment of Inertia Analysis of a Circular Plate

Reference

Beer, Ferdinand P. and Johnston, Jr., E. Russel, *Vector Mechanics for Engineers: Dynamics*, Third Edition, New York: McGraw-Hill, 1977, p. 936.

Problem Description

A .1" thick circular plate of 1" radius in the YZ plane is analyzed for weight, center of gravity and mass moment of inertia. This problem is the same as AVE - 108 where 2-D elements were used.

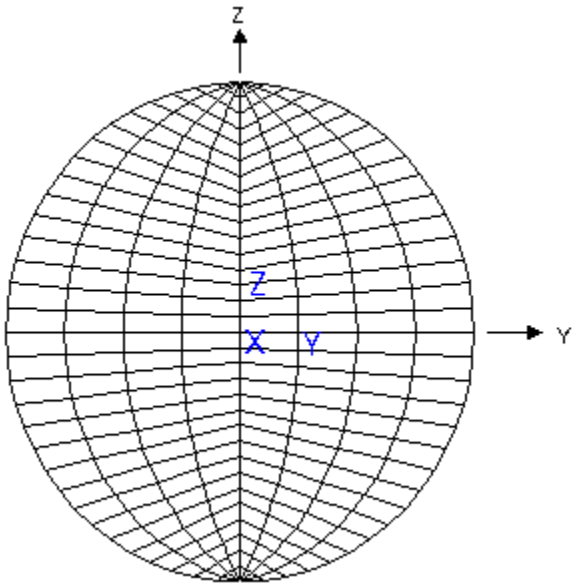

Figure 101-1. Circular plate model.

Theoretical Solution

The following gives the mass moment of inertia equation for a circular plate:

$$I = \frac{\rho\, t\, \pi\, d^4}{64}$$

Where:

- d = 2.0" (plate diameter)
- t = .1" (plate thickness)
- ρ = 7.34E-4 $\frac{lb\ s^2}{in^4}$ (mass density)

Autodesk Simulation Solution

The plate is modeled with 256 membrane elements. The theoretical moment of inertia for the axis perpendicular to the plane of the disk is twice the above thin plate approximation moment of inertia. This example verifies the accuracy of the Mass Properties Analysis Processor for membrane elements.

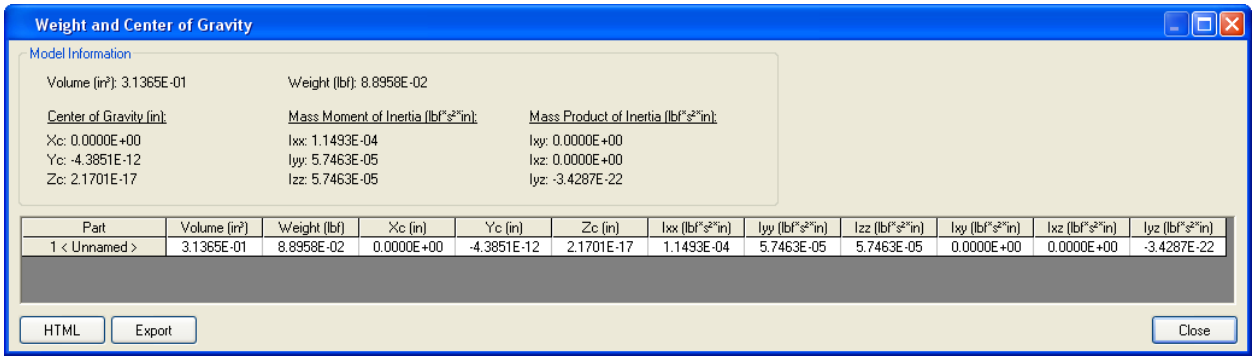

Figure 101-2. "Weight and Center of Gravity Calculation" screen.

Table 101-1. Comparison of Results

	Theory	Analysis	% Difference
Volume, V (in^3)	0.31416	0.31365	0.16
Weight, W (lb)	0.089101	0.088958	0.16
X_c (inch)	0.00	0.00	0.00
Y_c (inch)	0.00	-4.E-12	-
Z_c (inch)	0.00	-4.E-17	-
Mass Moment of Inertia: X Axis (lb in sec^2)	1.15296E-4	1.1493E-4	0.32
Mass Moment of Inertia: Y Axis (lb in sec^2)	5.76482E05	5.7463E-5	0.32
Mass Moment of Inertia: Z Axis (lb in sec^2)	5.76482E-5	5.7463E-5	0.32

AVE - 102 Thick-walled Cylinder under Both Pressure and Temperature Loadings

Reference

Tuba, I. S. and Wright, W. B., ed., "ASME Pressure Vessel and Piping 1972 Computer Program Verification," *ASME Publication I-24*, New York: The American Society of Mechanical Engineers, 1972.

Problem Description

This example involves a thick-walled cylinder with temperature and pressure applied.

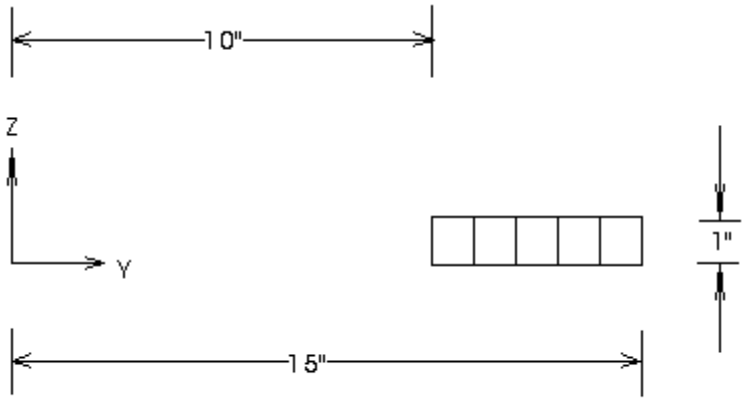

Figure 102-1. Axisymmetric model of the thick-walled cylinder.

Theoretical Solution

$E = 28 \times 10^6$ psi (modulus of elasticity)
$\nu = 0.25$ (Poisson's ratio)
$\alpha = 7.5 \times 10^{-6}$ in/in/°F (coefficient of thermal expansion)
$p = 2000$ psi (internal)
$T_i = 100\ ^oF$ (temperature of inside wall)
$T_o = 0\ ^oF$ (temperature of outside wall)

Temperature distribution:

$$T = \frac{T_i}{\log\left(R_0 / R_i\right)} \log\left(\frac{R_0}{R}\right)$$

Autodesk Simulation Solution

This AVE illustrates the axisymmetric form of the 2-D element. It also illustrates the use of the load case multipliers to apply both the thermal and pressure loads.

Since temperature varies with position, the temperature at each node had to be specified. Use of the element load multipliers sets up the pressure as load case 1, and the thermal load as load case 2. Since this is a portion of a long cylinder, the Z displacements are fixed, so only the Y degrees of freedom are active.

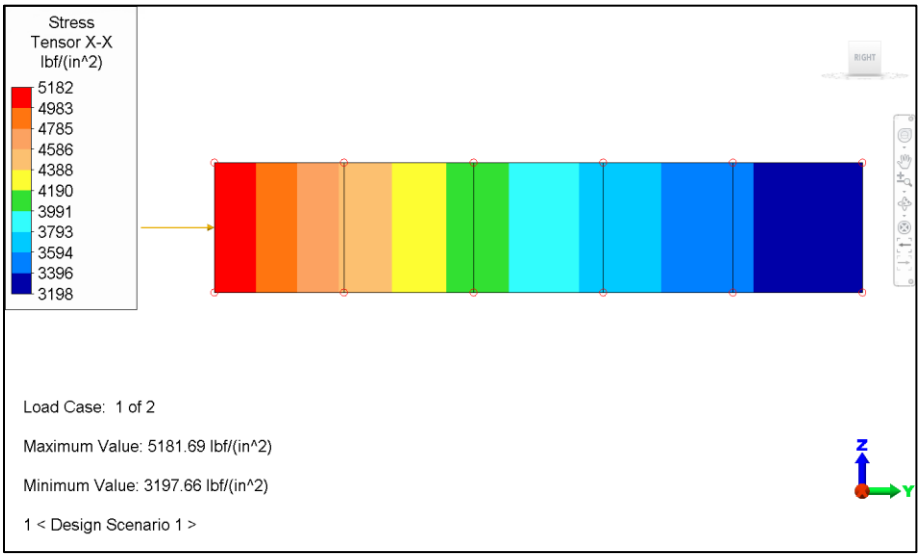

Figure 102-2. Stress tensor results for the pressure load case.

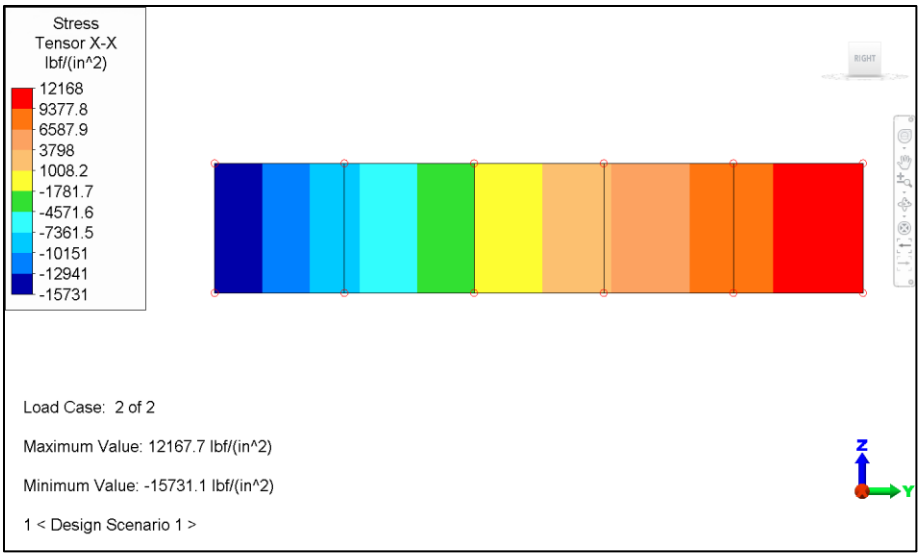

Figure 102-3. Stress tensor results for the temperature load case.

Table 102-1 Comparison of Results (Pressure Load Case)

	Theory	Analysis	% Difference
Inside Hoop Stress (psi)	5200	5181.7	0.35
Outside Hoop Stress (psi)	3200	3197.7	0.072

Table 102-2 Comparison of Results (Temperature Load Case)

	Theory	Analysis	% Difference
Inside Hoop Stress (psi)	-15,870	-15,731	0.88
Outside Hoop Stress (psi)	12,128	12,168	0.33

AVE - 103 Stress Concentration around a Hole

Reference

Zienkiewicz, O. C., *The Finite Element Method in Engineering Science*, 2nd ed., New York: McGraw-Hill, 1965.

Savin, G. N., *Stress Concentrations Around Holes*, London: Pergamon Press, 1961.

Problem Description

This example involves stress concentration around a hole obtained by a plane stress analysis. A uniform pressure load is applied. Orthotropic material properties are used.

Theoretical Solution

Orthotropic properties from Zienkiewicz:

$E_1 = 1$
$\nu_2 = 0.0$
$E_2 = 3$
$G = 0.42$
$G_{12} = 0.42$
$\nu_1 = 0.1$

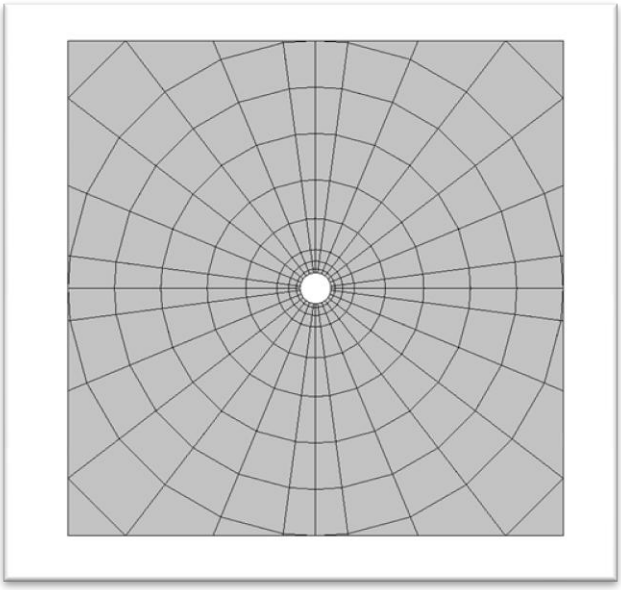

Figure 103-1. The mesh and geometry used to simulate this problem

Autodesk Simulation Solution

A quarter-symmetry model is built using 2-D elements. A uniform pressure of 1 psi is applied in the Y direction. The orthotropic properties are relative to the global coordinate system. The Y-Symmetry and Z-Symmetry boundary conditions were applied to the appropriate nodes along the Symmetry edges.

The stress values at each radius were calculated by taking the average of the two nodal stresses (nodes I and L for the Y-direction S-Tensor stress, with the "Smoothed" option active) for each element along the Z axis edge.

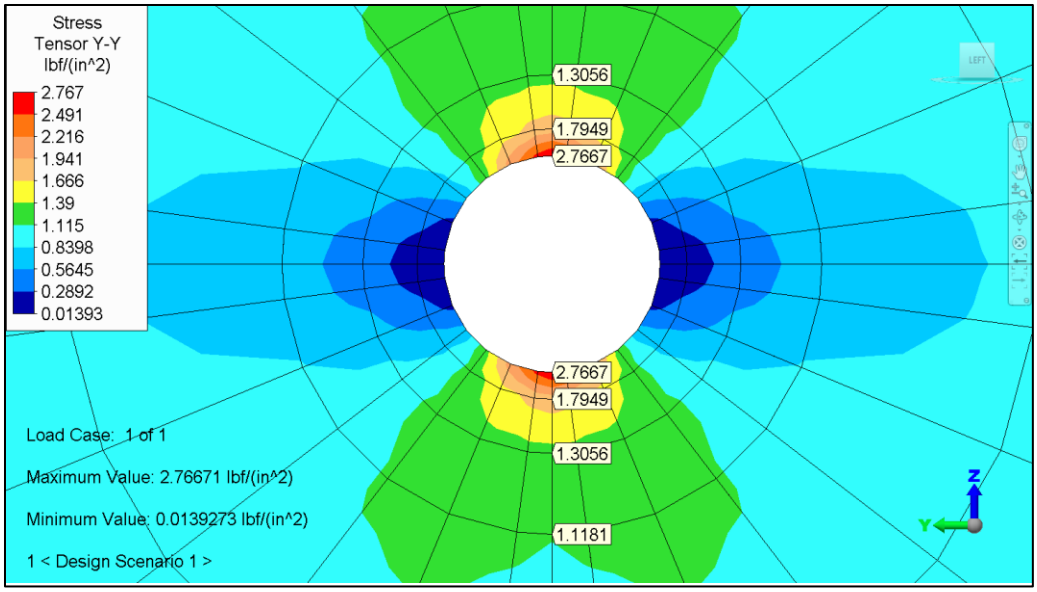

Figure 103-2. Inquiring on the Y-directed stress tensor results along the Z axis. probes were added to Z coordinates: 0.5, 0.625, 0.875 and 1.25 inches

Table 103-1. Comparison of results

Radius	σ_y along Y = 0		% Difference
	Theory	Analysis	
0.5625	2.21727	2.2808	2.87
0.75	1.51756	1.55025	2.15
1.0625	1.20289	1.21185	0.74
1.75	1.05714	1.076	1.78
2.875	1.01771	1.02485	0.70
4.25	1.00749	1.0118	0.43
5.75	1.00396	1.0054	0.14
7.25	1.00245	0.99705	0.54

AVE - 104 Spherical Cap with Pressure

Reference

Timoshenko, S. P. and Woinowsky-Krieger, S., *Theory of Plates and Shells*, Second Edition, New York: McGraw-Hill, 1959.

Problem Description

This example involves a spherical cap with uniform pressure. (See AVE - 113 for the same problem with the plate/shell element.)

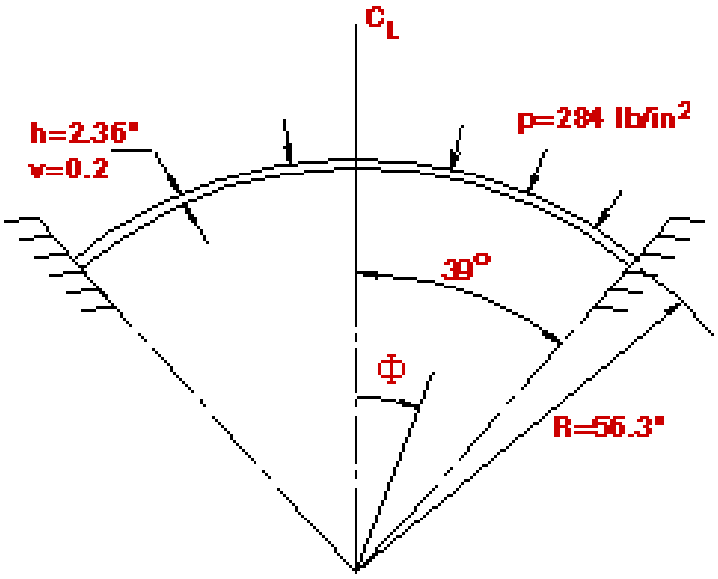

Figure 104-1. Cross section drawing of the spherical cap with a pressure load and boundary conditions.

Theoretical Solution

E = 9.6 x 10^6 psi (modulus of elasticity)
ν = 0.2 (Poisson's ratio)
h = 2.36" (thickness)
R = 56.3" (radius of sphere)
p = 284 psi (applied pressure)

Autodesk Simulation Solution

There are several ways to set up this problem. In this example we will be using 2-D axisymmetric elements. This problem verifies the accuracy of the 2-D element and shows how to apply uniform pressure to this type of element.

When analyzing such a problem with a 2D axisymmetric element, the use of incompatible displacement modes gives the best results. However, incompatible displacement modes should not be used on an element that has one edge coincident with the axis of revolution. Since the use or non-use of incompatible displacement modes is controlled only by the part number, this example simulates the problem using 2 parts. Both are 2-D elements but one has only two elements and no incompatible modes (compatibility enforced), while the other uses incompatible modes (compatibility not enforced) with the remaining elements.

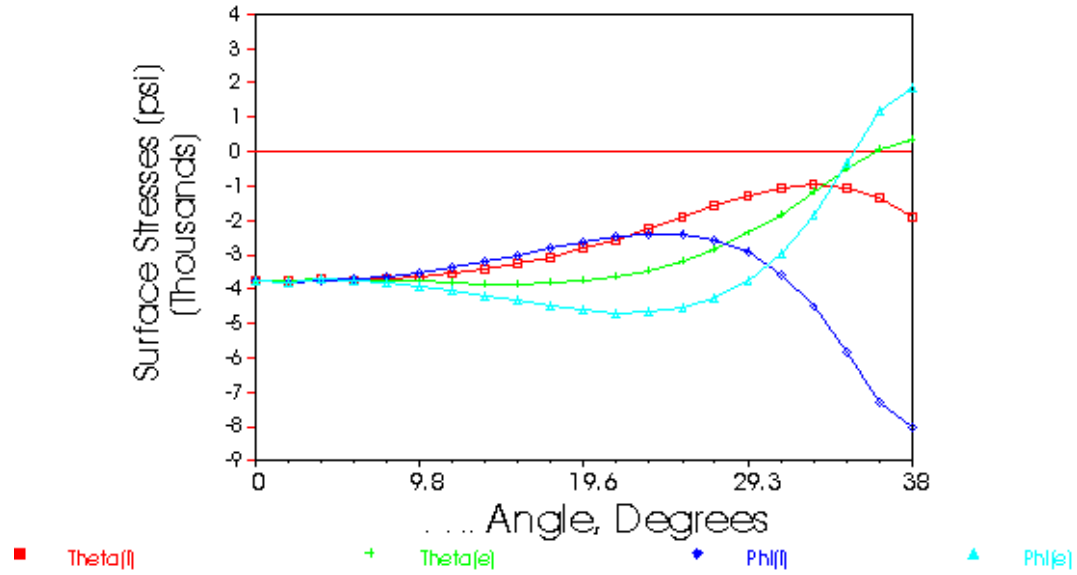

Figure 104-2. Surface stress distributions.

The surface stresses, σ_θ (hoop) and σ_Φ (tangential), on the external (e) and internal (i) surfaces are shown in Figure 104-2. The values used to plot these curves are obtained directly from the results environment by taking the S-tensor stress in the hoop (S33) and tangential (S11) directions. See Figure 104-1 for a definition of the Φ angle. The stress values shown are those produced by the analysis.

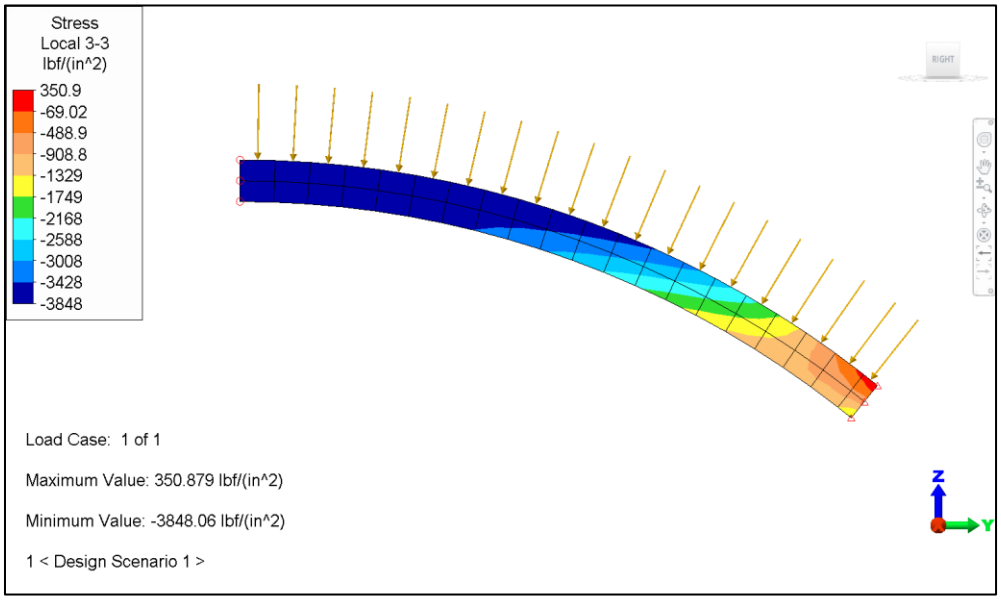

Figure 104-3. S-tensor stress in the hoop (S33) direction.

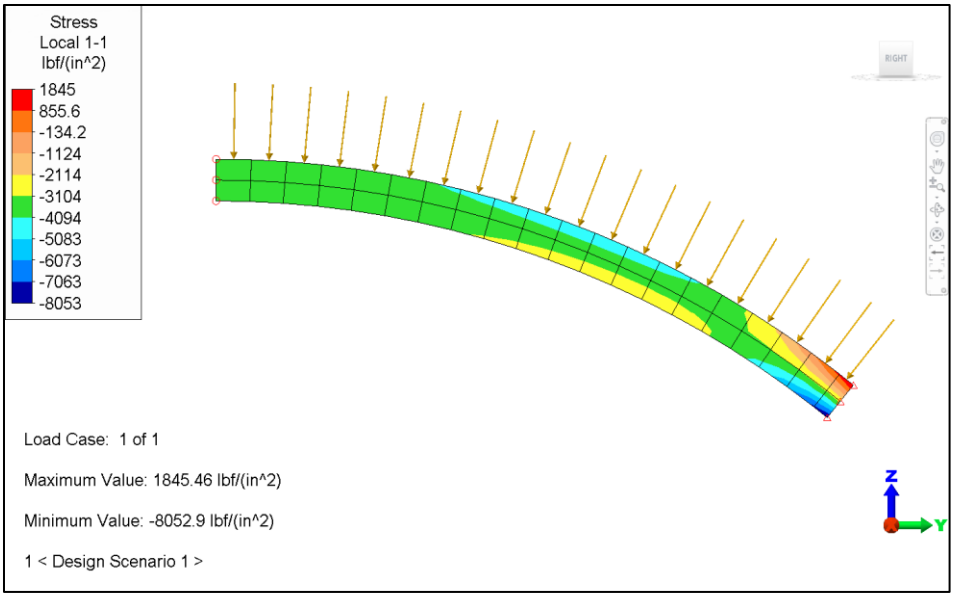

Figure 104-4. S-tensor stress in the tangential (S11) direction.

AVE - 105 Cylindrical Tube under Forced Response with Direct Integration

Reference

Reismann, H. and Padlog, J., "Forced Axisymmetric Motions of Cylindrical Shells", *Journal of the Franklin Institute*, 284, November 1967.

Problem Description

A cylindrical tube with a suddenly applied constant radial load is analyzed using the direct integration method. (The same example is analyzed in AVE - 106 using the modal combination method.)

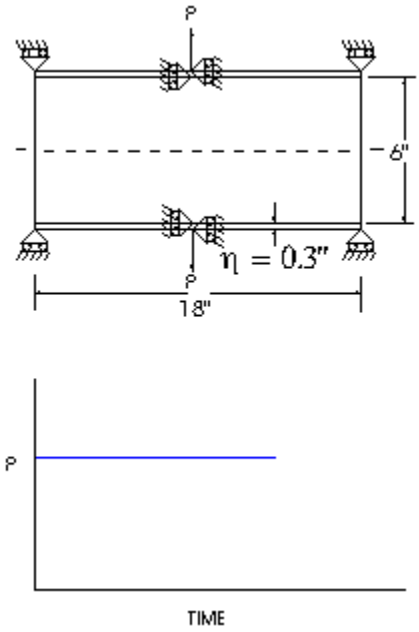

Figure 105-1. 2-D axisymmetric model of the cylindrical tube under forced response.

Theoretical Solution

$E = 30 \times 10^6$ psi (modulus of elasticity)
$P = 1000$ lb/in $= 3000$ lb/radian (applied radial force)
$\nu = 0.3$ (Poisson's ratio)
$\rho = 3.663 \times 10^{-2}$ lb/sec^2/in^4 (mass density)

Autodesk Simulation Solution

Due to symmetry, only half the length is needed for the model. Note that the use of symmetry (including axial symmetry) to reduce the size of dynamics problems can result in missing modes that do not have the symmetry of the reduced model. For this problem, those modes would not be excited by the symmetrical loading.

A two-dimensional axisymmetric element is used. The dynamic load is applied as a unit step function at time = 0.0. Only half the load needs to be applied since it is on the symmetry boundary. The method of analysis is direct integration.

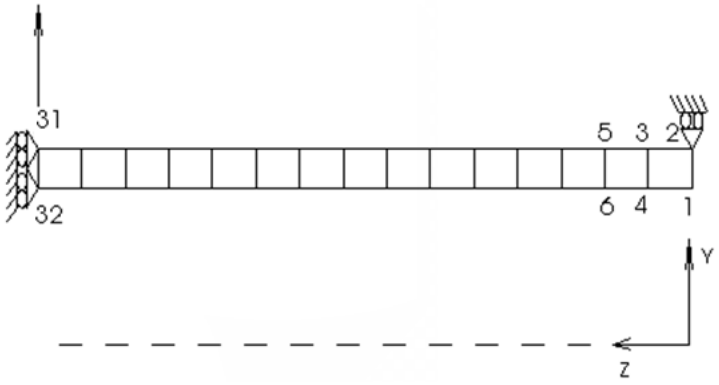

Figure 105-2. FEA model of the cylindrical tube with boundary conditions.

In Figure 105-3, displacement versus time for node 32 is compared to the results in the reference for direct integration and modal combination solutions. (The modal combination solution is obtained in AVE - 106.)

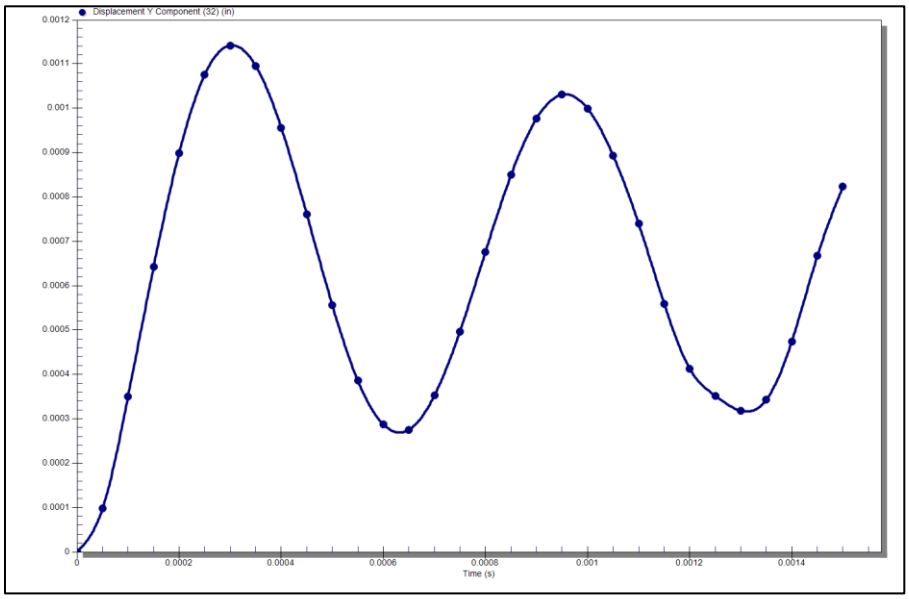

Figure 105-3. Radial displacement (i.e., displacement in the Y direction for node 32) versus time.

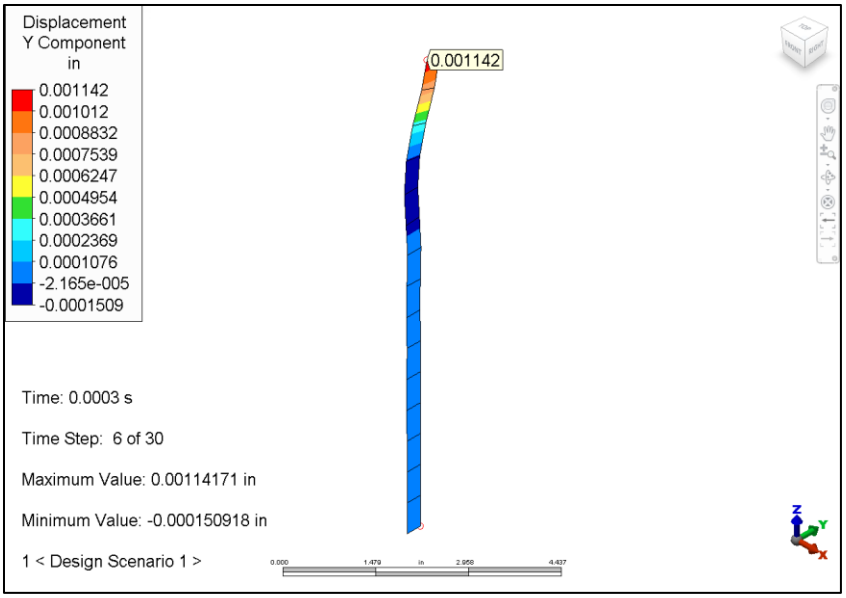

Figure 105-4. Y displacement result of node 32 at time = 0.003 seconds.

AVE - 106 Cylindrical Tube under Forced Response with Modal Combination

Reference

Reismann, H. and Padlog, J., "Forced Axisymmetric Motions of Cylindrical Shells", *Journal of the Franklin Institute*, 284, November 1967.

Problem Description

A cylindrical tube with a point load is analyzed using the modal combination method. (The same problem is analyzed in AVE - 105 using the direct integration method.)

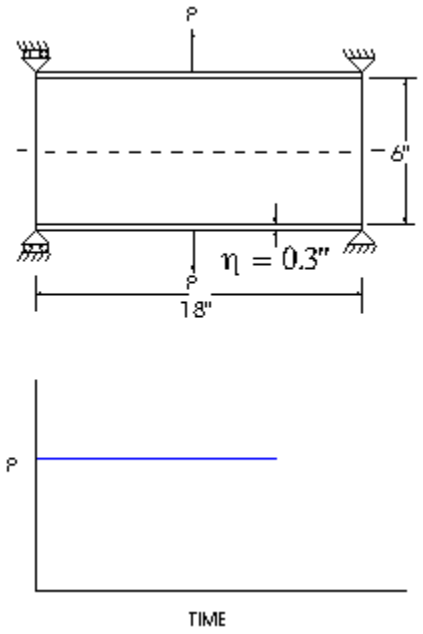

Figure 106-1. 2-D axisymmetric model of the cylindrical tube under forced response.

Theoretical Solution

$E = 30 \times 10^6$ psi (modulus of elasticity)
P = 1000 lb/in = 3000 lb/radian (applied force)
$\nu = 0.3$ (Poisson's ratio)
$\rho = 3.663 \times 10^{-2}$ lb/sec^2/in^4 (mass density)

Autodesk Simulation Solution

Due to symmetry, only half the length is needed for the model. Note that the use of symmetry (including axial symmetry) to reduce the size of dynamics problems can result in missing modes that do not have the symmetry of the reduced model. For this problem, those modes would not be excited by the symmetrical loading.

A two-dimensional axisymmetric element is used. The dynamic load is applied as a unit step function at time = 0.0. Only half the load needs to be applied since it is on the symmetry boundary. The method of analysis is modal combination.

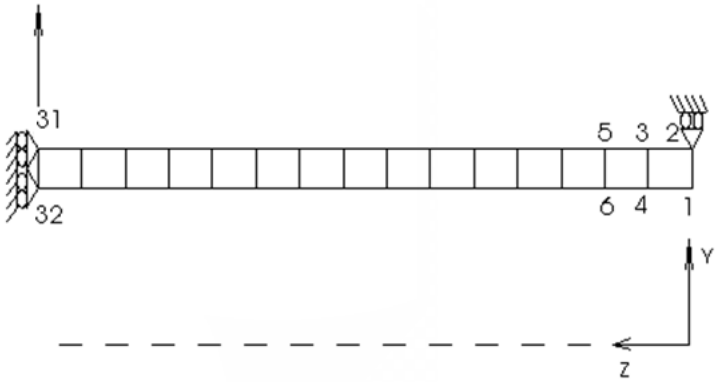

Figure 116-2: FEA model of the cylindrical tube with boundary conditions.

In Figure 106-2, displacement versus time for node 32 is compared to the results in the reference for direct integration and modal combination solutions. (The direct integration solution is obtained in AVE - 105.)

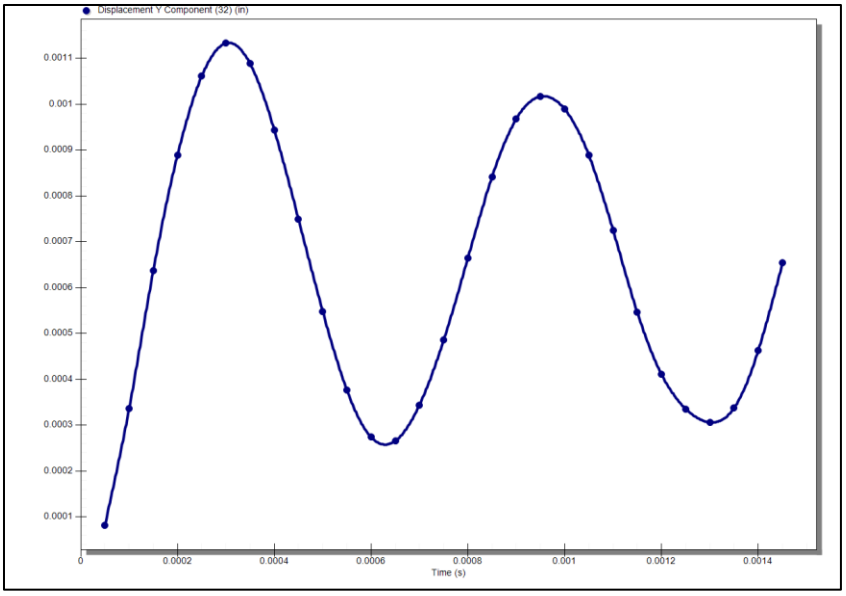

Figure 106-2. Radial displacement (i.e., displacement in the Y direction for node 32) versus time.

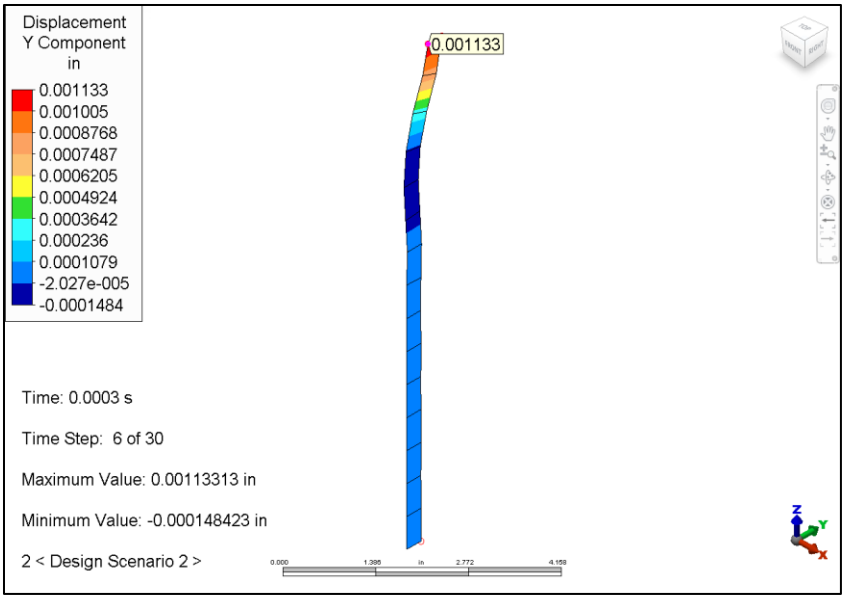

Figure 106-3. Y displacement result of node 32 at time = 0.003 seconds.

AVE - 107 Patch Test with Constant Stress

Reference

MacNeal, R. H. and Harder, R. L., "A Proposed Set of Problems to Test Finite Element Accuracy", *Finite Element Analysis and Design*, 1985.

Problem Description

This patch test consists of applying a constant stress loading to a group (patch) of elements and showing that all elements in the patch will have the same stress. Incompatible modes are suppressed in this example.

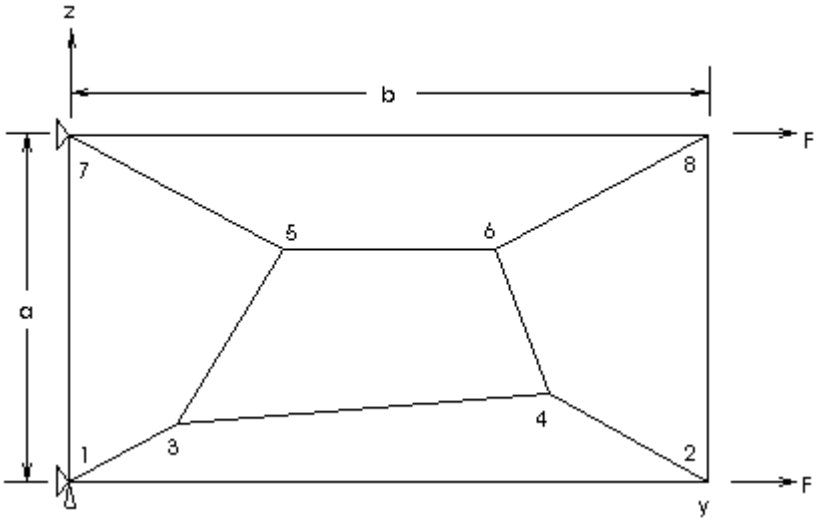

Figure 107-1. FEA Mesh of the 2-D Plane Stress Model

Theoretical Solution

$E = 1.0^6$ psi (modulus of elasticity)

$\nu = 0.25$ (Poisson's ratio)

a = 0.12" (patch height)

b = 0.24" (patch length)

t = 0.001" (patch thickness)

F = 12 lb (applied force at each corner)

$$\sigma_y = \frac{2 \times 12}{0.12 \times 0.001} = 200{,}000 \text{ psi}$$

$\sigma_z = 0.0$ psi

Autodesk Simulation Solution

A static analysis using 2-D plane stress elements was performed.

Location of Inner Nodes		
Node Number	**X**	**Y**
3	0.04	0.02
4	0.18	0.03
5	0.08	0.08
6	0.16	0.08

Because only one of the elements (element 5) has local axes that are parallel to the global axes, the smoothed stress tensor display in the global Y and Z directions has been used for the analysis results below.

Note that the biggest Z direction stress value is more than nine orders of magnitude smaller than the Y direction stress value, showing the Z direction stress values are within round-off error of zero.

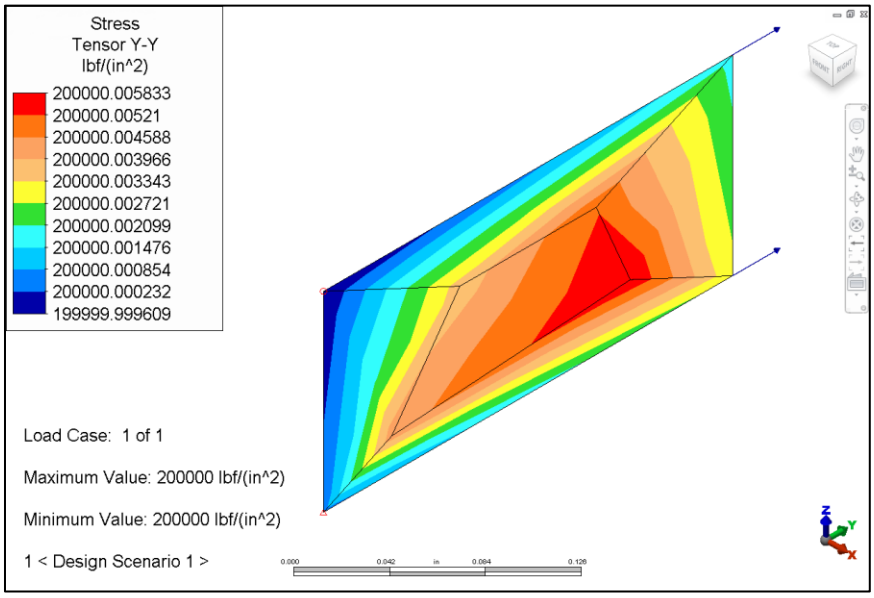

Figure 107-2. Stress tensor display in the global Y direction.

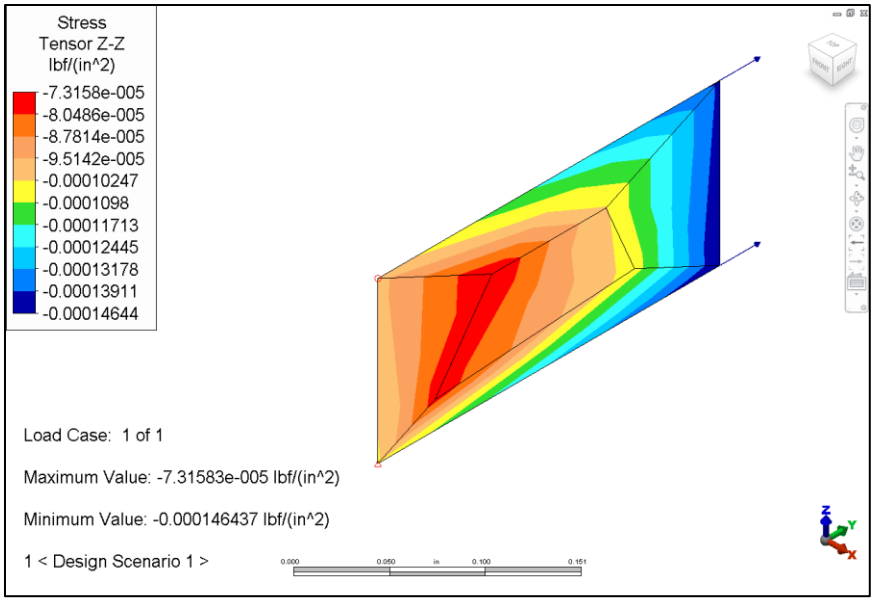

Figure 107-3. Stress tensor display in the global Z direction.

Table 107-1. Comparison of Results

	Theory	Analysis	% Difference
Stress Tensor (Y Direction)	200,000	200,000	0.0
Stress Tensor (Z Direction)	0.00	-0.0001	0.0

AVE - 108 Weight, Center of Gravity and Mass Moment of Inertia Analysis of a Circular Plate

Reference

Beer, Ferdinand P. and Johnston, Jr., E. Russel, *Vector Mechanics for Engineers: Dynamics*, Third Edition, New York: McGraw-Hill, 1977, p. 936.

Problem Description

A 0.1" thick circular plate of 1" radius in the YZ plane is analyzed for weight, center of gravity, and mass moment of inertia.

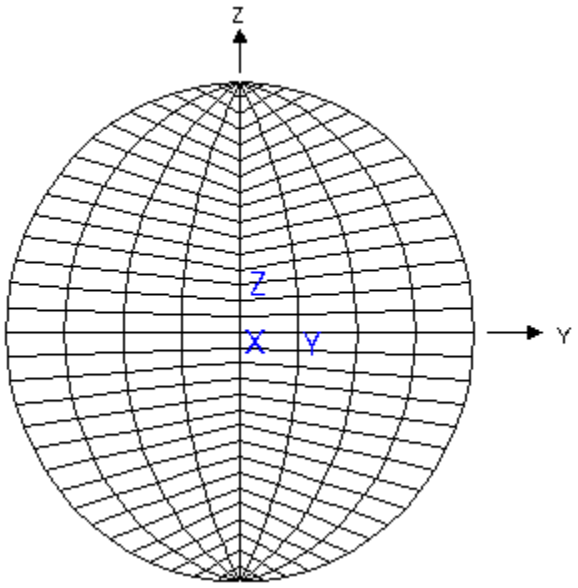

Figure 108-1. FEA model of the circular plate.

Theoretical Solution

Mass moment of inertia equation for a circular plate:

$$I = \frac{\rho t \pi d^4}{64}$$

Where:

- d = 2.0" (plate diameter)
- t = 0.1" (plate thickness)
- ρ = 7.34e-4 lb s^2/in^4 (mass density)

Autodesk Simulation Solution

The plate is modeled with 256 2-D plane stress elements. The theoretical moment of inertia for the axis perpendicular to the plane of the disk is twice the above in plane thin plate approximation moment of inertia.

In FEA Editor, the "Analysis: Weight and Center of Gravity…" command sequence was used to perform a weight, center of gravity and mass moment of inertia analysis. This example verifies the accuracy of the Mass Properties Analysis Processor for 2-D plane stress elements.

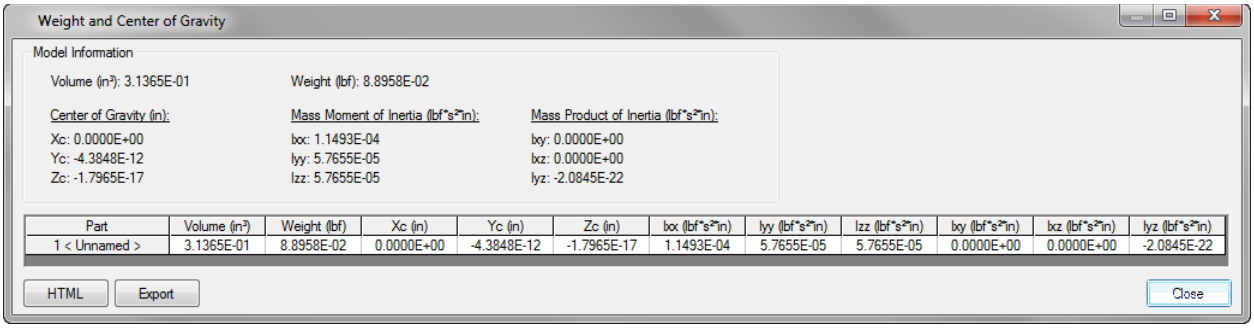

Figure 108-2. "Weight and Center of Gravity Calculation" screen in FEA Editor.

The values for weight, volume, and mass moment of inertia about the X axis are slightly low due to the volume missed by approximating the circle by straight line segments. The values for the mass moments of inertia about the Y and Z axes are slightly higher than theoretical because the 2-D element calculation takes some account of the moment of inertia due to the thickness, which the thin plate theory used here does not.

Table 108-1. Comparison of Results

	Theory	Analysis	% Difference
Volume, V	0.31416 in^3	0.31365 in^3	0.16
Weight, W	0.089095 lb	0.088958 lb	0.16
X_c	0.00"	0.00"	-
Y_c	0.00"	-4.38E-12"	-
Z_c	0.00"	-1.79e-17"	-
Mass Moment of Inertia: X axis	1.15288 E-4 lb in sec^2	1.1493 E-4 lb in sec^2	0.31
Mass Moment of Inertia: Y axis	5.7644 E-5 lb in sec^2	5.7655 E-5 lb in sec^2	0.02
Mass Moment of Inertia: Z axis	5.7644 E-5 lb in sec^2	5.7655 E-5 lb in sec^2	0.02

AVE - 109 Thick-walled Cylinder under Centrifugal and Pressure Loading

References

Tuba, I. S. and Wright, W. B., ed., "ASME Pressure Vessel and Piping 1972 Computer Programs Verification", *ASME Publication I-24*, New York: The American Society of Mechanical Engineers, 1972.

Timoshenko, S. P., *Strength of Materials*, Third Edition, New York: Van Nostrand, 1955.

Problem Description

This example is an analysis of a thick-walled cylinder with centrifugal force and pressure applied as two separate load cases.

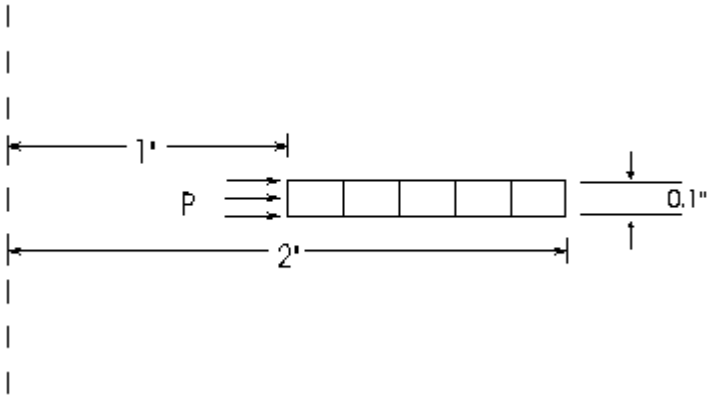

Figure 109-1. Sectional view of the cylinder with loading and dimensions.

Theoretical Solution

$E = 30 \times 10^6$ psi (modulus of elasticity)
$\nu = 0.3$ (Poisson's ratio)
$\rho = 0.286$ lb/in^3 (weight density)

Structure Load Case 1: $\omega = 100$ *rad*/*sec* (angular velocity)
Structure Load Case 2: p = 3000 psi (internal pressure)

Autodesk Simulation Solution

This problem illustrates how centrifugal forces could be emulated by using load case multipliers to apply a different gravitational force to each element based on its distance from the axis of rotation. (However, this is no longer necessary due to the ability to automatically generate centrifugal loading.) This is a good illustration of the multiple part concept (note that every brick element in the model is element number "1").

To model this problem, the 8-node bricks are arranged as a 0.1 radian segment.

Since boundary conditions in the software are globally oriented, boundary elements were added to insure that the nodes do not move tangentially across the non-globally aligned pie-cut symmetry plane. One element group was used for each brick element, allowing, in the old formulation of this problem, the appropriate amount of gravity loading in the Y direction for each element to be applied using element load multipliers to act like centrifugal loading. The mesh is coarse, due to this history.

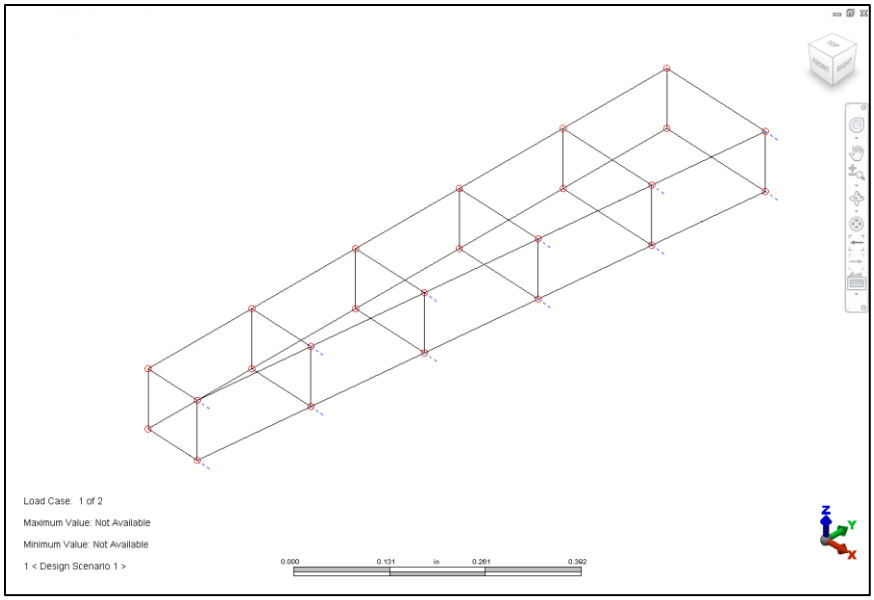

Figure 109-2. Isometric view of the model with node numbers and boundary elements displayed.

Centrifugal loading is applied directly by giving the axis and the angular velocity in RPM. The following figures show stress results for load cases 1 (centrifugal force) and 2 (pressure loading).

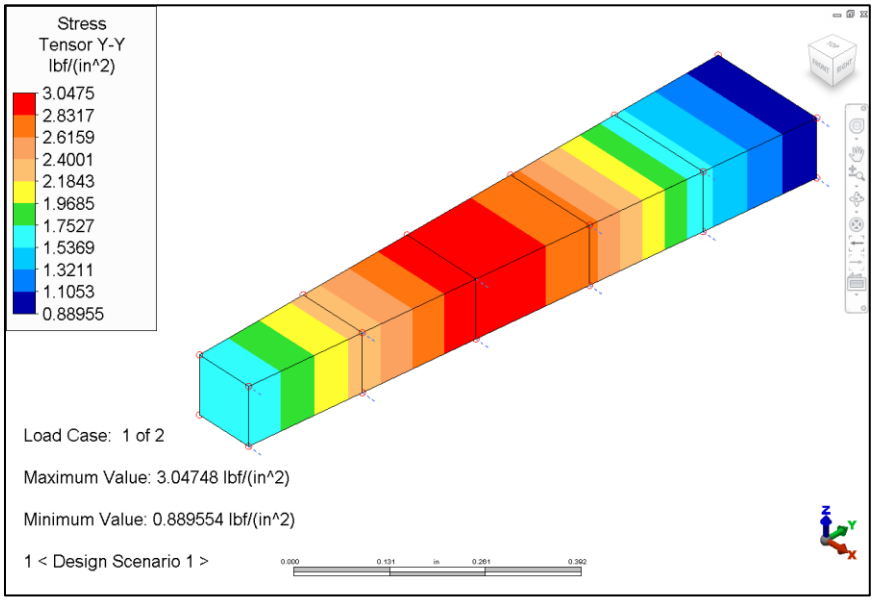

Figure 109-3. Radial stress results of an element for Load Case 1 (centrifugal force).

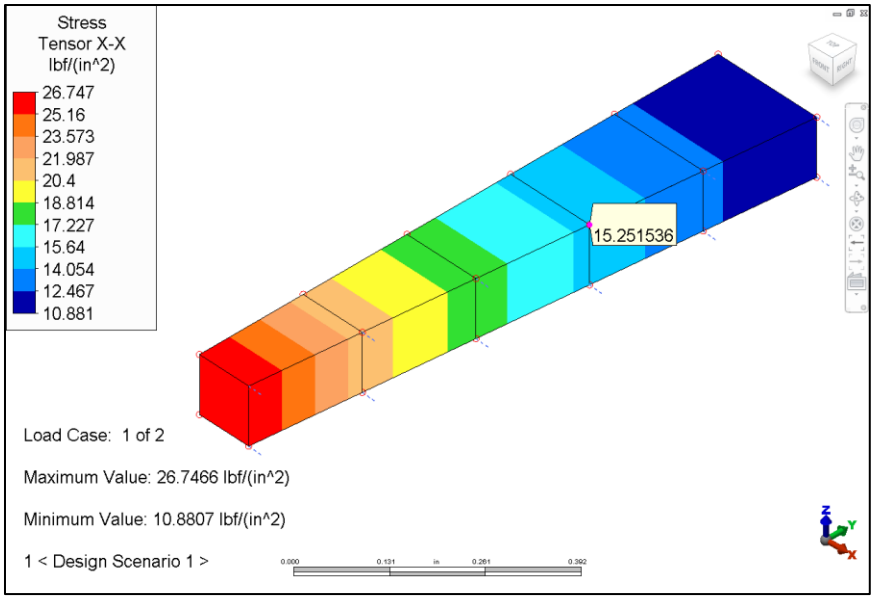

Figure 109-4. Hoop stress results of an element for Load Case 1 (centrifugal force).

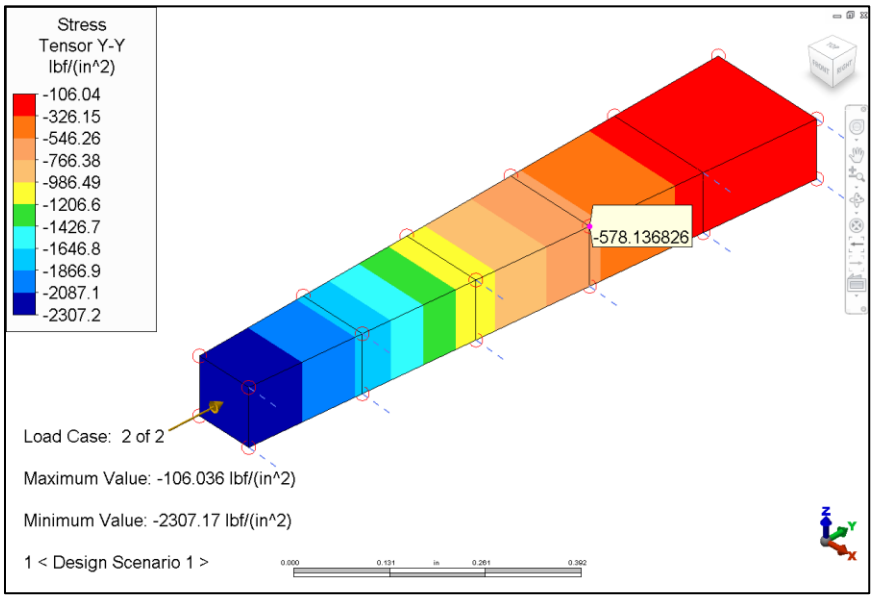

Figure 109-5. Radial stress results of an element for Load Case 2 (pressure loading).

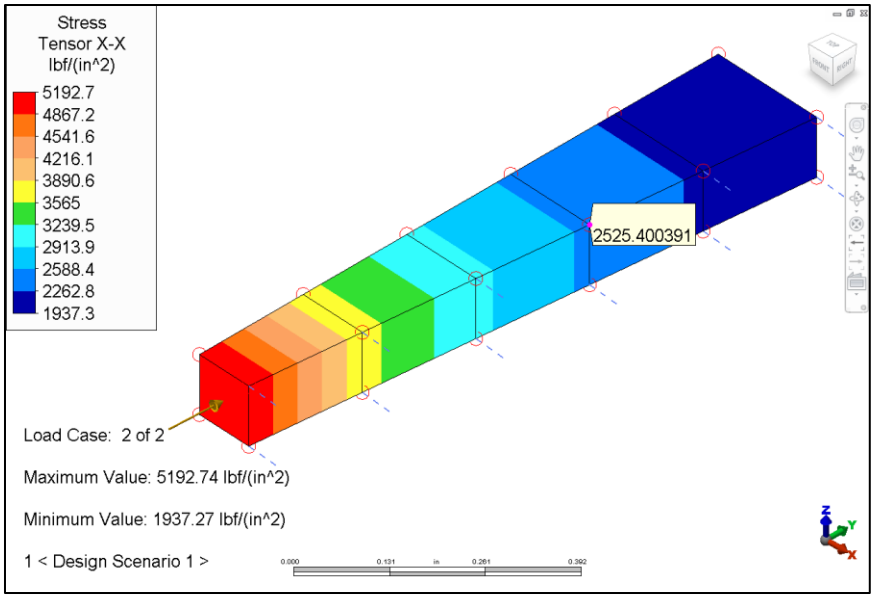

Figure 109-6. Hoop stress results of an element for Load Case 2 (pressure loading).

The stress results reported in the tables below are the stress tensor vector stresses averaged from all the nodes of an element.

Table 109-1. Comparison of Centrifugal Force Results

R	Centrifugal Force					
	σ_r (near σ_{22})			σ_θ (near σ_{11})		
	Theory	Analysis	% Difference	Theory	Analysis	% Difference
1.1	1.4799296	1.5315	3.48	23.256107	23.92	2.85
1.3	2.8825521	2.97825	3.32	19.541775	19.84	1.53
1.5	2.971449	3.06525	3.16	16.755884	16.75	-0.03
1.7	2.2186548	2.2805	2.79	14.4264	14.135	-2.02
1.9	0.8617883	0.8700	0.95	12.315703	11.725	-4.80

Table 109-2. Comparison of Pressure Loading Results

R	Pressure Loading					
	σ_r (near σ_{22})			σ_θ (near σ_{11})		
	Theory	Analysis	% Difference	Theory	Analysis	% Difference
1.1	-2305.7851	-2302.25	-0.15	4305.7851	4351.5	1.06
1.3	-1366.8639	-1366.25	-0.04	3366.8639	3387.5	0.62
1.5	-777.7778	-778.25	0.06	2777.7778	2787.5	0.35
1.7	-384.083	-385.275	0.31	2384.083	2388.5	0.19
1.9	-108.0332	-109.675	1.52	2108.0332	2109.5	0.07

Note: Because the stress values are provided at nodes, and the legacy theoretical radius values used here occur at the middle of the elements, the stress values in this table were arrived at by averaging the nodal values for each element.

AVE - 110 Cantilever Beam Eigenvalues

Reference

Carnegie, W. and Thomas, J., "The Effects of Shear Deformation and Rotary Inertia on the Lateral Frequencies of Cantilever Beams in Bending", *ASME Journal of Engineering for Industry*, February 1972.

Problem Description

A cantilever beam is modeled with 3-D solid elements to verify natural frequencies.

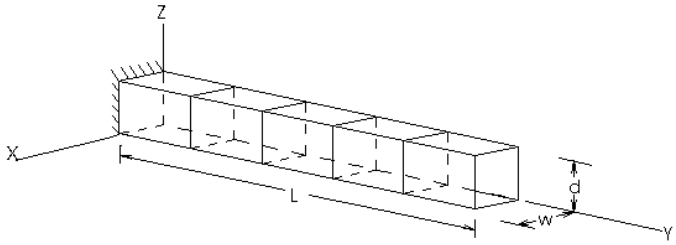

Figure 110-1. FEA model of the cantilever beam.

Theoretical Solution

- $E = 10^6$ psi (modulus of elasticity)
- L = 10 in (length of beam)
- $\nu = 0.3$ (Poisson's ratio)

Displacements in the X direction are suppressed.

- d = 1 in (beam height)
- w = 1.2 in (beam width)
- $\gamma = 0.386$ lb/in^3 (weight density)

Frequencies for the flexural vibrations of a cantilever beam:

$$f_i = \frac{\lambda_i^2}{2\pi}\sqrt{\frac{EI}{\gamma l^4}}$$

Extensional vibration frequencies:

$$f_i = \frac{i}{4l}\sqrt{\frac{E}{\gamma}}$$

However, the flexural frequencies are too high because of neglecting shear and rotary inertia. This effect is more pronounced for the higher modes. The results for a Timoshenko beam were obtained by multiplying the Euler beam frequencies by a factor obtained from Figure 1 in the article by Carnegie and Thomas.

Autodesk Simulation Solution

The cantilever beam is modeled with 3-D solid elements. A Linear Mode Shapes and Natural Frequencies analysis is performed.

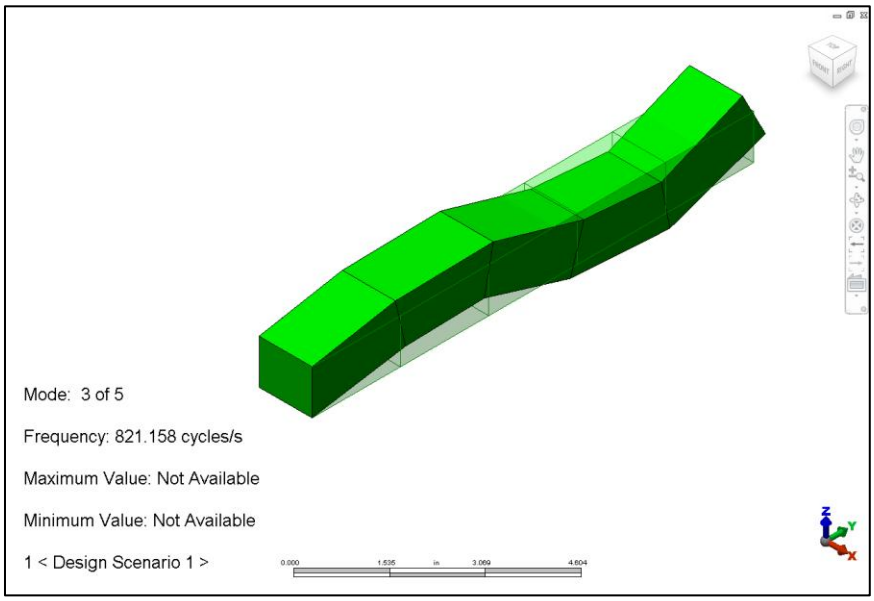

Figure 110-2. Third mode shape.

Table 110-1. Comparison of Results

Mode Number	Type	Natural Frequencies, Hz			% Difference	
		Euler Beam	Timoshenko Beam	Analysis	Euler-Analysis	Timoshenko-Analysis
1	Flexural	55.96	55.6	52.43	4.52	3.90
2	Flexural	350.7	332.0	309.4	11.78	6.81
3	Flexural	982.0	876	821.2	16.37	6.26
4	Extensional	790.6	---	834.8	-5.59	---
5	Flexural	1924.0	1590.0	1537.0	20.11	3.33

AVE - 111 Weight, Center of Gravity and Mass Moment of Inertia Analysis of a Square Beam

Reference

Beer, Ferdinand P. and Johnston, Jr., E. Russel, *Vector Mechanics for Engineers: Dynamics,* Third Edition, New York: McGraw-Hill, 1977, pp. 937-938.

Problem Description

A square 10" long steel beam of 1 in^2 cross-sectional area oriented along the Y axis is analyzed for weight, center of gravity and mass moment of inertia. (This problem is the same as AVE - 99 where beam elements were used.)

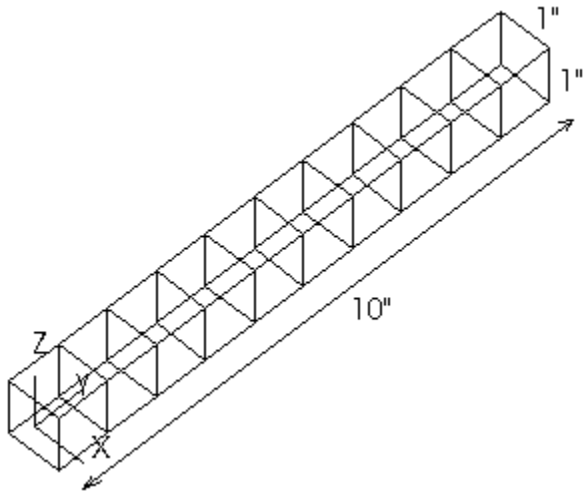

Figure 111-1. FEA model of the square beam.

Theoretical Solution

The mass moment of inertia about a transverse axis through one end of the square cross section beam is given by the following:

$$I_x = \rho a^2 l\left(\frac{a^2}{12} + \frac{l^2}{3}\right)$$

$$I_z = \rho a^2 l\left(\frac{a^2}{12} + \frac{l^2}{3}\right)$$

Where:

- l = 10.00" (length of beam)
- α = 1.00 (side of square beam)
- ρ = 7.3395 E-4 (lb s^2 / in^4) (mass density)

Autodesk Simulation Solution

The beam is modeled with 10, brick elements. The volume of each brick is 1 in^3. A weight, center of gravity and mass moment of inertia analysis was performed.

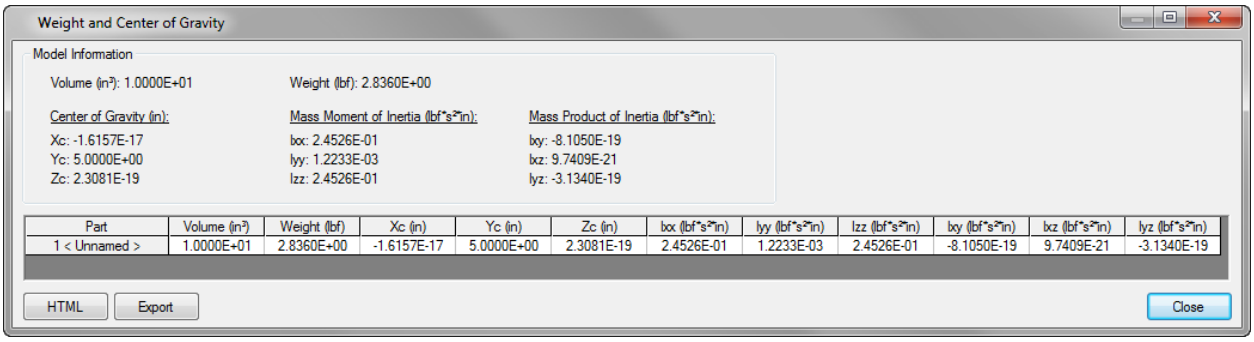

Figure 111-2. "Weight and Center of Gravity Calculation" screen.

Table 111-1. Comparison of Results

	Theory	Analysis	% Difference
Volume, V	10.00 in^3	10.00 in^3	0.0
Weight, W	2.836 lb	2.836 lb	0.0
X_c	0.00"	0.00"	0.0
Y_c	5.00"	5.00"	0.0
Z_c	0.00"	0.00"	0.0
Mass Moment of Inertia X axis	0.24526 lb in sec^2	0.24526 lb in sec^2	0.0
Mass Moment of Inertia Y axis	1.2233 E-3 lb in sec^2	1.2233 E-3 lb in sec^2	0.0
Mass Moment of Inertia Z axis	0.24526 lb in sec^2	0.24526 lb in sec^2	0.0

AVE - 112 Weight, Center of Gravity and Mass Moment of Inertia Analysis of a Solid Sphere

Reference

Ellis, R., and Gulick, D., *Calculus with Analytic Geometry*, New York: HBJ, 1978.

Problem Description

A 1.0" radius solid sphere is analyzed for weight, center of gravity and mass moment of inertia. (This problem is the same as AVE - 40 where 2-D axisymmetric elements were used.)

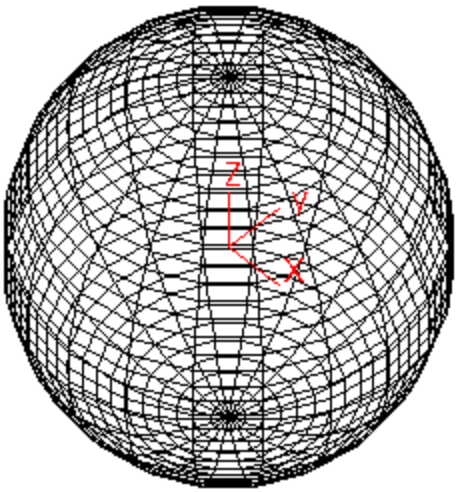

Figure 112-1. FEA model showing the surface mesh of the solid sphere.

Theoretical Solution

The mass moment of inertia equation for a solid sphere is given by the following:

$$I = \frac{8\rho\pi r^5}{15}$$

Where:

- r = 1.0" (sphere radius)
- ρ = 7.3395 E-4 lb s^2/in^4 (mass density)

Autodesk Simulation Solution

The solid sphere is modeled with 8000 brick elements. A weight, center of gravity and mass moment of inertia analysis is performed.

The errors are due to the lost volume inherent in representing a sphere by a polyhedral shape with vertices on the sphere surface. All volume between the flat surfaces and the sphere is missed. A finer surface mesh would reduce the error.

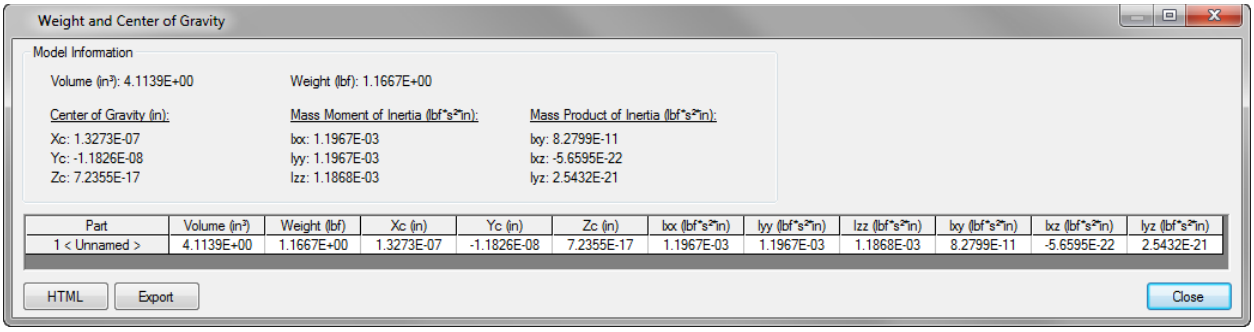

Figure 112-2. "Weight and Center of Gravity Calculation" screen.

Table 112-1. Comparison of Results

	Theory	Analysis	% Difference
Volume, V	4.189 in^3	4.114 in^3	1.79
Weight, W	1.1879 lb	1.1667 lb	1.78
X_c	0.00"	0.00"	0.0
Y_c	0.00"	0.00"	0.0
Z_c	0.00"	0.00"	0.0
Mass Moment of Inertia X axis	1.23 E-3 lb s^2 in	1.20 E-3 lb s^2 in	2.44
Mass Moment of Inertia Y axis	1.23 E-3 lb s^2 in	1.20 E-3 lb s^2 in	2.44
Mass Moment of Inertia Z axis	1.23 E-3 lb s^2 in	1.19 E-3 lb s^2 in	3.25

AVE - 113 Spherical Cap with Uniform Pressure

Reference

Timoshenko, S. P. and Woinowsky-Krieger, S., *Theory of Plates and Shells*, Second Edition, New York: McGraw-Hill, 1959.

Problem Description

This example involves a spherical cap with uniform pressure. (Refer to AVE - 104 for an alternate way of setting up this problem using the solid of revolution element.)

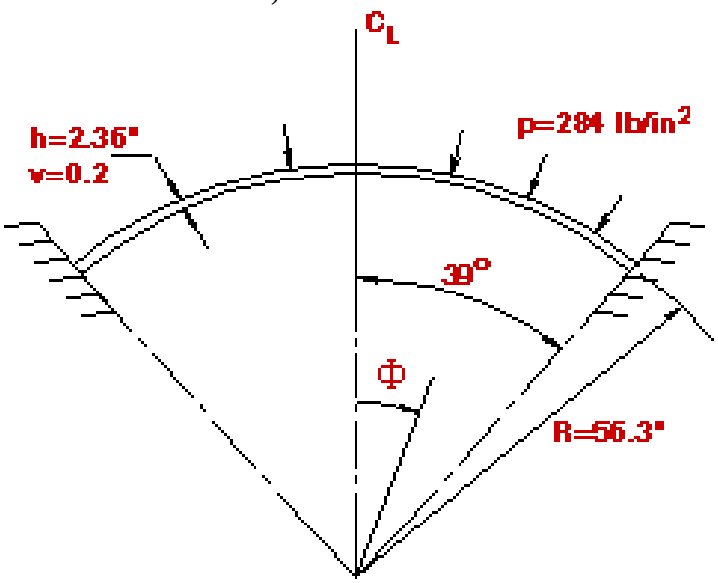

Figure 113-1. Cross section drawing of the spherical cap with a pressure load and boundary conditions.

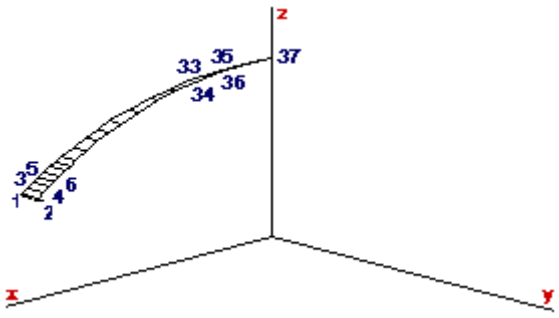

Figure 113-2. Five-degree wedge of the shell (used to perform the analysis).

Theoretical Solution

- E = 9.6 x 10^6 psi (modulus of elasticity)
- ν = 0.2 (Poisson's ratio)
- h = 2.36" (thickness)
- R = 56.3" (radius)
- p = 284 psi (applied pressure)

Autodesk Simulation Solution

This problem is modeled by a 5-degree wedge of the shell. The wedge of plate/shell elements is constrained by orthogonal degrees of freedom restrictions on one side and by two-node boundary elements on the other. Boundary elements are used to force radial displacements of the nodes and to set the appropriate rotations to zero. The coordinates are in the Cartesian system. Also, the element load case multipliers are used to apply the uniform pressure.

> **Note:** The apex element is a triangle. The triangular plate element is permitted, although the quadrilateral element is preferable, when possible.

The surface stresses, σ_θ (hoop) and σ_Φ (tangential), on the external and internal surfaces are shown in Figure 113-3. The values used to plot these curves are obtained from the Results environment by taking the S-tensor stress in the radial and tangential directions. The stress values shown are those produced by the analysis.

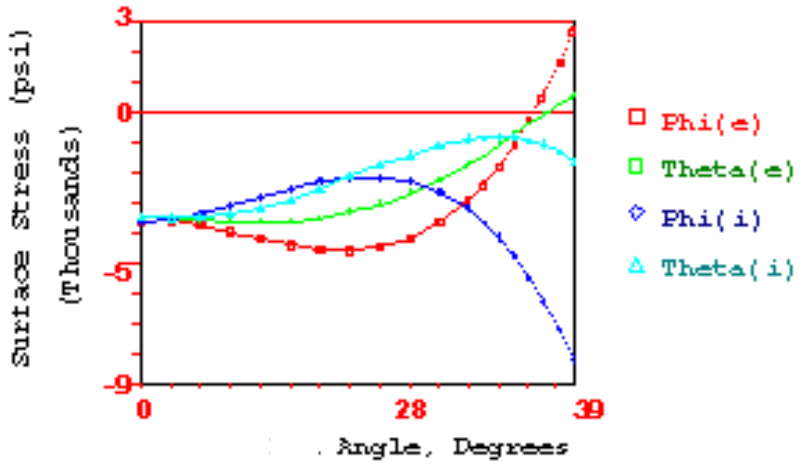

Figure 113-3. Surface stress distributions.

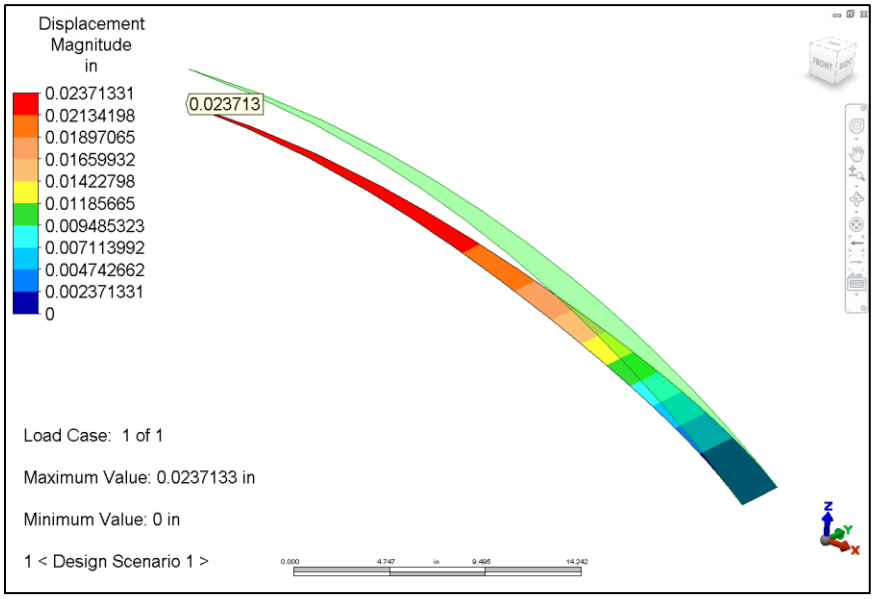

Figure 113-4. The deflected and undeflected shapes with a probe on the apex point.

AVE - 114 Equilateral Triangle with Linear Thermal Gradient

Reference

I. S. Tuba and W. B. Wright, ed., "ASME Pressure Vessel and Piping 1972 Computer Programs Verification", *ASME Publication I-24*, New York: The American Society of Mechanical Engineers, 1972.

J. L. Maulbetsch, "Thermal Stresses in Plates", *Journal of Applied Mechanics*, 2, June 1935.

Problem Description

This problem is a rare example of the application of temperature difference through thickness in plate element analysis. In this case, a triangular wing is modeled and a temperature gradient through the thickness is applied using the element load case multipliers. Find the deflections along the X axis.

Theoretical Solution

The following material data are used:

- $E = 10 \times 10^6$ psi (modulus of elasticity)
- $\nu = 0.3$ (Poisson's ratio)
- $a = 12 \times 10^{-6}/^oF$ (coefficient of thermal expansion)
- $T_1 - T_2 = 450\ ^oF$ (temperature difference)
- $t = 0.1$" (plate thickness)

All edges are simply supported.

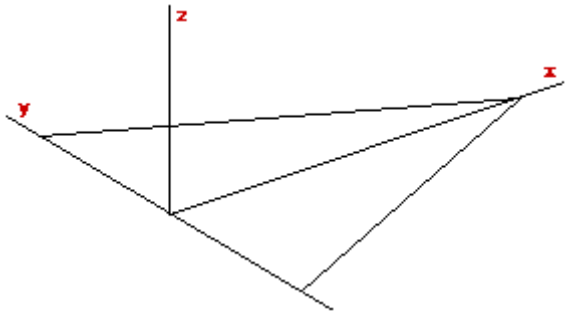

Figure 114-1. FEA model of the equilateral triangle.

The temperature gradient is:

$\delta T/\delta Z = 450/0.1 = 4500^oF/in$

Autodesk Simulation Solution

The deflections are given in the following table. (**Note:** the theoretical values shown are from Maulbetsch.)

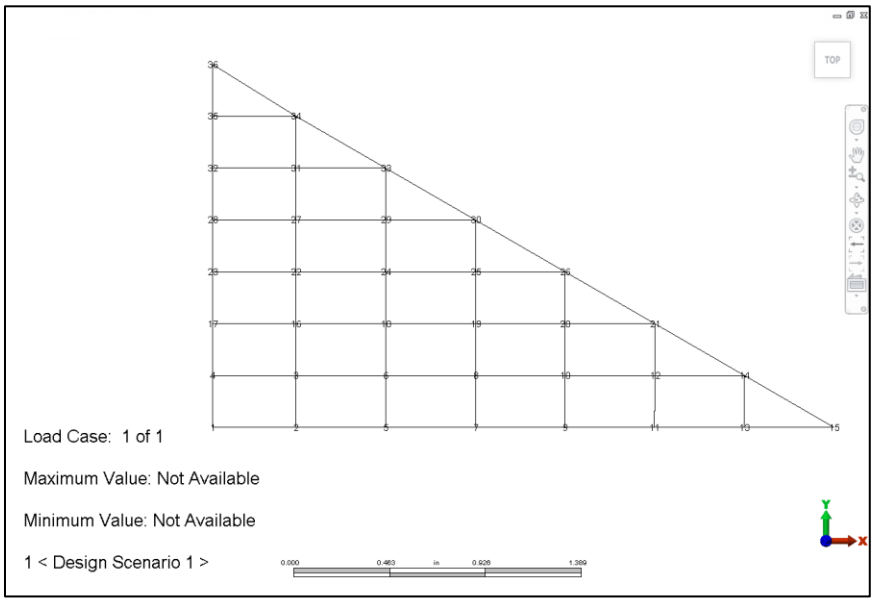

Figure 114-2. Node numbering scheme.

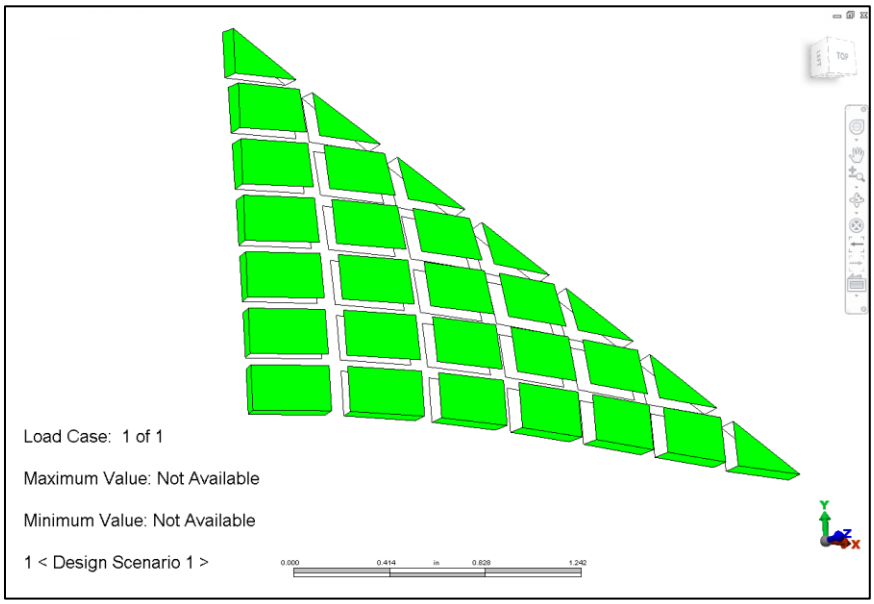

Figure 114-3. Deflected shape using the "Shrink" option

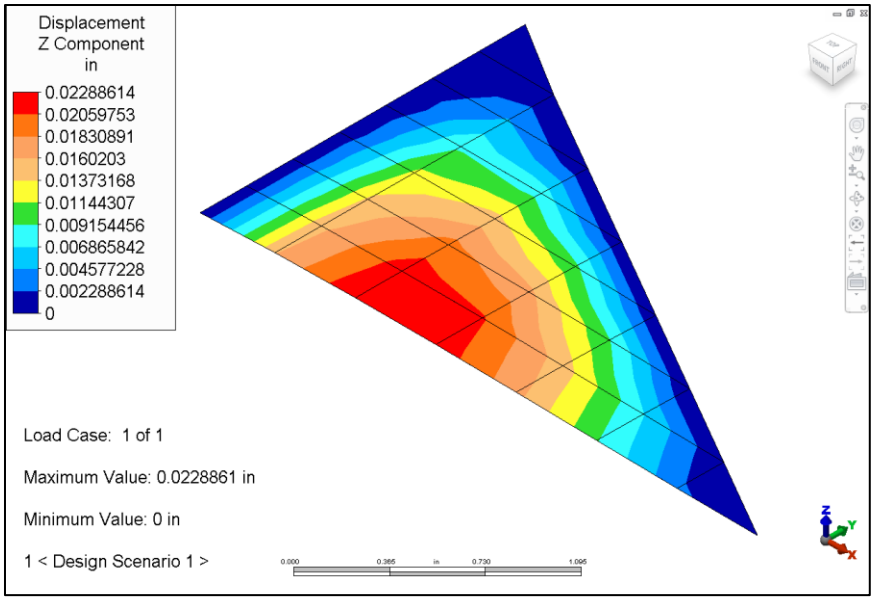

Figure 114-4. Z-Displacement contour.

Table 114-1. Z Deflection at Nodes along the X Axis

Node Number	X Coordinate	DZ Theoretical	DZ Analysis	% Difference
2	0.403	0.0159003	0.01589	0.06
5	0.836	0.0229002	0.02289	0.07
7	1.269	0.0222439	0.02223	0.06
9	1.702	0.0167751	0.01678	0.03
11	2.134	0.0093451	0.009336	0.10
13	2.567	0.0028036	0.002832	1.01

AVE - 115 Simply Supported Anisotropic Plate

Reference

Timoshenko, S. P. and Woinowsky-Krieger, S., *Theory of Plates and Shells*, Second Edition, New York: McGraw-Hill, 1959.

Problem Description

This example involves a simply supported plate with anisotropic material properties. This example demonstrates the capabilities of the software to engineers who are interested in the elasticity matrix. In this problem there is a flat plate with simple supports and a uniform pressure applied perpendicular to the surface. Results are compared with the Timoshenko method. Also, this example shows the use of orthogonal boundary conditions to model with quarter symmetry.

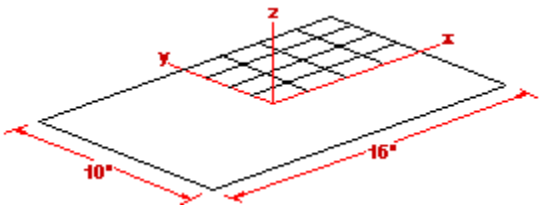

Figure 115-1. FEA model of the simply supported plate (dimensions shown).

Theoretical Solution

Using Timoshenko's notation:

$E_1 = 1.87 \times 10^6$ psi
$E_2 = 0.6 \times 10^6$ psi
$E_{12} = 0.073 \times 10^6$ psi
$G = 0.159 \times 10^6$ psi
h = 0.5" (plate thickness)
p = 5 psi (applied pressure)

Timoshenko's elasticity constants become:

$C_{xx} = E_1 = 1.87 \times 10^6$psi
$C_{yy} = E_2 = 0.6 \times 10^6$psi
$C_{xy} = E_{12} = 0.073 \times 10^6$psi
$G_{xy} = G = 0.159 \times 10^6$psi

Autodesk Simulation Solution

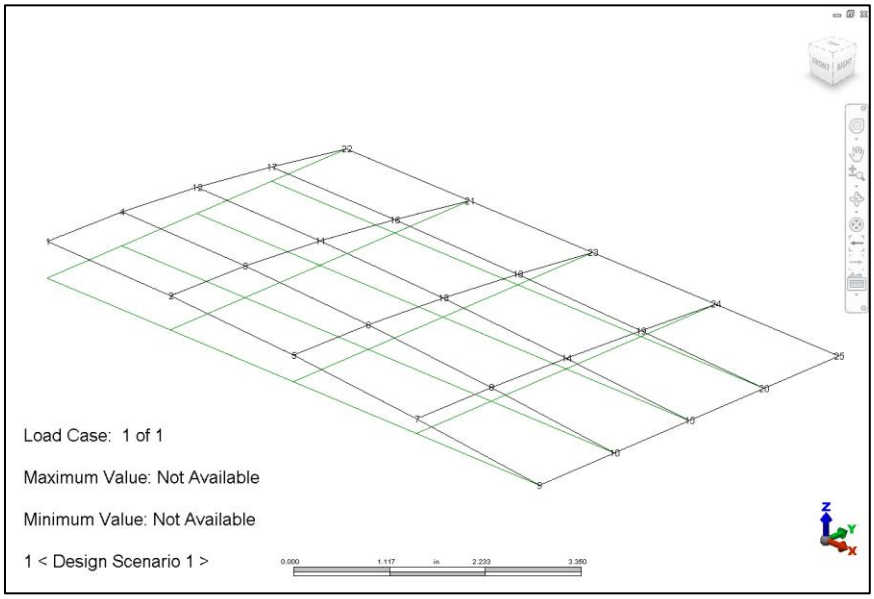

Figure 115-2. Deflected shape superimposed on original model.

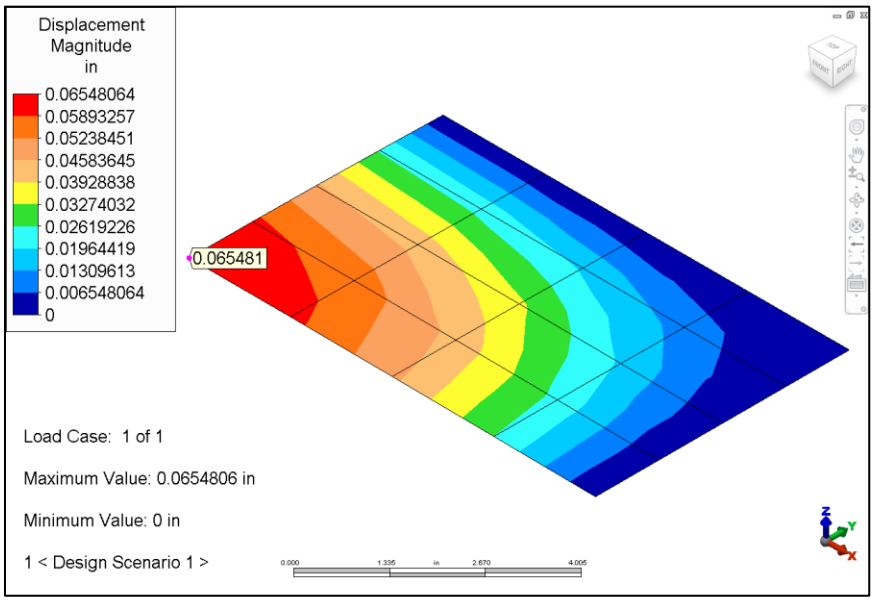

Figure 115-3. Inquiring on the deflection result at a node.

Table 115-1. Comparison of Results

Node	x	y	DZ Theoretical	DZ Analysis	% Difference
1	0	0	0.065654	0.06548	0.27
2	2	0	0.061151	0.06088	0.44
5	4	0	0.047717	0.04737	0.73
7	6	0	0.026319	0.02614	0.68

AVE - 116 Rectangular Plate with All Edges Clamped

Reference

Timoshenko, S. P. and Woinowsky-Krieger, S., *Theory of Plates and Shells*, Second Edition, New York: McGraw-Hill, 1959.

Problem Description

A square plate with all of its edges clamped is subjected to a uniform pressure load normal to the plate. Various mesh densities are used, and the resulting maximum deflection is compared to that predicted by the Timoshenko method. This example shows the reliability of the plate/shell element in bending analysis.

A 0.1" thick square plate with clamped edges is subjected to a uniform pressure.

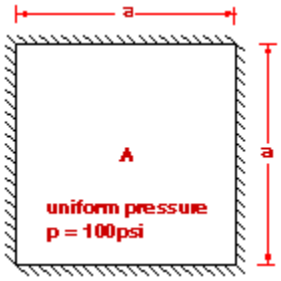

Figure 116-1. The rectangular plate with loading and boundary conditions.

Theoretical Solution

a = 10" (edge length)
p = 100 psi (applied pressure)
t = 0.1" (plate thickness)
E = 300.0 x 10^6 psi (modulus of elasticity)
ν = 0.3 (Poisson's ratio)

Timoshenko predicts deflection at the plate's center to be the following:

$\Delta = 0.00126\ pa^4/D$

Where:

$D = [Et^3] / [12\ (1-\nu^2)] = 27472.53$

Therefore:

Δ = 4.5864E-2

Autodesk Simulation Solution

This problem was analyzed using various mesh densities. The resulting maximum deflection occurring at point A is compared to the theoretical result predicted by Timoshenko.

Based on the symmetrical nature of the example, only 1/4 of the problem needs to be modeled. Figure 116-2 shows the 1/4 model.

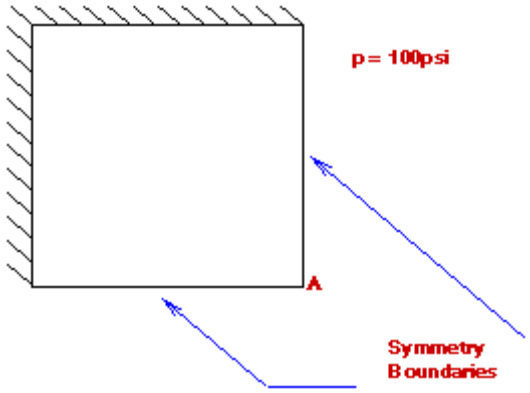

Figure 116-2. FEA model of the plate using symmetric boundary conditions.

Full models were used for the first two design scenarios. Quarter models were used for the third and fourth design scenarios.

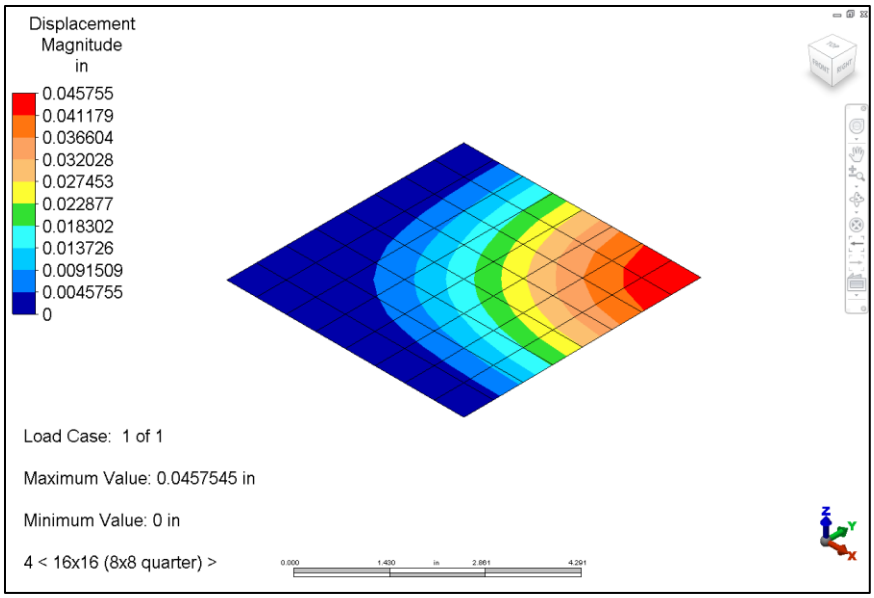

Figure 116-3. Displacement results in the 8x8 quarter simulation model.

The following table shows the maximum deflection calculated for various mesh densities, and the percent error when compared to Timoshenko.

Table 116-1. Comparison of Results

Design Scenario	Mesh Density	Number of Elements	Maximum Deflection	Theoretical Result	% Difference
1	4x4 (full)	16	4.2426E-2	4.5864E-2	7.5
2	8x8 (full)	64	4.4853E-2	4.5864E-2	2.2
3	12x12 (6x6 quarter)	36	4.5515E-2	4.5864E-2	0.76
4	16x16 (8x8 quarter)	64	4.5755E-2	4.5864E-2	0.24

AVE - 117 Linear Mode Shape Analysis with Load Stiffening, Simply Supported Beam

Reference

Timoshenko, S., Weaver, W. and Young, D. H., *Vibration Problems in Engineering*, New York: Wiley, 1974.

Problem Description

This beam load stiffening problem models a 0.25" x 12" x 96" steel beam which is simply supported under compressive axial loading. This example verifies the accuracy of the Linear Mode Shapes and Natural Frequencies Analysis with Load Stiffening processor for plate elements.

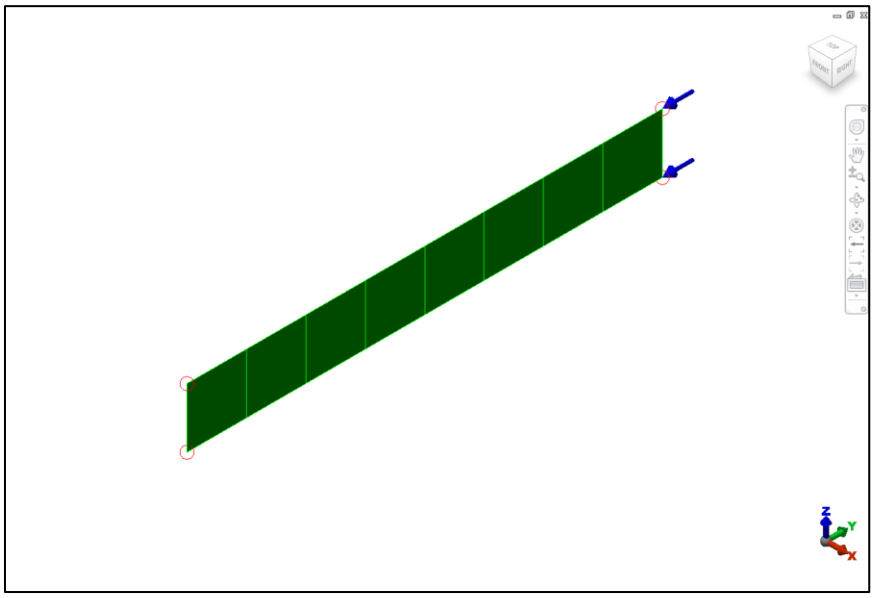

Figure 117-1. FEA model for the beam with nodal boundary conditions.

Theoretical Solution

The beam theory frequency equation is given by the following:

$$\omega_1 = \frac{i^2\pi^2}{l^2}\sqrt{\frac{EI}{\rho A}\left(1 \pm \frac{Sl^2}{i^2 EI\pi^2}\right)}$$

Where:

- i = (1,2,3 ...) for different mode shapes,
- l = 96" (length of the beam)
- E = 30E6 psi (modulus of elasticity),
- I = $bh^3/12$ in^4 (area moment of inertia)
- ρ = 7.34E-4 lb s^2/in^4 (Mass density)
- A = 3 in^2 (cross sectional area)
- S = 15 lb (axial load)
- +/- = Denotes tensile or compressive load respectively

Autodesk Simulation Solution

The beam is modeled with 8 plate elements. Appropriate translational and rotational nodal boundary conditions are used at the ends to constrain the beam.

The beam element load stiffening problem models a 0.25" x 12" x 96" steel beam which is simply supported under compressive axial loading of 15 lb. This load is about 3% of the buckling load for this model and lowers the lowest frequency about 1.5%. Results below show good agreement. Higher modes are affected less, though the model has a rather coarse mesh for the higher modes as it has only 8 plate elements. Modes 3 and 5 are torsional modes, which are not covered by the simple beam theory formula shown above.

The following table gives both the theoretical and computed frequencies for different mode shapes. (Results show comparative frequencies obtained for different mode shapes as obtained using the software and the theoretical solutions using the FORTRAN program developed from the reference.)

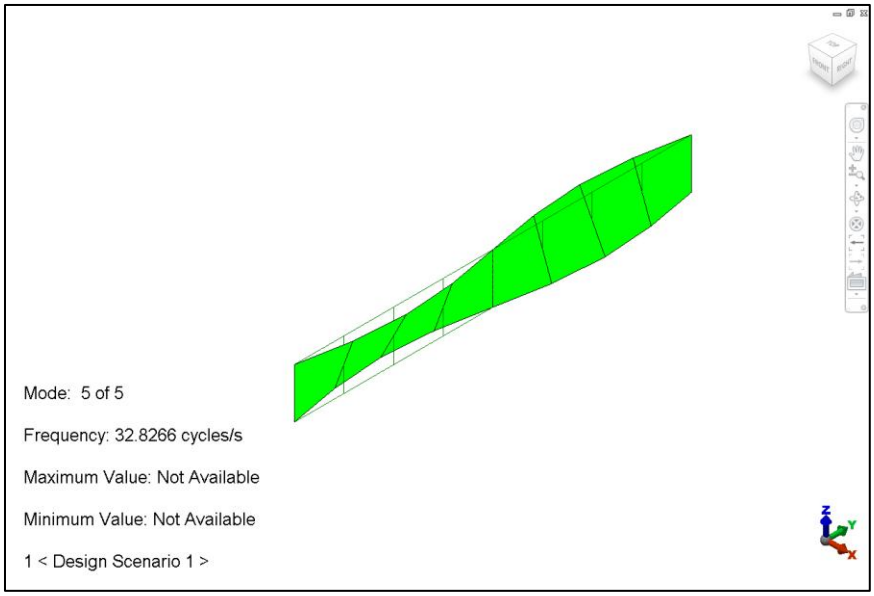

Figure 117-2. Mode shape and frequency for mode 5.

Table 117-1. Comparison of Results

Mode Number	Mode	Frequency (Hz)		% Difference
		Theory	Analysis	
1	weak 1	2.4494	2.4456	-0.16
2	weak 2	9.910	9.838	-0.72
3	-	-	15.91	-
4	weak 3	22.34	21.93	-1.84
5	-	-	32.83	-

AVE - 118 Thin-walled Cylinder with a Uniform Axial Load

Reference

Roark, R. J. and Young, W. C., *Roark's Formulas for Stress and Strain*, Fifth Edition, New York: McGraw-Hill, 1975.

Problem Description

This example is taken from formulas for membrane stresses and deformations in thin-walled pressure vessels. It is a thin-walled cylinder with a uniform axial loading, which is analyzed for axial stress and deflection. This example is the same as AVE - 3 where membrane elements were used.

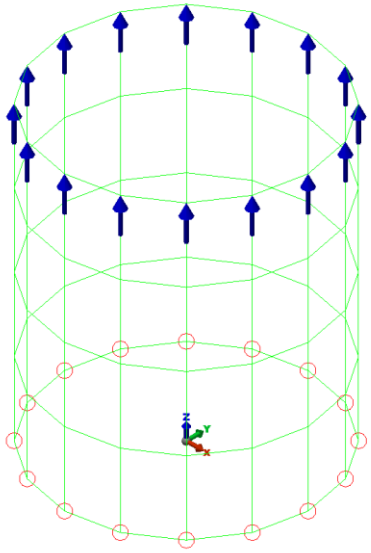

Figure 118-1. FEA model of the cylinder with loading and boundary conditions.

Theoretical Solution

For this example the following values are used:

- p = 1000 lb/in (uniform axial load)
- t = 0.1" (cylinder thickness)
- E = 30E6 lb/in^2 (Young's Modulus)
- L = 12" (half length of cylinder)
- r = 5" (cylinder radius)
- σ_1 = p/t = 1000 / 0.1 = 10000 psi
- Δ_z = pz/Et = (1000 *12) / 30E6 * 0.1 = 0.004 in

Autodesk Simulation Solution

The cylinder is modeled in FEA Editor as a cylindrical surface with a radius of 5" and length of 12". There are 4 elements along the length of the cylinder and 15 elements around the circumference. The cylinder is fully fixed at the base and the axial force applied as linear point loads at each of the nodes at the free end. The nodal loads are calculated as

Total load = 1000 lb/in * 2 * π * 5 = 31415.93 lb
F/node = 31415.93 / 15 = 2094.4 lb

The model is constructed using plate elements and with E and t as stated above. The stress result below is the Z direction plate membrane stress from the Results environment.

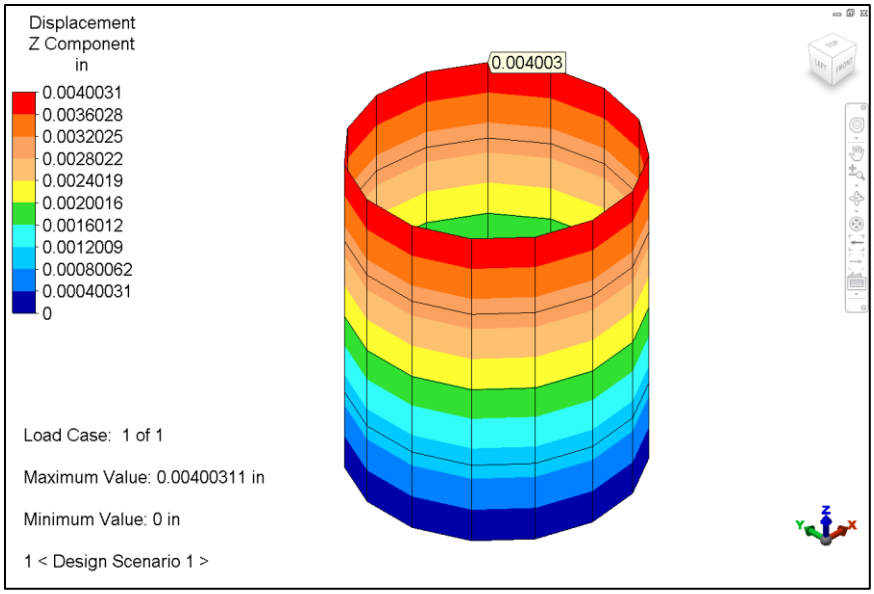

Figure 118-2. Inquiring on the Z displacement result at a node.

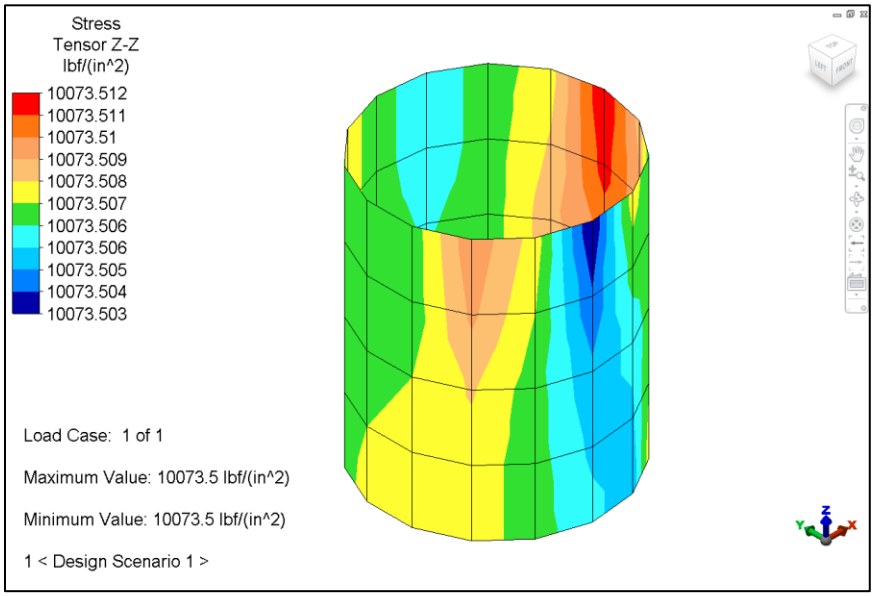

Figure 118-3. Stress tensor display of Z-direction. plate membrane stress option is activated.

Table 118-1. Comparison of Results

	Theory	Analysis	% Difference
z (in)	0.004000	0.004003	0.07
l (psi)	10000.0	10073.5	0.74

AVE - 119 Thick-walled Cylinder under Centrifugal and Pressure Loading

Reference

Tuba, I. S., and Wright, W. B., ed. "ASME Pressure Vessel and Piping 1972 Computer Programs Verification", *ASME Publication I-24*, New York: The American Society of Mechanical Engineers, 1972.

Timoshenko, S. P., *Strength of Materials*, Third Edition, New York: Van Nostrand, 1955.

Problem Description

This verification example is a thick-walled cylinder with pressure and centrifugal force applied as two separate load cases modeled using tetrahedral elements.

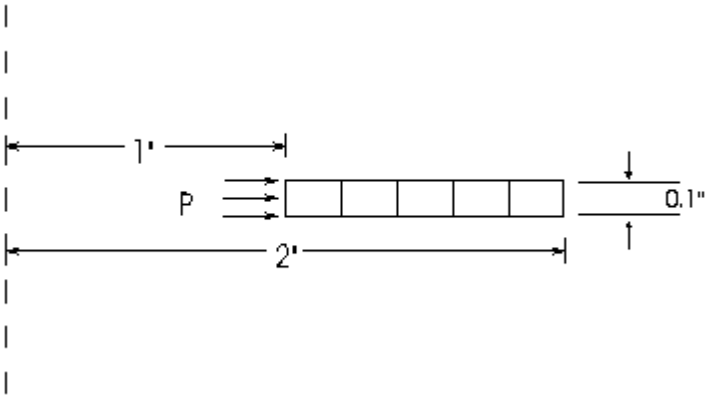

Figure 119-1. FEA model of the cylinder with pressure loading.

Theoretical Solution

- $E = 30 \times 10^6$ psi
- $\nu = 0.3$
- $\rho = 0.286$ lb/in^3 (weight density)
- Structure Load Case 1: (centrifugal force) = 100 rad/sec
- Structure Load Case 2: p = 3000 psi

Autodesk Simulation Solution

This problem is the same as AVE - 109, which was modeled using brick elements. To generate the FEA model for this problem, A quarter symmetry model was generated using Autodesk Fusion and the model was meshed in Autodesk Simulation with an absolute mesh size of 0.1 in and a "All tetrahedral" mesh type was used. 2nd order elements were generated and midside nodes were activated. Symmetry boundary conditions wer applied to the cut planes.

Load Case One was assigned a multiplier of 1 for the Pressure load, whereas Load Case Two was assigned a multiplier of 1 for "Angular rotation" load.

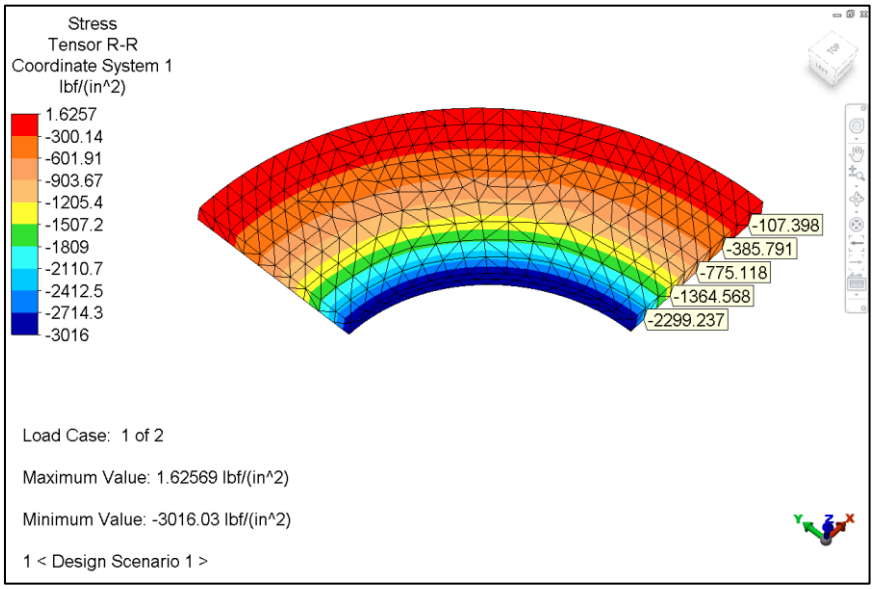

Figure 119-2. Inquiring on radial stress results at a node for Load Case 1.

Table 119-1. Comparison of Results – Pressure Loading

Radius	σ_r (σ_{22})			σ_{theta} (σ_{11})		
	Theory	Analysis	% Difference	Theory	Analysis	% Difference
1.1	-2305.79	-2299.24	0.28	4305.79	4299.187	0.15
1.3	-1366.86	-1364.57	0.17	3366.86	3366.20	0.02
1.5	-777.778	-775.12	0.34	2777.78	2775.386	0.09
1.7	-384.083	-385.79	0.44	2384.08	2385.367	0.05
1.9	-108.033	-107.398	0.59	2108.03	2107.114	0.04

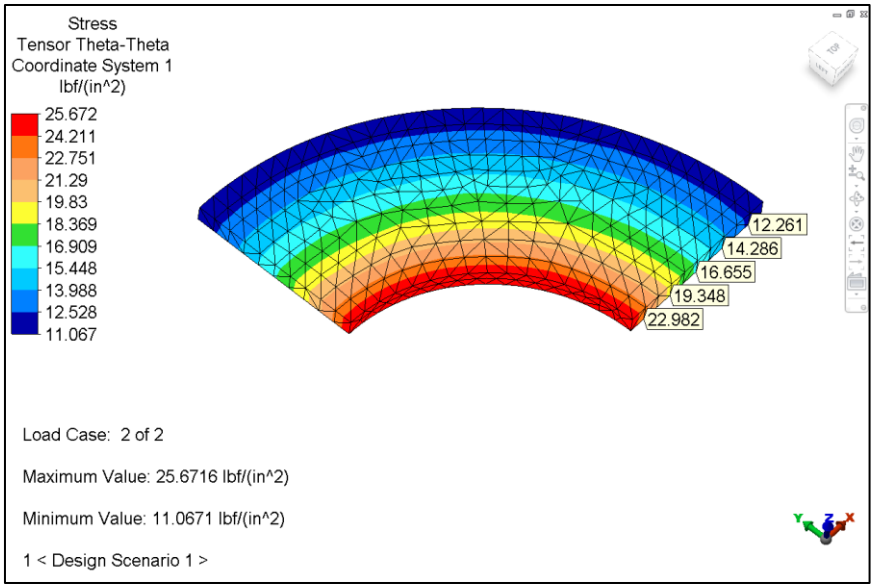

Figure 119-3. Inquiring on tangential stress results at a node for load case 2.

Table 119-2. Comparison of Results – Centrifugal Force

Radius	σ_r (σ_{22})			σ_{theta} (σ_{11})		
	Theory	**Analysis**	**% Difference**	**Theory**	**Analysis**	**% Difference**
1.1	1.47993	1.469	0.74	23.2561	22.982	1.18
1.3	2.88255	2.919	1.26	19.5418	19.348	0.99
1.5	2.97145	3.065	3.15	16.7559	16.655	0.60
1.7	2.21865	2.058	7.24	14.4264	14.286	0.97
1.9	0.861789	0.881	2.23	12.3157	12.261	0.44

AVE - 120 Weight, Center of Gravity and Mass Moment of Inertia Analysis of a Solid Sphere

Reference

Ellis, R. and Gulick, D., *Calculus with Analytic Geometry*, New York: HBJ, 1978.

Problem Description

This example involves a weight, center of gravity and mass moment of inertia analysis of a solid spherical model using tetrahedral elements. This example verifies the accuracy of the Mass Properties Analysis Processor for tetrahedral elements.

A 1.0" radius solid sphere is analyzed for weight, center of gravity and mass moment of inertia. This problem is the same as AVE - 40 where 2-D axisymmetric elements were used.

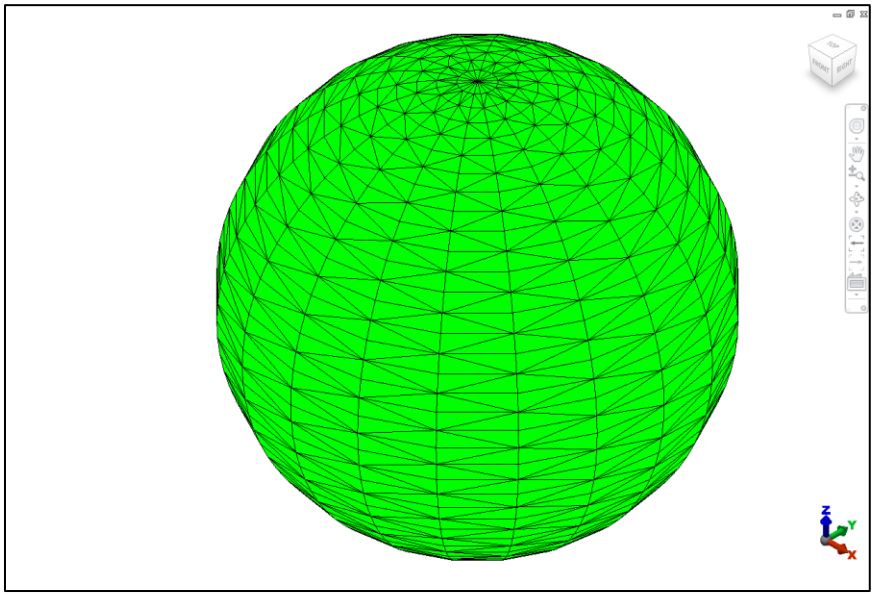

Figure 120-1. FEA model of the solid sphere.

Theoretical Solution

The mass moment of inertia equation for a solid sphere is given by the following:

$I = 8\rho\pi r^5 / 15$

Where:

- r = 1.0" (sphere radius)
- ρ = 7.3395 E-4 lb s^2/in^4 (mass density)

Autodesk Simulation Solution

The solid sphere is modeled with 17,572 10-node tetrahedral elements. In FEA Editor, the "Analysis : Weight and Center of Gravity…" command was used to access the capability for analyzing the weight, center of gravity and mass moment of inertia.

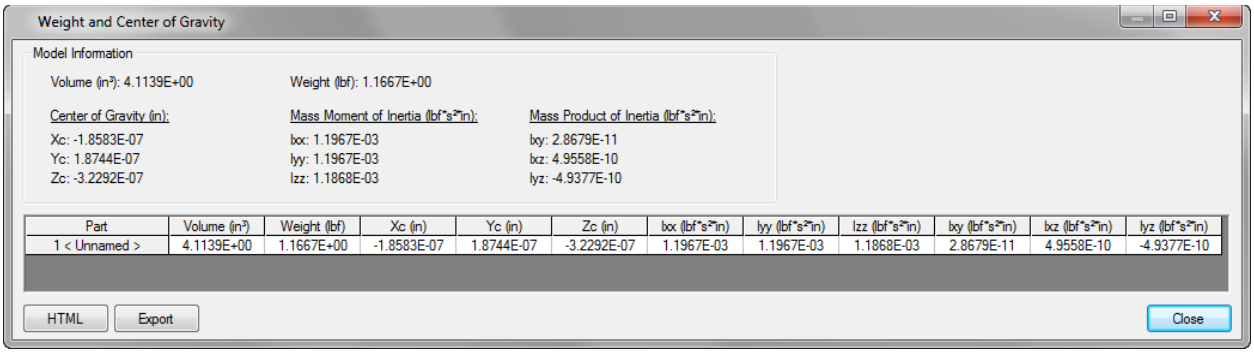

Figure 120-2. The "Weight and Center of Gravity Calculation" window.

Table 120-1. Comparison of Results

	Theory	Analysis	% Difference
Volume, V	4.19 in^3	4.1139 in^3	-1.8
Weight, W	1.1883 lb	1.1667 lb	-1.8
X_c	0.00"	-2.E-7"	0.0
Y_c	0.00"	2E-7"	0.0
Z_c	0.00"	-3E-7"	0.0
Mass Moment of Inertia X axis	1.23 E-3 lb s^2 in	1.1967 E-3 lb s^2 in	-2.7
Mass Moment of Inertia Y axis	1.23 E-3 lb s^2 in	1.1967 E-3 lb s^2 in	-2.7
Mass Moment of Inertia Z axis	1.23 E-3 lb s^2 in	1.1868 E-3 lb s^2 in	-3.5

The errors are due to the lost volume inherent in representing a sphere by a polyhedral shape with vertices on the sphere surface. All volume between the flat surfaces and the sphere is missed. A finer surface mesh would reduce the error.

AVE - 121 Two Cantilever Beams Connected by a Tension-Only Element at the Tip

Reference

Roark, R. J. and Young, W. C., *Roark's Formulas for Stress and Strain*, Fifth Edition, New York: McGraw-Hill, 1975.

Problem Description

Two 100" long cantilever beams connected by a 1" long tension-only cable at the free ends are subjected to a concentrated load of 10 lb at 20" from the tip. A tension-only gap element is used to find the tip deflection.

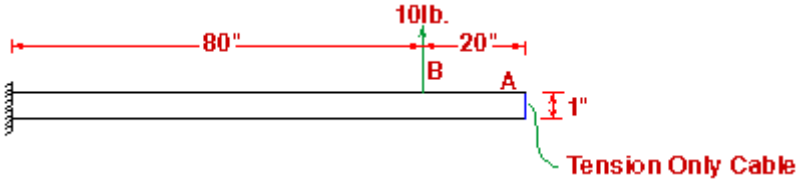

Figure 121-1. FEA model of the coupled cantilever beam with a tension-only gap element at the tip.

Theoretical Solution

The material properties for the beams are the following:

- E = 1.0 * 10^6psi (modulus of elasticity)
- ν = 0.1 (Poisson's ratio)
- Area = 1 in^2
- Iy = Iz = 1.0 in^4
- Sy = Sz = 0.2 in^3 (S = section modulus)

Find the displacements at points A and B.

The analytical solution can be found as follows: The deflections at points A and B due to a unit load at point B are the following:

$$dBB = \frac{P \times L1^3}{3 \times E \times I} = \frac{10 \times 80^3}{3 \times 1.0\,E6 \times 1.0} = 0.170667"$$

$$dAB = dBB + \frac{20.0 \times P \times L1^2}{2 \times E \times I} = 0.170667 + \frac{20.0 \times 10 \times 80^2}{2 \times 1.0\,E6 \times 1.0} = 0.234667"$$

$$dAA = \frac{P \times L^3}{3 \times E \times I} = \frac{10 \times 100^3}{3 \times 1.0\,E6 \times 1.0} = 0.333333"$$

dBA = dAB = -/234667"

The global stiffness matrix for points A and B is given as the following:

$$K = \begin{bmatrix} dBB & dBA \\ dAB & dAA \end{bmatrix}^{-1} = \begin{bmatrix} 0.17667 & 0.234667 \\ 0.234667 & 0.333333 \end{bmatrix}^{-1} = \begin{bmatrix} 183.120 & -128.917 \\ -128.917 & 93.758 \end{bmatrix}$$

After the gap element is activated, the stiffness contributed from the bottom beam is:

$$kAA = \frac{3 \times E \times l}{L^3} = \frac{3 \times 1.0\,E\,6 \times 1.0}{100^3} = 3.0 \text{ lb/in}$$

This needs to be added to the global stiffness matrix.

Therefore, the final solution is given as:

$$\begin{bmatrix} uB \\ uA \end{bmatrix} = \begin{bmatrix} 183.120 & -128.917 \\ -128.917 & 96.758 \end{bmatrix}^{-1} \begin{bmatrix} 10.0 \\ 0.0 \end{bmatrix} = \begin{bmatrix} 0.88065" \\ 1.17334" \end{bmatrix}$$

The reaction in the gap element is:

R = 3.0 * 1.17334 = 3.520 lb

Autodesk Simulation Solution

One tension gap element (zero gap) was used to model the tension-only element at the tip. Stiffness value of 1.0E7 lb/in was used for the gap element.

The results are:

- uB = 0.8806"
- uA = 1.1733"
- R = 3.520 lb

which match the analytical answer.

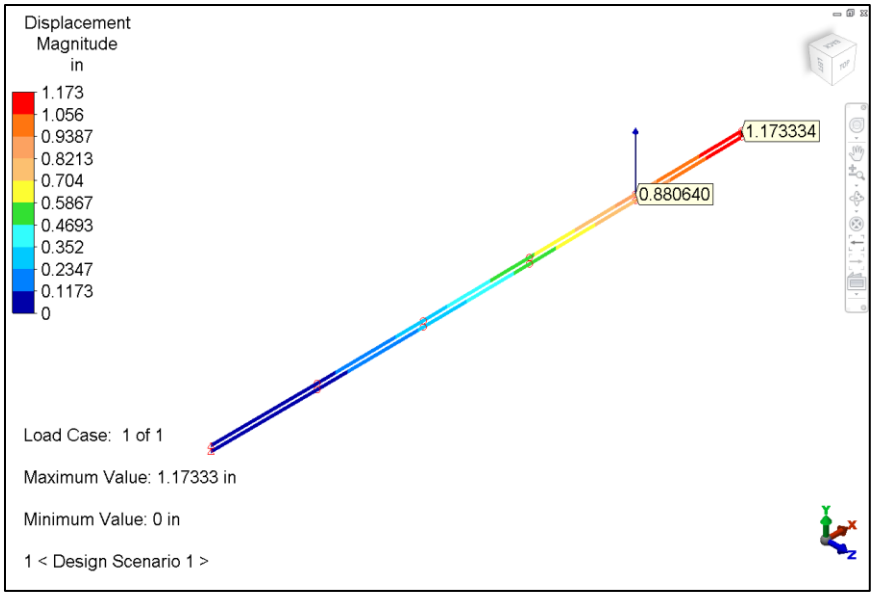

Figure 121-2. Inquiring on displacement results at point A and B.

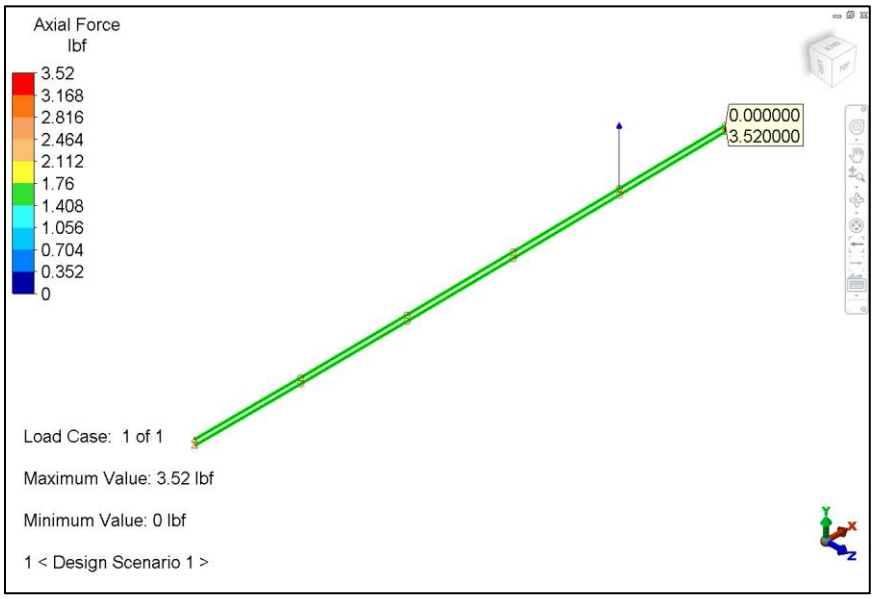

Figure 121-3. Displaying the reaction forces in the gap element.

Table 121-1. Comparison of Results

	Theory	Analysis	% Difference
uB (in)	0.88065	0.8806	0.0
uA (in)	1.17334	1.1733	0.0
R (lb)	3.520	3.520	0.0

AVE - 122 L-Shaped Pipe System Subjected to Temperature Load

Reference

No theoretical reference is needed for this problem.

Problem Description

An L-shaped pipe system with a 6.625" diameter and 0.280" wall thickness is subjected to a uniformly distributed load of 15 lb/in, a temperature increase of 120 ^{o}F, and gravity. Due to the interaction of the gravity, temperature load, and the uniformly distributed load, only a portion of the pipe contacts the support. Ten zero-gap compression-only gap elements are used to find the reactions.

This problem is modeled in two different ways: using beam and gap elements (Design Scenario 1) and using only beam elements (Design Scenario 2).

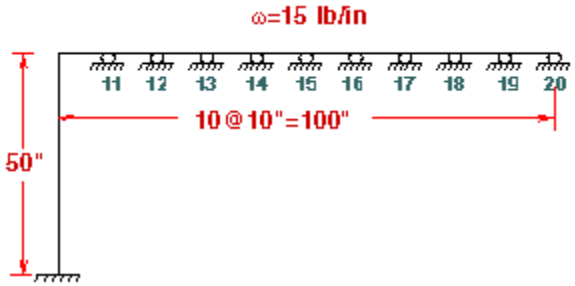

Figure 122-1. FEA model of the pipe system with gap elements and boundary conditions.

Theoretical Solution

The material properties for the pipe are:

- E = 30.0 * 10^{6} psi (modulus of elasticity)
- Thermal Expansion Coeff. = 6.5 * 10^{-6} / °F
- Area = 5.58 in^{2}
- $I_y = I_z$ = 28.1 in^{4}
- $S_y = S_z$ = 8.50 in^{3} (S = section modulus)

Find the reactions on the top support.

Autodesk Simulation Solution

For Linear Static Stress Analysis, 10 zero-gap compression elements are used. The pipe system was modeled by the beam element. Gravity and a uniformly distributed load on the horizontal beam elements were applied to give a downward deflection which was countered by growth due to thermal expansion.

The results show that only the last two gap elements, 9 and 10, are in action, ending up open for gap elements 1 to 8 (i.e., no contact).

A separate run (Design Scenario 2) using two boundary elements at the corresponding locations was performed.

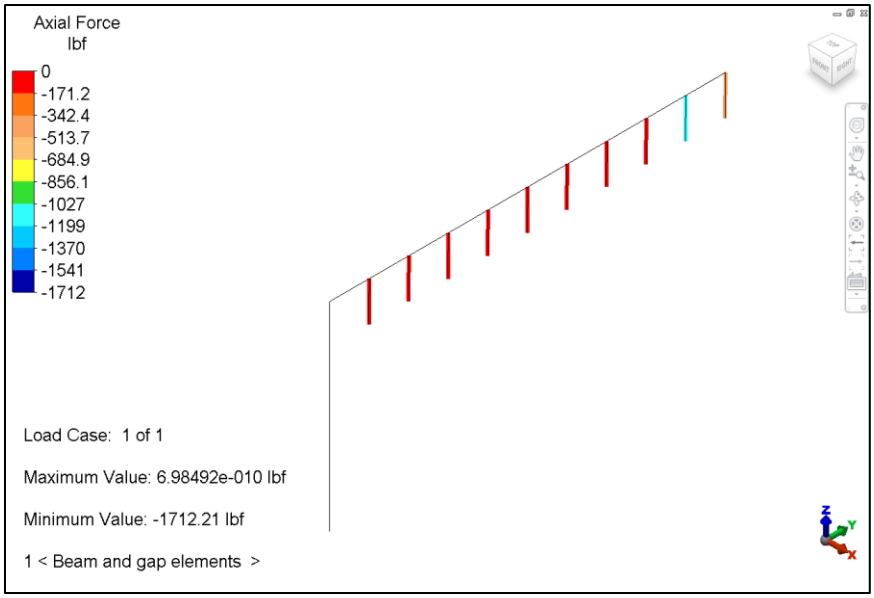

Figure 122-2. Axial forces for the gap and beam element model.

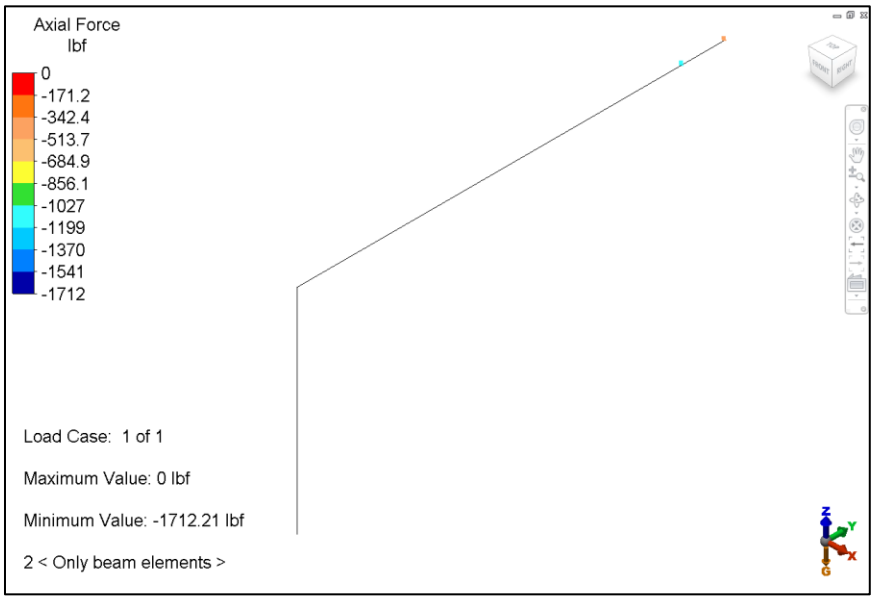

Figure 122-3. Axial forces for the all beam element model.

Table 122-1. Comparison of Results

Support Location	10 Gap Elements	2 Boundary Elements
11-18	0.0	---
19	-1065.0 lb	-1065.0 lb
20	-414.14 lb	-414.14 lb

AVE - 123 An Internally Pressurized Cylinder

Reference

Roark, R. J. and Young, W. C., *Roark's Formulas for Stress and Strain*, Fifth Edition, New York: McGraw-Hill, 1975.

Problem Description

This model represents a sector of an internally pressurized cylinder. The cylinder is free to expand along its axis. All rotations are fixed as the expected results are only radial and axial displacements. Find the radial displacement and hoop stress.

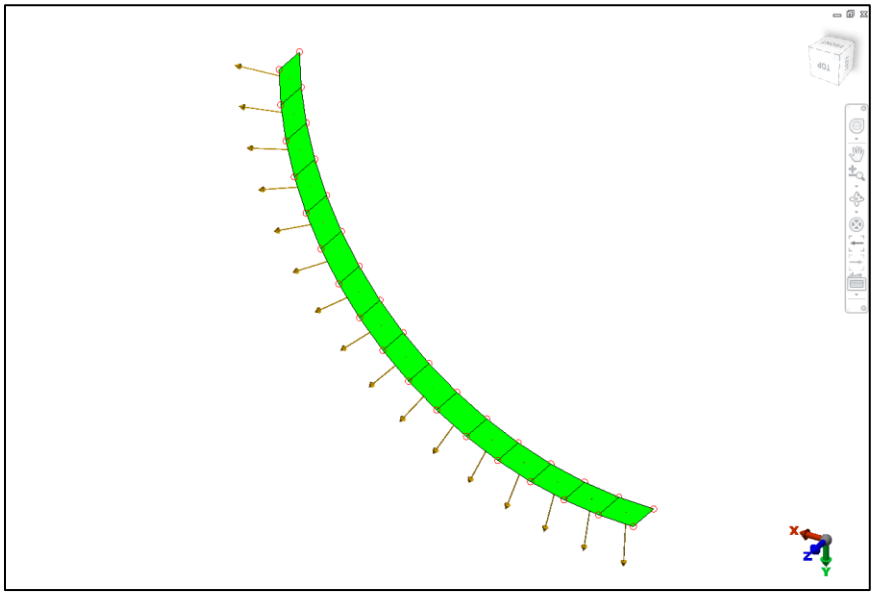

Figure 123-1. FEA model of the sector of the composite shell cylinder.

Theoretical Solution

P = 1000 psi (applied pressure)
t = 0.01" (wall thickness)
l = 1.0" (cylinder length)
R = 10.0" (cylinder radius)
E = 30.0 x 10^6 psi (modulus of elasticity)

Hoop Stress (for thin walled cylinders)
= Pressure * (Radius / Thickness)
= 1000 (10 / 0.1)
= 100,000 psi

Strain = Stress / Modulus
= 100,000 / 30E6
= 0.0033333

Radial Displacement
= Radius * Strain
= 10 * 0.0033333
= 0.033333"

Autodesk Simulation Solution

A sector of an internally pressurized cylinder is modeled using both thin and thick composite elements. Three different mesh densities are considered. The first used 4 elements; the second used 8, and the third used 16. (The supplied archive file represents the 1 x 16 mesh for the thin composite elements.)

The following table shows good agreement between the analysis and the theoretical results. Also, as the mesh is refined, the analysis results approach the theoretical values. This shows convergence of the results with increasing mesh density.

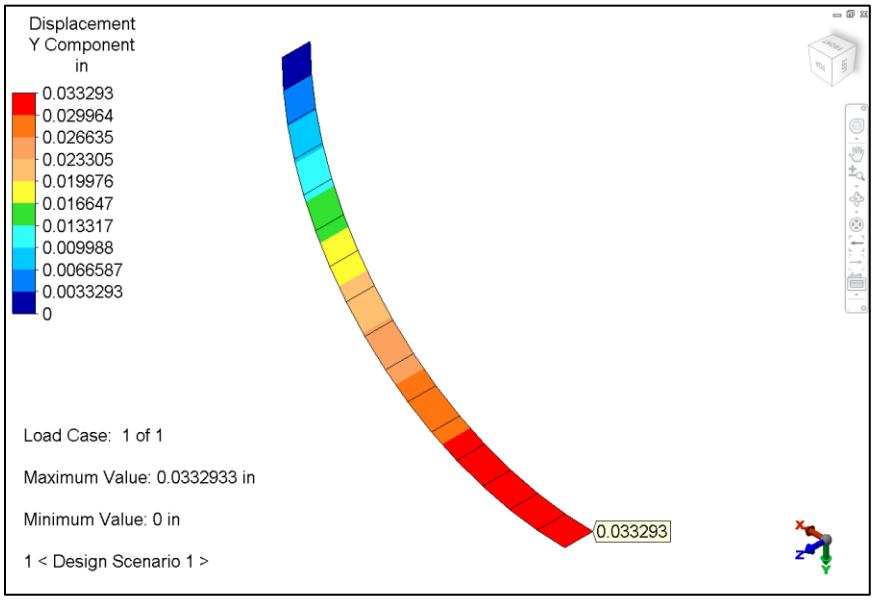

Figure 123-2. Inquiring on the Y displacement results at a node for the 1 x 16 mesh of thin composite elements.

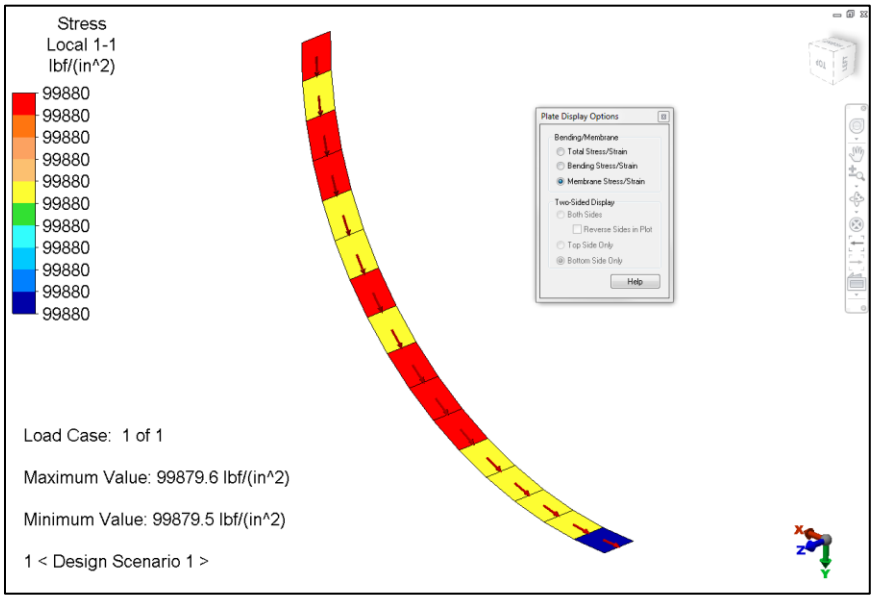

Figure 123-3. Hoop stress results for the 1 x 16 mesh of thin composite elements.

In Figure 123-3 the result contour is presented in the Local Coordinate system. “Plate Display Option : Membrane Stress/Strain” and “Element Orientation : Element Axis 1” are activated.

Table 123-1. Comparison of Results

Element Type	Mesh density	Radial Displacement (in)	% Difference	Stress (psi)	% Difference
Thin Composite	1 x 4 Mesh	0.0327	1.90	98,085.1	1.91
	1 x 8 Mesh	0.03317	0.49	99,508.3	0.49
	1 x 16 Mesh	0.033293	0.12	99,879.6	0.12
Thick Composite	1 x 4 Mesh	0.03269	1.93	98,078.6	1.92
	1 x 8 Mesh	0.03317	0.49	99,518.5	0.48
	1 x 16 Mesh	0.033293	0.12	99,879.6	0.12

AVE - 124 Simply Supported Square Laminate Subjected to a Uniform Pressure Load

Reference

Noor, A. K. and Mathers, M. D., "Shear Flexible Finite Element Models of Laminated Composite Plates and Shells", *NASA TN D-8044*, 1975.

Problem Description

A simply supported square laminate ($T_{xy}R_z$) (10" x 10") is subjected to a uniform lateral pressure. The laminate material is comprised of 9 different lamina (layers). Due to model symmetry, a quarter sector was modeled with symmetric boundary conditions.

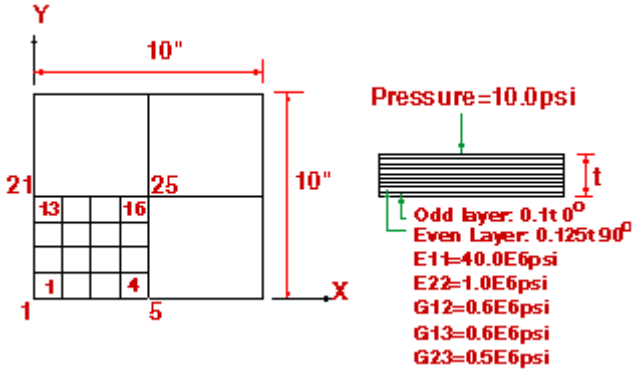

Figure 124-1. Quarter symmetric FEA model of the composite laminate plate.

Find the central laminate maximum deflection.

Autodesk Simulation Solution

This problem is modeled both as thin and thick composite elements. Two different laminate thicknesses and three different mesh densities are considered.

The model was analyzed with three different grid refinements and two thicknesses. The grid refinements were 1 x 1, 2 x 2, and 4 x 4 element meshes. The plate thicknesses used were 0.01" and 0.1". Both the thin and thick composite elements were used to model the plate.

The supplied model archive file represents the 4 x 4 mesh for the thin composite elements of 0.01" thickness with 10 psi applied over a model area of 25 square inches. This is a linear small deformation analysis, though the numbers call for a large deformation non-linear analysis. However, even though the calculated displacement is hundreds of inches and the stress is about 9 million psi, the small deformation analysis result can be reasonably checked against small deformation theory, since both are completely scalable with respect to loading. If the pressure were reduced by a factor of 1.0E-4 to 0.001 psi, the displacement and stress would be reduced by exactly the same factor. That would be a more appropriate size of load to be supported by what is something like a sheet of paper in bending.

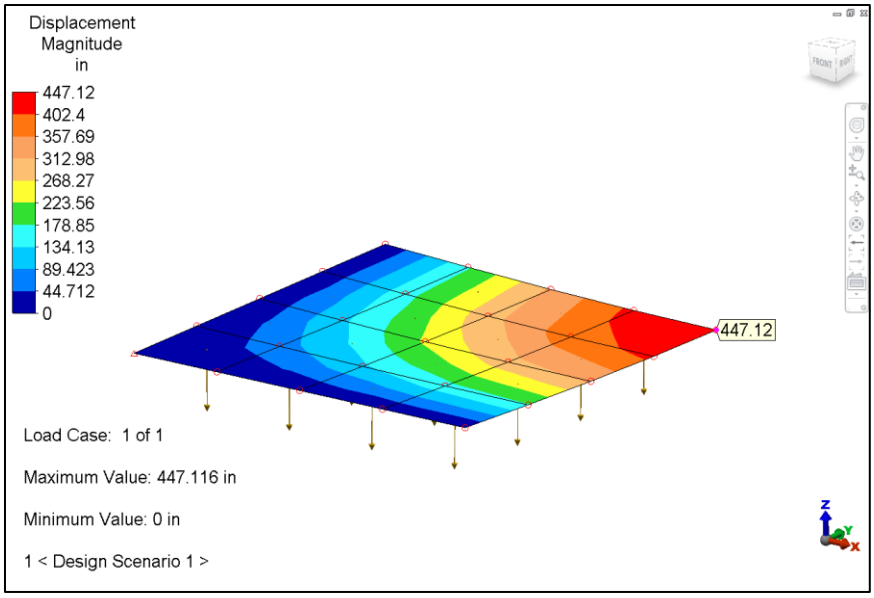

Figure 124-2. Inquiring on displacement results at the central node of the quarter-symmetry model. The 4x4 mesh of thin composite elements with thickness of 0.01 is shown.

Table 124-1. Comparison of Results

Description		Central Deflection (in)		% Difference
		Theory	Analysis	
Thin Laminate	1x1 Mesh, t = 0.01	447	417.0	6.8
	2x2 Mesh, t = 0.01	447	446.0	0.3
	4x4 Mesh, t = 0.01	447	447.12	0.03
	1x1 Mesh, t = 0.1	0.459	0.417	9.2
	2x2 Mesh, t = 0.1	0.459	0.446	2.8
	4x4 Mesh, t = 0.1	0.459	0.447	2.6
Sandwich Panel (Transverse shear deflections in 1 ply only)	1x1 Mesh, t = 0.01	447	323.0	27.8
	2x2 Mesh, t = 0.01	447	428.0	4.3
	4x4 Mesh, t = 0.01	447	443.0	0.9
	1x1 Mesh, t = 0.1	0.459	0.351	23.6
	2x2 Mesh, t = 0.1	0.459	0.446	2.8
	4x4 Mesh, t = 0.1	0.459	0.459	0.0

The table above shows a good correlation between the analysis and the predicted values. The mesh refinement demonstrates the convergence of solutions for both element types with increasing mesh. The thin composite finer mesh is closer to theory for the thinner examples, and the thick composite finer mesh is closer to theory for the thicker examples, as should be expected.

AVE - 125 Clamped Circular Plate with a Point Load

Reference

Reddy, J. N., *Energy and Variational Methods in Applied Mechanics,* New York: John Wiley and Sons, Inc., 1984.

Problem Description

A thick circular plate, 2" thick with a radius of 5", is subjected to a center point load of 4 lb. Due to the symmetric nature of this problem, a quarter-symmetry section was modeled with symmetry boundary conditions.

Find displacements at various points along the plate radius.

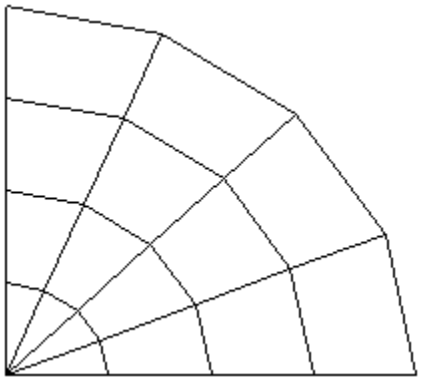

Figure 125-1. Quarter-symmetric FEA model of the thick shell composite circular plate.

Theoretical Solution

The analytic solution for the deflections is:

$$w = \left(\frac{P \times R^2}{16 \times \pi \times D} \right) \times \left[1 - \left(\frac{r}{R} \right)^2 - 2 \left(\frac{r}{R} \right)^2 \times \ln\left(\frac{R}{r} \right) - \left(\frac{8 \times D}{K^2 \times G \times h \times R^2} \right) \ln\left(\frac{r}{R} \right) \right]$$

Where:

- w = lateral deflection
- P = 4 lb (point load)
- R = 5" (plate radius)
- D = plate bending constant [(E * h^3) / (12 * (1 - ν^2))]
- E = modulus of elasticity (E11 = E22 = 10 E6 psi)
- ν = 0.3 (Poisson's Ratio)
- h = 2.0" (plate thickness)
- G = E / [2 (1 + ν)] (shear modulus)
- K = shear correction factor (K^2 = 5/6)

Autodesk Simulation Solution

For analysis with the Linear Static Stress Analysis processor, 20 thick composite elements were used to model the quarter plate. These elements include a transverse shear deflection for the core layer. A small hole of radius 0.001" is located at the center of the plate in order to maintain four-noded plates at the center. The point load is distributed over the five nodes at this radius.

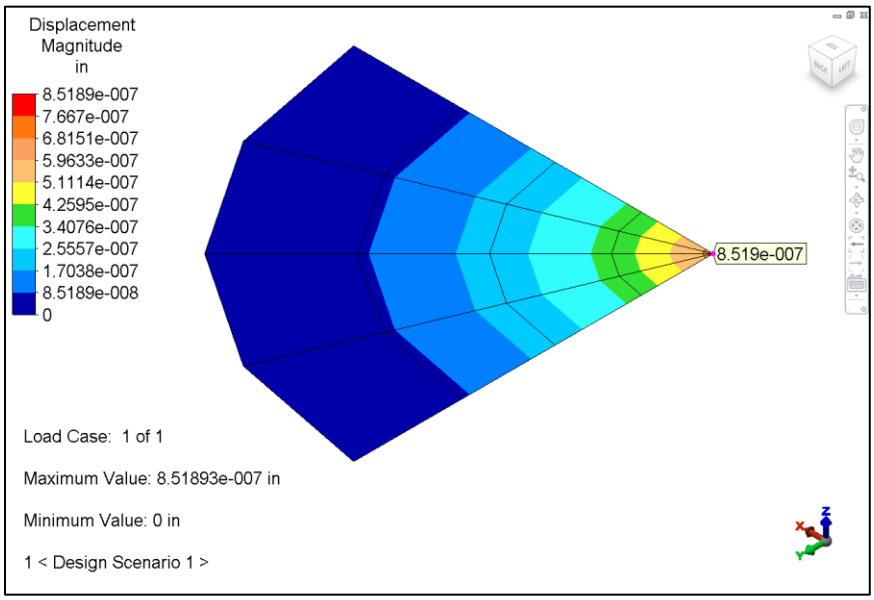

Figure 125-2. Inquiring on the displacement results at a node.

Table 125-1. Comparison of Results

r/R	Deflection (in x E-7)		% Difference
	Theory	Analysis	
0.0002	11.174	8.519	23.8
0.02	6.5911	5.926	10.1
0.20	3.8557	3.690	4.3
0.44	2.1419	2.035	5.0
0.70	0.78996	0.7404	6.3
1.00	0.0	0.0	0.0

The above table shows good agreement between the analysis results and the theoretical ones. The analysis results do not correspond as closely to the theoretical results at the plate center because the theoretical equation has a singularity at that location.

AVE - 126 Large Deformation and Large Strain for a Rubber Sheet

Reference

Iding, R. H., *Identification of Nonlinear Materials by Finite Element Methods*, SESM Report No. 73-4, Berkeley: Department of Civil Engineering, University of California, January 1973.

Problem Description

A 0.125" thick, bell-shaped rubber sheet is subjected to a uniformly distributed load of 111.493 psi at the end surface. The rubber material is assumed to be a Mooney-Rivlin type with the material constants C1 = 21.605 psi and C2 = 15.7465 psi.

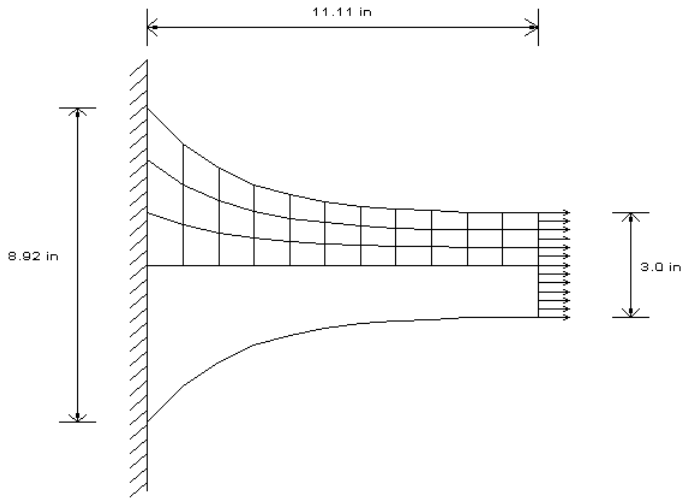

Figure 126-1. FEA model of a rubber sheet under pressure loading.

Theoretical Solution

The following values were used for the analytical solution:

Thickness = 0.125 in
p = 111.493 psi

Autodesk Simulation Solution

Because the sheet is symmetrical, only half of it is modeled using 33 plane stress elements (4-node 2-D continuum) with "incompressible elastic (Mooney-Rivlin)" material properties. The total number of nodes is 48. The final solution was obtained in 4 equal load steps. Total Lagrangian formulation and 2 *2 integration points were used.

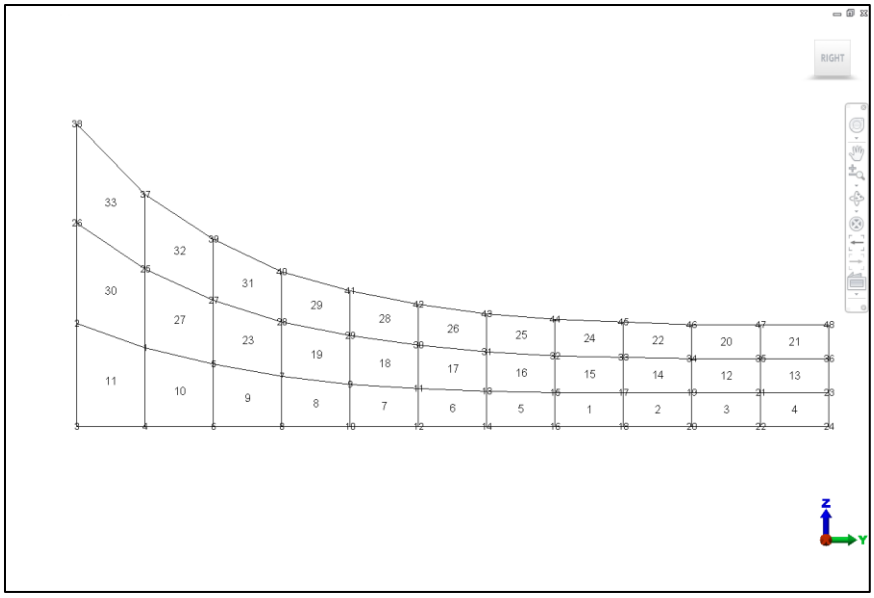

Figure 126-2. Node and element numbering in the FEA model.

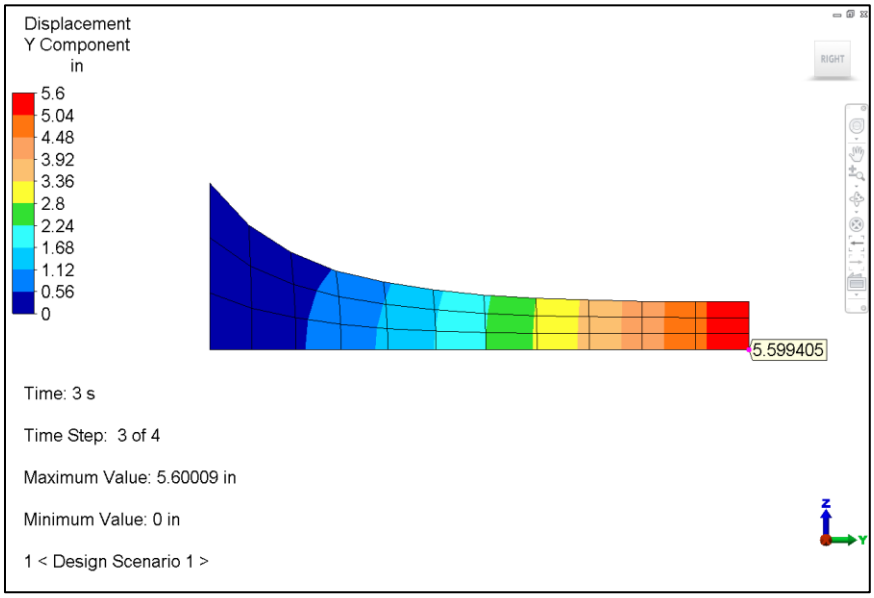

Figure 126-3. Inquiring on Y-displacement results at node 24 for load case 3.

Table 126-1. Comparison of Results

Step	Load (psi)	Displacement (inches) at Load End (Node 12)		% Difference
		Theory	Analysis	
1	27.873	1.26	1.281	1.67
2	55.747	3.17	3.075	3.00
3	83.620	5.57	5.599	0.52
4	111.493	8.31	8.974	7.99

Note: The theory data were measured from the figure in the published paper.

AVE - 127 Plastic Analysis of a Thick-walled Cylinder

Reference

Hodge, P. G. and White, G. H., "A Quantitative Comparison of Flow and Deformation Theories of Plasticity." *Journal of Applied Mechanics*, 17 (1950) 180-184.

Problem Description

A thick-walled hollow cylinder with an inner radius of 1" and an outer radius of 2" was subjected to internal pressure that varied with time. The material of the cylinder was assumed to obey the von Mises yield condition with an equivalent uniaxial yielding stress of 17.32 psi.

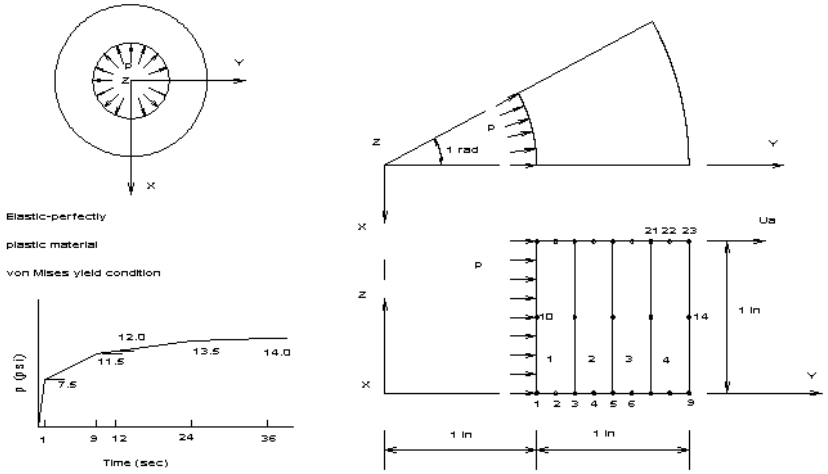

Figure 127-1. Thick-walled cylinder.

Theoretical Solution

The following values were used for the analytical solution:

- outside diameter = 4.0 in
- inside diameter = 2.0 in
- E = 86666.0 psi (modulus of elasticity)
- ν = 0.3 (Poisson's ratio)
- Sy = 17.32 psi (yield stress)
- G = E / 2 (ν+1) = 33333 psi

Autodesk Simulation Solution

Because the cylinder is axisymmetrical, only one sector of it with a one radian angle was modeled using four axisymmetric elements (8-node 2-D continuum). There are 23 nodes in the model. The uniformly distributed pressure was added in FEA Editor as a surface load to element 1. There were 20 load steps used for the solution, and results were printed at every fourth load step. Since displacements and strains were small, the analysis of the cylinder was carried out using the materially nonlinear-only formulation with a 2 *2 integration scheme.

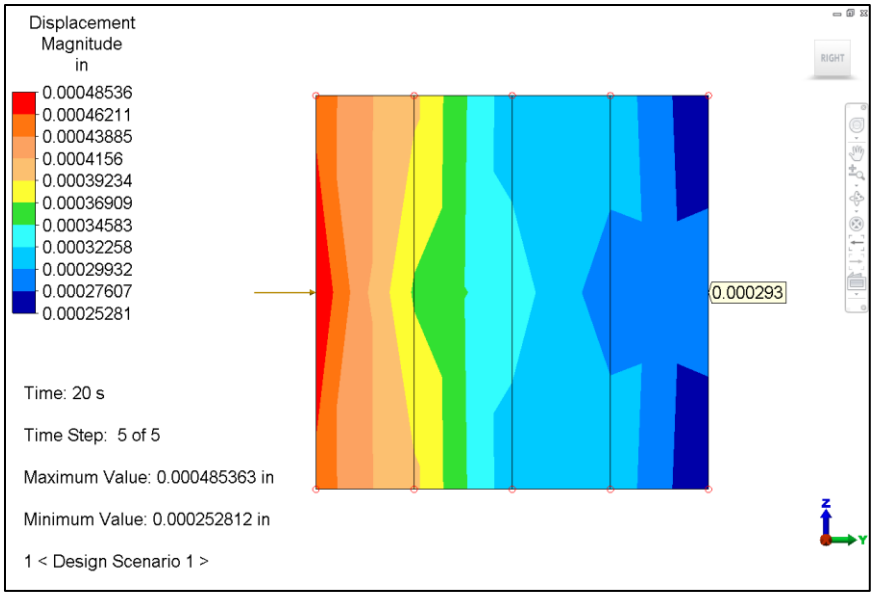

Figure 127-2. Inquiring on the displacement results at node 14 for Time step 5.

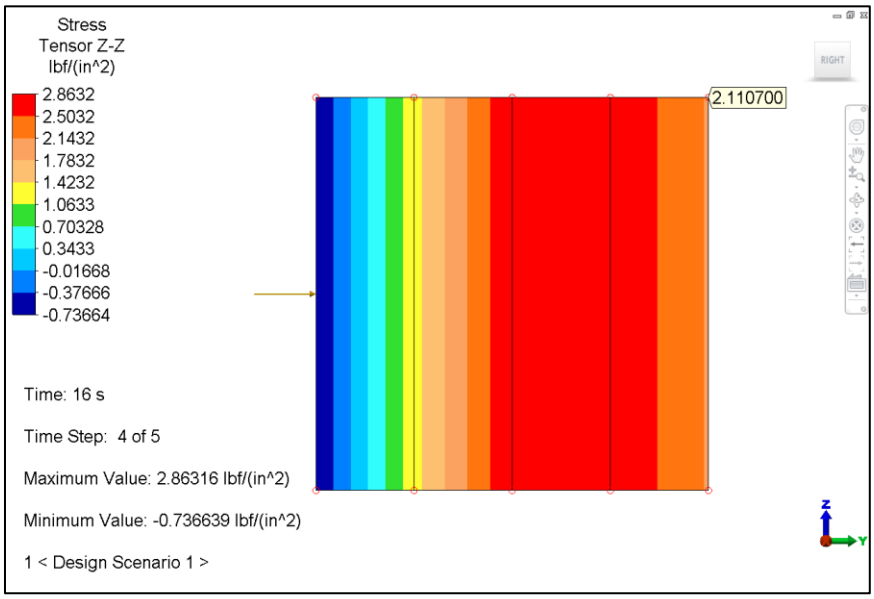

Figure 127-3. Inquiring on the stress tensor results in the Z direction at node 23 for Time step 4.

Table 127-1. Radial Displacement Results

The radial displacements (Ua) on the outer surface of cylinder (Y-displacement at nodes 9, 14, 23)			
Time Step	**Pressure (psi)**	**Ua (10E-4 In)**	**2*G*Ua (lb/In)**
1	9.0	1.275	8.500
2	11.0	1.716	11.44
3	12.0	2.074	13.83
4	12.5	2.314	15.43
5	13.0	2.664	17.76

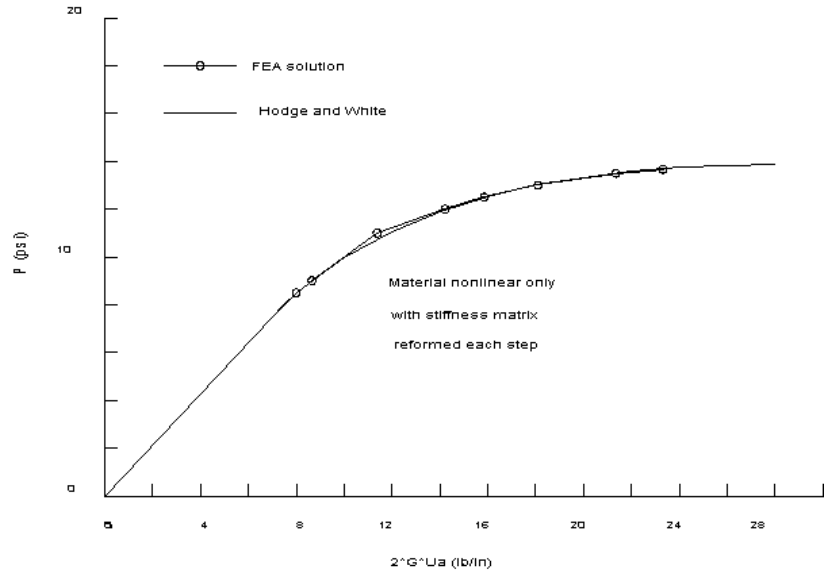

Figure 127-4. Comparison of Results.

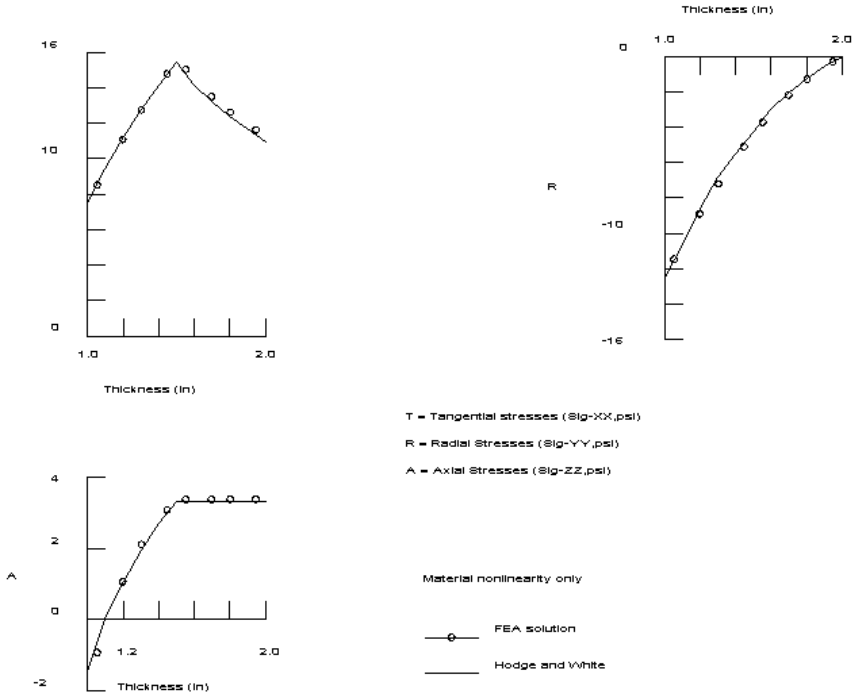

Figure 127-5. Elastic-plastic stress distribution through thickness of thick-walled cylinder at p = 12.5 psi.

AVE - 128 Static Large Displacement Analysis of a Spherical Shell

Reference

Stricklin, J. A., "Geometrically Nonlinear Static and Dynamic Analysis of Shells of Revolution", High Speed Computing of Elastic Structures, *Proceedings of the Symposium of IUTAM*, University of Liege, August 1970.

Mescall, J. F., "Large Deflections of Spherical Shells Under Concentrated Loads", *Journal of Applied Mechanics*, 32 (1965): 936-938.

Problem Description

A spherical shell, 0.01576" thick, was subjected to a concentrated apex load up to 100 lb. The material was assumed to be isotropic, but the shell may experience a large displacement. Young's modulus = 1.0E+09 psi and Poisson's ratio = 0.3 were assumed. The deflection at the apex of the shell will be determined.

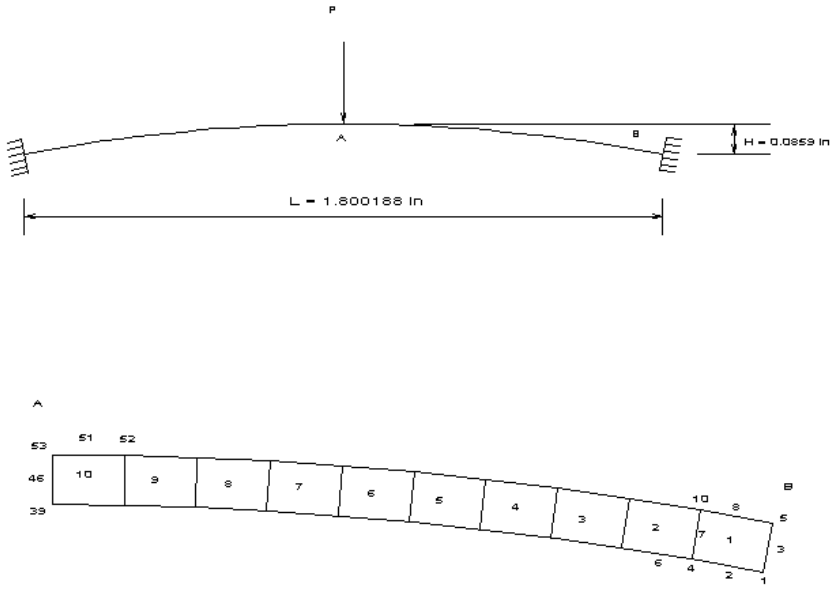

Figure 128-1. Axisymmetric FEA model of a spherical shell.

Theoretical Solution

The following values were used for the analytical solution:

Radius of Shell = 4.76 in.
Young's Modulus = 1.0E+7 psi
Poisson's Ratio = 0.3
Thickness of Shell = 0.01576 in.

Autodesk Simulation Solution

The shell is axisymmetrical, therefore 10 axisymmetric elements (8-node 2-D continuum) were used. There were 53 nodes in the model. The total load of 100 lb was applied to a node over 25 time steps. A 2 *2 integration scheme and Updated Lagrangian formulation was used. Element stiffness was reformed in every time step.

Force applied to a node on 2D axisymmetric model = 100 lbf /(2π) = 15.9155 lbf/radian

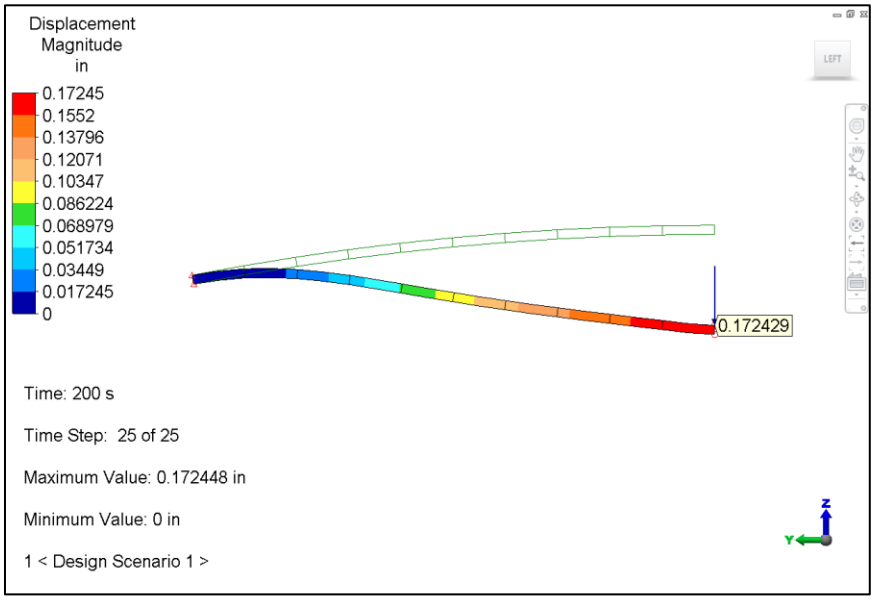

Figure 128-2. Inquiring on the displacement results at point A for time step 25/25.

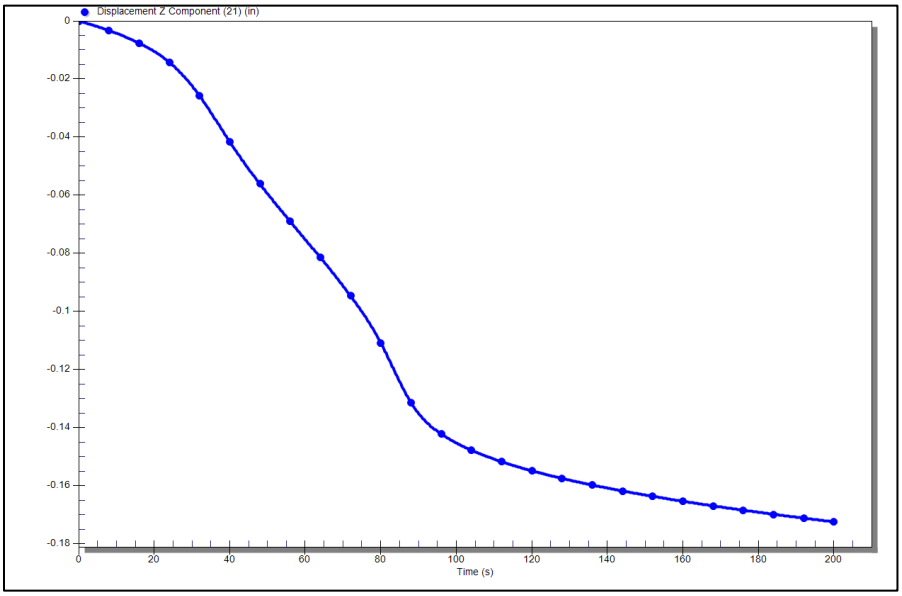

Figure 128-3. Z Displacements at Point A

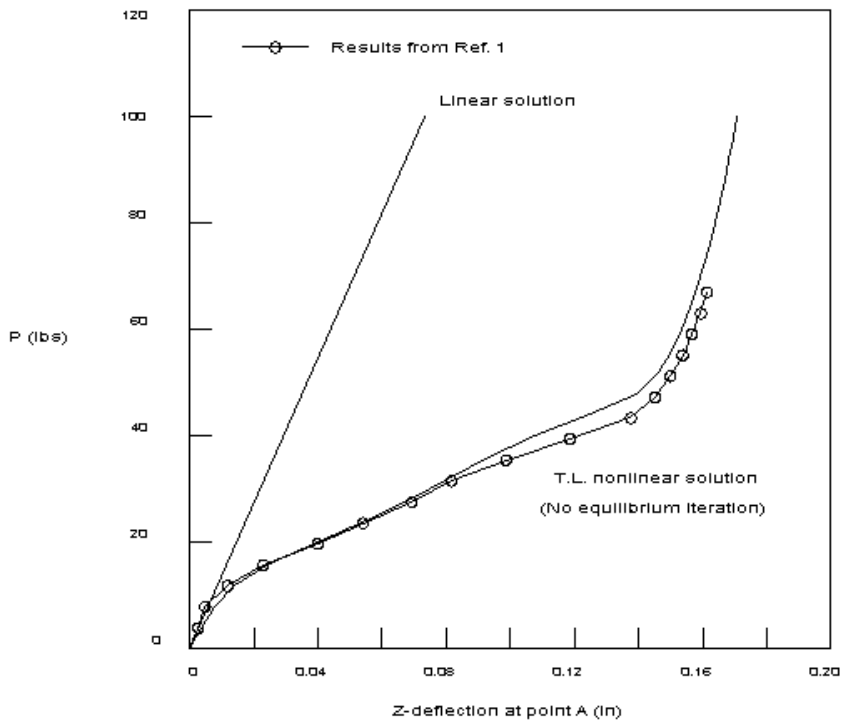

Figure 128-4. Comparison of Results

AVE - 129 Static Analysis of a Simply Supported Plate

Reference

Volterra, E. and Gaines, J. H., *Advanced Strength of Materials*, Prentice-Hall, Englewood Cliffs, NJ: 1971.

Problem Description

A simply supported, 1.0" thick plate was subjected to a concentrated load of 40 lb applied at the center. The material was assumed to be isotropic with Young's Modulus = 30000 psi and Poisson's Ratio = 0.25. Only the small displacement was considered. The deflection at the plate center was to be determined. Note that this problem is similar to AVE - 69 by design with a different loading condition.

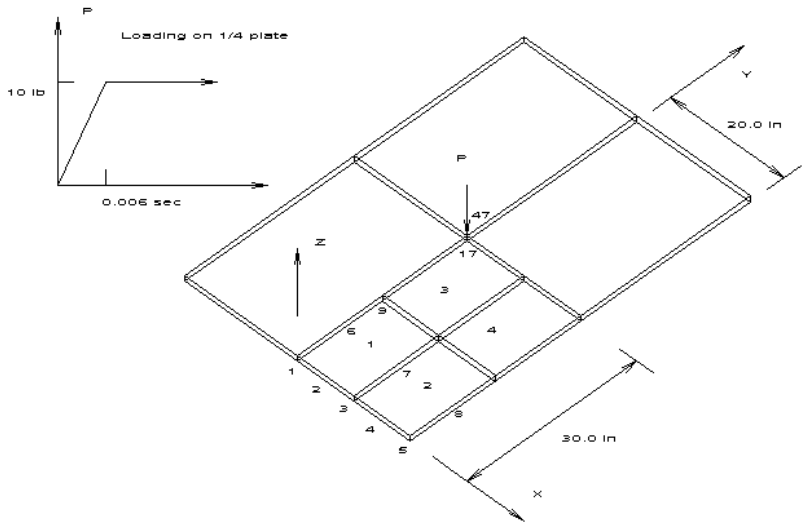

Figure 129-1. FEA model of a simply supported plate.

Theoretical Solution

The following values were used for the analytical solution:

- Thickness = 1.0 in
- Poisson's Ratio = 0.25
- E = 30000 psi (Young's Modulus)
- $\rho = 0.0003 \ \frac{\text{lb sec}^2}{\text{in}^4}$

Autodesk Simulation Solution

Because the plate is symmetrical, only a quarter of it was modeled. Four elements (20-noded Brick elements), 51 nodes, and a 2*2*2 integration scheme were used.

You should note that the finite element model was rather coarse, yet the results are fairly close to theoretical, due to the midside nodes being used on all element edges.

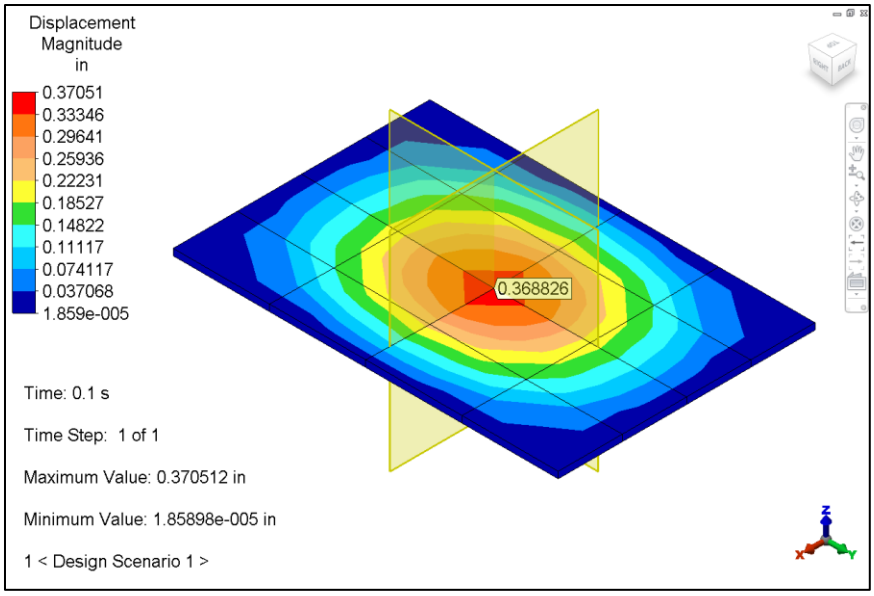

Figure 129-2. Inquiring on displacement results at the center node.

Note that 2 mirror planes were activated in the above figure to show the full model

Table 129-1. Comparison of Results

Deflection at the center node		% Difference
Theory	Analysis	
0.3684	0.3688	0.11

AVE - 130 Natural Frequencies for a Simply Supported Plate

Reference

Young, Warren C., *Roark's Formulas for Stress and Strain*, Sixth Edition, McGraw-Hill Book Company, New York: 1989, 717.

Problem Description

The geometric and material properties for this plate are identical to those in AVE - 129. Three natural frequencies were determined.

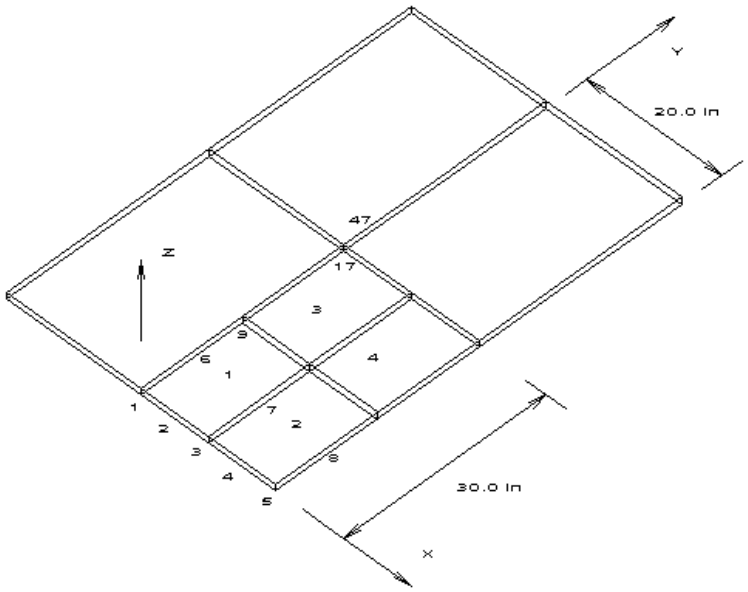

Figure 130-1. FEA model of a simply supported plate.

Theoretical Solution

The analytical solution from Kirchhoff plate theory is as follows.

$$f(Hz) = 1.5708 \times \sqrt{\left(\frac{D}{m}\right)\left(\frac{p^2}{a^2} + \frac{n^2}{b^2}\right)}$$

Where:

- f = natural frequencies $\left(\frac{cycles}{sec}\right)$
- D = $\frac{Eh^3}{12\left(1-\nu^2\right)}$
- E = 30000 psi (Young's Modulus)
- h = 1.0 in (thickness of plate)
- ν = 0.25 (Poisson's Ratio)

- a = 60 in (width of plate)
- b = 40 in (height of plate)
- p,n = math number
- T = $\frac{1}{f}\sec(\text{period})$
- m= 0.72 lb*s^2/in (mass of the plate)

Autodesk Simulation Solution

Because the plate geometry and boundary conditions were symmetrical, only a quarter of the plate needed to be modeled for the static analysis AVE - 129 and the dynamic analysis AVE - 131. The same mesh is used for this modal analysis. However, the use of symmetry to decrease model size restricts the mode shapes that can be found to those having the same symmetry as the model. Therefore, antisymmetric modes are predictably missed by this particular analysis. Four elements (20-noded Brick elements), 51 nodes, and a 2*2*2 integration scheme were used. Two separate analyses, one with consistent masses and the other with lumped masses, were performed. Only the input model database for consistent masses is included with the software, but it is easy in the "Analysis Parameters" screen to change to a lumped mass analysis.

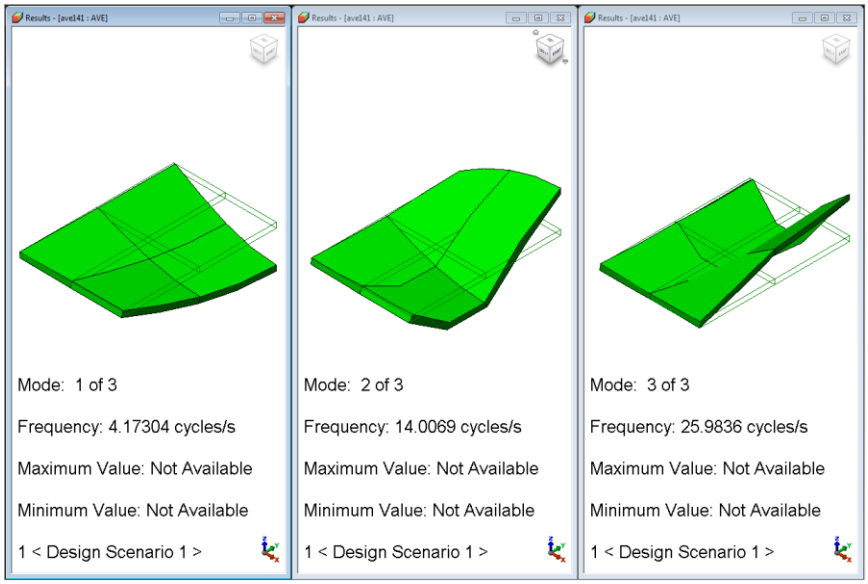

Figure 130-2. Displaying the frequency for the first 3 modes.

The period is the reciprocal of the frequency (1/4.1662 for mode 1). Note that the finite element model was rather coarse and high accuracy in the model could not be expected. With more elements the accuracy would improve substantially.

Table 130-1. Comparison of Results

Mode Number	Vibration Period (sec)		% Difference	Vibration Period (sec)	% Difference
	Theory	Analysis (Consistent)		Analysis (Lumped)	
1	0.2365	0.2396	1.31	0.2396	1.31
2	0.0683	0.0714	4.54	0.0714	4.54
3	0.0362	0.0385	6.35	0.0385	6.35

AVE - 131 Dynamic Analysis of a Simply Supported Plate under Concentrated Load

Reference

Volterra, E. and Gaines, J. H., *Advanced Strength of Materials*, Prentice-Hall, Englewood Cliffs, NJ, 1971.

Problem Description

A simply supported, 1.0" thick plate was subjected to a concentrated load of 40 lb applied at the center. The material was assumed to be isotropic. (The geometric and material properties for this plate are identical to those in AVE - 130.) The dynamic displacement at the point of applied load until time = 0.3 sec was to be determined.

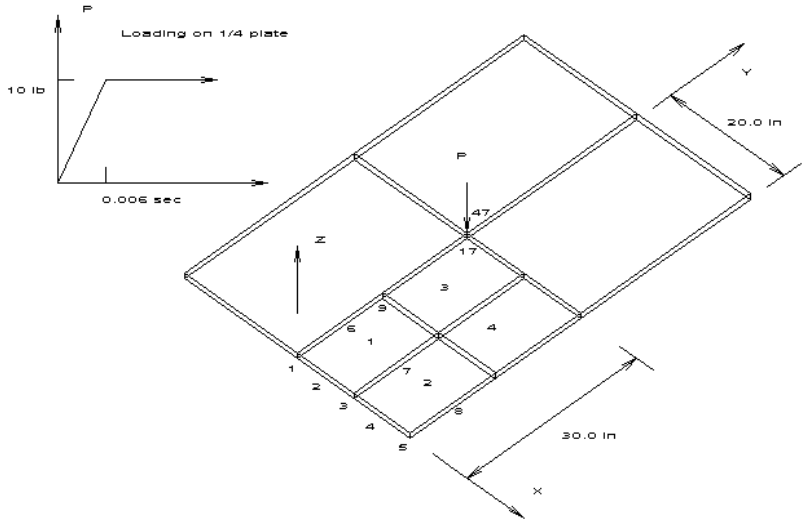

Figure 131-1. FEA model of a simply supported plate.

Theoretical Solution

The following values were used for the analytical solution:

- Thickness = 1.0 in
- Poisson's Ratio = 0.25
- E = 30000 psi (Young's Modulus)
- $\rho = 0.0003 \ \frac{\text{lb sec}^2}{\text{in}^4}$

Autodesk Simulation Solution

Because the plate is symmetrical, only a quarter of it was modeled. The previous form of this model did not include midside nodes through the thickness; therefore there are now 9 more nodes, and flexibility, displacements, and period are somewhat increased compared to the previous results. Four elements (20-noded Brick elements), 51 nodes, and 2 *2 *2 integration scheme were used. Only the response with consistent masses was considered.

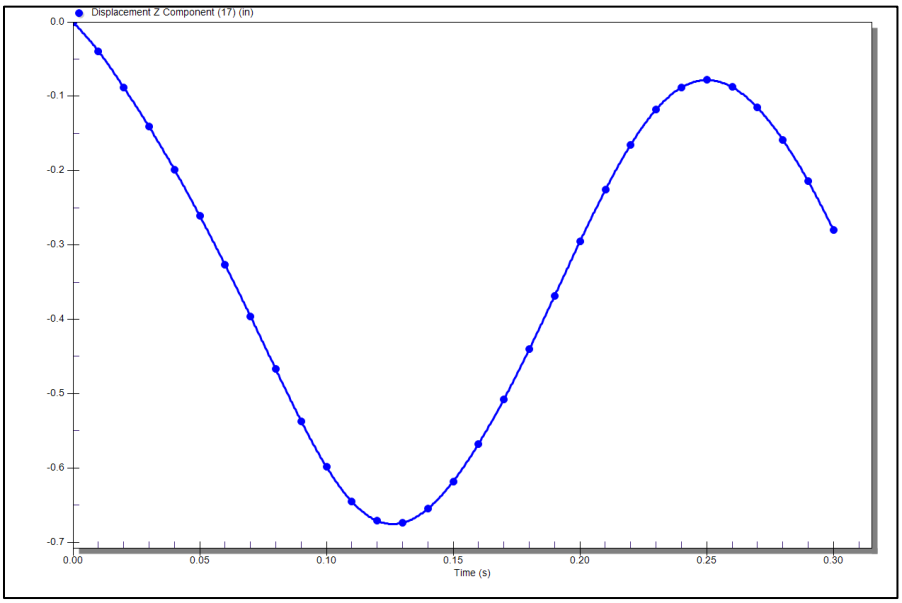

Figure 131-2. Dynamic response of the simply supported plate (at the center node).

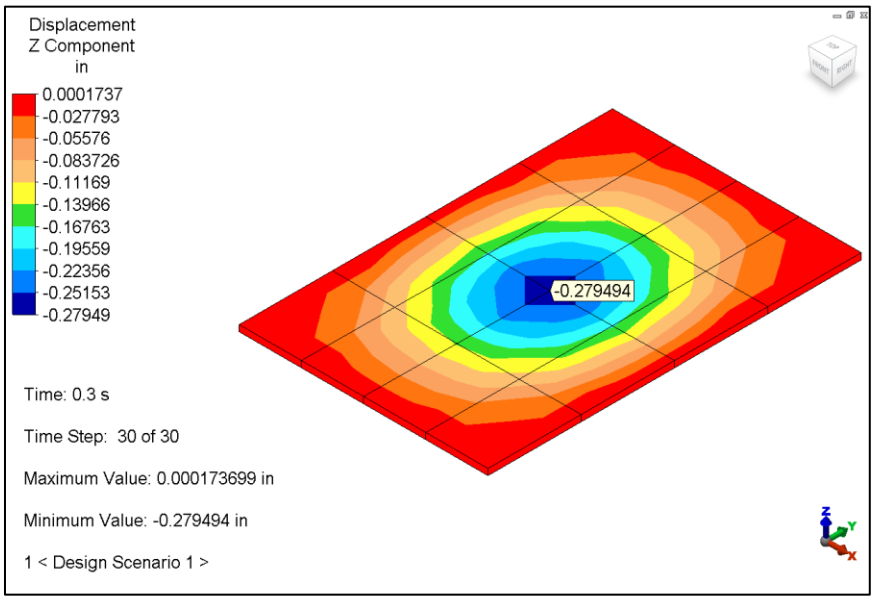

Figure 131-3. Inquiring on the displacement results at the center node for the last step.

Note that 2 mirror planes were activated in the above figure to show the full model

AVE - 132 Wall with Internal Heat Generation

Reference

Holman, J. P., *Heat Transfer*, Third Edition, New York: McGraw-Hill, 1981.

Problem Description

A plane wall 40" thick has a distributed internal heat generation of 1 BTU / in^3 hr. The temperature distribution inside the wall is desired. The conductivity of the material is 0.5 BTU / hr in ^oF. The external temperature is held at 70 ^oF.

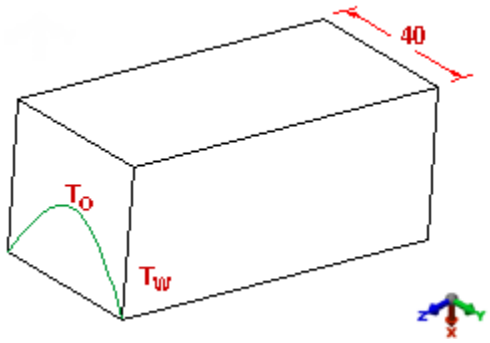

Figure 132-1. Thermal FEA model of the wall with internal heat generation.

Theoretical Solution

q = 1 BTU / in^3 hr
K = 0.5 BTU / in hr ^oF
t = 40 in (wall thickness)
T_w = 70^oF

It can be shown (by using an offset with the steady state terms of the formula for AVE - 58) that the temperature is a parabolic function of distance and that the maximum temperature is at the midplane, and that this maximum temperature is 470^o.

Autodesk Simulation Solution

Taking advantage of symmetry, only half the thickness of the wall needs to be analyzed. At the center, the derivative of temperature with respect to thickness is 0, which means that the midplane can be treated as an insulated surface. Four temperature boundary elements are used to maintain a temperature of 70^{o}F at the outside of the wall. A stiffness of 10,000 BTU/(F.hr) is used. (This is equivalent to the stiffness of a boundary element in a stress analysis.)

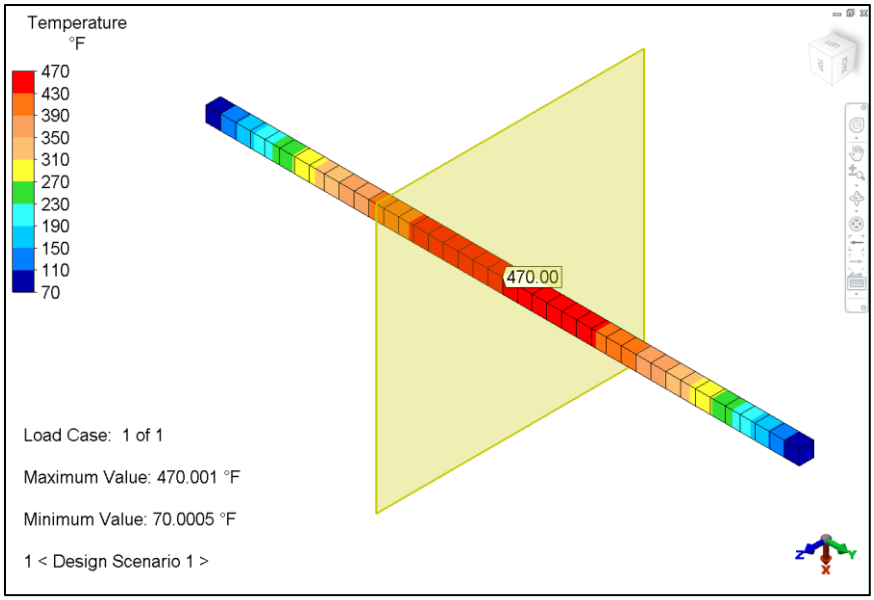

Figure 132-2. Inquiring on temperature results at a node.

Note that 1 mirror plane was activated in the above figure to show the full model

Table 132-1. Comparison of Results

Maximum Temperature (°F)		% Difference
Theory	**Analysis**	
470	470	0.0

AVE - 133 Plane Couette Flow with pressure gradient

Reference

Panton, R. L., *Incompressible Flow*, New York: John Wiley & Sons, Inc., 1984.

Problem Description

This example involves steady-state viscous flow between two parallel plates (Couette flow with pressure gradient). The top plate moves with constant speed, and the bottom plate is stationary. The left and right boundaries are set as zero velocity at vertical direction and free at horizontal direction.

Figure 133-1. FEA mesh of the moving wall.

Theoretical Solution

The bottom wall in **Error! Reference source not found.** is fixed at zero velocity. The top wall is moving at a constant velocity of 1.0 in/s X_1 (Y) direction. The left end input velocity profile is linear. Determine the local fluid velocity U everywhere else.

The exact analytical solution is:

U_1 (x1,x2) = x2

U_2 (x1,x2) = 0

Theoretical velocity profile in X2 direction

With considering the viscosity and pressure gradient in incompressible viscous flow (this is the basic assumption in Autodesk Multiphysics fluid flow simulation), the theoretical velocity profile has to be the formula of "Couette flow with pressure gradient".

The velocity profile formula is list below, refer to http://en.wikipedia.org/wiki/Couette_flow

$$u(y) = u_0 \frac{y}{h} + \frac{1}{2\mu}\left(\frac{dp}{dx}\right)(y^3 - hy) \qquad \textbf{(Eqn 133- 1)}$$

Where dp/dx is the pressure gradient in flow direction, and μ is the fluid viscosity.

Fluid pressure drop dp/dx = [-0.763452-(-1.145304)]lbf/in^2 /2.0in = 0.190926 lbf/in^3

(Refer to Figure 133-2. Pressure gradient in the flow. The 2 nodes probed have a distance of 0.2 in.)

Fluid viscosity	μ	=0.1 lbf*s/in^2
Top driving velocity	u_0	=1 in/s
Height	h	=1 in

Substitute above parameter into Eqn 133- 1, yielding the theoretical velocity profile in the vertical direction formula.

$$\mathbf{u(y) = y[1+0.95462(y-h)]} \qquad \textbf{(Eqn 133- 2)}$$

Autodesk Simulation Solution

The model consisted of 250 2-D planar fluid elements. Appropriate boundary conditions were applied along the perimeter to specify velocity. A Steady Fluid Flow analysis was performed.

The results obtained are very accurate to the theoretical solution with all node velocity relative error smaller than 0.002%.

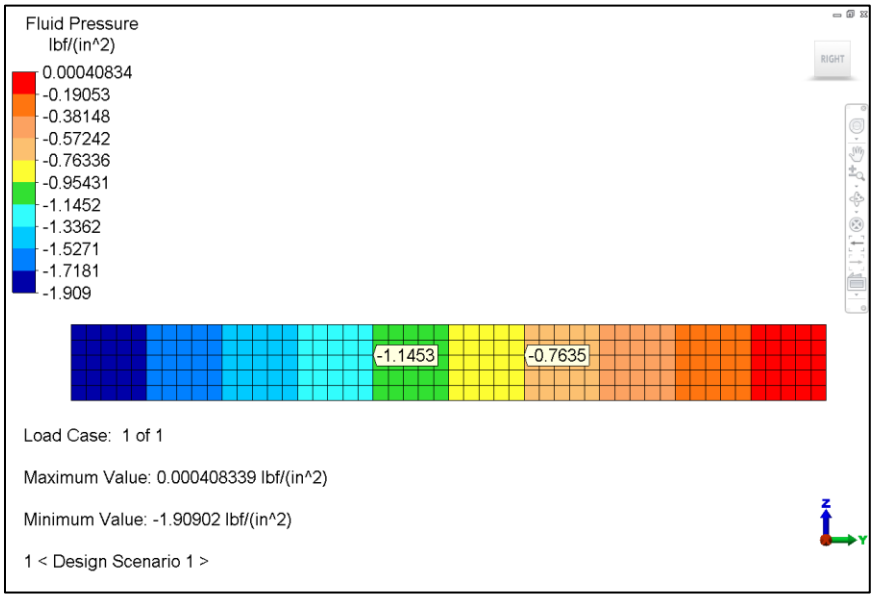

Figure 133-2. Pressure gradient in the flow. The 2 nodes probed have a distance of 0.2 in

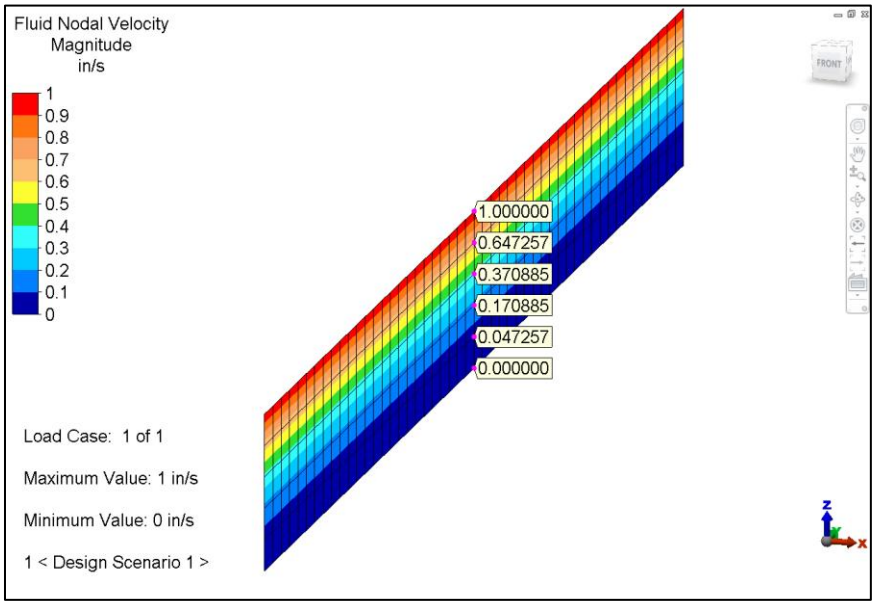

Figure 133-3: Velocity distribution in Z direction

Table 133-1: Comparison of Results

Y coordinate	Velocity in/s		% Difference
	Theory	Analysis	
1(Top)	1.0	1.0	0
0.8	0.647259	0.647257	0.00031%
0.6	0.370889	0.370885	0.00108%
0.4	0.170888	0.170885	0.00175%
0.2	0.047258	0.047257	0.00211%
0(Bottom)	0	0	0

AVE - 134 Axisymmetric Flow through a Circular Pipe

Reference

Batchelor, G. K., *An Introduction to Fluid Mechanics*, Cambridge: Cambridge University Press, 1990.

Problem Description

This example involves steady-state viscous flow in a circular pipe (Poiseuille flow). Figure 134-1 shows an axisymmetric view of a circular pipe. The fixed wall is on the right and the center of the pipe is along the left. This corresponds to the Poiseuille flow through a pipe. Determine the fluid velocity in the Z direction, U_2.

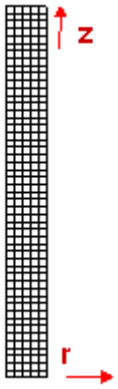

Figure 134-1. FEA mesh of the axisymmetric moving pipe.

Theoretical Solution

The exact analytical solution is:

$U_1 (r,z) = 0$

$U_2 (r,z) = 1 - r^2$

The Vorticity is:

$\omega_\theta = -2r$

Autodesk Simulation Solution

The axisymmetric option yields a reasonable solution.

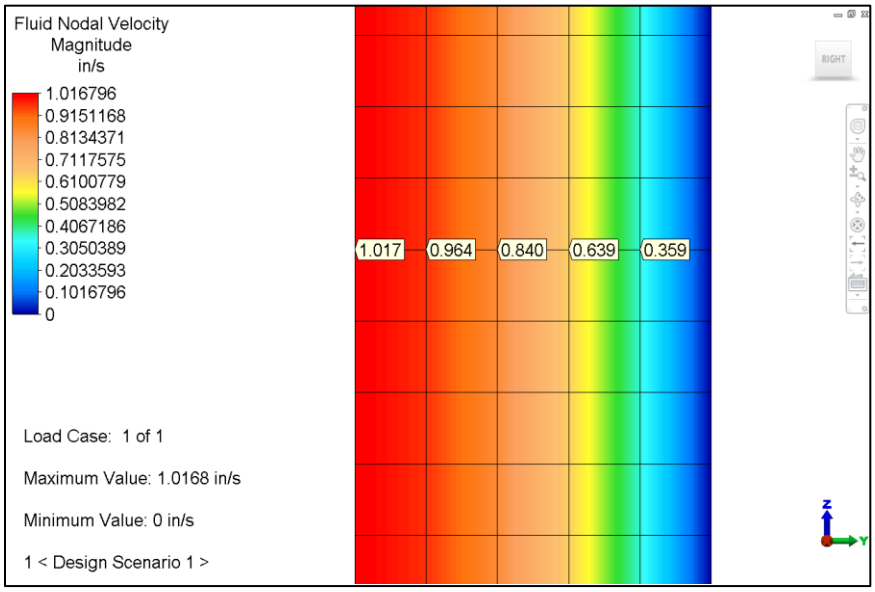

Figure 134-2. Inquiring on the velocity results at a node.

Table 134-1. Comparison of Results

Node Number	Velocity (U_2)		% Difference
	Theory	Analysis	
187	1.0	1.01679628 E+00	1.6
188	0.96	9.63829457 E-01	0.40
189	0.84	8.40240012 E-01	0.02
190	0.64	6.38965833 E-01	0.16
191	0.36	3.58997879 E-01	0.28

AVE - 135 Axisymmetric Flow past a Sphere at Re=10

Reference

Brooks, A., Hughes, T. J. R. and Liu, W. K., *Review of Finite Element Analysis of Incompressible Viscous Flows by the Penalty Function Formulation*, Journal of Computation Physics, 30 (1979).

Dennis, S. C. R. and Walker, J. D. A., Calculation of the Steady Flow Past a Sphere at Low and Moderate Reynolds Numbers, Journal of Fluid Mechanics, 48 (1971).

Problem Description

This example involves an axisymmetric flow past a sphere at Reynolds number = 10. Pressure and vorticity matches closely with other numerical results.

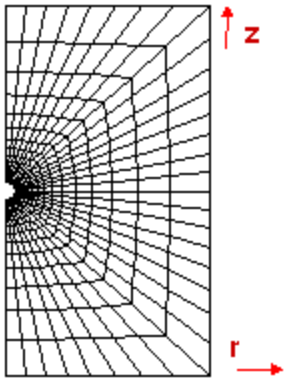

Figure 135-1. FEA mesh of the axisymmetric flow past a sphere.

Theoretical Solution

The flow field is assumed to be uniform (i.e., $U_2 = U = 1.00$ upstream and $\rho = 1$). The Reynolds number based on sphere diameter D is:

- $Re = (DU_\infty) / \nu$
- $\rho = 1$, Mass Density $[(lb - in^2) / sec^4]$
- $\nu = \mu / \rho$ = Kinematic viscosity (in^2/sec)

There are analytical solutions available for creeping flow (Stokes) i.e., Re = 0, which are not accurate beyond Re = 1.0. Dennis and Walker solved the infinite domain problem at Re = 10. This problem has also been solved by Hughes et al by the penalty method (using downstream boundary conditions, $t_1 = 0$, $u_2 = 0$). We compare our results to those of Hughes et al and Dennis et al in the following figures.

Autodesk Simulation Solution

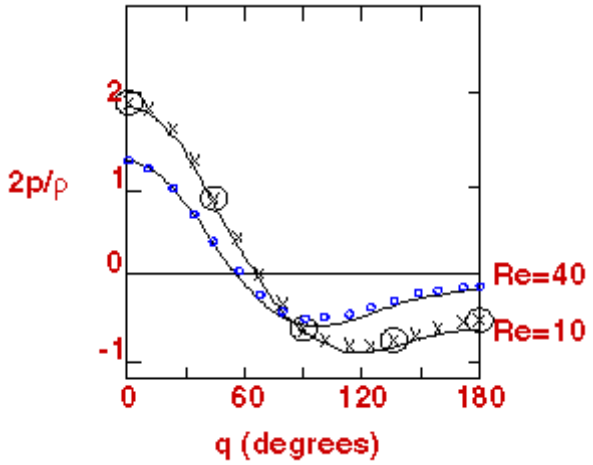

Figure 135-2. Pressure distribution on the sphere. The analysis results are superimposed as circles.

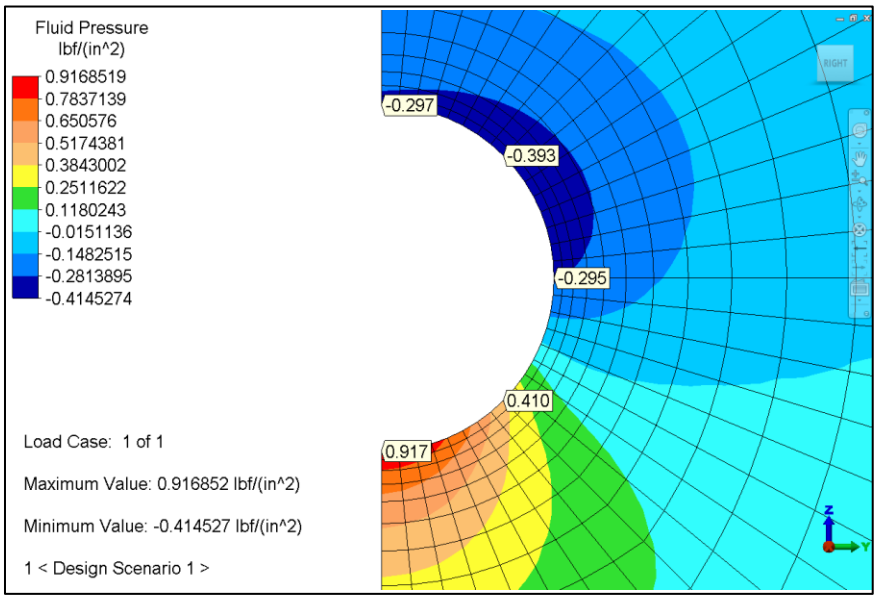

Figure 135-3. Inquiring on the pressure results at a node.

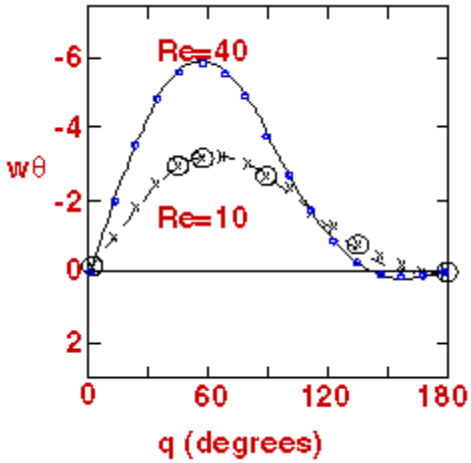

Figure 135-4. Vorticity distribution on the sphere. The analysis results are superimposed as circles.

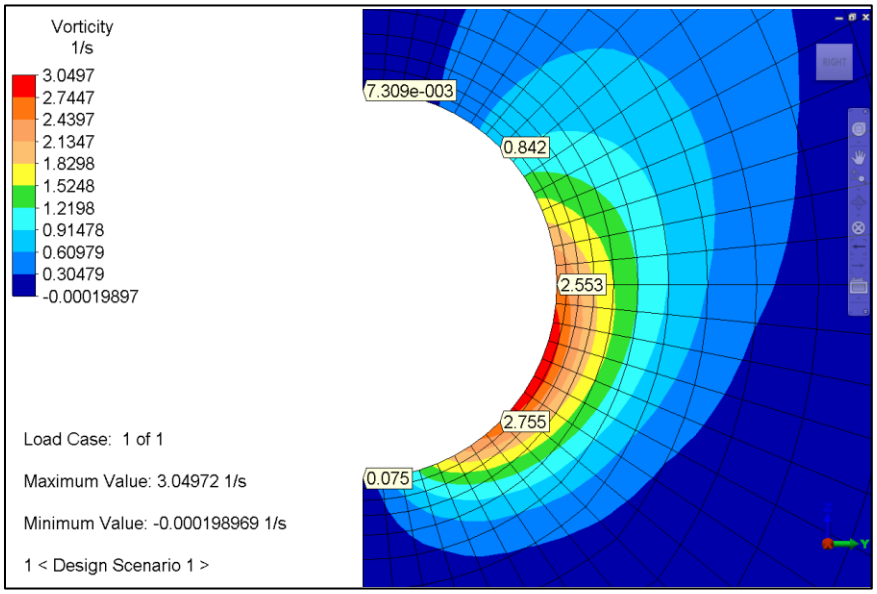

Figure 135-5. Inquiring on vorticity results at a node.

AVE - 136 Flow past a Circular Cylinder at Re=40, 100

Reference

M. Braza, P. Chassaing and H. H. Minh, *Numerical Study and Physical Analysis of the Pressure and Velocity Fields in the Near Wake of a Circular Cylinder*, Journal of Fluid Mechanics, 165 (1979).

T. E. Tezduyar, J. Liou and D. K. Ganjoo, *Incompressible Flow Computations Based on the Vorticity-Stream Function and the Velocity-Pressure Formulations*, University of Minnesota Supercomputer Institute Report UMSI, 89/86 (May 1989).

White, Frank M., *Fluid Mechanics*, P455, Fourth Edition, McGraw-Hill, Inc., (1997).

Problem Description

In fluid mechanics, the wake behind a body is of interest to many engineers. This example involves a flow past a circular cylinder at Reynolds number = 100. A reasonable flow field is obtained showing the formation of eddies. The analysis results agree quite well at lower Reynolds numbers.

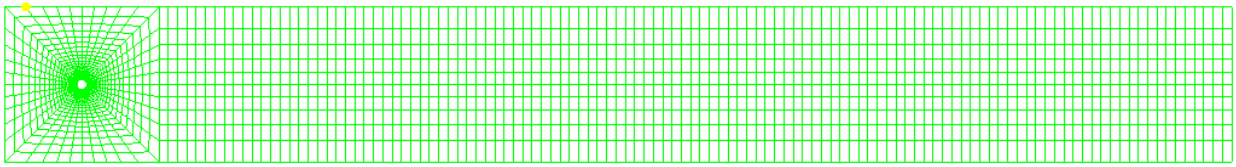

Figure 136-1. Mesh of the flow past the circular cylinder

Theoretical and experimental Solution

In this problem, the flow field is assumed to be uniform upstream, using a prescribed velocity of 1 at the left edge, (u_1 = U = 1.0), and the Reynolds number is defined as:

$$Re = (D\ U_\infty) / \nu$$

Where:

- $\rho = 1$ and $\nu = \mu / \rho$
- ν = Kinematic viscosity (in^2 / sec)
- D = Diameter of the cylinder (in)
- ρ = Mass density (lb sec^2 / in^4)
- μ = Viscosity (lb sec/ in^2)
- P = Pressure (stagnation)

Other quantities of interest are:

- $P_\infty = P_0 - 0.5\ \rho\ U_\infty^2$
- Pressure coefficient $C_p = (P - P_\infty) / 0.5\ \rho\ U_\infty^2$

Where U_∞ is inlet velocity and P_0 is stagnation pressure at forefront node on upstream side of the cylinder.

Figure 136-1 illustrates the pressure coefficient distribution for inviscid fluid flow and viscous laminar/turbulence flows respectively. For a detailed comparison, the viscous laminar flow at Reynolds number 100 is showed in Figure 136-2, the experimental data were extracted to compare and verify Autodesk Simulation result. Note that the theoretical solution is for inviscid fluid only, considering viscous flow in real physics, the simulation result should compare to experimental result.

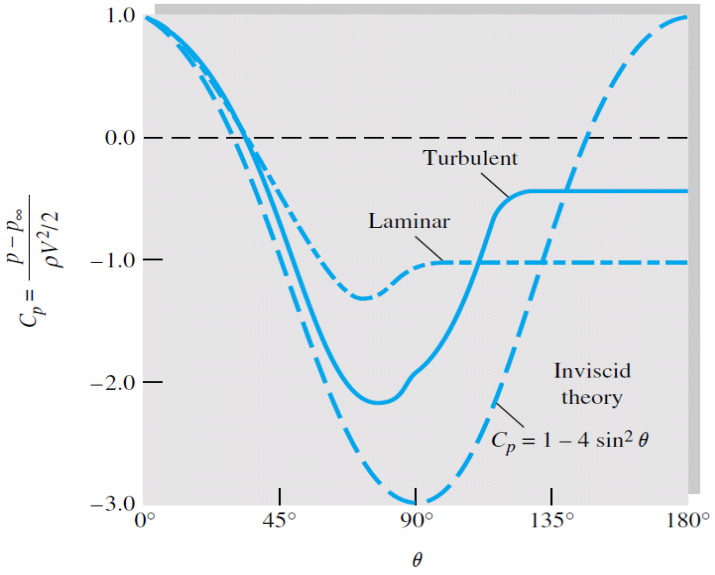

Figure 136-2. Pressure coeffcient distribution on cyclinder surface (Frank M. White, "Fluid dynamics", Fourth Edition, P455)

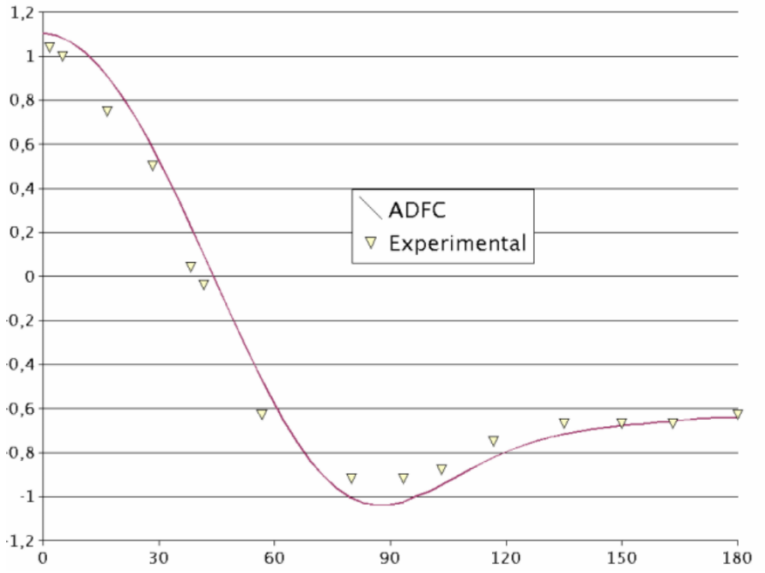

Figure 136-3. Pressure coeffcient distribution on cyclinder surface (Re=100)

(http://adfc.sourceforge.net/img/cil2D-cp-Re100.gif)

Autodesk Simulation Solution

Note that only half of the domain is needed since the solution is symmetric. Nevertheless, a full domain is used in order to verify that the resulting numerical solution is symmetric up to a reasonable number of digits. The pressure results on cylinder nodes were probed to obtain the simulation result. The nodes were selected at the angle from 0, 18, 36, 54, 72, 90, etc. degrees with incremental value as 18 degrees. The forefront node on upstream side of the cylinder was picked to obtain the stagnation pressure results. The reference pressure was then calculated using the following formula:

$P_\infty = P_0 - 0.5\ \rho\ U_\infty^2$

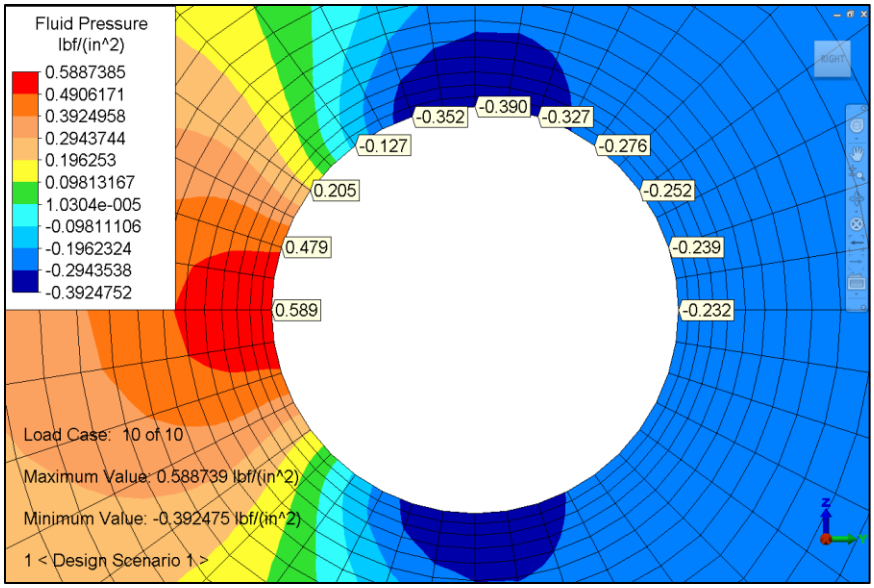

Figure 136-4. Stagnation Pressures at various nodes

Table 136-1. Comparison of Results

Angle	Reference Pressure		% Difference
	Theory	Analysis	
0	1	1	0.00
18	0.7796	0.8	2.55
36	0.2319	0.270889	14.39
54	-0.431	-0.4	7.75
72	-0.8812	-0.83	6.17
90	-0.9565	-0.92	3.97
108	-0.8301	-0.81	2.48
126	-0.73	-0.72	1.39
144	-0.6824	-0.654	4.34
162	-0.6544	-0.62	5.55
180	-0.6415	-0.61	5.16

AVE - 137 3-D Fluid Flow

Reference

Brooks, A., Hughes, T. J. R. and Liu, W. K., *Review of Finite Element Analysis of Incompressible Viscous Flows by the Penalty Function Formulation*, Journal of Computational Physics, 30 (1979).

Problem Description

This verification example is a driven 3-D cavity flow at Reynolds number = 400. Fluid is entrapped in a 3-D box, and the top wall moves, setting the fluid in motion.

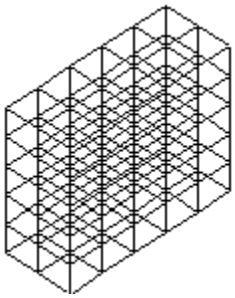

Figure 137-1. FEA mesh for the 3-D driven cavity.

Theoretical Solution

This problem is a 3-D version of the 2-D driven cavity problem (AVE - 13). Essentially a 2-D problem, it is generated by extruding the model and imposing zero velocity in the third direction.

There is no analytical solution available for this problem. However, since this problem is widely used to test fluid flow problems, we can compare the solution with those obtained by Hughes et al.

Autodesk Simulation Solution

The mesh used consists of 50 3-D fluid elements (length=5 x width=2 x height=5). The results are in close agreement with results from the equivalent 2-D problem.

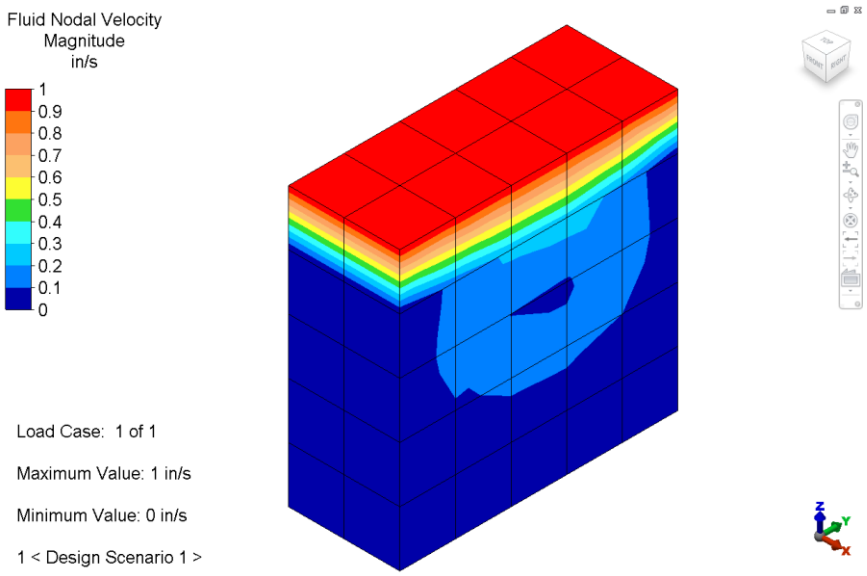

Figure 137-2. Displaying velocity results.

AVE - 138 DDAM Shock Analysis of Heavy Equipment Mounted on the Deck of a Surface Ship

Reference

Belsheim, R. O. and O'Hara, G. J., "Shock Design of Shipboard Equipment: Dynamic Design-Analysis Method", Naval Ship Systems Command, Department of Navy, Washington, D.C., NAVSHIPS 250-423-30, May 1961.

Problem Description

Consider a piece of previously shock-tested equipment that weighs 20,000 lbs. It is deck mounted on a surface ship and a design check of a proposed foundation is to be made for the elastic-plastic category in the athwartship direction. Assume that, the equipment can be considered to be a rigid body, but because of unsymmetrical foundation stiffness and location of the center of gravity that the system rotates as it translates (see Figure 138-1). Then a system of two degrees of freedom will be used to check the foundations. Figure 138-2 is the system under consideration and shows its schematic model for shock design purposes.

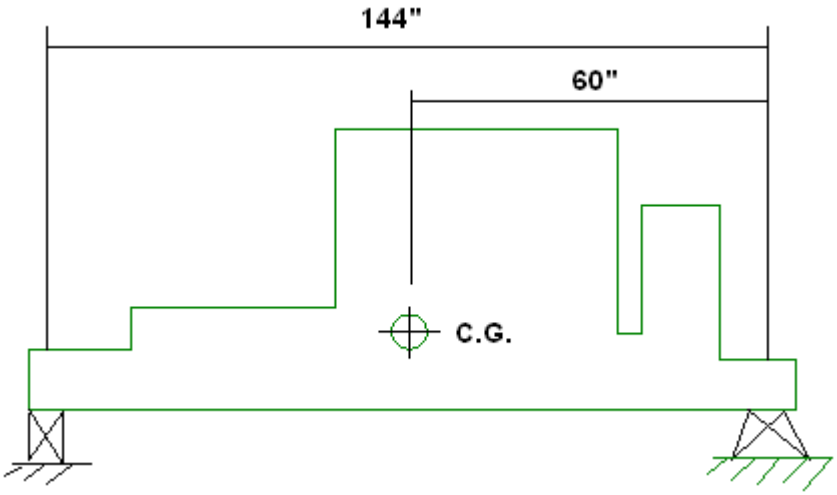

Figure 138-1. Rigid equipment.

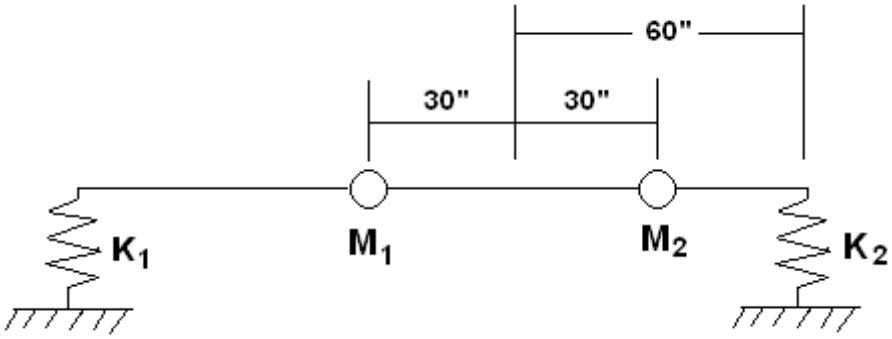

Figure 138-2. Considered system.

Theoretical Solution

First the moment of inertia I_g of the equipment was found about the center of gravity. Since only unidirectional motion is being considered, the "rigid" equipment was then divided into two equal masses that were located about the center of gravity such that $\sum_i M_i d_i^2 = I_g$, where d_i is the distance to the mass center from the center of gravity. Assume this is 30 inches. Then if the spring constants for the left and right hand foundations are, $K_1 = 1.3\times10^6$ lbs/in and $K_2 = 3.9\times10^6$ lbs/in, the normal node equations become:

$$\begin{Bmatrix} x_1 \\ x_2 \end{Bmatrix} = \frac{10^{-2}\,\omega^2}{386} \begin{bmatrix} 0.336539 & 0.176282 \\ 0.176282 & 0.194088 \end{bmatrix} \cdot \begin{bmatrix} 1 & 0 \\ 0 & 1 \end{bmatrix} \cdot \begin{Bmatrix} x_1 \\ x_2 \end{Bmatrix}$$

This matrix equation has two solutions:

Mode 1	Mode 2
$\omega_1^2 = 84753$	$\omega_2^2 = 513393$
$\omega_1 = 291.123$ rad/sec	$\omega_2 = 716.514$ rad/sec
$f_1 = 46.3$ cps	$f_2 = 114.0$ cps
$\bar{x}_{11} = 1.0$	$\bar{x}_{12} = 1.0$
$\bar{x}_{21} = 0.674506$	$\bar{x}_{22} = -1.482584$

The procedure outlined previously, along with that in the reference, is now followed.

Table 138-1. Mode 1 – Analysis Table

Mass	M_i	$\bar{x}_{i1}$	$M_i\bar{x}_{i1}$	$M_i\bar{x}_{i1}^2$	$M_i\bar{x}_{i1}\bar{P}_1D_1$
1	25.906736	1.0	25.906736	25.906736	69054 lbs
2	25.906736	0.674506	17.474249	11.786486	46577 lbs
		Σ	43.380985	37.693222	

$$\bar{P}_1 = \frac{43.360985}{37.693222} = 1.150896$$

$$\overline{W}_1 = \frac{386}{1000} \times 43.380985 \times 1.150895 = 19.272 \text{ kips}$$

The reference equations provide

$$A_{01} = 27.798\,g$$
$$V_{01} = 37.123\,\text{in/sec}$$

From Table V:
$$A_1 = 0.4\,A_0 = 11.119\,g$$
$$V_1 = 0.2\,V_0 = 7.425\,\text{in/sec}$$

Now
$$A_1 g = 4292\,\text{in/sec}^2$$
$$V_1\omega_1 = 2162\,\text{in/sec}^2$$

The lesser of these two values is $V_1\omega_1$, but this is less than $2316\,\text{in/sec}^2$, so $D_1 = 2316$.

To complete the table, please notice that $D_1\overline{P}_1 = 2665.475$, and proceed with column $M_i\overline{x}_{i1}\overline{P}_1 D_1$ to find the forces applied to each mass.

The displacement at each mass is:
$$\Delta_{11} = \frac{x_{11}D_1P_1}{\omega_1^2} = \frac{1.0\times 2665.475}{291.123^2} = 3.145\times 10^{-2}$$
$$\Delta_{21} = \frac{x_{21}D_1P_1}{\omega_1^2} = \frac{0.674506\times 2665.475}{291.123^2} = 2.121\times 10^{-2}$$

Table 138-2. Mode 2 – Analysis Table

Mass	M_i	$\overline{x}_{i1}$	$M_i\overline{x}_{i1}$	$M_i\overline{x}_{i1}^2$	$M_i\overline{x}_{i1}\overline{P}_1 D_1$
1	25.906736	1.0	25.906736	25.906736	-31794 lbs
2	25.906736	-1.482584	-38.408912	56.944438	47138 lbs
		Σ	-12.502176	82.851174	

$$\overline{P}_2 = \frac{-12.5021765}{82.851174} = -0.150899$$
$$\overline{W}_2 = \frac{386}{1000}\times(-0.150899)\times(-12.502176) = 0.728\,\text{kips}$$

The reference equations provide $\begin{cases} A_{02} = 107.490\,\text{g} \\ V_{02} = 56.754\,\text{in/sec} \end{cases}$

Using the factors of Table V produces $\begin{cases} A_2 = 0.4\,A_0 = 42.996\,\text{g} \\ V_2 = 0.2\,V_0 = 11.351\,\text{in/sec} \end{cases}$

Then D_2 is the lesser of $\begin{aligned} A_2 g &= 16596\,\text{in/sec}^2 \\ V_2 \omega_2 &= 8133\,\text{in/sec}^2 \end{aligned}$

Then $D_2 = 8133$ in/sec^2. Since it is greater than 2316 in/sec^2, it becomes the Shock Design Value. Then $D_2 \bar{P}_2 = -1227.262$ and the modal analysis table for mode 2 can be completed.

The displacement at each mass is:

$$\Delta_{12} = \frac{x_{12} D_1 P_1}{\omega_2^2} = \frac{1.0 \times (-1227.262)}{716.514^2} = -2.390 \times 10^{-3}$$

$$\Delta_{22} = \frac{x_{22} D_1 P_1}{\omega_2^2} = \frac{-1.482584 \times (-1227.262)}{716.514^2} = 3.544 \times 10^{-3}$$

The forces found by this method are used to design check the foundations. After the stresses in each mode for each of the foundations are found they are combined by the method in the later section.

Autodesk Simulation Solution

DDAM (Dynamic Design Analysis Method) is a restart analysis processor that calculates a combination of peak responses of given spectra through all considered frequency modes calculated by a previous modal analysis on the model. The user selects shock spectra based on ship type, mounting method, material type, and direction. The Naval Research Laboratory (NRL) combination method is used to determine the resultant response. By default, shock spectra are calculated using unclassified equations and coefficient that are "hard coded" into the DDAM application. It is also possible for the user to define the shock spectra using an ASCII format input file. A sample copy of this file is provided with the software. It can have an arbitrary name, but the provided file is called DDAM.DEF. This ASCII definition file can also be used to avoid the default English (inch based) units system.

A DDAM model that is equivalent to the example is shown in Figure 138-3:

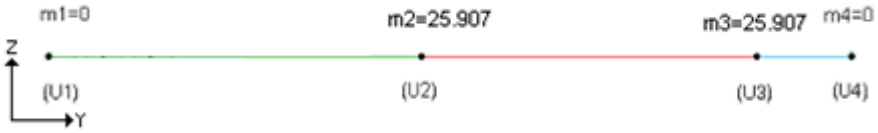

Figure 138-3. Model of the DDAM system.

Three massless beams were used for the structure with two lumped masses of 10,000/386 added at the appropriate locations. (Note: Although the modal analysis defaults to a gravity constant of 386.4, the gravity value for DDAM can be set to 386.0 to match the hand calculation.) Because the rigidity of the structure is not part of the hand solution, the beam element properties were made "rigid" (A=100, I_2=I_3=1000, E=12x10^{10}). The end nodes were fixed in X and Y translation and Y and Z rotation, while node 1 and node 4 are constrained by elastic boundary elements in the Z direction. Ty and Tx might be considered too but they will not make too much different because the model is a one-dimensional problem. The DDAM analysis gives:

Mode	Frequency	% of Total Mass	Participation	Direction
1	46.3	96.36	7.0659	Z
2	114.0	3.64	-1.3737	Z

Note that all participation factors in Rx get dropped because they are too small (relative values to the maximum participation factor are less than 10^{-6}). The eigenvector sets from the modal analysis are different from the ones used in hand calculations above. The ones DDAM gets from the modal analysis are normalized by mass matrix, i.e., generalized mass is unit, $X_\alpha^T M X_\alpha = 1$. So the participation factors in DDAM are different from what are used in hand calculations too. In fact participation factors, P_a is calculated by

$$\overline{P}_\alpha = \frac{\sum_{i=1}^{n} M_i \overline{X}_{i\alpha}}{\sum_{i=1}^{n} M_i \overline{X}_{i\alpha}^2}$$

If we replace the eigenvector X_α by Y_α = s* X_α, then P_a will vary by 1/s, too. But since the responses are calculated by multiplying the participation factor by the design value times the eigenvector, the scale s will cancel 1/s from the participation factor in Y_α. So the response should be same even though the eigenvector scale is different.

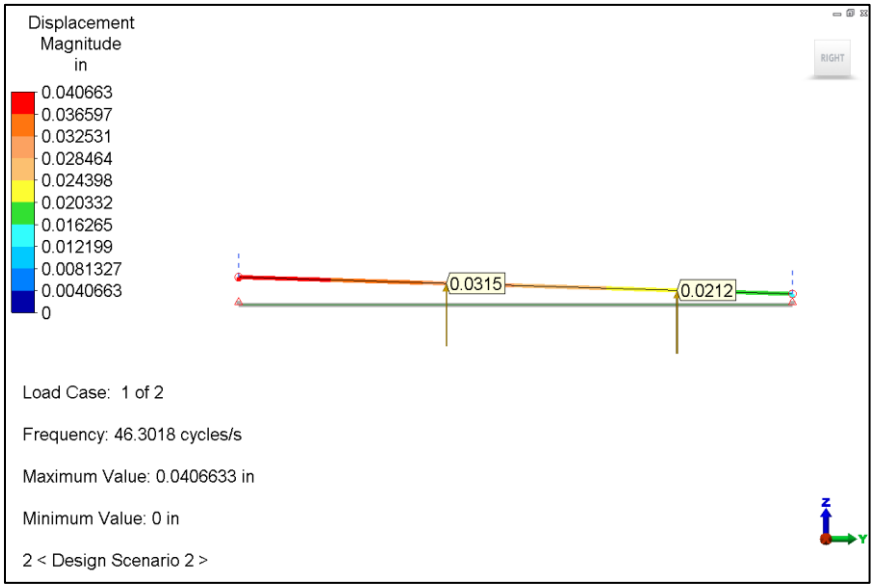

Figure 138-4. Displacement results for mode 1.

Where {U1, U2, U3, U4}$_{a=1}$ = {0.0406, 0.0315, 0.0212, 0.0161}.

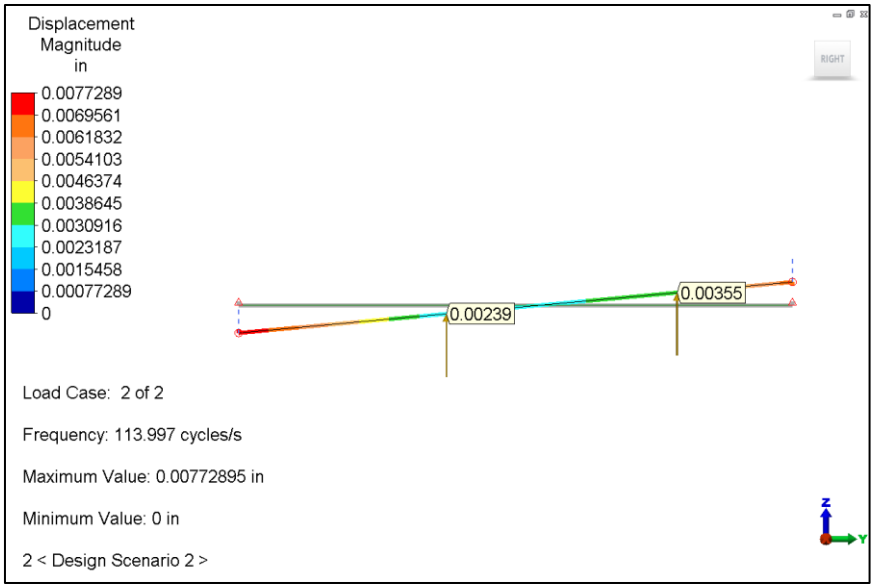

Figure 138-5. Displacement results for mode 2.

Where $\{U1, U2, U3, U4\}_{\alpha=2} = \{-0.00773, -0.00239, 0.00355, 0.00651\}$.

Table 138-3. Comparison of Results

Mode	Value	Theory	Analysis	% Difference
1	Δ_{11}	0.03145	0.0315	0.16
1	Δ_{21}	0.02121	0.0212	-0.05
2	Δ_{12}	-2.39E-3	-0.00239	0.0
2	Δ_{22}	3.544E-3	0.00355	0.17

AVE - 139 DDAM Shock Analysis of a Ship's Rudder System

Reference

"Shock Design Criteria for Surface Ships", Naval Sea Systems Command, NAVSEA 0908-LP-000-3010, Rev. 1, Appendix I, May 1976.

Problem Description

The rudder system of a surface ship is supported vertically at the deck level by the upper bearing housing (see Figure 139-1). The rudder is secured to the rudder stock by the carrier key. This means that the flexibilities to be considered are in the bearing housing and foundation, the rudder stock and the rudder carrier key. Hence, the system can be modeled as an elastic mass-spring system shown in Figure 139-2.

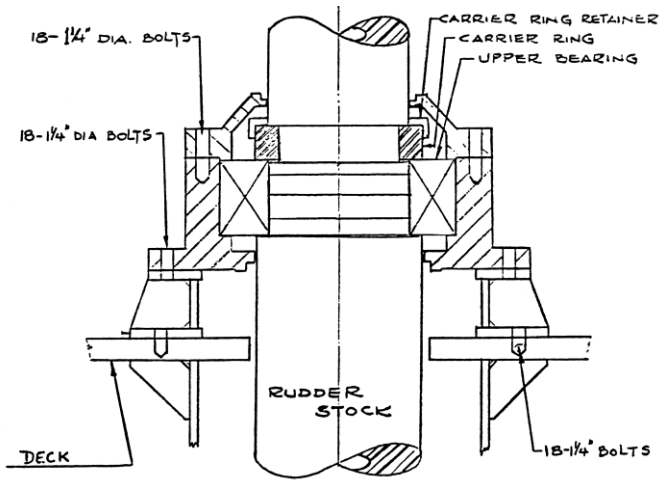

Figure 139-1. Diagram of the vertical rudder system.

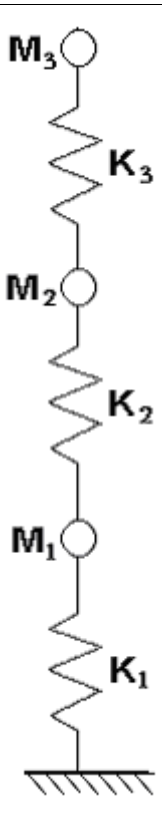

Figure 139-2. 3-mass, vertical rudder system.

Theoretical Solution

The mass assignments are as follows. For the spring-mass system shown in Figure 139-2, mass 1 includes:

Table 139-1. Weight of mass 1.

Mass 1	**Weight (lb_f)**
Crosshead	5,200
Upper bearing	500
½ Foundation (upper bearing)	315
Carrier ring, retainer and seal	143
Upper bearing housing	1785
Upper ½ of rudder stock	7413
Total	15,356

Converting to mass units,

$M_1 = 15{,}356 / 386.4 = 39.742\ lb_f\ sec^2 / in$

Mass 2 is the rudder stock (lower half), which weighs 7,413 lb_f. Hence,

$M_2 = 7{,}413 / 386.4 = 19.185\ lb_f\ sec^2 / in$

Finally, mass 3 includes the rudder and rudder hub casting, which weighs 11,500 lb_f. Therefore,

$M_3 = 11{,}500 / 386.4 = 29.762\ lb_f\ sec^2 / in$

The total model weight is 34,269 lb_f.

Stiffness K_1 comes from serial combination of the upper bearing housing stiffness K_H and the foundation stiffness K_F so that, since $K = \frac{AE}{L}$,

$$K_H = \frac{0.7845\left(31^2 - 23.623^2\right)\times 30\times 10^6}{11.25} = 592.61\times 10^6\ lb_f / in$$

$$K_F = \frac{\left[0.7845\left(30^2 - 28.5^2\right) + \left(0.75\times 4\times 18\right)\right]\left(30\times 10^6\right)}{7.5} = 491.64\times 10^6\ lb_f / in$$

$$K_1 = \frac{1}{1/K_H + 1/K_F} = \frac{K_H\times K_F}{K_H + K_F} = \frac{592.61\times 491.64}{592.61 + 491.64} = 268.72\times 10^6\ lb_f / in$$

Stiffness K_2 is for the rudder stock so that,

$$K_2 = \frac{\text{Average Area} \times E}{\text{Length}} = \frac{300.835\left(30 \times 10^6\right)}{140} = 64.46 \times 10^6 \text{ lb}_f / \text{in}$$

Stiffness K_3 comes from the carrier key, which is a parallel combination of the stock stiffness and the casting stiffness on the left side (K_L) and the right side (K_R) so that,

$$K_L = \frac{34.7\left(12 \times 10^6\right)}{4.625} = 90.03 \times 10^6 \text{ lb}_f / \text{in}$$

$$K_R = \frac{39.075\left(12 \times 10^6\right)}{4.625} = 101.38 \times 10^6 \text{ lb}_f / \text{in}$$

$K_3 = K_L + K_R = 90.03\text{x}10^6 + 101.38\text{x}10^6 = 191.41\text{x}10^6$ lb$_f$ / in

Then, using the following definition of the ship:

Ship type: surface
Shock direction: vertical
Input: deck mount
Material: elastic

Final results are obtained from the reference as:

Mode 1

Frequency: $\omega_1 = 965.814$ rad/sec, $f_1 = 153.75$ cps

Participation Factor $P_1 = 1.18603$

Modal Effective Mass $M_1 = 63.5876$, 71.6238% of total mass

Modal Effective Weight $W_1 = 24.5448$ kips

Table 139-2. Results for Mode 1.

Mass	M_i	Displacement (in)	Force (lbs)
1	39.752	2.21989E-3	82376.9
2	19.205	1.01959E-2	182652.0
3	29.793	1.19276E-2	331478.0

Mode 2

Frequency: ω_2 = 2870.56 rad/sec, f_2 = 456.972 cps

Participation Factor P_2 = 0.767363

Modal Effective Mass M_2 = 25.0237, accumulated 99.8099% of total mass

Modal Effective Weight W_2 = 9.65914 kips

Table 139-3. Results for Mode 2.

Mass	M_i	Displacement (in)	Force (lbs)
1	39.752	1.49736E-3	490847.0
2	19.205	1.24543E-4	19709.1
3	29.793	-4.4074E-4	-108201.0

Mode 3

Frequency: ω_3 = 4353.13 rad/sec, f_3 = 692.986 cps

Participation Factor P_3 = 7.76597E-2

Modal Effective Mass M_3 = 0.163735, accumulated 100.0% of total mass

Modal Effective Weight W_3 = 0.163735 x 386.4 = 63.20171 lb_f
63.20171 / 1000 = 6.320171e-2 kips

Table 139-4. Results for Mode 3.

Mass	M_i	Displacement (in)	Force (lbs)
1	39.752	2.98639E-5	22513.1
2	19.205	-1.94902E-4	-70930.5
3	29.793	9.99739E-5	56442.2

NRL Combined Displacements

Table 139-5. Results for NRL Combined Displacements

Mass	Displacement (in)
1	3.718E-3
2	1.0427E-2
3	1.2379E-2

Mode 2 Forces = 490847.0
+ 19709.1
- 108201.0
402355.1

$$\frac{P}{A} = \frac{402355.1}{(18)0.969} = 23068.17\,psi$$

Autodesk Simulation Solution

DDAM (Dynamic Design Analysis Method) is a restart analysis processor that calculates a combination of peak responses of given spectra through all considered frequency modes calculated by a previous modal analysis on the model. The user selects shock spectra based on ship type, mounting method, material type, and direction. The Naval Research Laboratory (NRL) combination method is used to determine the resultant response. By default, shock spectra are calculated using unclassified equations and coefficient that are "hard coded" into the DDAM application. It is also possible for the user to define the shock spectra using an ASCII format input file. A sample copy of this file is provided with the software. It can have an arbitrary name, but the provided file is called DDAM.DEF. This ASCII definition file can also be used to avoid the default English (inch based) units system.

For the rudder system model, to satisfy the equation,

$$K = \frac{AE}{L}$$

assume the following:

- A = 1
- L = 1
- $E_i = K_i$

An DDAM model that is equivalent to the example is shown in Figure below.

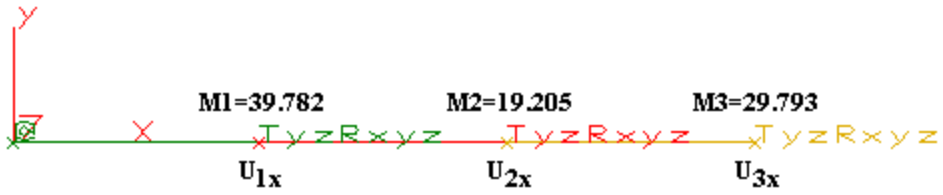

Figure 139-3. Three mass model.

At each node, *Tx* is the only degree of freedom considered as unknown while node 1 is fully fixed. Modal analysis (by the Linear Mode Shapes and Natural Frequencies processor) gives:

Table 139-6. Modal analysis results.

Mode	Frequency	Modal Effective Mass	% of Total Mass	Participation
1	153.7141	0.64E02	71.62	0.7974E01
2	456.8640	0.25E02	28.19	0.5002E01
2	692.8220	0.17E00	0.19	0.4108E00

Notice that all participation factors are different from hand-calculations above because DDAM uses SSAP1 eigenvectors that are normalized by mass matrix, i.e. their generalized mass is unit, $X_\alpha^T M X_\alpha = 1$. The eigenvector sets used in fact are,

$$\boldsymbol{X}_I = \begin{matrix}\{2.768147381977E\text{-}02\}\\ \{1.271395959713E\text{-}01\}\\ \{1.487343220827E\text{-}01\},\end{matrix} \quad \boldsymbol{X}_{II} = \begin{matrix}\{1.534000376710E\text{-}01\}\\ \{1.275904251113E\text{-}02\}\\ \{-4.515254351314E\text{-}02\},\end{matrix} \quad \boldsymbol{X}_{III} = \begin{matrix}\{2.896826084630E\text{-}02\}\\ \{-1.890568794670E\text{-}01\}\\ \{9.697567444345E\text{-}02\}\end{matrix}$$

In the DDAM "Analysis Parameters" screen, on the "General" tab, the "Shock uses" field is set to "Vertical spectrum only". On the "Advanced" tab, its "Spectrum Coordinate Directions" are set as X. Also in the DDAM "Analysis Parameters" screen, on the "General" tab, we set "Type of ship" as "Surface", "Mounting Locations" as "Attached to deck", and "Type of material" as "Elastic". Then results are obtained:

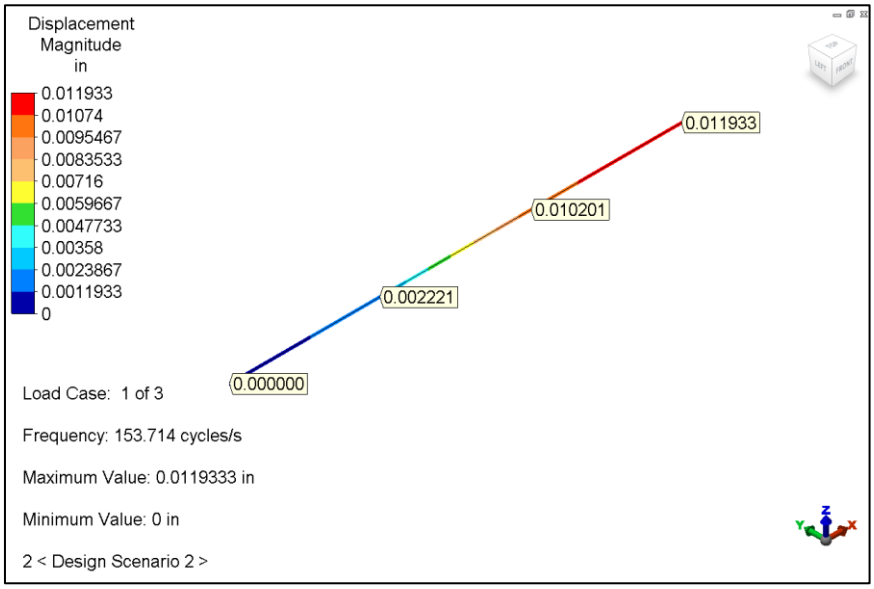

Figure 139-4. Displacements for mode 1.

where $\{U_{1x}, U_{2x}, U_{3x}\}_{a=1}$={2.220951663958E-03, 1.020071760145E-02, 1.193331476019E-02}, notice they match hand-calculated results in table 2.

Table 139-7. Comparison of displacement results for mode 1.

Mass	Theory	Analysis	% Difference
1	2.21989E-3	2.220952E-3	0.47%
2	1.01959E-2	1.02007E-2	0.047%
3	1.19276E-2	1.19333E-2	0.048%

Response of mode 2:

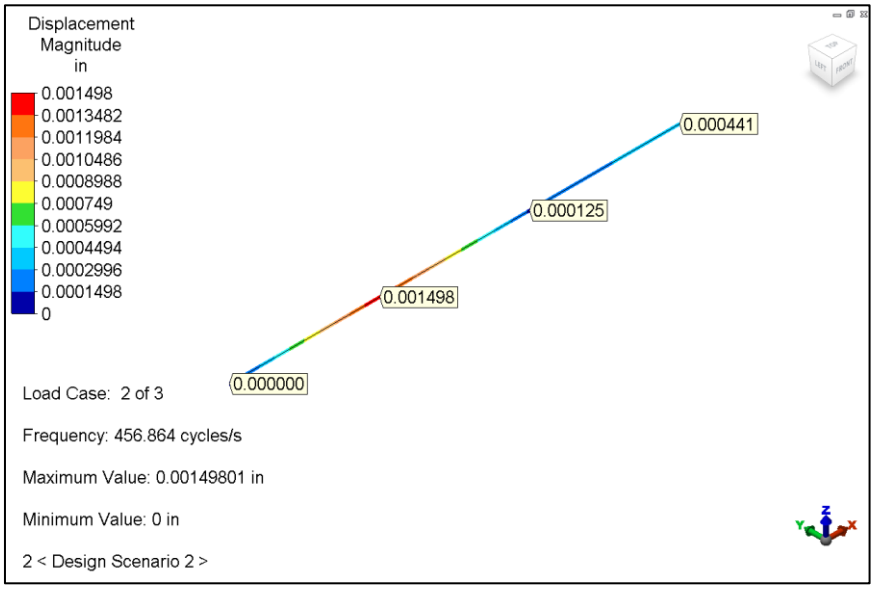

Figure 139-5. Displacements for mode 2.

Where $\{U_{1x}, U_{2x}, U_{3x}\}_{a=2}$ = {1.498006079610E-03, 1.245966007692E-04, -4.409306915399E-04}, they match hand-calculation results in table 3.

Table 139-8. Comparison of displacement results for mode 2.

Mass	Theory	Analysis	% Difference
1	1.49736E-3	1.498E-3	0.04%
2	1.24543E-4	1.246E-2	0.05%
3	-4.4074E-4	-4.409E-2	-0.13%

Response of mode 3:

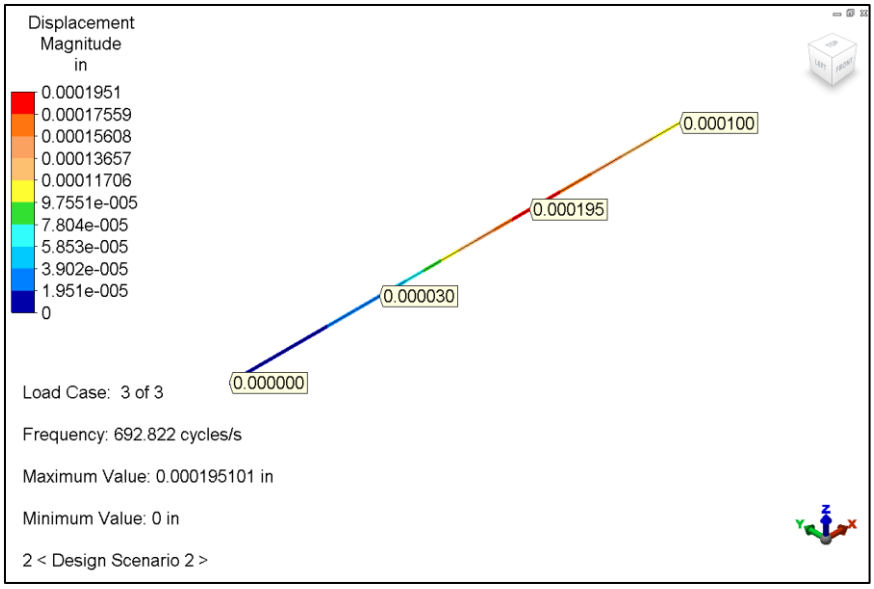

Figure 139-6. Displacements in mode 3.

Where $\{U_{1x}, U_{2x}, U_{3x}\}_{a=3}$ = {2.989439189336E-05, -1.951011306791E-04, 1.000760394736E-04}, they match hand-calculation results in table 4.

Table 139-9. Comparison of displacement results for mode 3.

Mass	Theory	Analysis	% Difference
1	2.98539E-5	2.989E-5	0.12%
2	-1.94902E-4	-1.951E-4	-0.06%
3	9.99739E-5	1.001E-4	0.13%

Then, the NRL combined response is as follows:

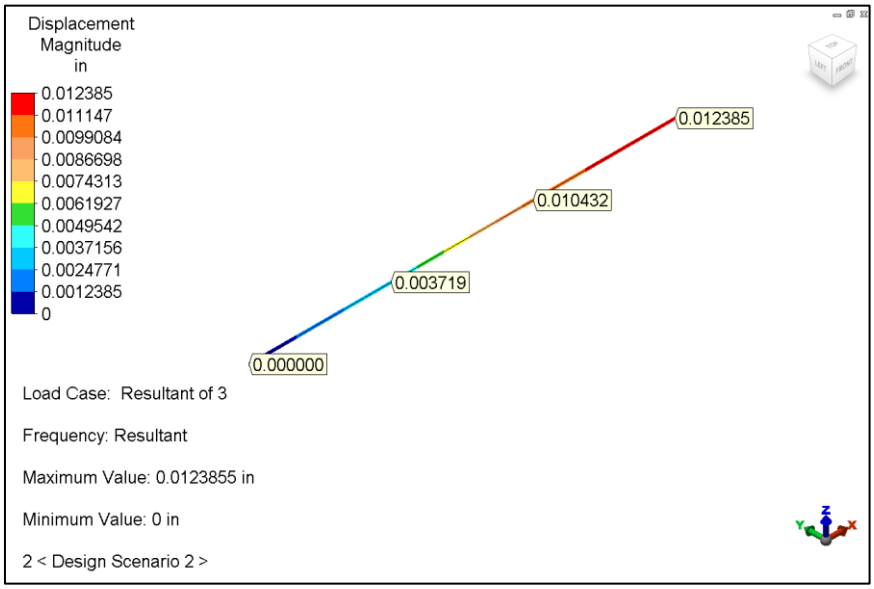

Figure 139-7. NRL combined displacements.

Where $\{U_{1x}, U_{2x}, U_{3x}\}_{comb}$ = {3.719E-3, 1.043E-2, 1.239E-2}.

Table 139-10. Comparison of NRL combined displacement results.

Mass	Theory	Analysis	% Difference
1	3.718E-3	3.719E-3	0.03%
2	1.0427E-2	1.043E-2	0.03%
3	1.2379E-2	1.239E-2	0.09%

AVE - 140 Pressure Drop in a Straight Pipe

Reference

White, Frank M., *Fluid Mechanics*, Third Edition, McGraw-Hill, Inc., 1994, page 311.

Problem Description

Determine the pressure drop from frictional losses for a 10" long straight pipe with a 2" diameter. The flow is fully developed at the inlet and the parabolic velocity profile has a maximum velocity of 1 in./sec. at the center (see Figure 140-1).

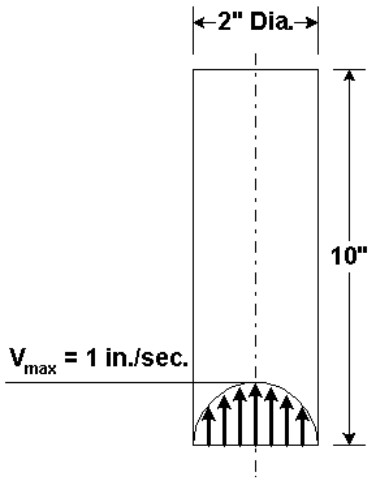

Figure 140-1. Overall dimensions of the pipe.

Theoretical Solution

The input variables are listed as follows:

- D = 2 in. (Diameter of Pipe)
- L = 10 in. (Length of Pipe)
- ρ = 9.34e-5 lb_m/in^3 (Fluid Mass Density)
- μ = 9.34e-5 lb_f*sec^2/in (Fluid Dynamic Viscosity)
- V_{max} = 1 in./sec (Maximum Fluid Velocity)

The first step is to calculate the Reynold's number in order to determine whether the flow is turbulent or laminar in nature.

$$R_e = \frac{\rho V D}{\mu} = 2$$

A Reynold's number of 2 indicates that the flow is laminar. The following formula provides the pressure drop for laminar flow in a circular pipe:

$$\Delta P = \frac{32 * \mu * L * V_{avg}}{D^2} = .003736 \frac{lb_f}{in^2}$$

where

$$V_{avg} = \frac{V_{max}}{2} = 0.5 \frac{in}{sec}$$

Autodesk Simulation Solution

The pipe is modeled as a two-dimensional (2-D) axisymmetric problem (see Figure 140-2). The mesh is comprised of 320 elements, with 8 elements in the radial direction (Y) and 40 elements in the axial direction (Z). An arithmetic ratio of 3 was used for the mesh spacing in the radial direction to refine the mesh at the outer wall in order to accurately capture the frictional losses.

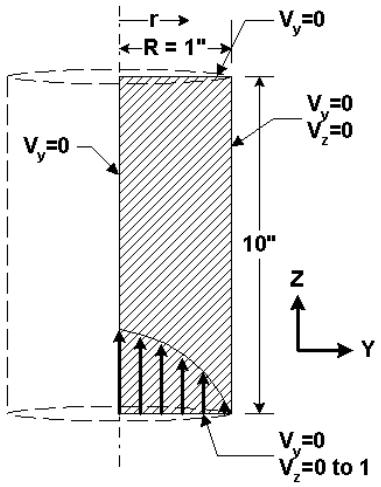

Figure 140-2. FEA model.

The prescribed velocities in the axial direction (Z) for the nine nodes at the inlet, which has a parabolic velocity profile for the fully developed flow, were calculated using the following formula:

$$V_r = V_{max} * \left(1 - \frac{r^2}{R^2}\right)$$

This formula provides the velocity (V_r) for any node based on its position (r) along the radius (R) (see Figure 140-2). The calculated nodal velocities are listed in Table 140-1.

Table 140-1. Nodal Inlet Velocities.

Distance from Center (in.)	Velocity (in./sec.)
0.0	1.0
0.1875	0.967
0.3571	0.872
0.5089	0.741
0.6428	0.587
0.7589	0.424
0.8571	0.265
0.9375	0.121
1.0	0.0

The model was analyzed using the Steady Fluid Flow processor. The prescribed inlet velocity was ramped up from zero to full velocity using a load curve with ten steps. Pressure results are shown in Figure 140-3.

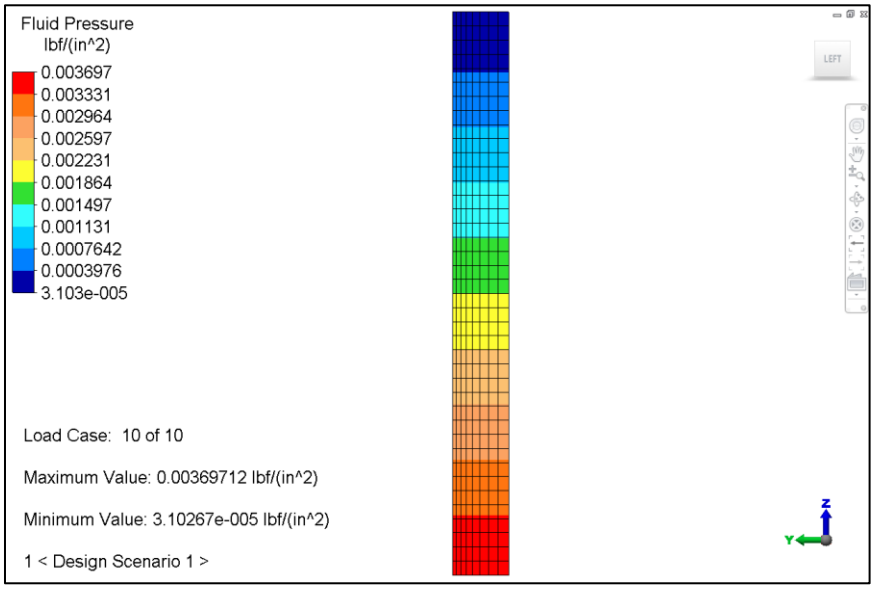

Figure 140-3. Pressure results.

Table 140-2 compares theoretical results to the analysis results.

Table 140-2. Comparison of Results.

Output	Theoretical	Analysis	% Difference
Pressure Drop (psi)	0.003736	0.003697	1.04%

AVE - 141 Linear Static Stress Analysis of a Laminated Strip

Reference

"NAFEMS Composite Benchmarks", NAFEMS, Reference R0031, Test No. R0031/1, Date/Issue 28.11.94/1.

Problem Description

A 1mm thick laminated strip, which is 50 mm long and 10 mm wide, is simply supported 10 mm inward from each end (see Figure 141-1). The strip is subjected to a 10 N/mm line load at the center. The material lay-up for the laminate is comprised of seven layers of the same orthotropic material in a 0/90/0/90/0/90/0 material orientation (see Figure 141-2). The middle layer is 0.4 mm thick while the outer six layers are 0.1 mm in thickness.

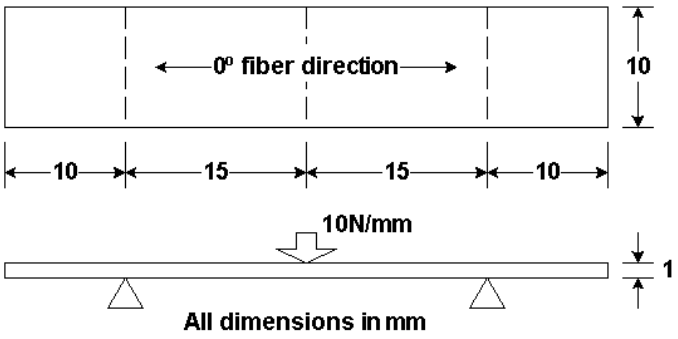

Figure 141-1. Overall dimensions of the laminated strip.

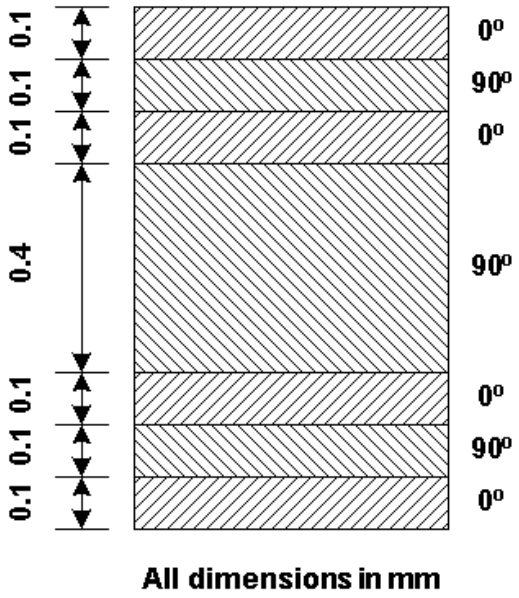

Figure 141-2. Material lay-up.

The orthotropic material properties are as follows:

E_1 = 1.0E5 MPa
E_2 = 5.0E3 MPa
G_{12} = 3.0E3 MPa
ν_{12} = 0.40
ν_{21} = 0.02 (calculated based on $\nu_{12}/E_1 = \nu_{21}/E_2$)

Theoretical Solution

There is no exact analytical solution for this problem. An approximation can be developed by modifying fundamental beam bending theory to include the effects of layered construction and shear loading. These equations are presented in Appendix A of the reference.

Autodesk Simulation Solution

A 10x50 grid of 500 thin composite elements was created in the XY plane in FEA Editor. Simply supported boundary conditions (TxyzRyz) were added at the designated locations. The line load was created by adding nodal forces of 10 N in the negative Z direction at the center nodes. Note that the 2 nodes at each end of the line load have a magnitude of 5 N (see Figure 141-3).

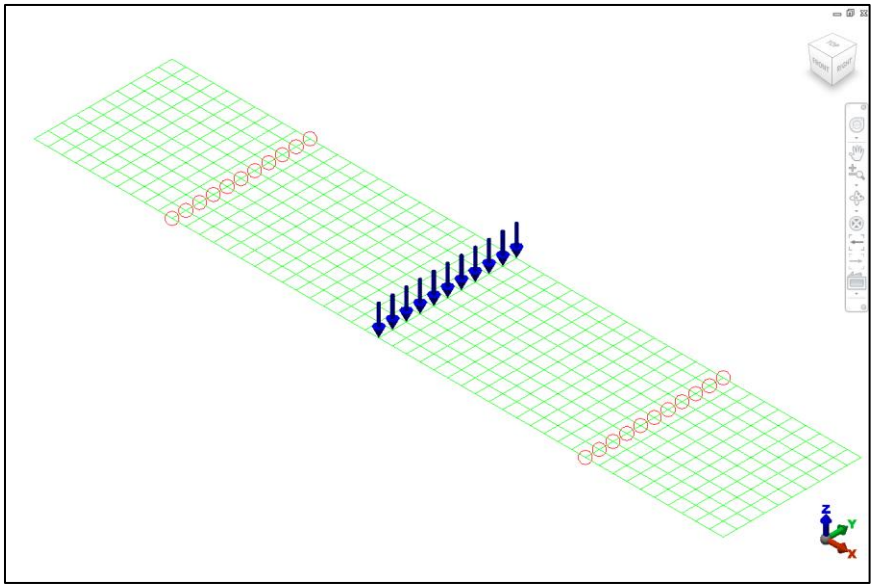

Figure 141-3. FEA model.

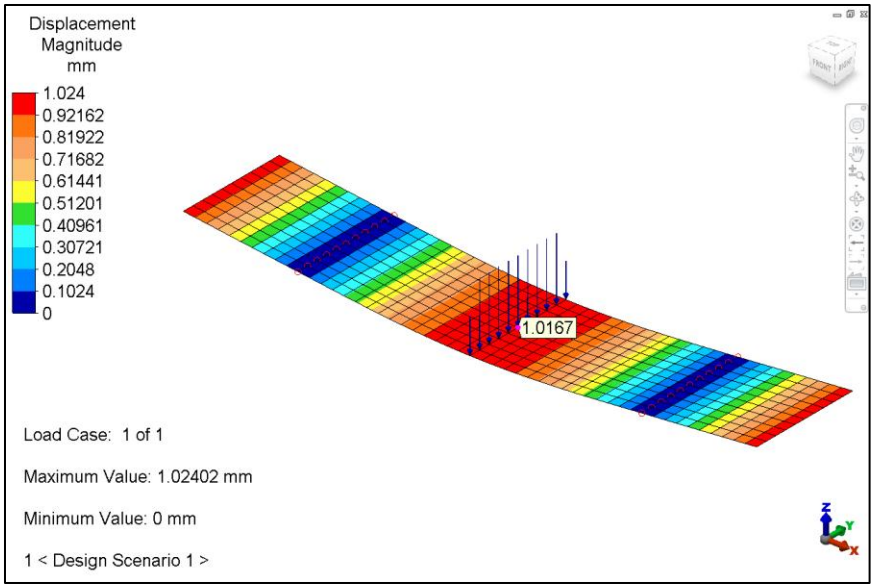

Figure 141-4. Displacement magnitude.

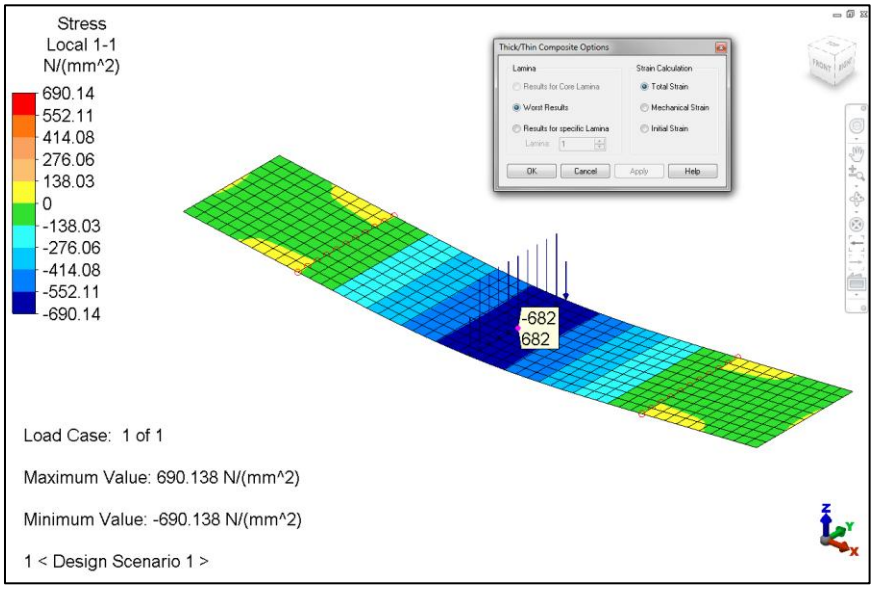

Figure 141-5. Composite stress in local 11 direction.

The reference provides only the results at the center node of the laminate strip, which corresponds to node #281 in the meshed model. Stresses in 1-1 direction (see Figure 141-5) are obtained by looking at the Composite stresses for the Local 11 direction. A comparison of the results is provided in Table 141-1.

Table 141-1. Comparison of Results.

Output at center node	NAFEMS	Analysis	% Difference
Displacement (mm)	-1.06	-1.02	3.7%
Stress (MPa)	683.9	680.1	0.056%

AVE - 142 Distance for Stopping a Car

Reference

Shames, Irving H., *Engineering Mechanics: Volume II Dynamics*, Third Edition, Prentice-Hall, Inc., 1980, page 509.

Problem Description

Determine the distance it takes to stop a 2895-lb weight traveling at 88 ft/s if the coefficient of friction between the weight and the concrete is 0.6.

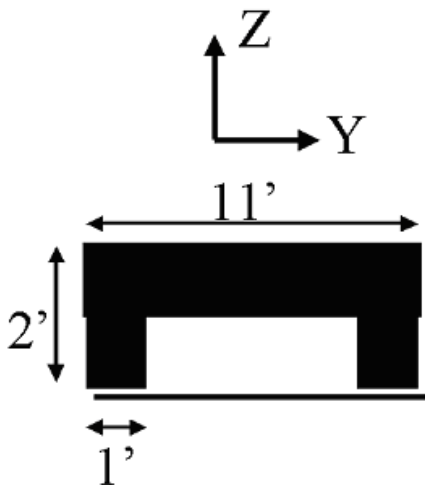

Figure 142-1. Diagram of the problem.

Theoretical Solution

The input variables are listed as follows:

- Weight of car (W) = 2895 lb
- Dynamic friction coefficient (μ) = 0.60
- Gravity (g) = 32.2 ft/s^2
- Initial velocity (v_{y1}) = 88 ft/s
- L = Stopping distance

$$\int_0^L F_y \, dy = \frac{m}{2}\left[v_{y2}^2 - v_{y1}^2\right]$$

$$L * W * \mu = \frac{W}{2 * g}\left[v_{y2}^2 - v_{y1}^2\right]$$

where

$$L * 2895 \text{ lb} * 0.6 = -\frac{2895 \text{ lb}}{2 * 32.2 \text{ ft/s}}\left[0 - 88^2\right]$$

$$L = 200.4 \text{ ft}$$

Autodesk Simulation Solution

The weight is modeled as a two-dimensional (2-D) plane stress problem. The mesh is comprised of 3 parts and a total of 123 elements. Part 1 is made of Aluminum. Part 2 has Steel A-36 material properties and Part 3 is considered to be concrete. Parts 1 and 2 are connected together while a 0.01-foot gap is between parts 1 and 3. Surface to surface contact was added between parts 1 and 3 with the specified friction coefficient.

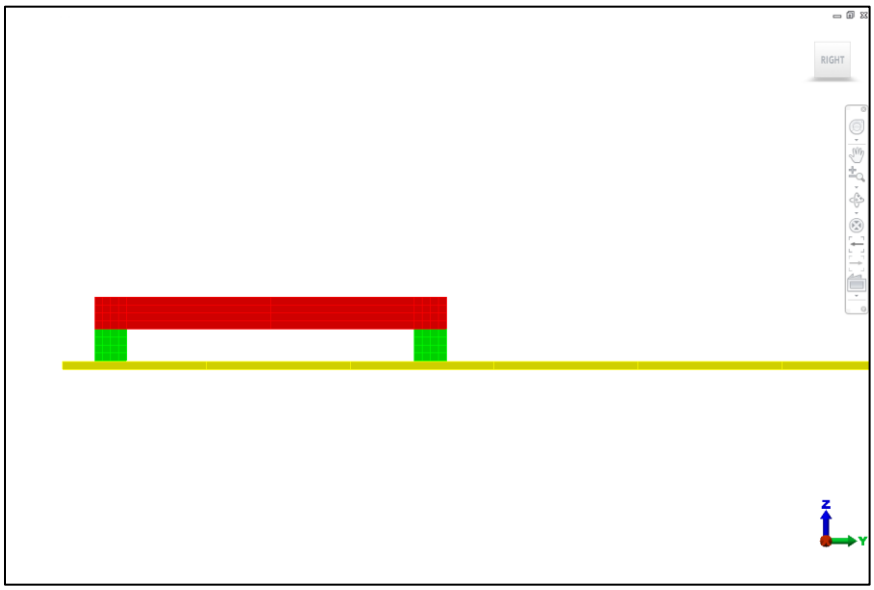

Figure 142-2. FEA model.

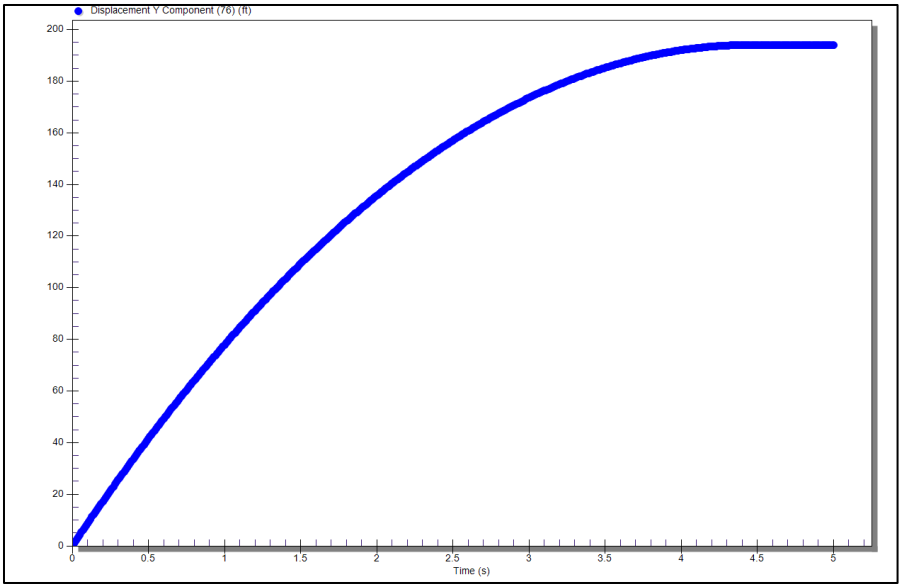

Figure 142-3. Graph Results

Table 142-1. Comparison of results.

Output	Theoretical	Analysis	% Difference
Length to stop	200.4 feet	194.02 feet	3.18 %

AVE - 143 Body-to-Body Radiation between Two Cylinders

Reference

Holman, J.P., *Heat Transfer*, Seventh Edition, McGraw-Hill Inc, 1990, pages 424-425.

Problem Description

Two concentric cylinders each have a length of 20 cm and diameters of 10 cm and 20 cm, respectively. The inner cylinder is maintained at a temperature of 1000 K. The inner cylinder has an emissivity of 0.8 and the outer cylinder has an emissivity of 0.2. The cylinders are in a room at 300 K. The outer cylinder is in radiant balance. Calculate the temperature of the outer cylinder.

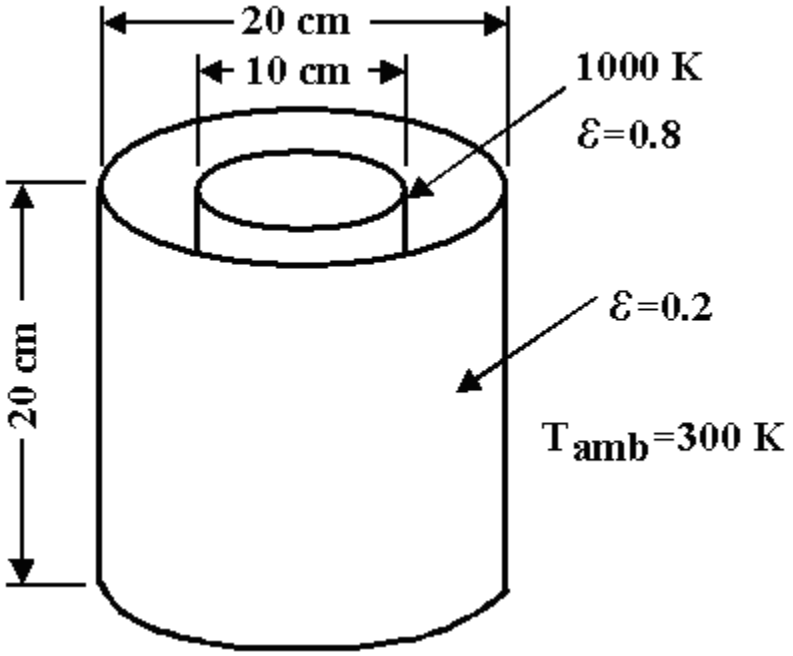

Figure 143-1. Overall dimensions of the cylinders.

Theoretical Solution

The problem is solved with the aid of the following network, where the inner cylinder is designated as body 1, the outer cylinder is designated as body 2, and the room is designated as body 3. The view factors between the bodies are calculated as follows:

- F_{12} = 0.86 (inner cylinder to outer cylinder)
- F_{13} = (2)(0.07) = 0.14 (inner cylinder to room)
- F_{23i} = (2)(0.12) = 0.24 (inside of outer cylinder to room)
- F_{23o} = 1.0 (outside of outer cylinder to room)

Also,

- $A_1 = 0.06283\ m^2$ (area of inner cylinder)
- $A_2 = 0.12566\ m^2$ (area of outer cylinder)
- $E_{b1} = (5.669 \times 10^{-8})(1000)^4 = 5.669 \times 10^4\ W/m^2$ (emissive power of inner cylinder)
- $E_{b3} = (5.669 \times 10^{-8})(300)^4 = 459.2\ W/m^2$ (emissive power of the room)

Solving the network as a series-parallel circuit yields three equations for node J_1, J_{2i} and J_{2o} gives the following results:

- $J_1 = 50{,}148\ W/m^2$
- $J_{2i} = 27{,}811\ W/m^2$
- $J_{2o} = 3498\ W/m^2$

From the network, the emissive power of the outer cylinder is the following:

$$E_{b2} = (J_{2i} + J_{2o})/2 = 15{,}655\ W/m^2$$

and

$$T_2 = (15{,}655 / 5.669 \times 10^{-8})^{1/4} = 724.9\ K \quad \text{[Answer]}$$

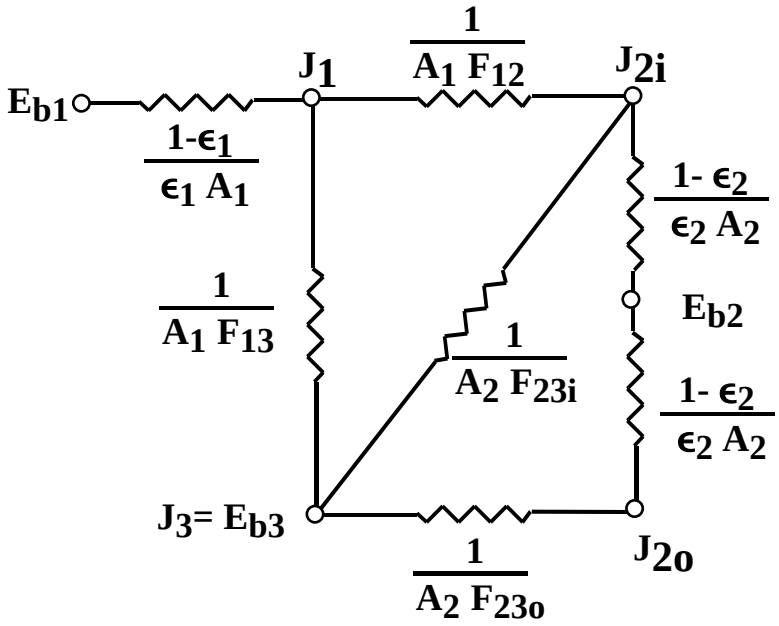

Figure 143-2. Radiation network for concentric cylinders.

Autodesk Simulation Solution

The cylinders are modeled using plate elements. A mesh of 40 elements around the perimeter and 10 elements along the length was created. The model was analyzed with the Steady-State Heat Transfer processor.

The theoretical example assumes that the outer cylinder is at a uniform temperature. In reality, the temperature would vary along the length because the view factor with the room and inner cylinder changes along the length. To compensate for this effect, a large conductivity (180E3 J/(s m K), or 1000 times as conductive as aluminum) was used for the cylinders.

The temperature of the inner cylinder was set by using a large convection coefficient (1E8 J/(s m^2 K)) at 1000 K. Body to body radiation was set for the radiation between the outside of the inner cylinder, the inside of the outer cylinder, and the room. To calculate a more accurate view factor between the closely spaced cylinders, the view factor calculation method was set to "string rule/contour integration". Radiation from the outside of the outer cylinder could also be handled with the body to body radiation, but it is more efficient to use the surface-based radiation since the view factor is known (1).

Since the model includes nonlinear effects (radiation), the "Advanced" tab of the "Analysis Parameters" screen was used to specify the iteration controls. The input used was the following:

- Criteria: Stop when corrective norm < E1 (case 1)
- Maximum number of iterations: 40
- Corrective tolerance: 0.1
- Relaxation parameter: 0.3

Also, to aid the convergence, the "Default nodal temperature" was set to 724.9 K, which is the expected temperature of the outer cylinder. An initial temperature of 1000 K was specified for the inner cylinder as its expected temperature.

The temperature results are shown in Figure 143-3.

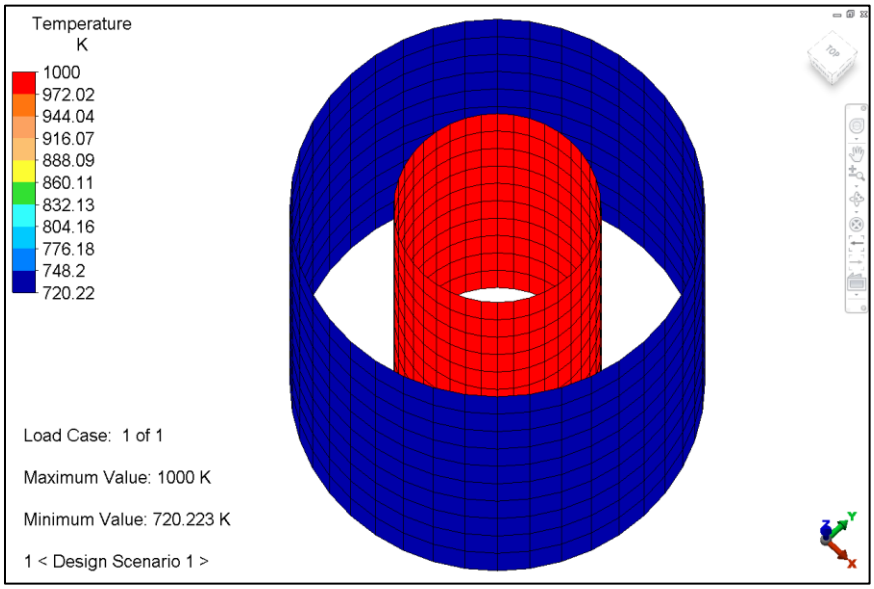

Figure 143-3. Temperature results.

Table 143-1. Comparison of results.

Output	Theoretical	Analysis	% Difference
Outer cylinder temperature (K)	724.9	720.2	-0.65%

AVE - 144 Nonlinear Displacement of a Bar with an Axial Load

Problem Description

Determine the displacement of a bar that has an axial load (4000 N) applied to it and has gone past the yield point of the material. The model will demonstrate nonlinear material capabilities.

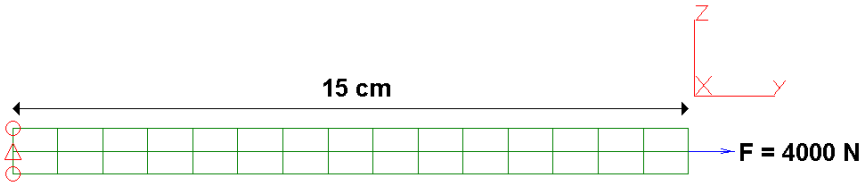

Figure 144-1. Diagram of the bar made of nonlinear material with an axial loading.

Theoretical Solution

The material and geometry properties are as follows:

- Modulus of Elasticity = 1e7 N/cm^2
- Poisson's Ratio = 0.3
- Strain Hardening Modulus = 1e5 N/cm^2
- Yield stress = 3000 N/cm^2
- Area = 1.0 cm^2

The theoretical solution will be based on the linear and nonlinear solution.

The linear solution using Hooke's law is:

$$F = k * x$$

solving for x

$$x = \frac{F}{k}$$

where

$$k = \frac{AE}{L}$$

The nonlinear solution is:

$$x_{nl} = \frac{LF_l}{AE_l} + \frac{LF_{nl}}{AE_{nl}}$$

When the force is equal to 3000 Newtons, the model is still in the linear range. The following shows the hand calculations:

Axial Displacement = (15cm* 3000 N)/(1cm^2*1e7 N/ cm^2)
Axial Displacement = 0.0045 cm

When the force is equal to 4000 Newtons, part of the model has yielded and now uses nonlinear material properties. The following shows the hand calculations:

Axial Displacement = (15cm* 3000 N)/(1cm^2*1e7 N/ cm^2)+(15*1000N)/(1cm^2*1e5 N/ cm^2)
Axial Displacement = 0.1545 cm

Autodesk Simulation Solution

The model is constructed using two-dimensional (2-D) plane stress elements. The mesh is made of 30 elements, with 15 elements in the axial direction (Y) and 2 elements in the vertical direction (Z). The material model chosen was von Mises with isotropic hardening. The force on the end of the model was applied as 0.5 Newtons on the top and bottom nodes and 1.0 Newton on the middle node. The total load of 4000 Newtons was achieved by scaling the load curve from 0 at time 0 seconds to 2000 at time 2 seconds. The analysis formulation for the 2-D elements was changed to nonlinear material only. Ty constraints were added to the top and bottom nodes on the left-hand side of the model. Ty and Tz constraints were added to the middle node on the left-hand side.

A Mechanical Event Simulation with Nonlinear Material Models was performed. The results for the model were captured at node number 47 as shown in Figure 144-2 and Figure 144-3. Table 144-1 shows a comparison of the analysis results and the theoretical solution.

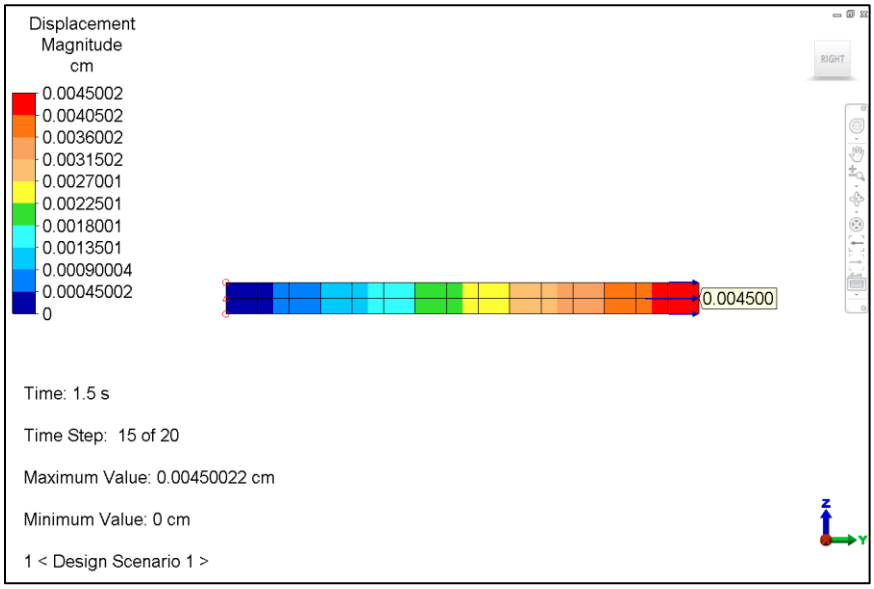

Figure 144-2. Displacement results at node 47 for time step = 15, which corresponds to force = 3000 N.

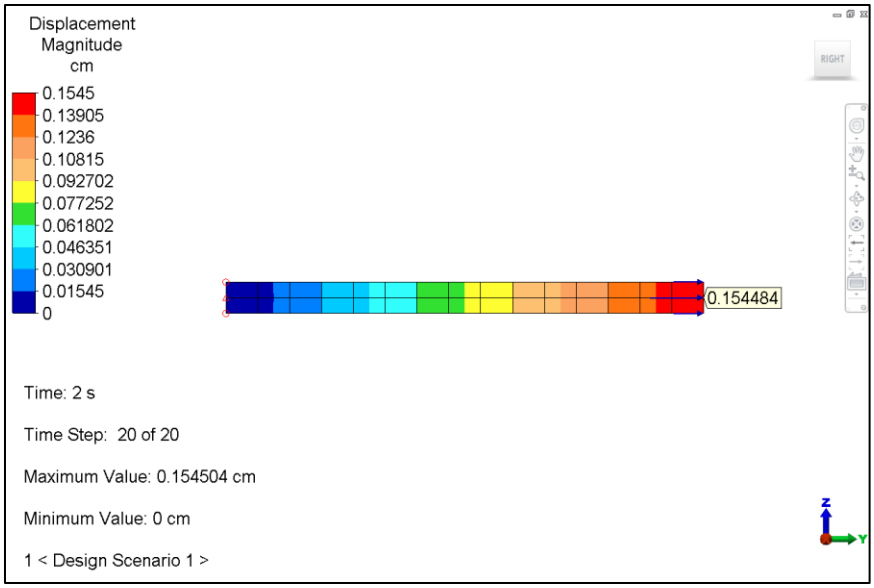

Figure 144-3. Displacement results at node 47 for time step = 20, which corresponds to force = 4000 N.

Table 144-1. Comparison of Results

Output			Displacement (cm)		% Difference
Node Number	Load Step	Force (N)	Analysis	Theoretical	
32	15	3000	0.0045	0.0045	0.00
32	20	4000	0.1545	0.1545	0.00

AVE - 145 Tapered Axisymmetric Thick Shell Subjected to a Pressure Load

Reference: *NAFEMS (C1 REV1) – Benchmarks Test for Various Finite Element Assemblies*, Glasgow, UK, November 1986, pp 13-15.

Problem Description

Determine the hoop stress of a tapered axisymmetric thick shell that has a pressure load of 100E6 N/m^2 applied to it.

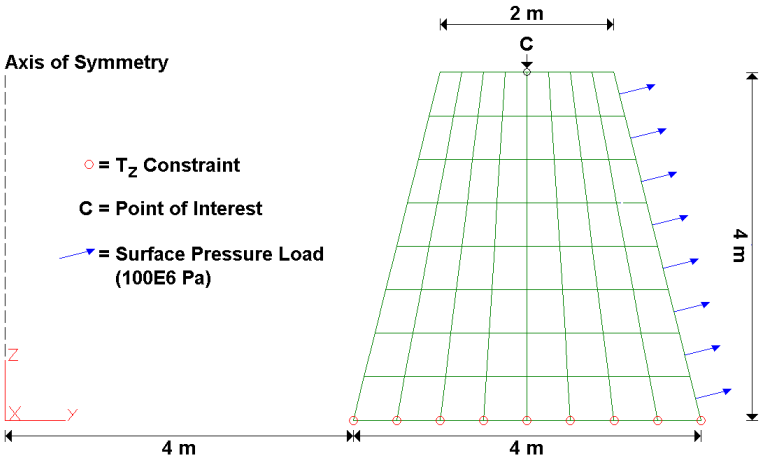

Figure 145-1. Diagram of the tapered axisymmetric thick shell problem.

The material and geometry properties are as follows:

- Modulus of Elasticity = 210e9 Pa
- Poisson's Ratio = 0.3
- Density = 7e3 kg/m^3

Reference Solution

The reference solution yielded the following result:

- Hoop stress at point C (labeled in Figure 145-1) = 2.28E8 Pa

Autodesk Simulation Solution

The model is made of two-dimensional (2-D) axisymmetric elements. The mesh consists of 64 elements, with 8 elements in the radial direction (Y) and 8 elements in the vertical direction (Z). The pressure of 100E6 N/m^2 was applied to the outside surface of the model. Boundary conditions of Tz were applied to the bottom of the model.

A Static Stress with Linear Material Models analysis was run. The hoop stress results for the model were examined by displaying the stress tensor in the X-X direction and inquiring on the results at node number 37 as shown in Figure 145-2.

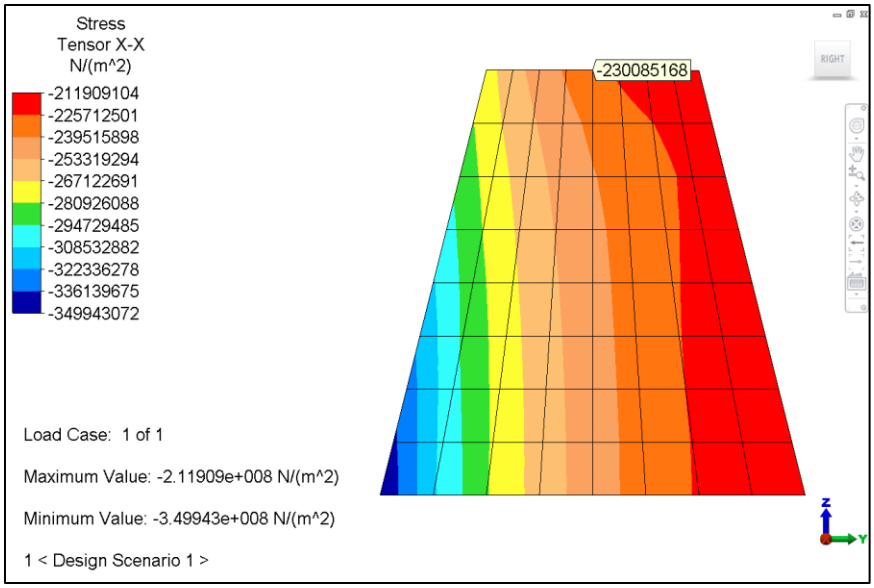

Figure 145-2. Hoop stress results displayed in the model.

The following table shows a comparison of the analysis results to the reference solution.

Table 145-1. Comparison of Results.

Node Number	Hoop Stress (Pa)		% Difference
	Analysis	Theoretical	
37	2.3E8	2.28E8	0.8

AVE - 146 Contact Pressure Analysis of a Punch-Foundation System

Reference

Feng, Q. and Prinja, N. K., *NAFEMS Benchmark Tests for Finite Element Modelling of Contact, Gapping and Sliding*, Ref: R0081, Issue: 1, CGS-1.

Problem Description

Calculate the contact pressure when a punch contacts the foundation. The punch and the foundation combine to make a 1.0-m cube. The entire bottom of the foundation is constrained in the vertical direction and the center node on the bottom of the foundation has all rotations and translations constrained. A pressure of Q = 40,000 N/m^2 is applied to the top of the punch.

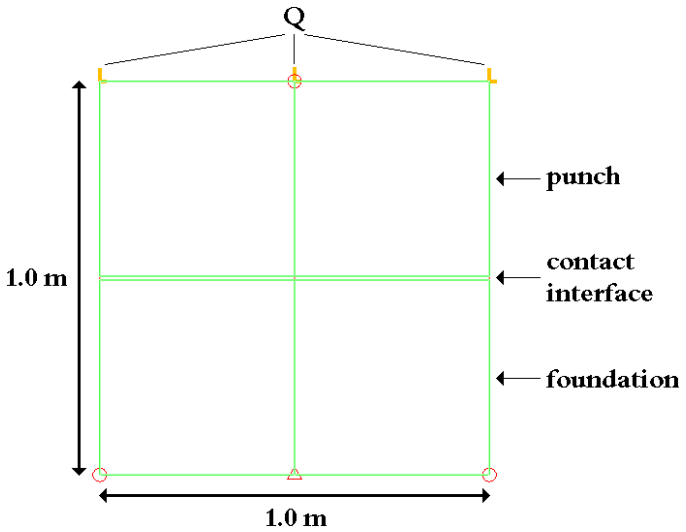

Figure 146-1. Diagram of the punch-foundation model.

The material properties are as follows:

- Modulus of Elasticity = E_{punch} = $E_{foundation}$ = 100 MPa
- Poisson's Ratio = ν_{punch} = $\nu_{foundation}$ = 0.3

Reference Solution

The reference solution yielded the following result:

- Applied pressure = contact pressure = 40,000 N/m^2

Autodesk Simulation Solution

The model was drawn in the YZ plane using 2D elements. The constraints as described in the problem description were applied. Additionally, the upper middle node of the punch was constrained from translation in the horizontal (Y) direction to provide additional stability. Gap elements were drawn between the punch and the foundation to facilitate calculation of the contact force. A pressure of 40,000 N/m^2 was applied to the top of the punch. A Linear Static Stress analysis was performed. Then, the inquire results capability was used to sum the forces in the three gap elements, which equaled -40,000 N.

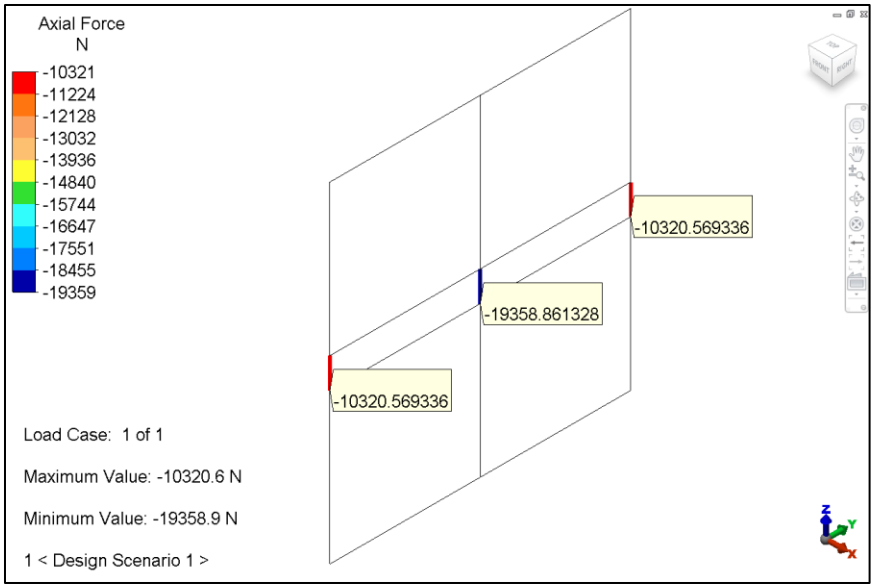

Figure 146-2. Sum of the contact forces.

Dividing the total force by the area of 1 m^2 gives a contact pressure of 40,000 N/m^2, which matches exactly the reference solution as shown in the following table.

Table 146-1. Comparison of results.

Contact Pressure (N/m^2)		% Difference
Analysis	**Theoretical**	
40,000	40,000	0.0

AVE - 147 Acceleration Analysis of a Piston-Crank Mechanism

Reference

Hibbeler, R.C., *Engineering Mechanics:Dynamics, (7th Edition)*, Prentice-Hall, Inc., 1995, p. 322.

Problem Description

Calculate the acceleration of point C of the piston-crank mechanism shown below if the rotational velocity of link AB is 10 rad/s (95.493 RPM), the rotational velocity of link BC is 2.43 rad/s (23.205RPM) and the geometry is known. Point C can only move in the vertical direction. There is no angular acceleration.

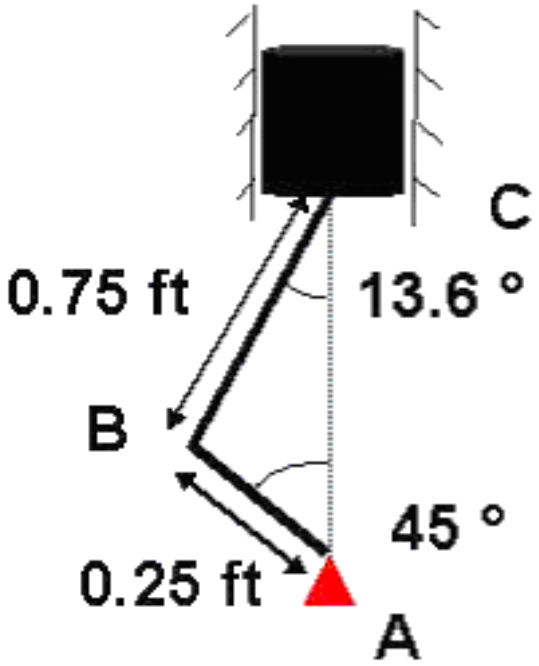

Figure 147-1. Diagram of the piston-crank mechanism.

Theoretical Solution

From the reference:

$$a_B = \alpha_{AB} \times r_{B/A} - \omega_{AB}^2 r_{B/A}$$
$$a_C = a_B + \alpha_{BC} \times r_{C/B} - \omega_{BC}^2 r_{C/B}$$

Using trigonometry, we can find horizontal (i) and vertical (j) components of the displacement vectors from point A to point B and from point B to point C.

$$r_{B/A} = \{-0.177\,i + 0.177\,j\}\ ft$$
$$r_{C/B} = \{0.176\,i + 0.729\,j\}\ ft$$

Solving for a_B,

$$a_B = \{17.7\,i - 17.7\,j\}\frac{ft}{s^2}$$

Solving for a_C,

$$a_C = \{-17.97\,j\}\frac{ft}{s^2}$$

Autodesk Simulation Solution

The mechanism was drawn in the XY plane using truss and beam elements. Point A was constrained in all three translations. Point B was constrained in the Z translation. Point C was constrained in the X and Z translations. Aluminum material properties were defined for all parts; however, the choice of material was arbitrary because inertial effects were not considered and mass was irrelevant for this purely kinematic analysis. A prescribed rotation of 1 rev magnitude was applied to point A by defining a load curve that ramped from 0 to –1.59155 in 1 second. A Mechanical Event Simulation with Nonlinear Material Models analysis was performed to analyze the motion of the piston-crank mechanism. The acceleration at 0.628 s, which is when the mechanism is at the location shown in Figure 147-1, is –18.046 ft/s for point C as shown in Figure 147-2.

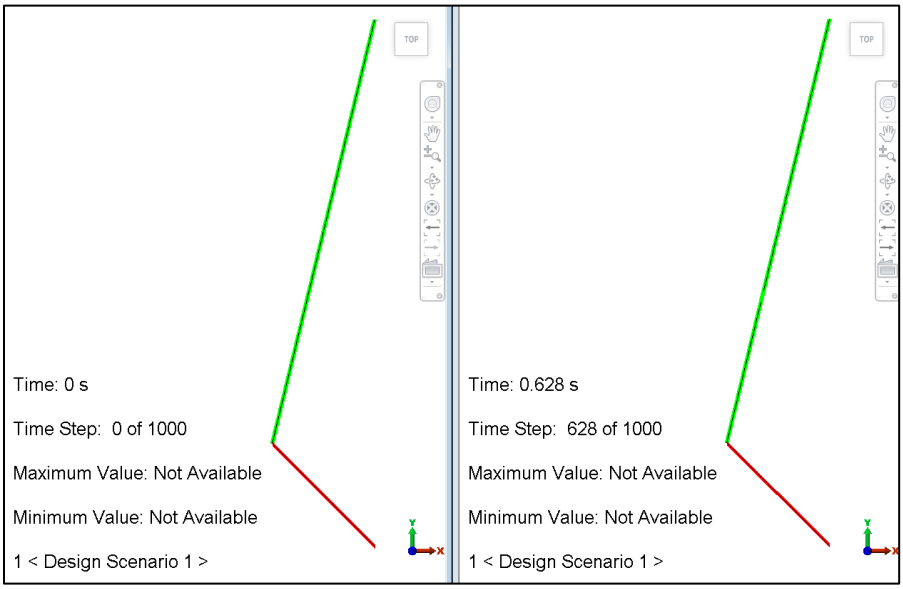

Figure 147-2. Position of point C at the time of interest.

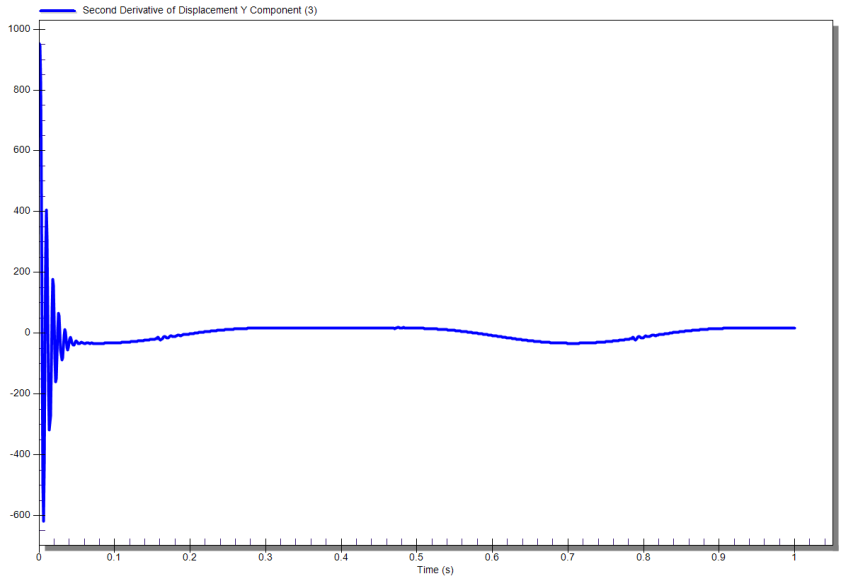

Figure 147-3. Acceleration of point C throughout the simulation.

Alternatively, the graph values can be saved as a Comma Separated Value output list and examined in a spreadsheet utility. Table 147-1 provides a comparison of the theoretical and analysis results.

Table 147-1. Comparison of Results.

Acceleration (ft/s^2)		% Difference
Theoretical	**Analysis**	
-17.97	-17.835	0.85

AVE - 148 Natural Frequencies Analysis of a Pin-Ended Double Cross Structure

Reference

Abbassian, F., Dawswell, D. J. and Knowles, N. C., *NAFEMS Free Vibration Benchmarks*, November 1987, Test 2, pp. 60-79

Problem Description

Calculate the first 16 natural frequencies of the double cross structure shown below. The ends of the beams are pinned, each arm is 5.0m long and the cross section of each beam is a 0.125m x 0.125m square.

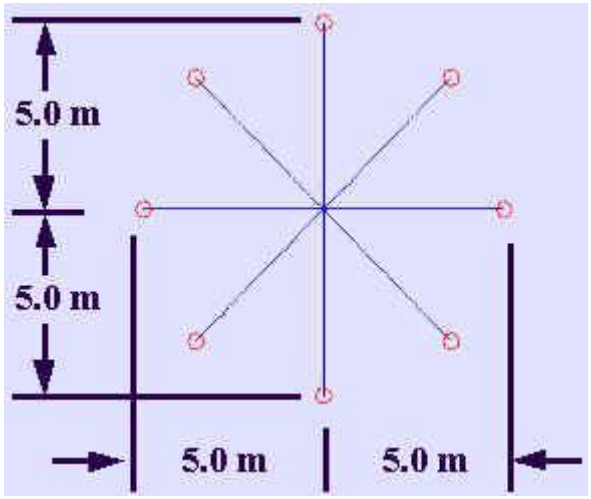

Figure 148-1. Schematic of the pin-ended double cross structure.

Material properties are as follows:

- Modulus of elasticity (E) = 200 x 10^9 N/m^2
- Poisson's ratio = 0.3
- Mass density (ρ) = 8000 kg/m^3

Theoretical Solution

The classical beam theory prediction of the natural frequencies is given by:

$$f_1 = \frac{\lambda i^2}{2\pi L^2}\left(\frac{EI}{\rho A}\right)^{\frac{1}{2}}$$

Autodesk Simulation Solution

The model was drawn in the XY plane using beam elements. The ends of the beams were constrained in all translations. The rest of the nodes were constrained in the Z translation. A Linear Mode Shapes and Natural Frequencies analysis was performed and the natural frequencies were obtained as shown in Figure 148-2.

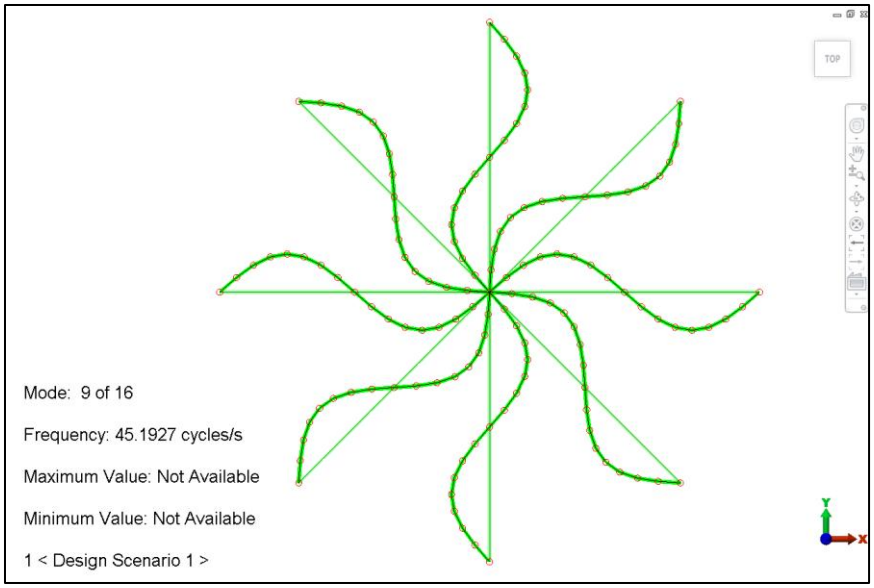

Figure 148-2. Natural frequency and mode shape for mode 9.

Below is a table comparing the analysis results to the reference results.

Table 148-1. Comparison of Results.

Mode Number	NAFEMS (Hz)	Analysis (Hz)	% Difference
1	11.336	11.325	0.09
2	17.709	17.639	0.39
3	17.709	17.639	0.39
4	17.709	17.666	0.25
5	17.709	17.668	0.23
6	17.709	17.668	0.23
7	17.709	17.668	0.23
8	17.709	17.670	0.22
9	45.345	45.193	0.34
10	57.39	56.741	1.13
11	57.39	56.741	1.13
12	57.39	57.044	0.60
13	57.39	57.052	0.59
14	57.39	57.052	0.59
15	57.39	57.052	0.59
16	57.39	57.059	0.58

AVE - 149 Electrostatic Field Strength Analysis of a Spherical Electron Cloud

Reference

Pohang University of Science and Technology, *Example Problems on Electrostatic Field*, pp. 9-10

Problem Description

Calculate the electrostatic (E) field caused by a spherical cloud of electrons with a volume charge density $\rho = -\rho_0$ for $0 \leq R \leq b$ (both ρ_0 and b are positive) and $\rho = 0$ for $R < b$.

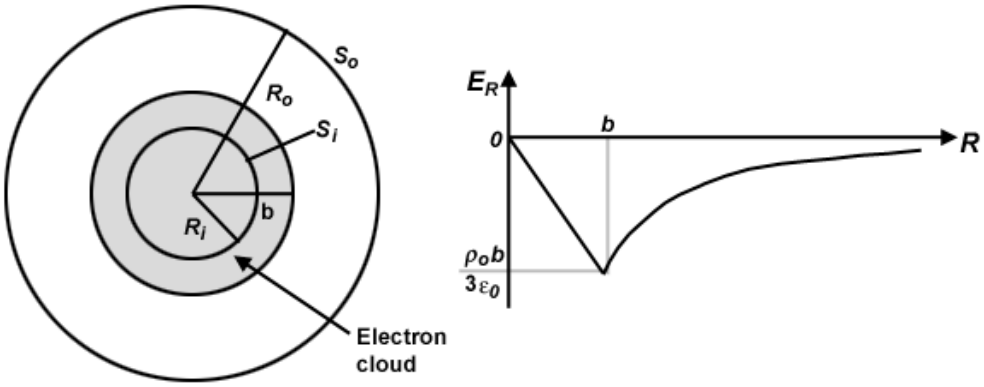

Figure 149-1. Electric field intensity of a spherical electron cloud.

Theoretical Solution

From the reference, the following assumptions are made:

- spherical symmetry
- the Gaussian surfaces must be concentric spherical surfaces

There are two cases to solve for:

1. $0 \leq R \leq b$
2. $R > b$

Case 1: $0 \leq R \leq b$

The outward E flux can be expressed as:

$$\int_{S_i} \underline{E} \cdot ds = E_R \int_{S_i} ds = E_R \, 4\pi R^2$$

The total enclosed charge is:

$$Q = \int_V \rho d\upsilon = -\rho_0 \int_V d\upsilon = -\rho_0 \frac{4\pi}{3} R^3$$

Substituting gives us:

$$E = -\frac{\rho_0}{3\varepsilon_0} R,\ 0 \le R \le b$$

Case 2: R > b

The outward E flux can be expressed as:

$$\int_{S_0} \underline{E} \cdot d\underline{s} = E_R \int_{S_0} d\underline{s} = E_R\ 4\pi R^2$$

The total enclosed charge is:

$$Q = -\rho_0 \frac{4\pi}{3} b^3$$

Substituting gives us:

$$E = -\frac{\rho_0 b^3}{3\varepsilon_0 R^2},\ R \ge b$$

Autodesk Simulation Solution

A two-dimensional (2-D) axisymmetric section of the plate was modeled in the YZ plane using 2-D elements for the inner and outer parts. The dimension b was chosen to be 1 meter, and the outer boundary had a radius of 2 meters. Dielectric constants of 1.0 were assigned and the inner area was given a charge density of 8.8545E-11 C/m^3. Voltages of 0 were applied along the outer edge with a stiffness of 100,000. An Electrostatic Field Strength and Voltage analysis was performed to obtain the E field magnitude as shown in Figure 149-2.

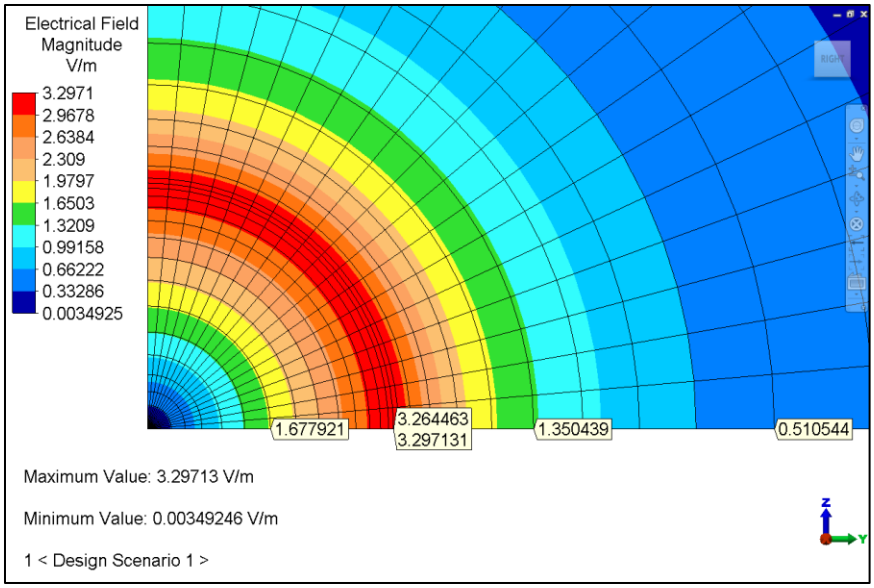

Figure 149-2. Electric field magnitude for R = 0.5, 1.0, 1.57 and 2.55.

The analysis results are compared to the theoretical solution in the following table.

Table 149-1. Comparison of Results.

Radius	Electric Field Magnitude in Radial Direction V/m		% Difference
	Theoretical	Analysis	
0.50	1.67	1.68	0.60
1.00	3.33	3.28	1.50
1.57	1.35	1.35	0.0
2.55	0.51	0.51	0.0

AVE - 150 Steady-State Heat Transfer Analysis of a Rod with an Adiabatic Tip

Reference

Lindeberg, Michael R., *Mechanical Engineering Reference Manual, (10th Edition)*, Professional Publications, 1997, pp. 34-18 – 34-19

Problem Description

Calculate the temperature 3 inches in from the base of a 0.5 in x 0.5 in x 10 in long rectangular rod, which has its base maintained at 300°F by heating equipment, as shown in Figure 150-1.

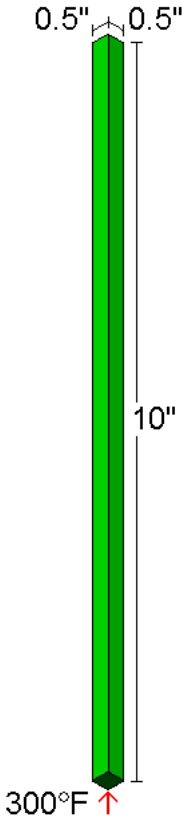

Figure 150-1. Setup of the rod.

The problem specifications are as follows:

- Conductivity = 80 Btu-ft/hr-ft^2-°F
- Ambient air temperature = 80°F
- Average film coefficient = 1.65 Btu/hr-ft^2-°F

Theoretical Solution

Because the tip area is approximately 1% of the total surface, the rod is assumed to have an adiabatic tip.

The perimeter length is:

$$P = (2)(w+t) = \frac{(2)(0.5\text{ in} + 0.5\text{ in})}{12\frac{\text{in}}{\text{ft}}} = 0.167\text{ ft}$$

The cross-sectional area of the fin at its base is:

$$A_b = wt = \frac{(0.5\text{ in})(0.5\text{ in})}{\left(12\frac{\text{in}}{\text{ft}}\right)^2} = 0.00174\text{ ft}^2$$

From heat transfer theory:

$$m = \sqrt{\frac{hP}{kA_b}} = \sqrt{\frac{(1.65)(0.167)}{(80)(0.00174)}} = 1.41/\ ft$$

Hence, the temperature 3 in from the base is:

$$T_x = T_\infty + (T_b - T_\infty)\left[\frac{\cosh(m(L-x))}{\cosh(mL)}\right]$$

$$= 80 + (300 - 80)\left[\frac{\cosh\left(\frac{(1.41)(10-3)}{12}\right)}{\cosh\left(\frac{1.41(10)}{12}\right)}\right] = 248.4°F$$

Autodesk Simulation Solution

The rod was drawn in the XY plane and extruded in the Z direction. It was constructed of brick elements. The film coefficient, conductivity and ambient temperature were applied and one tip was kept at 300°F. A Steady-State Heat Transfer analysis was performed to obtain the temperature distribution. In the Results environment, the "Inquire Results" capability was used to obtain the temperature at 3 inches from the base.

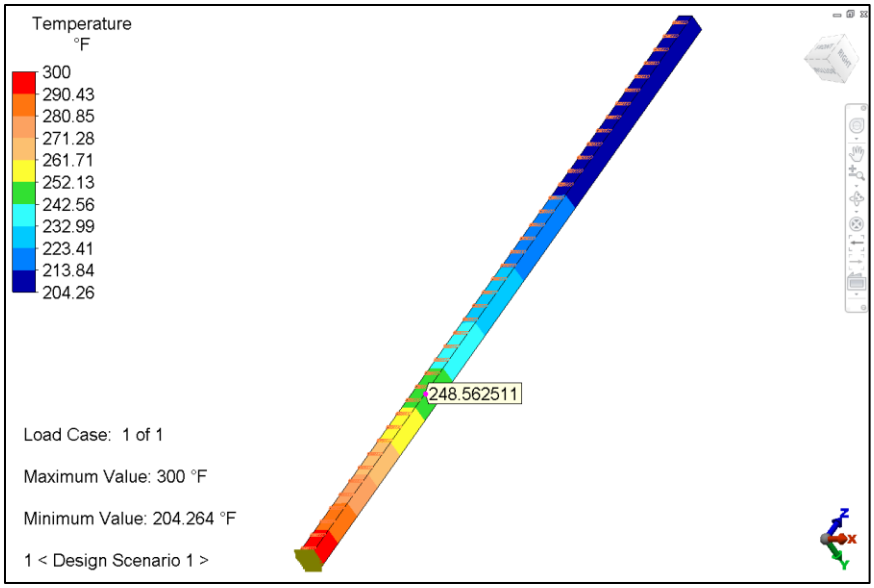

Figure 150-2. Probing the temperature at 3 inches from the base.

The analysis results are compared to the theoretical results in the following table.

Table 150-1. Comparison of results.

Temperature (°F) at 3 in from base		% Difference
Theoretical	**Analysis**	
248.4	248.6	0.08

AVE - 151 Natural Frequency Analysis of a Flat Circular Plate

Reference

Young, Warren C., *Roark's Formulas for Stress & Strain, (6th Edition)*, McGraw-Hill, 1989, case 10a, p. 716

Problem Description

Calculate the first natural frequency of a flat circular plate of uniform thickness (t) and radius (r). There is a uniform load (w) per unit area including its own weight. The outer edge is fully fixed.

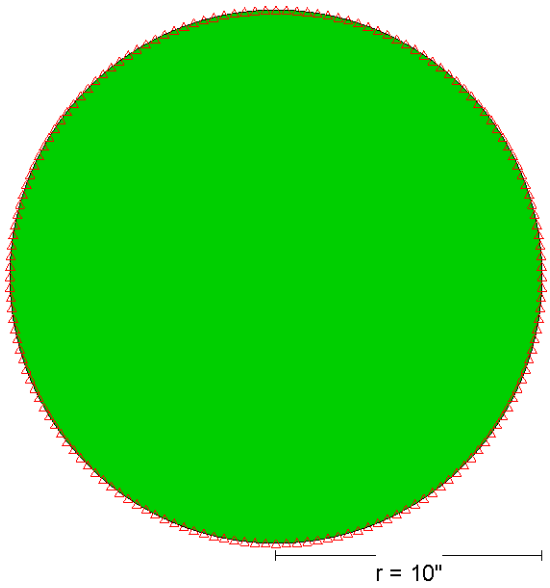

Figure 151-1. Setup of the circular plate.

For this example, the following specifications are used:

- r (radius) = 10 in
- t (thickness) = .01 in
- ρ (mass density) = 2.61E-4 lbf*s^2/in/in^3
- E (modulus of elasticity) = 10E6 lbf/in^2
- ν (Poisson's ratio) = 0.397
- g (gravity) = 386.4 in/s^2
- w (uniform load per unit area) = g * ρ * t = 1.009E-3 lbf

Theoretical Solution

From the reference:

$$f = \frac{K_n}{2\pi}\sqrt{\frac{Dg}{wr^4}}$$

where

K1 = 10.2 (fundamental)
K2 = 21.3 (one nodal diameter)
K3 = 34.9 (two nodal diameter)
K4 = 39.8 (one nodal circle)

or

$$K = \begin{bmatrix} 10.2 \\ 21.3 \\ 34.9 \\ 39.8 \end{bmatrix}$$

and

$$D = \frac{E \cdot t^3}{12\left(1 - v^2\right)}$$

Hence, solving for the first natural frequency gives:

$$f_1 = 10.29 \text{ cycles/s}$$

Autodesk Simulation Solution

The plate was drawn in the FEA Editor and assigned to plate elements with a thickness of 0.01 in. Material properties were manually entered based on the problem description. The outer edge was fully constrained. A Natural Frequency analysis was performed to obtain the natural frequencies.

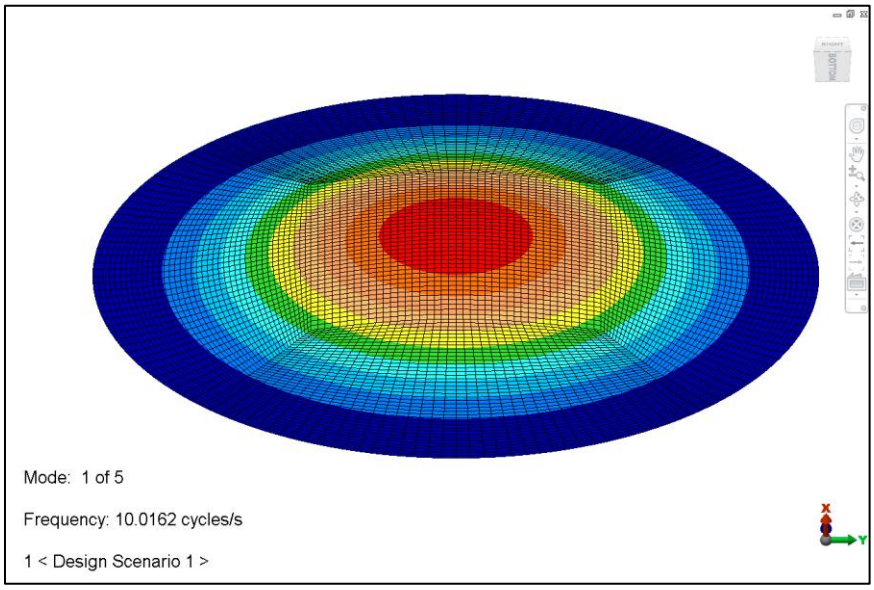

Figure 151-2. First natural frequency of the flat circular plate.

The analysis results are compared to the theoretical solution in the following table.

Table 151-1. Comparison of results.

First Natural Frequency (cycles/s)		% Difference
Theoretical	**Analysis**	
10.29	10.0162	2.66

AVE - 152 Cylinder/Sphere under Uniform Internal Pressure

Reference

Hitchings, D., Kamoulakos, A., Davies, G. A. O., *Linear Statics Benchmarks, Volume 1*, National Agency for Finite Element Methods & Standards (NAFEMS), October 1987, Example 27.

Problem Description

A thin-shelled cylinder/sphere combination is subjected to a uniform internal pressure of 1 MPa. Calculate the hoop stress (s_{tt}) on the outer surface at point D as shown in Figure 152-1.

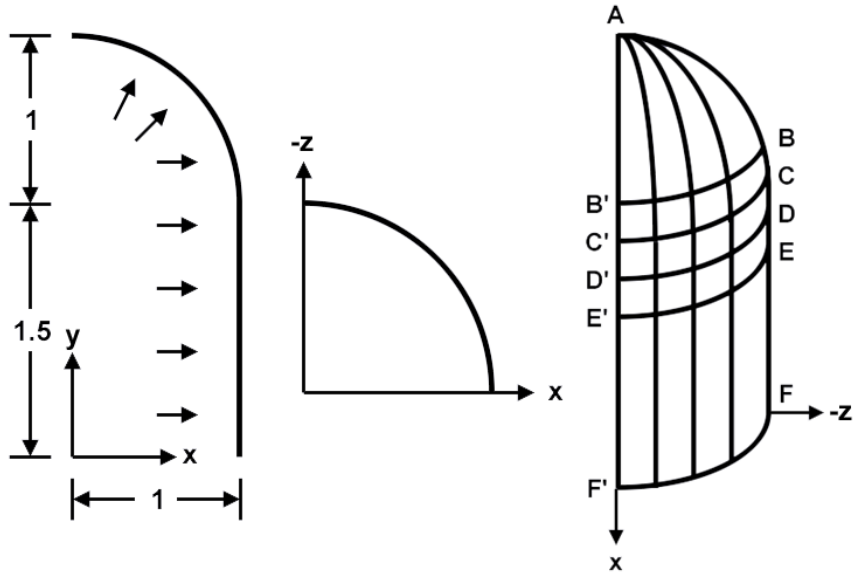

Figure 152-1. Drawing and setup of the cylinder/sphere model.

The following specifications were used:

- thickness = 0.025 m
- uniform internal pressure = 1 MPa
- material properties = isotropic
- E (modulus of elasticity) = 210 x 10^3 MPa
- ν (Poisson's ratio) = 0.3

Theoretical Solution

Data coordinates for points B, D and E were specified as shown in Table 152-1.

Table 152-1. Data coordinates for points B, D and E.

Point	X	Y
B	0.9814	1.6920
D	1.0	1.4034
E	1.0	1.1136

The boundary conditions were specified as follows:

- Edge AC'D' was given boundary conditions of zero y displacement and zero rotations about the x and y axes.

- Edge ACD was given boundary conditions of zero x displacement and zero rotations about the y and z axes.
- Edge FF' was given a boundary condition of zero z displacements.

An isotropic material model was used with general thin shell quadrilateral and triangular elements.

Solving for an analysis type of linear elastic thin shell, the pressure on the outer surface at point D is 38.5 MPa.

Autodesk Simulation Solution

For the model, the profile was drawn in the XY plane using the coordinates shown in Table 152-2.

Table 152-2. Data coordinates for points A, B, C, D and E.

Point	X	Y
A	0	2.5
B	0.9814	1.6920
C	1.0	1.5
D	1.0	1.4034
E	1.0	1.1136

The line AB was divided into 12 segments; the line BC was divided into 8 segments; the line CD was divided into 6 segments; and the line DE was divided into 8 segments. The profile was then copied 8 times over a 90-degree angle to meet the –z axis. Plate elements were assigned to the part with a thickness of 0.025 m, and an isotropic material model was chosen with E = 210 x 10^3 MPa, v = 0.3. The edge of the part on the XY plane was given Z symmetry, the edge on the YZ plane was given X symmetry, and the edge on the XZ plane was constrained from moving in the Y direction. A Linear Static Stress analysis was performed and a cylindrical Local Coordinate system was used in the results environment to obtain the hoop stress at point D as shown in Figure 152-2.

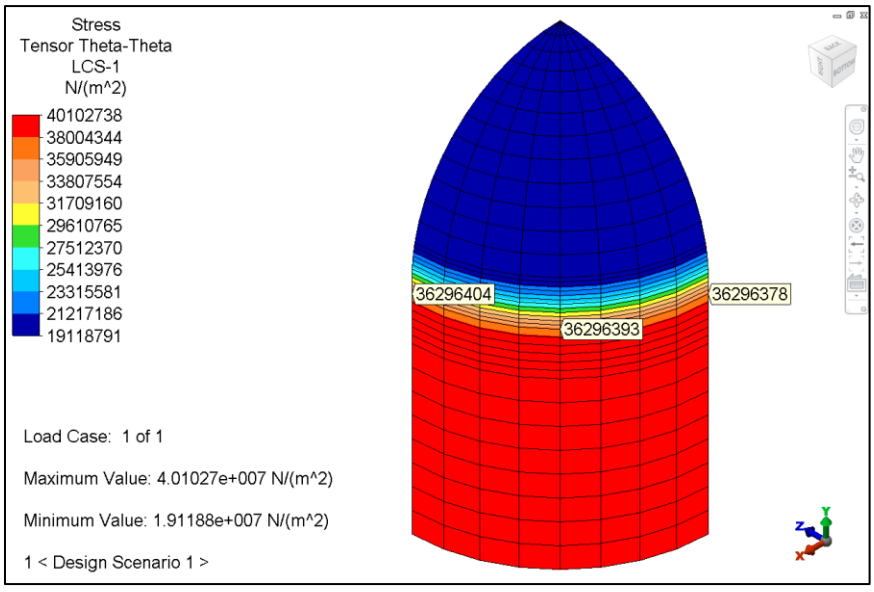

Figure 152-2. Hoop stress on outer surface at point D.

Table 152-3. Comparison of Results.

Analysis	Theory	% Difference
38.0	36.3	4.47

AVE - 153 Heat Generation in a Wire due to Electrical Current

Reference

Holman, J. P., *Heat Transfer, (7th Edition)*, McGraw-Hill, 1981, p. 42

Problem Description

A stainless steel wire, which is 1 m long with a 3 mm diameter, passes an electrical current of 200 A and is submerged in a 110°C fluid. The convection coefficient between the fluid and the wire is 0.004 W/(mm^2°C). Calculate the temperature at the center of the wire.

As shown in Figure 153-1, an axisymmetric cross-section of the wire, measuring 10 mm long and 1.5 mm wide, was analyzed.

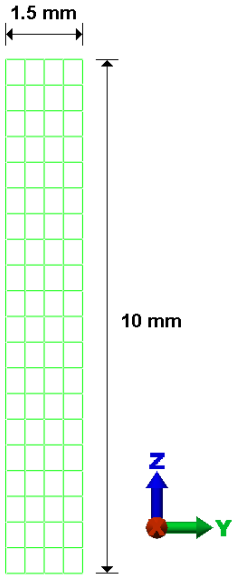

Figure 153-1. Setup of the wire model.

The following material properties were used:

- Thermal Conductivity = 0.019 W/(mm^2°C)
- Resistivity = 0.0007 Ω mm (1428.57 A/Vmm)

Theoretical Solution

All of the power generated in the wire must be dissipated by convection to the liquid:

$$P = I^2R = q = hA\left(T_w - T_\infty\right)$$

The resistance of the wire can be calculated from

$$R = \rho\frac{L}{A} = \frac{\left(70\times10^{-6}\right)(100)}{\pi(0.15)^2} = 0.099\,\Omega$$

where ρ is the resistivity of the wire. The surface area of the wire is π *d*L, so

$$(200)^2(0.099) = 4000\,\pi\left(3\times10^{-3}\right)(1)\left(T_w - 110\right) = 3960\,W$$

Hence,

$$T_w = 215°C$$

The heat generated per volume, $\dot{q}$ can be calculated from

$$P = \dot{q}V = \dot{q}\pi r^2L$$

Hence,

$$\dot{q} = \frac{3960}{\pi\left(1.5\times10^{-3}\right)^2(1)} = 560.2\,\frac{MW}{m^3}$$

Finally, the center temperature can be calculated

$$T_0 = \frac{\dot{q}r_o^{\,2}}{4k} + T_w = \frac{\left(5.602\times10^8\right)\left(1.5\times10^{-3}\right)^2}{(4)(19)} + 215 = 231.6°C$$

Autodesk Simulation Solution

The analysis of the model required a two-step multiphysics approach:

1. An Electrostatic Current and Voltage analysis would be performed to get the voltage distribution for the 200 Amp current.
2. The voltage results would be used as input to a Steady-State Heat Transfer analysis to get the temperature distribution.

A planar rectangular section of 1.5 X 10 mm was drawn in the YZ plane and assigned to 2-D elements. Element divisions of AB = 4 and BC = 20 were used. The 2-D elements were set to axisymmetric (about the Z axis).

The analysis type was specified as Electrostatic Current and Voltage. The given thermal conductivity was converted to get an electrical conductivity value of 14.2857 A(V/mm). A loading was specified as a voltage drop of 0.198 by applying voltages of 0.198 to the top row of vertices in the model and applying voltages of 0 to the bottom row. The electrostatic analysis was performed to obtain the voltage distribution results.

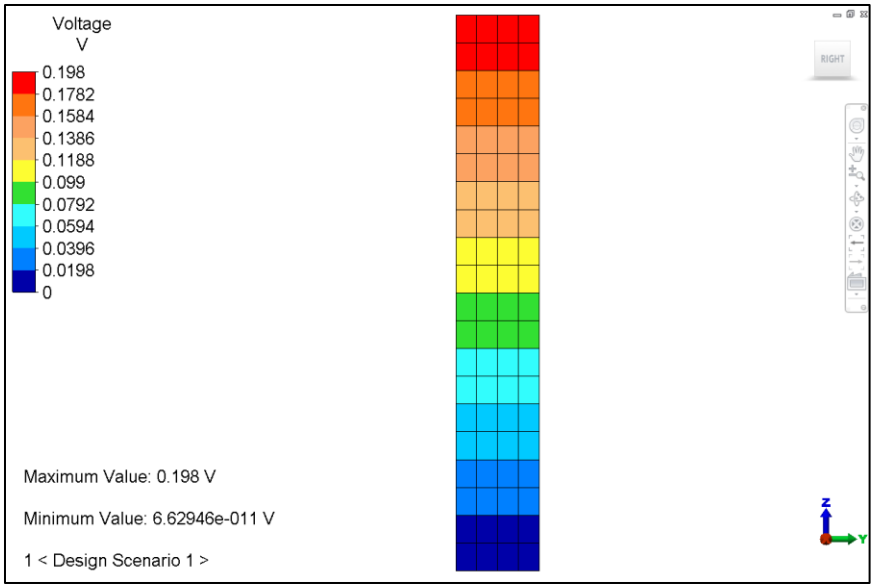

Figure 153-2. Voltage distribution in the wire model.

Next, the analysis type was changed to Steady-State Heat Transfer. A convection coefficient of 0.004 was applied to the outer edge of the wire. The ambient temperature was specified as 110°C. In the "Analysis Parameters" dialog, on the "Multipliers" tab, load case multipliers were activated for a convection multiplier and a heat generation multiplier. On the "Electrical" tab, under "Joule Effects", the "Use electrostatic results to calculate Joule Effects" option was activated and the location of the source model (.efo file) was specified as shown below.

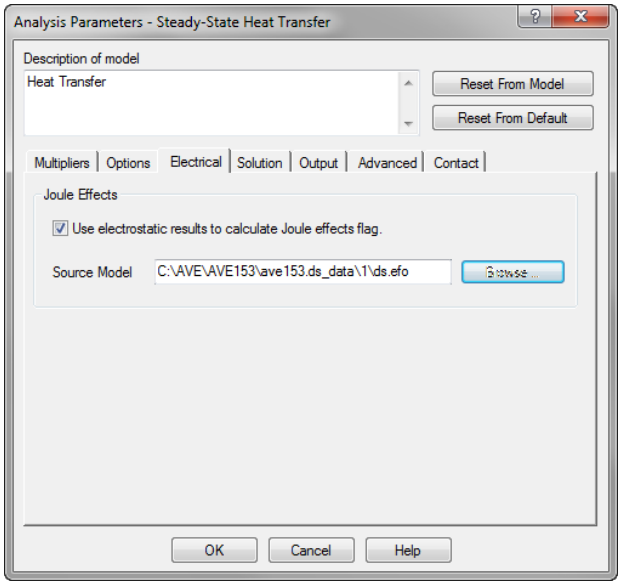

Figure 153-3. Specifying the use of electrostatic results to calculate Joule effects.

The heat transfer analysis was run to obtain the temperature distribution. In the Results environment, the "Inquire Results" capability was used to obtain the temperature at the center of the wire.

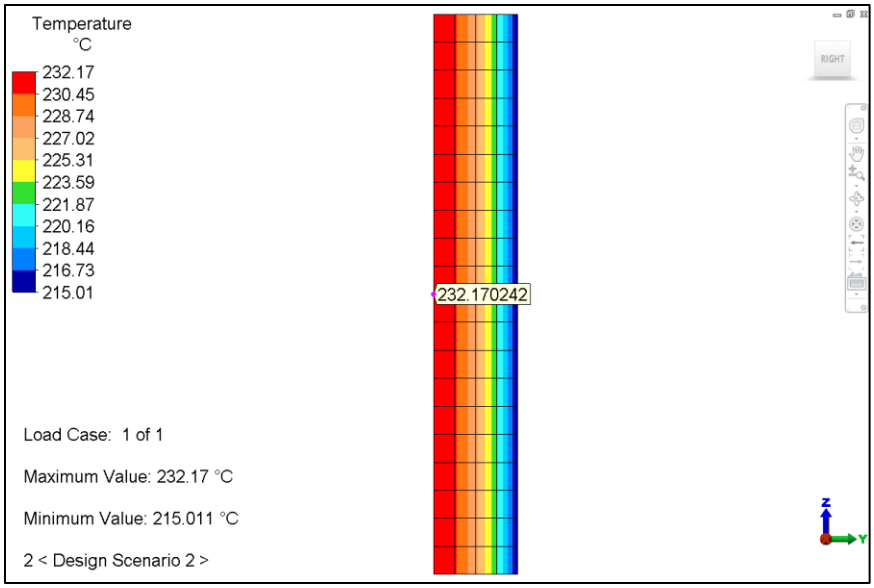

Figure 153-4. Inquiring on the temperature result at the center of the wire.

Table 153-1. Comparison of Results.

Temperature (°C)		% Difference
Theoretical	**Analysis**	
231.6	232.17	0.25

AVE - 154 Natural Frequency (Modal) Analysis of a Cantilevered Beam

Reference

Abbassian, F., Dawswell, D. J., Knowles, N. C., *Selected Benchmarks for Natural Frequency Analysis*, National Agency for Finite Element Methods & Standards (NAFEMS), November 1987, Test 71.

Problem Description

A 10-m beam with a square cross section of 0.125 m x 0.125 m is rigidly supported at one end as shown in Figure 154-1. The material properties are:

- Young's modulus of elasticity (E) = 200e9 N/m^2
- Density (ρ) = 8000 kg/m^3

Calculate the first modal frequency.

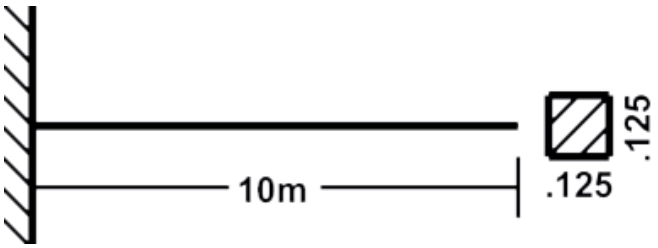

Figure 154-1. Diagram of the cantilevered beam problem.

Theoretical Solution

The beam is modeled as 8 equal-length segments using 2-D beam elements. Boundary conditions of Tx = Ty = Rz = 0 are specified at the wall. The natural frequency analysis result for the first mode of vibration is given in the reference as 1.010 Hz.

Autodesk Simulation Solution

The profile was drawn from the origin to (0, 10, 0) and split into 8 equal-length beam elements. The left end was given a fully fixed boundary condition, and the rest of the segments in the model were given boundary conditions of Tx = Ry = Rz = 0 to simulate a 2-D beam element.

A Natural Frequency (Modal) analysis was performed. In the Results environment, the first mode for the beam was displayed as shown in Figure 154-2.

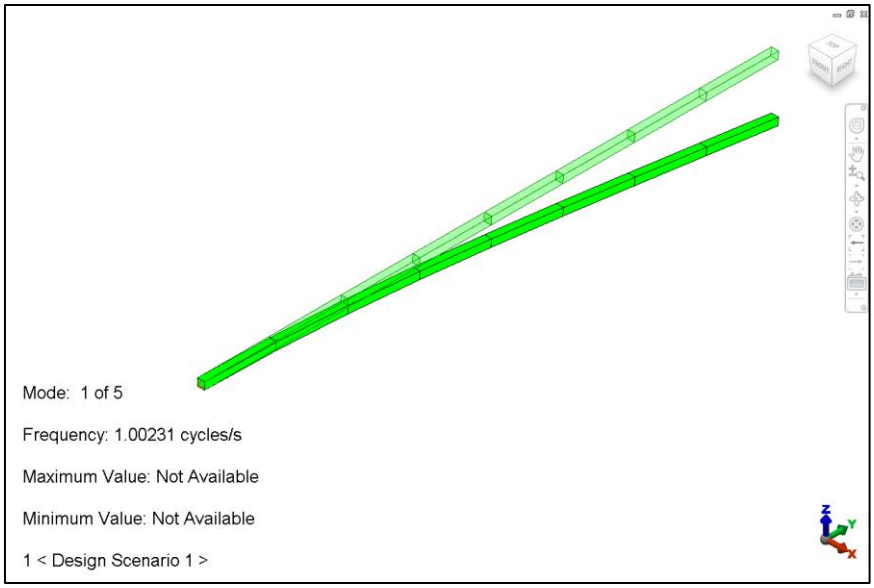

Figure 154-2. Results for the first mode of vibration. (3D beam visualization was activated)

Table 154-1. Comparison of Results.

Frequency (Hz)		% Difference
Theoretical	**Analysis**	
1.010	1.00231	0.69

AVE - 155 Tapered Plate with Gravity

Reference

Hitchings, D., Kamoulakos, A. and Davies, G. A. O., *Linear Statics Benchmarks*, National Agency for Finite Element Methods & Standards (NAFEMS), October-November 1987 (LSB1 and LSB2), Test 11.

Problem Description

A flat tapered plate (4 m x 4 m x 2 m) is fixed at edge ABC as shown in Figure 166-1. Find the stress in the X direction (Sxx) at point B due to the acceleration of gravity.

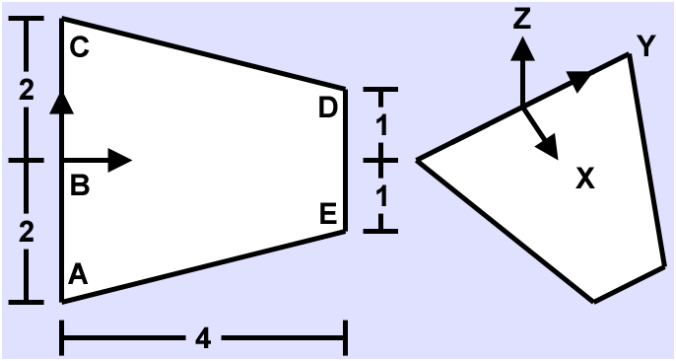

Figure 155-1. Diagram of the flat tapered plate problem.

Specifications used in this example include the following:

- Thickness = 0.1 m
- E = $210x10^3$ MPa
- $\nu = 0.3$
- $\rho = 7$ Mg/m^3
- Gravity = 9.81 m/s^2 in the Z direction

Theoretical Solution

According to the NAFEMS report, the stress at point B is 26 MPa.

Autodesk Simulation Solution

The plate was drawn in the XY plane and meshed with 64 divisions along each edge. These were defined as plate elements. Edge ABC was fully constrained. The materials and loads were applied as described above. A Static Stress with Linear Material Models analysis was performed to determine the stress tensor results in the X direction as shown in Figure 155-2.

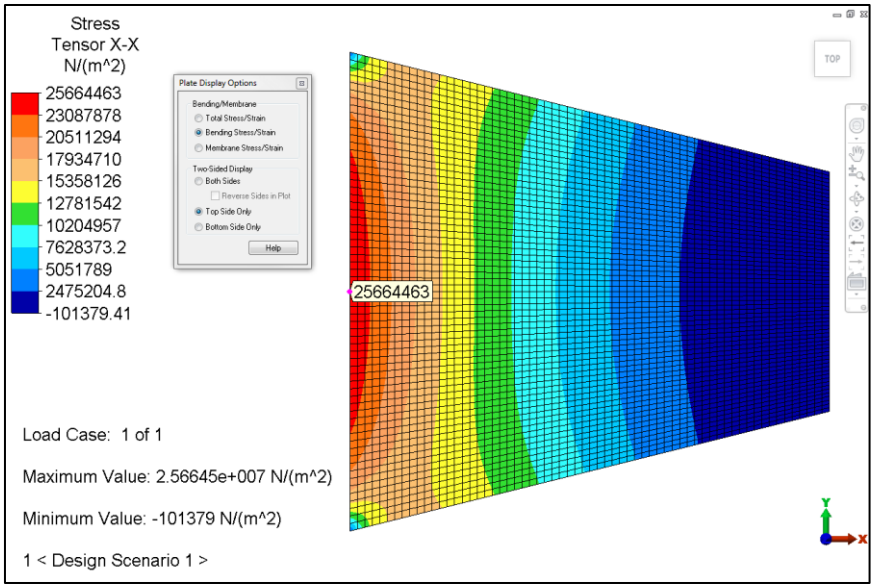

Figure 155-2. Stress tensor results in the X direction. Bending stress for the Top side of the plate is shown.

Table 155-1. Comparison of Results.

Stress Tensor in the X Direction (MPa)		% Difference
Theoretical	**Analysis**	
26.0	25.7	-1.2

AVE - 156 Rectangular Plate Held by Three Wires

Reference

Beer, Ferdinand P. and Johnston, Jr., E. Russell, *Vector Mechanics for Engineers: Statics and Dynamics*, Third Edition, McGraw-Hill Book Company, 1977, Sample Problem 16.2, p. 739

Problem Description

As shown in Figure 156-1, the thin rectangular plate ABCD has a mass of 50 kg and is held in position by three inextensible wires AE, BF and CH.

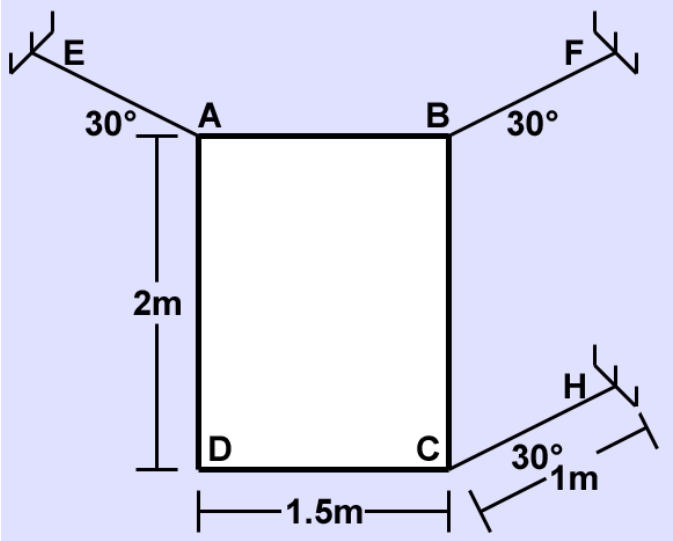

Figure 156-1. Diagram of the plate held by three wires.

Properties of the plate include the following:

- AB, DC = 1.5 m
- AD, BD = 2 m
- Thickness = 0.25 m
- Mass = 50 kg
- Gravity = -9.81 m/s^2
- Mass density = 66.667

Properties of the wires include the following:

- AE, BF, CD = 1 m
- Mass density = 0

Calculate the acceleration of a plate and the tension in two cables when a third cable is cut.

Theoretical Solution

The plate is 0.25m thick and has a mass of 50 kg. Cable AE is cut. The force in cable BF can be calculated to be 175.9N. The force in cable CH can be calculated to be 69.6N.

Autodesk Simulation Solution

The plate was drawn in the XY plane and meshed with 8 divisions along the AD edge and 6 divisions along the AB edge. These were defined as shell elements. Two cables were modeled with truss elements. Points F and H were constrained with boundary conditions. Point A was constrained with prescribed displacements of 0. Gravity was applied to the model. Once the gravity has been applied, the prescribed displacement at point A is removed allowing the point to move freely. The image below shows the axial force in the truss elements after the prescribed displacement was removed.

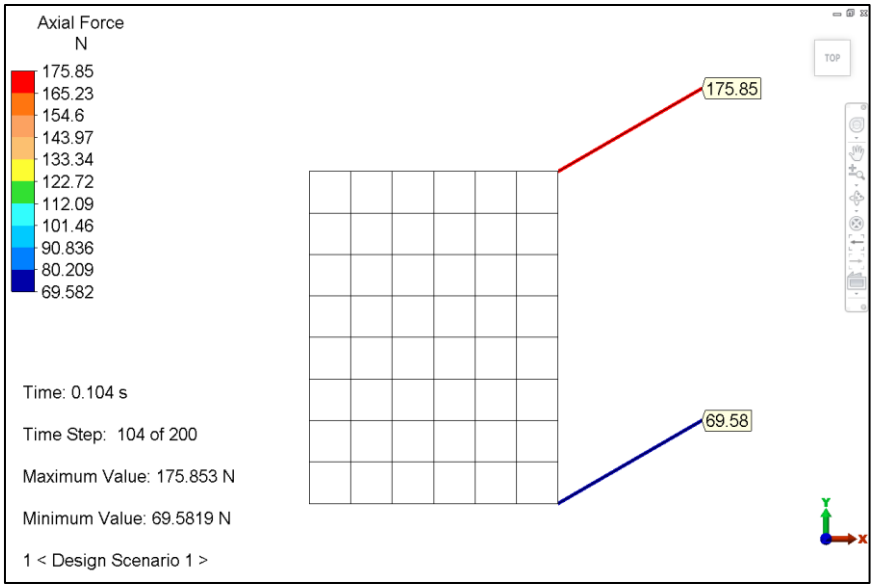

Figure 156-2. Axial force in the truss elements at Time = 0.104s.

Table 156-1. Comparison of Results.

	Theoretical	Analysis	% Difference
Axial Force in Cable BF at 0.104s (N)	175.9	175.85	0.03
Axial Force in Cable CH at 0.104s (N)	69.6	69.6	0.00

AVE - 157 Effect of Fins on Heat Transfer from a Steam Pipe

Reference

Cengel, Yunus A., *Heat Transfer: A Practical Approach*, WCB/McGraw-Hill, 1998, Example 3-14, pp. 191-192

Problem Description

Steam in a heating system flows through an aluminum pipe with an outer diameter of 3 cm and a temperature that is maintained at 120°C. Circular aluminum fins with a diameter of 6 cm and a thickness of 2 mm are attached to the pipe as shown in Figure 157-1. The space between the fins is 3 mm, and thus there are 200 fins per meter length of the pipe. The pipe and fins have thermal conductivity of k = 180 W/m·°C. The surrounding air temperature is 25°C with a combined heat transfer coefficient of h = 60 W/m^2·ºC.

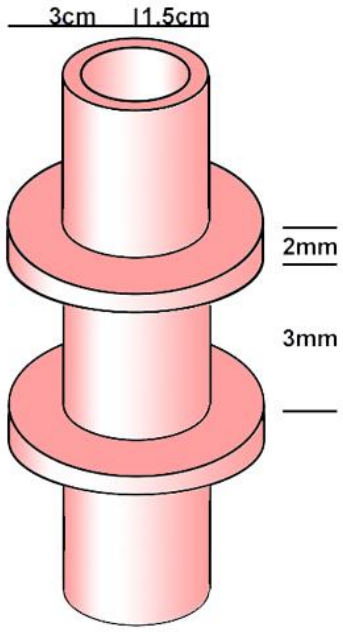

Figure 157-1. Diagram of the steam pipe with fins (not to scale).

The problem parameters include:

- Ambient Temperature (T_a) = 25°C
- Temperature of the Pipe = 120°C
- Thermal Conductivity (k) = 180 W/m·°C
- Convection Coefficient (h) = 60 W/m^2·°C

Determine the increase in heat transfer from the pipe per meter of its length as a result of adding 200 fins.

Theoretical Solution

The following assumptions are made:

1) Steady operating conditions exist.
2) The heat transfer coefficient is uniform over the entire fin surfaces.
3) Thermal conductivity is constant.
4) Heat transfer by radiation is negligible.

For the pipe without fins, the heat transfer can be determined as follows:

$$A_{nofin} = \pi D_1 L = \pi(0.03\,m)(1\,m) = 0.0942\,m^2$$

$$\dot{Q}_{nofin} = hA_{nofin}(T_b - T_\infty) = 537 \text{ Watts}$$

For the pipe with fins, the heat transfer can be determined as follows:

$$L = \frac{1}{2}(D_2 - D_1) = \frac{1}{2}(0.06 - 0.03) = 0.015\,m$$

Therefore, the efficiency of the circular fins is:

$$\frac{r_2 + \frac{1}{2}t}{r_1} = \frac{\left(0.03 + \frac{1}{2}\times 0.002\right)m}{0.015\,m} = 2.07$$

$$\left(L + \frac{1}{2}t\right)\sqrt{\frac{h}{kt}} = \left(0.015 + \frac{1}{2}\times 0.002\right)m \times \sqrt{\frac{60\frac{W}{m^2 \bullet ^\circ C}}{\left(180\frac{W}{m \bullet ^\circ C}\right)(0.002\,m)}} = 0.207$$

$$\eta_{fin} = 0.95$$

$$A_{fin} = 2\pi(r_2^2 - r_1^2) + 2\pi r_2 t = 0.00462\,m^2$$

$$\dot{Q}_{fin} = \eta_{fin}\dot{Q}_{fin,max} = \eta hA_{fin}(T_b - T_\infty) = 25.0\,W$$

If the space between the 2 fins is 3mm, then heat transfer from the finned portion is:

$$A_{unfin} = \pi D_1 S = \pi(0.03\,m)(0.003\,m) = 0.000283\,m^2$$

$$\dot{Q}_{unfin} = hA_{unfin}(T_b - T_\infty) = 1.60\,W$$

Since there are 200 fins and 200 interfin spacings per meter length, the total heat transfer from the finned pipe is:

$$\dot{Q}_{\text{total,fin}} = n\left(\dot{Q}_{\text{fin}} + \dot{Q}_{\text{unfin}}\right) = 200(25.0 + 1.6)\text{W} = 5320\,\text{W}$$

Autodesk Simulation Solution

A 1/200 m segment of the pipe length was modeled using quarter symmetry, both without fins and with fins. When meshing the fins, arithmetic meshing was used to create a finer mesh near the pipe because that area was expected to have the greatest change in heat transfer. Brick elements were used and, on the "Element Definition" dialog box, the "Heat Flow Calculation" option was set to "Linear Based on BC" to specify that the heat fluxes for the convection boundary conditions should be linearized. This option enabled examination of the heat flow through the convection boundary surfaces. Material properties were specified as noted in the problem description.

A Steady-State Heat Transfer analysis was performed to calculate the steady-state temperature distribution. In the Results environment, the heat flow rate was displayed as shown in Figure 157-2. The heat flow rate was summed for the elements of the pipe both without fins and with fins. The results were multiplied by 4 due to quarter symmetry and then by 200 to obtain the total heat loss in 1 meter of the pipe.

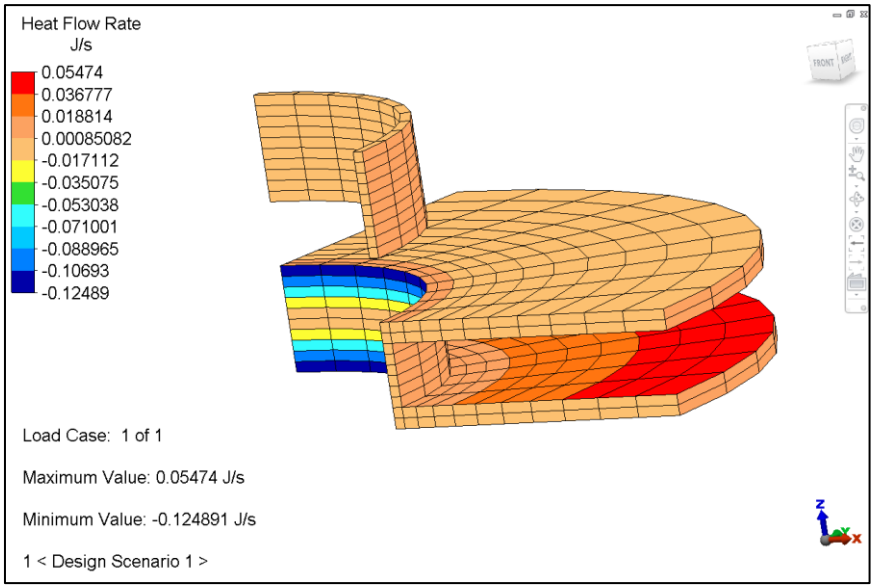

Figure 157-2. Display of heat flow rate. Smooth results deactivated

Table 157-1. Comparison of Results.

	Heat Transfer in 360°, 1-m section of Pipe (W/m)		% Difference
	Theoretical	Analysis	
without Fins	537	537	0.00
with Fins	5320	5340	0.38

AVE - 158 Velocity and Reaction Force from a Crate Being Dragged across the Floor

Reference

Hibbeler, R. C., *Engineering Mechanics:Dynamics*, *Seventh Edition*, Prentice-Hall, 1995, Example 15-1, p. 193

Problem Description

A 100-kg crate is initially at rest on a smooth horizontal floor. A force of 200 N, acting at an angle of 45°, is applied to the crate for 10 seconds, which drags the crate across the floor, as shown in Figure 158-1. Determine the final velocity of the crate.

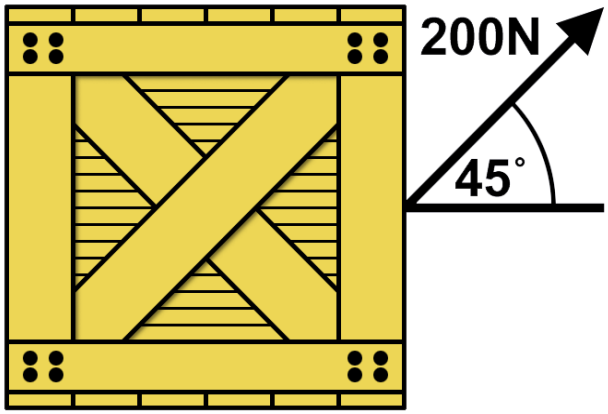

Figure 158-1. Diagram of the crate-dragging event.

Theoretical Solution

It is assumed that during the motion the crate remains on the floor. The vector along the X axis can be resolved as follows:

$$m(v_x)_1 + \sum \int_{t1}^{t2} F_x dt = m(v_x)_2$$

$0 + 200\ \text{N}(10\ \text{s})\cos 45° = (100\ \text{kg})v_2$

$v_2 = 14.1\ \text{m/s}$

Autodesk Simulation Solution

A 1m x 1m cube was built in the YZ plane with a 6 x 6 mesh of 2-D elements. A thickness of 1 m and a mass density of 100 kg/m^3 were specified. A 200 N force was applied to the side of the crate at a 45 degree angle from the Y axis. A "slide no bounce" impact plane was setup at Z = -0.00001 to simulate the floor with a slight space beneath the crate to allow for impact from gravity. A Mechanical Event Simulation with Nonlinear Material Models was set up with duration of 10 s and a capture rate of 10 per second.

Figure 158-2 shows a graph of the first derivative of the displacement of node 1, which gives the velocity. The graph shows that, at time = 10 s, the final velocity is 14.14 m/s.

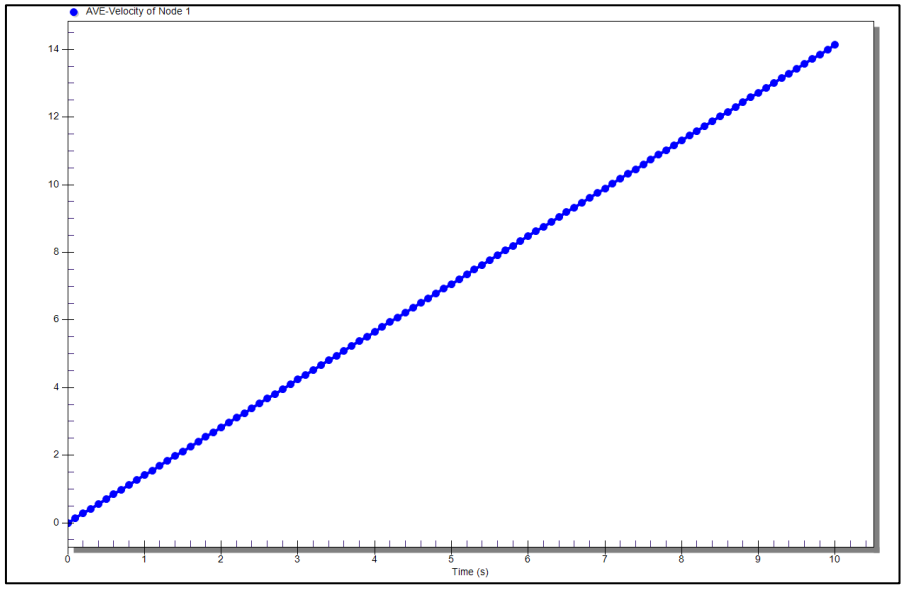

Figure 158-2. Graph of velocity.

Table 158-1. Comparison of Results

	Theoretical	Analysis	% Difference
Velocity (m/s)	14.1	14.14	0.28

AVE - 159 Heat Transfer between Hot- and Cold-Water Pipes

Reference

Cengel, Yunus, *Heat Transfer: A Practical Approach*, McGraw-Hill, 1998, p. 196

Problem Description

Two pipes run parallel to each other in a concrete block as shown in Figure 159-1. One pipe has hot water (70°C) running through it and the other pipe has running cold water (15°C). The pipes are each 5 cm in diameter and the distance between their centerlines is 30 cm. The thermal conductivity of the concrete is k = 0.75 W/m·°C. For a length of 5 m, calculate the rate of heat transfer between the pipes.

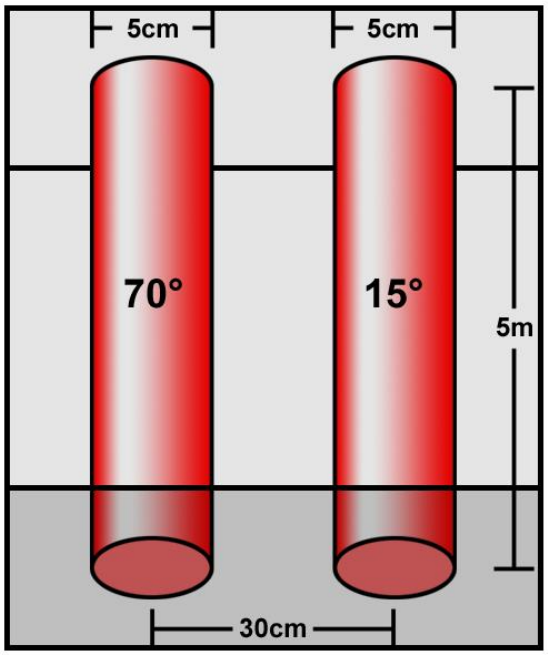

Figure 159-1. Diagram of the hot- and cold-water pipes in concrete.

Theoretical Solution

From the reference, the following assumptions are made:

1) Steady operating conditions exist.
2) The head transfer is two-dimensional (no change in the axial direction).
3) Thermal conductivity of the concrete is constant.

The shape factor for this configuration is

$$S = \frac{2\pi L}{\cosh^{-1}\left(\frac{4z^2 - D_1^2 - D_2^2}{2D_1D_2}\right)}$$

where z is the distance between the centerlines of the pipes and L is the length. Therefore,

$$S = \frac{2\pi \times (5\,\text{m})}{\cosh^{-1}\left(\frac{4\times 0.3^2 - 0.05^2 - 0.05^2}{2\times 0.05\times 0.05}\right)} = 6.34\,\text{m}$$

Thus, the steady rate of heat transfer between the pipes is

$Q = Sk(T_1-T_2) = (6.34\text{ m})(0.75\text{ W/m}\cdot°\text{C})(70\text{-}15°\text{C}) = 262\text{ W}$

Autodesk Simulation Solution

A model was built of a cross-section of the concrete block with holes to represent the pipes. Automatic mesh generation capabilities were used to generate a mesh using two-dimensional (2-D) elements. The mesh was finer around the holes, which was the area of interest. In the element definition, the heat flow calculation was changed to "linear Based on BC" for increased accuracy. Convection surface loads were specified for the two holes to simulate the hot and cold running water.

A Steady-State Heat Transfer analysis was performed to calculate the temperature distribution. Summing the heat rate of faces of a one-element radius from the hole provided the heat transfer between the pipes as shown in Figure 159-2.

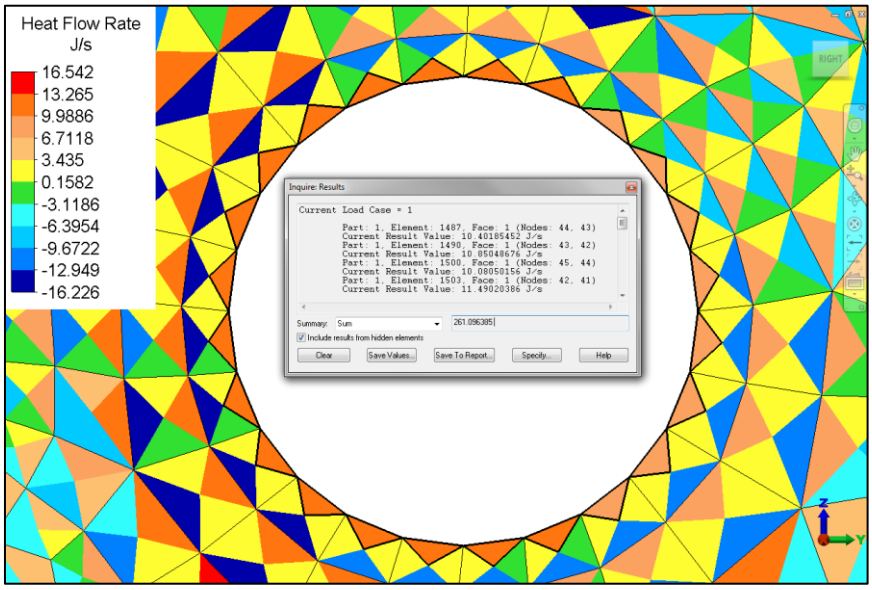

Figure 159-2. Summing the heat rate of faces at one of the holes.

Table 159-1. Comparison of Results.

Heat Transfer between Pipes (W)		% Difference
Theoretical	Analysis	
262	261.096	0.35

AVE - 160 Axisymmetric Vibration of a Simply Supported Annular Plate

Reference

Abbassian, F., Dawswell, D. J., Knowles, N. C., *Selected Benchmarks for Natural Frequency Analysis*, National Agency for Finite Element Methods & Standards (UK), November 1987, Test 43.

Problem Description

A simply supported annular plate has an inner radius of 1.8 m, radial length of 4.2 m and thickness of 0.6 m as shown in Figure 160-1. The plate is constrained in the Z direction at point A. The material properties are:

- Young's modulus of elasticity (E) = 200e9 N/m^2
- Poisson's ratio (ν) = 0.3
- Density (ρ) = 8000 kg/m^3

Calculate the first three modal frequencies.

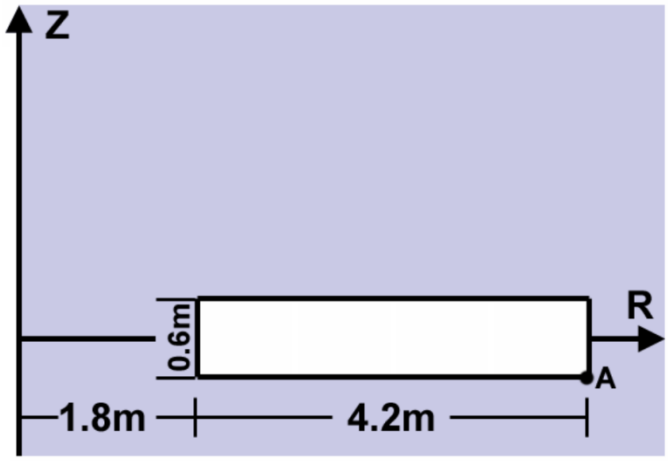

Figure 160-1. Diagram of the axisymmetric model of the simply supported annular plate.

Theoretical Solution

From the reference, using a 15 x 4 mesh of 4-noded isoparametric axisymmetric elements to model the plate, the first mode is 18.711 Hz, the second mode is 145.46 Hz and the third mode is 224.22 Hz.

Autodesk Simulation Solution

The profile was drawn from (0, 1.8, 0) to (0, 6, 0.6) and meshed with a mesh size of 15 x 4 using two-dimensional (2-D) elements. The bottom right corner was constrained from translation in the Z direction.

A Natural Frequency (Modal) analysis was performed to calculate the natural frequencies and mode shapes. The results for the first mode are shown in Figure 160-2.

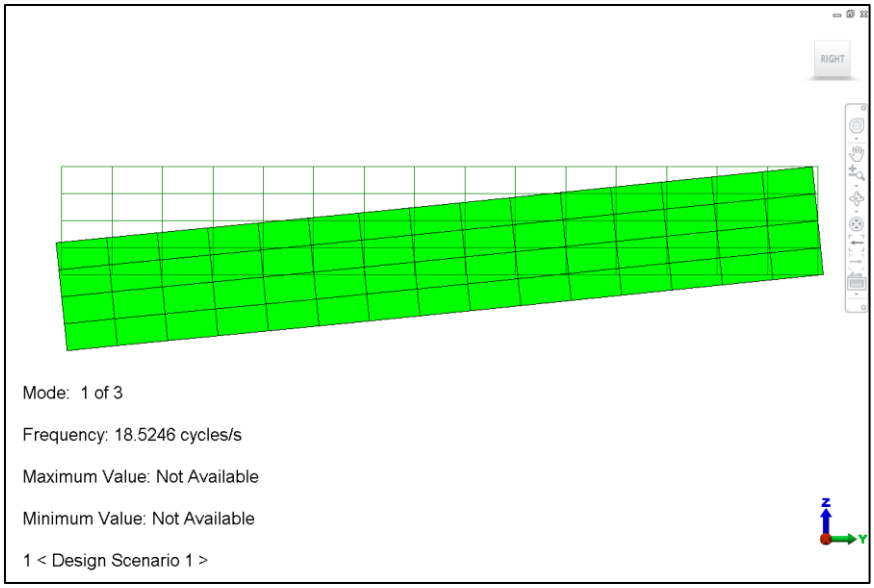

Figure 160-2. The frequency and mode shape of the first modal frequency.

Table 160-1. Comparison of Results.

Frequency (Hz)		% Difference
Theoretical	**Analysis**	
18.583	18.5246	0.31
140.15	138.467	1.20
224.16	224.042	0.05

AVE - 161 Natural Frequency (Modal) Analysis of a Cantilever Beam with Off-Center Point Masses

Reference

The Standard NAFEMS Benchmarks, National Agency for Finite Element Methods & Standards (UK), TNSB, Rev. 3, 5 October 1990, Test No. FV4.

Problem Description

A cantilever beam with a circular cross section is fixed at one end and has two off-center point masses at its free end as shown in Figure 161-1.

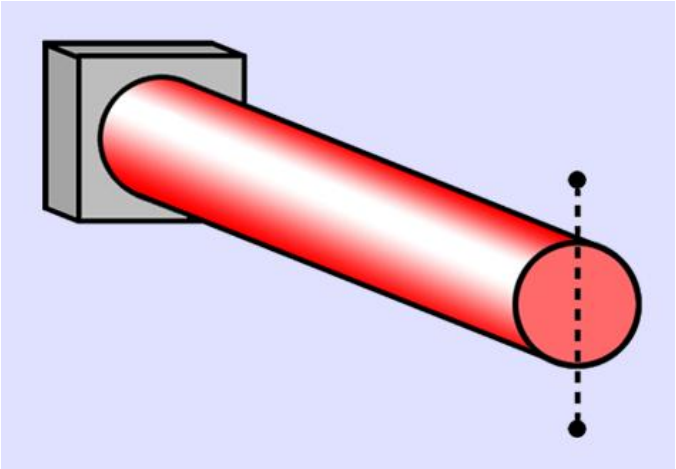

Figure 161-1. Illustration of the cantilever beam with circular cross section and two off-center point masses.

The beam is 10 m long and has a cross-sectional diameter of 0.5 m. The point masses are 10,000 kg and 1,000 kg, respectively, both 2 m from the end of the beam. (See Figure 161-2)

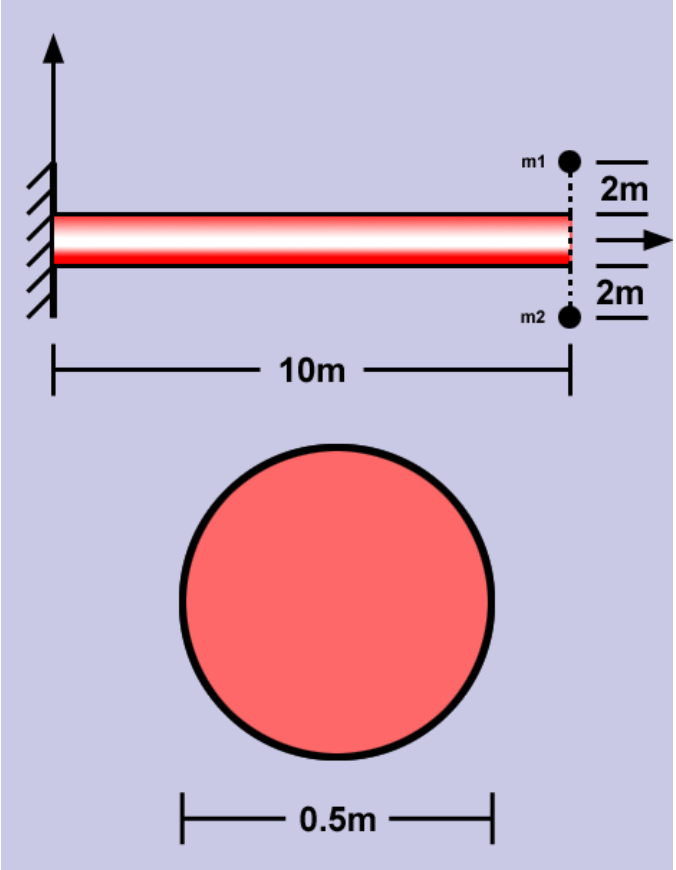

Figure 161-2. Dimensions of the beam with masses.

The material properties are:

- Young's modulus of elasticity (E) = 200e9 N/m^2
- Poisson's ratio (ν) = 0.3
- Density (ρ) = 8000 kg/m^3

Calculate the first six natural frequencies.

Theoretical Solution

According to the NAFEMS benchmark, using a mesh of 5 3-D beam elements along the beam length, the first natural frequency is 1.722 Hz, the second is 1.727 Hz, the third is 7.413 Hz, the fourth is 9.972 Hz, the fifth is 18.155 Hz and the sixth is 26.957 Hz.

Autodesk Simulation Solution

The beam was drawn as a line from (0, 0, 0) to (10, 0, 0) and meshed with 20 beam elements. The origin point was fully constrained. Offsets for the point masses were defined using beam elements with high stiffness and zero mass density so they would not affect the solution. Lumped masses were defined at (10, 2, 0) and (10, -2, 0).

A Natural Frequency (Modal) analysis was performed to calculate the first six natural frequencies and mode shapes. The results for the sixth mode are shown in Figure 161-3. The analysis results are compared to the NAFEMS solution in Table 161-1.

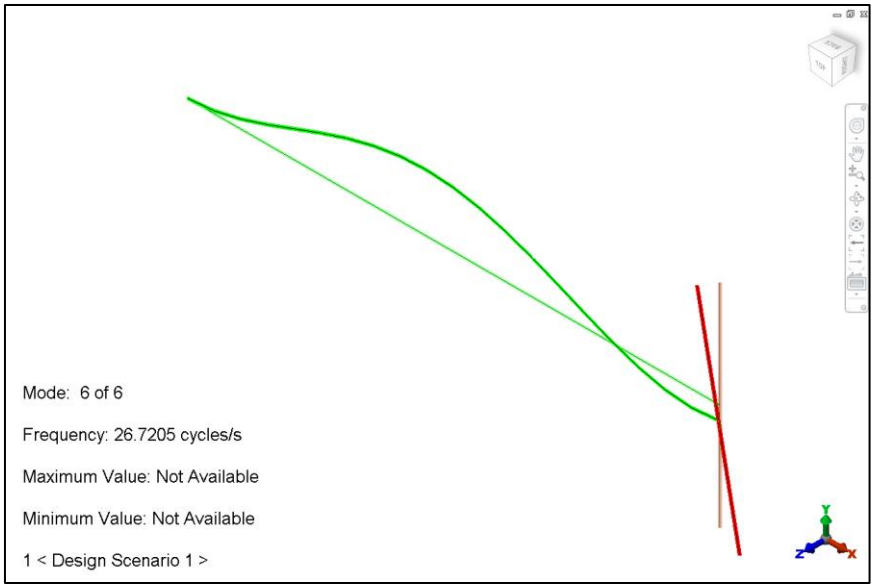

Figure 161-3. The frequency and mode shape of the sixth natural frequency.

Table 161-1. Comparison of Results.

Mode	Frequency (Hz)		% Difference
	NAFEMS	Analysis	
1	1.723	1.722	0.06
2	1.727	1.725	0.12
3	7.413	7.435	0.30
4	9.972	9.950	0.22
5	18.160	18.060	0.55
6	26.972	26.721	0.93

AVE - 162 Steady-State Heat Transfer Analysis of a Coal Powder Stockpile

Reference

Bejan, A., *Heat Transfer*, John Wiley & Sons, 1993, Example 1.2, p. 25.

Problem Description

A 2-m-deep layer of fine coal powder (as shown in Figure 162-1) generates heat volumetrically due to a reaction between the coal particles and atmospheric gases.

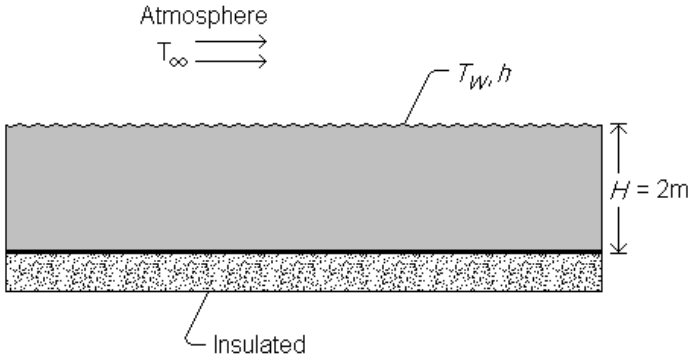

Figure 162-1. Illustration of the heat-generating coal powder stockpile.

The material properties are:

- Air temperature (T_∞) = 25 °C
- Heat transfer coefficient (h) = 5 W/m^2 K
- Heat generation ($\dot{q}$) = 20 W/m^3
- Conduction = 2 W/m C

Calculate the temperature of the upper surface, T_w.

Theoretical Solution

Expressed per unit of surface area covered by the coal pile, the heat generated by the entire layer of coal is

$$q'' = \dot{q}H = 20\frac{W}{m^3}2m = 40\frac{W}{m^2}$$

This heat transfer rate must escape through the upper surface of temperature T_w,

$$q'' = h(T_w - T_\infty)$$

because the lower surface has been modeled as insulated (zero heat flux). The unknown temperature of the upper surface of the coal stockpile is

$$T_w = T_\infty + \frac{q''}{h} = 25°C + 40\frac{W}{m^2}\frac{m^2 \cdot K}{5W}$$

$$= 25°C + 8°C = 33°C$$

Autodesk Simulation Solution

A cross-section of the coal stockpile (10 m long by 2 m wide) was modeled in FEA Editor using 80 two-dimensional (2-D) elements. The top surface was defined as a unique surface number to facilitate the application of the convection load. Element and material information was defined per the problem statement.

A Steady-State Heat Transfer analysis was performed to calculate the temperature distribution. The temperature at the top of the coal stockpile was 33 °C as shown in Figure 162-2. The analysis results are compared to the theoretical solution in Table 162-1.

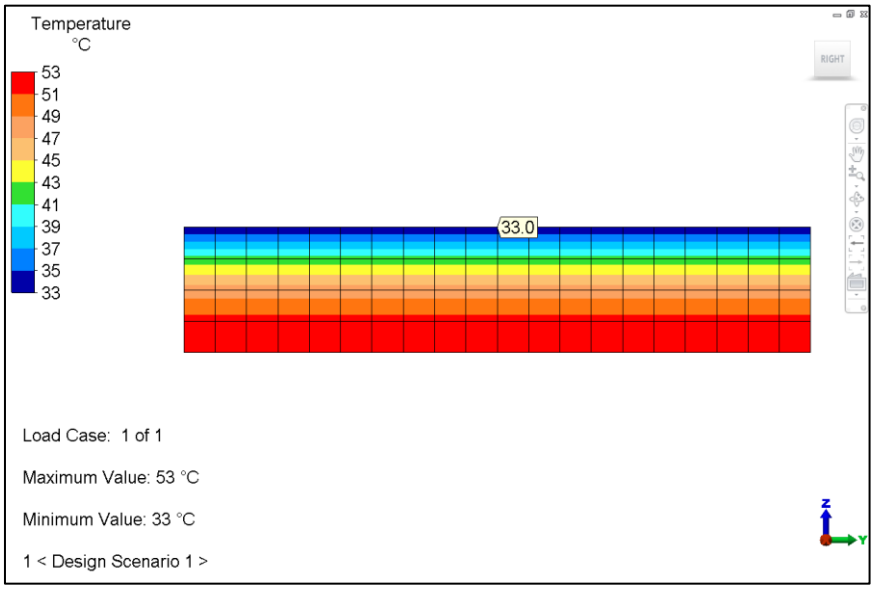

Figure 162-2. Inquiring on the temperature results at the top of the coal stockpile model.

Table 162-1. Comparison of Results.

Temperature (°C)		% Difference
Theoretical	**Analysis**	
33	33	0.00

AVE - 163 Bending and Wrinkling of a Pretensioned Beam-like Membrane

Reference

Miller, R. K., Hedgepeth, J. M., Weingarten, V. I., Das, P. and Kahyai, S., "Finite Element Analysis of Partly Wrinkled Membranes", *Computers and Structures*, 1985; 20:631-639.

Problem Description

A beam-like rectangular plane membrane, with width h and thickness t, is tensioned by a uniform normal stress σ_0 in both the x- and y-directions and subject to an in-plane bending moment M applied on its two ends. As the bending moment is increased, a band of vertical wrinkles with height b appears along the compressed edge.

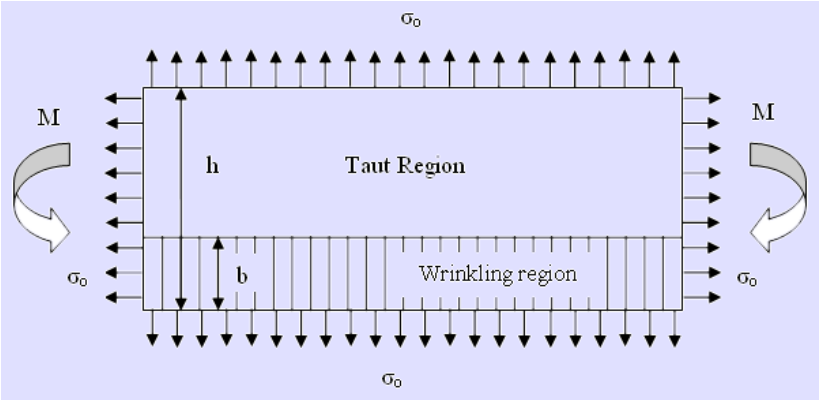

Figure 163-1. Diagram of the beam-like membrane.

Determine the stress in the membrane and the relation between the bending moment and the overall curvature of the beam-like membrane.

Theoretical Solution

The height b of the wrinkling region is given by

$$\frac{b}{h} = \begin{cases} 0, & \frac{M}{Ph} < \frac{1}{6} \\ \frac{3M}{Ph} - \frac{1}{2}, & \frac{1}{6} \le \frac{M}{Ph} < \frac{1}{2} \end{cases}$$

The stress within the membrane may be expressed as

$$\frac{\sigma_x}{\sigma_0} = \begin{cases} 2\left(\frac{y}{h} - \frac{b}{h}\right) \Big/ \left(1 - \frac{b}{h}\right)^2, & \frac{b}{h} < \frac{y}{h} \le 1 \\ 0, & 0 \le \frac{y}{h} \le \frac{b}{h} \end{cases}$$

$$\frac{\sigma_y}{\sigma_0} = 1$$

$$\tau_{xy} = 0$$

Let κ denote the overall curvature of the membrane acting as a beam. The relation between M and κ is given by

$$\frac{2M}{Ph} = \begin{cases} \frac{1}{3}\frac{Eth^2}{2P}\kappa, & \frac{Eth^2}{2P}\kappa \le 1 \\ 1-\frac{2}{3}\sqrt{\frac{2P}{Eth^2\kappa}}, & \frac{Eth^2}{2P}\kappa > 1 \end{cases}$$

where E is the Young's modulus of the membrane material.

Autodesk Simulation Solution

Taking advantage of symmetry, only half of the diagram shown in Figure 163-1 was modeled in FEA Editor using 200 membrane elements. When defining the element information, a thickness of 0.01 m was specified. Additionally, on the "Advanced" tab, the "No Compression" option was activated, which disabled the element's ability to support compressive loads (i.e., if the membrane elements are placed in compression, they should not resist the compressive load). This option is useful for simulating fabric materials such as sails or parachutes. The material was specified from the Autodesk Simulation Material Library as Plastics Nylon, Type 6/6.

Symmetry boundary conditions (Tx, Ry, Rz) were defined along the left edge of the model, which is the centerline of the diagram shown in Figure 174-1. Additionally, to give the model stability, nodal boundary conditions were specified for the bottom left corner node (Tx, Tz, Rx, Ry, Rz) that constrained the model from out of plane translation at the centerline.

Nodal forces of 0.01 N were added to the upper, right, and bottom edges to define the pretensioned tautness of the membrane. (At the corner nodes, the nodal force values were halved (0.005 N) because the nodal forces are shared by the adjacent elements.)

To simulate the moments shown in Figure 163-1, a nodal force of 0.0233 N was added to the top right corner node and a nodal force of -0.0233 N was added to the bottom right corner node.

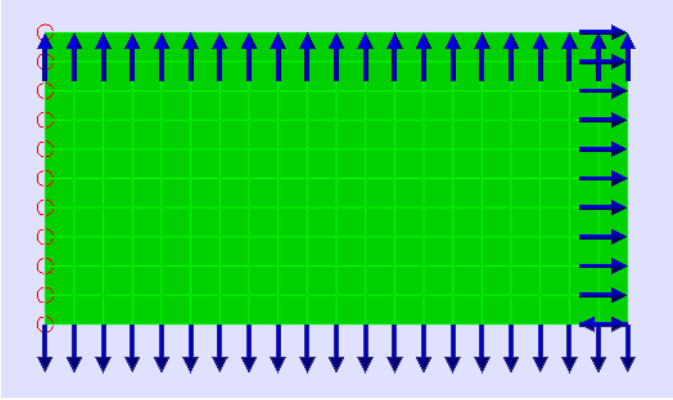

Figure 163-2. Half-symmetry model of the pretensioned membrane.

An MES with Nonlinear Material Models was set up with duration of 4 seconds and a capture rate of 10 steps per second. A load curve was defined to specify that the bending load should be applied after 2 seconds and remain in effect for the rest of the event. The analysis solved for motion and stresses.

In the Results environment, stresses were examined, which indicated that the upper region of the model is taut and the lower region may be buckled. A chart comparing the theoretical and analysis results is shown in Figure 163-4.

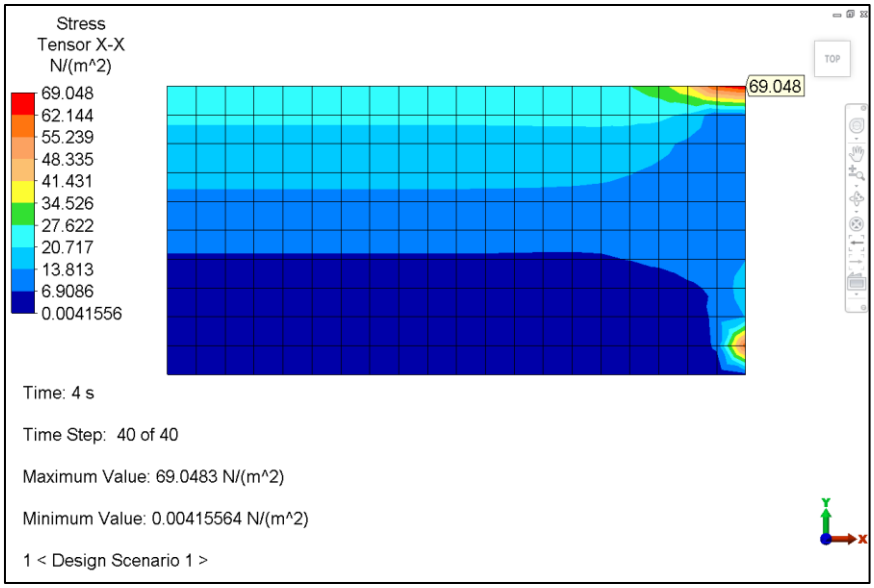

Figure 163-3. Stress tensor X-X results at a node in the buckling region.

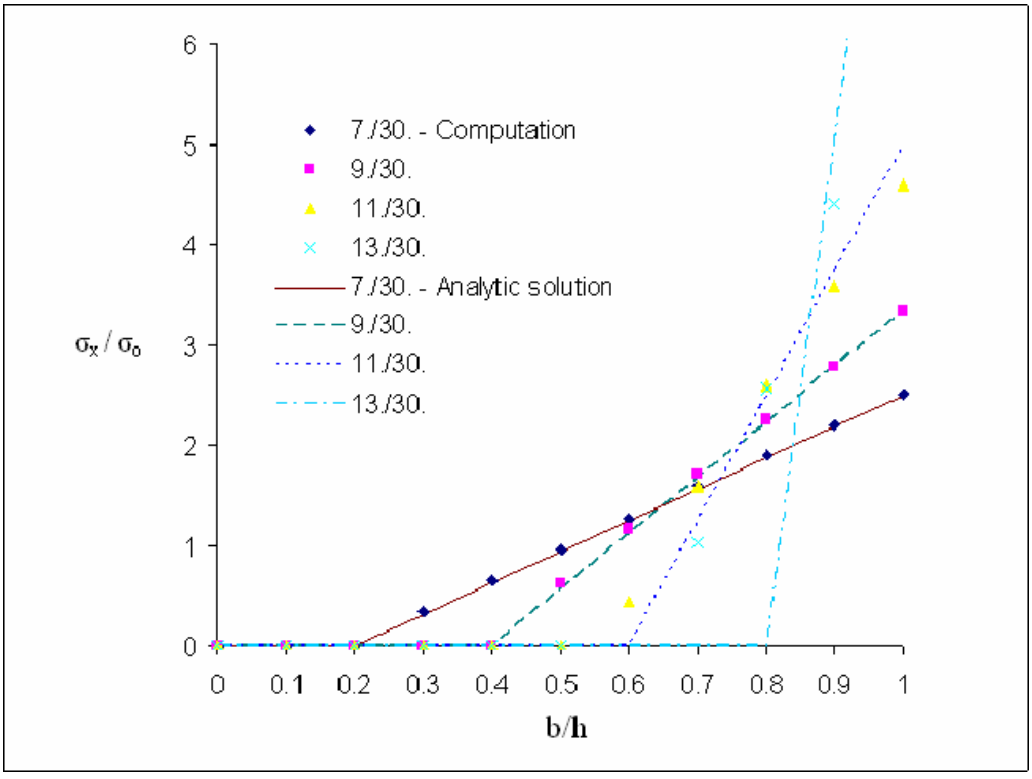

Figure 163-4. Comparison of Results.

AVE - 164 Displacement of a Restraining Rod Attached to a Beam

Reference

Lindeburg, Michael R., *EIT Review Manual*, #4073 594, Problem 13, p. 18-10.

Problem Description

A horizontal beam carries a triangular distributed load of 290 kN/m over section AB as shown in Figure 164-1. The beam has a mass of 148 kg/m and is simply supported at point B. The cantilever end BC is restrained by a thin aluminum rod, CD.

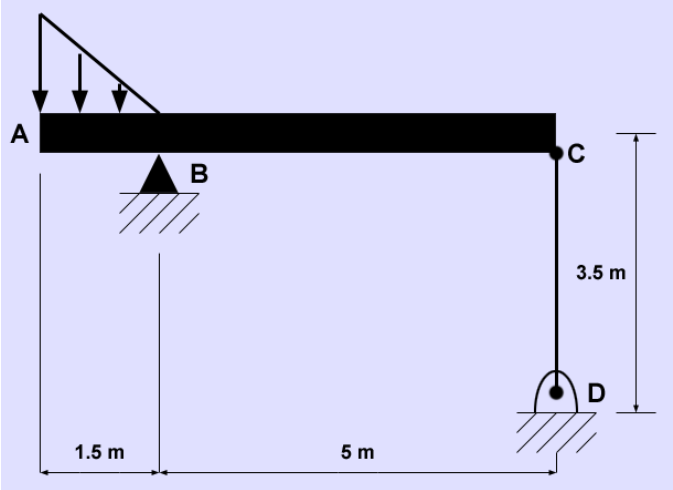

Figure 164-1. Diagram of the beam and restraining rod.

The material properties of aluminum rod CD are:
- Cross-sectional area (A) = 3.25 cm^2
- Modulus of elasticity (E) = 6.9×10^{10} Pa

Determine the change in length of the rod.

Theoretical Solution

The triangular distribution has a total magnitude of

$$\frac{1}{2}\text{bh} = \left(\frac{1}{2}\right)(1.5\text{m})\left(290\times10^3\,\frac{\text{N}}{\text{m}}\right) = 217500\,\text{N}$$

This force can be assumed to act through the centroid of the triangular distribution located 2/3 of the length AB from support B. This is at

$$\left(\frac{2}{3}\right)(1.5\text{m}) = 1\text{m}$$

The beam self-loading for 1.5 m on either side of support B is equal. Only the last 3.5 m of the right side of the beam are unbalanced. The unbalanced beam load is

$$\left(148\frac{\text{kg}}{\text{m}}\right)\left(9.81\frac{\text{m}}{\text{s}^2}\right)(3.5\text{m}) = 5082\,\text{N}$$

Measuring distance from point B to the right, this unbalanced beam load acts at

$$1.5\text{m}+\left(\frac{1}{2}\right)(3.5\text{m}) = 3.25\text{m}$$

Take moments about point B to determine the tensile force in the aluminum rod CD.

$$M_B: (217500\,\text{N})(1\text{m}) - (5082\,\text{N})(3.25\text{m}) + R_C(5\text{m}) = 0$$

R_C = -40197 N [downward]

The elongation is

$$\delta = \frac{PL}{AE} = \frac{(40197\,\text{N})(3.5\text{m})\left(\frac{100\,\text{cm}}{1\text{m}}\right)^2}{(3.25\text{cm}^2)(6.9\times10^{10}\,\text{Pa})} = 0.00627\text{ m} = 6.27\text{ mm}$$

Autodesk Simulation Solution

The lines of the model were created by using the "Draw: Line..." capability in the FEA Editor environment.

The horizontal beam was modeled as part 1 using beam elements. The reference did not provide a cross-sectional area for the horizontal beam; however, in the "Element Definition" screen, a cross-sectional area of 1 was specified to allow easy calculation of mass density. The mass density was defined as 148 kg/m^3. (Multiplying the mass density times the area of 1 gives the density as 148 kg/m^3.)

The thin aluminum rod was modeled as part 2 using a single truss element. On the "Element Definition" screen, the cross-sectional area was specified as 0.000325 m^2. Because the rod was considered thin and massless, a very small value was entered for the mass density (0.00001 kg/m^3) on the "Element Material Specification" screen. The modulus of elasticity was defined as 6.9e10 N/m^2.

The bottom node of the rod (D in Figure 164-1) was fully constrained. Because truss elements have only translational degrees of freedom, the fixed node will act as a pin. To simulate the simple support of the beam at point B, the node was constrained in all degrees of freedom except for rotation about the Z axis.

The triangular distributed load over the 1.5-m section (AB) of the beam was defined by selecting the line and right clicking to access an options menu and then using the "Setup tab; Beam Loads panel; Beam Distributed Load" command sequence. The I-node magnitude was specified as -290000 N/m in the Y direction at the I side (the left hand side of the model) and the J-node magnitude was defined as 0 N/m in the Y direction at the J side to give the triangular distributed load.

To better simulate the gravity loading, the 5-m beam section (BC) was divided into five beam elements. The gravity loading was specified in the –Y direction.

A Static Stress with Linear Material Models analysis was run to determine the displacement of point C. In the Results environment, displacements were examined in the Y direction, which matched the reference solution. Table 164-1 shows a tabular comparison of the theoretical and analysis results.

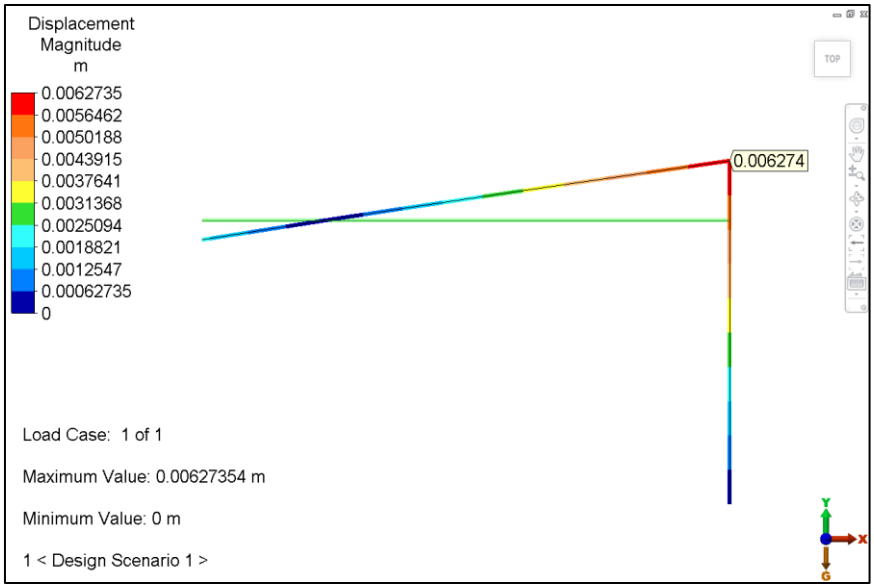

Figure 164-2. Inquiring on displacement results at point C. Results are shown on the displaced model with the undisplaced model shown as a mesh.

Table 164-1. Comparison of Results.

Displacement (m)		% Difference
Theoretical	**Analysis**	
6.27e-3	6.27e-3	0.00

AVE - 165 MES of a Parallelogram Linkage Used to Transfer a Crate between Platforms

Reference

Meriam, J. L., Kraige, L. G., *Engineering Mechanics: Dynamics*, Volume Two, problem 6/29, p. 426.

Problem Description

As shown in Figure 165-1, a parallelogram linkage (including rods CD and EF) is used to transfer crates from platform A to platform B and is hydraulically operated by an actuator.

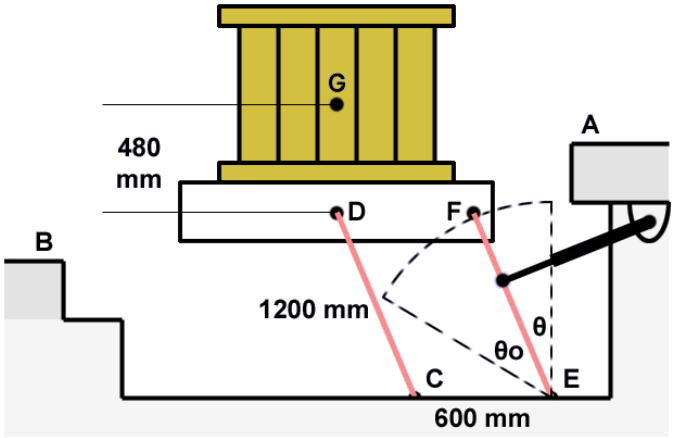

Figure 165-1. Diagram of the parallelogram linkage used to transfer a crate from platform A to platform B.

The oil pressure in the actuator cylinder is programmed to provide a smooth transition of motion from $\theta = 0$ to $\theta = \theta_0 = \pi/3$ rad given by

$$\theta = \frac{\pi}{6}\left(1 - \cos\frac{\pi t}{2}\right)$$ where t is in seconds.

The crate has a mass of 200 kg with mass center at point G. Assume that the mass of both the platform beneath the crate and the rods is negligible.

Determine the force at point D on the rod:
(a) just after the start of the motion with θ and t essentially zero; and
(b) when t = 1 s.

Theoretical Solution

The reference gives the solution as:
(a) D = 1714 N; and
(b) D = 2178 N

Autodesk Simulation Solution

Rod CD was modeled as part 1 using a single truss element. On the "Element Definition" screen, a cross-sectional area of 1 m^2 was specified. The material was defined as "Aluminum (6061-T6)" with a small value for the mass density (0.00001 kg/m^3) to because the problem description specified that the rod is considered massless.

The platform that supports the crate was modeled as part 2 using 2-D elements with dimensions (1.6 m wide and .25 m thick) that were not specified in the problem description. On the "Element Definition" screen, plane stress geometry was specified along with a thickness of 1 m. The material was defined as "Aluminum (6061-T6)" with mass density of 0.00001 kg/m^3 to simulate masslessness.

The crate was modeled as part 3 using 2-D elements with the center point of the crate at 0.48 m above point D. Same as for the platform, plane stress geometry and a thickness of 1 m were specified. The material was defined as "Aluminum (6061-T6)" with the mass density as 352.113 kg/m^3, which was calculated from the volume to give mass = 200 kg as specified in the problem description.

Rod EF was modeled as part 4 using a single beam element. A cross-sectional area of 1 m^2 was specified. The material was defined as "Aluminum (6061-T6)" with mass density as 0.00001 kg/m^3 to simulate masslessness.

Fully fixed nodal boundary conditions were added to the node at point C. Per the problem description, point C should be free to rotate about the X axis; however, because rod CD is a truss element and truss elements do not have rotational degrees of freedom, there is no need to define rotational degrees of freedom and it is satisfactory to use the fully fixed condition.

The node at point E was constrained in all degrees of freedom except for rotation in the X direction.

A prescribed rotation was added to the node at point E with a magnitude of 1 revolution in the Scalar X direction. The Timeline Event Editor was used to define an equation to represent the motion. In the "Equation Editor" dialog, a start time of 0.00, end time of 1.00 and interval of 0.001 were specified and the equation was input (the equation given in the problem description was converted from radians to revolutions). (See Figure 165-2)

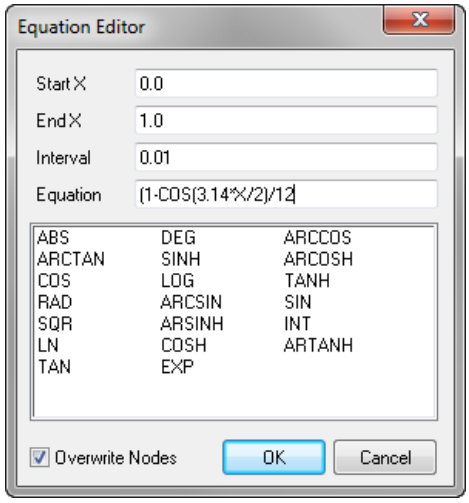

Figure 165-2. Defining the event curve in the "Equation Editor" dialog of the Timeline Event Editor.

The active range for the prescribed rotation was defined as a birth time of 0 and death time of 100 so that it was always active throughout the event.

On the "Analysis Parameters" screen, the duration of the event was specified as 1 s and the capture rate as 100 steps/s. On the "Accel/Gravity" tab, a standard gravity load was specified in the –Z direction.

A Mechanical Event Simulation with Nonlinear Material Models was performed to solve for the force at point D at time = 0.01 s and 1.00 s. In the Results environment, axial forces were examined for the relevant time steps. The axial force on point D at time = 0.01 s was calculated as -1714.88 N as shown in Figure 165-3. The axial force on point D at time = 1 s was calculated as -2174.48 N as shown in Figure 165-4. Table 165-1 shows a tabular comparison of the theoretical and analysis results.

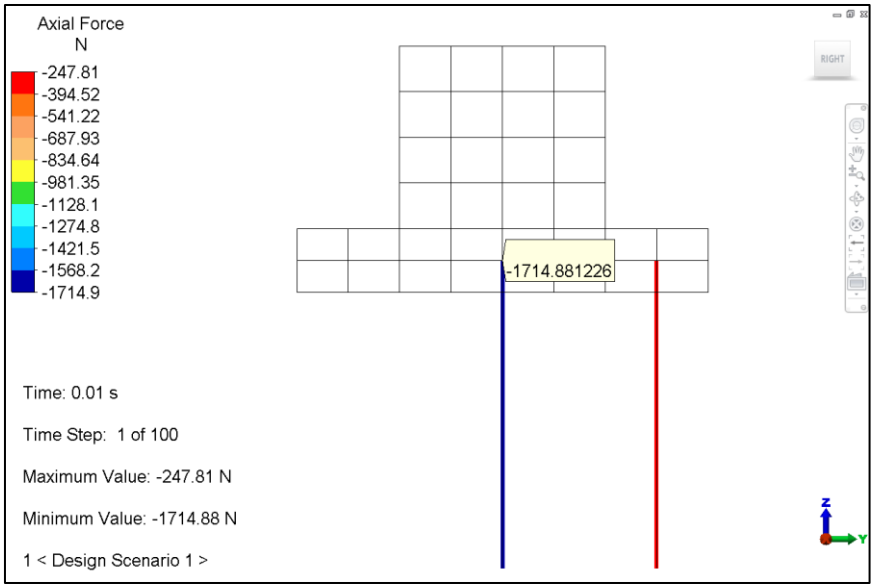

Figure 165-3. Inquiring on axial force results at point D for time = 0.01 s.

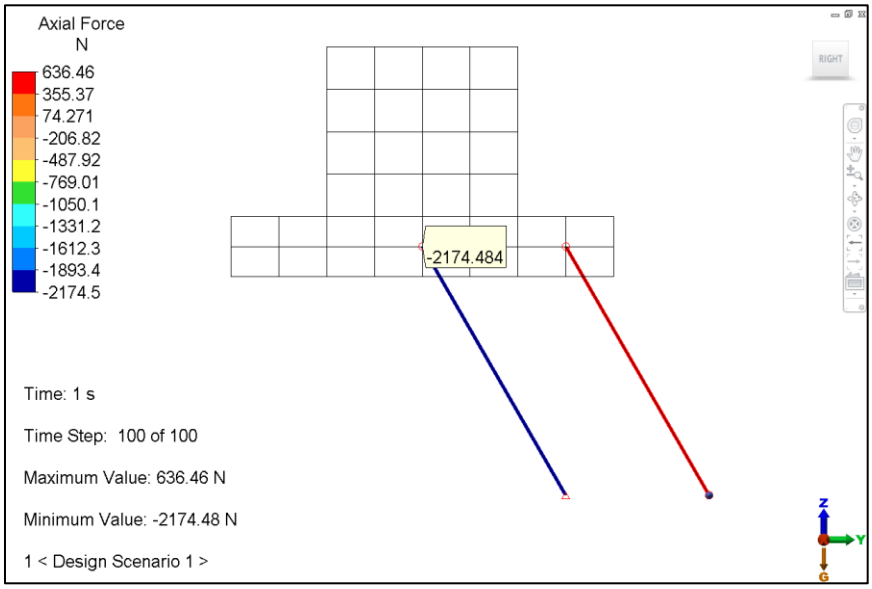

Figure 165-4. Inquiring on axial force results at point D for time = 1 s.

Table 165-1. Comparison of Results

Time (s)	Axial Force (N)		% Difference
	Theoretical	Analysis	
0.01	1714	1714.88	0.05
1	2178	2174.48	0.16

AVE - 166 Beam with Spring Support under Distributed Load

Reference

Formulae used in this example are available in any mechanical engineering handbook.

Problem Description

A horizontal beam (length = 30 in, width = 0.5 in and height = 0.75 in) is fixed on one end and supported by a spring (with stiffness k = 54 lb/in) at the other end. A distributed load (w = 5 lb/in) is applied on the top of the beam as shown in Figure 166-1.

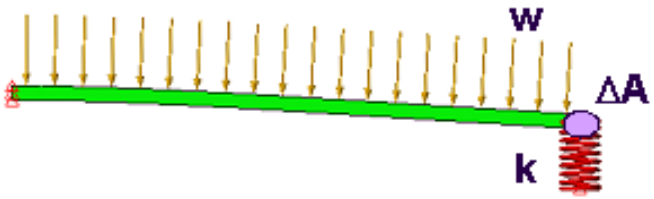

Figure 166-1. Diagram of the beam with a spring support under a distributed load.

The material properties of the beam include:

- Modulus of elasticity (E) = 30×10^6 Pa
- Poisson's ratio = 0.3

Find the deflection at point A (the free end of the beam) and the force in the spring.

Theoretical Solution

The method of modal superposition was used for the theoretical solution of this problem. As shown in Figure 166-2, the problem was broken down into two problems:

1. a cantilever beam with the distributed load (causing a larger deflection at the free end); and
2. a force (equal to the spring stiffness times the deflection in the spring) applied to the end of the beam.

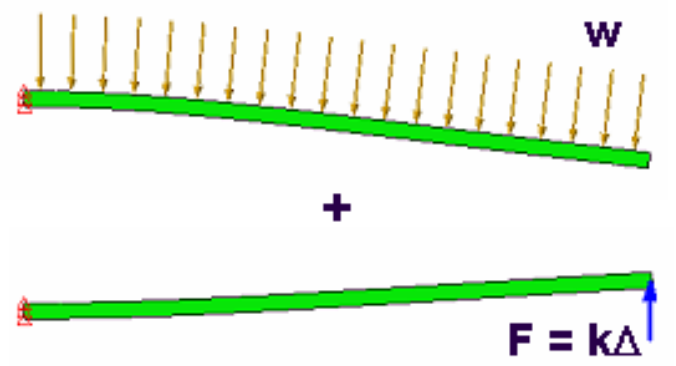

Figure 166-2. The results of these two problems were added to solve for the system shown in Figure 166-1.

The results of these two problems were added together to yield the solution for the system shown in Figure 166-1.

First, the deflection at point A due solely to the distributed load was solved for as shown in Figure 166-3.

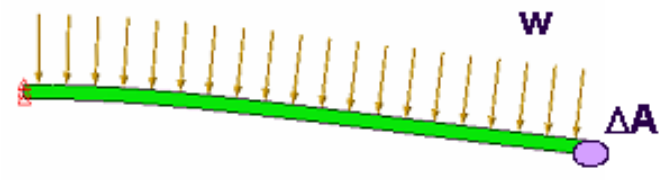

Figure 166-3. Diagram of the deflection at point A in the beam due to the distributed load.

This value can be found in mechanical engineering handbooks or calculated as follows

$$\Delta A_w = \frac{w * L^4}{8 * E * I} = -0.9599 \,\text{inch}$$

The above equation gives a deflection of nearly one inch in the downward direction.

The moment of inertia (the beam cross section) is based on the width and height given and is calculated as

$$I = \frac{(0.5)(0.75)^3}{12} = 0.01758 \,\text{in}^4$$

Next, as shown in Figure 166-4, the deflection due to the spring load (the force F) is unknown because the amount of downward deflection in the beam (ΔA) is not known.

Figure 166-4. Diagram of the deflection at point A in the beam due to the spring load.

The deflection due to the load at the end of a cantilever beam is

$$\Delta A_F = \frac{F * L^3}{3 * E * I} = (k * \Delta A) * 0.0171$$

where the force at the end of the beam is a function of how much deflection occurs in the spring.

Finally, the two problems were put together to calculate the total deflection at point A as shown in Figure 166-5.

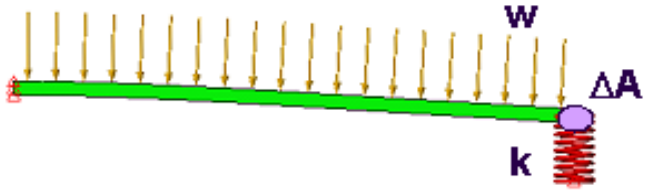

Figure 166-5. Diagram of the total deflection at A in the beam with support spring.

The total deflection at point A due to both loads is

$$\Delta A = \Delta A_w + \Delta A_F$$

$$\Delta A = -0.9599\,\text{in} + (k * \Delta A) * 0.0171$$

$$\Delta A = -0.499\,\text{in}$$

Thus, the final deflection at point A was calculated as just under a half inch.

With the deflection of the spring known, it was used to find the force in the spring:

$$F = k * \Delta A = -26.95\,\text{lb}$$

Thus, the force in the spring was calculated as nearly 27 pounds compression.

Autodesk Simulation Solution

The beam was modeled in FEA Editor as using Brick elements. The Brick model represented the ends of the beam as four rectangular surfaces with a point at the center of the beam. The center point was where the spring would be attached, which would not introduce any twisting effects that were not covered in the theoretical solution. A line (with a length of 5 inches in the –Z direction) was added as part 2 to represent the support spring.

Translational constraints (Tx, Ty and Tz) were applied to the free end of the spring to pin it to the ground. Fully fixed constraints were applied to the free end of the beam. A uniform pressure load of 10 lbf/in^2 was applied to the top surface of the beam.

For part 1, the beam, material properties were specified for the modulus of elasticity (30e6 lbf/in^2), which was given, and Poisson's ratio (0.3). For part 2, the spring, the spring element type was specified. In the "Element Definition" dialog, the spring stiffness was defined as 54 lbf/in and the "Axial" option was chosen for the element type to describe the spring's movement. On the "Visualization" tab, options were specified to visualize spring elements as a spring with coils rather than as a line. The finite element model of the beam and spring support is shown in Figure 166-6.

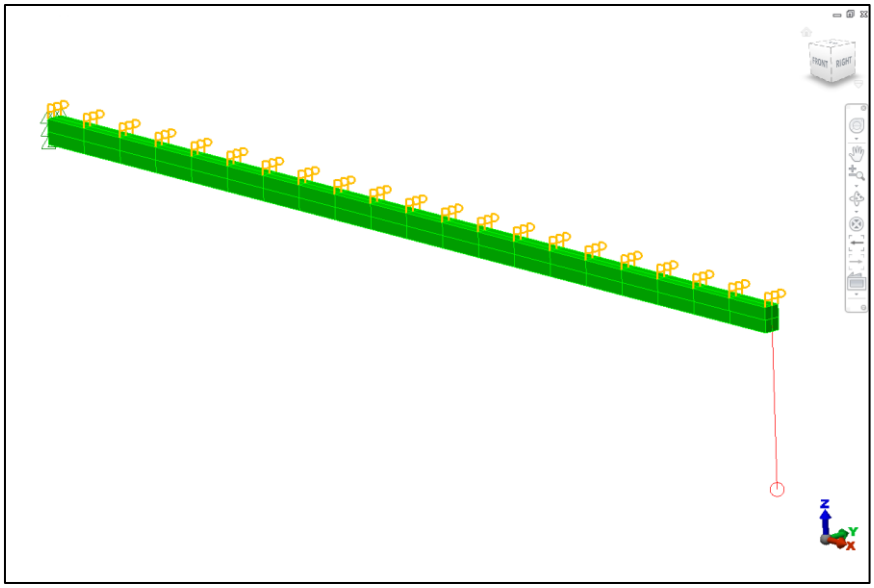

Figure 166-6. The finite element model of the beam and spring support.

A Static Stress with Linear Material Models analysis was performed. In the Results environment, the deflection in the Z direction at the center of the spring end of the beam was examined as shown in Figure 166-7.

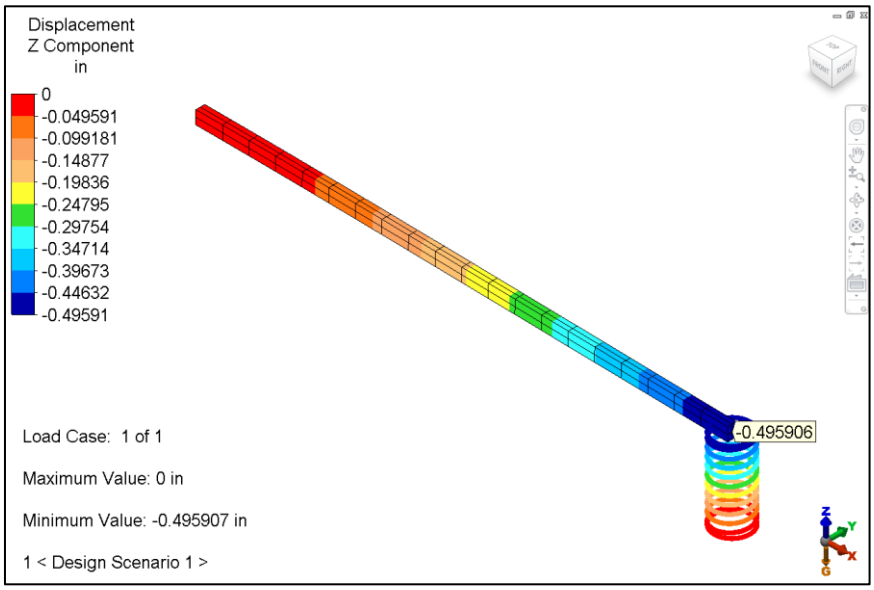

Figure 166-7. Displacement results at the center of the spring end of the beam.

The force in the spring was examined as shown in Figure 166-8.

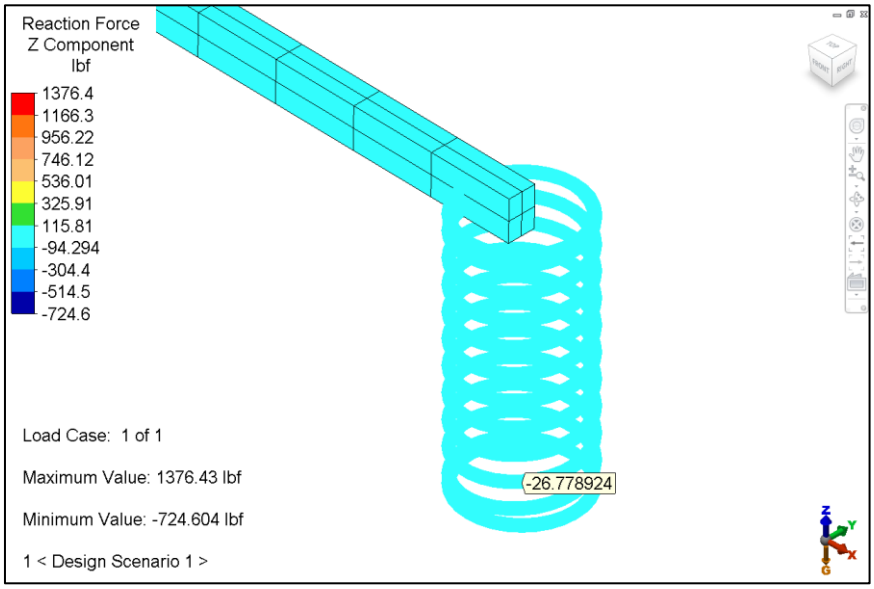

Figure 166-8. Inquiring on the force result of the spring.

Table 166-1 shows a tabular comparison of the theoretical and analysis results. The results matched the theoretical solution to within one percent.

Table 166-1. Comparison of Results

	Theoretical	Analysis	% Difference
Displacement (in)	-0.499	-0.496	-0.60
Force (lb)	-26.95	-26.78	-0.63

AVE - 167 Flow through a Tube with Fixed Heat Flux

Reference

Incropera, F. P. and Dewitt, D. P., *Fundamentals of Heat and Mass Transfer*, 2nd Edition, John Wiley & Sons, 1985, pp. 390-391.

Problem Description

Water flows through a tube (length = 2.0 m and diameter = 60 mm) at a flow rate of 0.01 kg/s with an inlet temperature of 20 °C. The outer surface of the tube is subjected to a heat flux load of 2 kW/m^2 as shown in Figure 167-1

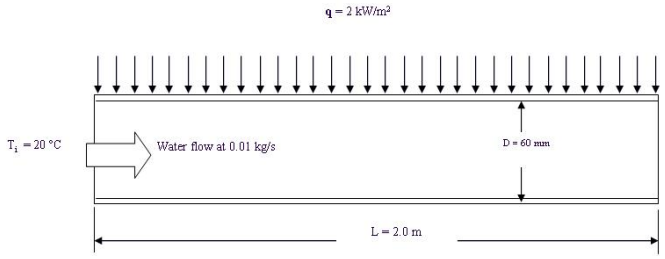

Figure 167-1. Diagram of the flow through a tube with fixed heat flux.

The material properties of the fluid include:

- Mass density (ρ) = 1000 kg/m^3
- Thermal conductivity (k) = 0.67 J/kg/K/s
- Specific heat (Cp) = 4181 J/kg/K
- Viscosity (μ) = 3.52e-4 N/s/m^2

Find the temperature at the outlet of the tube.

Theoretical Solution

In the reference, the theoretical solution is calculated as 79.1 °C.

Autodesk Simulation Solution

To simulate this problem, coupled fluid flow and steady-state heat transfer analysis capabilities were used. As an overview, first a Steady Fluid Flow analysis was performed to obtain the velocity results for the fluid that flows through the tube. Then, the fluid flow results were input as a load to the Steady-State Heat Transfer analysis.

Steady Fluid Flow Analysis

To simplify the model, the pipe material was not included; only the fluid was modeled.

A three-dimensional (3-D) model of the fluid that flows through the tube was built using FEA Editor. First, the cross section (with a 60-mm diameter) was drawn and a small rectangle was added in the center to facilitate meshing as shown in Figure 167-2.

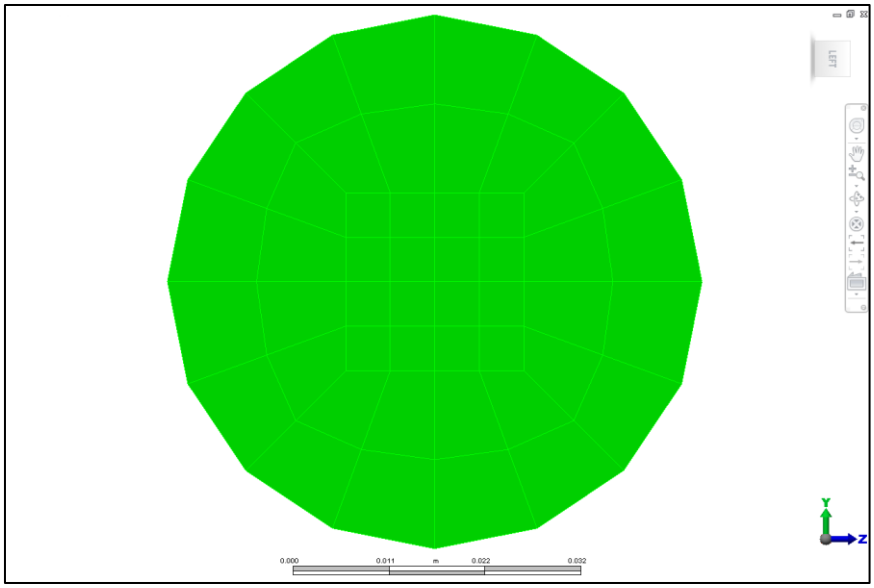

Figure 167-2. The cross-sectional mesh of the fluid that flows through the tube.

Next, the two-dimensional (2-D) mesh of the cross section was extruded along the X axis to generate a 3-D model with length = 2.0 m.

3-D elements were used with the default Newtonian viscosity model and integration order. For material properties, the mass density and dynamic viscosity were specified with values given in the problem description.

A fan surface with a inlet flow rate of 0.00001 m^3/s was added to the inlet surface to match the mass flow rate of 0.01 kg/s that was specified in the problem description. At opposite end a Surface prescribed Inlet/outlet condition was defined. The Steady Fluid Flow analysis was run and the velocity results were examined in the Results environment as shown in Figure 167-3.

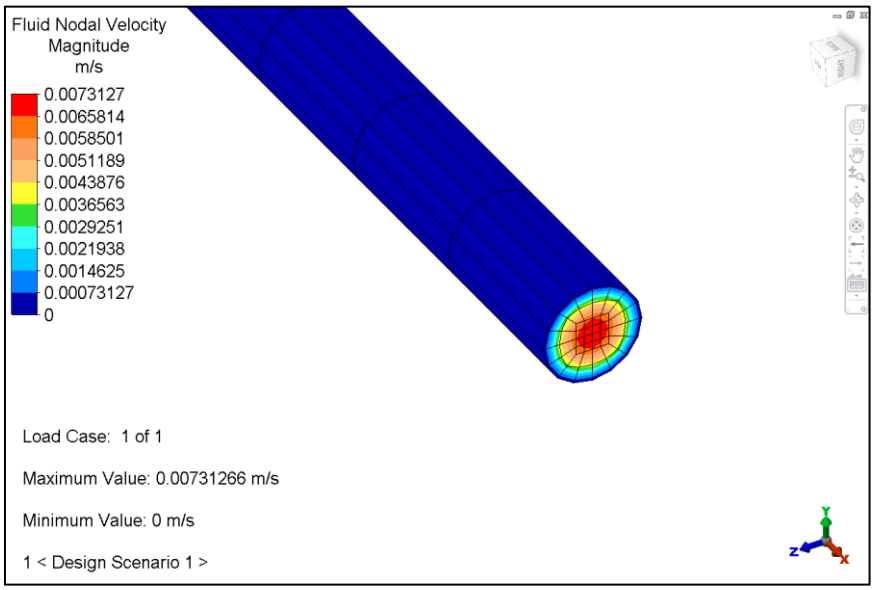

Figure 167-3. Fluid flow velocity results.

Steady-State Heat Transfer Analysis

The same model geometry from the fluid flow analysis was used for the steady-state heat transfer analysis. As a simplifying assumption, the effects of the heat flux passing through the pipe material were ignored as if the conductivity of the pipe material was infinite.

The outer surface of the cross-section (surface number 4) was used to add the heat flux load. Brick elements were used with the default element definition. For material properties, the mass density, thermal conductivity and specific heat were specified per the problem description.

> **Note:** Normally, for a Steady-State Heat Transfer analysis, only the thermal conductivity is needed. But, in this case, because we were modeling heat transfer from fluid flow with convective terms (the mass transfer of the fluid), all three properties (mass density, thermal conductivity and specific heat) were needed.

Three loads were applied to the model:

1. A heat flux load on the outer surface – A thermal surface load (heat flux =2000 J/(s*m^2)) added to surface 4.
2. A constant temperature at the inlet surface – Surface controlled temperature (magnitude = 20 °C) was added to the surface of the inlet face.
3. The heat transfer from the motion of the fluid – The results from the previous fluid flow analysis were applied as a load.

A Steady-State Heat Transfer analysis was performed and the temperature distribution results were examined in the Results environment.

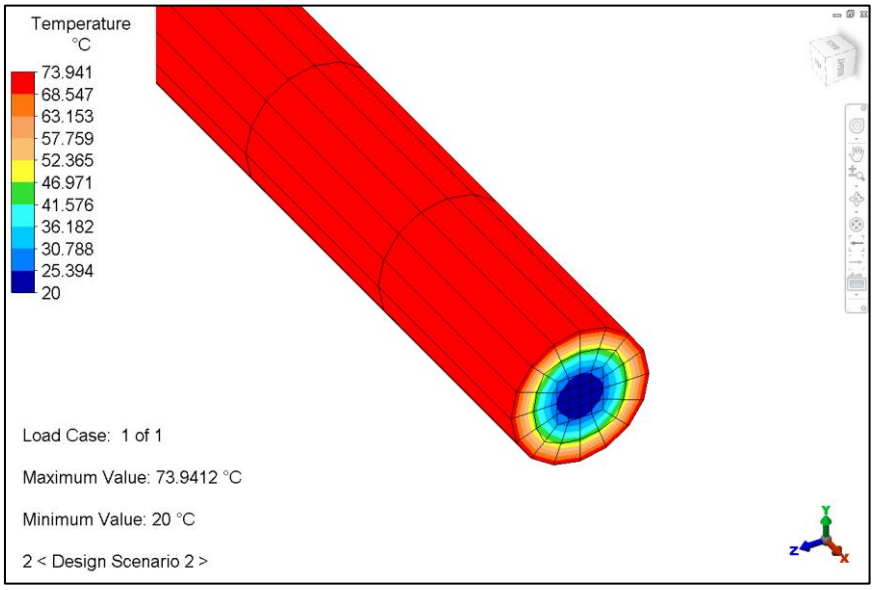

Figure 167-4. Temperature at the outlet.

Table 167-1. Comparison of Results

	Theory	**Analysis**	**% Difference**
Temperature at Outlet (°C)	79.1	73.94	6.52

AVE - 168 Body-to-Body Radiation Heat Transfer in the Frustum of a Cone

Reference

Siegel, Robert and Howell, John R., *Thermal Radiation Heat Transfer*, 3rd Edition, Taylor & Francis, 1992, Example 7-15, pp. 277-278.

Problem Description

A frustum of a cone has its base heated (heat flux of 3000 W/m^2) while its top is held at 550 °K and the side is perfectly insulated on the outside as shown in Figure 168-1. Each surface has a different emissivity as noted.

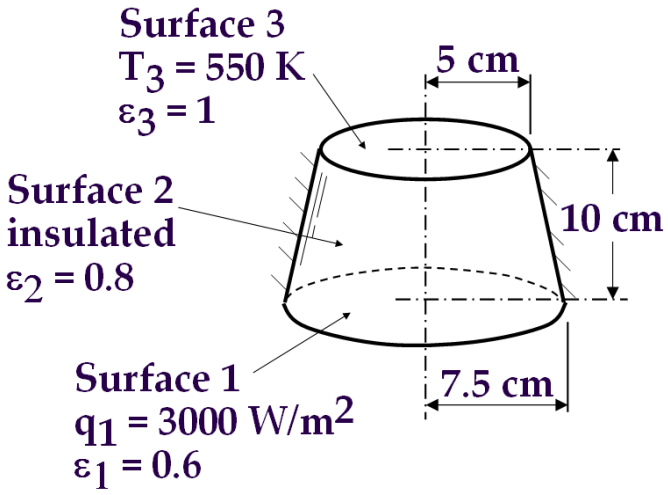

Figure 168-1. Diagram of the body-to-body radiation heat transfer in the frustum of a cone.

Find the temperature on the bottom surface and the temperature of the side surface.

Theoretical Solution

From Appendix C of the reference, the shape factor for surface 3 to surface 1 (the top to the bottom) is calculated as

F3-1 = 0.3249

All other view factors are calculated either by using reciprocity because the view factors must sum to 1. With the view factors known and based on the given, the equation for the temperature of the bottom surface can be written as

$$\frac{3000}{0.6} = \sigma\left[T_1^4 - 0.8556T_2^4 - 0.1444(550)^4\right]$$

and the equation for the temperature of the side surface can be written as

$$-3000(0.3735)\frac{1-0.6}{0.6} = \sigma\left[-0.3735T_1^4 + (1-0.4955)T_2^4 - 0.1310(550)^4\right]$$

Solving the two equations for the unknowns gives

- $T_{\text{bottom surface}}$ = 721.6 °K
- $T_{\text{side surface}}$ = 667.4 °K

Autodesk Simulation Solution

A two-dimensional (2-D) model of the cone frustum was built using FEA Editor. 3-D view with a slice plane is shown in Figure 168-2. The top, side and bottom parts were modeled using different part numbers and the inner and outer surfaces were specified to have distinct surface numbers to facilitate applying loads and examining results.

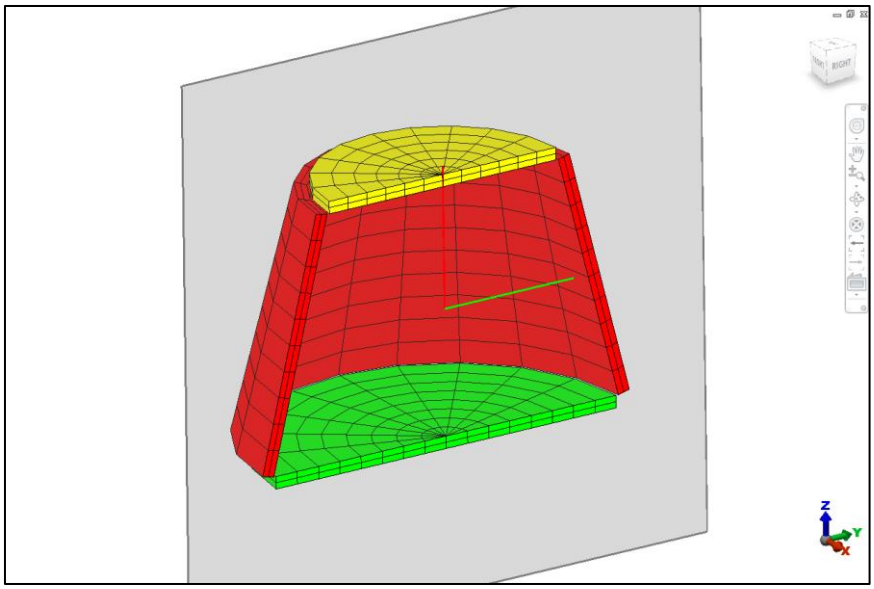

Figure 168-2. A cross section of the cone frustum.

For units, the standard Metric mks (SI) unit system was modified to use Kelvin (K) for temperature in order to match the problem description. 2D axisymmetric elements were used for all three parts.

Although the material was not specified in the reference source, it was assumed that all three parts had uniform temperatures. This was simulated by using a material with a high thermal conductivity, copper, for all three parts.

Three loads were applied to the model:

- Controlled temperature (550 °K) on the top part – A stiffness of 500e4 J/°K was used to ensure that the calculated temperature would approach the specified magnitude.
- Heat flux load (3000 J/(s*m^2)) on the bottom part
- Body-to-body radiation for the three parts – The Analysis Parameters dialog was used to define surfaces and specify emissivity values per the problem description. Then, the surfaces were assigned to enclosures, which are collections of surfaces that can "see" each other and radiate amongst themselves. Because the interior of the cone frustum is a completely enclosed body, no shadowing or ambient temperature parameters needed to be specified. However, because the surfaces are relatively close to each other, the view factor tolerance was set to 0.2 to avoid a warning message.

Additional analysis parameters were specified:

- On the "Multipliers" tab, a radiation multiplier of 1 was specified to activate the radiation load.
- On the "Options" tab, under "Nodal Temperatures", the default nodal temperature was specified as 667 °K to help the solver converge on the final solution. (This value, which is near the theoretical result, would be used by the solver for the first iteration.)
- On the "Advanced" tab, under "Non-Linear Iterations", the "Perform" option was activated to specify that nonlinear calculations should be performed. In the "Criteria" field, the "Stop when corrective norm < E1 (case 1)" option was specified. Values were specified for the maximum number of iterations (500), the corrective tolerance (0.1) and relaxations parameter (0.15).

A Steady-State Heat Transfer analysis was performed and the temperature distribution results were examined in the Results environment.

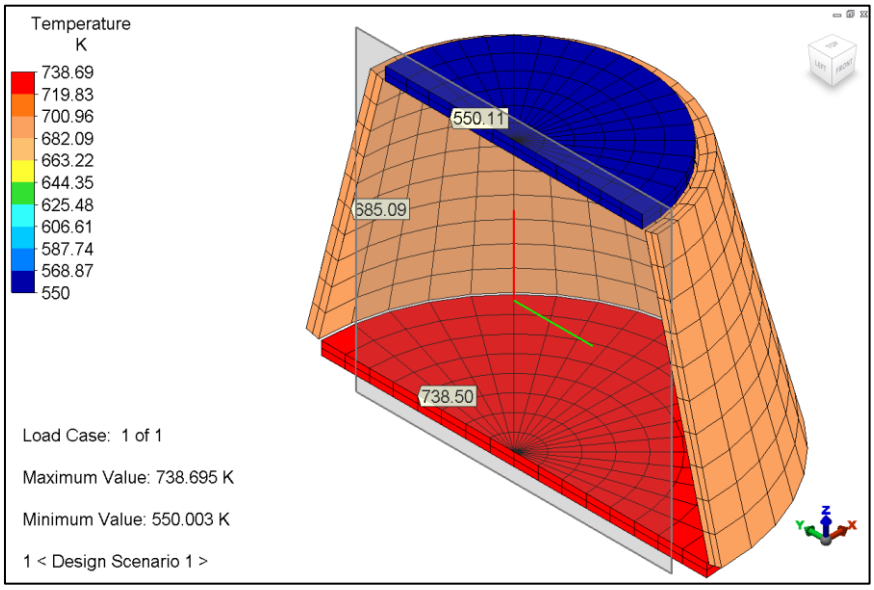

Figure 168-3. Temperature results (3D visualization + slice plane).

Table 168-1. Comparison of Results

	Theory	Analysis	% Difference
Temperature of Bottom Surface (°K)	721.6	738.5	2.34
Temperature of Side Surface (°K)	667.4	685.1	2.65

AVE - 169 Steady Fluid Flow through a Circular Tube

Reference

Formulae used in this example are available in any engineering handbook about fluid flow.

Problem Description

A circular tube (diameter = 2m, length = 4m) has fluid flowing through it (inlet pressure = 2000 N/m^2 and outlet pressure = 1 N/m^2) as shown in Figure 169-1.

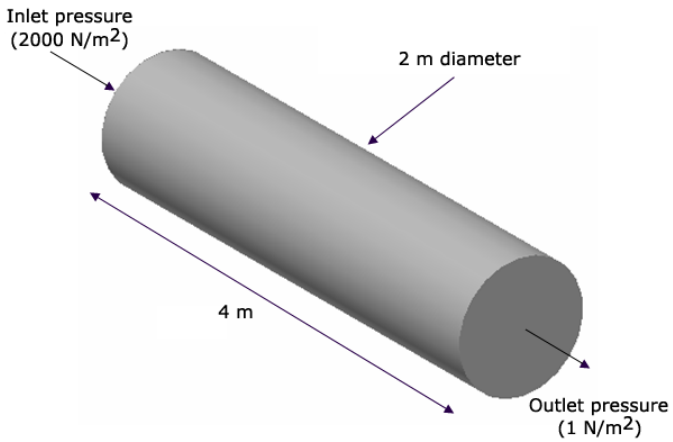

Figure 169-1. Diagram of the fluid flow through a circular tube.

The material properties of the fluid include:

- Mass density (ρ) = 1 kg/m^3
- Dynamic viscosity (μ) = 1 $N*s/m^2$

Find the maximum velocity of the fluid flow in the circular tube.

Theoretical Solution

The radial velocity is calculated as

$$u_x = \frac{2U_\infty}{R^2}\left(R^2 - r^2\right)$$

Solving the equation gives

radial velocity = 124.9 m/s

Autodesk Simulation Solution

A two-dimensional (2-D) axisymmetrical model of the fluid flow inside the circular tube was built using FEA Editor. (The tube itself was not included in the model.) The mesh was made finer near the tube and coarser at the center of the fluid. This meshing technique ensured there would be more elements near the surface constraints of the tube, which would provide a more efficient and accurate solution. Unique surface numbers were specified for the inlet and the outlet in order to facilitate applying the pressure loads.

2-D Axisymmetric element type was used and the "Geometry Type" specified as "Basic Axisymmetric" in the "Element Definition" dialog. For material properties, the mass density and dynamic viscosity were specified per the problem description.

The following loads were applied to the model:

- Nodal prescribed velocities were added to the nodes of the inlet and the outlet to specify that fluid would not flow in the Y direction (Y Magnitude = 0).
- Nodal prescribed velocities were added to the nodes along the tube boundary to simulate a fixed wall (Y Magnitude = 0 and Z Magnitude = 0).
- Surface pressure loads were added to the inlet and the outlet per the problem description.

The following analysis parameters were specified:

- On the "Load Curves" tab, in the "Custom Load-Stepping Settings" table, The "Steps" field was set to 10 to specify that the analysis processor should solve for every tenth of a step in order to converge on the answer.
- The "Maximum length scale" was set to 0.1 m to help the solver converge on the final solution.

The 2-D axisymmetrical finite element model is shown in Figure 169-2.

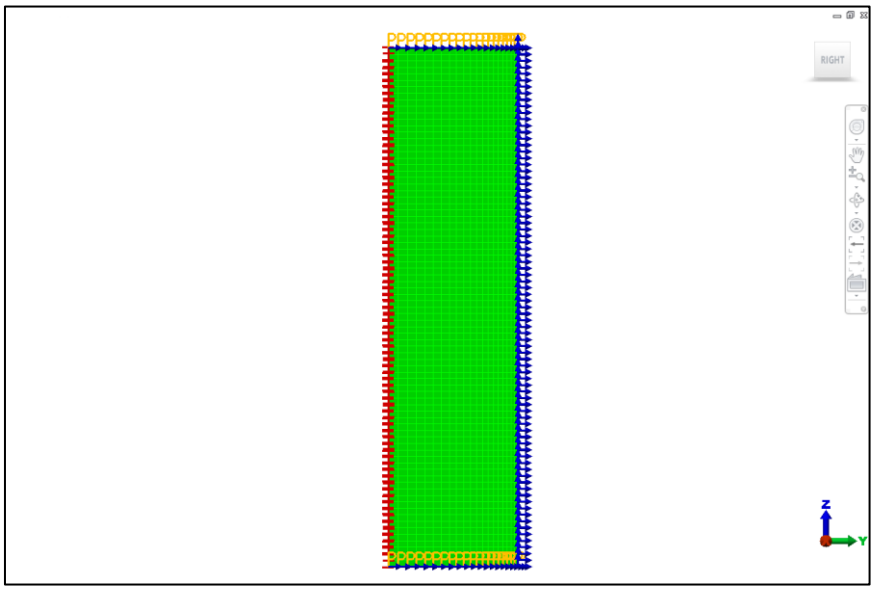

Figure 169-2. The 2-D axisymmetrical finite element model of fluid flow through the circular tube.

A Steady Fluid Flow analysis was performed and the fluid velocity distribution results were examined in the Results environment. The maximum velocity was found furthest from the tube wall, at the center of the fluid flow as shown in Figure 169-3.

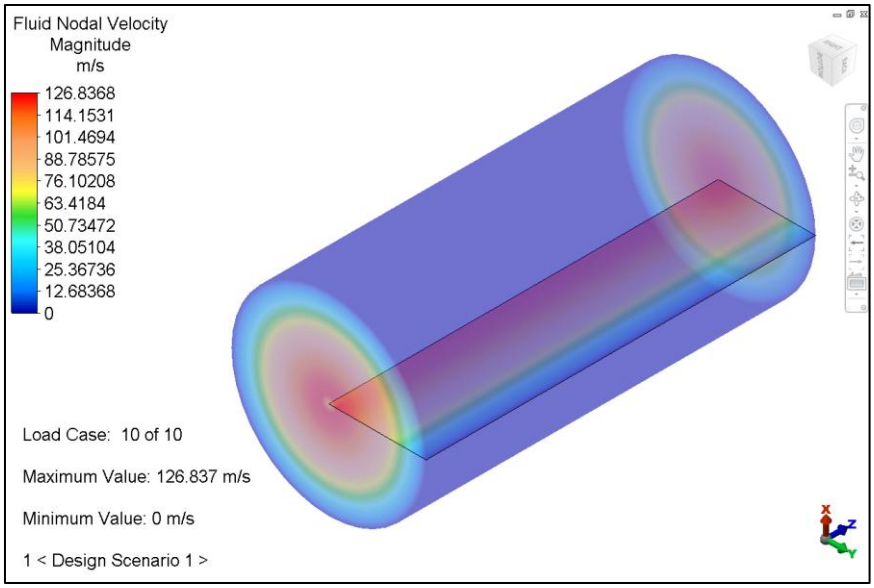

Figure 169-3. Fluid nodal velocity magnitude results for the flow through the circular tube.

Table 169-1 shows a tabular comparison of the theoretical and analysis results. The results matched the theoretical solution to less than two percent.

Table 169-1. Comparison of Results

	Theory	**Analysis**	**% Difference**
Radial velocity (m/s)	124.9	126.8	1.5

AVE - 170 Circular Plate with Fixed Edges under Uniform Pressure Load

Reference

Boresi, Arthur P., Schmidt, Richard J. and Sidebottom, Omar M., *Advanced Mechanics of Materials*, Fifth Edition, John Wiley & Sons, Inc., 1993, Example 13.3, pp. 548-550.

Problem Description

A circular plate (diameter = 200 mm, thickness = 10 mm) is fixed at the edges and is subjected to a uniform pressure load of 4.2 MPa as shown in Figure 170-1.

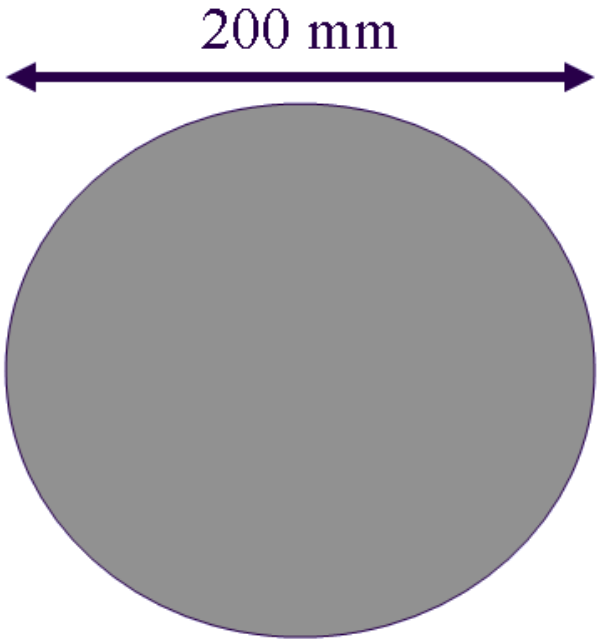

Figure 170-1. Diagram of the circular plate with fixed edges under uniform pressure load.

The material properties of the plate include:

- Modulus of Elasticity (E) = 200 GPa
- Poisson's Ratio (ν) = 0.29

Find the maximum displacement in the circular plate due to the pressure load.

Theoretical Solution

The maximum deflection of the plate under the uniform applied pressure is

$$w_{max} = \frac{3}{16}\left(1-\nu^2\right)\frac{p_y a^4}{Eh^3} = \frac{3\left(1-0.29^2\right)(4.20)(100)^4}{16\left(200\times10^3\right)(10)^3} = 0.361\,\text{mm}$$

Autodesk Simulation Solution

A plate element model of the circular plate was built using the Sketching features in FEA Editor. A sufficiently fine mesh was created by drawing a rectangle inside the circle and then meshing between the arcs of the circle and the sides of the rectangle as well as inside the rectangle as shown in Figure 170-2.

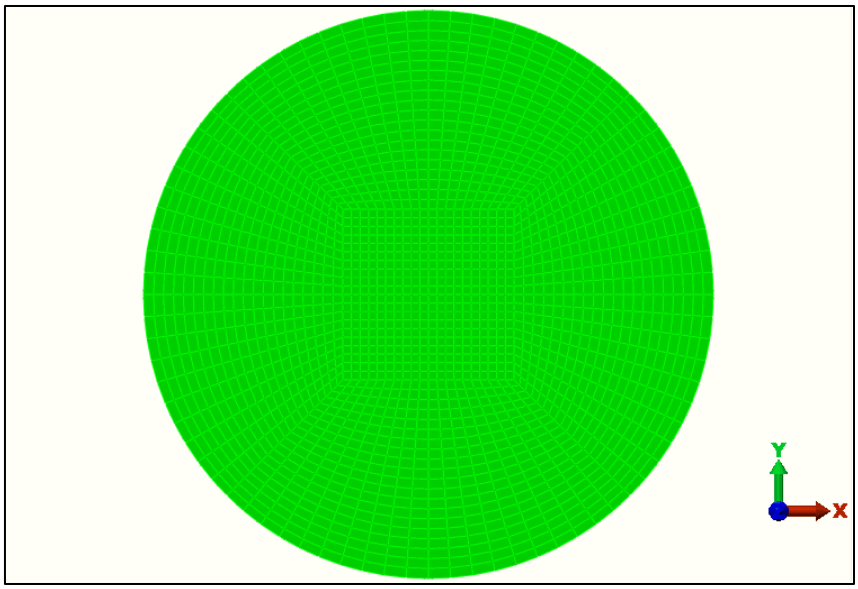

Figure 170-2. The finite element mesh.

the problem description, the unit system was customized for length in millimeters to correspond with how the model was drawn. Plate elements were used with the thickness specified as 10 mm per the problem description. For material properties, the modulus of elasticity and Poisson's ratio were specified per the problem description.

A uniform pressure load (4.2 N/mm^2) was added to surface 1 of the model. The outermost nodes of the model were fully constrained.

A Static Stress with Linear Material Models analysis was performed and the maximum displacement results were examined in the Results environment. The maximum displacement was found at the center of the plate as shown in Figure 170-3.

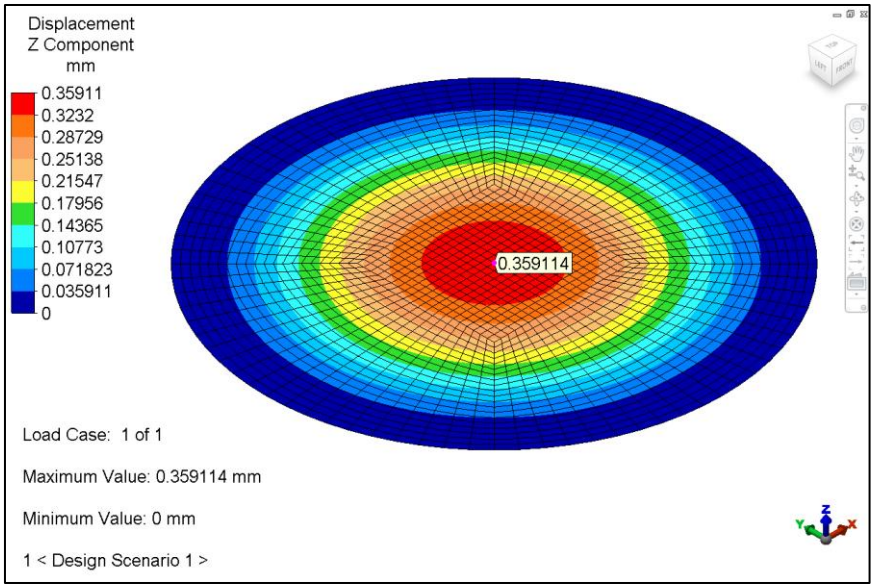

Figure 170-3. Inquiring on nodal displacement results in the Z direction for the circular plate with fixed edges under uniform pressure load.

Table 170-1 shows a tabular comparison of the theoretical and analysis results. The results correlated with the theoretical solution to less than one percent.

Table 170-1. Comparison of Results

	Theory	**Analysis**	**% Difference**
Displacement (mm)	0.361	0.359	-0.55

AVE - 171 Force on the Actuator of a Hydraulic-Lift Table

Reference

Beer, Ferdinand P., Johnston, Jr., E. Russell, Eisenberg, Elliot R. and Clausen, William E., *Vector Mechanics for Engineers: Statics and Dynamics*, Seventh Edition, McGraw-Hill, 2004, Problem 6.7, pp. 332-333.

Problem Description

A hydraulic-lift table is used to raise a 1000-kg crate. It consists of a platform and two identical linkages on which hydraulic cylinders exert equal forces. (Only one linkage and one cylinder are shown in Figure 171-1.) The two vertical members are each 1.4 m in length and the horizontal member is 1.6 m in length. Half of the weight of the crate acts as a downward force of 4905 N on the table.

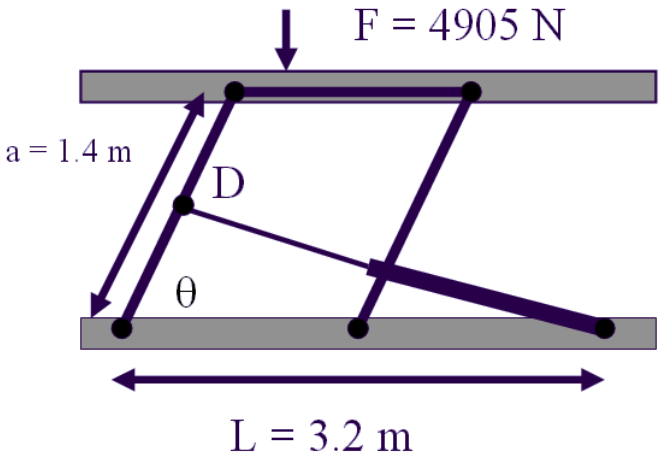

Figure 171-1. Diagram of half of the hydraulic-lift table.

Determine the force on the actuator at D when $\theta = 60°$.

Theoretical Solution

Free-body diagrams were used to solve for the force on the actuator as

$$F_{DH} = W\frac{DH}{EH}\cot\theta = (9.81\,\text{kN})\frac{2.91\,\text{m}}{3.20\,\text{m}}\cot 60° = 5.15\,\text{kN}$$

Autodesk Simulation Solution

A model of half of the hydraulic-lift table was built using FEA Editor. The crate was not modeled because its weight would be simulated by the downward force of 4905 N on the table top.

Beam elements were used for the two 1.4-m long vertical members. Because results in this part of the model were not of interest and because cross-sectional properties were not given in the problem description, these beam elements were made very rigid (a thick cross-section was specified [1 m x 1 m]; the mass density was made very small [.00000001 kg/m^3]; and the modulus of elasticity was made an order of magnitude stiffer than normal steel [1999500000000 N/m^2]).

2-D elements were used to represent the table top. A thickness of 1 m was specified and the same material properties were specified as for the beam elements in order to make the table top very rigid.

An actuator element was used to simulate the hydraulic actuator. The type of actuation was specified as displacement (rather than rotation) and a distinct load curve number was used for the specified length.

The bottom three nodes (at the base of the vertical members and the actuator) were constrained except for rotation about the X axis. The other three nodes of the model (at the midpoint of the leftmost vertical member and at the top of the vertical members) were constrained from translation in the X direction in order to make the 3-D beam and actuator elements remain in the YZ plane along with the 2-D elements.

A nodal force (magnitude = -4905 N in the Z direction) was added to the table top to simulate the weight of the crate. (The location of the force was arbitrary because it could be applied to any node along the top of the table without changing its effect.)

Analysis parameters were defined including the event duration (1 second) and capture rate (1000 time steps/second). Load curve information was specified for the force load and for the actuator movement (extend the actuator by 0.3 m, which would move the leftmost vertical member to an angle slightly greater than $\theta = 60°$). The finite element model is shown in Figure 171-2.

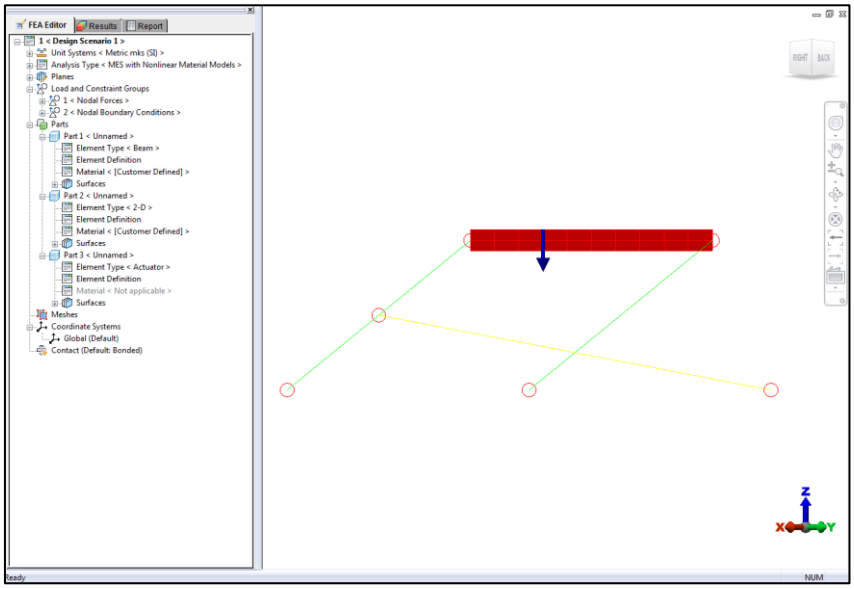

Figure 171-2. The finite element model of the hydraulic-lift table.

A Mechanical Event Simulation with Nonlinear Material Models was performed. The "Tools tab: Inquire panel: Measure command" was used to determine at what time step was the angle of the leftmost vertical member nearest to $\theta = 60°$ (see Figure 171-3).

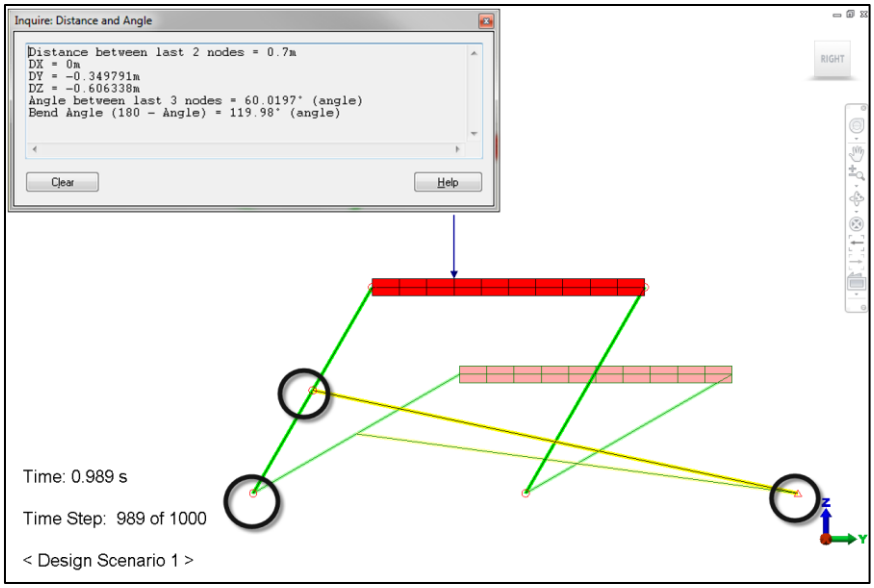

Figure 171-3. Inquiring on the distance and angle of circled nodes.

It was found that θ was nearest to 60° at time step 989. Inquiring on the reaction force magnitude at point D for time step 989 (as shown in Figure 171-4) gave the answer that was asked for in the problem description.

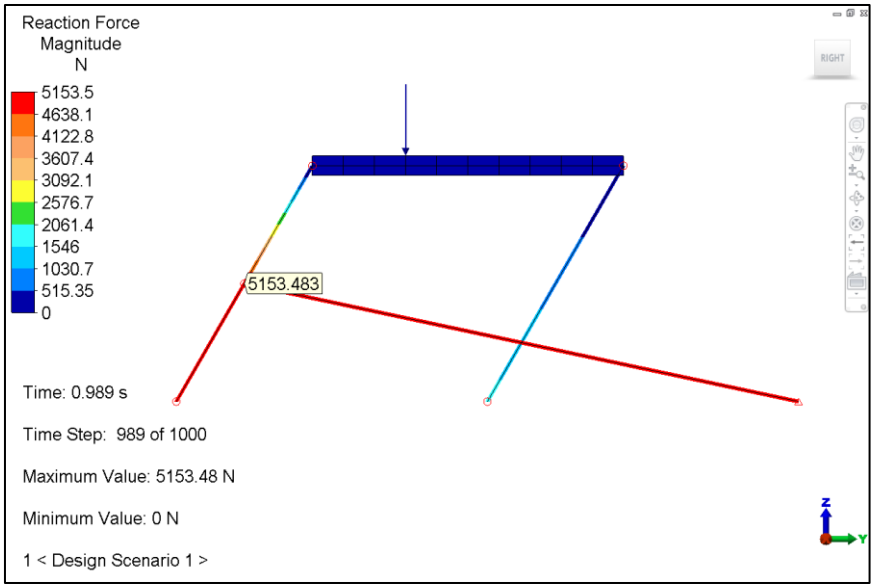

Figure 171-4. Inquiring on the reaction force magnitude at point D when θ was nearest to 60°.

Table 171-1 shows a tabular comparison of the theoretical and analysis results. The results matched the theoretical solution.

Table 171-1. Comparison of Results

	Theory	Analysis	% Difference
Force (kN)	5.15	5.15	0.00

AVE - 172 Heat Transfer Rate of a Heat Exchanger Wall with Pin Fins on One Side

Reference

Bejan, Adrian, *Heat Transfer*, John Wiley & Sons, Inc., 1993, Example 9.1, pp. 456-457.

Problem Description

A heat exchanger wall separates a stream of hot liquid (T_h = 100 °C, h_h = 200 W/m^2*K) from a stream of cold gas (T_c = 30 °C, h_c = 10 W/m^2*K). The wall has a thickness of 0.8 cm and a square frontal area (length = 0.5 m). The cold side has 625 pin fins (each with length = 5 cm and diameter = 0.5 cm) arranged in a square pattern (see Figure 172-1). The effects of convection on both sides of the wall are negligible.

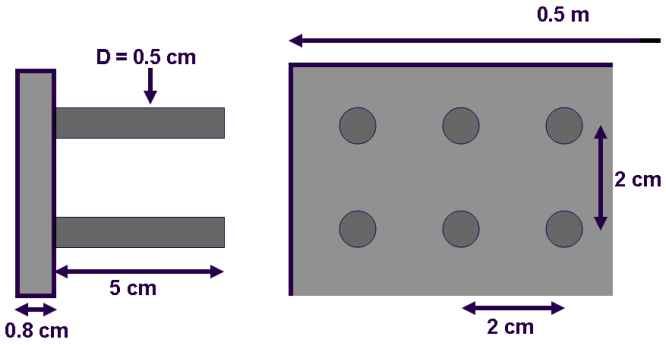

Figure 172-1. Diagram of the heat exchanger wall with pin fins on one side.

The wall and fins are made of a metal with the following material properties:

- Conductivity (k) = 40 W/m*K

Determine the total heat transfer rate (q) for the entire 625-pin finned heat exchanger wall.

Theoretical Solution

The total heat transfer rate through the entire arrangement is calculated as

$$q = U_h A_h (T_h - T_c) = \frac{(100 - 30)\text{K}}{0.169\ \text{K/W}} = 415\ \text{W}$$

Autodesk Simulation Solution

Due to symmetry, only a section of the wall with one fin was modeled using FEA Editor. First, a 2-D cross section of the wall and fin was drawn and meshed. Then, the wall and fin were extruded separately to create the 3-D mesh. Different surfaces were specified to facilitate adding convective loads to the hot side and the cold side (see Figure 172-2).

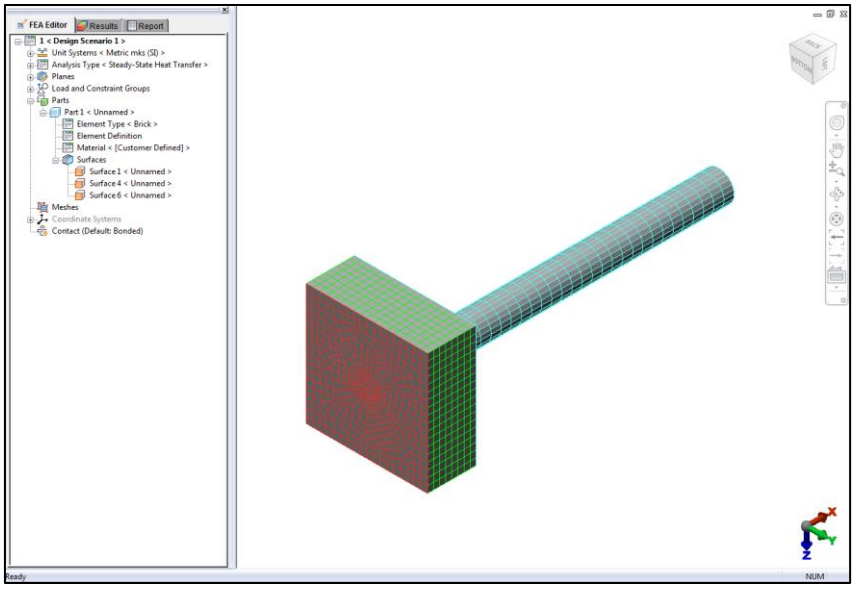

Figure 172-2. The surfaces of the heat exchanger wall and pin fin.

Brick elements were used and material properties were specified including the thermal conductivity per the problem description. Convective loads were specified for the surfaces of the cold side and the hot side. A Steady-State Heat Transfer analysis was performed to determine the temperature results for the model under the two convective loads. The results were examined in the Results environment. Inquire capabilities were used to sum the heat flow rate results for only the nodes of the hot-side surface (see Figure 172-3). The summed value was multiplied by 625 to give the total heat flow rate for the entire heat exchanger wall with 625 pins.

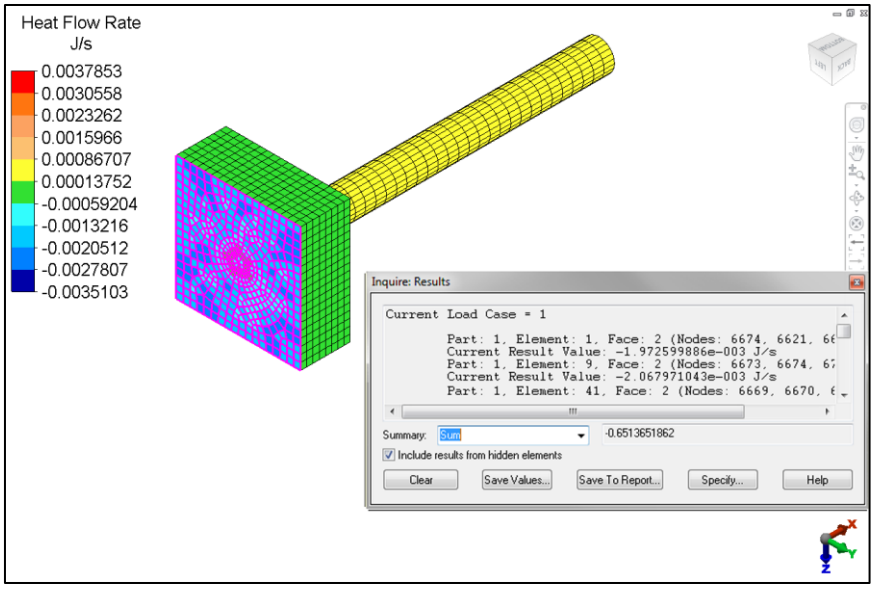

Figure 172-3. Summing the heat flow rate for the hot-side surface.

Table 172-1. Comparison of Results

	Theory	Analysis	% Difference
Total Heat Transfer Rate (q)	415	407	1.9

AVE - 173 First Natural Frequency of a Rectangular Flat Plate with All Edges Fixed

Reference

Young, Warren C., *Roark's Formulas for Stress and Strain*, Sixth Edition, McGraw-Hill Book Company, 1989, Table 36, Case Number 15, p. 717.

Problem Description

A rectangular flat plate (in this case, a square with sides of length = 10 in as shown in Figure 173-1) has all four edges fixed.

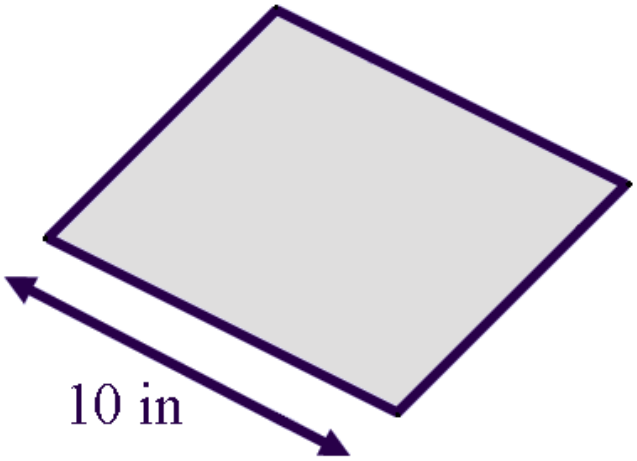

Figure 173-1. Diagram of the rectangular flat plate with all edges fixed.

Find the first natural frequency of vibration (cycles per second) due to the plate's own weight.

Theoretical Solution

The first natural frequency of the plate is calculated as

$$f = \frac{K_1}{2\pi}\sqrt{\frac{Dg}{wa^4}} = 351.0\,\text{Hz}$$

Autodesk Simulation Solution

The reference allows for the rectangle to have different length and width, but, for this example, a 10 in x 10 in square was used. The model of the square plate was drawn within FEA Editor. A 100 x 100 mesh was created using automatic meshing capabilities.

Plate elements were used and a thickness of 0.1 inch was specified arbitrarily because the problem description did not specify the thickness. The problem description also did not specify material properties, so properties for Steel (4130) from the Autodesk Simulation Material Library were used. The nodes along all four edges were fully constrained.

A Natural Frequency (Modal) analysis was performed to determine the mode shapes and natural frequencies for the model due to its own weight under gravity loading. The results were examined in the Results environment including the first natural frequency.

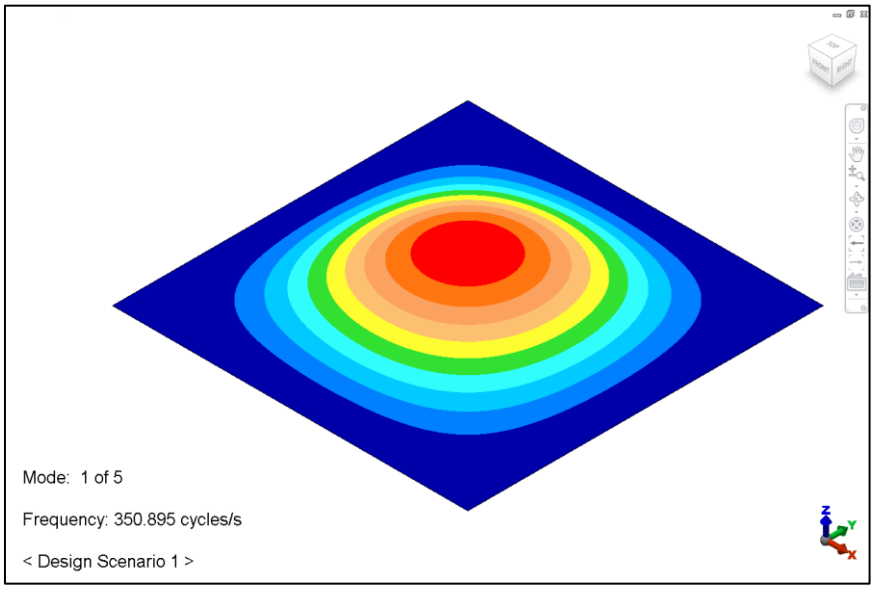

Figure 173-2. The first natural frequency.

Table 173-1 shows a tabular comparison of the theoretical and analysis results. The results nearly matched the theoretical solution.

Table 173-1. Comparison of Results

	Theory	**Analysis**	**% Difference**
First Natural Frequency (Hz)	351.0	350.9	0.03

AVE - 174 Heat Transfer through Thin Plate

Reference

Bejan, Adrian, *Heat Transfer*, Second Edition, John Wiley and Sons, 1993, Example 2.3, p. 68

Problem Description

A 3in diameter circular battery of 6in in length is placed on one circular face on a heated plate with temperature of 50 C. The surrounding air is 20 C and sufficiently large that can be considered infinite thermal well for the battery. A thin shell of .5 mm surrounds the interior of the battery. The convection coefficient for this shell and the contact with surrounding air is 5 W/K*m^2. The thermal conductivity value is 15 W/K*m. The Heat transfer between the battery shell and contents of the battery can be ignored.

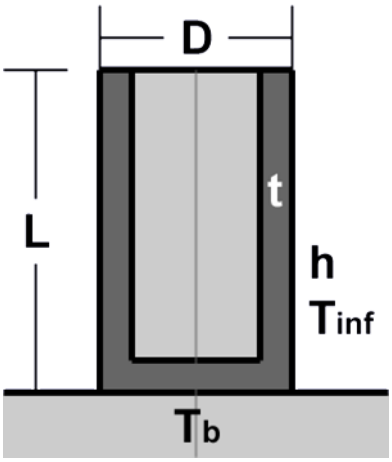

Figure 174-1. Diagram of Problem

Theoretical Solution

This situation is clearly an application of an extended surface or a fin. Since we have the choice of equations on how to treat fins, first the situation is tested for the long-fin criteria:

$$mL = (25.8) * (0.06) = 1.55$$

$$m = \left(\frac{h}{kt} \right)^{1/2}$$

Since *mL* is not significantly larger than 1, the model should be considered a fin with heat transferring tip rather than a long fin:

$$\frac{\theta}{\theta_b} = \frac{1}{\cosh(mL) + \frac{h}{mk}\sinh(mL)} = 0.402 = \frac{T_{top} - T_\infty}{T_b - T_\infty}$$

$$T_{top} = 32.1 C$$

Autodesk Simulation Solution

The model was created in the sketching environment of FEA Editor by first sketching a radial cross section of the model. This rectangle is then meshed using the "4 points rectangular" function of the FEA editor. The lines on the outside of the mesh are selected and designed as Part 2. The entire system is then selected and the entire cross section is revolved around the center axis. The element type of the center part, Part 1, is assigned as brick and the battery shell, Part 2, is assigned as a plate element. The plate element is assigned a thickness of 0.0005 m. This does make the overall battery have a diameter of 0.0305 m rather than the 0.03 m specified as plate elements create thickness on both sides of the mesh, but this difference is too minor for major concern. The bottom surface of the shell is selected using Line select and assigned a new surface number.

A convection load of 5 W/K*m^2 and 20 C is applied to the outside surface of the shell. A temperature is applied to the bottom surface of the shell. Thermal Conductivity for the parts must be set for this type of analysis. The interior of the battery, part 1, should have an extremely low conductivity, 1E-9, as the problem states that its heat conduction is negligible. The outer shell has a thermal conductivity of 15 W/K*m.

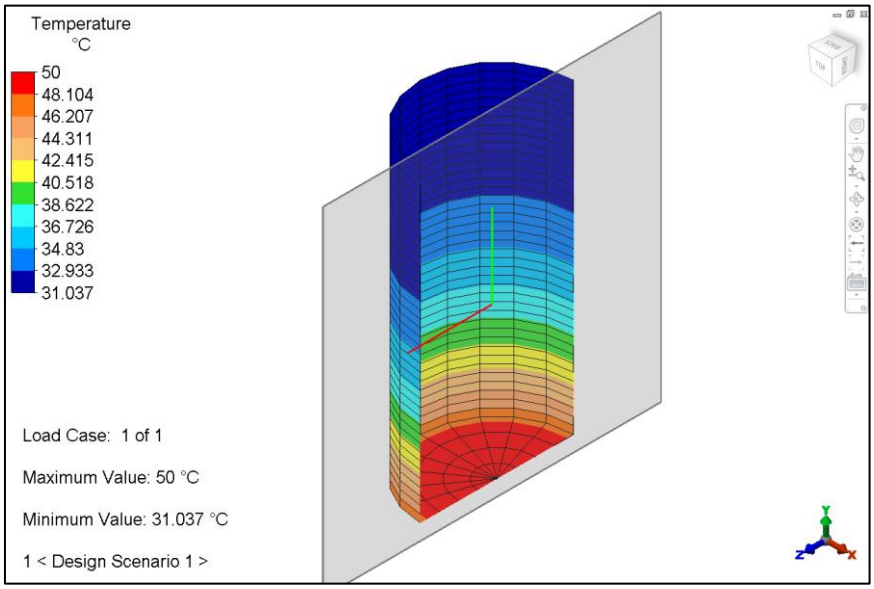

Figure 174-2. Temperature results on the outer surface of the Plate

Table 174-1. Comparison of Results

	Theory	Analysis	%Difference
Temperature (C)	32.1	31.04	3.3

AVE - 175 Maximum Fluid Velocity

Reference

White, Frank, *Fluid Mechanics*, McGraw-Hill, Inc, 1994, p. 213, 235, 236

Problem Description

Find the maximum velocity of a fluid in a simple tube with a diameter of 2 meters. The fluid has properties of 1 kg/m^3 density and a kinematic viscosity of 1 Ns/m^3. The pressure drop is a continuous 1 N/m^2 per 3 m of pipe.

Theoretical Solution

Simple pipe flow is solved using the Navier-Stokes momentum equation for incompressible fluids:

$$\rho\frac{dV}{dt} = \rho g - \nabla p + \mu\nabla^2 V$$

From removal of change in velocity (steady state flow), gravity (assume no gravity change), and radial terms (assume velocity profile is symmetrical across centerlines of cross section). Since pressure drop is constant, a homogenous linear differential equation is left:

$$\frac{dp}{dz}\frac{1}{\mu} = \frac{1}{r}\frac{dV}{dr} + \frac{d^2V}{dr^2}$$

Since the velocity profile is parabolic and that velocity is a max when r=0 and 0 when r=1 (due to no slip conditions, we can assume:

$$V(r) = C_1 r^2 + C_2 = -C_2 r^2 + C_2$$

Substituting the first and second derivates into the differential equation yields:

$$\frac{dp}{dz}\frac{1}{\mu} = -2C_2 + -2C_2$$

$$C_2 = \frac{dp}{dz}\frac{1}{-4\mu} = \frac{-1}{3*-4*1} = \frac{1}{12} = 0.0833$$

The maximum velocity at the center of the tub is 0.0833 m/s.

Autodesk Simulation Solution

This model is created using the sketching environment of FEA Editor. First a circle of radius 1 m is created in a sketch. Then in the same sketch, a square is created with side length of 1 m. The circle is then divided into 4 pieces and rotated such that the 4 arcs break along the lines y=x and y=-x. This means they are co-linear with the 4 corners of the square. Finishing the sketch, use the "Structured mesh: Between Two Objects" to create meshes of 4x4 for the inner circle and 4x2 for each side to arc segment. This mesh will allow for more elements in the interior of the model. To complete the overall mesh, select all the lines first on the outside of the circle. Designate these as a new surface number. Then select all the lines of the model and use the Copy command to make a pipe which has a length of 3 meters with 10 divisions. Select the lines at both ends and designate each as different new surfaces.

A pressure of 2 N/m^2 is applied at one circular surface and a pressure of 1 N/m^2 to the other to create the needed pressure drop. Each of the surfaces is prescribed as a surface inlet/outlet. The material properties need to be set using the material library. Finally, the number of steps is increased in the Analysis Parameters screen. The Model is now ready to run.

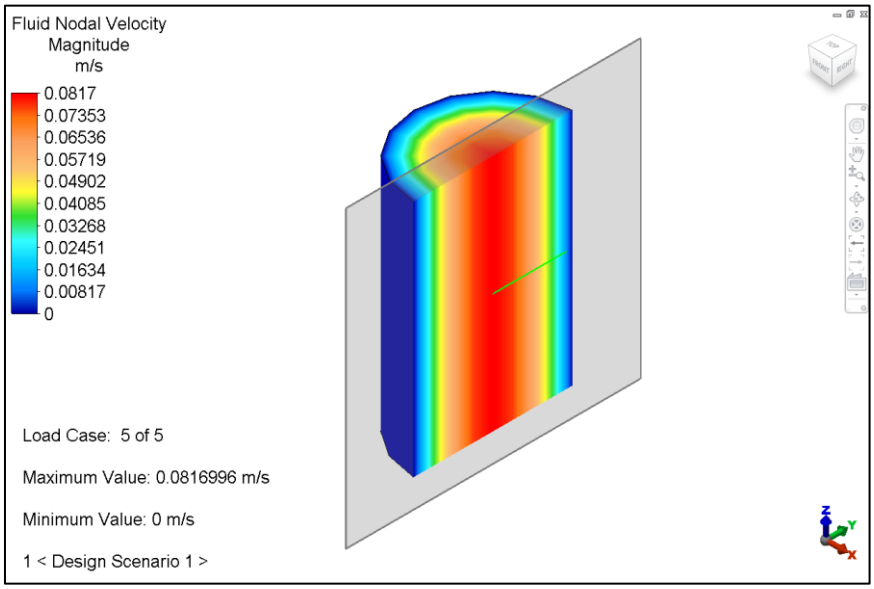

Figure 175-1. Velocity pattern by default (segregated) formulation

The results match with theory. Inquiring on the maximum value on the outlet side of the pipe yielded a maximum velocity of 0.0817 m/s

Table 175-1. Comparison of Results.

	Theory	**Analysis**	**% diff**
Maximum Fluid Flow (m/s)	0.083	0.0817	1.57

AVE - 176 Angular Deflection of Steel Step Shaft

Reference

Popov, E.P. *Mechanics of Materials*, Second Edition, Prentice-Hall, 1976, Example 3-7, p. 609-611.

Problem Description

A stepped shaft with properties of steel is attached to a wall at one end. Torsion loads are applied at two points along the shaft.

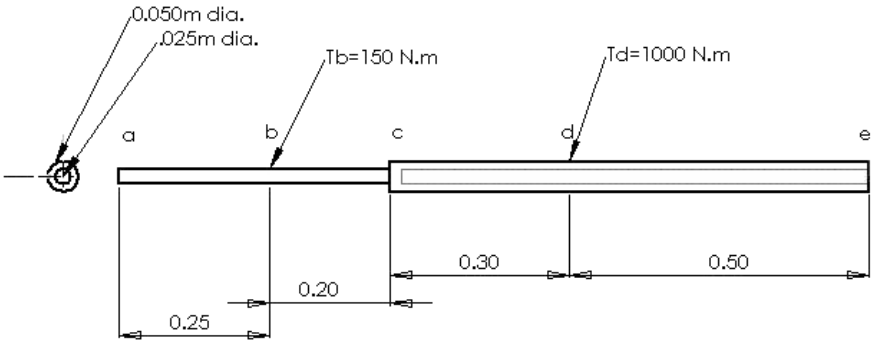

Figure 176-1. Diagram of Problem

Theoretical Solution

This example uses prismatic beams, thus the simple torsion formula equations:

$$\theta = \frac{TL}{GJ} = \left[\frac{T_{de}L_{de}}{J_{de}} + \frac{T_{cd}L_{cd}}{J_{cd}} + \frac{T_{bc}L_{bc}}{J_{bc}} + \frac{T_{ab}L_{ab}}{J_{ab}} \right] / G$$

Where T is the combined value of torsion, L is the length of the shaft, G is the Shear Modulus, and J is the polar moment of inertia.

$$G = 80E9 \;\; N/m^2$$

$$J_{ab} = J_{bc} = \frac{(\pi)(d^4)}{32} = 383.5E-6 \;\; m^4$$

$$J_{cd} = J_{de} = \frac{\pi}{32}\left(d_o^4 - d_i^4\right) = 57.52E-6 \;\; m^4$$

These values result in a total angular deflection at *a* of:

$$\theta = 1.33^0$$

Autodesk Simulation Solution

The CAD model was imported to FEA Editor to be meshed. Since the default mesh of this part was too coarse, the model was re-meshed using an absolute mesh size of 0.005. A split line was added from along the centerline of the shaft for later use in adding coupled forces. In addition, two splits were created at the points where the loads need to be added.

The bottom surface of the shaft is fully constrained as specified by a wall connection. Since the shaft is modeled as solid brick elements and brick elements do not accept moments and torsional loads, there are a few options available to apply the loads to the model such as adding beam elements. In this case, coupled forces were chosen to mimic

the torsion loads. First a cylindrical coordinate system was defined along the centerline of the shaft. This coordinate system was then applied to the edges created by split lines added earlier. Then the proper forces were applied to the edges in the tangential (Y in the cylindrical coordinate) direction. To complete the shaft part, typical steel material properties were assigned.

Since rotational displacement measures the twist of each element, beam elements were added at the top such that the center of the beam part was aligned with the center of the part. The beams were directly attached to nodes on the top end of the shaft and given very stiff properties to prevent possible deflections. The rotational displacement of the beams gives an accurate description of the rotation of the end face of the shaft.

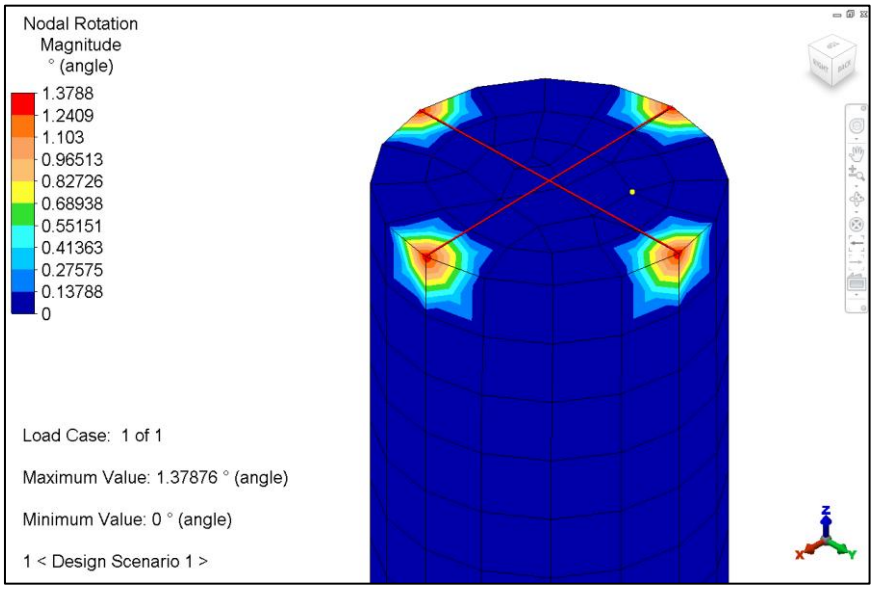

Figure 176-2. Angular Deflection of Beam Elements

Table 176-1. Comparison of Results in Degrees

	Theory	Analysis	%Difference
Deflection Angle	1.33	1.3788	3.67

AVE - 177 Deflection of Simply Supported Beam and Spring System

Reference

Higdon, Archie; Ohlsen, Edward; Stiles, William; Weese, John; Riley, William, *Mechanics of Materials*, Third Edition, John Wiley and Sons, 1976, Example 11-2, p. 609-611.

Problem Description

A 50-lb block drops 2in onto the center of a 6061-T6 aluminum alloy beam. The beam has a cross section of 3in wide by 1in high and is simply supported. In the center of the beam a helical spring, *k*=100 lb/in, is in contact with the beam but is unstressed before impact. The beam and spring system absorb 90% of the energy elastically.

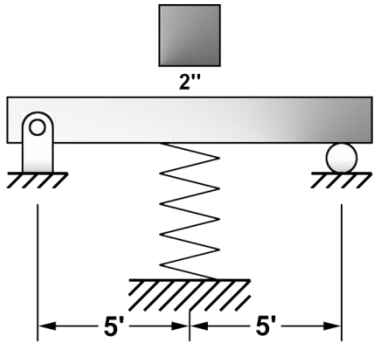

Figure 177-1. Diagram of Problem

Theoretical Solution

Since the action is assumed to be elastic and the materials obey Hooke's law the load-deflection relation will be linear. Using deflection relationships, contact force and flexural stress can be determined.

$$50(2+\Delta)(.9) = P\Delta/2$$

$$\delta_A = \frac{(P-Q)L^3}{48EI} = \frac{(P-Q)(10^3)(12^3)}{48(10^7)(3)(1^3)/12} = \frac{(P-Q)(144)}{(10^4)}$$

$$\delta_B = \frac{Q}{100}$$

$$\Delta = \delta_A = \delta_B$$

Where P is the dynamic contact force and Q is the force exerted by the spring. From these equations and a few simple algebraic steps,

$P = 225.3\ lb$ and $Q = 133.0\ lb$

Flexural Stress

$$\sigma = \frac{Mc}{I} = \frac{R(60)}{3(1^3)/12} = 5540\,psi$$

Where R is the reaction force at one end of the beam

$$R = (P-Q)/2 = 46.15\ lb$$

Autodesk Simulation Solution

A model was created in the FEA Editor. There are three parts in this system; a beam, a spring, and a falling block. The beam was created using the "Draw tab: Draw panel: Line button" and assigned a user-specified rectangular cross section in the elements definition section of the tree control window. The material was originally defined as Aluminum 6061-T6 and the density was edited to 0 to match the mass of the beam model used in the test. The beam was also divided into 8 segments using the "Draw tab: Modify panel: Divide button". The spring was also created using the "Draw tab: Draw panel: Line button" and defined with an axial spring stiffness of 100 lb/in. Lastly, the block of brick elements was created 2in above the height of the beam using the Sketching functions of FEA Editor. Again, the density of the brick was set to 0 to mimic the ideal situation of the text. Since the other properties of the block were not specified, the values for Poisson's Ratio and Modulus of Elasticity of Aluminum 6061-T6 were used.

The model was analyzed using the MES with Nonlinear Material models analysis type with duration of 0.2 seconds and a capture rate of 500 frames per second. The ends of the beam element were constrained for the pin joint at one end and the roller support at the other. The spring was also constrained at its lower end as the upper end is attached to the beam.

The block was constrained to prevent movement out of the Z plane. A lumped mass was added to the block to simulate the weight force of 50 lb * 90% specified by the problem. Gravity was set at standard values in the –Z direction. Results were observed using the Graph function at the center node of the beam.

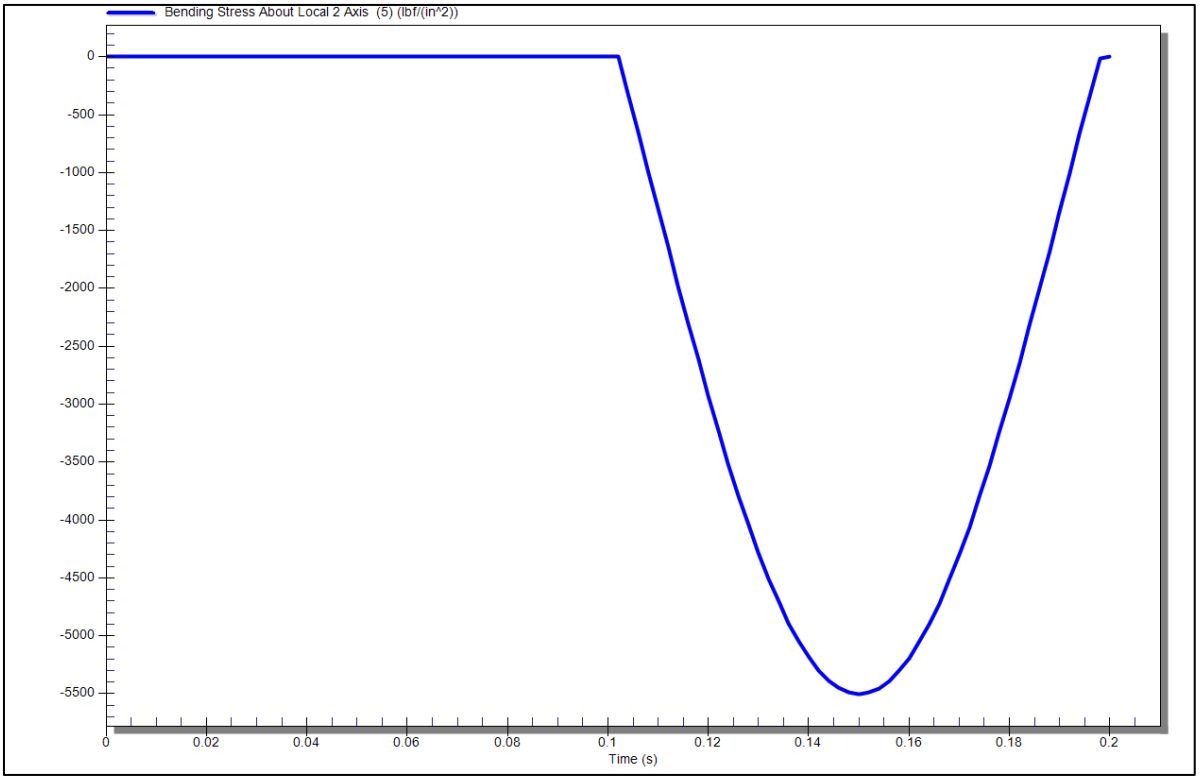

Figure 177-2. Bending Stress at Center Point

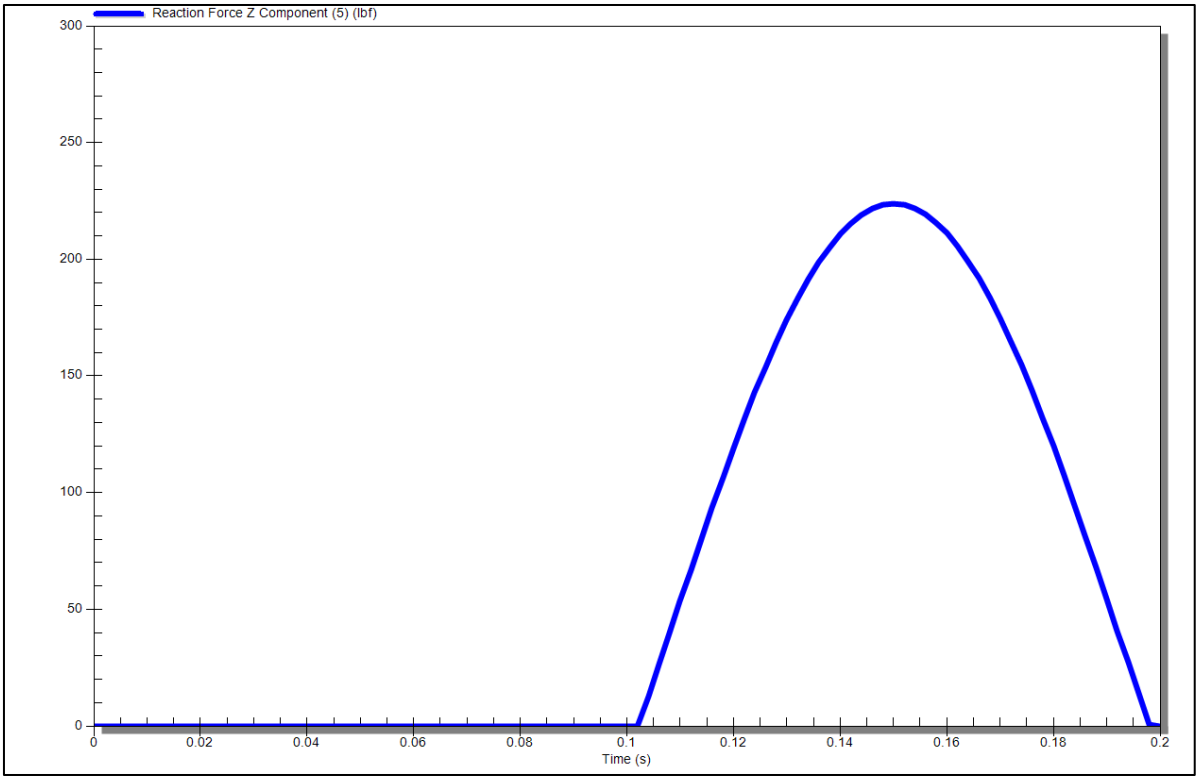

Figure 177-3. Dynamic contact force at Center Point

Table 177-1. Comparison of Results

	Theory	Analysis	% Difference
Bending Stress	5525	5502	0.42
Contact Force	225.3	223.8	0.67

AVE - 178 Temperature Drop across Contact

Reference

Holman, J.P., *Heat Transfer*, McGraw-Hill, Inc, 1981, Example 2-8, p. 51

Problem Description

Two 3 cm diameter bars made of 304 Stainless Steel are placed such that each has an end face completely touching an end face of the other bar. A temperature of 100 degree Celsius is applied to one free end face and 0 degree Celsius is applied to the opposite end face. With a contact resistance of 5.28e-4 m^2C/W find the temperature drop across the contact region.

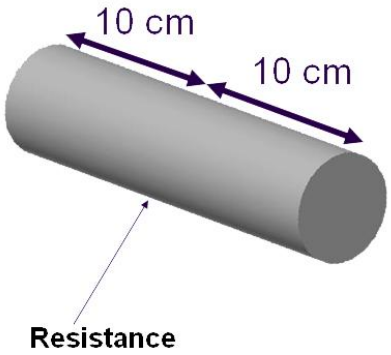

Figure 189-1: Diagram of Problem

Theoretical Solution

This is a simple heat transfer problem so 1-D heat transfer equations are appropriate. In this case, ratios of resistances can be used:

$$\Delta T_c = \frac{R_c}{\Sigma R_{th}} \Delta T$$

Where ΔT is the total temperature difference of 100 C, and R_c is the contact resistance, 5.28 x 10^{-4} m^2C/W

$$R_{rod} = \frac{l}{k} = \frac{.1}{16.2}$$

$$\Sigma R_{total} = 2 * R_{rod} + R_c = 0.01287$$

$$\Delta T_c = 4.10$$

Autodesk Simulation Solution

The model is generated in inventor Fusion and the geometry is transferred to Autodesk Simulation. A contact is specified between the cylinders with a Total Resistance of 0.746967 C/W.

Total resistance = [Distributed resistance] ÷ [Contact area]

A Steady-State Heat Transfer analysis must be specified before heat contact resistance is an available setting. A 25% mesh is applied to the model. Temperatures are applied both on the top surface and the bottom surface of the model. The material is specified for both cylinders as AISI Type 304 Stainless Steel. After the analysis has been performed, results are found by selecting nodes along the contact plane of the two cylinders. Then the "Inquire:Results:Range" function is used to find a temperature difference of 4.09 C.

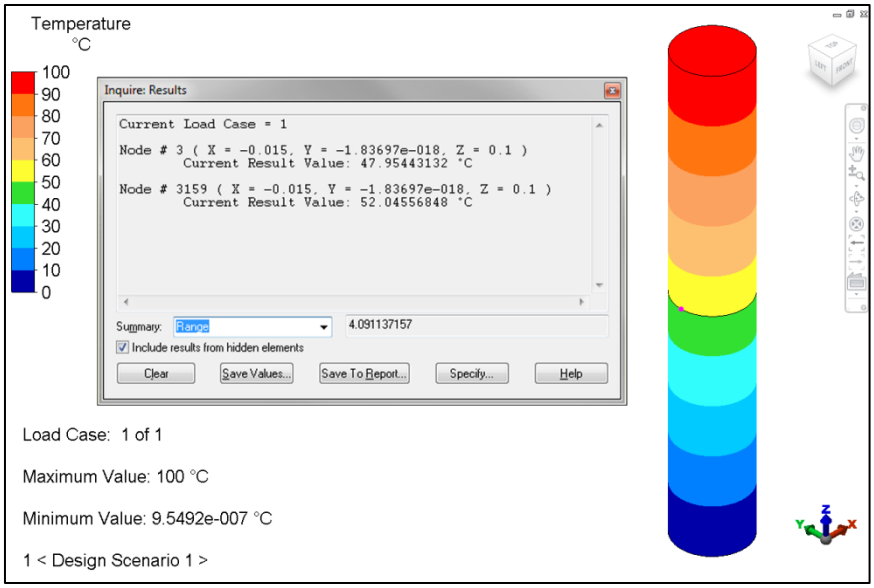

Figure 178-1. Inquiring results at the contact plane

Table 178-1. Comparison of Results in Degrees C

	Theory	Analysis	%Difference
ΔT	4.10	4.09	0.24

AVE - 179 Natural Frequency of a Flat Plate

Reference

Young, Warren C., *Roark's Formulas for Stress and Strain*, Sixth Edition, Case Number 17, p 717.

Problem Description

A flat metal plate 2 in by 10 in made from A36 Steel is fixed at three ends and simply supported on the fourth. Find the first natural frequency of the plate.

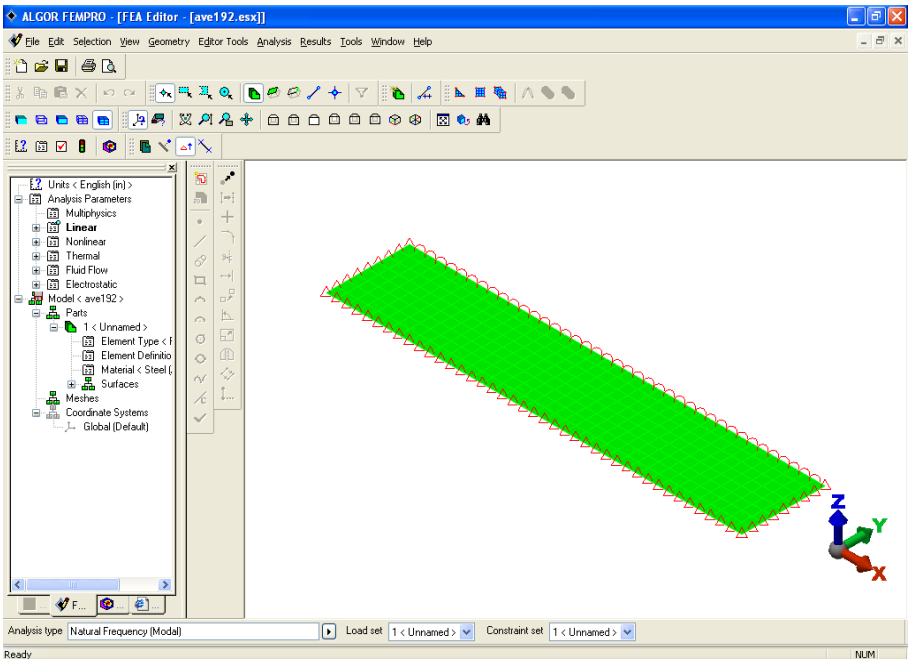

Figure 179-1. FEA Model of the Plate

Theoretical Solution

The first natural frequency of the plate is calculated as

$$f = \frac{K_1}{2\pi}\sqrt{\frac{Dg}{wa^4}} = 3862\,\text{Hz}$$

Autodesk Simulation Solution

The model of the rectangular plate was created using the "Mesh Tab: Structured Mesh panel: 4-Point Rectangular" command in the FEA Editor. A 8 x 40 Mesh was created with 4 mesh division per inch. The element type of this part is assigned as a plate.

Plate elements were used and a thickness of 0.1 inch was specified arbitrarily because the problem description did not specify the thickness. Material properties of Steel (ASTM A36) were used in both the Analysis and the Theory calculations.

A Natural Frequency analysis was performed to determine the mode shapes and natural frequencies for the model. The results were examined in the Results environment including the first natural frequency.

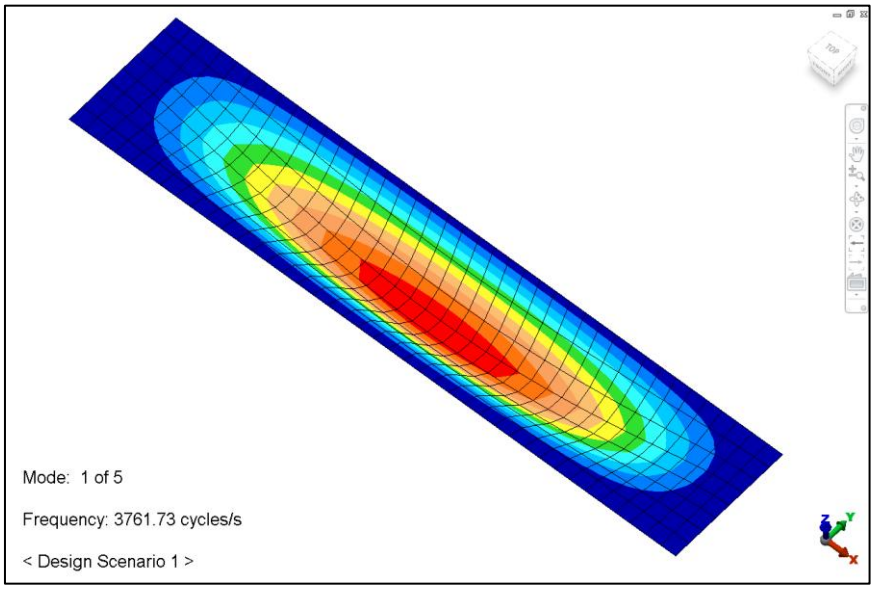

Figure 179-2. Displaced Model

To obtain more accurate answers, the mesh can be redefined with more division per inch.

Table 179-1. Comparison of Results in Hertz (Hz)

	Theory	Analysis	% Difference
frequency	3862	3762	-2.6

AVE - 180 Deflection of Truss

Reference

Young, Warren C., *Roark's Formulas for Stress and Strain*, Sixth Edition, Example 6-2, p. 83.

Problem Description

A truss is constructed of tubular steel members of various thicknesses. Loads of 1200 lb and 600 lb are applied and the truss is fixed on one end to a wall. Find the maximum displacements in both the vertical and horizontal directions. The truss has dimensions of 3 ft by 8 ft with a member running through the midpoint of the long dimension. E=30E6

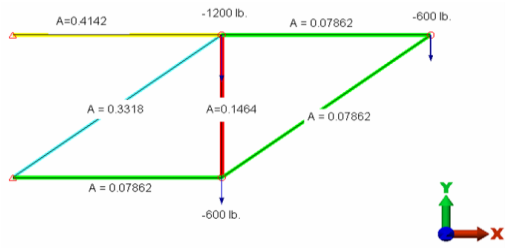

Figure 180-1. FEA Model

Theoretical Solution

The deflections in this truss can be solved using the following method

$$D = \sum Pe = P_1 e_1 + P_2 e_2 \ldots = \sum \frac{P^2 l}{AE}$$

Where *D* is the total deflection, *P* is the force applied to a truss, *e* is the deformation, *l* is the length, *A* is the cross sectional area, and *E* is Young's Modulus. For this situation the total deflection can be broken into x and y components.

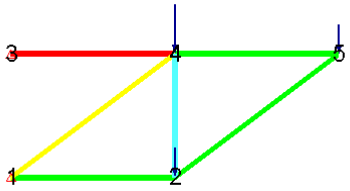

Figure 180-2. Node Numbers of Truss Elements

$$d_x = Px_{12}\frac{P_{12}l_{12}}{A_{12}E} + Px_{25}\frac{P_{25}l_{25}}{A_{25}E} + Px_{54}\frac{P_{54}l_{54}}{A_{54}E} + Px_{41}\frac{P_{41}l_{41}}{A_{41}E} + Px_{42}\frac{P_{42}l_{42}}{A_{42}E} + Px_{43}\frac{P_{43}l_{43}}{A_{43}E} = 0.0317 \ in$$

$$d_y = Py_{12}\frac{P_{12}l_{12}}{A_{12}E} + Py_{25}\frac{P_{25}l_{25}}{A_{25}E} + Py_{54}\frac{P_{54}l_{54}}{A_{54}E} + Py_{41}\frac{P_{41}l_{41}}{A_{41}E} + Py_{42}\frac{P_{42}l_{42}}{A_{42}E} + Py_{43}\frac{P_{43}l_{43}}{A_{43}E} = 0.1769 \ in$$

Autodesk Simulation Solution

The truss model was created using the "Draw tab: Draw panel: Line button" of FEA Editor. Different parts were used for different cross section values. Since there are 4 cross sections, there are 4 parts in the FEA model. Each part is designated as a truss element type and assigned the appropriate cross sectional area. Since the material is not important for this problem, a custom material was created. Only the Modulus of Elasticity, 30E6 psi, was defined. Forces were applied at the nodes 2, 4, and 5 with values of -600 y, -1200 y and -600 y respectfully. The ends attached to the wall are given fixed nodal boundary conditions. After the analysis is performed, the deflection results were inquired using the probe function.

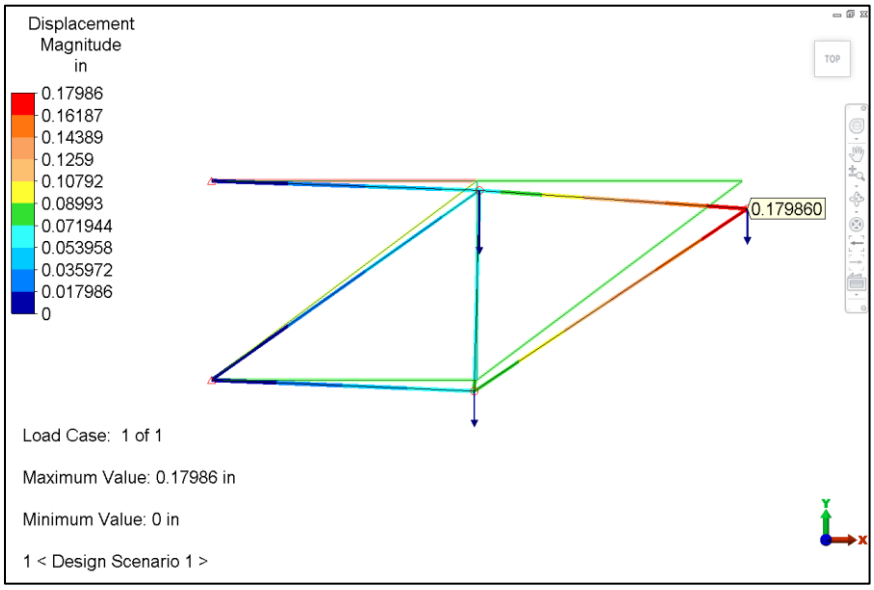

Figure 180-3. Displaced Model

Results are compared in the following table

Table 180-1. Comparison of Results

	Theory	**Analysis**	**% Difference**
Dx (inches)	0.0317	0.0317	0.00
Dy (inches)	-0.1769	-0.1770	0.06

AVE - 181 MES Thermal Loading of Shell Composite

Problem Description

A temperature load of 100 F is applied to a thin composite of two materials which is fixed by clamps on all edges. The composite has dimensions 10 in by 20 in and is composed of material 1, 0.75 in thick, and material 2, 0.25. Although the materials have different properties, they share a stress free reference temperature of 25 F. Find the stress tensors in the thin composite.

Table 181-1. Temperature Dependent Material Properties

		Material 1		Material 2	
	Symbol	**T=0**	**T=200**	**T=50**	**T=150**
Young's Modulus	E1	1.50E+06	2.50E+06	1.75E+06	2.25E+06
	E2	5.00E+05	1.50E+06	7.50E+05	1.25E+06
Poisson's Ratio	υ12	0.2	0.3	0.225	0.275
Shear Modulus	G12	1.00E+05	2.00E+05	1.20E+04	1.20E+05
	G13	1.00E+04	2.00E+04	1.30E+04	1.30E+05
	G23	2.00E+04	3.00E+04	2.30E+04	2.30E+05
Coefficient of thermal expansion	α1	5.00E-07	1.50E-06	7.50E-07	1.25E-06
	α2	1.50E-06	2.50E-06	1.75E-06	2.25E-06

Theoretical Solution

This is a situation of thermoelastic materials:

$$[\sigma]=[C]([\varepsilon]-\langle\alpha\rangle\Delta T)$$

Where σ is the stress tensor, ε is the strain tensor, α is the vector of thermal expansion coefficients, C is the matrix of material stiffness and ΔT is the temperature difference from applied to stress free. In this situation, the laminate can be modeled using single layer orthogonal plane stress:

$$\begin{bmatrix}\sigma_1\\ \sigma_2\\ \sigma_{12}\end{bmatrix}=\frac{1}{1-\nu_{12}\nu_{21}}\begin{bmatrix}E_1 & \nu_{12}E_2 & 0\\ \nu_{12}E_2 & E_1 & 0\\ 0 & 0 & G_{12}\end{bmatrix}\left(\begin{bmatrix}\varepsilon_1\\ \varepsilon_2\\ \varepsilon_{12}\end{bmatrix}-\left\langle\begin{matrix}\alpha_1\\ \alpha_2\\ 0\end{matrix}\right\rangle\Delta T\right)=\begin{bmatrix}-193.55\\ -174.19\\ 0\end{bmatrix}$$

When ε is 0 because of clamped ends and ΔT is 75 C.

Autodesk Simulation Solution

The model of the square plate was drawn using sketching function of FEA Editor. A 4 x 4 mesh was created using the Mesh tab: Structured mesh: 4 point rectangular button. This option allows for the creation of a mesh with specified divisions between 4 specified points. The analysis type was set as Mechanical Events Simulator (MES) with time duration of 1s and a capture rate of 1 frame per second. Combined with the simple loading curve of 0 multiplier to 1 multiplier over the course of the analysis will achieve fast and accurate results.

The element type of the mesh is set as a shell element, which allows for composites in the MES analysis type. In the Element Definition screen, the material model of this shell element is changed to "Temperature Dependent Composite" and the element formulation was set to "Co-rotational". In the Thermal tab of the Element Definition screen, the stress free reference temperature is set to 25 F. In the Composite Tab, the thickness, orientation angle and material properties of the composite are defined. Since there was no designation for orientation angle, we will assume that the materials have the same orientation angle. Material properties can be set by clicking inside the material column and row of appropriate material.

Every edge was constrained by adding fixed nodal boundary conditions on each edge node. The load condition of 100 F was set on the Thermal/Electrical tab of the Analysis Parameters screen as the "Default Nodal Temperature".

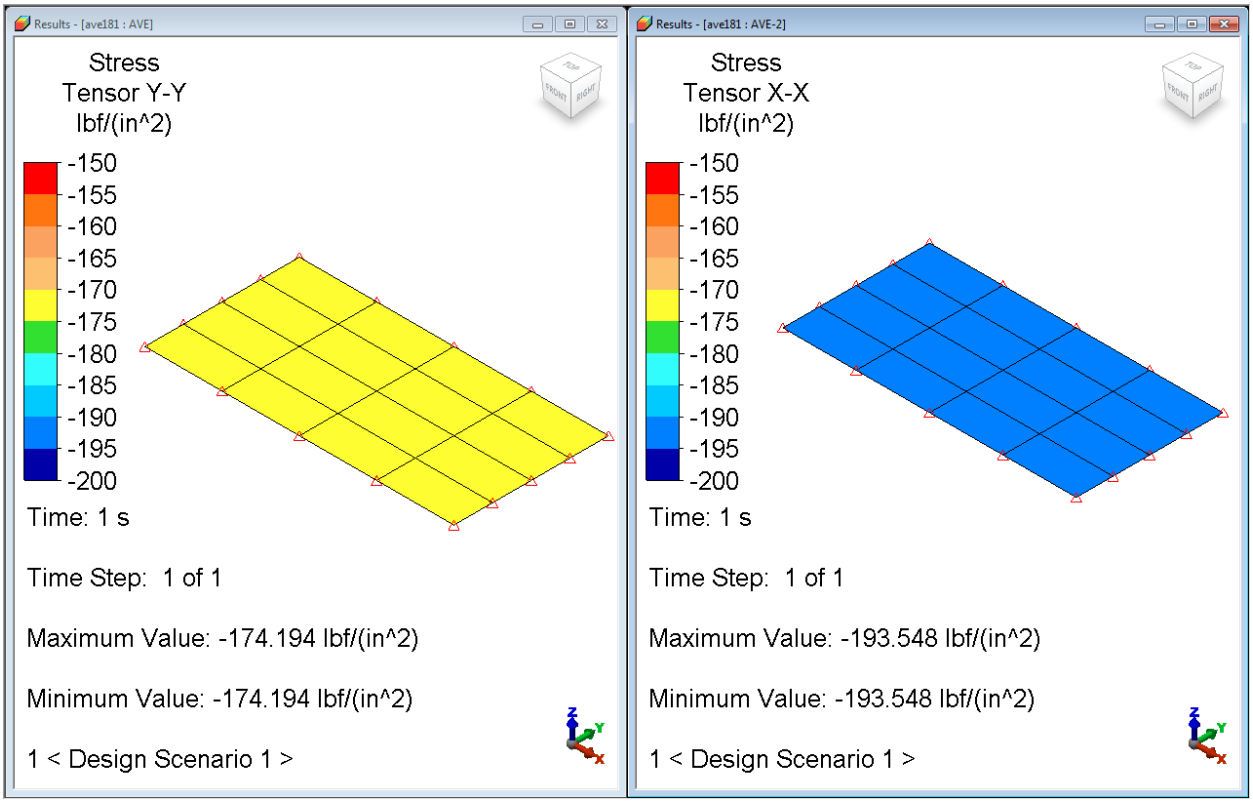

Figure 181-1. Stress Tensors in the YY and XX direction is consistent with a uniform load

A comparison of the results with the Theoretical is found in the following table.

Table 181-2. Comparison of Stress Tensor results in psi

	Theory	Analysis	% diff
σ_{11}	-193.55	-193.548	0
σ_{22}	-174.19	-174.194	0
σ_{12}	0	0	0

AVE - 182 Deflection of a Spring Supported Beam

Reference

Bourni, Scmidt, and Sidebottom. *Advanced Mechanics of Materials*, Fifth Edition, Example 10-2.

Problem Description

A square cross-section beam of length 6.8 meters is supported by 7 springs with a load of 12 kN applied in the center. Find the maximum deflection and bending stress. The beam has a moment of inertia around the bending plane of 2.46e6 mm^4 and is made out of a material with a modulus of elasticity of 72 GPa. The springs each have a stiffness of 110 kN/m and are spaced evenly under the beam.

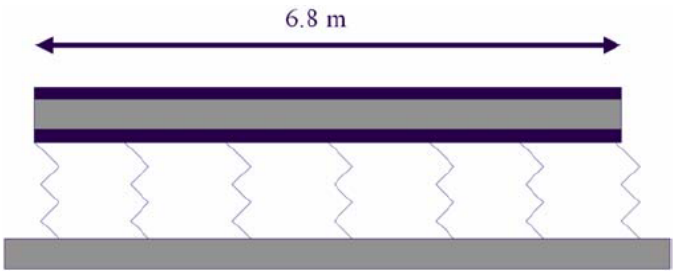

Figure 182-1. Problem Geometry

Theoretical Solution

Beam:
P=12 kN
I=2.45e6 mm^4
S=4.9e-5 m^3 section modulus
L=6.8 m

Springs:
k= 110 kN/m
n= 7

Autodesk Simulation Solution

The initial beam is modeled using the “Draw tab: Draw panel: Line button”. The initial line, of total length 6.8 m, is placed into part 1, surface 1, layer 1. Using the line selection tool, the initial single line is divided into six equal segments to produce nodes at each spring attachment point. Part 1 is then defined as having an element type of beam and assigned appropriate cross-section and material properties using the element definition and material definition screens respectively.

The seven springs are modeled in a similar fashion. Using the “Draw tab: Draw panel: Line button”, seven single lines are placed into part 2, surface 1, layer 1. Each of the single lines begins at a node on the beam and is defined at a relative distance of 1 m from the beam in the negative Z direction. Part 2 is then assigned the element type of spring. This defines each of the 7 lines as springs of the same type. Using the element definition screen, the springs are assigned a stiffness value of 1,100,000 N/m. No additional material definition is needed for spring elements.

FEA loads and constraints are applied to the model at appropriate points. A nodal force load of 12000 N is applied to the central node of the beam element in the negative Z direction. The ends of the seven spring elements are fully fixed.

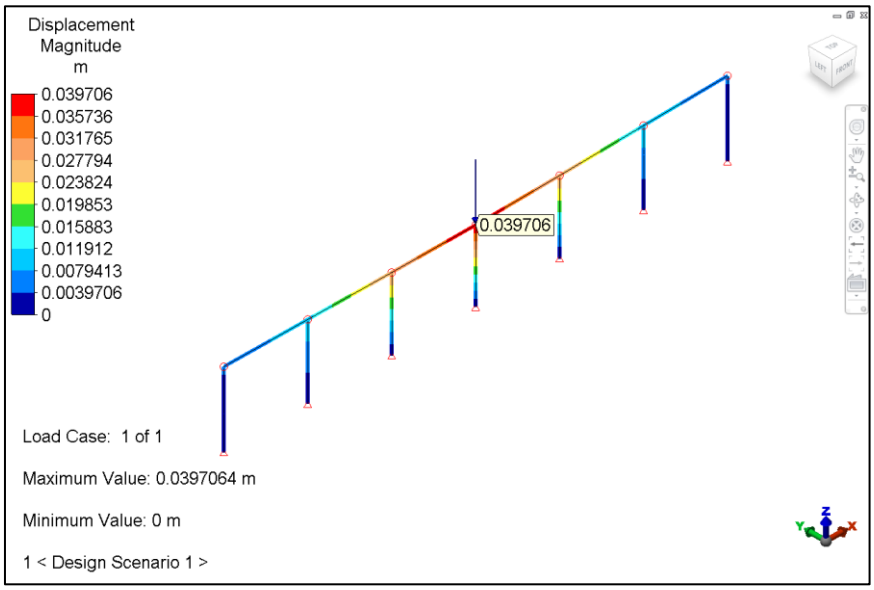

Figure 182-2. Deflection in Meters

A comparison of the results with the theoretical is found in the following table.

Table 182-1. Comparison of Results

	Theory	Analysis	% diff
Deflection (mm)	38.98	39.7	1.8
Bending Stress (MPa)	93.5	93.4	0.1

AVE - 183 MES of Force Accelerated Block

Reference

Lindeburg, Michael R. *EIT Review Manual*. p. DE V-4.

Problem Description

A 100 kg block resting on a surface is pulled by a 500 N force. The force is oriented at a 30º angle from the surface. The kinematic coefficient of friction between the block and the surface is 0.15. Find the acceleration of the block.

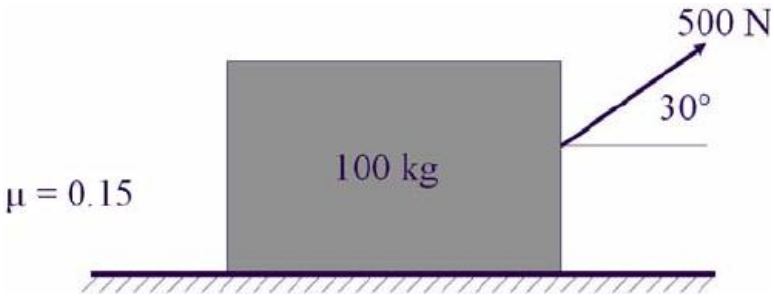

Figure 183-1. Problem Geometry

Theoretical Solution

$$a_h = \frac{\sum F_h}{m} \qquad \sum F_h = 500 * \cos\theta - \mu * (mg - 500 * \sin(\theta))$$

M=100 kg
g=9.8 m/s^2
F=500 N
θ=30
μ=0.15

$$a_h = 3.235\,\text{m/s}^2$$

Autodesk Simulation Solution

Since the model has no displacement or forces in one plane, 2-D elements can be used to simplify both model creation and analysis. To create the 2 separate parts, two "4 Point Rectangular" meshes were generated using the "Structured Mesh" panel within the Mesh tab of the ribbon user interface.

The element definition screen will allow the user to select any thickness for the 2-D elements. The thickness is irrelevant outside of determining the mass of each object. After the element definition has been defined, the material properties can be set for the 2-D parts. The material can be the same for both parts, but the density must allow the block rectangle to have a mass of 100 kg. Additionally, since the object is assumed to be rigid, a high value should be set for a modulus of elasticity and a 0.3 value for Poisson's ratio.

FEA loads, constraints and surface contact pairs need to be applied to the model. The bottom edge of the surface rectangle is constrained as fixed. Surface to surface contact (slide no bounce frictional) is defined between the bottom surface of the upper block and the upper edge of the surface rectangle. A nodal load of 500 N is defined with a Y component of 0.866 and a Z component of 0.5 to account for the 30 degree angle. In the analysis parameters screen, gravity loading needs to be defined in the negative Z direction. A load curve , event duration and capture rate

need to be set up as well. In this situation, it is appropriate to analyze the event 1.5 second at 50 captures per second. At time 0, the force will have a multiplier of 1 and at 3 seconds, the multiplier for the forces should remain as 1.

The model is now ready for analysis. Results can be viewed either upon completion or monitored as the analysis progresses. To view a graph of the acceleration, simply change the result type to displacement in the Y direction, select a node, right-click to access the bump-out menu, and select the "Graph" option. A graph will appear with displacement plotted against time. Using the "Results Inquire tab; Graph panel: Graph option pull-down menu", the graph can be made to display the second derivative, or acceleration, versus time.

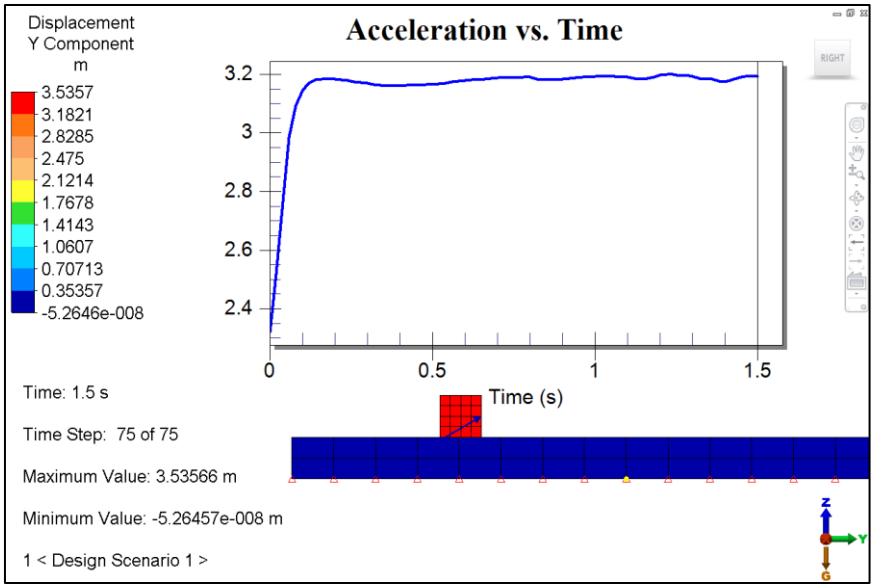

Figure 183-2. Embedded Graph of Acceleration versus Time

A comparison of the results with the theoretical is found in the following table.

Table 183-1. Comparison of Results

	Theory	**Analysis**	**% diff**
Acceleration (m/s^2)	3.235	3.193	1.3

AVE - 184 Radiation between two Cylinders

Reference

Holman, J.P., *Heat Transfer*, Seventh Edition, 1990, pages 424-425.

Problem Description

Two concentric cylinders radiating to each other. Find the temperature of the outer cylinder.

Theoretical Solution

This type of problem is usually solved using a radiation network. The radiation network of this problem follows:

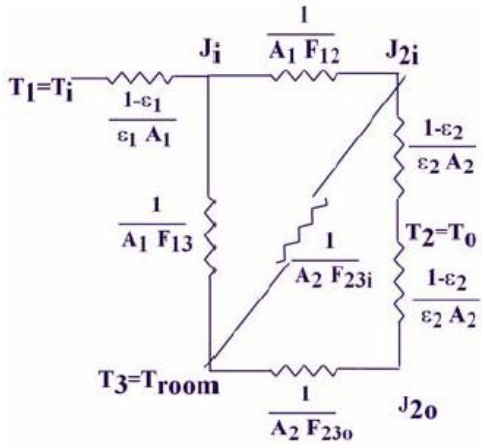

Figure 184-1. Radiation Chart

Inner Cylinder:
r=5 cm
T_i=1000 K
ε=0.8

Outer Cylinder:
r=10 cm
ε=0.2

L=20cm
T_{amb}=300 K

In addition to these variables, view factors are needed to solve the above radiation network.

T_{final}=724.9 K

Autodesk Simulation Solution

Since this model is symmetric about an axis, 2-D axisymmetric elements can be used to simplify building the model as well as the analysis. 2-D elements can be created using the "4 Point Rectangular: Structured Mesh" command as long as the mesh falls completely within the YZ plane. Build two parts, one rectangle 5 by 20 starting from the origin and the second a 1 by 20 mesh starting a distance of 10 in the Y direction from the origin. The element definition for each element should set the element type to 2-D axisymmetric. Since the theoretical solution does not take into consideration potential differences in temperature along the length, a material property with extremely high thermal conductivity is set for each part.

To prepare the model for FEA loads, surfaces need to be defined in the appropriate areas. A surface can be defined by selecting a set of lines, and modifying their surface number. In this situation, a surface should be set up on the outer edge of the inner cylinder and the inner edge of the outer cylinder.

An applied temperature needs to be added along the center line of the inner cylinder. Applying a high stiffness factor will keep the inner cylinder close to 1000 K. In addition, a radiation enclosure needs to be defined. This is done by ensuring no objects are selected within the FEA Editor, right-clicking and selecting "Body-to-Body Radiation…" from the bump-out menu. In this screen, surfaces defined earlier need to be defined as "Radiation surfaces" and the appropriate emissivity applied. Each surface then needs to be selected to participate in the enclosure, and an ambient temperature needs to be defined as 300 K. The model is now ready for analysis.

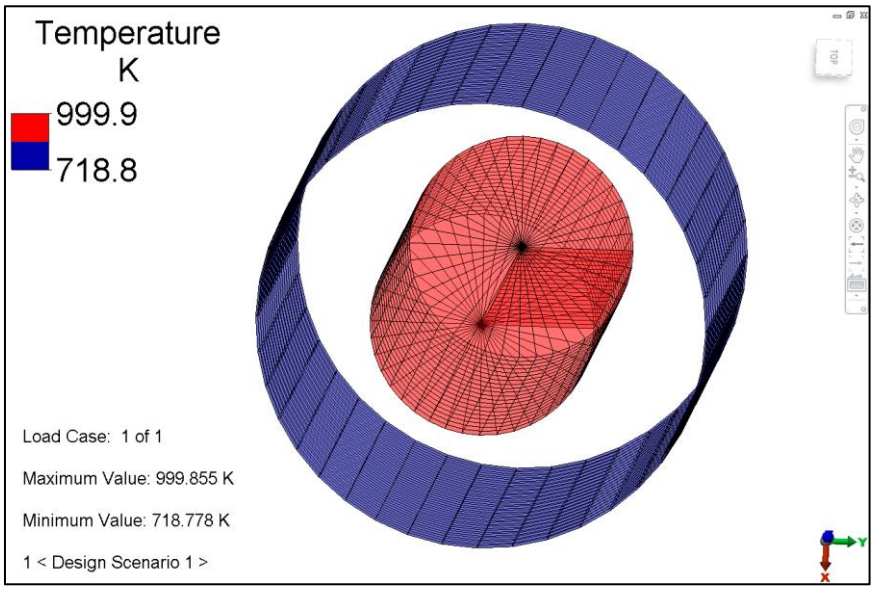

Figure 184-2. Temperature in K

A comparison of the results with the theoretical is found in the following table.

Table 184-1. Comparison of Results

	Theory	Analysis	% diff
Temperature (K)	724.9	718.8	0.84

AVE - 185 Outlet Velocity of 3D Fluid Tank with Sudden Contraction Loss

Reference

White, Frank M., Fluid Mechanics, P372 to P373, Fourth Edition, McGraw-Hill, Inc., (1997).

Problem Description

A large water tank drains through a tube attached to the lowest point on the tank. Given the diameter, length of tube and water height, find the velocity of fluid exiting the tube after four seconds.

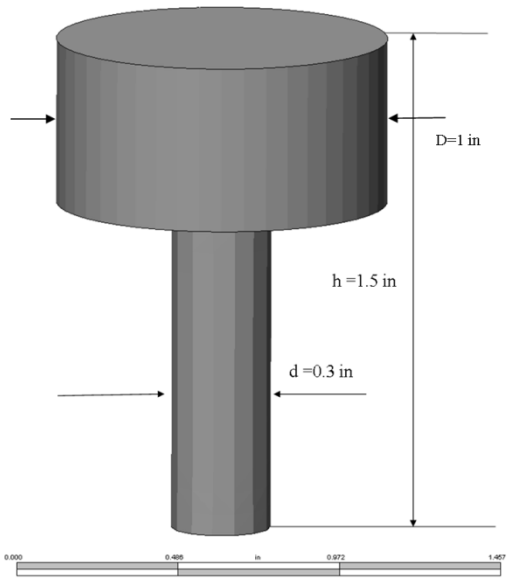

Figure 185-1. Problem Description

Theoretical Solution

Height h = 1.5 in

Gravity acceleration g=386 in/s2

(a) Theoretical solution without energy loss

$$\rho gh = \frac{1}{2}\rho v^2$$

This theoretical solution is based on the assumption of perfect energy transfer between potential energy and kinetic energy. In other words, it ignores any energy loss which cannot be avoided in real physics, and typically loss from flow sudden contraction.

(b) Simi-empirical solution with correction considering sudden contraction

$$\rho gh = \frac{1}{2}\rho v^2 + \frac{1}{2}k_{sc}\rho v^2$$

Where ksc is loss coefficient due to sudden contraction
This equation is derived from Frank. White's textbook "Fluid dynamics", with considering the energy loss from sudden contraction.

The flow separation in downstream pipe causes main stream to contract through a minimal diameter d_{min}, called the vena contracta, which is illustrated in Figure 185-2. There are no theoretical solution for vena contracta, the experimental data of loss coefficient in sudden contraction is showed in in Figure 185-2 or fits the empirical formula as below,

$$k_{sc} = 0.42(1-\frac{d^2}{D^2})$$

Substitute d and D in this model, get k_{sc}=0.382
Substitute k_{sc}, h, g into corrected semi-empirical solution formula, get v=28.95 in/s, this is the expected average velocity at outlet.

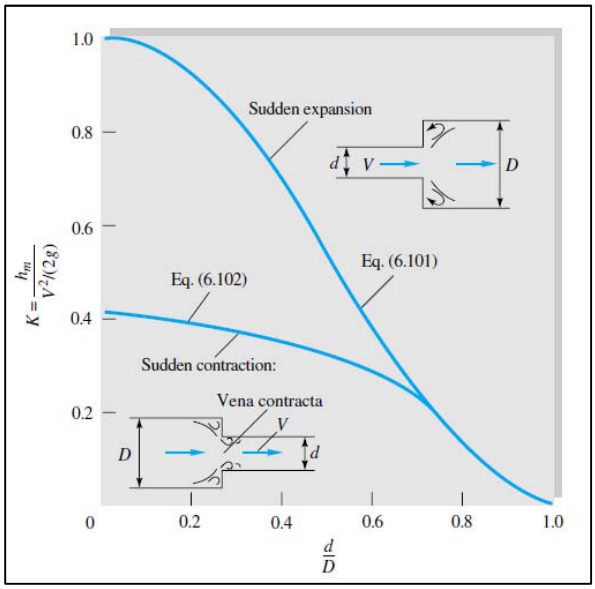

Figure 185-2. Sudden expansion and contraction head losses. (Frank. White, "Fluid dynamics", page: 372,)

Autodesk Simulation Solution

Starting from N-S equation, incompressible viscous flow simulation can automatically count all factors including entrance/exit loss due to the sudden expansion and sudden contraction, minor losses and friction losses in pipe system. The energy loss details could be referred from Chapter 6 Viscous flow in ducts from Frank. White's text book "Fluid Mechanics".

Trying to compare the theoretical solution, the model is designed to minimize the factors from minor losses between theoretical solution and simulation, hence the exit nozzle is modeled as short as possible and flow turning is minimized as well.

The top surface and bottom outlet are modeled as "inlet/outlet" boundary conditions, they are identical to zero pressure boundary conditions which is used simulate the reference pressure open to atmosphere. It needs to note that the two surfaces have to be modeled as horizontal to gravity direction so that it does not need extra pressure compensation from gravity compensation; this is one of the current limitations to handle gravity in software.

This is another model where 2-D elements can be used to simplify the analysis. To create the 2-D elements, the sketching environment can be utilized to draw the outline of the tube and a 3 m tank attached to the tube. The sketch is then changed into a 2-D mesh, by selecting the finished sketch and selecting the 2-D mesh engine. In this situation, a finer mesh than the default is desirable. Initially, the mesh density needs to be set to 2000. To finish the geometry information, the default values for element definition need to be accepted and a material of water applied to the model.

Since there are no additional loads on the model outside of gravity, the only FEA loads and constraints that need to be applied to the model are specified inlets and outlets. Surface inlet/outlets need to be defined at the end of the tube and at the top of the tank. The gravity loading is applied from the analysis parameters screen in the "Gravity" tab.

To prepare the model for analysis, an appropriate load curve and load curve duration need to be applied. This is accomplished by having two rows in the "Time-Stepping Settings" table under the "Load Curves" tab of the analysis parameters screen. One row will represent the condition at time zero, and an additional row will represent the condition from time 0 to time 4. A capture rate of 10 steps per second is recommended for this analysis.

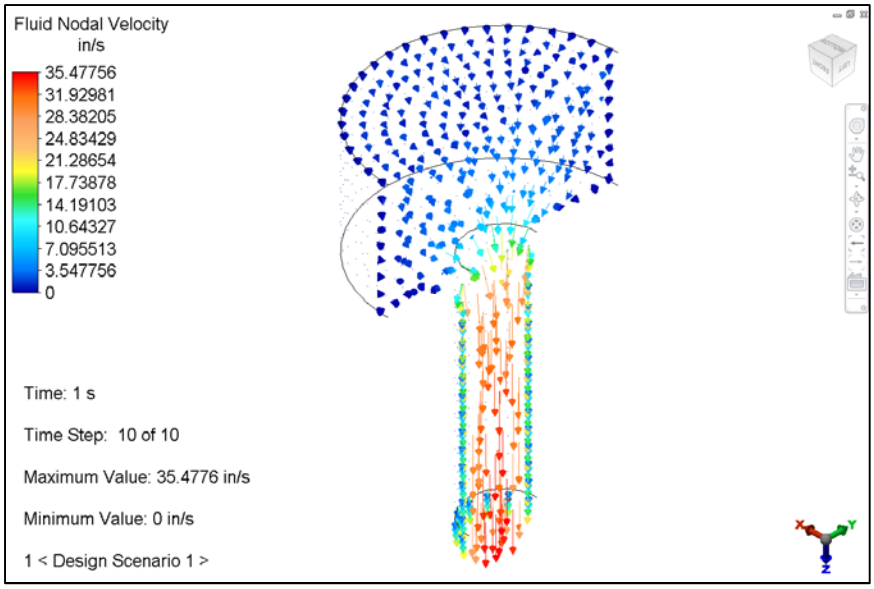

Figure 185-3. Velocity Profile

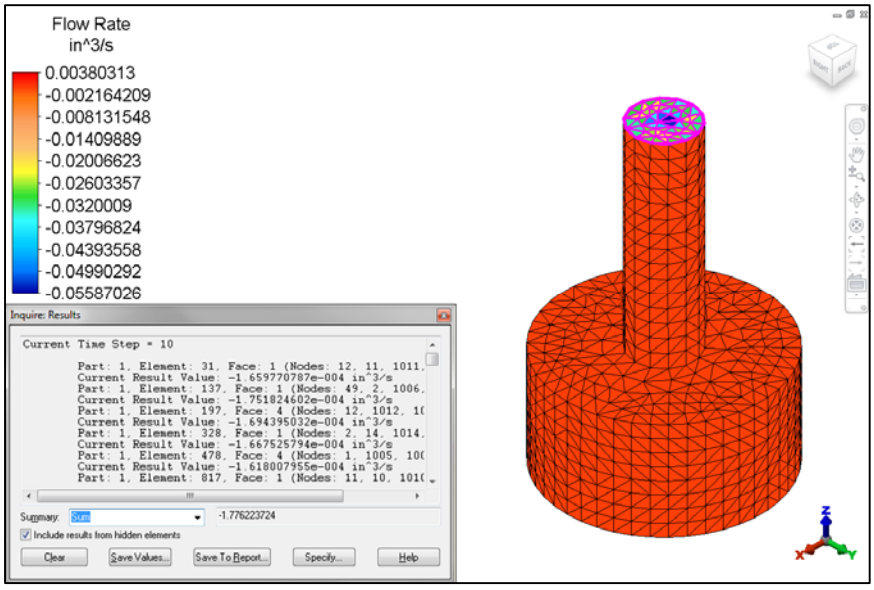

Figure 185-4. Outlet flow rate

Outlet surface area=0.25*3.14159*d2 =0.25*3.14159*0.32=0.0707 in2
Average velocity at outlet = Volume flow rate summation/Area
= 1.776 (in3/s) / (0.0707 in2)
= 25.12 in/s

A comparison of the results with the empirical result is found in the following table. Note that the analysis result is smaller than empirical estimate, considering the ignored wall friction from empirical calculation which makes the empirical result has less energy loss and bigger outlet result than reality value. The 13.2% result discrepancy is reasonable and acceptable.

Table 185-1. Comparison of Result

	Empirical	**Analysis**	**% diff**
Outlet Average Velocity (in/s)	28.95	25.12	13.2%

Simulation notes and tips:

- Use small time step for solution stability
- The total simulation time has to be large enough to ensure stable result achieved
- Outlet surface has to be in horizontal plane. i.e., no hydrostatic pressure changes on this surface. This is a limitation of software.
- Verify average velocity on outlet instead of picking maximal velocity, since the verification formulation is based on the system energy balance with considering loss in sudden contraction.
- Set the model in relative small scaling so that the flow is laminar flow, it has relative less energy loss from friction than turbulence flow which has much larger velocity gradient on the wall and more friction and energy loss.
- The summation of outlet flow rate is used to calculate average velocity, which automatically counts the non-uniform velocity on this surface.
- The energy loss from friction is minor than the sudden contraction loss. Since this factor has no good empirical estimation, so we allow relative large tolerance in result comparison. In the meantime, we have considered the offset trend from this factor.
- The verification result and conclusion should be robust under further verifications by mesh study.

AVE - 186 Steady-State Heat Transfer along a Rod

Reference

Lindeburgh, Michael R., *Mechanical Engineering Reference Manual for the PE Exam*, Tenth Edition, p 34-18 and 34-19.

Problem Description

A 0.5 in by 0.5 in by 10 in rod has an applied temperature of 300 ºF at one end and exists in an ambient environment of 80 ºF. The rod has a thermal conductivity of 80 BTU/(hr-ft-ºF) and a convection coefficient with the environment of 1.65 BTU/(hr-ft^2-ºF). Find the temperature 3 in from the base of the rod.

Theoretical Solution

$$T_3 = T_{amb} + (T_{base} - T_{amb}) * \frac{\cosh(m(L-3))}{\cosh(mL)} \qquad m = \sqrt{\frac{h * P}{k * A}}$$

$T_3 = 248.2F$

Autodesk Simulation Solution

Because heat differences across the cross-section of the rod are unimportant, a rod element type can be used for this analysis. A 10 in long rod is created by using the "Draw tab: Draw panel: Line button". This line is then divided into 10 line segments, to allow sampling at 3 in along the length. The element type is set to rod. The cross-sectional area of 0.25 in^2 and the cross-section perimeter of 2 in need to be set in the element definition screen. Finally, the material needs to be defined as having a thermal conductivity of 80 BTU/(hr-ft-ºF). A nodal controlled temperature of 300 ºF was applied to one end of the rod. A relatively high stiffness of 80e3 BTU/hr/F was used to ensure that the temperature of this node stays constant. In addition, a convection load was applied to the surface of the rod.

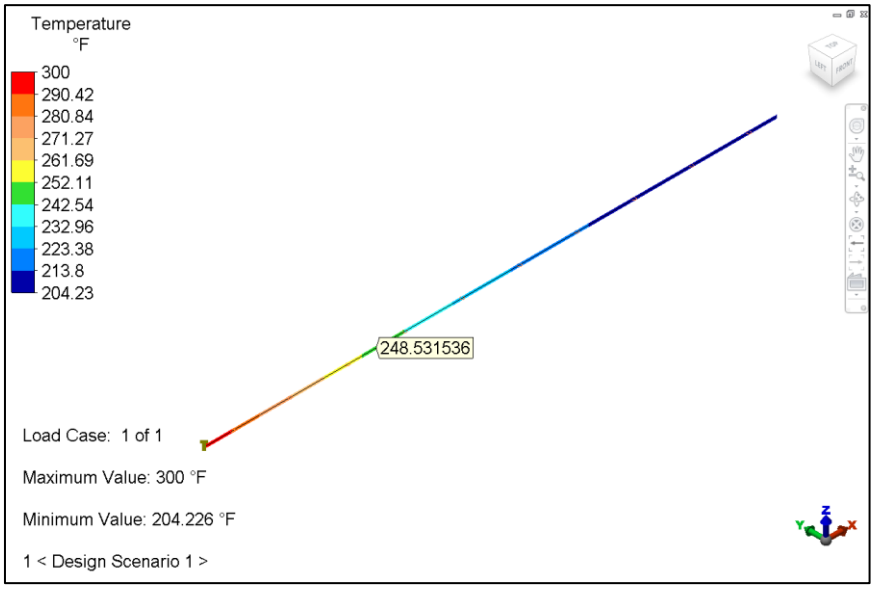

Figure 186-1. Temperature contour

Table 186-1. Comparison of Results

	Theory	Analysis	% diff
Temperature (F)	248.4	248.5	0.04

AVE - 187 Natural Frequency of a Beam, Spring and Mass System

Reference

Lindeburgh, Michael R., *Mechanical Engineering Reference Manual for the PE Exam*, Eleventh Edition, p 58-6.

Problem Description

A ten meter beam is attached to a wall at one end, a spring at the middle and a 10 kg mass at the opposite end. The spring has a stiffness of 2e8 N/m. Find the natural frequency of the beam.

Theoretical Solution

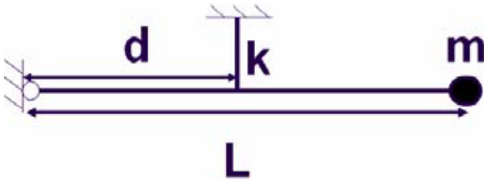

Figure 187-1. Problem Geometry

$$f = \sqrt{\frac{kd^2}{mL^2}}$$

k= 2e8 N/m
m=10 kg
L=10 m
d=5 m

f=355.9 Hz

Autodesk Simulation Solution

The initial beam is modeled using the "Draw tab: Draw panel: Line button". The initial line, of total length 10 m, is placed into part 1, surface 1, layer 1. Using the line selection tool, the initial single line is divided into 10 equal segments. An appropriate cross-section needs to be defined for the beam through the beam element definition screen. This system should be governed by the stiffness of the spring, so high values such as 100 are entered for moments of inertia. In addition, a material with a high modulus of elasticity but low mass is defined for the beam.

The spring is modeled in a similar fashion. Using the "Draw tab: Draw panel: Line button", a line is added to the middle node of the beam. A spring element is defined and a stiffness value is associated with the spring through the element definition screen.

FEA loads and constraints are applied to the model at appropriate points. A nodal constraint which fixes the end of the beam except in rotation around the Z-axis is applied to the end node of the beam. A fixed boundary condition is applied to the free end of the spring. A lumped mass is attached to the other end of the beam with a mass of 10 kg. In addition, out-of-plane movement of the beam should be restrained across the entire model. Out-of-plane in this situation is translation in the Z direction.

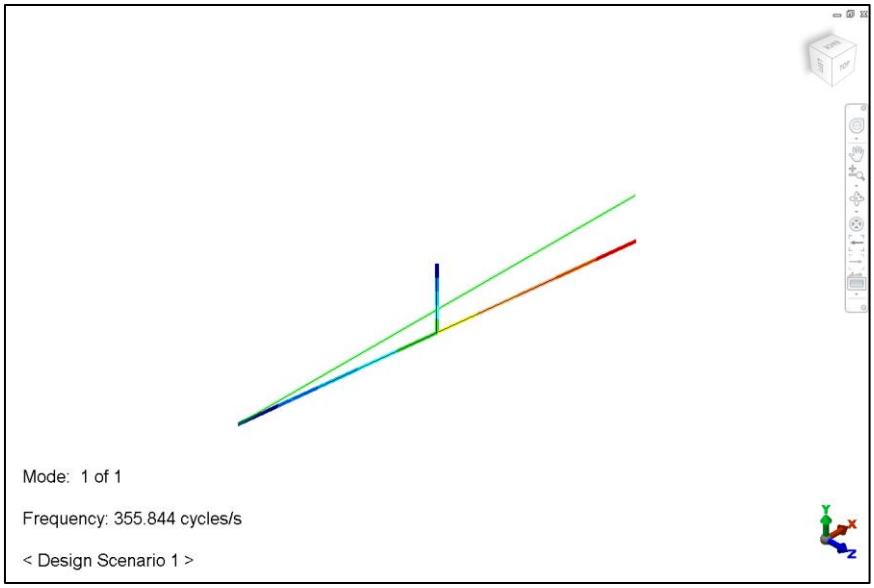

Figure 187-2. First Mode Shape

A comparison of the results with the theoretical is found in the following table.

Table 187-1. Comparison of Results

	Theory	Analysis	% diff
1st mode Frequency (Hz)	355.9	355.8	0.03

AVE - 188 Notched Plate

Reference

Young, Warren C., *Roark's Formulas for Stress and Strain*, Sixth Edition, p. 728.

Problem Description

A flat steel plate is fixed on one end and pulled with a 1000 psi load on the other. The plate is 4.0 in by 1.5 in with a thickness of 1.0 in. Notches of radius 0.45 in intersect the plate at the midpoint on both sides. Find the maximum stress.

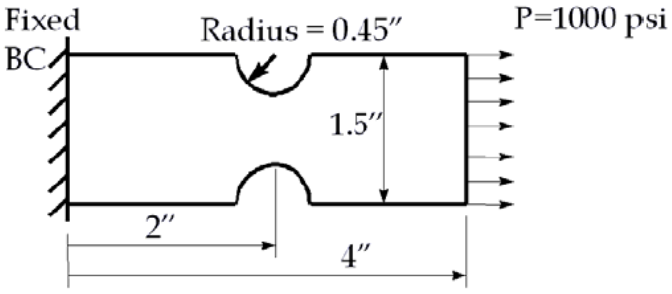

Figure 188-1. Problem Geometry

Theoretical Solution

$$\sigma_{max} = k * P * \frac{Area}{R.Area}$$

k= 1.418, stress concentration factor
P=1000 psi
Area= 1.5 in^2
R. Area= 0.6 in^2

σ_{max}=3545 psi

Autodesk Simulation Solution

This problem considers deflection and stress only in one direction. Therefore, 2-D elements can be used to speed model creation time and analysis time. An outline of the plate with the notches is created in the sketching environment. A 2-D mesh is created from the sketch by selecting the sketch in the tree view and selecting the Generate 2-D Mesh button within the Mesh tab, Mesh panel. A thickness of 1 in is assigned for the element in the element definition screen and material properties of Steel (ASTM – A36) are assigned in the material properties screen.

To constrain the fixed end of the model, a fixed surface boundary condition is applied to one end. A pressure load of -1000 psi is applied to the other end of the plate. A negative value is used to indicate the load should be in tension rather than compression.

Since we are looking for a surface stress located directly on the edge of the notches, the smoothing option should be turned off in order to sample individual nodal results. Smoothing would be more consistent if the objective was a general stress, or a stress located inside the model or not at a specific nodal location.

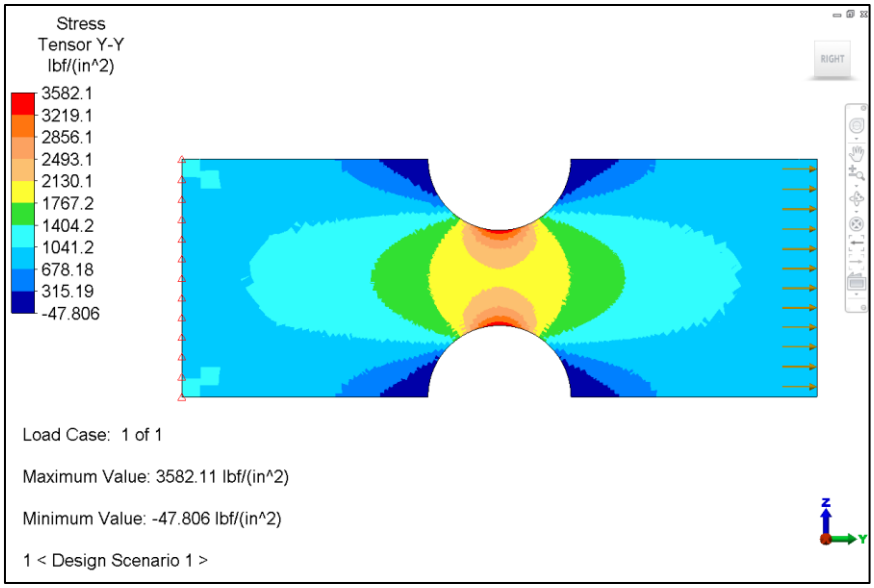

Figure 188-2. Stress tensor Y-Y

A comparison of the results with the theoretical is found in the following table.

Table 188-1. Comparison of Results

	Theory	Analysis	% diff
Maximum Stress (psi)	3545	3582	1.04

AVE - 189 MES Deflection of a Spring Supported Beam

Reference

Spyrakos, Constantine C., Raftoyiannis, John. *Linear and Nonlinear Finite Element Analysis in Engineering Practice*, p 399, 454-467.

Problem Description

A steel cantilever beam of length 100 in has an initial position such that its free end is 0.5 in above a spring. A force of 810 pounds is applied at the end of the beam, which has a square cross-section of 3 in on a side. Find the end deflection of the system.

Theoretical Solution

Figure 189-1. Problem Geometry

Deflection = (F+kd)/((3EI/L^3)+k)

Autodesk Simulation Solution

The initial beam is modeled using the "Draw tab: Draw panel: Line button”. The initial line, of total length 100 in, is placed into part 1, surface 1, layer 1. Using the line selection tool, the initial single line is divided into ten equal segments. Part 1 is then defined as having an element type of beam and assigned appropriate cross-section and material properties using the element definition and material definition screens respectively.

The spring is modeled in a similar fashion. Using the "Draw tab: Draw panel: Line button”, a single line is placed into part 2, surface 1, layer 1. The single line begins at the node at the end of the beam and is defined at a relative distance of 10 in from the beam in the negative Z direction. Part 2 is then assigned the element type of truss. In the element definition screen, the truss element is assigned a curve material model. This will allow for a stress/strain curve to be defined for the truss to simulate quick yielding for the distance specified in the problem and then a spring-like stiffness for the remainder of the event.

FEA loads and constraints are applied to the model at appropriate points. A nodal force load of 810 lb is applied to the end node of the beam element in the negative Z direction. The end of the truss element and the end of the cantilever beam are fully fixed. In addition, the nodes of the beam element should be constrained from out-of-plane movement at every node. Since this is a MES analysis, the analysis parameters must be defined to specify an event duration of 100 seconds and a capture rate of 1 per second. A ramped load curve with a constant slope is applied from Time 0 to Time 100.

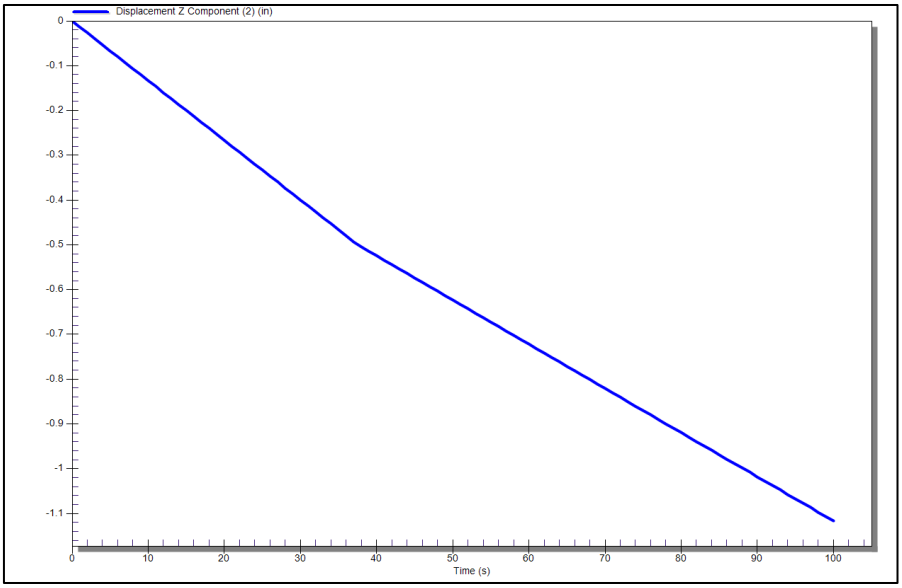

Figure 189-2. Deflection in the Z direction at the node where the force is applied

A comparison of the results with the theoretical is found in the following table.

Table 189-1. Comparison of Results

	Theory	Analysis	% diff
Deflection (mm)	1.13	1.1168	1.17

AVE - 190 Flow of Steam through an Insulated Pipe

Reference

Chapman, A.J., *Heat Transfer*, Fourth Edition, p 442.

Problem Description

Steam at 300ºC is flowing through an insulated pipe at a velocity of 5 m/s. The pressure is 2000 kN/m^2. The pipe has and inside diameter of 15.41 cm, and outside diameter of 16.83 cm and has a conductivity of 45 W/m-ºC. The insulation is 3.5 cm thick and has a conductivity of 0.075 W/m-ºC. The convection coefficient between the pipe and the surroundings at 20ºC is 5.75 W/m^{2}ºC. Find the temperature at the inside surface of the pipe and at the outside surface of the insulation.

Theoretical Solution

The convection coefficient between the steam and the pipe can be calculated using the material and flow properties. For steam at 2000 kN/m^2, the density is 7.9681 kg/m^3, the viscosity is 20.1e-6 kg/m-s, the conductivity is 49.95e-3 W/mºC and the Prandtl number is 1.02. These values can be used in the following three equations to calculate the convection coefficient.

$$\mathrm{Re} = \frac{v D \rho}{\mu} = 3.055e5$$

$$\mathrm{Nu} = 0.023 \mathrm{Re}^{0.8} \mathrm{Pr}^{0.3} = 564.9$$

$$h = \mathrm{Nu} \frac{k}{D} = 168.5 \ \mathrm{W/m^2{}^oC}$$

The overall heat transfer coefficient, U, for the pipe can be calculated using the following equation where r_1 is the inside radius of the pipe, r_2 is the outside radius of the pipe and r_3 is the outside radius of the insulation.

$$U = \left[\frac{r_3}{r_1 h_{inside}} + \frac{r_3 \ln\left(\frac{r_2}{r_1}\right)}{k_{pipe}} + \frac{r_3 \ln\left(\frac{r_3}{r_2}\right)}{k_{ins}} + \frac{1}{h_{outside}} \right]^{-1} = 1.36 \mathrm{W/m^2{}^oC}$$

The outside temperature of the pipe, $T_{outside}$, can be calculated from the following equation.

$$h_{outside}(T_{outside} - T_{amb}) = U(T_{steam} - T_{amb})$$

$$T_{outside} = 86^oC$$

The inside temperature of the pipe, T_{inside}, can be calculated from the following equation.

$$h_{inside}(T_{steam} - T_{inside}) = U(T_{steam} - T_{amb})$$

$$T_{inside} = 297^oC$$

Autodesk Simulation Solution

Since the thickness of the pipe is irrelevant, 2-D elements can be used for this analysis. The cross-sections of the pipe and insulation will be drawn as separate sketches in FEA Editor. The sketches will be meshed by selecting the headings in the tree view, and accessing the 2-D Mesh Generation utility. Any thickness value can be input in the element definition screen. The appropriate thermal conductivities for the pipe and insulation must be input in the material specification screen.

Convection loads must be applied to the surfaces on the interior of the pipe and exterior of the insulation. When defining the convection load on the interior of the pipe, the Film/Convection Coefficient Calculator can be used to calculate the convection coefficient between the steam and the pipe based on the fluid properties and geometry of the flow.

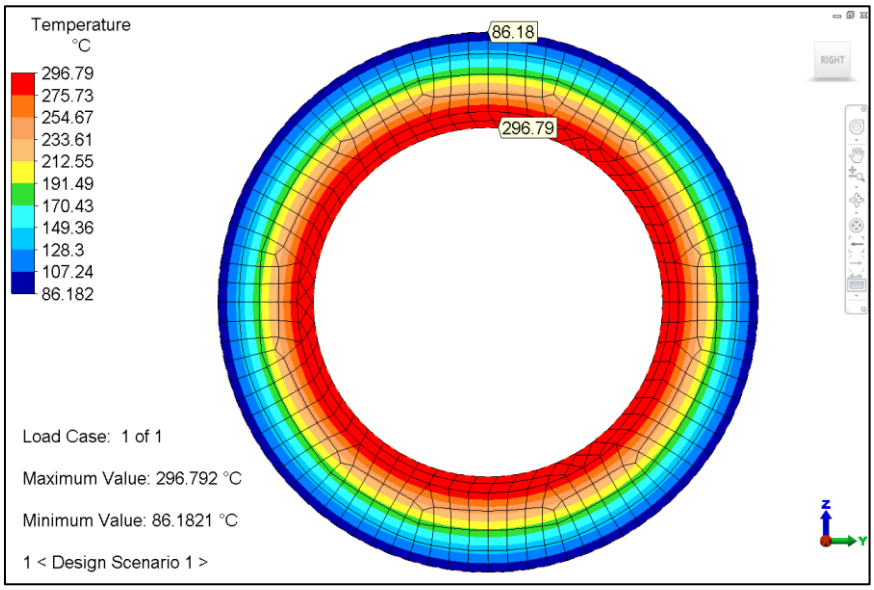

Figure 190-1. Temperature Profile

A comparison of the results with the theoretical is found in the following table.

Table 190-1. Comparison of Results

	Theory	Analysis	% diff
Inside Temperature (°C)	297	296.8	0.0
Outside Temperature (°C)	86	86.2	0.2

AVE - 191 Airflow over a Hill

Reference

Munson, Bruce R., Young, Donald F., Okiishi, Theodore H., *Fundamentals of Fluid Mechanics*, p 360-361.

Problem Description

The shape of a hill rising from a plain can be approximated with the top section of a half-body as illustrated in Figure 202-1. The height of the hill approaches 200 ft. When a 40 mph wind blows toward the hill, what is the magnitude of the air velocity at a point directly above the origin (Point 2)?

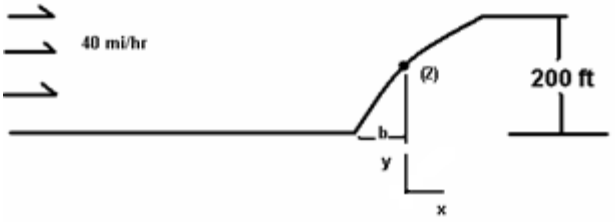

Figure 191-1. Profile of the Hill

Theoretical Solution

The equation for the velocity at Point 2, v_2, is

$$v_2^2 = u^2\left(1+2\frac{b}{r}\cos\theta+\frac{b^2}{r^2}\right)$$

where u is the velocity of the flow before it contacts the half-body. The vertical location, r, can be calculated using the equation

$$r=\frac{b(\pi-\theta)}{\sin\theta}$$

At Point 2, the angle θ from the X axis is π/4. Therefore r=1.061b

Substituting the values for u, q and r gives,

$$v_2=\sqrt{40^2\left(1+3*1.061*0.707+\frac{1}{1.061^2}\right)}=73.6\,\text{mph}=107.9\,\text{ft/s}$$

Where 1 mph=1.4667ft/s

It has to be noted that this solution is based on the inviscid flow assumption. To have simulation result comparing to this theoretical solution, one needs to understand to have certain tolerance for the real viscous laminar or turbulence flow, and this equation is applied to the pressure side (face the wind) of the hill where it has no adverse pressure gradient and no boundary layer separation.

Autodesk Simulation Solution

A steady fluid flow analysis will be performed using 2-D elements. The profile of the hill will be created using a sketch in FEA Editor. The sketch will be meshed by selecting the heading in the tree view, and accessing the 2-D Mesh Generation utility. The fluid properties for air will be input in the material definition screen.

Prescribed velocities of 58.7 ft/s (40 mph) in the horizontal direction will be applied to the left edge of the model. The velocity in the vertical direction will be kept at 0. An inlet/outlet condition will be applied to the right edge of the model. The top surface is modeling to specify zero velocity at Z direction but free in Y direction, this can reduce partial wall effect on the external flow. As the comparison theoretical solution is flow through half-body, the bottom surface is specified the symmetric boundary velocity boundary condition, in this model, Z direction velocity is constrained to zero and Y velocity is free. Here is the slight difference between the flow through half-body and flow over a hill, the later needs no-slip (zero velocity) boundary condition on the bottom surface while the former needs symmetric boundary condition.

However, this difference does not change the flow pattern, so the flow through half-body could be used to simulate a flow over a hill.

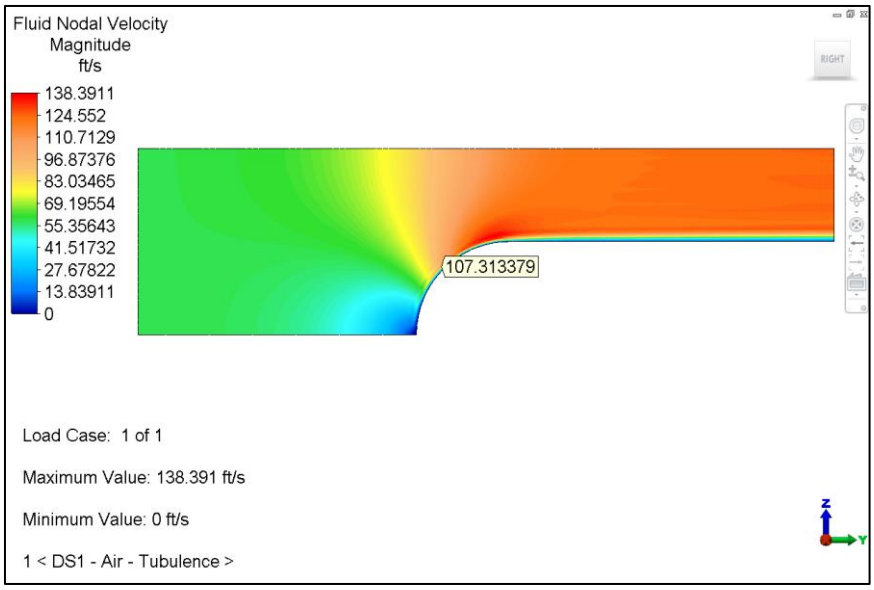

Figure 191-2. Velocity profile for Design Scenario 1. Fluid is Air. Turbulence flow calculation.

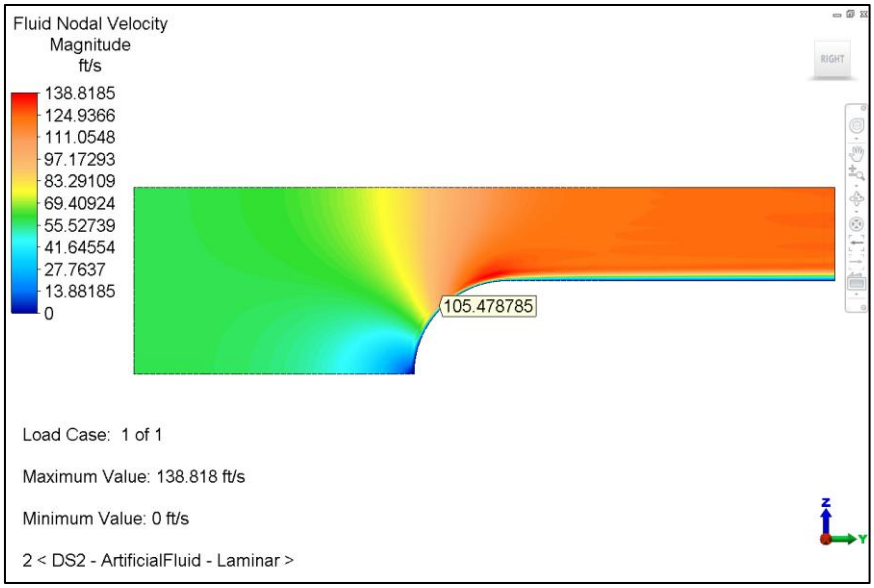

Figure 191-3. Velocity profile for Design Scenario 2 An artificial fluid is used. Laminar flow calculation.

Notes on selecting check point (comparison node)

- The theoretical solution is based on inviscid flow, which does not need no-slip boundary condition on the hill. Therefore a velocity probe can be located on the hill surface.
- The simulation is based on the assumption of incompressible viscous flow. It is more in line with reality. However, since we define a no-slip boundary condition on the hill, and the probe location was selected 1 node into the flow path. Note that this picked node has to be just out of the boundary layer to avoid the velocity gradient inside boundary layer.

A comparison of the results with the theoretical is found in the following table.

Table 191-1. Comparison of Results

Flow pattern	Theory	Analysis	% diff
DS1, Air, turbulence flow	107.9 (ft/s)	107.3 (ft/s)	0.56%
DS2, Artificial fluid, laminar flow	107.9 (ft/s)	105.5 (ft/s)	2.22%

Note that it is suggested to extend the outlet to improve the simulation solution stability. Since the vertical plane is very close to the ending location of the hill top, this simulation does not have stable velocity and pressure profile and is prone to having “converge with stagnation due to oscillation”.

AVE - 192 Heat Lost through the Walls of a Furnace

Reference

Holman,J.P., *Heat Transfer*, Seventh Edition, p 86.

Problem Description

A small cubic furnace which is 50 cm x 50 cm x 50 cm on the inside, is made of fireclay brick (k = 1.04 W/m-ºC) with a thickness of 10 cm. The interior and exterior temperatures are kept constant at 500ºC and 50ºC, respectively. Calculate the heat lost through the walls.

Theoretical Solution

The total shape factor for the furnace is the sum of the six wall sections, twelve edges and eight corners. These components can be calculated using the equations below.

$$S_{wall} = \frac{A}{L} = \frac{(0.5m)(0.5m)}{0.1m} = 2.5m$$
$$S_{edge} = 0.54D = (0.54)(0.5m) = 0.27m$$
$$S_{corner} = 0.15L = (0.15)(0.1m) = 0.015m$$

Summing these values for all of the walls, edges and corners results in a total shape factor of 18.36 m. The heat loss can be calculated using the equation below.

$$q = kS\Delta S = (1.04)(18.36)(450) = 8.592kW$$

Autodesk Simulation Solution

A CAD solid model of 1/8th of the furnace was created and meshed in the FEA Editor as shown in Figure 192-1.

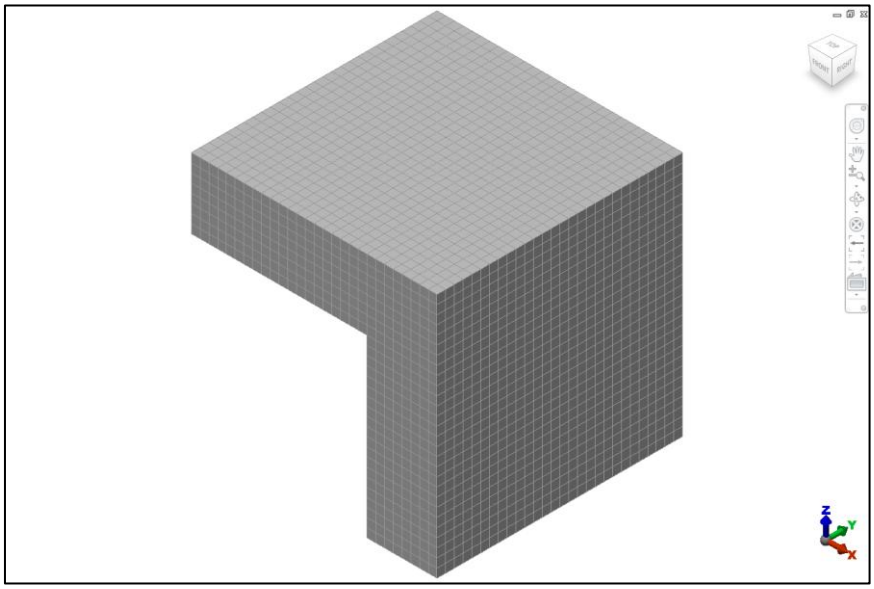

Figure 192-1. CAD Solid Model of 1/8th of the Furnace

Applied temperatures are applied to the interior and exterior surfaces of the model. No temperatures are applied to the symmetry planes.

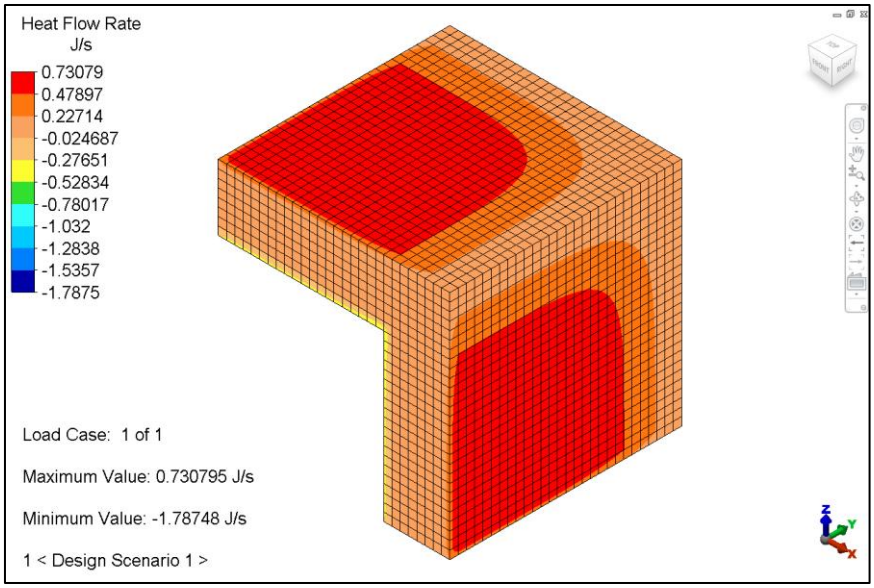

Figure 192-2. Heat Rate of Face Profile

The simulation results output a heat loss of 361.359 J/s per exterior surface. This is a 1/8th geometry, and the full model is made up of 6 exterior surfaces. Each exterior surface is made up of 4 1/4th sections. So we have to multiply 361.359 J/s by 24 in order to calculate the heat loss for the full model.

(361.359 J/s per section) x (24 sections) = 8672.616 J/s = 8.673 kW

A comparison of the results with the theoretical is found in the following table.

Table 192-1. Comparison of Results

	Theory	Analysis	% diff
Heat Loss (kW)	8.592	8.673	0.9

AVE - 193 Natural Frequency of a Simply Supported Beam with a Mass in the Middle

Reference

Avallone, Eugene A., Baumeister III, Theodore, *Mark's Standard Handbook for Mechanical Engineers*, Ninth Edition, p 5-70.

Problem Description

A simply supported beam is 48 in long and has a circular cross-section of 0.125 inch radius. The mass density is 0.0007324 lbf-s^2/in/in^3. The modulus of elasticity is 30e6 psi and Poisson's Ratio is 0.3. A uniform lumped mass of 0.1 lbf-s^2/in is placed at the center of the beam. Determine the first natural frequency of the system.

Theoretical Solution

The natural frequency, ω, can be calculated using the cross-sectional and material properties of the beam, the lumped mass, m, and the mass of the beam, m_{beam}. The equation is shown below.

$$\omega = \sqrt{\frac{48EI}{(m + 0.5m_{beam})L^3}} = 0.792\,\text{Hz}$$

Autodesk Simulation Solution

The beam is modeled using the "Draw tab: Draw panel: Line button". A line was created from the origin (0,0,0) to (48,0,0) and divided into 40 segments. The cross-sectional properties were defined in the element definition screen using the Cross-Section Libraries (0.125" radius round). The material properties were input in the material definition screen (per the Problem Description on the preceding page).

The end at the origin was constrained against translation in all three global directions and against rotation about the X-axis (to prevent rigid-body rotation about the beam axis). The opposite end was constrained against translation in the Y and Z directions. A lumped mass of 0.1 lbf-s^2/in is added to the center node of the beam and is applied equally in all three global directions.

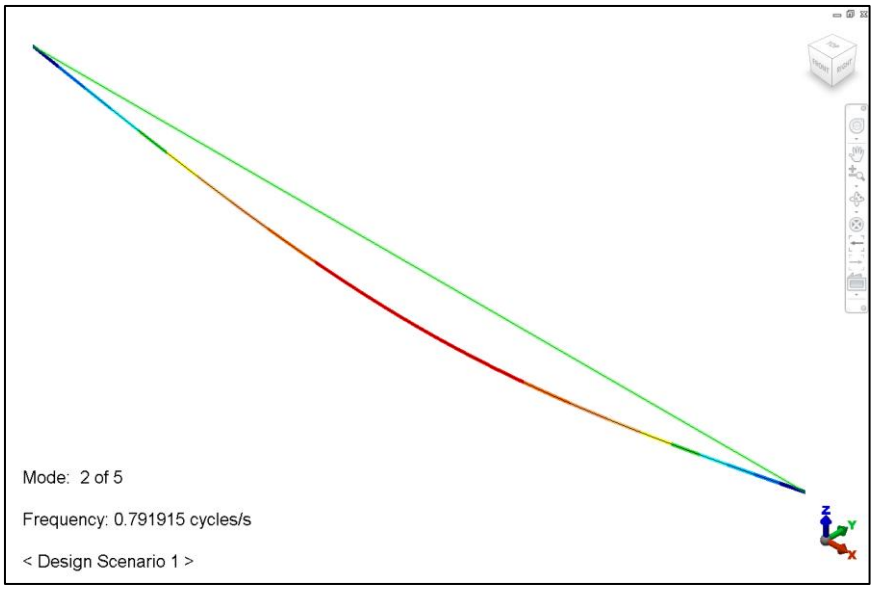

Figure 193-1. Natural Frequency

A comparison of the results with the theoretical is found in the following table.

Table 193-1. Comparison of Results

	Theory	Analysis	% diff
Natural Frequency (Hz)	0.792	0.792	0.0

AVE - 194 Contact Pressure between a Punch and Foundation

Reference

Feng, Q., Prinja, N.K., *NAFEMS Benchmark Tests for Finite Element Modeling of Contact, Gapping and Sliding*, Ref: R0081, Issue: 1, CGS-1.

Problem Description

A 40,000 N/m^2 pressure is applied to a punch which causes it to contact the foundation. The contact area is 1.0 m^2. The modulus of elasticity for both materials is 100 MPa and Poisson's ratio is 0.3. Determine the contact pressure.

Theoretical Solution

In order for static equilibrium to exist, the contact pressure must be equal to the applied pressure. Therefore the contact pressure must be 40,000 N/m^2. Since the area is 1 m^2, the contact force is 40,000 N.

Autodesk Simulation Solution

Please refer to AVE - 146 for the 2 D version of the same problem. The punch and foundation were built using a CAD solid model program. Surface contact was defined between the parts by right clicking on the contact heading in the tree view. The model was meshed. The specified material properties were defined in the material definition screen. The bottom surface of the foundation was constrained against translation in the vertical (Y) direction. The center lines of nodes along the top of the punch and bottom of the foundation parallel to the X axis were constrained against translation in the Z direction. The center lines of nodes along the top of the punch and bottom of the foundation parallel to the Z axis were constrained against translation in the X direction. These constraints make the model statically stable. A 40,000 N/m^2 pressure was applied to the top surface of the punch.

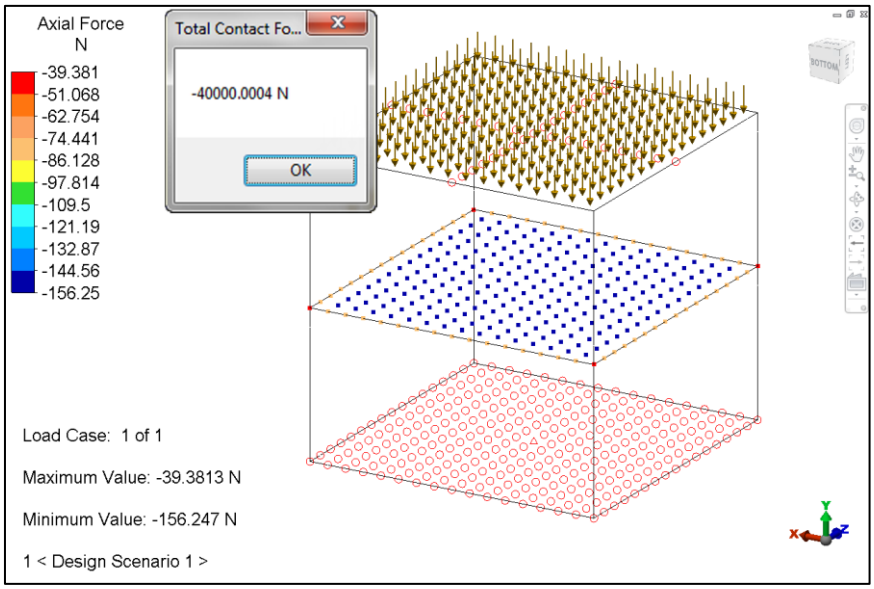

Figure 194-1. Contact Force

Table 194-1. Comparison of Results

	Theory	Analysis	% diff
Contact Force (N)	40000	40000	0.0

AVE - 195 MES Deflection of a Pointer Due to Thermal Expansion

Reference

Higdon, Ohlsen, Stiles, Weese, Riley, *Mechanics of Materials*, Third Edition, p 119.

Problem Description

Determine the movement of the pointer in Figure 195-1 with respect to the scale zero when the temperature increases 50ºC. The coefficients of thermal expansion for the steel and aluminum are 12e-6 per ºC and 23e-6 per ºC, respectively.

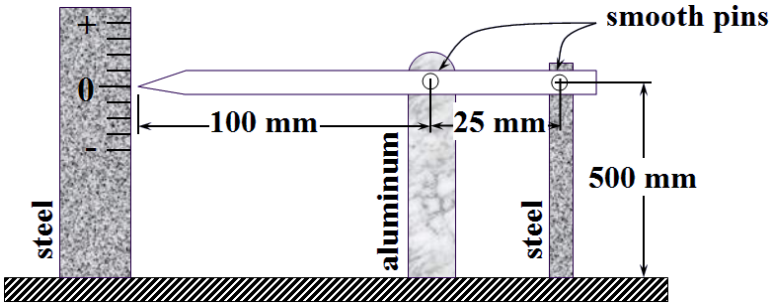

Figure 195-1. Problem Geometry

Theoretical Solution

The elongation,δ, for each part can be calculated from the coefficient of thermal expansion, α, temperature difference, ΔT, and the original length, L, using the following equation.

$$\delta = L\alpha\Delta T$$

Using the coefficients of thermal expansion for steel and aluminum, it can be calculated that the aluminum bar elongates 0.575 mm and the steel bars elongate .3 mm. Since both the scale and the steel bar elongate the same distance, the pin attaching the pointer to the aluminum bar is 0.275 mm above the scale zero. The ratio below can be used to calculate the location of the end of the pointer with respect to the scale zero.

$$\frac{0.275\text{mm}}{25\text{mm}} = \frac{d_{end}}{125\text{mm}}$$

$$d_{end} = 1.375\text{mm}$$

Autodesk Simulation Solution

The model will be analyzed with Autodesk Simulation using beam elements and will be drawn in the XZ plane. The beams for the scale and the steel part can be placed in the same part number since they are of the same material. The beams for the aluminum part and pointer must be placed in separate parts. Two beam elements will be required for the pointer because a vertex will be needed where it meets the aluminum part.

The steel and aluminum parts will have a thermoelastic material model defined in the element definition screen. The pointer will have an isotropic material model defined. A rectangular cross-section was also defined in the element definition screen for all three parts. The specified thermal coefficients of expansion were defined for the entire temperature range for the steel and aluminum parts. 200,000 N/mm^2 was defined for the modulus of elasticity of

steel and 68,900 N/mm^2 was used for the modulus of elasticity of aluminum. Steel material properties were used for the pointer, however no coefficient of thermal expansion was defined.

The bottom node of each of the vertical parts was fully constrained. Beam end releases were added to the steel and aluminum parts (not the scale). The rotational constraint about the Y axis was released. An event duration of 1 s and capture rate of 10 per second were defined. A default nodal temperature of 1ºC was defined and follows a load curve that starts at 20 at 0 seconds and increases to 70 at 1 second.

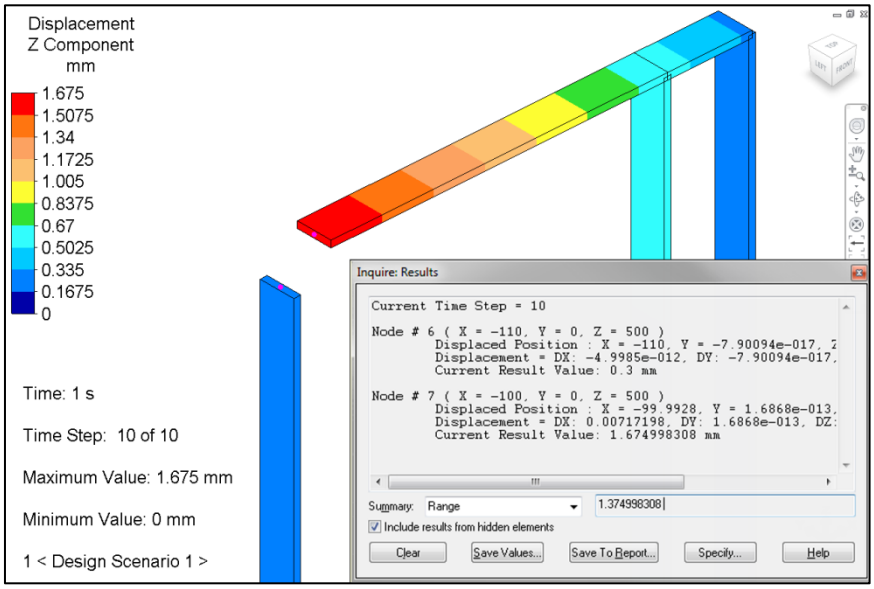

Figure 195-2. Deflection in the Z direction

A comparison of the results with the theoretical is found in the following table.

Table 195-1. Comparison of Results

	Theory	Analysis	% diff
Delta Z with respect to pointer (mm)	1.375	1.375	0.0

AVE - 196 Natural Frequency of a Weighing Platform

Reference

Meriam, J. L., Kraige, L. G., *Engineering Mechanics: Dynamics*, Fourth Edition, p. 616.

Problem Description

The weighing system shown in Figure 196-1 has a mass, m, of 0.02588 lbf-s^2/in and a spring stiffness, k, of 0.4 lbf/in. The distance b is 2 in and the distance c is 8 in. Determine the period of the system.

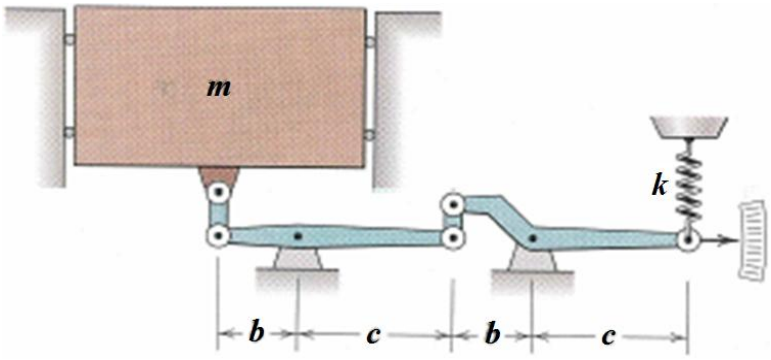

Figure 196-1. Problem Geometry

Theoretical Solution

Let y be the vertical displacement of the mass. Using the ratio of the two levers between the spring and the mass, the displacement of the spring, y_{spring}, can be calculated to be

$$y_{spring} = y\left(\frac{c}{b}\right)^2 .$$

Therefore the force of the spring can be calculated as

$$F_{spring} = ky_{spring} = ky\left(\frac{c}{b}\right)^2 .$$

The force on the block, F, can be calculated using the ratio of the two levers and the spring force as

$$F = F_{spring}\left(\frac{c}{b}\right)^2 = ky\left(\frac{c}{b}\right)^4 .$$

The differential equation for the system is

$$\ddot{y} + \frac{k}{m}\left(\frac{c}{b}\right)^2 y = 0 .$$

The period, τ, can be calculated as

$$\tau = 2\pi\left(\frac{b}{c}\right)^2\sqrt{\frac{m}{k}} = 2\pi\left(\frac{2}{8}\right)^2\sqrt{\frac{0.02588}{0.4}} = 0.0998s$$

Autodesk Simulation Solution

The entire model was built in the FEA Editor environment of Autodesk Simulation. The mass was constructed from an extruded four point mesh and was defined as brick elements. The dimensions were 2 in x 2 in x 1 in. The two levers were defined as rigid elements. The links connecting the two levers and the left lever to the mass were defined as truss elements. The spring was created as a spring element.

The brick elements were assigned a mass density of 0.00647 lbf-s^2/in^4 in the material specification screen. This will result in the required mass. The rigid elements were assigned a high stiffness of 1e10 lbf/in in the element definition screen. The truss elements were assigned a cross-sectional area of 10 in^2 in the element definition screen and a modulus of elasticity of 1e6 psi in the material specification screen. The spring element was assigned a 0.4 lbf/in stiffness in the element definition screen.

The mass was constrained so that it can only translate vertically. The nodes at the pivots were constrained so that they can only rotate about the axis perpendicular to the system. The node at the end of the spring not attached to the lever was constrained against translation in all directions.

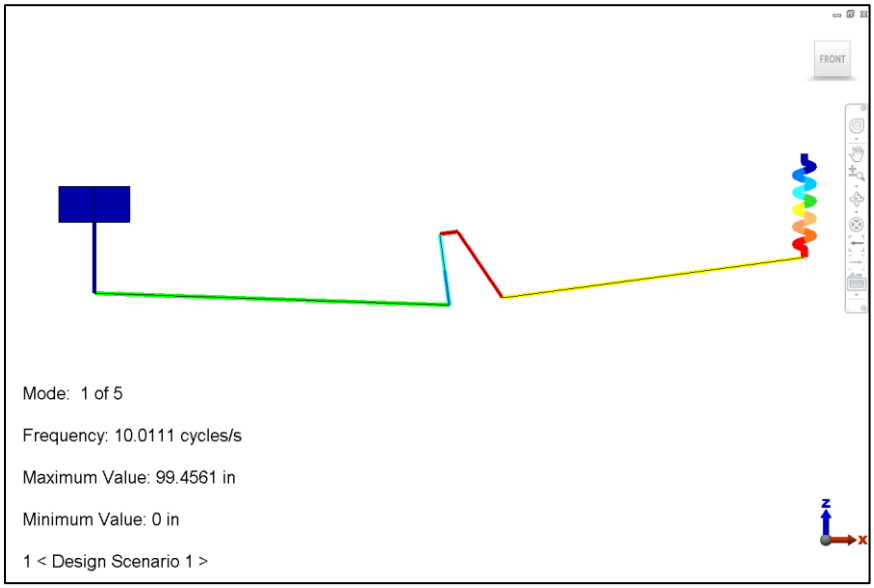

Figure 196-2. First Natural Frequency

A comparison of the results with the theoretical is found in the following table.

Table 196-1. Comparison of Results

	Theory	Analysis	% diff
Period (s)	0.0998	0.0998	0.0

AVE - 197 Axial and Bending Forces Acting on a Wide Flanged Beam

Reference

Hibbeler, R.C., *Mechanics of Materials*, Fourth Edition, p 801.

Problem Description

A wide flanged beam is 40 feet long and has a cross-section shown in Figure 197-1. The beam is fixed at one end and has three 500 lbf forces applied in the X, Y and Z directions at the opposite end. Determine the worst stress in the beam.

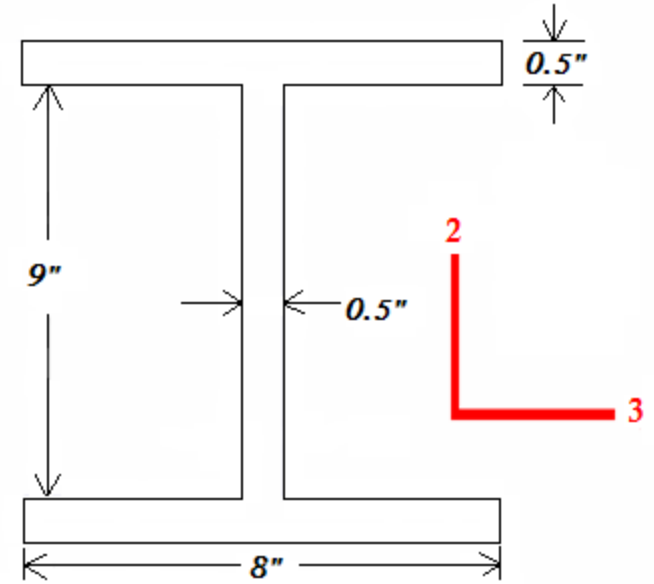

Figure 197-1. Problem Description

Theoretical Solution

We must first calculate the moments of inertia of the cross-section about the local 2 and 3 axes. These can be calculated using the following equations.

$$I_2 = \frac{1}{12}(9)(0.5)^3 + \frac{1}{12}(0.5)(8)^3 + \frac{1}{12}(0.5)(8)^3 = 42.76\text{in}^4$$

$$I_3 = \frac{1}{12}(0.5)(9)^3 + 2\left(\frac{1}{12}(8)(0.5)^3 + (8)(0.5)(4.75)^2\right) = 211.04\text{in}^4$$

The formula for the maximum stress is

$$\sigma_{max} = \frac{P}{A} + \frac{My_2}{I_3} + \frac{My_3}{I_2}.$$

The force, P, is 500 lbf. The area, A, is 12.5 in^2.The moment, M, is the product of the beam length and the force which is 240,000 in-lbf. The values y_2 and y_3 are the distances for the centroid of the cross section to the point of maximum bending stress along the local 2 and 3 axes, respectively. The value for y_2 is 5 in and the value for y_3 is 4 in. Substituting these values into the maximum stress equation results in

$$\sigma_{max} = \frac{500}{12.5} + \frac{(240000)(5)}{211.04} + \frac{(240000)(4)}{42.76} = 28{,}177 \text{psi}$$

Autodesk Simulation Solution

The beam was built in FEA Editor. The line was created in Surface 1. This will cause the local 2 axis to be parallel to the global Y axis. The 40 foot long beam was divided into 40 segments. The cross-section library in the element definition screen was used to input the cross-section dimensions. The material was set to Steel A36 in the material specification screen.

The node at the left end of the beam was constrained against translation and rotation in all directions. Three 500 lbf nodal forces were applied to the other end of the beam along each of the global directions.

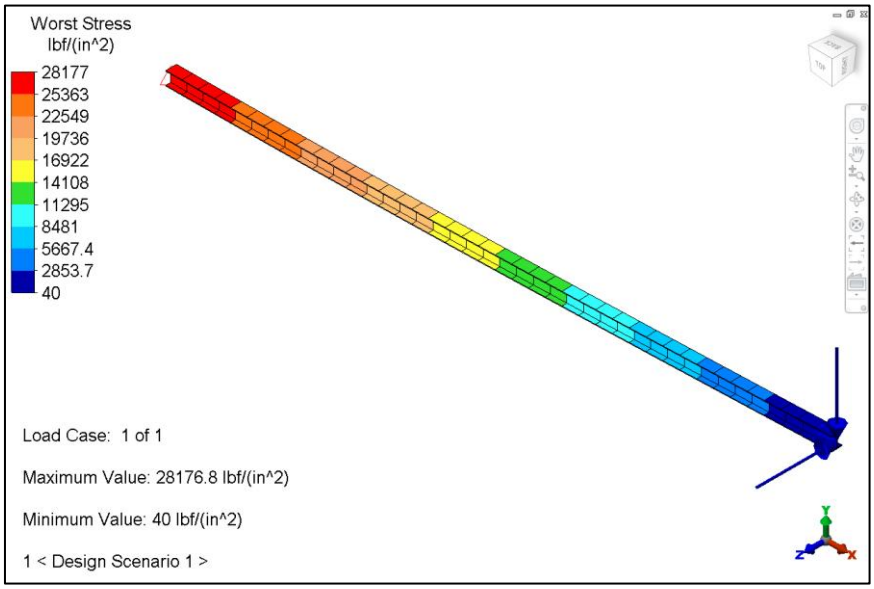

Figure 197-2. Worst Beam Stress

A comparison of the results with the theoretical is found in the following table.

Table 197-1. Comparison of Results

	Theory	Analysis	% diff
Worst Stress (psi)	28177	28176.8	0.0

AVE - 198 MES of a Pinned Rod Released from Rest

Reference

Lindeburg, M. R., *EIT Review Manual*, 1997-98 Edition, p. 17-6.

Problem Description

A uniform rod is 1 m long and has a mass of 10 kg. It is pinned at one end by a frictionless pivot. The rod is originally at a 45º angle with the horizontal. If it is released from rest, find the velocity of the tip when it becomes horizontal.

Theoretical Solution

Initially, all of the rod's energy is potential energy. When the rod is horizontal, the potential energy will have been converted to rotational kinetic energy. Therefore the conservation of energy principle can be used as shown in the equation below.

$$mg\left(\frac{1}{2}L\sin 45\right) = \left(\frac{mL^2}{3}\right)\left(\frac{\omega^2}{2}\right)$$

$$(10)(9.81)\left(\frac{1}{2}(1)\sin 45\right) = \left(\frac{(10)(1)^2}{3}\right)\left(\frac{\omega^2}{2}\right)$$

$$\omega = 4.56 \text{rad/s}$$

The velocity at the end of the rod can be calculated using the relationship

$$v = r\omega = (1)(4.56) = 4.56 \text{m/s}$$

Autodesk Simulation Solution

A single line was drawn in the FEA Editor environment in the XY plane at a 45º angle. This line was assigned an element type of beam. An appropriate combination of cross-section and mass density was defined so that the mass of the rod would be 10 kg. The end at the pivot was constrained so that only rotation about the Z axis was allowed. Standard gravity was applied to the model.

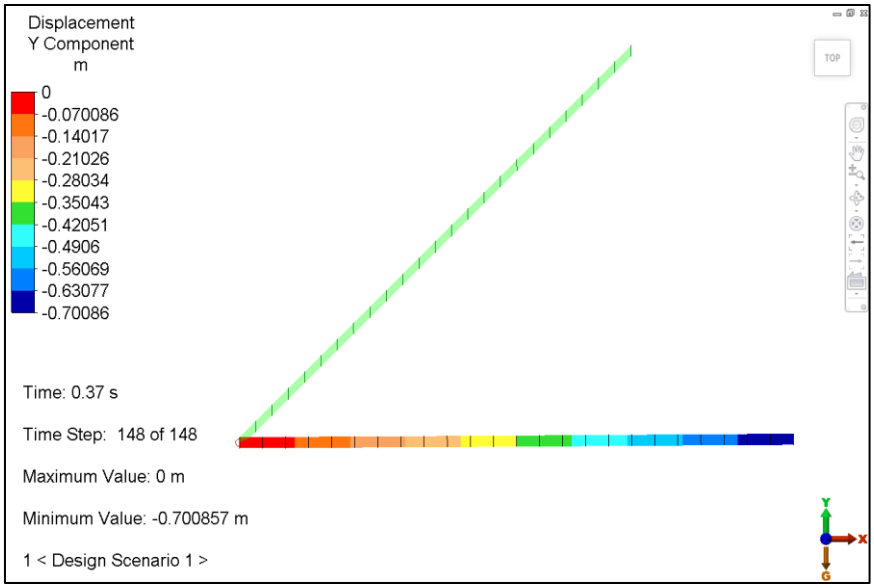

Figure 198-1. Y displacement after 0.37 seconds.

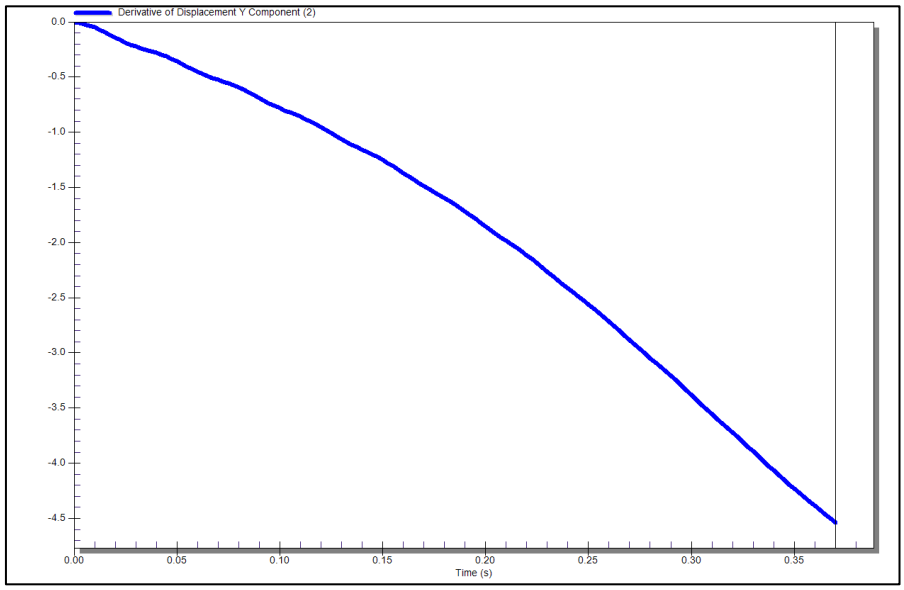

Figure 198-2. Graph of the Y Velocity

Table 198-1. Comparison of Results

	Theory	Analysis	% diff
Y Velocity (m/s)	4.56	4.54	0.44

AVE - 199 MES of a Reinforced Concrete Beam

Reference

Biggs, M. R., *Finite Element Modeling and Analysis of Reinforced-Concrete Bridge Decks*, p. 5-7.

Problem Description

A concrete beam has a span of 20ft, a width of 10 in and a depth of 25 in. The concrete has a strength, f `c, of 6,000 psi and a modulus of 4,420 ksi. The reinforcing steel has a modulus of 29,000 ksi, a yield stress of 60 ksi and a cross-sectional area of 2.37 in^2. A uniform loading of 4,260 lbf/ft is applied over the length of the beam.

Theoretical Solution

Maximum stresses attributable to the applied load were calculated in accordance with the code of the American Concrete Institute. The vertical displacement results are plotted along the length of the beam in Figure 199-1.

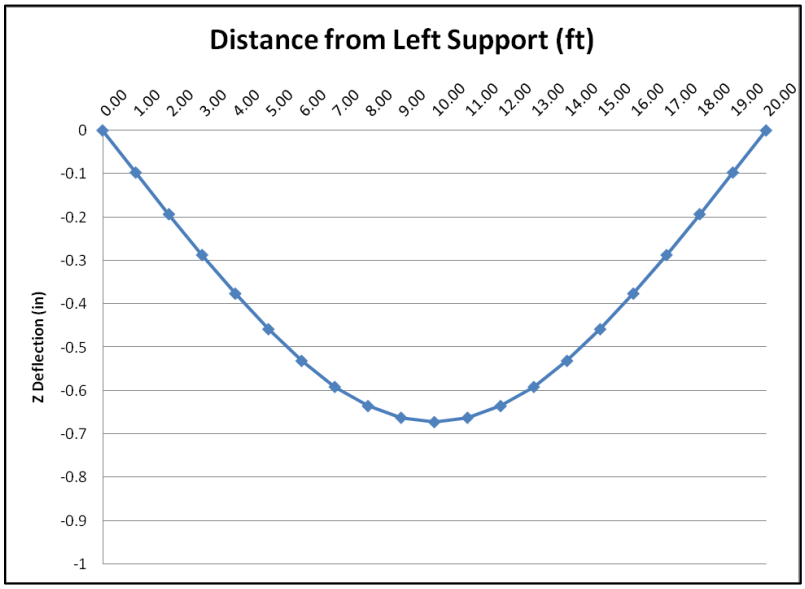

Figure 199-1. Graph of the Z deflection along the length of the beam

Autodesk Simulation Solution

A brick element model was created in FEA Editor with dimensions of 240 in x 10 in x 25 in. There were 20 elements along the 240 inch length (Y axis), 2 elements along the 10 in length (X axis) and 4 elements along the 25 in length (Z axis). A normal pressure of 35.5 psi was applied to the 240 in x 10 in surface. This corresponds to the 4,260 lb/ft distributed load. Boundary conditions were applied along the centerline of each end constraining the Y and Z translations.

A duration of 1 second and a capture rate of 100 1/s were used. The load curve for the pressure was ramped up from 0 magnitude to full magnitude over 1 second.

The reinforced concrete material model was assigned in the element definition dialog. The following material properties were assigned:

- General Tab
  - Mass density: 2.2e-4 lbf*s^2/in/in^3
  - Young's modulus: 4,420,000 psi
  - Poisson's ratio: .15
- Strength Tab (Only the uniaxial compressive strength, f '$_c$, was provided. For the uniaxial tensile strength, the value 0.1f '$_c$ was used. For the biaxial compressive strength, the value 1.2f '$_c$ was used.)
  - Uniaxial tensile strength: 600 psi
  - Uniaxial compressive strength: 6,000 psi
  - Biaxial compressive strength: 7,200 psi
  - Tension stiffening: Fracture energy, Linear
    - Fracture energy/area: 10 in*lbf/in^2
- Hardening Tab

Strain	Stress
0	-4,800
-0.004	-6,000

- Rebar Tab
  - Number of rebars: 1
  - Volume ratio: 0.00948
  - Mass density: 0.00074 lbf*s^2/in/in^3
  - Modulus of elasticity: 29,000,000 psi
  - Strain hardening modulus: 59,000 psi
  - Yield stress: 60,000 psi
  - Rebar direction: Y

A comparison of the results with the theoretical is found in the following table.

Table 199-1. Comparison of Results

	Theory	**Analysis**	**% diff**
Vertical Displacement at Center of Beam (in)	-0.669	-0.672	0.45

AVE - 200 Riks Analysis of a Curved Cylindrical Shell

Reference

Surana, K.S., *Geometrically Nonlinear Formulation for the Curved Shell Elements*, p. 603-607.

Problem Description

A force is applied to the center of a cylindrical shell section. The longitudinal edges are hinged and the curved edges are free. The cylinder has a radius of 2540 mm and depth of 508 mm. The thickness is 12.7 mm. The section spans an arc of 0.1 radians on either side of the force location. The material has a modulus of elasticity of 3.10275 kN/mm^2 and a Poisson's ratio of 0.3.

Theoretical Solution

In the technical paper, twelve equal displacements increments were applied. Equilibrium iterations were performed at each increment until the following tolerances were met: $\Delta 1 \leq 0.00001$, $\Delta 2 \leq 0.001$. The total force is plotted against the vertical deflection at the center point in Figure 200-1.

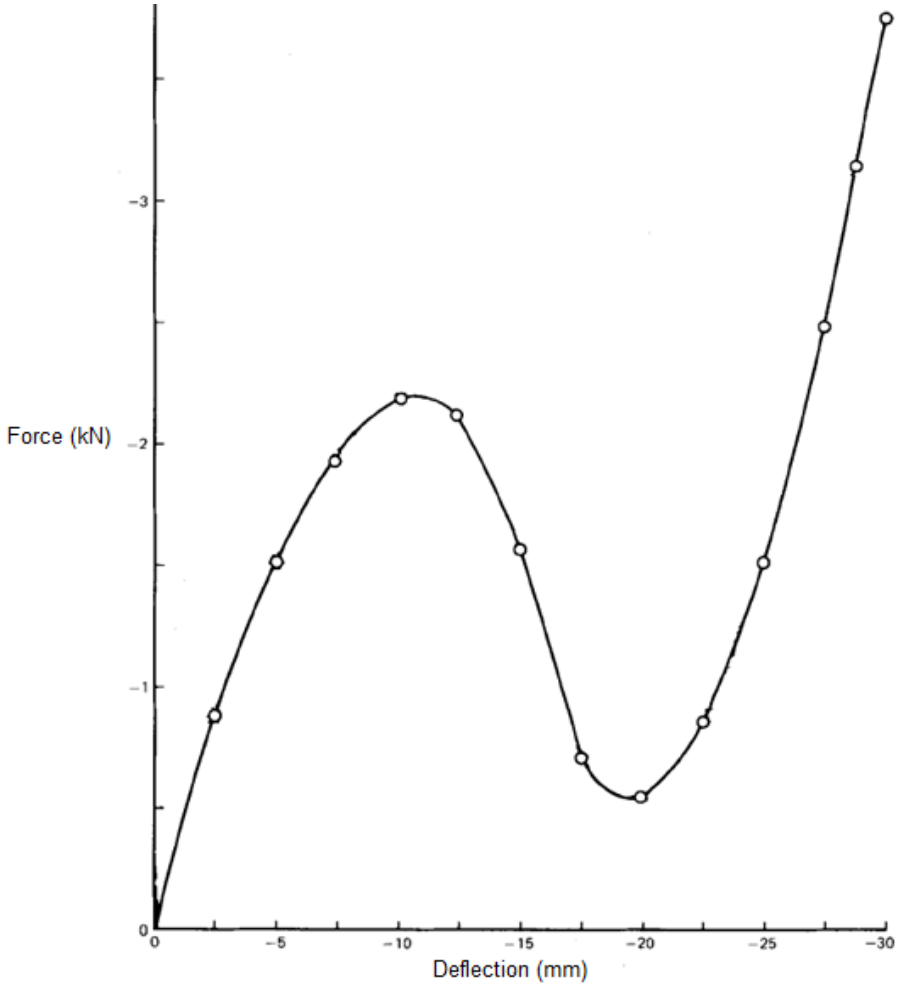

Figure 200-1. Graph of the Force vs. Y Deflection at Center Point

Autodesk Simulation Solution

A quarter symmetry model was created using a two-object mesh with 3 divisions along each length. A 1,000 N force was applied to the center node. Hinged constraints were applied along the longitudinal edge. Symmetry boundary conditions were applied along each of the symmetry planes. Thin shell elements were defined with the specified material and thickness parameters. For the Riks analysis, an initial load factor increment of 0.06 was used and a total of 100 steps were requested.

A comparison of the results with the theoretical is found in the following table.

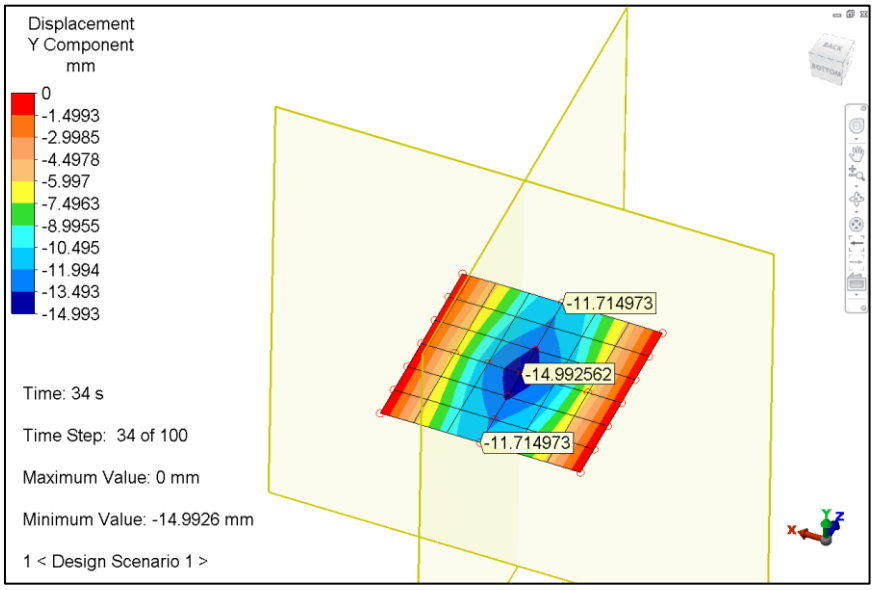

Figure 200-2. Y displacement when center node displaces 15 mm due to applied force.

Figure 200-3. Load level table from the log file

Time	Percent	DT	L	Iter.	Residual	Load level
1.000000	1.00	1.000000	1	1	1.0000E+00	6.0000E-02
1.000000	1.00	1.000000	1	2	3.6482E-02	6.0000E-02
1.000000	1.00	1.000000	1	3	5.8780E-05	6.0000E-02c
2.000000	2.00	1.000000	1	1	1.0000E+00	1.2000E-01
2.000000	2.00	1.000000	1	2	4.0793E-02	1.2000E-01
2.000000	2.00	1.000000	1	3	8.3324E-05	1.2000E-01c
32.000000	32.00	1.000000	1	3	6.3965E-06	4.0700E-01c
33.000000	33.00	1.000000	1	1	1.0000E+00	3.9041E-01
33.000000	33.00	1.000000	1	2	5.4067E-03	3.9017E-01
33.000000	33.00	1.000000	1	3	5.4334E-06	3.9017E-01c
34.000000	34.00	1.000000	1	1	1.0000E+00	3.7313E-01
34.000000	34.00	1.000000	1	2	4.1472E-03	3.7296E-01
34.000000	34.00	1.000000	1	3	4.3084E-06	**3.7296E-01c**
35.000000	35.00	1.000000	1	1	1.0000E+00	3.5560E-01
35.000000	35.00	1.000000	1	2	2.8553E-03	3.5550E-01
35.000000	35.00	1.000000	1	3	3.0525E-06	3.5550E-01c

The force applied at a given time has to be calculated using the following equation:

= [Load Level from the LOG file] x [Applied force] x [symmetry multiplier]
= 0.37296 x 1000 N x 4
= 1492 N
= 1.492 kN

Table 200-1. Comparison of Results When Vertical Deflection at the Force Location is -15 mm

	Theory	**Analysis**	**% diff**
Force Applied at Center (kN)	1.5584	1.492	-4.2
Vertical Deflection (Y) of Point Along the Center of the Edge (mm)	-11.3711	-11.715	-2.9